CARLETON
TECHNOLOGIES INC

A Cobham plc company

REDESIGNED GAS MASS FLOW SENSORS

FOR

SPACE SHUTTLE PRESSURE CONTROL SYSTEM

AND

FUEL CELL SYSTEM

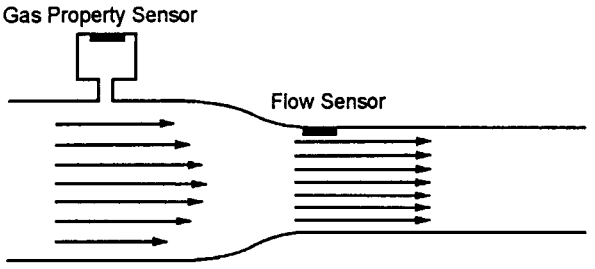

NASA Contract No. NAS9-19322

Date: 6/25/96
Report No: CRT-1311

CARLETON
TECHNOLOGIES INC

A Cobham plc company

REDESIGNED GAS MASS FLOW SENSORS FOR SPACE SHUTTLE PRESSURE CONTROL SYSTEM AND FUEL CELL SYSTEM

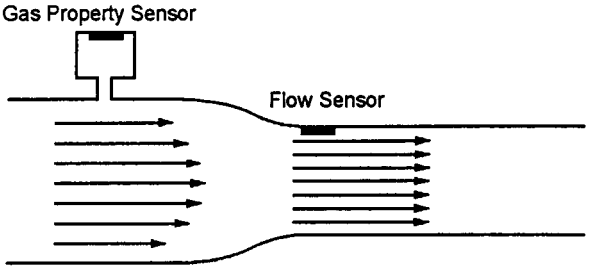

NASA Contract No. NAS9-19322

Date: 6/25/96
Report No: CRT-1311

Approved:

SUMMARY

A program was conducted to determine if a state of the art micro-machined silicon solid state flow sensor could be used to replace the existing space shuttle orbiter flow sensors. The rather aggressive goal was to obtain a new sensor which would also be a multi-gas sensor and operate over a much wider flow range and with a higher degree of accuracy than the existing sensors. Two types of sensors were tested. The first type was a venturi throat design and the second was a bypass design. The accuracy of venturi design was found to be marginally acceptable. The bypass sensor was much better although it still did not fully reach the accuracy goal. Two main problems were identified which would require further work.

Introduction

The Gas Mass Flow Sensor Proof of Concept Testing for Space Shuttle Orbiter Flow Measurement program was conceived as a means of demonstrating that a commercially available state of the art micro-machined silicon solid state flow sensor would meet the stringent environmental requirements of the Orbiter. And also, hopefully, exceed the capabilities of the existing flow sensors by having a multi-gas capability and an improved flow range, improved accuracy, reduced power consumption and drift rate. Because of certain unforeseen problems, which will be discussed later, the program quickly became more development oriented rather than proof of concept oriented. As a result the time scale of the program was greatly extended and, although the program was intended to be fully funded by NASA, it became necessary for both the Honeywell Technology Center and Carleton Technologies Inc. to invest substantially in order to ensure that the results of the program approached the original goals as closely as possibly. Both Carleton and Honeywell were prepared to make this investment because of their continuing commitment to the concept of producing a space qualified flow sensor with currently unrivaled capabilities.

The original program called for the manufacture and test of two through flow venturi design units (identified as Unit 1 and Unit 2) in order to estimate unit to unit variation. Fortunately this was done because a significant difference was found between the units (this will be discussed in the section on unit 2) which invalidated the premise that a multi-gas sensor could be produced. Also, substantial noise was found with this approach as well as great difficulty in reaching the accuracy requirements. For these reasons Honeywell recommended that a different approach be adopted. Honeywell had developed at their own expense a bypass type of flow sensor for another application and based on their estimation of its improved performance in the areas of noise, accuracy and unit to unit repeatability proposed that it be used as a replacement for the venturi type units. Honeywell offered to loan this bypass unit (identified as Unit 3) to Carleton and NASA for test purposes and as a result NASA agreed for the original plan to be modified to conduct only spot checks on unit 2 and introduce unit 3 into the program in place of unit 2. Unfortunately, because of a chip manufacturing problem (micro-cracks which are the subject of further discussion later) much time was lost in obtaining a properly functioning unit 3 and so the full range of tests was not conducted but rather a sufficient subset.

This report shows an approximate time line of the testing which was conducted and mentions some of the minor problems encountered which are not addressed elsewhere. A discussion of the test results for each of the three units tested are presented in turn. The actual results plots are contained in three appendices (B,C & D respectively) to avoid cluttering the report. Appendix A contains a red-lined test plan and a red-lined test procedure and a paper which was prepared based upon the preliminary test data and presented at the 1996 ICES conference. The test plan shows a test setup schematic and details the testing methodology which was adopted in order to conduct a thorough and rational low cost test program. The paper shows cross sections for the two sensor types and gives a description of the principle of operation of each type thus this information is not repeated in the body of the report. Appendix E contains the Honeywell final technical report which was delivered to Carleton in March 1996. Finally, the conclusions section summarizes Carleton's findings and recommendations for further means of advancing the technology to a point where it can be utilized to supplant the extant sensors.

A Short Summary of the History of the Testing Conducted

As the program was originally conceived it was believed that Honeywell would deliver a fully calibrated unit to Carleton for testing. However, Honeywell's flow standard proved to be incapable of handling the wide range of flows to be covered, as a result, Carleton was forced to run all calibration tests before any significant testing could be conducted. These calibration tests consisted of six or seven flow sweeps covering ambient nitrogen, hot and cold nitrogen, oxygen and helium. Occasionally the cold nitrogen sweep would be dispensed with. After the calibration data was obtained a significant amount of manipulation was required to transform the data into a form easy for Honeywell to deal with. This calibration effort occupied between 4 and 5 days of work and as will be seen was repeated many times during the program.

The original test program was scheduled to start in March 1995 but was postponed to September 1995 because Honeywell experienced problems with the first batch flow sensor chips produced. These produced a large orientation error and Honeywell believed that by reducing the size of the chips by an order of magnitude the error would be significantly reduced.

The first unit was delivered at the beginning of September and preliminary testing was started to try and get any bugs in the test setup worked out. The unit was observed to be very noisy. Also, the unit temperature sensor was observed to respond to unit body temperature rather than gas temperature. This latter fact caused an immediate change in the DOE structure as it had been planned to conduct tests in which the gas temperature and the unit temperature were different. Because it was essential for accuracy for the unit temperature sensor to give an accurate gas temperature reading it was necessary to only run tests in which the unit body and gas temperatures were identical.

Calibrate unit 1.

Second unit delivered in middle of September. Unit observed to be extremely noisy.

Calibrate unit 2.

Visit by Honeywell to review test setup. Agreed that unit 2 be returned to Honeywell to improve noise.

Commenced testing on unit one. Observed that voltage out put not operating. Unit returned to Honeywell for rework.

Unit 1 returned to Carleton with working voltage output. Commenced unit 1 calibration and observed that voltage output flipped to zero at maximum flow. Unit 1 returned to Honeywell for rework.

Unit 1 returned to Carleton. Checked voltage output working correctly and noise improved by new software code.

Honeywell by studying calibration data determine that there is a problem with unit 2 in that helium gas flow error performance is different from unit 1 by approximately a factor of 2. This is believed to be a function of the flow channel.

Carleton flow measurement equipment damaged by improper use by new technician. Equipment returned to vendor for repair (November 95). Repaired unit returned end of December. Equipment recalibrated and accuracy checked.

Unit 1 calibrated and the first meaningful test data begins to be collected.

Honeywell state that flow channel problem with unit 2 is insurmountable and offer loan of bypass unit (unit 3) as a potential solution.

Unit 1 DOE tests run (March 1996)

Unit 1 flow, pressure, temperature, gas type sweeps run.

Unit 1 step response tests run.

Unit 3 received and calibrated.

Preliminary testing shows pressure sensitivity and lack of repeatability. Unit returned to Honeywell. It is discovered that flow sensor chip is cracked (according to Honeywell caused by a flaw in manufacturing process). Inspection shows many other chips from same batch also cracked. Honeywell find one which is not and repair unit 3.

Unit 2 calibrated. It is observed that the noise on this unit is substantially improved. A subset of flow, pressure, temperature and gas type sweeps is run as a spot check per agreement with NASA. The helium gas factor of two flow error is still present.

Unit 3 returned to Carleton.

Unit 3 calibrated.

A subset of flow, pressure, temperature and gas type sweeps is run as a spot check taking into account the limited time left in the program. Some stand alone pressure sweeps are run at constant flow and a representative step response is run mid May 1996. Also, a number of temperature experiments run where the effect of small gas to unit body temperature differences is investigated.

Finally, during the first two weeks of June some repeat flow sweeps are run to investigate the effect of zero drift/shift.

Test Results Unit 1

The DOE results data and plots are presented in appendix B. The figure and table numbers presented in this section refer only to appendix B. Calibration data is not included. The data is presented in approximately chronological order.

Prior to commencing the main test program a preliminary flow test, using nitrogen at room temperature, was conducted to verify correct operation of the sensor and the test equipment. The results are shown in Figures 1 and 2. Figure 1 is Honeywell mass flow versus actual measured mass flow and Figure 2 is the error (as a percentage of reading) plot for figure 1. These show that the sensor gives an output with a linear trend over the required flow range but with a maximum deviation of 19% of reading. It was determined that, apart from a narrow flow range, the deviation was significantly constant and thus could be attributed to a potentially correctable calibration error. Therefore the test program was continued knowing that absolute errors would be unacceptable but in the knowledge that average error could be improved by more accurate calibration.

The first structured experiment (L8), which was designed to verify that humidity, ambient air pressure and X-axis orientation did not influence performance, was successful in that it did demonstrate that these factors had a negligible effect on the sensor output as expected. The results are shown in Table 1 (the actual DOE matrix is in figure 3 of the test procedure). The ANalysis Of VAriance (ANOVA) of the flow signal is in Table 2 and showed that 98.43% of the variation in flow was due to the flow changes within the experiment which indicates, not unexpectedly, that as a flow sensor the unit is very good. And also, that the other factors within the experiment, humidity, gas pressure, gas temperature, ambient pressure and X-axis orientation produced output variation of only 1.42% and so had almost no effect on the flow signal. The experimental error was only 0.15% of the variation within the experiment showing that the conditions were accurately set and that there were no significant effects from outside sources. An ANOVA was also performed on the flow error (as a percentage of reading) and is shown in Table 3 and indicates that 31.8% of the variation in error was due to flow, 6.4% due to gas pressure, 17.1% due to gas temperature, 6.0% due to ambient air pressure, 25.5% due to humidity and 3.8% due to X-axis orientation with 9.4% experimental error. None of these effects were statistically significant and it was hypothesized that the apparent effects, particularly the large and unexpected effect of humidity on the error were due to the use of a saturated experiment and to the difficulty in maintaining consistent gas and unit temperatures. To verify this a full factorial L4 experiment was run with flow and humidity as the only factors. The results are shown in Table 4 and the DOE matrix in Table 5. The ANOVA of the flow signal for this DOE is presented in Table 6 and shows that the flow changes accounted for 99.9% of the variation in flow and humidity for only 0.05%. The main effects plot is shown in Figure 3 and shows that changing relative humidity from 25 to 85% has an imperceptible effect on flow rate. The ANOVA for the flow error is given in Table 7 and shows that error variation was 49.5% due to flow, 10.7% due to humidity which again is not statistically significant and 39.9% due to experimental error and other factors not included within the experiment.

The results for the L18 experiment are shown in Table 8. Because the flow levels selected for nitrogen and oxygen were beyond the capability of the sensor for helium, the helium runs were conducted at flow levels one-tenth of the nitrogen levels. As a result, to analyze the data, the helium results had to be coded (multiplied by 10) to make them comparable with the nitrogen and oxygen. The flow signal ANOVA (Table 9) showed that 99.43% of the flow variation was due to flow changes within the experiment with no statistically significant effects from other sources. The flow error ANOVA (Table 10) showed no statistically significant effects, and a residual of 55.6% which indicates that there was more variation in flow error due to experimental error and outside factors than there was due to the factors within the experiment. Of the five factors within the experiment, the gas pressure and the flow level, were the main contributors to flow error. The main effects plots (Figure 4) show that the sensor output is significantly linear with flow and virtually not affected by the other factors. Figure 5 shows the interaction plots which seem to indicate the presence of many interactions.

The L18 experiment was found to have been poorly designed because the flow levels selected were not equally spaced and because the interactions are uniformly distributed across all columns which gave the indication of many interactions. The lack of equal flow level spacing was

overcome by analysis of the logarithmic flow value. A series of five L4 experiments were subsequently necessary in order to establish which interactions were real and which were spurious. The interactions indicated by the L18 were between gas pressure and gas temperature, between gas temperature and Y attitude, between gas pressure and Y attitude, between gas pressure and gas type and between gas temperature and gas type. The results and test matrices for the five L4 experiments are shown in Tables 11 through 15. The ANOVA results for the five DOE's are shown in Tables 16 through 20. The main effects plots are shown in Figures 6, 8, 10, 12 and 14 and the interaction plots in Figures 7, 9, 11, 13 and 15. It was recognized that DOE 3D, the gas type and gas temperature interaction DOE, had been incorrectly run by using helium flow rates which were out of range so it was re-run and the revised matrix and results are shown in Table 21, the ANOVA in Table 22 the main effects plot in Figure 16 and the interaction plot in Figure 17. The interaction plots for the 5 DOE's show that the only real interactions are between gas pressure and gas temperature and between gas pressure and Y attitude. Both of these interactions are relatively weak being about 1.4% and 4.5% of flow reading respectively but together make it almost impossible to achieve the target 3% of reading requirement.

The gas pressure and Y attitude interaction is caused by the well known gravitational effect and was already identified by previous testing by Honeywell. The L4 results show that at low pressure (100 psi) the gravitational effect is almost zero but at high pressure (900 psi) is quite large such that when gas is flowing up through the unit the measured flow rate is approximately 4.5% higher than when nitrogen gas is flowing down through the unit.

The gas pressure and gas temperature interaction was previously unknown and shows what appears to be a gas density related effect such that at low temperature and high pressure (when gas density is a maximum) the unit measured flow rate output is about 1.4% higher than when the pressure is low or the temperature is high. As will be seen in the section on Unit 3 test results this was proven to be not a real unit interaction but a spurious one caused by lack of chip thermal isolation combined with the inability to keep the actual gas temperature and unit temperature exactly equal throughout the test. The DOE result was real but the cause was unfortunately not understood at the time. The program should have been halted to really understand this effect and then, in the long run, much time would have been saved.

Table 23 is a summary of the data found in the following figures 18 through 145. The Table shows clearly that average error and standard deviation is relatively constant throughout gas type and pressure and temperature ranges covered. This indicates the potential to improve the performance of unit 1 by calibration and filtering in the flow range covered by the Gdu signal. It was this information which gave confidence that the unit 3 results would be much better than unit 1 and the realization that attempting to cover the flow range by merging different flow sensor methodologies was not the best way to proceed.

Figures 18 through 145 are plots of the smart sensor flow signal output versus the actual measured flow for each of the seven laminar flow elements (LFE's) necessary to cover the flow range. These graphs show the linearity and hysteresis performance for one particular gas type, pressure and temperature combination and are representative of the other data collected. Included for each of the 12 cases shown in Table 23 is a figure which shows a concatenation of the seven individual tests and a figure which shows the error as a percentage of reading. These graphs show clearly the problems associated with measuring flow rate over such a wide range and problems with this particular unit.

Noise at the low and high flow ends of the flow range is seen. The low end noise is caused by poor signal to noise ratios and electrical noise on very low signals. The high end noise is caused by flow turbulence and the inability to create a single flow passage capable of maintaining laminar flow over such a wide flow and pressure range.

On the low flow plots (below 0.03 lb./hr for nitrogen) with LFE 1 a phenomenon is observed in which a vertical line of data points lies off to the side of the main response line. This is an error with the Flo-Dynamics computer used to convert the LFE signals into actual mass flows. It is caused by noise on the delta p transducer at very low flows causing the transducer signal to become negative signaling reverse flow through the transducer. The computer, instead of clipping or zero limiting these spurious values, took the absolute value and thus reflected them back so they appear to be valid data in the actual flow range.

The concatenated error plot shows that the concept of using two different flow measurement methodologies to cover the high and low flow ranges with a merging of the two methods in the middle is not capable of producing low errors in the merged area. This may be capable of being corrected by use of multiple lookup tables instead of curve fitted equations but a superior approach appears to be that which is embodied in the by-pass unit which uses only a single measurement methodology and avoids the merging of two separate range signals completely.

Figures 146 through 159 show step response tests for the sensor for the particular gas type, gas temperature and pressure conditions covered by the flow sweep tests shown in Table 23. The flow rate selected for the test was 8 lb./hr for oxygen and nitrogen and 1 lb./hr for helium. The sensor does not exhibit a typical linear system exponential time response, instead having a pure time delay of about 2.5 seconds before rising (or falling) instantly to the final value. The sensor uses a digital sampling and averaging technique to minimize the effect of flow noise and calculate the output mass flow signal, and thus changes the output once every 2 to 3 seconds. This low update rate is related to the use of non-optimized electronics in the unit and would be expected to be increased in a production unit by the use of a more powerful micro-processor.

Because of the averaging method used to reduce the noise levels the time delay associated with changing signals makes it very difficult to distinguish between true hysteresis and time delay effects. The faster a sweep is run the wider the apparent hysteresis band due to the time delay. The best estimate of hysteresis is obtained by assuming that the narrowest band is representative of the hysteresis and is least affected by the time delay. Figures 160 through 163 show a selection of flow sweeps in which the direction of increasing and decreasing flow has been shown. Figure 164 shows a segment of one of these flow curves with best fit straight lines for increasing and decreasing flow. The hysteresis is defined as half the difference between the two best fits and is approximately 0.7% of reading. The flow standard used has hysteresis of 0.1% of reading thus, the unit 1 hysteresis is estimated to be 0.6% of reading.

The power consumption of the unit was measured by measuring the current on each of the three power inputs in turn. The results are tabulated below.

Voltage level	Current	Wattage
-15 V	69 mA	1.035 W
+15 V	64 mA	960 mW
+5V	70 mA	350 mW

The total power consumption is about 2.35 watts. However, as the electronics are commercial and non-optimized it is expected that this figure will be capable of reduction in a flight unit. Also, several extra circuits related to heater power measurement and control are included in this design which would not be required in a bypass type of unit.

The pressure differential across the unit was measured at various flow rates. The values obtained were quite large, much larger than the target maximum values. For example, the pressure drop for nitrogen at 150 lb./hr is required not to exceed 28 psid and the unit measured value was 42 psid. It was theorized that the these large values were due to the filters and not to any inherent problem with the unit. This was tested by utilizing the existing Shuttle engineering unit flow sensor. It was equipped with the filters taken from unit 1 and the pressure differential was measured. The filters were then removed and the test repeated. The results are tabulated below.

Flow rate (lb./hr)	Drop with filter (psid)	Drop without filter (psid)
15	1.0	0.2
75	12.7	1.6
150	49.2	5.0

Thus it was concluded that the bulk of the measured pressure drop was due to the filters and not the unit. Because it is not feasible to test unit 1 without the filters in place actual pressure drops cannot be measured until the filter problem is corrected but based on the current

observations it is concluded that the actual unit 1 pressure drop will be slightly less than the existing Shuttle flow sensor.

Test Results on Unit 2

The plots of the test data are presented in appendix C. The figure numbers presented in this section refer only to this appendix. Calibration data is not included. The data is presented in approximately chronological order.

As already discussed in the introduction, due to changes in the test plan and limited testing time available only a few spot checks were run on unit 2. Just sufficient to see that the unit is functional and to obtain a rough measure of the performance. Figure 1 is a plot of unit 2 mass flow versus actual measured mass flow at a number of discrete points across the flow range for nitrogen gas at 200 psig and room temperature. As can be seen the unit is, like unit 1, approximately linear from 0.1 to 8 lb./hr and then deviates substantially. The deviation occurs at the point where the unit begins to transition from a differential flow measurement methodology to a heater power methodology.

Figure 2 is an error plot for the flow sweep shown in figure 1. Error is presented as a % of reading and the different values obtained from each of the seven laminar flow elements LFE's used to cover the range are separately identified. As can be seen the unit is not very accurate with the range for reasonable accuracy being only 0.1 to 2 lb./hr.

Figure 3 is a flow sweep for nitrogen at 200 psig and 130 degrees Fahrenheit and is similar to figure 1. The error plot for figure 3 shown in figure 4 indicates about the same degree of accuracy.

Figure 5 is again similar to figure 1 but is for helium at 200 psig and room temperature. Notice that the unit 2 measured flows are shifted relative to the actual measured flows by about a factor of 1.53. This is the reason the type 1 sensor cannot be used as a multi-gas sensor. Although unit 1 was acceptable as a multi-gas sensor unit 2 cannot be calibrated for both nitrogen and helium simultaneously because of this factor of 1.53 error. For sensors operating correctly, such as unit 1, a series of sensor signals versus flow can be obtained as a function of temperature and gas type. At constant temperature the differences in these sensor flow signatures for different gases amounts to a simple zero shift which allows all of the signatures to be collapsed into a single calibration curve. For the unit 2 sensor this was not possible as there appears to be an approximately constant multiplication factor relating the different gas flow signatures. Figure 6 is the related error plot and highlights the problem by showing the error plot is centered about 35% (1-1/1.53) instead of 0 as with the nitrogen error plot.

Figure 7 is a flow sweep for helium at 200 psig and 40 degrees F. It shows the same trend as the helium at room temperature. Figure 8 is the associated error plot which is again centered around 35% instead of zero.

Figure 9 is a flow sweep for oxygen at 900 psig and 40 degrees F. It shows a similar trend to the nitrogen plots with a fair degree of linearity up to the sensor transition point. The equivalent error plot is centered about zero as expected and shows reasonable accuracy from 0.05 to 9 lb./hr.

Test Results Unit 3

The plots of the test data are presented in appendix D. The figure numbers presented in this section refer only to this appendix. Calibration data is not included. The data is presented in approximately chronological order.

Due to the short time scale remaining in the test program only a limited amount of testing was accomplished, but, it is hoped sufficient to enable an appreciation of both the problems associated with and the capabilities of the unit. No designed experiments (DOE's) were run on unit 3, however, as a full range of DOE's was run on unit 1 and as unit 1 and 3 used identical flow sensing chips, simply arranged in a different geometry, it is believed that no loss of information occurred. The environmental factors covered by the DOE's should have generated the same results when applied to the chips in unit 3 as were obtained with the chips in unit 1. Unfortunately only one version of unit 3 was available and so no estimate of unit to unit variability was capable of being obtained. This is the major shortfall in the testing conducted on the bypass unit.

One reason for the short time scale is that a lot of time was lost due to the fact that the first time unit 3 was delivered to Carleton by Honeywell it contained a cracked flow chip which apparently caused many anomalies related to non-repeatable results. In general, data collected with the cracked chip is not presented. The cracks are the product of a defective manufacturing process utilized in the manufacture of prototype chips and not representative of production units.

The tests which were conducted on unit 3 consisted of a series of pressure, temperature and flow range sweeps. The sweeps were not continuous as were the sweeps which were performed on unit 1 but were a series of discrete data points collected over the flow range. The flow sweeps were run for different gases, (nitrogen, oxygen and helium) at different pressures and temperatures. A similar spectrum was covered to that which has already been discussed in the test results for unit 1.

One of the first points to mention, with regard to unit 3, is that it was not optimized for the flow range requirements as units 1 and 2 were. Its main flow channel diameter is 25 mm whereas in units 1 and 2 the throat is 10 mm. Thus, theoretically unit 3 should be able to handle much higher flow rates than the venturi type units. However, Figure 1, which is a plot of the raw sensor signal Gdu versus flow, shows a characteristic curl over at a flow rate of about 170 lb./hr. This represents the absolute limiting flow rate of the unit because beyond this point the relationship between flow rate and Gdu is multi-valued and hence indeterminate. So it appears that although theoretically this flow channel should handle flows up to nearly 1000 lb./hr it is only capable of 170. This is an unexplained anomaly which requires further investigation. Although these particular results were obtained with the cracked flow chip the replacement chip also showed a very similar trend in this area with an apparent curl over at about 190 lb./hr.

The second most important point to mention is that the unit is highly sensitive to small differences in temperature between the gas and the chip on board temperature sensor. Unfortunately this effect was not recognized until very late in the testing and so all calibration data was collected with only nominally similar gas and unit temperatures. This will probably explain much of the difficulty in obtaining a good unit calibration. This effect was misdiagnosed originally as either drift, or pressure sensitivity. Ultimately it was realized that the apparent lack of repeatability or pressure sensitivity was totally due to these temperature differences which were not being controlled as tightly as necessary because the result of very small temperature differences was not understood.

Figure 2 is a flow sweep for nitrogen at 200 psig and 100 degrees F. Figure 3 is the associated error plot and Figure 4 is an enlargement of the error in the range ±10%. As can be seen the unit is not calibrated properly because there is a distinct trend with error moving from negative to positive as flow increases, in other words a slope error. Also, because of the curvature at the low flow end it is obvious that the unit has an incorrect value of Gdu-zero. The range of flows where the unit remains in the approximately ±3% range is from 2 lb./hr to about 80 lb./hr. Figure 5 is a flow sweep for oxygen at 900 psig and room temperature and Figure 6 is the related error plot again showing good accuracy between 2 and 80 to 100 lb./hr. Figure 7 is a flow sweep for nitrogen at 200 psig and room temperature and Figure 8 is again the error plot showing good accuracy between about 1 and 150 lb./hr. Figure 9 is a flow sweep for helium at 200 psig and room temperature and Figure 10 is the error plot showing good accuracy between about 4 and 7

lb./hr. Figure 11 is a flow sweep for oxygen at 900 psig and 150 degrees F and Figure 12 is the related error plot. Figure 12 is the same error plot with an expanded scale and shows good accuracy between 1 and 40 lb./hr. Figure 13 is a flow sweep for helium at 200 psig and 30 degrees F and Figure 14 is the related error plot and shows good accuracy between about 9 and 22 lb./hr. Figure 15 is a flow sweep for nitrogen at 200 psig and 150 degrees F and Figure 16 is the related error plot. Figure 17 is the same error plot with an expanded scale and shows good accuracy between about 3 and 30 lb./hr. This data is summarized in Table 1 below.

Table 1 - Flow Accuracy Summary

Gas	Pressure	Temperature	Accurate Flow Range
Nitrogen	200	Ambient	1 to 150
Nitrogen	200	100	2 to 80
Nitrogen	200	150	3 to 30
Oxygen	900	Ambient	2 to 90
Oxygen	900	150	1 to 40
Helium	200	Ambient	4 to 7
Helium	200	30	9 to 22

What these flow sweep plots and the table show is that the unit is capable of covering the flow range over a range of pressures and temperatures for all three gases tested. All of the plots show the similar trend of incorrect calibration at the low flow end. This is caused by a value of Gdu-zero (the basic sensor zero offset) which is incorrect. The fact that this bias value was set incorrectly is a combination of two factors, firstly, as already mentioned, the unit is very temperature sensitive and the gas to unit temperature difference was not sufficiently tightly controlled during the calibration runs. Secondly, the unit was suffering from a burn-in transition drift which was not recognized at the time as will be explained later. As a result the unit was not in a stable situation for calibration or for subsequent testing.

Figures 17 and 18 show a representative step response for the unit. The demonstrated characteristic is, as expected, identical to that which was obtained from unit 1 and reference to the section on unit 1 test results will provide expanded comment.

Figure 19 is one of the many pressure sweep tests which were initially run and which caused considerable worry because they seemed to show that the unit mass flow output was a function of pressure and/or also varied widely with time (the ±3% of reading band is also shown for reference). However, Figure 20 shows that while the gas and unit temperatures were nominally kept constant throughout the test the temperature difference actually changed with pressure (time) and an almost perfect correlation is seen between the apparent flow variation and the extremely small temperature difference variation.

Figures 21 through 27 show the results of a series of tests designed to investigate this temperature sensitivity. For these tests the actual mass flow, gas pressure and unit temperature were rigorously held constant. Initially the gas temperature was set as closely as possible to the unit temperature. After a suitable stabilization period the gas temperature was given a slight positive disturbance followed by a negative disturbance and finally returned to the unit temperature value. The curves show large flow reading changes (up to 40% for a 7 degree F temperature change). The flow variations show good correlation with the temperature difference variations as shown in Table 2. These results show excellent agreement with the results of the

Table 2 - Flow to Temperature Difference Correlation

Pressure	Flow Rate	Correlation Coefficient
200	2	0.6852
900	2	0.9783
900	10	0.9758

DOE which was run of unit 1. The DOE highlighted an unknown pressure and temperature interaction and indicated that flow rate was more sensitive to temperature at high pressure than at low pressure. As can be seen here, at low pressure, the correlation is not as good as at high pressure.

It was decided to determine whether this effect could be corrected by temperature compensation. Because the unit temperature sensor was mainly responding to unit body temperature changes instead of gas temperature changes the unit effectively had no compensation. In these tests, where unit sensor temperature was deliberately kept completely constant, it was definitely completely ineffective. Thus the 900 psig and 10 lb./hr case was manipulated on a spread sheet and a temperature compensation algorithm based on the actual gas temperature was applied. Figures 28 and 29 show the before and after results for mass flow and flow rate error as a function of time. It can be seen that application of the algorithm was capable of reducing the 14% flow deviation to about ± 2%. Unfortunately, the coefficients used in the algorithm were much larger than expected and would probably be inappropriate for larger temperature variations. Thus the whole question of temperature compensation for the unit is something which does require further investigation. Honeywell have provided the curve shown in Figure 30 which shows that the temperature compensation algorithm with normal coefficients works quite well over a very wide temperature range for their standard production unit.

Normally, when Honeywell manufacture flow units the chips are subjected to a proprietary hardening or burn-in process. However, because the chips used in units 1 through 3 were new prototype chips not manufactured by the standard process they were not subjected to this accelerated burn-in cycle. (These prototype chips were used because they were designed to reduce or eliminate the orientation error.) Honeywell's experience suggested that natural burn-in could be accomplished by normal operational use over a number of days. However, it appears that in the case of these new chips that was not true and as the testing cycled the units through higher and higher temperatures the zero offset continued to change. This effect is illustrated by the final two figures 31 and 32. The initial flow sweep was run after calibration at a maximum temperature of 130 degrees F and showed a large negative error at low flow. The unit was subsequently tested at 150 degrees and then the ambient test was repeated on 6/7/96 and showed a large positive error (the zero offset of the unit was noticed to have changed by about 3 milli-volts between runs). One week later (the unit was kept continually powered) the test was repeated again on 6/14/96 with almost no change indicating that the unit had stabilized and could now be accurately calibrated at low flow. The high flow calibration accuracy would still be dependent on obtaining proper temperature compensation.

Conclusions

New programs seldom move to completion as originally planned and this one was no different. Hindsight indicates that more preparatory work/testing should have been carried out before launching such an ambitious program. None-the -less, much work was accomplished and much information was gained so that although the program was only partially successful in reaching the original goals, enough was learned to enable some cogent observations and recommendations to be made.

The Accomplishments:

It has been determined that both the venturi and bypass types of sensor are capable of operating over the required gas type, pressure, temperature, orientation attitude and flow ranges required. Also it has been demonstrated that the units utilize little power, have a fairly low pressure drop and a relatively fast response time. It has been shown that the units are insensitive to relative humidity and ambient pressure. In terms of flow accuracy and noise the venturi type is marginal but may have the potential to be improved to a point where it could meet the accuracy goal for a specific gas type. The bypass type can definitely meet the accuracy target over very wide flow ranges and for various gas types. The unit's orientation sensitivity in a gravitational environment has been established and measured. The units have been shown to be both robust, having survived many shipments between Carleton and Honeywell, and capable of operating over extended periods without maintenance. The importance and required avoidance of certain manufacturing defects, such as micro-cracks, has been highlighted.

The Remaining Work:

What has not been achieved is that no measure of unit to unit variation has been obtained for the bypass unit and as was seen with the venturi sensor type this could be crucial. Satisfactory temperature compensation has not been demonstrated for either sensor type. Although Honeywell have supplied data showing good temperature compensation for production units the data do not address either high pressure or very small temperature differences, which effects have been seen to be large. Further, the ability to satisfactorily thermally isolate the chip from the unit body, to allow proper temperature compensation, has not been demonstrated. Also, related to this feature, the effect of thermal gradients caused by gas to unit body temperature differences has not been investigated. Finally, it has not been demonstrated that the bypass type of sensor can accommodate the required flow ranges when the flow channel is sized according to recognized theoretical guidelines.

Recommendations:

Carleton and Honeywell are still committed to the long term goal of producing a space qualified flow sensor with capabilities which are not available from other products. However, being both pragmatic and averse to taking unnecessary risks Carleton believes that before launching into a full flight development and qualification program a further small development/demonstration program should be completed to address all of the items listed above in the remaining work section. Carleton therefore proposes that Carleton and Honeywell be funded by NASA to modify the two units (Unit 1 and Unit 2 which are NASA owned products of the current program) for further development. This modification would involve re-using the existing electronics but replacing the flow channels with properly sized bypass type flow channels fitted with actual production chips (not prototypes). The programmed modification would be designed to allow initially, investigation of chip thermal isolation, and subsequently, the use of a separated temperature sensor located in the flow path as a fall back position, should sufficient thermal isolation for satisfactory temperature compensation prove impossible.

In addition, to further lower risk, funds should be made available for the design, building and stand alone testing of a set of prototype flight type electronics.

RED LINED
R.7.

FLOW SENSOR TEST PLAN

Introduction

The purpose of the flow sensor program is to determine if the solid state flow sensors can meet the target specifications for accuracy and response time and to characterize their overall performance (not including EMI and vibration) within the NASA defined operating conditions as shown in Table 1.

The purpose of the test plan is to define the testing to be conducted to enable accuracy, response time data and sensor characterization to be obtained. The testing of the flow sensors will be divided into two categories, design of experiments (DOE), to obtain the sensor characterization, and one factor at a time testing to obtain the accuracy (linearity, hysteresis and repeatability) and response time data. The designed experiments will be tailored to obtain the maximum amount of information as inexpensively and as quickly as possible. The DOEs will determine sensor sensitivity factors and interaction effects for all of the pertinent parameters. The one factor at a time test will also tend to act as a verification of the DOE testing to further boost the test confidence level.

Figure 1 shows the proposed test configuration. A data acquisition system will be used to both control the experimental conditions and to collect the data.

Three DOEs will be run on the sensors. The first will be an L8 run on one sensor only to carry out some preliminary screening and hence enable more efficient and accurate data to be subsequently collected by enabling some of the potential factors to be eliminated. Then a three level L18 DOE will be used in order to obtain curvature data for the sensitivity factors. Finally a second L8 will be run as a full factorial, again on one sensor only, to test for interactions on the main factors. For the L18 the same test conditions will be applied to both sensors in order to obtain replicate information which will be used to improve the overall accuracy of the experiment and as a confidence factor.

The factors considered in the DOEs will be ambient pressure, ambient temperature, relative humidity, gas flow rate, gas temperature, gas pressure, gas type (three gases used in the DOEs will be oxygen, nitrogen and helium) and orientation about each of the X and Y axes. (Figure 2 shows the orientation axes definition.) These nine parameters are judged to be the only ones which might affect operation of the sensor. The responses to be collected and analyzed will be flow rate, pressure drop, power consumption, flow rate error, thermal conductivity error, pressure and temperature.

The experimental factor test levels (conditions) are selected to be slightly different for the three experiments so that the data can be merged to give more complete curvature indications by having 7 points on the curve instead of only 3.

The one factor at a time testing will consist of flow rate sweeps for each of the three gases in which the flow rate will be both increased from minimum to maximum and then decreased from maximum to minimum to obtain hysteresis data. Also, flow rate step response tests will be carried out for each of the three

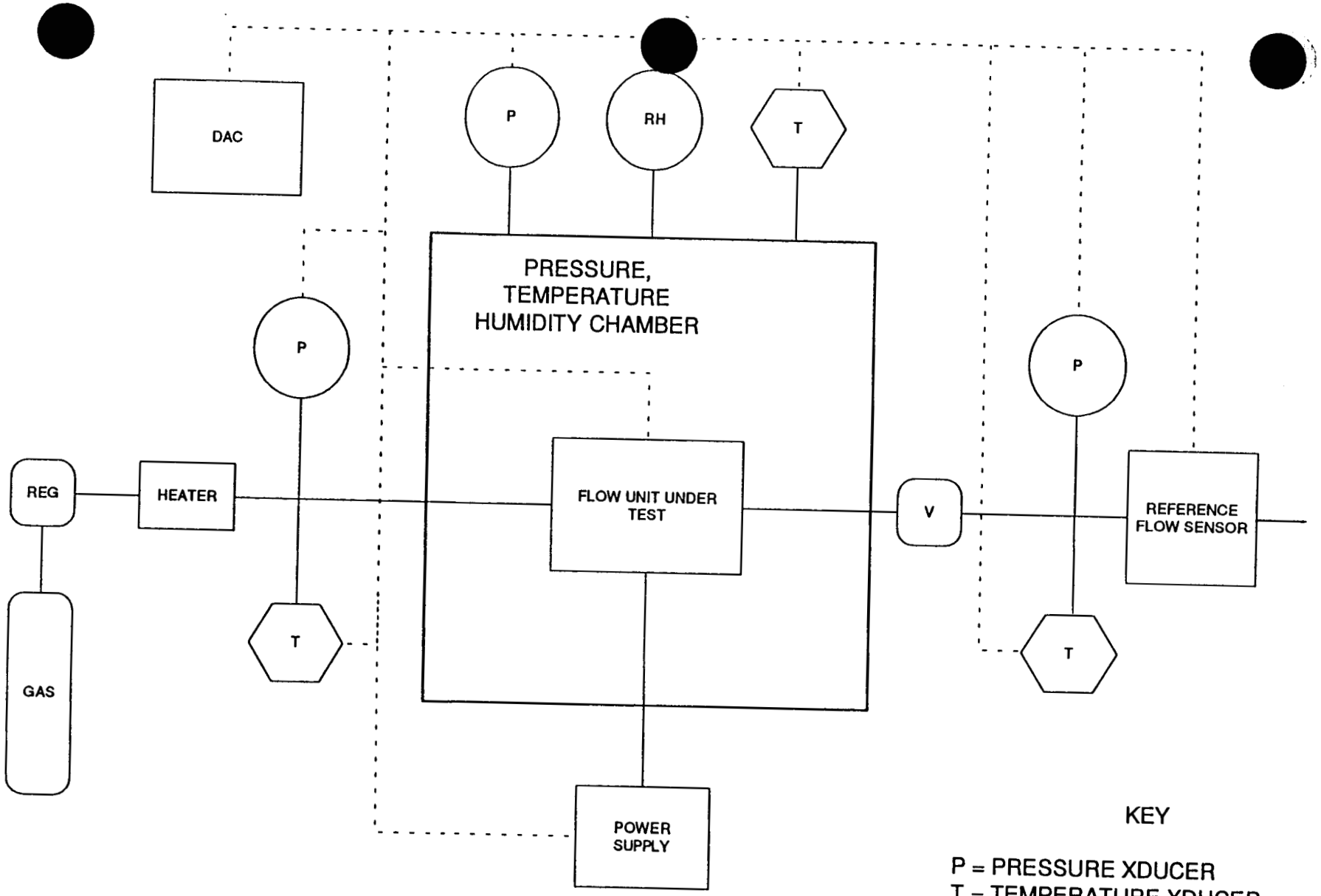

Figure 1

HONEYWELL FLOW SENSOR TEST SETUP

gases . The one factor at a time tests will be repeated at NASA for a fourth gas (hydrogen) after all testing at Carleton is completed.

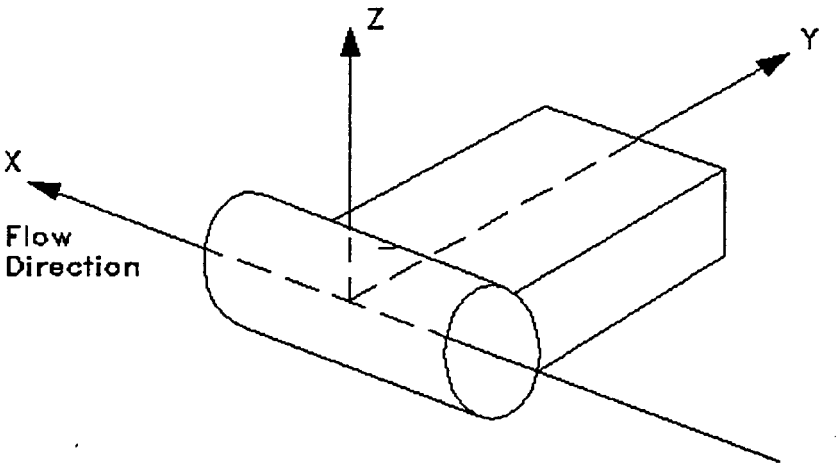

Figure 2 Orientation Axes Definition

Parameter	Requirement
Operating Fluids	Nitrogen/Oxygen/Hydrogen/Helium
Flow Range	0.01 to 150 lb/hr
Pressure Range	100 to 1000 psig
Max Pressure Drop Oxygen	0.5 psid @ 900 psig & 15 lb/hr
	2.0 psid @ 900 psig & 75 lb/hr
Max Pressure Drop Nitrogen	0.5 psid @ 200 psig & 15 lb/hr
	28.0 psid @ 200 psig & 150 lb/hr
Max Pressure Drop Hydrogen	0.5 psid @ 200 psig & 15 lb/hr
Max Pressure Drop Helium	0.5 psid @ 200 psig & 15 lb/hr
Gas Temperature Range	35 to 175 degrees F
Ambient Pressure Range	0 to 15 psia
Ambient Temperature Range	40 to 90 degrees F
Accuracy	< ± 3% of reading
Offset at Zero Flow	< ± 0.01 lb/hr
Drift	Unit remains in calibration > 5 years
Response Time	< 3 seconds
Maximum Power	1.5 Watts @ 28 VDC
Output Voltage Range	0 to 5 VDC
Acceleration	* 4.4 vertical, 4.8 lateral g's
EMI	* TBD
Volume	* < 30 cubic inches
Weight	* < 1.35 lbs
Particle Impact Sensitivity	* Oxygen safe
Service Life	* > 10 years

Table 1 - Flow Sensor Requirements (* Not Required for Demonstration)

File: FLOW1 .DAT
Title: Solid State Flow Sensor Screening Test
Comment: Screening to Reduce Number of Factors
Response: Flow & Err, Pwr, Delta P & Thermal Err

Design Listing:

TC#

	1	2	3	4	5	6
	Flow Rate	Pressure	Gas Temp	Air Press	Humidity	X Attitude
1:	5	100	50	14.5	85	+90
2:	50	100	50	~~0.5~~ 1.7	25	+90
3:	5	800	50	~~0.5~~ R.7	85	-90
4:	50	800	50	14.5 3/5/96	25	-90
5:	5	100	150	14.5	25	-90
6:	50	100	150	~~0.5~~	85	-90
7:	5	800	150	~~0.5~~	25	+90
8:	50	800	150	14.5	85	+90
	Flow Rate	Pressure	Gas Temp	Air Press	Humidity	X Attitude

Figure 3

Measurement Accuracy for all Test Parameters

The following list shows the available measurement accuracy for each of the test parameters.

Ambient pressure	± 0.016 psia
Ambient temperature	~~± 1 degree F~~ 2 R.T. 3/5/96
Relative humidity	± 0.5 %
Gas pressure	± 1 psig
Gas temperature	± 2 degrees F
Flow rate	± 0.7% of reading

Detailed Test Description For DOEs

L8 Screening Experiment

With nine factors to be considered, in order to obtain interaction and curvature data, a large L81 experiment utilizing excessive resources would be required. However, it is suspected that orientation about the X axis, relative humidity and possibly ambient pressure are less likely to affect the sensor performance so this L8 will be designed to find out if this is, in fact, so and hence enable the deletion of these factors from the main experiment. Also, flow rate, gas pressure and gas temperature will be included to guard against the possibility of interactions between these factors (which are believed to be the primary factors affecting sensor performance) and the factors which we wish to drop from the main experiment.

This L8 will be run with only nitrogen and only one sensor because it is believed that sensor performance with one gas and one sensor will be characteristic and show the same trends with any gas or any sensor.

Figure 3 shows the actual experimental treatment combinations and levels.

L18 Main Experiment

Assuming that the L8 screening experiment verifies the expectation that orientation about the X axis, relative humidity and ambient pressure can be eliminated then the L18 main experiment will obtain curvature and sensitivity data for gas type, flow rate, gas pressure, gas temperature, ambient temperature and orientation about the Y axis for each of the two sensors.

Figure 4 shows the actual experimental treatment combinations and levels. This experiment can accept up to 7 three level parameters and one 2 level parameter so that with only 6 parameters actually utilized a measure of experimental error can be obtained because the experiment is not saturated. However, because any interactions between any pair of parameters in columns 3 through 6 are partially confounded with columns 3 through 8 there is a risk that if

File: FLOW .DAT
Title: Solid State Flow Sensor Screening Test
Comment: Preliminary Sensitivity Identification
Response: Flow & Err, Pwr, Delta P & Thermal Err

D[redacted]n Listing:

R.7. 3/5/96

TC#	1	2	3	4	5	8
	Gas	Flow	Press	Gas Temp	Air Temp	Y Attitude
1:	Oxygen	1	40	30	55	Up
2:	Oxygen	10	475	105	75	Up
3:	Oxygen	100	910	180	95	Up
4:	Nitrogen	1	40	105	75	Up
5:	Nitrogen	10	475	180	95	Up
6:	Nitrogen	100	910	30	55	Up
7:	Helium	1	475	30	95	Up
8:	Helium	10	910	105	55	Up
9:	Helium	100	40	180	75	Up
10:	Oxygen	1	910	180	75	Down
11:	Oxygen	10	40	30	95	Down
12:	Oxygen	100	475	105	55	Down
[redacted]	Nitrogen	1	475	180	55	Down
[redacted]	Nitrogen	10	910	30	75	Down
[redacted]	Nitrogen	100	40	105	95	Down
16:	Helium	1	910	105	95	Down
17:	Helium	10	40	180	55	Down
18:	Helium	100	475	30	75	Down
	Gas	Flow	Press	Gas Temp	Air Temp	Y Attitude

Figure 4

the interactions exist and are large then experimental error will be confused with them. Thus, a full factorial, follow on experiment will be run to identify the interactions.

L8 Full Factorial Experiment

The assumption is made that if interactions exist they are most likely between flow rate and gas temperature and flow rate and gas pressure. Thus with three factors an L8 is required for no fractionalization to occur. If the L18 shows any possible interactions between orientation and any parameter then this experiment may have to be expanded to an L16. Figure 5 shows the actual experimental treatment combinations and levels. Like the L8 screening experiment this experiment only needs to be run for nitrogen and one sensor because it again is assumed that trends for one gas and one sensor are characteristic for all gases.

One Factor At A Time Tests

These tests will utilize the same test setup as shown in figure 1 and will be run with ambient temperature at normal factory room temperature of approximately 72 degrees F $\pm$ 7 degrees and with orientation normal with the X axis horizontal (parallel to the factory floor). Each flow sensor will be subjected to the same tests. The tests will be repeated for each of the three gases nitrogen, oxygen and helium. Each test will consist of a flow sweep from zero flow up to maximum flow for the particular gas and back to zero while attempting to maintain gas temperature and gas pressure relatively constant. The test will be run at each of four conditions of gas temperature and pressure comprising all combinations of high and low. Thus high gas pressure and temperature, low gas pressure and temperature, high gas pressure and low gas temperature and finally, low gas pressure and high gas temperature. This will then require a total of 24 flow sweeps to complete all tests. This test data will be analyzed for linearity, error and hysteresis.

The test setup will then be modified to place a quick opening ball valve between the flow sensor and the pressure regulator. The data acquisition data collection rate will be set to maximum and the number of parameters collected will be reduced to flow rate and gas pressure only to facilitate data collection. The ball valve will be rapidly opened and then closed to simulate rising and falling step inputs to the sensor. The collected data will be analyzed to estimate the sensor response time. This series of tests will be repeated at an average gas temperature only but otherwise will cover the same combinations and conditions as the flow sweep tests and so will require 12 tests to complete the sequence. The volume between the ball valve and the sensor and between the sensor and the handvalve will be measured and hence by knowing the pressure rise and fall rates of these volumes the theoretical flow rates versus time can be computed

File: FLOW2 .DAT
Title: Solid State Flow Sensor Screening Test
Comment: Identification of Interactions
Response: Flow & Err, Pwr, Delta P & Thermal Err

Design Listing:

TC#

	1	2	3
	Flow Rate	Pressure	Gas Temp
1:	2	70	40
2:	80	70	40
3:	2	850	40
4:	80	850	40
5:	2	70	165
6:	80	70	165
7:	2	850	165
8:	80	850	165
	Flow Rate	Pressure	Gas Temp

Figure 5

and compared with the actual and by this means obtaining a measure of sensor response time.

Red LINED
R.7.

FLOW SENSOR TEST PROCEDURE

Required Test Condition Tolerances for all Experiments and Tests

Ambient pressure	± 0.25 psia
~~Ambient temperature~~	~~± 2 degrees F~~ R.7. 3/5/96
Relative humidity	± 5 %
Gas pressure	± 8 psig
Gas temperature	± 5 degrees F
Flow rate	± 1% of setting
Gas purity	± 0.1 %

Measurement Accuracy for all Test Parameters

Ambient pressure	± 0.016 psia
Ambient temperature	~~± 1 degree F~~ 2 R.7. 3/5/96
Relative humidity	± 0.5 %
Gas pressure	± 1 psig
Gas temperature	± 2 degrees F
Flow rate	± 0.7% of reading

L8 Screening Experiment

1. Use only the Honeywell unit A for this experiment.
2. Setup the test equipment in the configuration shown in figure 1.
3. To ensure thermal stability, allow the Honeywell unit and the reference flow sensor to warm up for 10 minutes after power up before any readings are taken.
4. Use a multi-turn handvalve with a maximum orifice capable of flowing 1000 LPM at 40 psig.
5. Set the DAC to collect data once every 10 seconds. Ensure that the DAC data is saved to disk, ensure that all actual test condition data is recorded as well as the electrical current to the unit under test and the following outputs from the unit; flow rate, pressure, temperature and thermal conductivity.
6. Use nitrogen as the supply gas.
7. For the reference flow sensor use the laminar flow elements for 5 and 50 lb/hr ranges (refer to table 1 for the correct elements). For the first test in the experiment use the 5 lb/hr element.
8. Refer to figure 3 for the test conditions required for this screening experiment. Note that the screening tests may be conducted in whichever order is most economical.

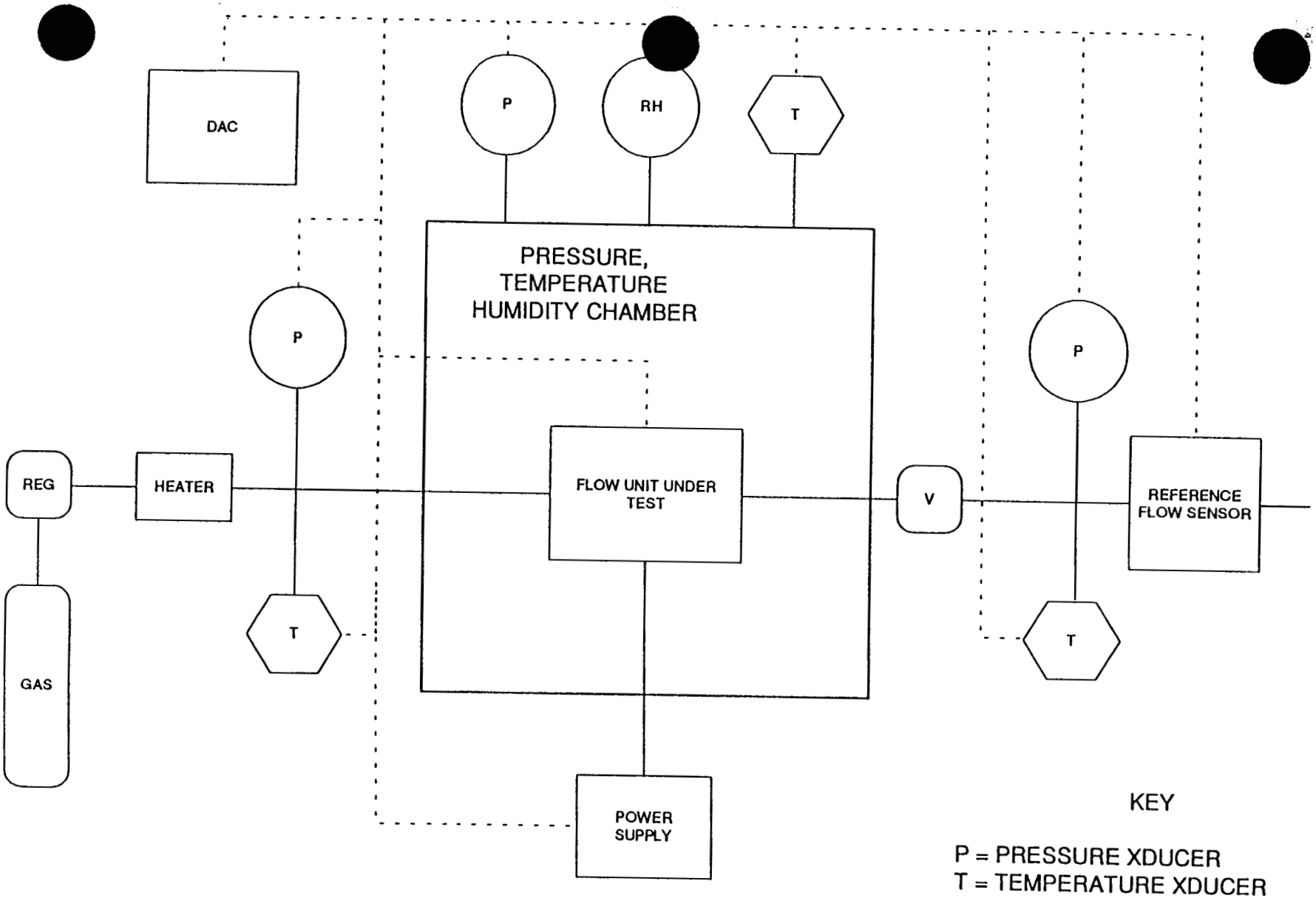

Figure 1

HONEYWELL FLOW SENSOR TEST SETUP

METER NUMBER	VOLUMETRIC FLOW RANGE (cfm)		NITROGEN FLOW RANGE (lb/hr)		OXYGEN FLOW RANGE (lb/hr)		HELIUM FLOW RANGE (lb/hr)	
	LOW	HIGH	LOW	HIGH	LOW	HIGH	LOW	HIGH
1	0.002	0.0081	0.0088	0.0352	0.0100	0.0403	0.0012	0.0050
2	0.008	0.0326	0.0352	0.1418	0.0403	0.1621	0.0050	0.0202
3	0.033	0.1313	0.1418	0.5710	0.1621	0.652	0.0202	0.081
4	0.131	0.5287	0.5710	2.2990	0.6525	2.627	0.0815	0.328
5	0.529	2.1286	2.2988	9.2550	2.6268	10.5754	0.3281	1.321
6	2.13	8.5695	9.2545	37.2580	10.5754	42.575	1.3207	5.317
7	8.57	34.5000	37.2579	150.0000	42.5754	171.4000	5.3170	21.410

Table 1 - Flow Meter Ranges

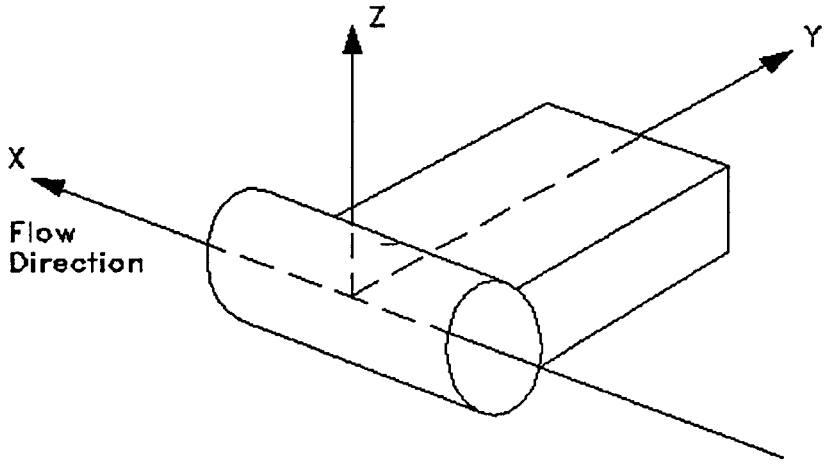

Figure 2 Orientation Axes Definition

9. Establish on the Honeywell unit A the location of the sensing element (the TO18 can on the side of the venturi) and arrange the unit in the PTH chamber so that the TO18 can is pointing in the up direction per figure 6 for all tests where the X attitude is required to be +90 degrees and in the down direction for tests where the attitude is -90 degrees.

10. Adjust the pressure regulator for 100 psig and adjust the hand valve for 5 lb/hr on the reference flow sensor. Re-adjust the pressure to compensate for any droop.

11. Adjust the PTH chamber to the correct conditions, ambient pressure 14.5 psia and relative humidity 85 %. Maintain the chamber temperature at 70 degrees F at all times.

12. Adjust the temperature of the gas heater/chiller until the gas temperature is 50 degrees F and recheck the flow and pressure. Allow the unit to stabilize for 2 minutes after all test conditions are stabilized.

File: FLOW1 .DAT
Title: Solid State Flow Sensor Screening Test
Comment: Screening to Reduce Number of Factors
Response: Flow & Err, Pwr, Delta P & Thermal Err

Design Listing:

TC#

	1	2	3	4	5	6
	Flow Rate	Pressure	Gas Temp	Air Press	Humidity	X Attitude
1:	5	100	50	14.5	85	+90
2:	50	100	50	~~0.5~~ 1.7	25	+90
3:	5	800	50	~~0.5~~ R.7	85	-90
4:	50	800	50	14.5	25	-90
5:	5	100	150	14.5 3/5/96	25	-90
6:	50	100	150	~~0.5~~	85	-90
7:	5	800	150	~~0.5~~	25	+90
8:	50	800	150	14.5	85	+90
	Flow Rate	Pressure	Gas Temp	Air Press	Humidity	X Attitude

Figure 3

File: FLOW .DAT
Title: Solid State Flow Sensor Screening Test
Comment: Preliminary Sensitivity Identification
Response: Flow & Err, Pwr

Data Listing:

TC#

	1	2	3	4	8
	Gas	Flow	Press	GasTemp	Y Attitude
1:	Oxygen	1	40	30	Up
2:	Oxygen	10	475	105	Up
3:	Oxygen	100	910	180	Up
4:	Nitrogen	1	40	105	Up
5:	Nitrogen	10	475	180	Up
6:	Nitrogen	100	910	30	Up
7:	Helium	1	475	30	Up
8:	Helium	10	910	105	Up
9:	Helium	100	40	180	Up
10:	Oxygen	1	910	180	Down
11:	Oxygen	10	40	30	Down
12:	Oxygen	100	475	105	Down
[illegible]	Nitrogen	1	475	180	Down
[illegible]	Nitrogen	10	910	30	Down
[illegible]	Nitrogen	100	40	105	Down
16:	Helium	1	910	105	Down
17:	Helium	10	40	180	Down
18:	Helium	100	475	30	Down
	Gas	Flow	Press	GasTemp	Y Attitude

File: FLOW .DAT
Title: Solid State Flow Sensor Screening Test
Comment: Preliminary Sensitivity Identification
Response: Flow & Err, Pwr, Delta P & Thermal Err

[redacted] Listing:

TC#

R.7 3/5/96

	1	2	3	4	5	8
	Gas	Flow	Press	Gas Temp	Air Temp	Y Attitude
1:	Oxygen	1	40	30	55	Up
2:	Oxygen	10	475	105	75	Up
3:	Oxygen	100	910	180	95	Up
4:	Nitrogen	1	40	105	75	Up
5:	Nitrogen	10	475	180	95	Up
6:	Nitrogen	100 R.7.	910	30	55	Up
7:	Helium	~~1~~ .1	475	30	95	Up
8:	Helium	~~10~~ 1	910	105	55	Up
9:	Helium	~~100~~ 10	40	180	75	Up
10:	Oxygen	1	910	180	75	Down
11:	Oxygen	10	40	30	95	Down
12:	Oxygen	100	475	105	55	Down
[redacted]	Nitrogen	1	475	180	55	Down
[redacted]	Nitrogen	10	910	30	75	Down
[redacted]	Nitrogen	100	40	105	95	Down
16:	Helium	~~1~~ .1	910	105	95	Down
17:	Helium	~~10~~ 1	40	180	55	Down
18:	Helium	~~100~~ 10	475	30	75	Down
	Gas	Flow	Press	Gas Temp	Air Temp	Y Attitude

Figure 4

13. Adjust the test conditions for the next test and repeat the above procedure, steps 9 through 12 being careful to always use the correct laminar flow element.

L18 Main Experiment

1. Use both the Honeywell units A and B in turn for this experiment.
2. Setup the test equipment in the configuration shown in figure 1.
3. To ensure thermal stability, allow the Honeywell unit and the reference flow sensor to warm up for 10 minutes after power up before any readings are taken.
4. Use a multi-turn handvalve with a maximum orifice capable of flowing 1000 LPM.
5. Set the DAC to collect data once every 10 seconds. Ensure that the DAC data is saved to disk, ensure that all actual test condition data is recorded as well as the electrical current to the unit under test and the following outputs from the unit; flow rate, pressure, temperature and thermal conductivity.
6. For the reference flow sensor use the laminar flow elements for 1,10 and 100 lb/hr ranges (refer to table 1 for the correct elements). For the first test in the experiment use the 1 lb/hr element.
7. Refer to figure 4 for the test conditions required for this main experiment. Note that the individual tests may be conducted in whichever order is most economical.
8. Arrange the plumbing in the chamber so that the Honeywell units can be installed with the flow direction pointing up or down as required for the test configuration. See figure 7 for orientation. Initially install in the up direction for the first test.
9. Connect the oxygen (or nitrogen or helium) gas supply to the pressure regulator.
10. Adjust the pressure regulator for 40 psig.
11. Adjust the hand valve for 1 lb/hr on the reference flow sensor. Re-adjust the pressure to compensate for any droop.
12. Adjust the PTH chamber to the correct condition, temperature at ~~55~~ 30 R.T. degrees F. Maintain the ambient pressure at approximately 14.7 psia and relative humidity at approximately 30 % at all times, try and keep constant. 3/5/96
13. Adjust the temperature of the gas heater/chiller until the gas temperature is 30 degrees F and recheck the flow and pressure. Allow the unit to stabilize for 2 minutes after all test conditions are stabilized.
14. Adjust the test conditions for the next test and repeat the above procedure, steps 8 through 13 being careful to always use the correct laminar flow element.

L8 Full Factorial Experiment

1. Use only one of the Honeywell units A or B for this experiment. (Which one will be decided after main experiment test results are obtained.)
2. Setup the test equipment in the configuration shown in figure 1.
3. To ensure thermal stability, allow the Honeywell unit and the reference flow sensor to warm up for 10 minutes after power up before any readings are taken.
4. Use a multi-turn handvalve with a maximum orifice capable of flowing 1000 LPM at 40 psig.
5. Set the DAC to collect data once every 10 seconds. Ensure that the DAC data is saved to disk, ensure that all actual test condition data is recorded as well as the electrical current to the unit under test and the following outputs from the unit; flow rate, pressure, temperature and thermal conductivity.
6. Use nitrogen as the supply gas.
7. For the reference flow sensor use the laminar flow elements for 2 and 80 lb/hr ranges (refer to table 1 for the correct elements). For the first test in the experiment use the 2 lb/hr element.
8. Refer to figure 5 for the test conditions required for the full factorial experiment. Note that the tests may be conducted in whichever order is most economical.
9. Plumb the unit under test so that the flow direction is horizontal and the sensing element is also horizontal (Y axis orientation).
10. Adjust the pressure regulator for 70 psig and adjust the hand valve for 2 lb/hr on the reference flow sensor. Re-adjust the pressure to compensate for any droop.
11. Adjust the PTH chamber to the correct conditions, ambient pressure 14.7 psia, temperature at 70 degrees F and relative humidity 30 %. Maintain the chamber at these conditions at all times.
12. Adjust the temperature of the gas heater/chiller until the gas temperature is 40 degrees F and recheck the flow and pressure. Allow the unit to stabilize for 2 minutes after all test conditions are stabilized.
13. Adjust the test conditions for the next test and repeat the above procedure, steps 10 through 12 being careful to always use the correct laminar flow element.

File: FLOW2 .DAT
Title: Solid State Flow Sensor Screening Test
Comment: Identification of Interactions
Response: Flow & Err, Pwr, Delta P & Thermal Err

Design Listing:

TC#

	1	2	3
	Flow Rate	Pressure	Gas Temp
1:	2	70	40
2:	80	70	40
3:	2	850	40
4:	80	850	40
5:	2	70	165
6:	80	70	165
7:	2	850	165
8:	80	850	165
	Flow Rate	Pressure	Gas Temp

Figure 5

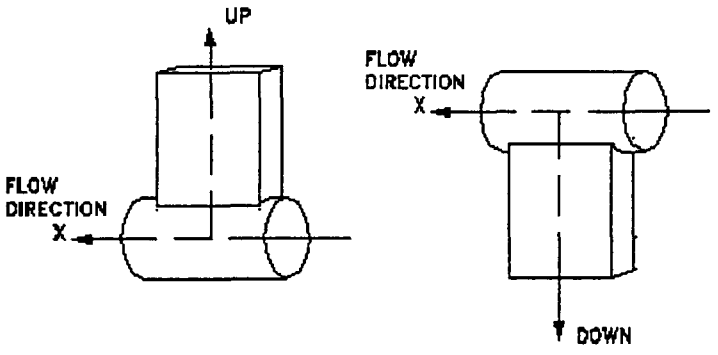

Figure 6 X Axis Orientation

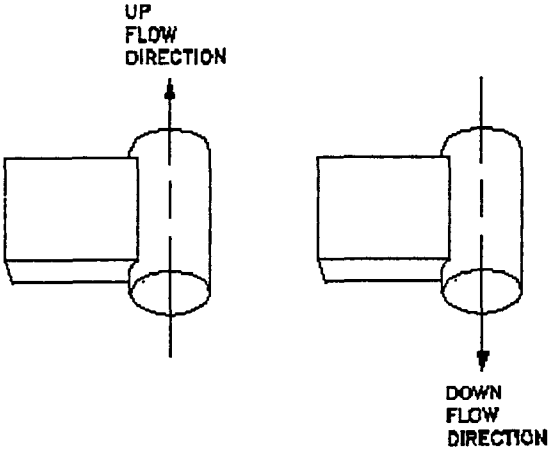

Figure 7 Y Axis Orientation

One Factor At A Time Tests

Linearity, Accuracy and Hysteresis

1. Use both the Honeywell units A and B in turn for these tests.
2. Setup the test equipment in the configuration shown in figure 1.
3. To ensure thermal stability, allow the Honeywell unit and the reference flow sensor to warm up for 10 minutes after power up before any readings are taken.
4. Use a multi-turn handvalve with a maximum orifice capable of flowing 1000 LPM at 40 psig.
5. Set the DAC to collect data once every 1 second. Ensure that the DAC data is saved to disk, ensure that all actual test condition data is recorded as well as the electrical current to the unit under test and the following outputs from the unit; flow rate, pressure, temperature and thermal conductivity.

6. Plumb the unit under test so that the flow direction is horizontal and the sensing element is also horizontal (Y axis orientation- see figure 2).
7. For the reference flow sensor use the appropriate laminar flow elements for the flow range (refer to table 1 for the correct elements). Note that this test will probably require the use of all nine elements in turn.
8. Connect the nitrogen, oxygen and helium gas supply in turn as required to the pressure regulator.
9. Adjust the pressure regulator for 40 psig with the hand valve closed.
10. Adjust the PTH chamber to the correct conditions, ambient pressure 14.7 psia, temperature at 72 degrees F and relative humidity 30 %. Maintain the chamber at these conditions at all times.
11. Open the handvalve to obtain some flow and adjust the temperature of the gas heater/chiller until the gas temperature is 30 degrees F. Allow the unit to stabilize for 2 minutes after all test conditions are stabilized.
12. Close the handvalve and start the data recording. Slowly open the handvalve and increase the flow. Keep checking the pressure is constant. When the first laminar flow element has reached its maximum stop the handvalve motion and change elements. Continue increasing flow. When full flow of 150 lb/hr is reached reverse the process and start slowly reducing flow until zero is reached.
13. Test unit B in the same way.
14. Set the next test conditions for pressure and gas temperature (refer to table 2) and repeat the flow sweep.
15. After all table 2 tests are complete for nitrogen for both units A and B connect oxygen as the supply gas and repeat the table 2 tests.
16. Finally, repeat again for helium as the supply gas.

Pressure	Temperature
40	30
40	180
900	30
900	180

Table 2

Response Time

1. Modify the test setup to introduce a quick opening ball valve between the pressure regulator and the Honeywell unit.

2. Modify the DAC setup to record only the Honeywell unit parameters and the reference flow sensor parameters. Increase the DAC sample rate to its maximum, or 20 times per second, which ever is smaller.
3. Set the gas temperature to approximately 105 degrees F.
4. At a gas pressure of 40 psig for nitrogen and with Honeywell unit A quickly open, hold for 5 seconds and then quickly close the ball valve.
5. Repeat step 4 at a pressure of 900 psig.
6. Repeat both steps 4 and 5 (pressures of 40 and 900 psig respectively) for unit B.
7. Change the supply gas to oxygen and repeat the four tests.
8. Change the supply gas to helium and again repeat the four tests.

26th Int'l.Env.Syst.Conf. sponsored by SAE, AAAI, AIChE, Monterey, CA, 8-11 July 1996

GAS MASS FLOW SENSOR PROOF OF CONCEPT TESTING FOR SPACE SHUTTLE ORBITER FLOW MEASUREMENT

R. Frampton and J. Walleshauser
Carleton Technologies Inc.
Orchard Park, NY

U. Bonne and D.Kubisiak
Honeywell Technology Center
Plymouth, MN

D. Hoy
NASA Johnson Space Center
Houston, TX

I. Andu and K. Kelly
Rockwell International
Houston, TX and Downey, CA

Abstract

The Space Shuttle Orbiter Atmospheric Revitalization Pressure Control System (ARPCS) and the Fuel Cell System (FCS) use a hot wire anemometer type of gas mass flow sensor for flow measurement. In the ARPCS oxygen and nitrogen mass flows are measured and in the FCS oxygen and hydrogen mass flows are measured. The existing flow sensors suffer from certain accuracy limitations and potential failure modes. A new type of commercially developed solid state micro-machined silicon gas mass flow sensor developed by Honeywell was adapted to allow the technology to be assessed for the application.

A demonstration test program has been conducted to evaluate the performance characteristics of the new sensor for space system applications and environments. The testing was sponsored by the National Aeronautics and Space Administration (NASA) at the Johnson Space Center (JSC). The primary testing was conducted at Carleton Technologies Inc. using nitrogen, oxygen and helium (as a surrogate for hydrogen). Hydrogen testing will be conducted at JSC. The objective of the tests was to determine if the new flow sensing technology would benefit the Shuttle and Space Station programs.

The new "smart" sensor has many advantages over the existing technology. These include low power consumption, very low drift rate, measurement capability over a 15000:1 flow range (compared to less than 1000:1 for the existing technology), high accuracy and the ability to be used with different gas types without modification or recalibration. The sensor has built in temperature and gas composition compensation, based upon heat transfer measurements.

The paper discusses the sensor operating principle, the test methodology, the sensor operational requirements and the test results.

Introduction

The Space Shuttle Orbiter Atmospheric Revitalization Pressure Control System (ARPCS) and the Fuel Cell System (FCS) presently use a hot wire anemometer type of gas mass flow sensor for flow measurement. In the ARPCS oxygen and nitrogen mass flow are measured and in the FCS oxygen and hydrogen mass flow are measured. The measurement method utilized consists of sensing the amount of heat transferred from a heater to a sensing element by the flow of gas. The existing sensors suffer from three main deficiencies which affect their accuracy and have necessitated a search for a superior product. The problems experienced by the existing sensors are orientation sensitivity, limited range and long term drift. The orientation effect is caused by thermal micro-currents which are sensitive to the gravitational vector and hence to position. In addition, the existing unit offers an accuracy of 3% of full scale over a range of 0 to 5 lbs/hour while the goal is to achieve 3% of reading (with a minimum resolution of ± 1% of reading) over a range of 0.01 to 150 lbs/hour.

The flow sensing applications on the Space Shuttle present very severe requirements for almost any presently available technology. A recently developed

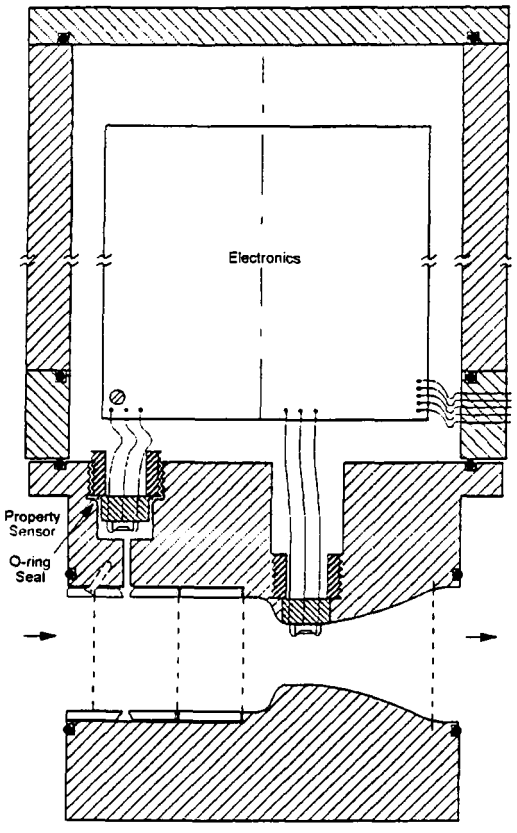

Figure 1 - Flow sensor type 1

micro-machined solid state silicon technology appears to have the potential to meet these requirements. Due to its small size, low heat dissipation and its inert material composition (Pt and Si_3N_4) it was expected that it would significantly reduce, or eliminate, both the orientation and long term drift errors. To verify this a program to demonstrate the ability of the new design to meet the Shuttle ARPCS and FCS accuracy, pressure drop, power consumption and response time requirements was conducted. In this program two types of existing "smart" sensor structures[1-7] were adapted and tested over a wide environmental range. Originally testing of only one type was envisaged but disappointing performance in certain areas led to the inclusion of the second type.

Type 1 consisted of one flow microsensor mounted at the throat of a Venturi nozzle[1-3] while type 2 had the same sensor mounted in a bypass[4-5]. The latter approach allows the use of a commercial sensor package and ensures that the microsensor: (1) is only exposed to flows driven by a multi-tap, averaged (piezometric sampling) pressure drop across a laminar flow restriction (honeycomb); and (2) is factory-assembled reproducibly in a well-defined flow microchannel. This approach also permits a wide enough flow range that the special high-flow measurement method (based on the measurement of heater power dissipation) could be eliminated, reducing hardware, software and calibration costs. Figures 1 and 2 show cross-sectional sketches of the respective flow sensor configurations.

Following the successful completion of the proof of concept program (with satisfactory accuracy performance measurements) the next stage would be a full development and qualification program during which other issues would be resolved, such as EMI and vibration.

This paper describes briefly the principle of sensor operation (a full description is available in past papers[1-7]), the requirements imposed on a flow sensor in the Space Shuttle environment, the strategy adopted for a short but thorough test of the concept, the test results obtained for both sensor configurations and

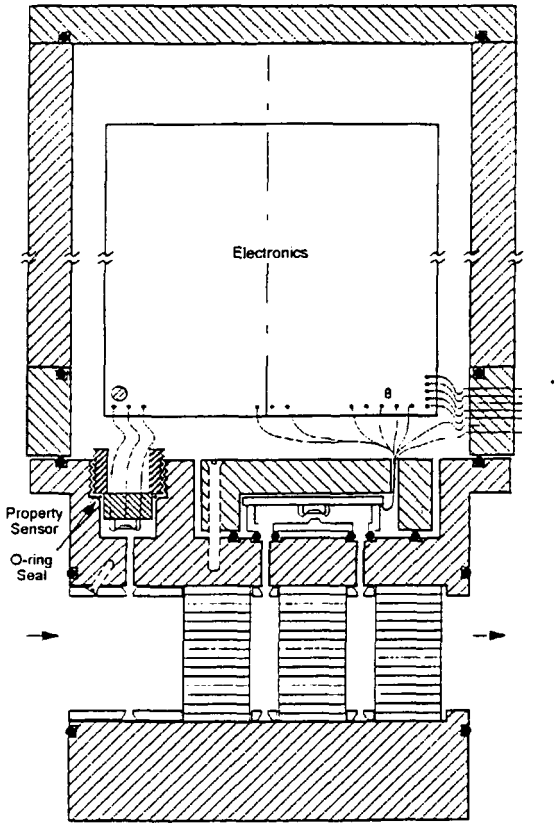

Figure 2 - Flow sensor type 2

finally, conclusions and recommendations for further work.

Flow Sensor Principle of Operation

The silicon based microbridge sensor uses a hot film element and a differential sensing approach that is more sensitive than existing hot wire anemometer designs. The "smart" microstructure sensor is micro-processor controlled and consists of two independent thermal sensing units. One sensing unit is placed upstream of a Venturi metering channel (figure 3), and the other is placed either at the throat of the Venturi for Type 1 (figure1) or in a bypass for Type 2 (figure 2) . The upstream sensing unit, or the property sensor, is

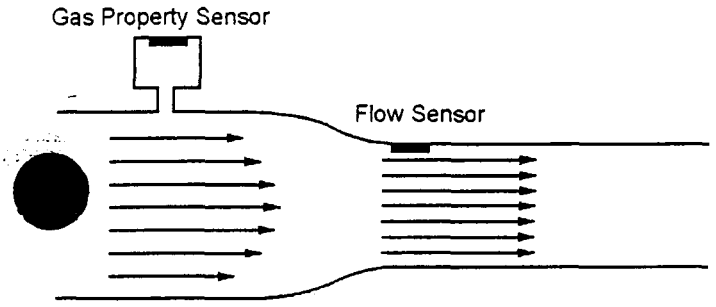

Figure 3 - Venturi flow channel

used to evaluate the gas properties (i.e. the temperature, the thermal conductivity and the specific heat of the gas). This allows the sensor output to be automatically compensated for different gas[1] types. The property sensor is recessed to avoid direct flow impingement, which would disturb its measurement function. The structure of the property sensor is identical to that of the flow sensor.

The flow sensing unit is used to measure the uncompensated flow. Each flow sensor consists of a heater located in the middle of two sensing elements which are positioned upstream and downstream with respect to the direction of gas flow (figure 4). The sensor can be operated in two modes, one of which gives best accuracy at low flows and one which gives best accuracy at high flows.

The first mode is that in which the differential signal between the upstream and downstream sensing elements is used. In the second mode the total heat dissipation of the heating element is used. The microprocessor merges the two flow outputs to generate a smooth changeover from one to the other as a function of flow.

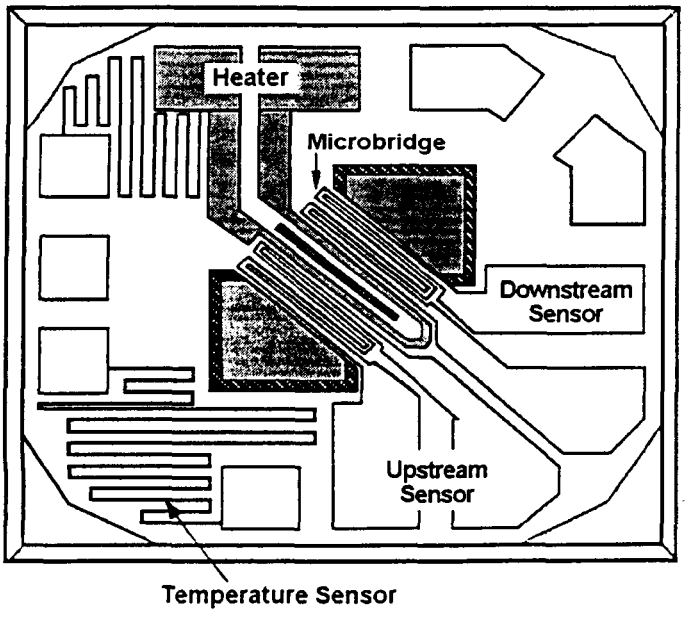

Figure 4 - Chip layout

The micro-processor also receives outputs from the property and temperature sensors and determines the values of k (thermal conductivity), c_p (specific heat) and temperature. It also receives the uncompensated signals from the flow sensor. The mass flow rate of the gas is then computed by correcting the flow signal for pressure, temperature, c_p and k. The sensor was configured with a 0 to 5 volt output to match the signals levels from the existing Shuttle sensor. However, because the existing sensor maximum range is only 5 lb/hr and the microbridge sensor maximum range is 150 lb/hr it was advantageous to convert the final micro-processor output to a voltage logarithmically proportional to flow so as to maintain the resolution and hence the required accuracy for low flows.

Sensor Characteristic Objectives

Listed below in Table 1 are the performance goals for the sensor. Table 2 specifies the environmental operating regime and in Table 3 the physical characteristic requirements are outlined.

Table 1 - Flow Sensor Performance Goals

Parameter	Requirement
Flow Range	0.01 to 150 lb/hr
Accuracy	< ± 3% of reading
Offset at Zero Flow	< ± 0.01 lb/hr
Drift	Unit remains in calibration > 5 years
Max Pressure Drop Oxygen	0.5 psid @ 900 psig & 15 lb/hr
	2.0 psid @ 900 psig & 75 lb/hr
Max Pressure Drop Nitrogen	0.5 psid @ 200 psig & 15 lb/hr
	28.0 psid @ 200 psig & 150 lb/hr
Max Pressure Drop Hydrogen	0.5 psid @ 200 psig & 15 lb/hr
Max Pressure Drop Helium	0.5 psid @ 200 psig & 15 lb/hr
Response Time	< 3 seconds (T90)
Maximum Power	1.5 Watts @ 28 VDC
EMI	TBD
Service Life	> 10 years

Table 2 - Flow Sensor Environmental Operating Regime

Parameter	Requirement
Operating Fluids	Nitrogen Oxygen Hydrogen Helium
Gas Temperature Range	35 to 175 degrees F
Ambient Pressure Range	0 to 15 psia
Ambient Temperature Range	40 to 90 degrees F
Acceleration	4.4 vertical, 4.8 lateral g's

It was decided that weight, volume, particle impact sensitivity, acceleration and EMI were outside the scope of proof of concept testing and were not included in the test program.

Table 3 - Flow Sensor Physical Characteristic Requirements

Parameter	Requirement
[redacted]put Voltage Range	0 to 5 VDC
[redacted]ume	< 30 cubic inches
[redacted]Weight	< 1.35 lbs
Particle Impact Sensitivity	Oxygen safe

Test Methodology

The purpose of the flow sensor program was to determine if the solid state flow sensors were able to meet the target specifications for accuracy, pressure drop, power consumption and response time and to characterize the overall performance (not including EMI and vibration) within the NASA defined environmental regime shown in Table 2.

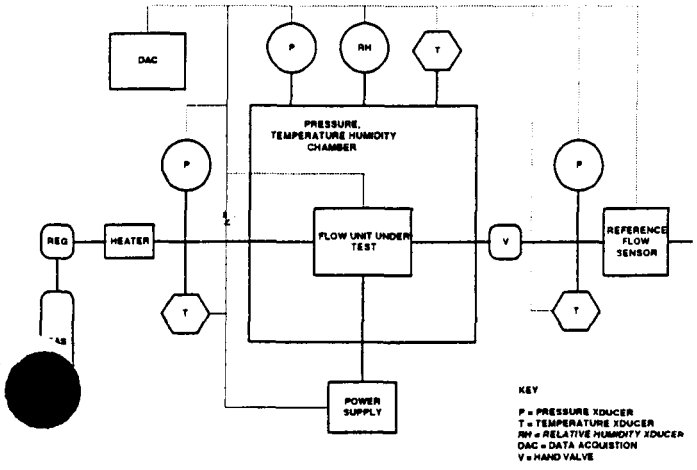

Figure 5 - Test Setup

The testing of the flow sensors was divided into two categories, Taguchi style statistical experimental designs (SED) to characterize the sensors, and "one factor at a time" testing to obtain the accuracy (linearity, hysteresis and repeatability) and response time data. The designed experiments were tailored to obtain the maximum amount of information as inexpensively and as quickly as possible. The SEDs were used to determine sensor sensitivity factors and interaction effects for all of the pertinent parameters. The one factor at a time tests also validated the SED testing to further boost the test confidence level.

Statistical experimental designs are used to determine variation due to predetermined parameters under study. These parameters are controlled in a manner such that a statistical evaluation will pinpoint which parameters or combinations of parameters are causing certain effects. An experiment matrix should be designed so there are enough columns (one for each) to accomodate the parameters under study, interactions [redacted]he results of combinations of parameters) and [redacted]erimental error. If the matrix is too small (saturated) [redacted] interactions and experimental error will be confused with individual parameters.

Three SEDs were planned. The first was a preliminary screening test, using one sensor, to identify unimportant factors which could then be eliminated from subsequent testing making this testing more efficient. A three level SED was used to obtain curvature data for the sensitivity factors. Finally one sensor was subjected to a full factorial SED to test for interactions of the main factors. The curvature experiment was performed twice, once for each sensor configuration. The test conditions were kept constant to obtain replicate information which was used to improve the overall accuracy of the experiment and as a confidence factor.

The factors considered in the SEDs were ambient pressure, ambient temperature, relative humidity, gas flow rate, gas temperature, gas pressure, gas type (three gases used in the SEDs were oxygen, nitrogen and helium) and orientation about the X and Y axes. These nine parameters are judged to be the only ones which might affect the accuracy of the sensor in the test scenario defined. The responses to be collected and analyzed were flow rate, pressure drop, power consumption and flow rate error.

The ranges of the experimental factor test levels (conditions) were selected for the three experiments to be similar, but not identical, so that the data could be merged to give more complete curvature indications.

The "one factor at a time" testing consisted of flow rate sweeps at all combinations of pressure and temperature limits for each of the three gases. For these tests the flow rate was increased from minimum to maximum and then decreased from maximum to minimum to obtain hysteresis data. Also, flow rate step response tests were carried out for each of the three gases . The one factor at a time tests will be repeated at Johnson Space Center for a fourth gas (hydrogen) after all testing at Carleton is completed.

Figure 5 shows the test configuration. A data acquisition system was used to both control the experimental conditions and to collect the data.

Because the result of the test program was intended to assess the accuracy of the flow sensor, the accuracy of the test equipment used was critical. This was especially true for the flow standard used. A series of seven laminar flow elements were used to cover the flow range from 0.01 to 150 pounds per hour for oxygen, nitrogen and helium. Laminar flow elements were chosen because of their ability to respond as fast as the smart sensor. The particular elements were chosen to give an accuracy of 3 to 4 times better than the specification flow accuracy requirement. Table 4 shows

Table 4 - Measurement Accuracy

Ambient pressure	± 0.016 psia
Ambient temperature	± 1 degree F
Relative humidity	± 0.5 %
Gas pressure	± 1 psig
Gas temperature	± 2 degrees F
Flow rate	± 0.7% of reading

the measurement accuracy for each of the test parameters.

The L18 three level main experiment was designed to obtain curvature and sensitivity data for gas type, flow rate, gas pressure, gas temperature, ambient temperature and orientation about the Y axis for each of the two sensors.

Table 5 - L18 Experimental Conditions

Gas	Flow	Pressure	Temp	Attitude
Oxygen	1	40	30	Up
Oxygen	10	475	105	Up
Oxygen	100	910	180	Up
Nitrogen	1	40	105	Up
Nitrogen	10	475	180	Up
Nitrogen	100	910	30	Up
Helium	0.1	475	30	Up
Helium	1	910	105	Up
Helium	10	40	180	Up
Oxygen	1	910	180	Down
Oxygen	10	40	30	Down
Oxygen	100	475	105	Down
Nitrogen	1	475	180	Down
Nitrogen	10	910	30	Down
Nitrogen	100	40	105	Down
Helium	0.1	910	105	Down
Helium	1	40	180	Down
Helium	10	475	30	Down

Table 5 shows the actual experimental treatment combinations and levels. This experiment can accept up to 7 three level parameters and one 2 level parameter so that with only 5 parameters actually utilized, a measure of experimental error can be obtained because the experiment is not saturated. However, because any interaction between pressure and temperature is partially confused with Y attitude and the spare columns used to collect experimental error there is a risk that if this interaction exists then experimental error will be confused with it. Thus, full factorial, follow on experiments were planned to identify interactions.

Test Results Unit 1

Prior to commencing the main test program a preliminary flow test, using nitrogen at room temperature, was conducted to verify correct operation of the sensor and the test equipment. The results are shown in Figures 6 and 7. These show that the sensor gives an output with a linear trend over the required flow range but with a maximum deviation of 21% of reading.

It was determined that, apart from a narrow flow range, the deviation was significantly constant and thus could be attributed to a correctable calibration error. Therefore the test program was continued knowing that absolute errors would be unacceptable but in the knowledge that average error could be improved by more accurate calibration.

The first structured experiment (L8), which was designed to verify that humidity, ambient air pressure and X-axis orientation did not influence performance, was successful in that analysis of the test results demonstrated that these factors had a negligible effect

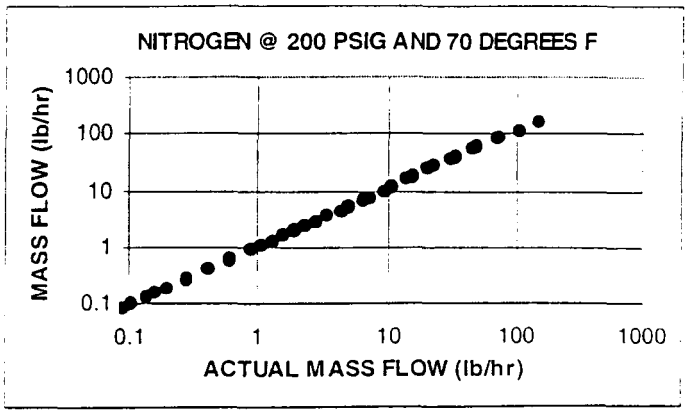

Figure 6 - Unit 1 Preliminary Flow Test

on the sensor output as expected. The test results are shown in Table 6.

The ANalysis Of VAriance (ANOVA) of the flow signal showed that 98.43% of the variation in flow was due to the flow changes within the experiment which indicates, not unexpectedly, that as a flow sensor the unit is very good. It also shows that the other factors within the experiment, humidity, gas pressure, gas

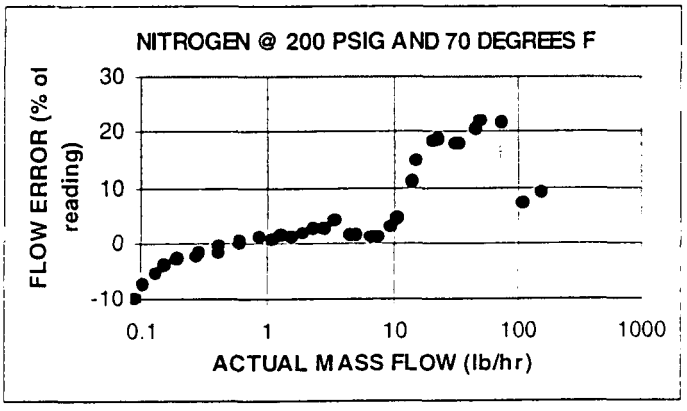

Figure 7 - Unit 1 Flow Error

temperature, ambient pressure and X-axis orientation produced output variation of only 1.42% and so had almost no effect on the flow signal. The experimental error was only 0.15% of the variation within the experiment

Table 6 - Screening Test Results

RUN NUMBER	ACTUAL FLOW	RS232 FLOW	ERROR % OF READING
1	5.06	5.307	4.88
2	50.6	54.2	7.11
3	5.02	5.375	7.07
4	50.65	54.2	7.01
5	5.015	5.279	5.26
6	50.14	57.53	14.74
7	5.074	5.245	3.37
8	49.36	65.7	33.1

showing that the conditions were accurately set and that there were no significant effects from outside sources. An ANOVA was also performed on the flow error (as a

percentage of reading) and showed that 31.8% of the variation in error was due to flow, 6.4% due to gas pressure, 17.1% due to gas temperature, 6.0% due to ambient air pressure, 25.5% due to humidity and 3.8% due to X-axis orientation with 9.4% experimental error. It was hypothesized that the apparent effects, particularly the large and unexpected effect of humidity on the error were due to the use of a saturated experiment and to the difficulty in maintaining consistent gas and unit temperatures. To verify this a full factorial L4 experiment was run with flow and humidity as the only factors. The results are shown in Table 7. The ANOVA showed that the flow changes accounted for 99.9% of the variation in flow and humidity for only 0.05%. The effect of flow error due to humidity in this experiment was not statistically significant.

Table 7 - Humidity Test

FLOW LB/HR	HUMIDITY % RH	ACTUAL FLOW	RS232 FLOW	ERROR % OF READING
5	25	5.02	5.355	6.67
50	25	50.79	54.07	6.46
5	85	5.056	5.438	7.56
50	85	50.21	52.05	3.66

The results for the L18 experiment are shown in Table 8. The flow signal ANOVA showed that 99.43% of the flow variation was due to flow changes within the experiment with no statistically significant effects from other sources. The flow error ANOVA showed no statistically significant effects, and a residual of 55.6% which indicates that there was more variation in flow error due to experimental error and outside factors than there was due to the factors within the experiment. Of the five factors within the experiment, the gas pressure and the flow level, were the main contributors to flow

Table 8 - L18 Test Results

RUN NUMBER	ACTUAL FLOW	RS232 FLOW	ERROR % OF READING
1	1.048	1.1326	8.07
2	9.9807	10.825	8.46
3	101.75	167.5	64.62
4	1.0	1.078	7.8
5	10.01	13.725	37.11
6	100.55	105.03	4.46
7	0.1067	0.1235	15.75
8	1.0023	1.043	4.06
9	9.998	9.115	-8.83
10	1.011	1.025	1.38
11	10.066	11.118	10.45
12	101.18	140.48	38.84
13	1.002	1.0972	9.5
14	9.997	11.235	12.38
15	100.64	108.32	7.63
16	0.10768	0.1222	13.48
17	0.978	1.0261	4.92
18	10.119	15.658	54.74

error. The main effects plots (Figure 8 on the next page) show that the sensor output is significantly linear with flow and virtually not affected by the other factors.

The main experiment was found to have been poorly designed because the flow levels selected were not equally spaced and because the interactions were uniformly distributed across all columns which gave the indication of many interactions. The lack of equal flow level spacing was overcome by analysis of the logarithmic flow value. A series of five "two-level" experiments was subsequently necessary in order to establish which interactions were real and which were spurious. The interactions indicated by the main experiment were between gas pressure and gas temperature, between gas temperature and Y attitude, between gas pressure and Y attitude, between gas pressure and gas type and between gas temperature and gas type. Subsequent full factorial experimentation using L4 SED's showed that the only real interactions are between gas pressure and gas temperature and between gas pressure and Y attitude. The results for these two L4 experiments are shown in Tables 9 and 10 and the interaction plots in Figures 10 and 12. Both of the interactions were relatively weak being about 1.4% and 4.5% of flow reading respectively but together made it almost impossible to achieve the target 3% of reading requirement.

The gas pressure and Y attitude interaction was caused by the gravitational effect previously discussed in the introduction and was identified by prior testing. The L4 results showed that at low pressure (100 psi) the gravitational effect was almost zero but at high pressure (900 psi) was quite large such that when gas was flowing up through the unit the measured flow rate was approximately 4.5% higher than when gas was flowing down through the unit. The gas pressure and gas temperature interaction was previously unknown and showed what appeared to be a gas density related effect such that at low temperature and high pressure (when gas density was a maximum) the unit measured flow rate output was about 1.4% higher than when the pressure was low or the temperature was high.

Table 9 - Pressure/Temperature Interaction

GAS TEMP	GAS PRESSURE	ACTUAL FLOW	CORR RS232	ERROR % OF READING
40	70	1.99	2.193	9.65
165	70	1.989	2.184	9.2
40	850	2.024	2.2243	11.22
165	850	1.9928	2.1798	8.99

Table 10 - Y Attitude/Pressure Interaction

GAS PRESSURE	Y ATTITUDE	ACTUAL FLOW	CORR RS232	ERROR % OF READING
100	UP	2.0166	2.2037	10.19
850	UP	2.014	2.2502	12.51
100	DOWN	2.008	2.1982	9.91
850	DOWN	2.006	2.1456	7.28

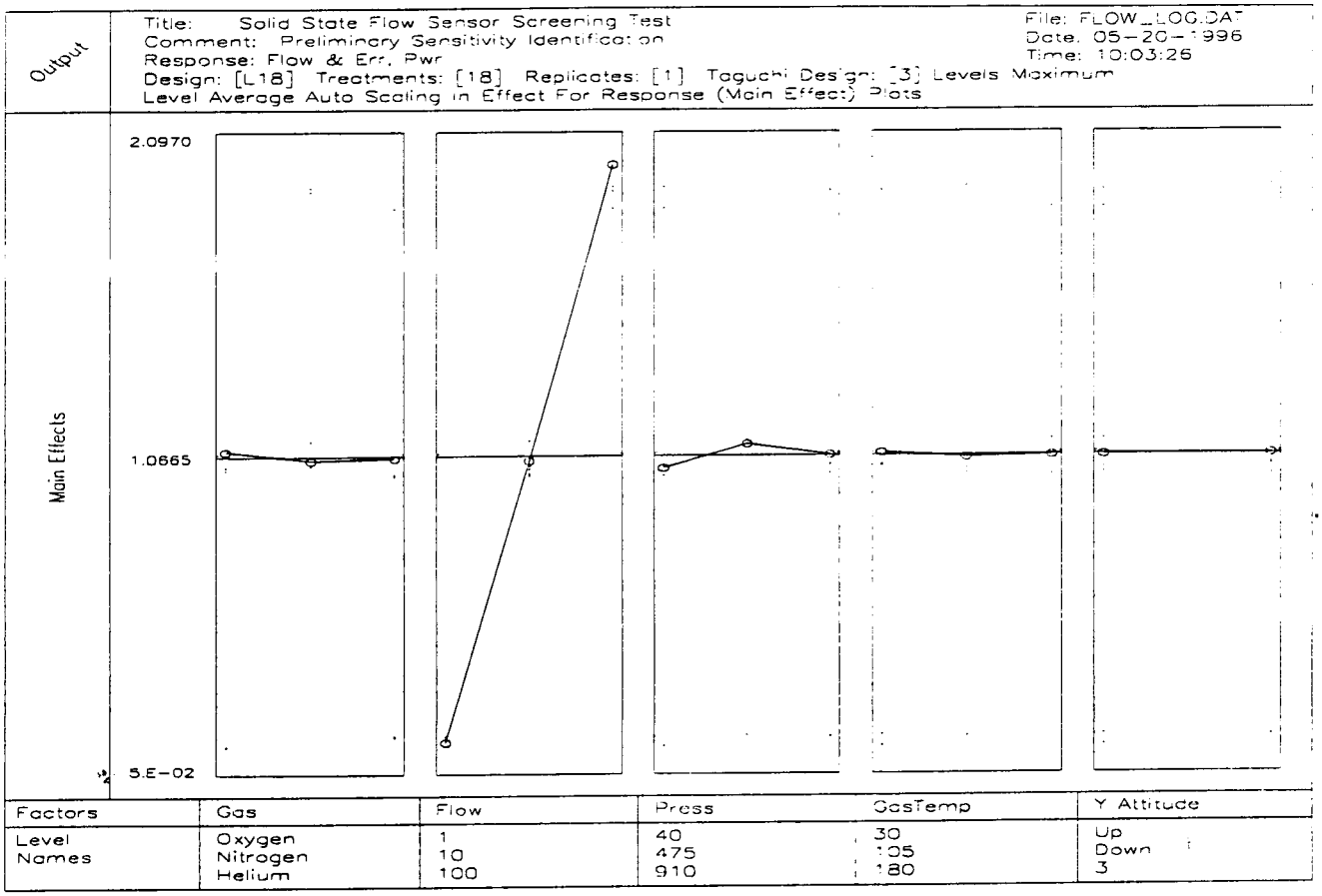

Figure 8 - Unit 1 Main Effects Plot

Plots of the smart sensor flow signal output versus the actual measured flow for each of the seven laminar flow elements (LFE's) necessary to cover the flow range were obtained. Figure 9 is a concatenation of the seven individual tests and shows the linearity and hysteresis performance for one particular gas type, pressure and temperature combination. This plot is representative of the other data collected.

Figure 11 shows the error as a percentage of reading. These graphs show clearly the problems associated with measuring flow rate over such a wide range and problems with this particular unit.

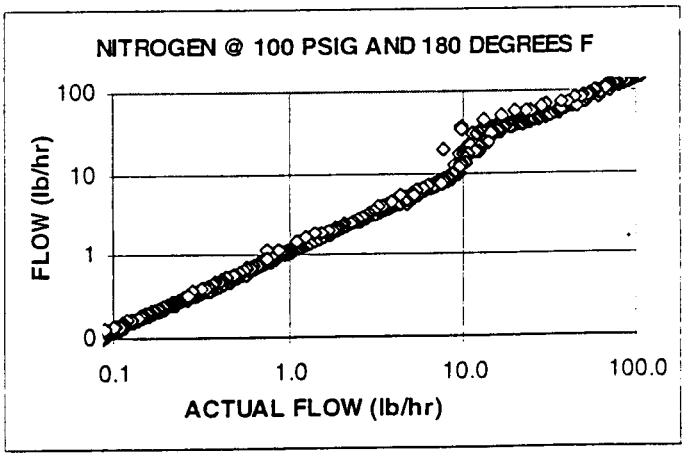

Figure 9 - Unit 1 Measured Flow

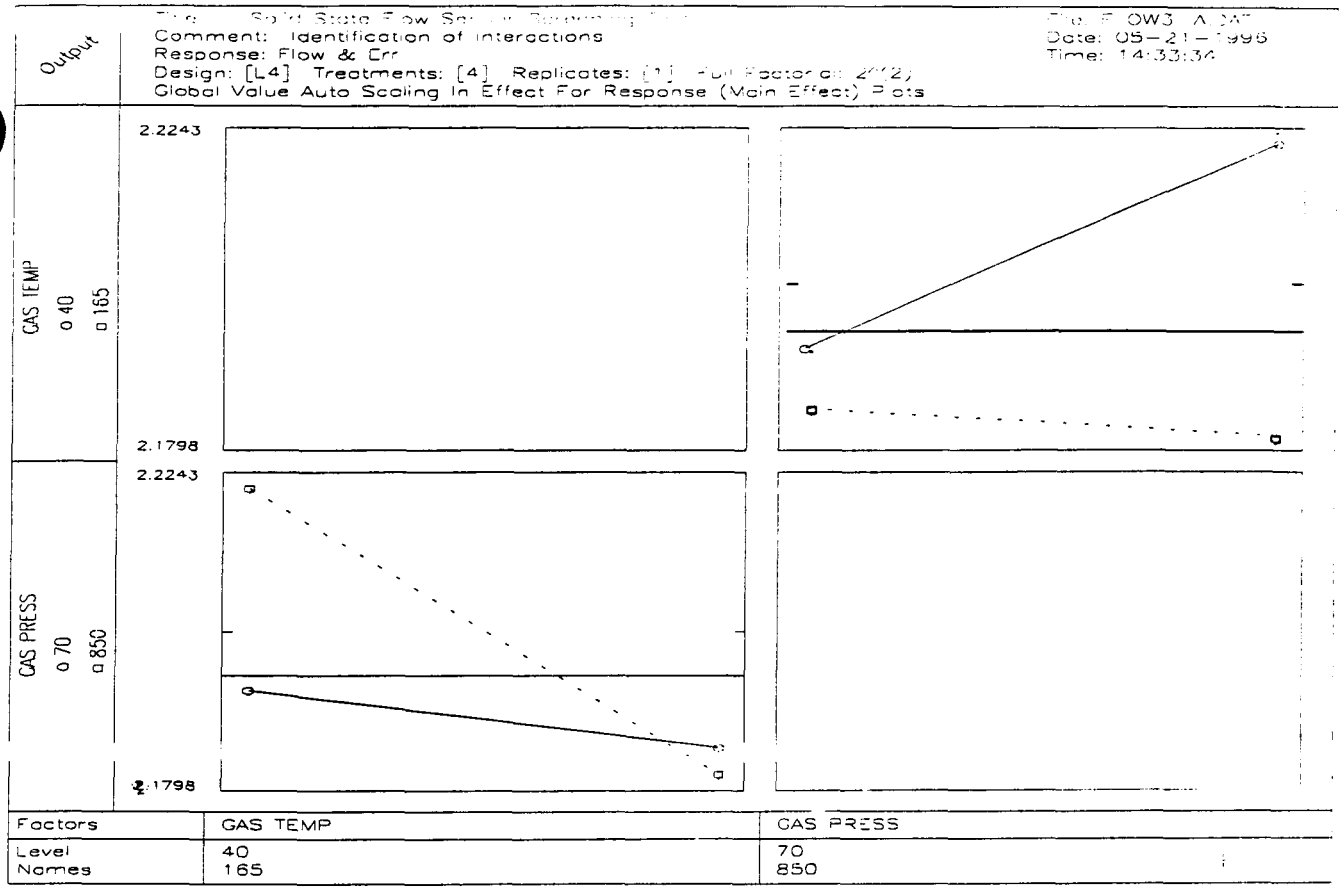

Figure 10 - Unit 1 Pressure and Temperature Interaction

Noise at the low and high ends of the flow range was seen. The low end noise was caused by poor signal to noise ratios and electrical noise on very low signals. The high end noise was caused by flow turbulence and the inability to create a single flow passage capable of maintaining laminar flow over such a wide flow and pressure range.

The concatenated error plot (Figure 11) shows that the concept of using two different flow measurement methodologies to cover the high and low flow ranges with a merging of the two methods in the middle was not capable of producing low errors in the merged area. This possibly could be corrected by use of multiple lookup tables instead of curve fitted equations but a superior approach appears to be that which is embodied in the by-pass unit which, uses only a single measurement methodology and avoids the merging of two separate range signals completely. Prior to actually testing the bypass unit a measure of its capability was obtained by studying the performance of unit 1 over a much narrower flow range (0.33 to 8 pounds per hour). Ignoring the large standard deviation due to noise, Figure 11 shows that the average error is almost constant and capable of falling within a ±3% of reading.

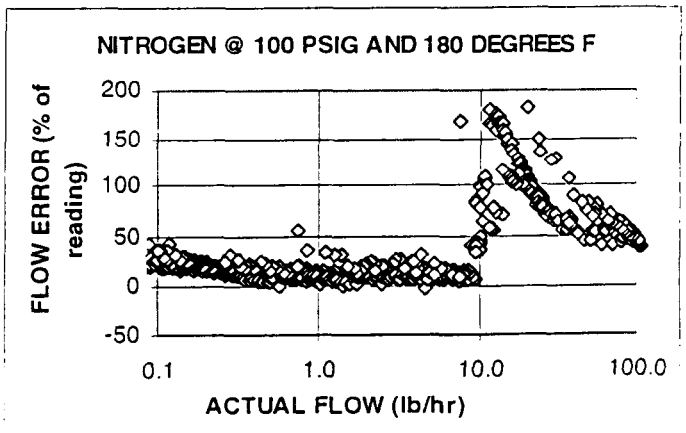

Figure 11 - Unit 1 Percentage Error

Because of the averaging method used to reduce the noise levels the time delay associated with changing signals made it very difficult to distinguish between true hysteresis and time delay effects. The

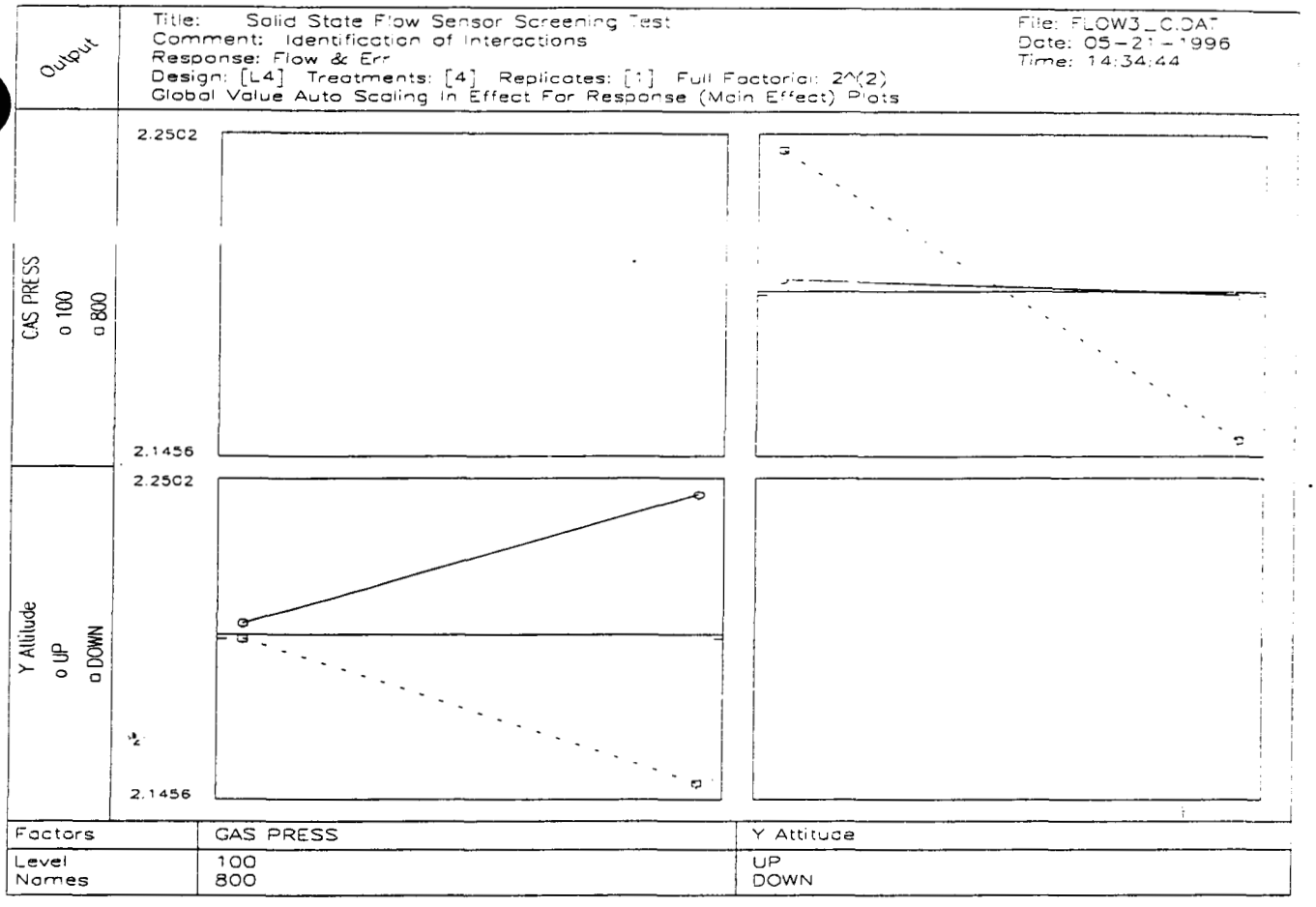

Figure 12 - Unit 1 Pressure and Y Attitude Interaction

faster a sweep is run the wider the apparent hysteresis band due to the time delay. The best estimate of hysteresis is obtained by assuming that the narrowest band is representative of the hysteresis and is least affected by the time delay. A best fit straight line for increasing flow and another for decreasing flow were computed for the linear segment of the flow curve shown in figure 9. The hysteresis is half the difference between the two best fits and is approximately 0.7% of reading. The flow standard used has hysteresis of 0.1% of reading; thus, the unit 1 hysteresis is estimated to be 0.6% of reading. Figure 13 shows a step response test for the sensor for one particular gas type, gas temperature, pressure and flow rate and is again representative of all of the data collected at other combinations of conditions. The sensor does not exhibit a typical linear system exponential time response, instead having a pure time delay of about 2.5 seconds before rising (or falling) instantly to the final value.

The sensor uses a digital sampling and averaging technique to minimize the effect of flow noise to calculate the output mass flow signal, and thus changes the output once every 2 to 3 seconds. This low

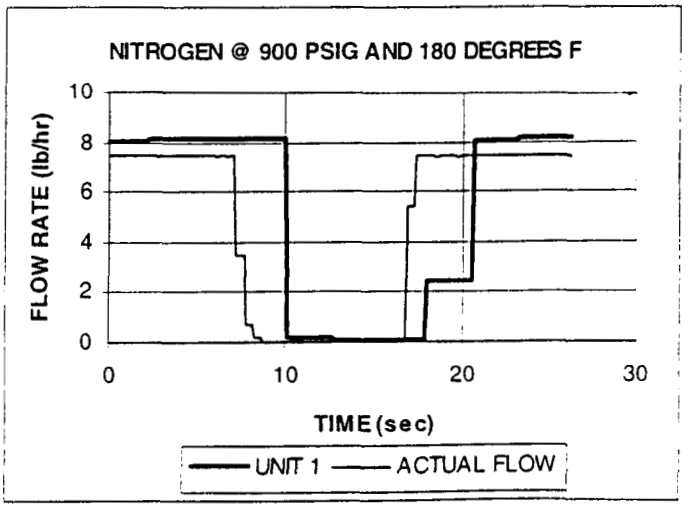

Figure 13 - Unit 1 Step Response

update rate is related to the use of non-optimized electronics in the unit and would be expected to be

increased in a production unit by the use of a more powerful micro-processor.

Conclusions

The existing unit can only be calibrated for a single gas and has a flow range of 0.15 to 5 lb/hr with an accuracy of ± 0.15 lb/hr. The goal for the new sensor was for a multi-gas capability and a range of 0.01 to 150 lb/hr with an accuracy of ± 3% of reading from 0.33 to 150 lb/hr and ± 0.01 lb/hr from 0.01 to 0.33 lb/hr. This goal represented a range multiplication of over 30 times the existing sensor and at 1 lb/hr an accuracy improvement of a factor of 5. These were aggressive objectives.

The test results for the type 1 sensor highlighted some specific problems with the unit but did confirm that the measurement principle is capable of operating over the flow, pressure and temperature ranges required. Furthermore, the testing verified that the unit is not affected by ambient pressure, temperature and humidity and by X-axis orientation. The problems identified by the testing were related to noise, accuracy, Y-axis orientation and unit to unit manufacturing repeatability. Preliminary evaluation of the data indicates that the problems with noise and accuracy can be alleviated and the problem with Y-axis orientation is not believed to be severe. However, the problem with unit to unit variation severely reduces the value of the unit by preventing interchangability. The problem related to accuracy is largely related to problems in the mid-flow range associated with the merging of signals generated by the different measurement methodologies.

The testing with the type 2 sensor is not sufficiently advanced to be included in the paper at this time but it is intended to include the data in an update of the paper. Nonetheless, the preliminary testing indicates, as expected, that this unit provides better accuracy and less sensitivity to orientation than the type 1 unit. The preliminary testing of the type 2 sensor which has been accomplished has covered a flow range of 0.01 to 150 lb/hr for oxygen, nitrogen and helium at pressures from 50 to 900 psig and temperatures from 30 to 150 degrees Fahrenheit. Generally from 2 lb/hr up to 150 lb/hr the unit accuracy is very good.

The test program has shown that the type 1 sensor probably will not be able to completely reach the goals which were set. But with correction of a temperature sensor isolation problem and improved calibration at the low flow end of the range the type 2 unit may be able to achieve the target objectives.

Acknowledgments

The authors are grateful to Ern Satren, HTC, Liese Dall-Bauman, NASA-Johnson and Bruce Siskowski, CTI, for their experimental contributions, and to NASA-Johnson for the funding provided under Phase I of a contract to Carleton and Honeywell entitled "Gas Mass Flow Sensor Redesign," for part of the work described above.

References

1. U.Bonne, "Fully Compensated Flow Microsensor for Electronic Gas Metering," Intl. Gas Research Conference, Orlando, FL, November 16–19, 1992, Proceedings, Vol.III p.859

2. U.Bonne and G.Havey, "Versatile Microbridge Flow Control Sensor Structure and Applications", SAE Technical Paper No. 921175, 22nd Int'l. Conf. Env. Syst., Seattle, WA, 13-16 July 92.

3. R. Hyoshi et al., "Microstructure Sensors for Flow, Differential Pressure and Energy Measurement", IGT Symposium on Natural Gas Energy Measurement, Chicago, IL, 30 April-2 May 1986, Proceedings; and U.Bonne, "Gas Composition Correction for Hot Element Flow Microsensors," 6th IGT Symposium on Gas Quality Measurement, Chicago, IL, June 10–12, 1991, Proceedings.

4. U.Bonne, "Sensing Fuel Properties with Thermal Microsensors," SPIE Conf. on Smart Electronics and MEMS, S.Diego, CA, 25-29 Feb.1996, Paper No. 2722-24

5. T.R.Ohnstein et al., "Environmentally Rugged, Wide Dynamic Range Microstructure Airflow Sensor," Solid-State Sensor and Actuator Workshop, IEEE Electr. Dev. Soc., Hilton Head, SC, 2-7 June 1990.

6. U.Bonne and D.Kubisiak, "Overpressure-Proof, Thermal Pressure Sensor for Gases," Solid-State Sensor and Actuator Workshop, Hilton Head Is., SC, 13-16 June 1994, Tech.Digest p.76

7. U.Bonne, V.Vesovic and W.A.Wakeham, "Sensing Thermophysical and Transport Properties of Natural Gas with Thermal Microsensors, " Int'l.Gas Research Conf., Cannes, France, 6-9 November 1995, Proceedings, Vol.III, p.152

UNIT # 1 NITROGEN FLOW AT 70 DEGREES F

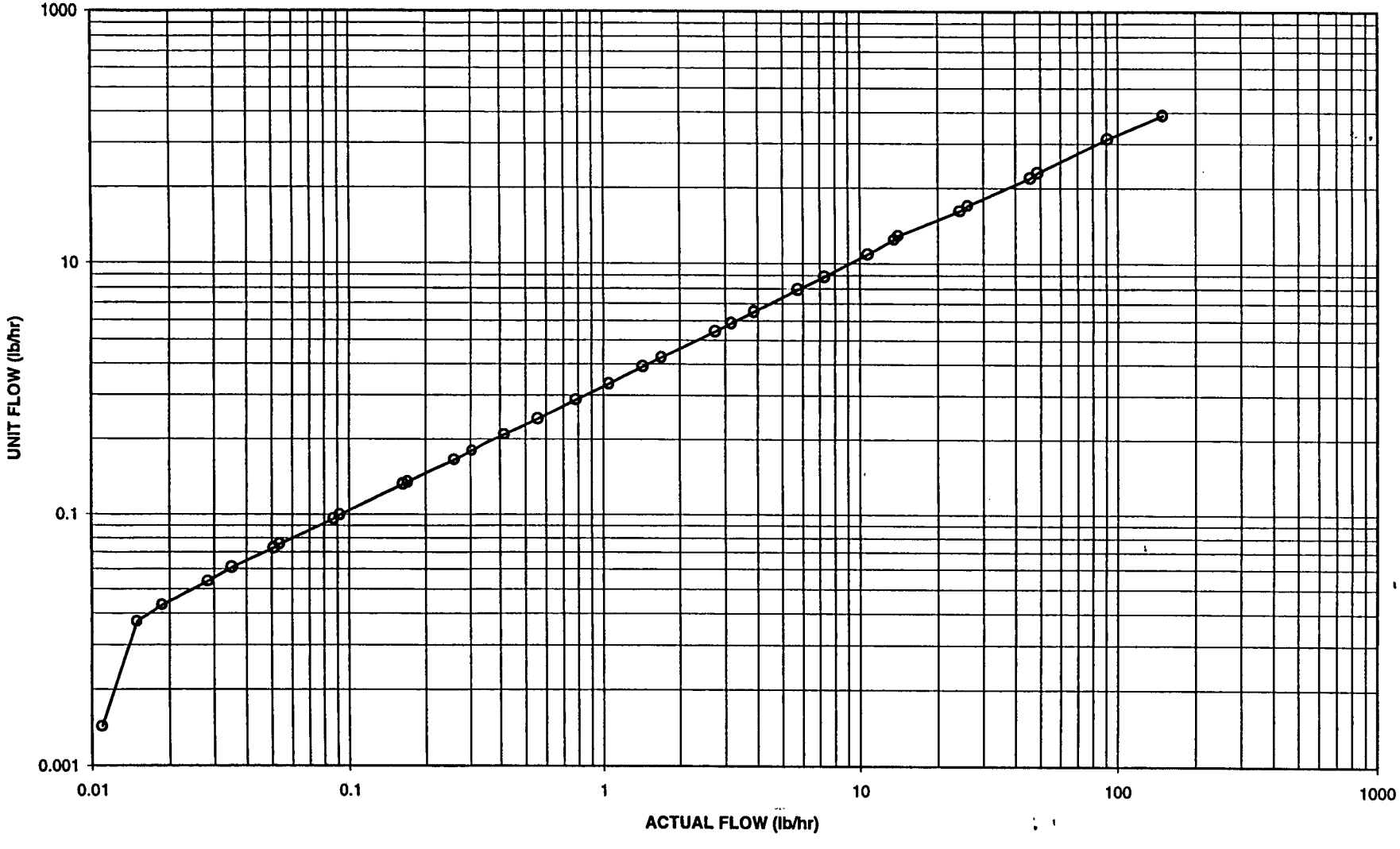

Figure 1

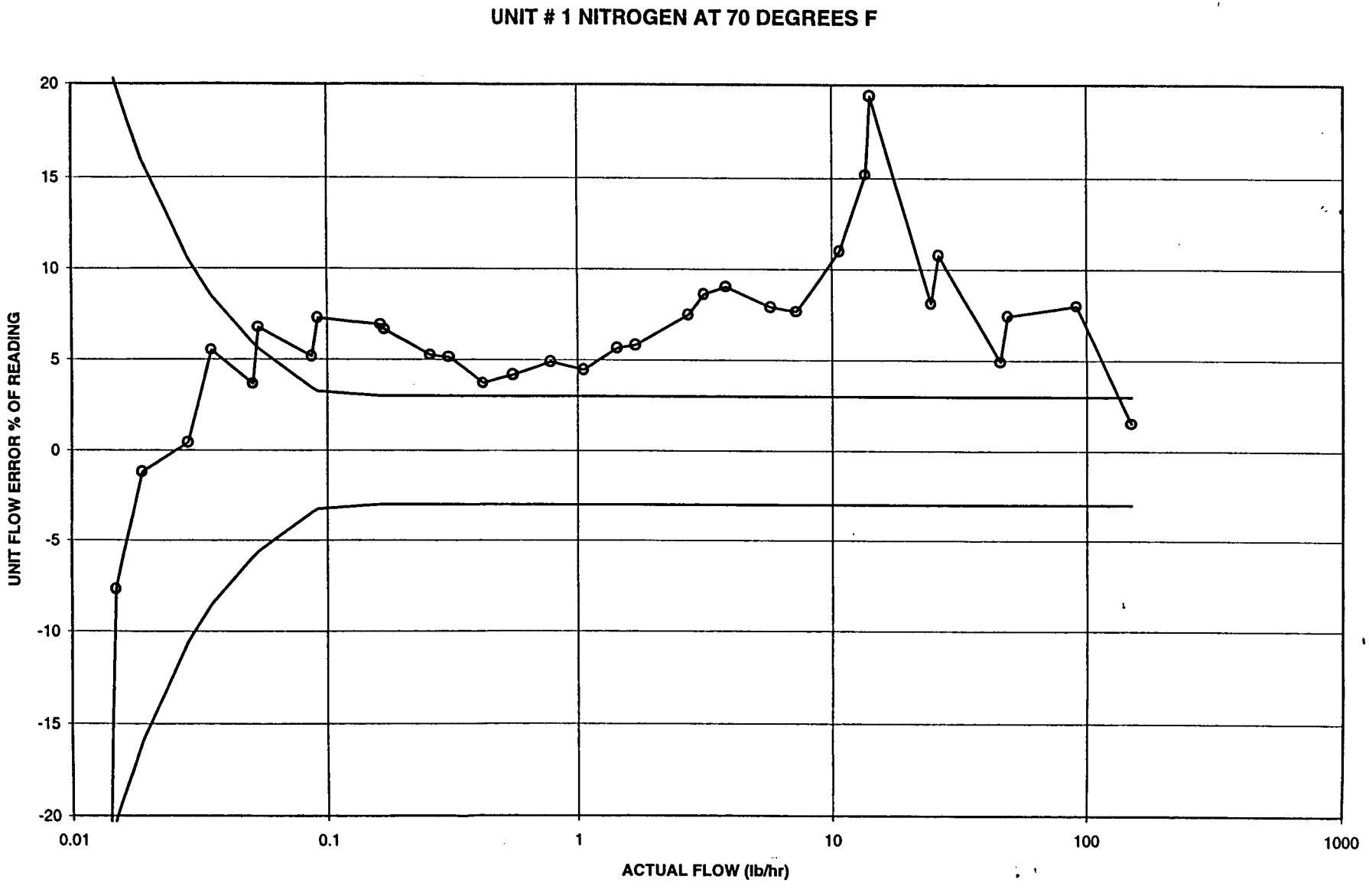
UNIT # 1 NITROGEN AT 70 DEGREES F
UNIT FLOW ERROR % OF READING
20
15
10
5
0
-5
-10
-15
-20
0.01
0.1
1
10
100
1000
ACTUAL FLOW (lb/hr)

Figure 2

UNIT 1 DOE 1

RUN NUMBER	FLOW ACTUAL	FLOW RS232	ERROR % READING	FLOW ANALOG	ERROR % READING
1	5.06	5.307	4.88	5.356	5.85
2	50.6	54.2	7.11	53.3	5.34
3	5.02	5.375	7.07	5.39	7.37
4	50.65	54.2	7.01	52.89	4.42
5	5.015	5.279	5.26	5.397	7.62
6	50.14	57.53	14.74	55.46	10.61
7	5.074	5.245	3.37	5.189	2.27
8	49.36	65.7	33.1	65.48	32.66

Table 1

File: FLOW1 .DAT
Title: Solid State Flow Sensor Screening Test
Comment: Screening to Reduce Number of Factors
Response: Flow & Err, Pwr, Delta P & Thermal Err

Analysis Of Variance (ANOVA) Table

#	Factor	DOF	SOS	Percent	Mean-Sqr	Fcalc	% Conf	Effect
1	Flow Rate	1	5534.78	98.43	5534.783	647.4	97.50	52.6060
	Ln	1	5534.78	98.43		647.4		
2	Pressure	1	8.41357	0.15	8.413574	.9841	-1.000	2.05100
	Ln	1	8.41318	0.15		.9841		
3	Gas Temp	1	26.9097	0.48	26.90967	3.148	67.32	3.66800
	Ln	1	26.9084	0.48		3.147		
4	Air Press	1	8.27490	0.15	8.274902	.9679	-1.000	2.03400
	Ln	1	8.27430	0.15		.9678		
5	Humidity	1	28.0806	0.50	28.08057	3.285	67.90	3.74700
	Ln	1	28.0800	0.50		3.284		
6	X Attitude	1	8.13721	0.14	8.137207	.9518	-1.000	2.01700
	Ln	1	8.13656	0.14		.9517		
	Residual	1	8.54932	0.15	8.549316			
	Replicate	0	.000000	0.00	.0000000			
	Pooled	1	8.54932	0.15	8.549316			
	Total	7	5623.15	100.00				

SOS Grand Total: 13613.9
SOS Mean (CF) : 7990.75
SOS Total : 5623.15

Table 2

File: FLOW1 .DAT
Title: Solid State Flow Sensor Screening Test
Comment: Screening to Reduce Number of Factors
Response: Flow & Err, Pwr, Delta P & Thermal Err

Analysis Of Variance (ANOVA) Table

#	Factor	DOF	SOS	Percent	Mean-Sqr	Fcalc	Fcrit	Effect
1	Flow Rate	1	214.038	31.77	214.0382	3.370	161.4	10.3450
	Ln	1	214.038	31.77		3.370		
2	Pressure	1	43.0593	6.39	43.05933	.6780	161.4	4.64000
	Ln	1	43.0592	6.39		.6780		
3	Gas Temp	1	115.520	17.14	115.5200	1.819	161.4	7.60000
	Ln	1	115.520	17.14		1.819		
4	Air Press	1	40.3203	5.98	40.32031	.6349	161.4	4.49000
	Ln	1	40.3202	5.98		.6349		
5	Humidity	1	171.495	25.45	171.4954	2.700	161.4	9.26000
	Ln	1	171.495	25.45		2.700		
6	X Attitude	1	25.8482	3.84	25.84821	.4070	161.4	3.59500
	Ln	1	25.8480	3.84		.4070		
	Residual	1	63.5058	9.43	63.50580			
	Replicate	0	.000000	0.00	.0000000			
	Pooled	1	63.5058	9.43	63.50580			
	Total	7	673.787	100.00				

SOS Grand Total: 1525.39
SOS Mean (CF) : 851.606
SOS Total : 673.787

Table 3

UNIT 1 DOE 1A

RUN NUMBER	FLOW ACTUAL	FLOW RS232	ERROR % READING	FLOW ANALOG	ERROR % READING
1	5.02	5.355	6.67	5.36	6.77
2	50.79	54.069	6.46	53.74	5.81
3	5.0556	5.438	7.56	5.429	7.39
4	50.21	52.05	3.66	51.66	2.89

Table 4

File: FLOW1A .DAT
Title: Solid State Flow Sensor Screening Test
Comment: Screening to verify humidity effect
Response: Flow & Err

Design Listing:

Design Name: [L4]
Design: Full Factorial [2^k], (K = 2)
Treatments: [4]

Extra DOF: [0], Extra DOF For > 2-Factor Ints

TC#

	1	2
	FLOW	HUMIDITY
1:	5	25
2:	50	25
3:	5	85
	50	85

	FLOW	HUMIDITY

Confounding/Aliasing Information:

No Confounding Exists Since P=0

Table 5

File: FLOW1A .DAT
Title: Solid State Flow Sensor Screening Test
Comment: Screening to verify humidity effect
Response: Flow & Err RS232

Analysis Of Variance (ANOVA) Table

#	Factor	DOF	SOS	Percent	Mean-Sqr	Fcalc	Fcrit	Effect
1	FLOW	1	2237.81	99.90	2237.811	1939.	161.4	47.3055
	Ln	1	2237.81	99.90		1939.		
2	HUMIDITY	1	1.01147	0.05	1.011475	.8765	161.4	-1.00550
	Ln	1	1.01103	0.05		.8761		
	Residual	1	1.15405	0.05	1.154053			
	Replicate	0	.000000	0.00	.0000000			
	Pooled	1	1.15405	0.05	1.154053			
	Total	3	2239.98	100.00				

SOS Grand Total: 5614.95
SOS Mean (CF) : 3374.97
SOS Total : 2239.98

Table 6

File: FLOW1A .DAT
Title: Solid State Flow Sensor Screening Test
Comment: Screening to verify humidity effect
Response: Flow & Err RS232

Analysis Of Variance (ANOVA) Table

#	Factor	DOF	SOS	Percent	Mean-Sqr	Fcalc	% Conf	Effect
1	FLOW	1	4.22301	49.46	4.223007	1.241	53.42	-2.05500
	Ln	1	4.22302	49.46		1.241		
2	HUMIDITY	1	.912018	10.68	.9120178	.2679	-1.000	-.955000
	Ln	1	.912025	10.68		.2679		
	Residual	1	3.40404	39.86	3.404037			
	Replicate	0	.000000	0.00	.0000000			
	Pooled	1	3.40404	39.86	3.404037			
	Total	3	8.53906	100.00				

SOS Grand Total: 156.770
SOS Mean (CF) : 148.231
SOS Total : 8.53906

Table 7

Output

Title. Solid State Flow Sensor Screening Test
Comment: Screening to verify humidity effect
Response: Flow & Err
Design: [L4] Treatments: [4] Replicates: [1] Full Factorial: 2^(2)
Level Average Auto Scaling In Effect For Response (Main Effect) Plots

File: FLOW1A.DAT
Date: 03-11-1996
Time: 11:13:46

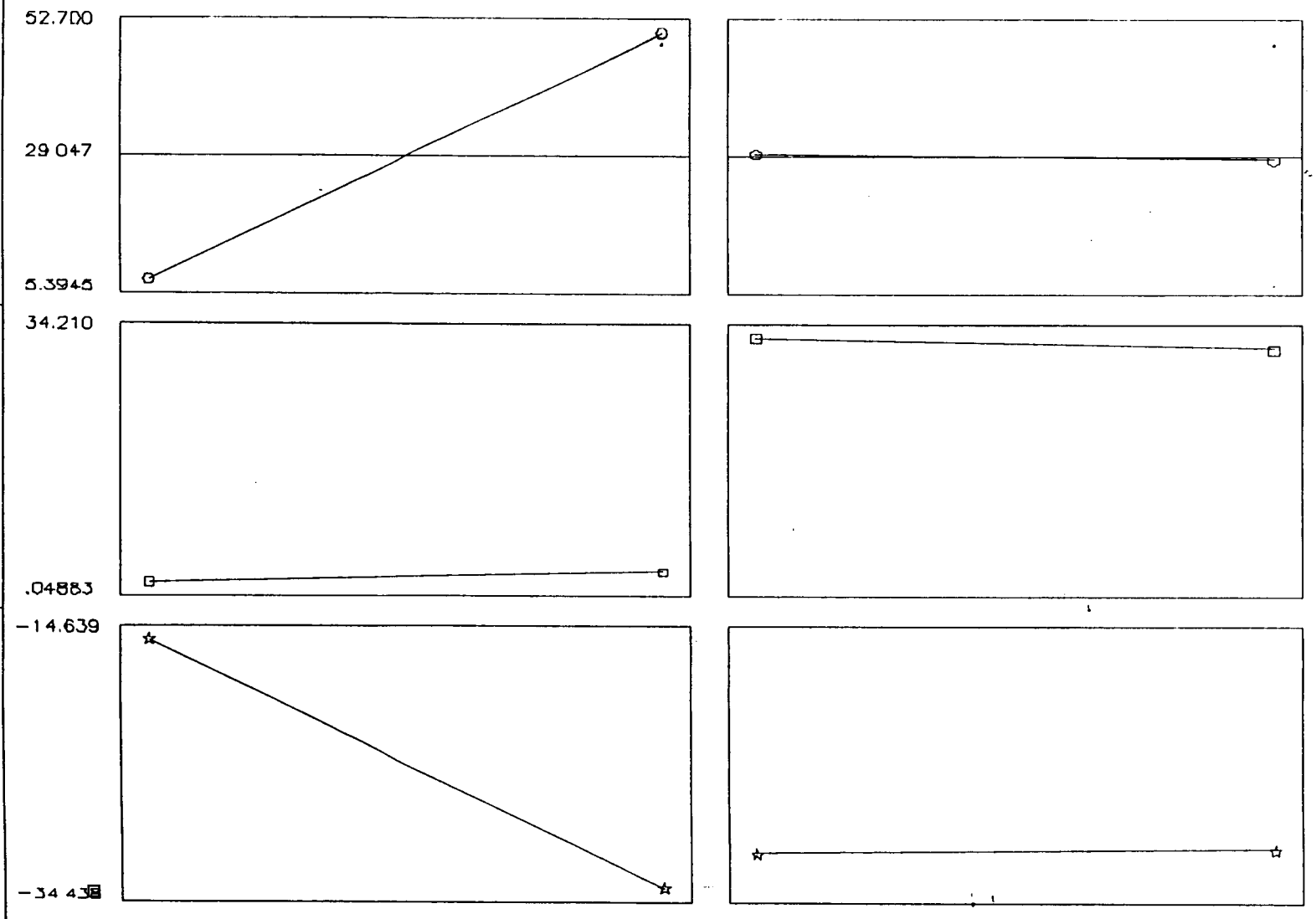

Factors	FLOW	HUMIDITY
Level Names	5 50	25 85

Figure 3

UNIT 1 DOE 2 HELIUM DATA CODED

RUN NUMBER	FLOW ACTUAL	FLOW RS232	ERROR % READING	FLOW ANALOG	ERROR % READING	LOG FLOW RS232	ERROR % LOG READING
1	1.048	1.1326	8.07	1.1305	7.87	0.0541	3.37
2	9.9807	10.825	8.46	10.845	8.66	1.0344	3.53
3	101.75	167.5	64.62	147.49	44.95	2.2240	21.65
4	1	1.078	7.80	1.078	7.80	0.0326	3.26
5	10.01	13.725	37.11	13.37	33.57	1.1375	13.71
6	100.55	105.03	4.46	104.43	3.86	2.0213	1.89
7	1.067	1.235	15.75	1.233	15.56	0.0917	6.35
8	10.023	10.43	4.06	10.4	3.76	1.0183	1.73
9	99.98	91.15	-8.83	90.35	-9.63	1.9598	-4.02
10	1.011	1.025	1.38	1.0222	1.11	0.0107	0.60
11	10.066	11.118	10.45	11.109	10.36	1.0460	4.32
12	101.18	140.48	38.84	139.89	38.26	2.1476	14.25
13	1.002	1.0972	9.50	1.089	8.68	0.0403	3.94
14	9.997	11.235	12.38	11.253	12.56	1.0506	5.07
15	100.64	108.32	7.63	106.78	6.10	2.0347	3.19
16	1.0768	1.222	13.48	1.21	12.37	0.0871	5.49
17	9.78	10.261	4.92	10.202	4.31	1.0112	2.09
18	101.19	156.58	54.74	156.9	55.05	2.1947	18.96

Table 8

File: FLOW_LOG.DAT
Title: Solid State Flow Sensor Screening Test
Comment: Preliminary Sensitivity Identification
Response: Flow & Err, Pwr LOG RS232 HELIUM CODED

Analysis Of Variance (ANOVA) Table

#	Factor	DOF	SOS	Percent	Mean-Sqr	Fcalc	Fcrit	Signif.
1	Gas	2	.003643	0.03	.0018215	.3176	4.459	_____
	Ln	1	.001976	0.02		.3446		
	Qd	1	.001676	0.01		.2922		
2	Flow	2	12.5396	99.43	6.269806	1093.	4.459	_____
	Ln	1	12.5371	99.41		2186.		
	Qd	1	.002544	0.02		.4435		
3	Press	2	.021526	0.17	.0107632	1.877	4.459	_____
	Ln	1	.006238	0.05		1.088		
	Qd	1	.015293	0.12		2.667		
4	GasTemp	2	.000948	0.01	.0004740	.0826	4.459	_____
	Ln	1	.000468	0.00		.0815		
	Qd	1	.000488	0.00		.0850		
5	Y Attitude	1	.000128	0.00	.0001278	.0223	5.318	_____
	Ln	1	.000134	0.00		.0234		
	Residual	8	.045879	0.36	.0057349			
	Replicate	0	.000000	0.00	.0000000			
	Pooled	8	.045879	0.36	.0057349			
	Total	17	12.6117	100.00				

SOS Grand Total: 33.0845
SOS Mean (CF) : 20.4728
SOS Total : 12.6117

Table 9

File: FLW_LG_E.DAT
Title: Solid State Flow Sensor Screening Test
Comment: Preliminary Sensitivity Identification
Response: Flow & Err, Pwr LOG RS232 HELIUM CODED

Analysis Of Variance (ANOVA) Table

#	Factor	DOF	SOS	Percent	Mean-Sqr	Fcalc	Fcrit	Signif.
1	Gas	2	31.7146	4.19	15.85730	.3015	4.459	_____
	Ln	1	24.4245	3.23		.4643		
	Qd	1	7.29000	0.96		.1386		
2	Flow	2	99.2856	13.12	49.64282	.9437	4.459	_____
	Ln	1	90.2557	11.92		1.716		
	Qd	1	9.03002	1.19		.1717		
3	Press	2	196.264	25.93	98.13184	1.866	4.459	_____
	Ln	1	48.8840	6.46		.9293		
	Qd	1	147.380	19.47		2.802		
4	GasTemp	2	6.60510	0.87	3.302551	.0628	4.459	_____
	Ln	1	.330008	0.04		.0063		
	Qd	1	6.27502	0.83		.1193		
5	Y Attitude	1	2.30414	0.30	2.304138	.0438	5.318	_____
	Ln	1	2.30409	0.30		.0438		
	Residual	8	420.820	55.59	52.60254			
	Replicate	0	.000000	0.00	.0000000			
	Pooled	8	420.820	55.59	52.60254			
	Total	17	756.993	100.00				

SOS Grand Total: 1421.66
SOS Mean (CF) : 664.666
SOS Total : 756.993

Table 10

Output

Title. Solid State Flow Sensor Screening Test
Comment: Preliminary Sensitivity Identification
Response: Flow & Err, Pwr LoG RS232
Design: [L18] Treatments: [18] Replicates: [1] Taguchi Design: [3] Levels Maximum
Level Average Auto Scaling In Effect For Response (Main Effect) Plots

File: FLOW_LOG.DAT
Date: 03-13-1996
Time: 09:53:59

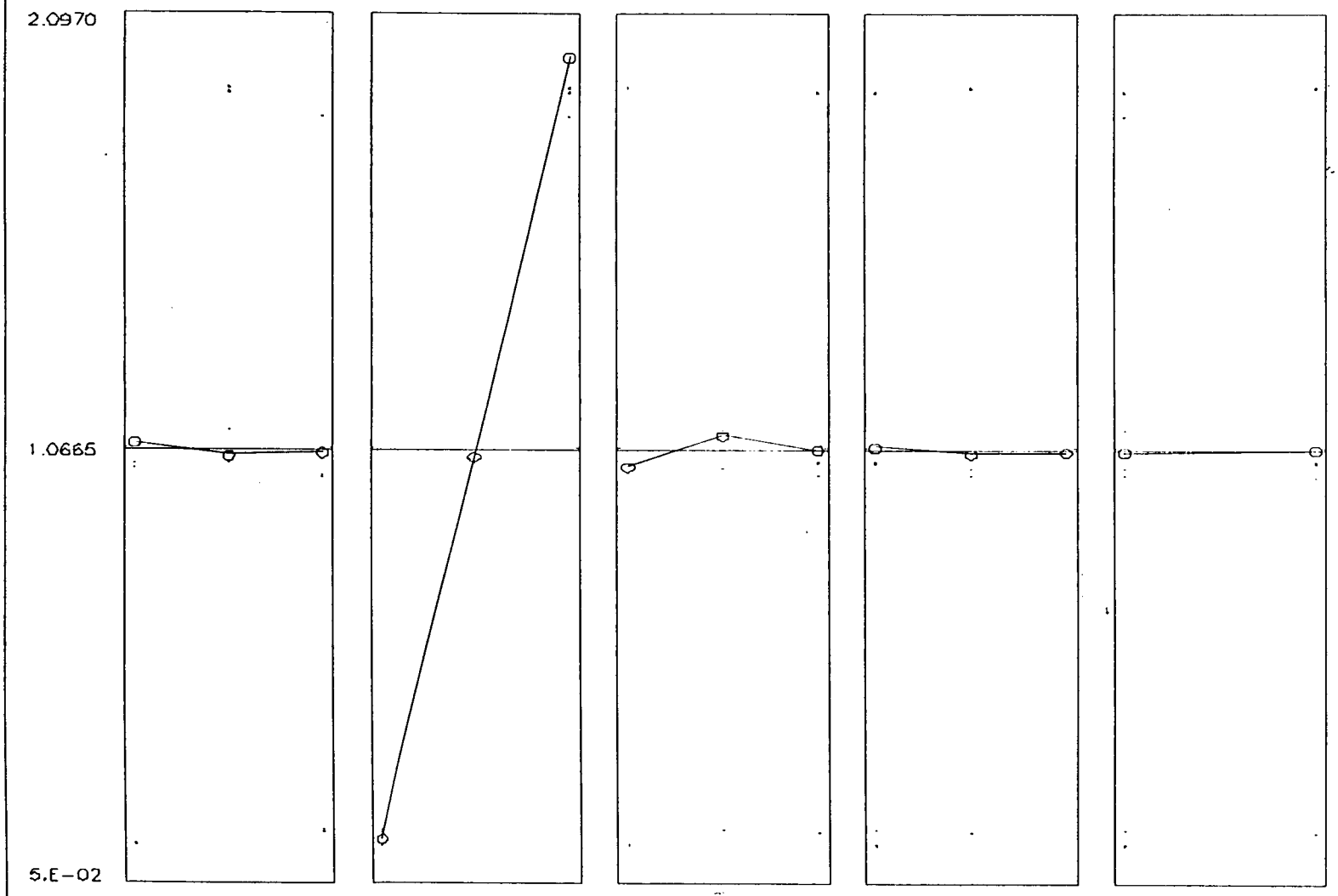

Factors	Gas	Flow	Press	GasTemp	Y Attitude
Level Names	Oxygen Nitrogen Helium	1 10 100	40 475 910	30 105 180	Up Down 3

Figure 4

Output

Title. Solid State Flow Sensor Screening Test
Comment: Preliminary Sensitivity Identification
Response: Flow & Err, Pwr LOG RS232
Design: [L18] Treatments: [18] Replicates: [1] Taguchi Design: [3] Levels Maximum
Global Value Auto Scaling In Effect For Response (Main Effect) Plots

File: FLOW_LOG.DAT
Date: 03-13-1996
Time: 09:55:24

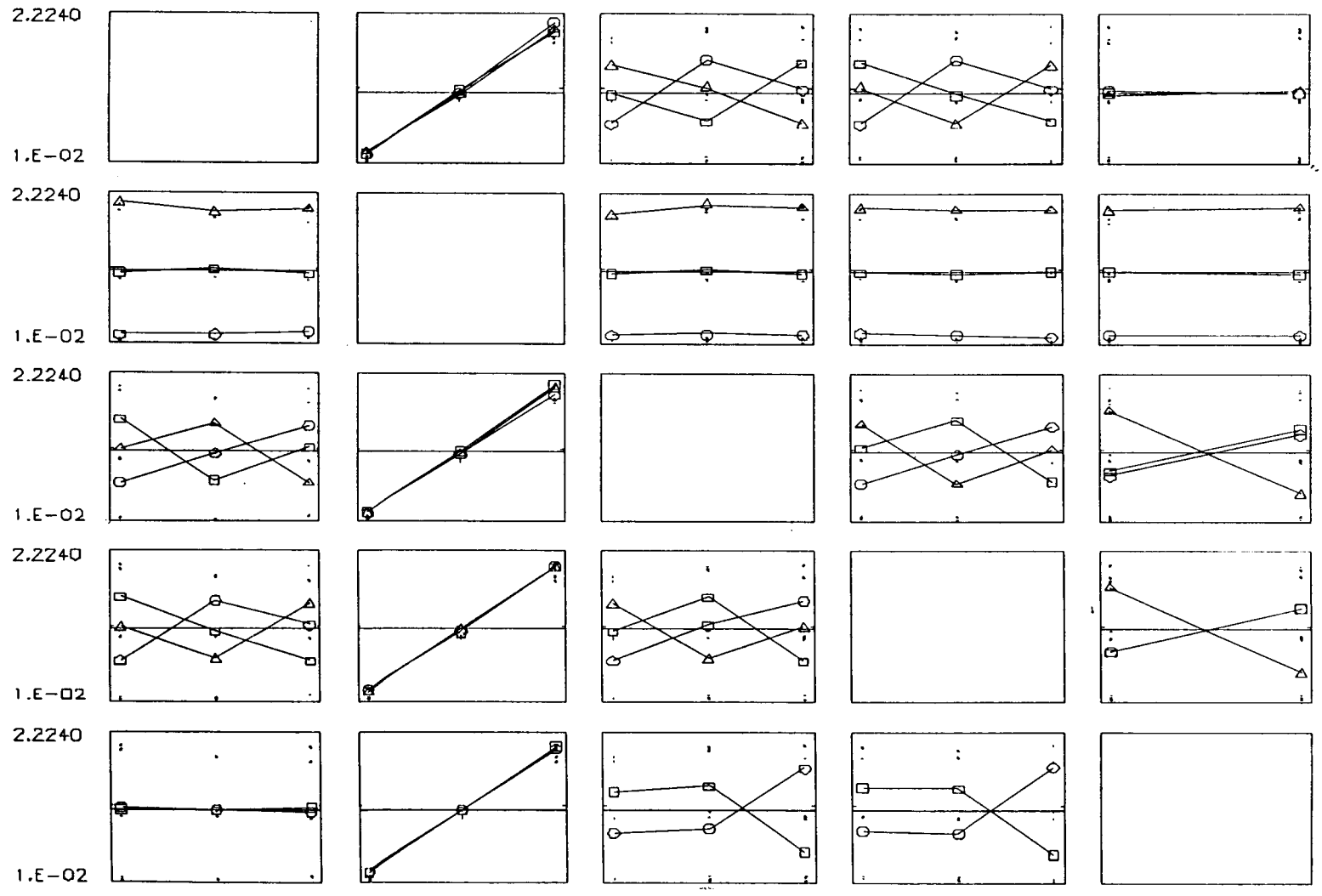

Factors	Gas	Flow	Press	GasTemp	Y Attitude
Level Names	Oxygen Nitrogen Helium	1 10 100	40 475 910	30 105 180	Up Down 3

Figure 5

UNIT 1 DOE 3A

RUN NUMBER	GAS TEMP	GAS PRESS	FLOW ACTUAL	FLOW RS232	CORR RS232	ERROR % READING	FLOW ANALOG	CORR ANALOG	ERROR % READING
1	40	70	1.99	2.182	2.1930	9.65	2.195	2.2060	10.30
2	165	70	1.989	2.172	2.1840	9.20	2.163	2.1750	8.75
3	40	850	2.024	2.251	2.2243	11.22	2.265	2.2381	11.91
4	165	850	1.9928	2.172	2.1798	8.99	2.165	2.1728	8.64

Table 11

UNIT 1 DOE 3B

RUN NUMBER	GAS TEMP	Y ATT'DE	FLOW ACTUAL	FLOW RS232	CORR RS232	ERROR % READING	FLOW ANALOG	CORR ANALOG	ERROR % READING
1	40	UP	2.014	2.266	2.2502	12.51	2.282	2.2661	13.31
2	165	UP	1.991	2.233	2.2431	12.15	2.234	2.2441	12.20
3	40	DOWN	2.006	2.152	2.1456	7.28	2.163	2.1565	7.83
4	165	DOWN	1.986	2.152	2.1672	8.36	2.155	2.1702	8.51

Table 12

UNIT 1 DOE 3C

RUN NUMBER	GAS PRESS	Y ATT'DE	FLOW ACTUAL	FLOW RS232	CORR RS232	ERROR % READING	FLOW ANALOG	CORR ANALOG	ERROR % READING
1	100	UP	2.0166	2.222	2.2037	10.19	2.239	2.2206	11.03
2	850	UP	2.014	2.266	2.2502	12.51	2.282	2.2661	13.31
3	100	DOWN	2.008	2.207	2.1982	9.91	2.221	2.2122	10.61
4	850	DOWN	2.006	2.152	2.1456	7.28	2.163	2.1565	7.83

Table 13

UNIT 1 DOE 3D

RUN NUMBER	GAS PRESS	GAS TYPE	FLOW ACTUAL	FLOW RS232	CORR RS232	ERROR % READING	FLOW ANALOG	CORR ANALOG	ERROR % READING
1	70	N2	1.989	2.172	2.1840	9.20	2.163	2.1750	8.75
2	850	N2	1.9928	2.172	2.1798	8.99	2.165	2.1728	8.64
3	70	He	2.098	3.064	2.9209	46.04	3.067	2.9237	46.19
4	850	He	1.996	2.1767	2.1811	9.05	2.177	2.1814	9.07

Table 14

UNIT 1 DOE 3E

RUN NUMBER	GAS TEMP	GAS TYPE	FLOW ACTUAL	FLOW RS232	CORR RS232	ERROR % READING	FLOW ANALOG	CORR ANALOG	ERROR % READING
1	40	N2	1.99	2.182	2.1930	9.65	2.195	2.2060	10.30
2	165	N2	1.989	2.172	2.1840	9.20	2.163	2.1750	8.75
3	40	He	1.9917	2.9597	2.9720	48.60	2.975	2.9874	49.37
4	165	He	2.098	3.064	2.9209	46.04	3.067	2.9237	46.19

Table 15

File: FLOW3_A .DAT
Title: Solid State Flow Sensor Screening Test
Comment: Identification of Interactions
Response: Flow & Err

Analysis Of Variance (ANOVA) Table

#	Factor	DOF	SOS	Percent	Mean-Sqr	Fcalc	Fcrit	Effect
1	GAS TEMP	1	.000719	59.09	.0007191	2.299	161.4	-.026750
	Ln	1	.000716	58.80		2.288		
2	GAS PRESS	1	.000185	15.20	.0001850	.5915	161.4	.013550
	Ln	1	.000184	15.09		.5870		
	Residual	1	.000313	25.71	.0003128			
	Replicate	0	.000000	0.00	.0000000			
	Pooled	1	.000313	25.71	.0003128			
	Total	3	.001217	100.00				

SOS Grand Total: 19.2781
SOS Mean (CF) : 19.2769
SOS Total : .001217

Table 16

Output

Title. Solid State Flow Sensor Screening Test
Comment: Identification of Interactions
Response: Flow & Err
Design: [L4] Treatments: [4] Replicates: [1] Full Factorial: 2^(2)
Level Average Auto Scaling In Effect For Response (Main Effect) Plots

File: FLOW3_A.DAT
Date: 03-14-1996
Time: 16:02:16

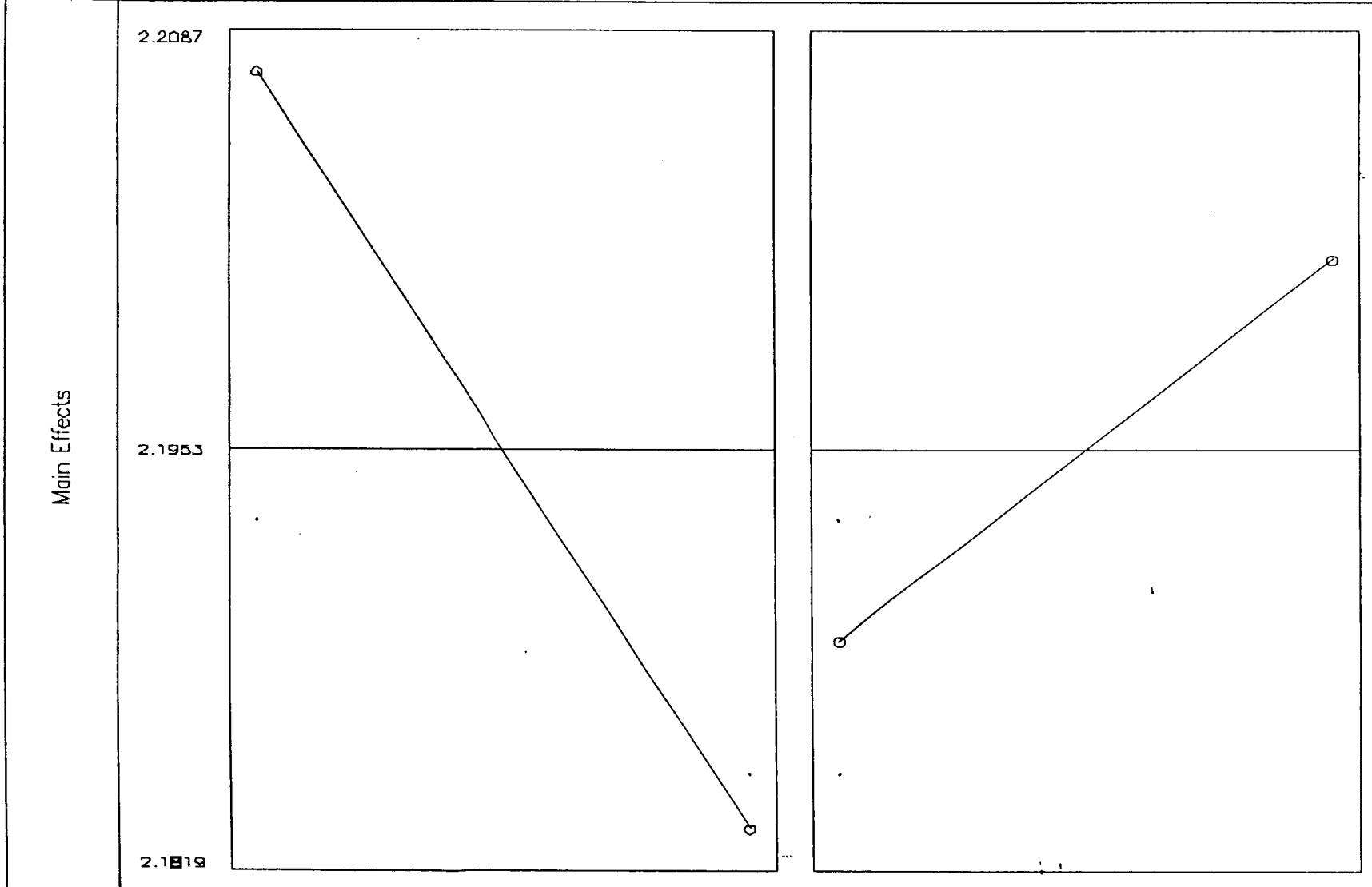

Factors	GAS TEMP	GAS PRESS
Level Names	40 165	70 850

Figure 6

Output

Title. Solid State Flow Sensor Screening Test
Comment: Identification of Interactions
Response: Flow & Err
Design: [L4] Treatments: [4] Replicates: [1] Full Factorial: 2^(2)
Global Value Auto Scaling In Effect For Response (Main Effect) Plots

File: FLOW3_A.DAT
Date: 03-14-1996
Time: 16:03:36

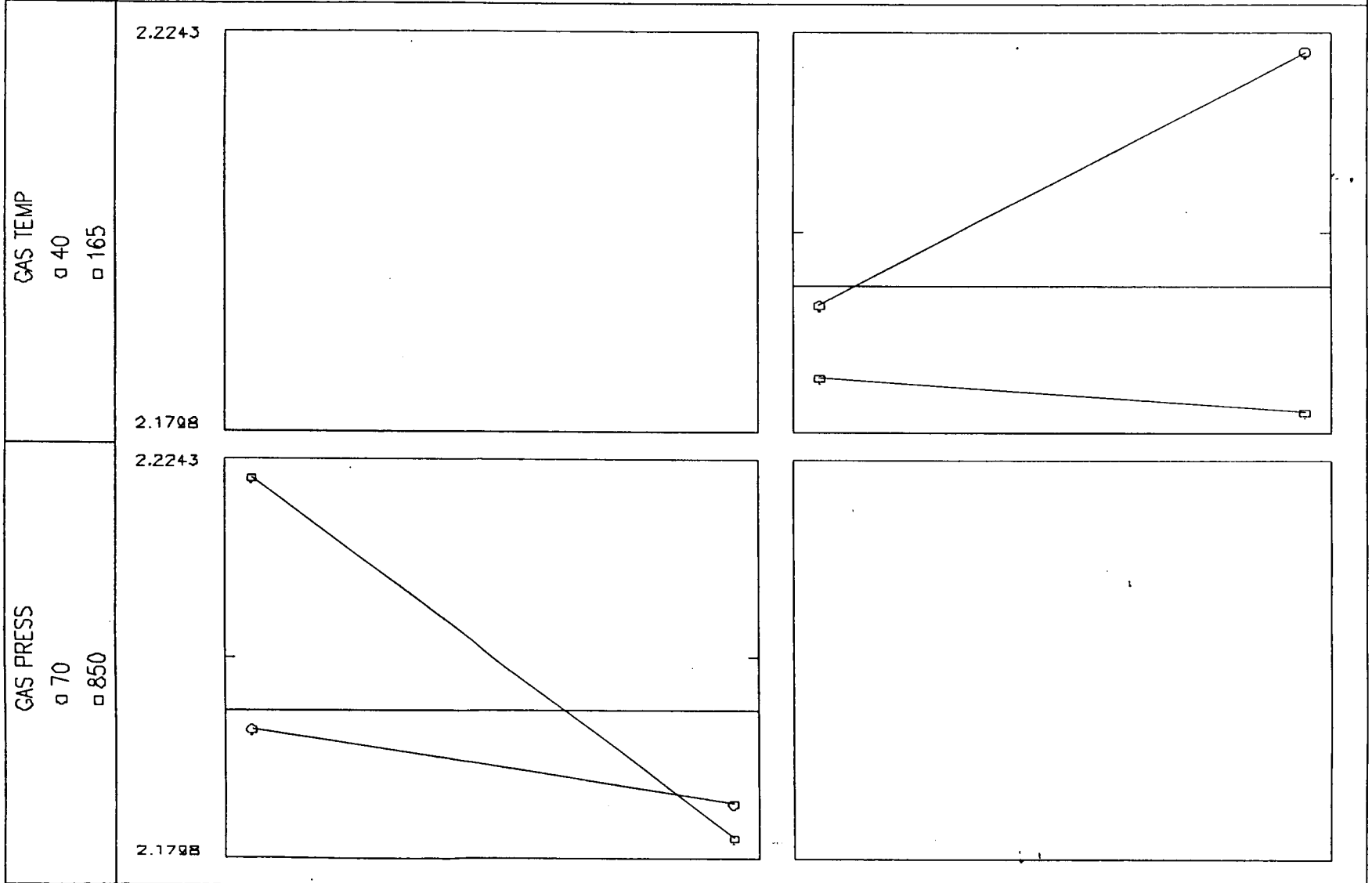

Factors	GAS TEMP	GAS PRESS
Level Names	40 165	70 850

Figure 7

File: FLOW3_B .DAT
Title: Solid State Flow Sensor Screening Test
Comment: Identification of Interactions
Response: Flow & Err

Analysis Of Variance (ANOVA) Table

#	Factor	DOF	SOS	Percent	Mean-Sqr	Fcalc	Fcrit	Effect
1	GAS TEMP	1	.000055	0.66	.0000553	.2762	161.4	.007250
	Ln	1	.000053	0.63		.2625		
2	Y Attitude	1	.008148	96.96	.0081482	40.69	161.4	-.090250
	Ln	1	.008145	96.92		40.67		
	Residual	1	.000200	2.38	.0002003			
	Replicate	0	.000000	0.00	.0000000			
	Pooled	1	.000200	2.38	.0002003			
	Total	3	.008404	100.00				

SOS Grand Total: 19.3953
SOS Mean (CF) : 19.3868
SOS Total : .008404

Table 17

Output

Title. Solid State Flow Sensor Screening Test
Comment: Identification of Interactions
Response: Flow & Err
Design: [L4] Treatments: [4] Replicates: [1] Full Factorial: 2^(2)
Level Average Auto Scaling In Effect For Response (Main Effect) Plots

File; FLOW3_B.DAT
Date: 03-14-1996
Time: 15:57:05

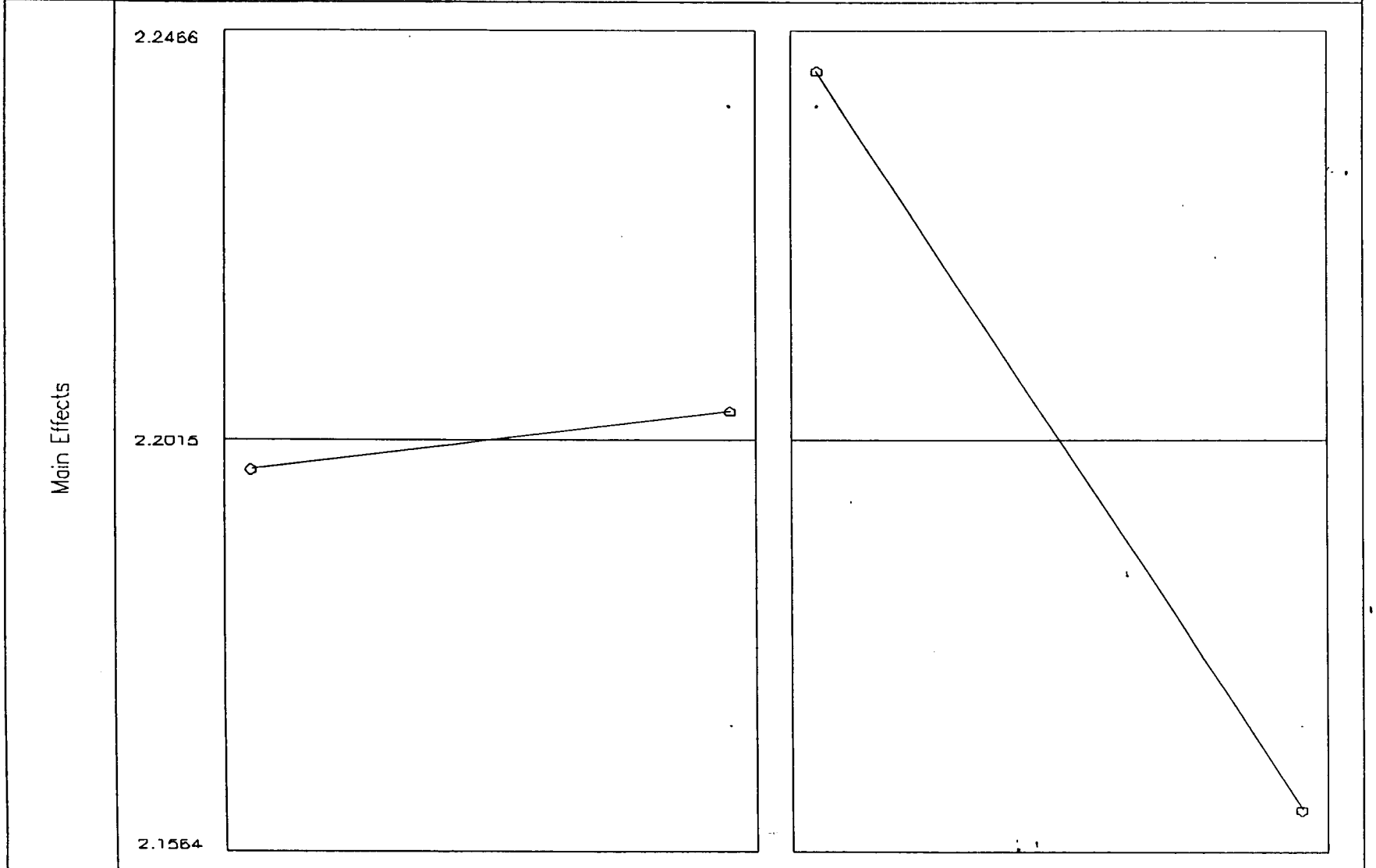

Factors	GAS TEMP	Y Attitude
Level Names	40 165	UP DOWN

Figure 8

Output

Title. Solid State Flow Sensor Screening Test
Comment: Identification of Interactions
Response: Flow & Err
Design: [L4] Treatments: [4] Replicates: [1] Full Factorial: 2^(2)
Global Value Auto Scaling In Effect For Response (Main Effect) Plots

File: FLOW3_B.DAT
Date: 03-14-1996
Time: 15:58:03

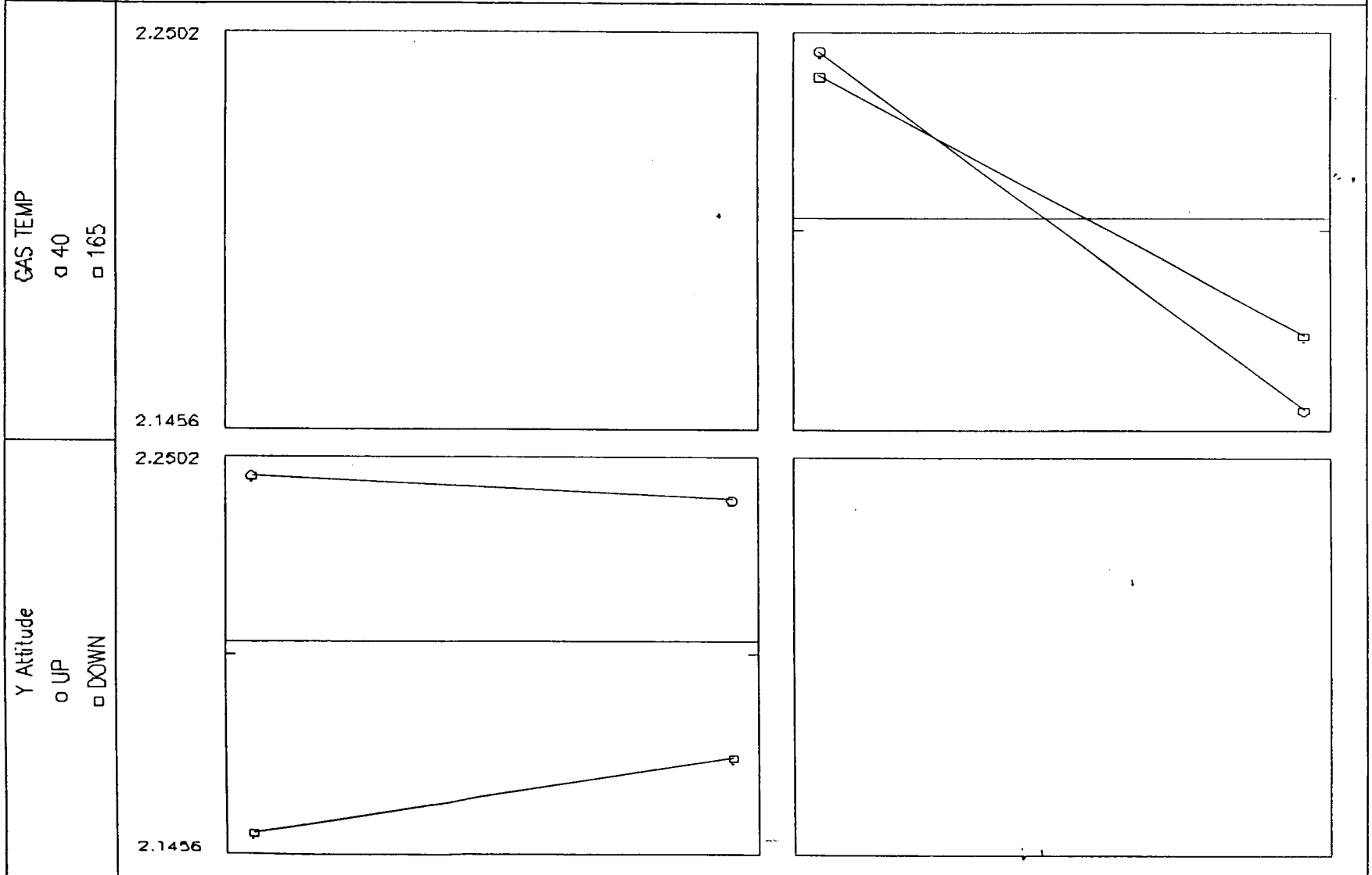

Factors	GAS TEMP	Y Attitude
Level Names	40 165	UP DOWN

Figure 9

File: FLOW3_C .DAT
Title: Solid State Flow Sensor Screening Test
Comment: Identification of Interactions
Response: Flow & Err

Analysis Of Variance (ANOVA) Table

#	Factor	DOF	SOS	Percent	Mean-Sqr	Fcalc	Fcrit	Effect
1	GAS PRESS	1	.000006	0.10	.0000057	.0023	161.4	-.003050
	Ln	1	.000009	0.17		.0038		
2	Y Attitude	1	.003027	55.12	.0030270	1.231	161.4	-.055050
	Ln	1	.003031	55.19		1.233		
	Residual	1	.002459	44.77	.0024586			
	Replicate	0	.000000	0.00	.0000000			
	Pooled	1	.002459	44.77	.0024586			
	Total	3	.005491	100.00				

SOS Grand Total: 19.3554
SOS Mean (CF) : 19.3499
SOS Total : .005491

Table 18

Output

Title. Solid State Flow Sensor Screening Test
Comment: Identification of Interactions
Response: Flow & Err
Design: [L4] Treatments: [4] Replicates: [1] Full Factorial: 2^(2)
Level Average Auto Scaling In Effect For Response (Main Effect) Plots

File: FLOW3_C.DAT
Date: 03-14-1996
Time: 15:19:48

Main Effects

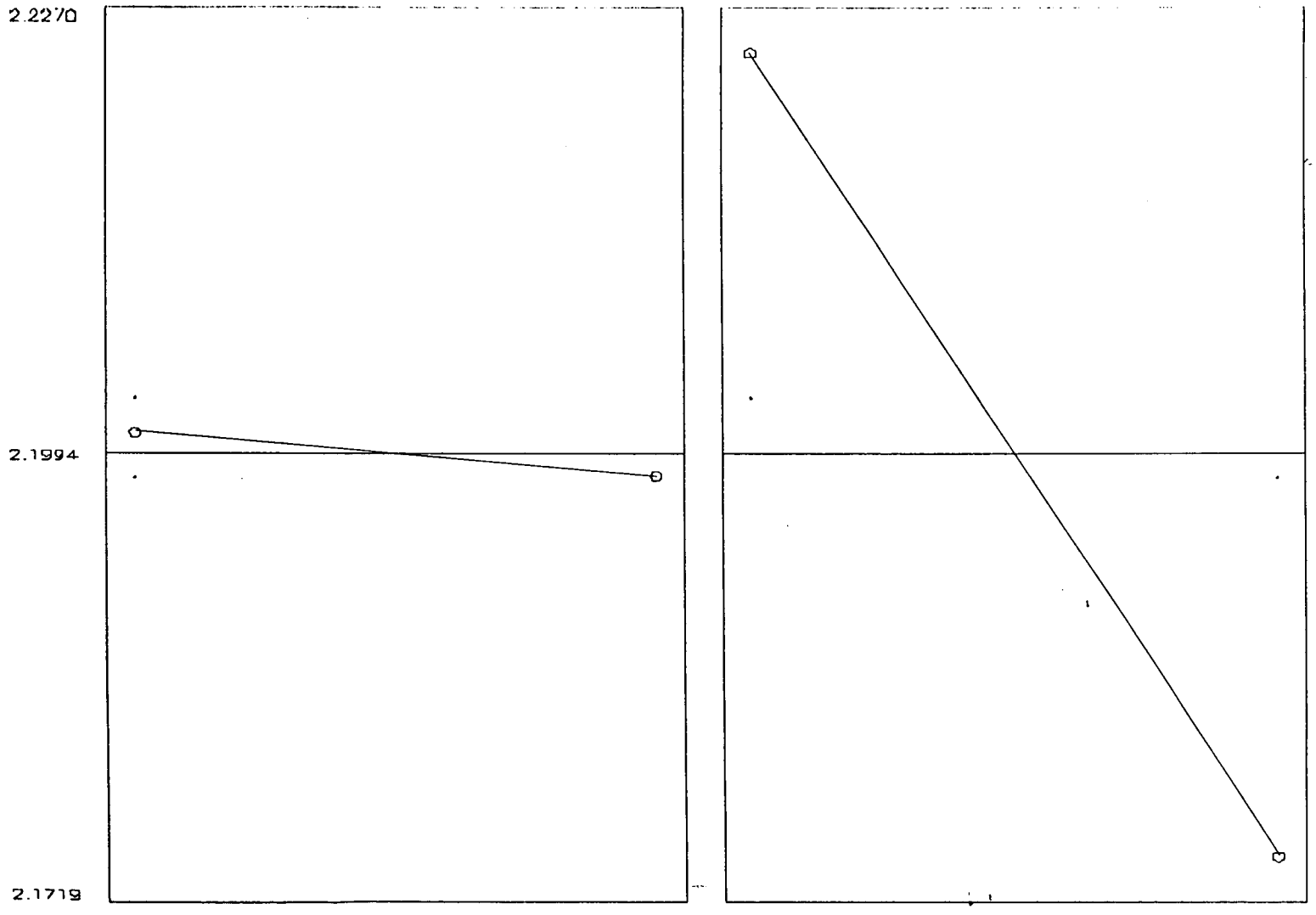

Factors	GAS PRESS	Y Attitude
Level Names	100 800	UP DOWN

Figure 10

Output

Title. Solid State Flow Sensor Screening Test
Comment: Identification of Interactions
Response: Flow & Err
Design: [L4] Treatments: [4] Replicates: [1] Full Factorial: 2^(2)
Global Value Auto Scaling In Effect For Response (Main Effect) Plots

File: FLOW3_C.DAT
Date: 03-14-1996
Time: 15:19:12

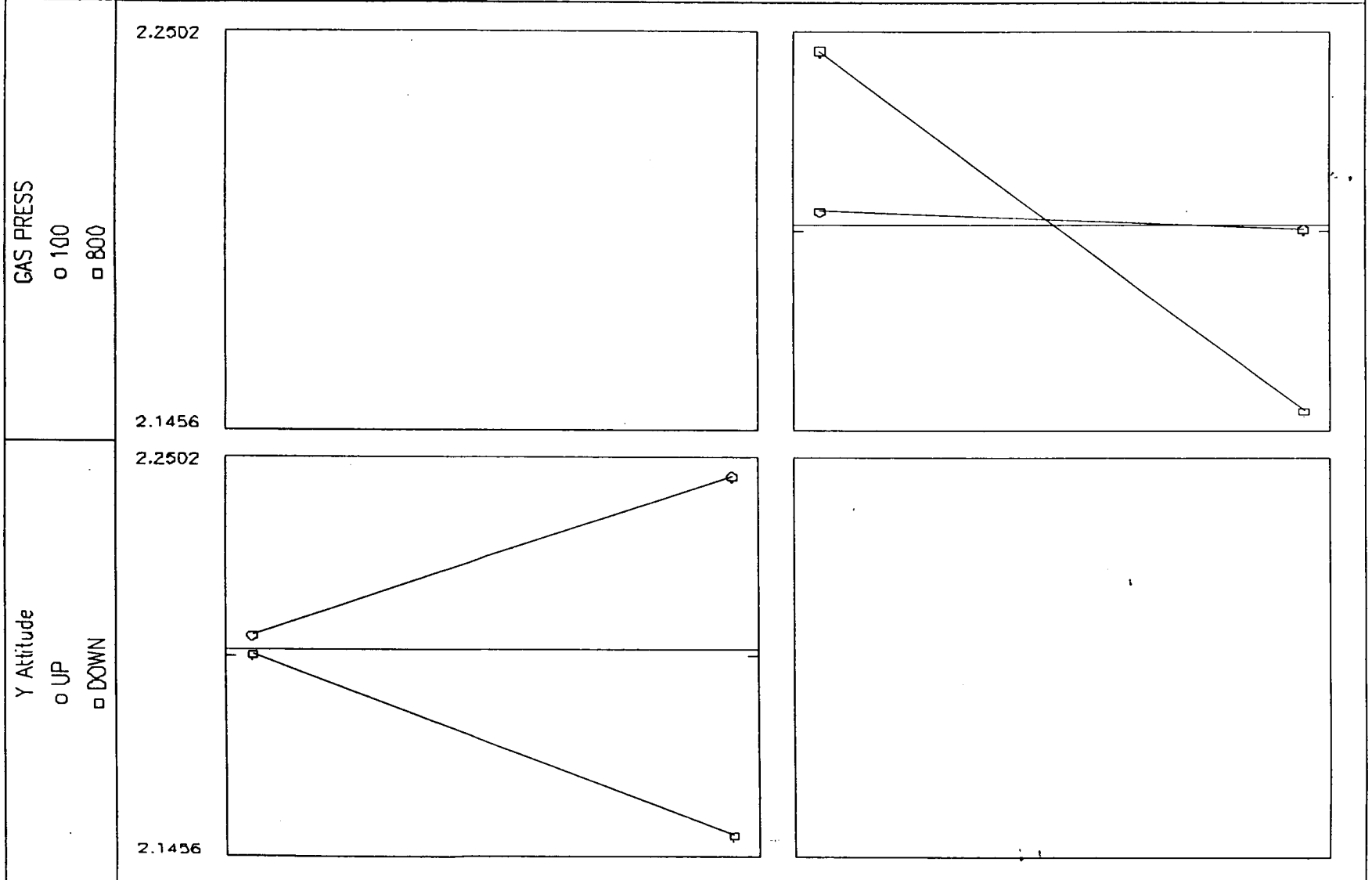

Factors	GAS PRESS	Y Attitude
Level Names	100 800	UP DOWN

Figure 11

File: FLOW3_D .DAT
Title: Solid State Flow Sensor Screening Test
Comment: Identification of Interactions
Response: Flow & Err

Analysis Of Variance (ANOVA) Table

#	Factor	DOF	SOS	Percent	Mean-Sqr	Fcalc	Fcrit	Effect
1	GAS PRESS	1	.138384	33.76	.1383839	1.023	161.4	-.372000
	Ln	1	.138384	33.76		1.023		
2	GAS TYPE	1	.136236	33.24	.1362362	1.007	161.4	.369100
	Ln	1	.136235	33.24		1.007		
	Residual	1	.135275	33.00	.1352749			
	Replicate	0	.000000	0.00	.0000000			
	Pooled	1	.135275	33.00	.1352749			
	Total	3	.409895	100.00				

SOS Grand Total: 22.8102
SOS Mean (CF) : 22.4003
SOS Total : .409895

Table 19

Output

Title. Solid State Flow Sensor Screening Test
Comment: Identification of Interactions
Response: Flow & Err
Design: [L4] Treatments: [4] Replicates: [1] Full Factorial: 2^(2)
Level Average Auto Scaling In Effect For Response (Main Effect) Plots

File: FLOW3_D.DAT
Date: 03-14-1996
Time: 16:05:27

Main Effects

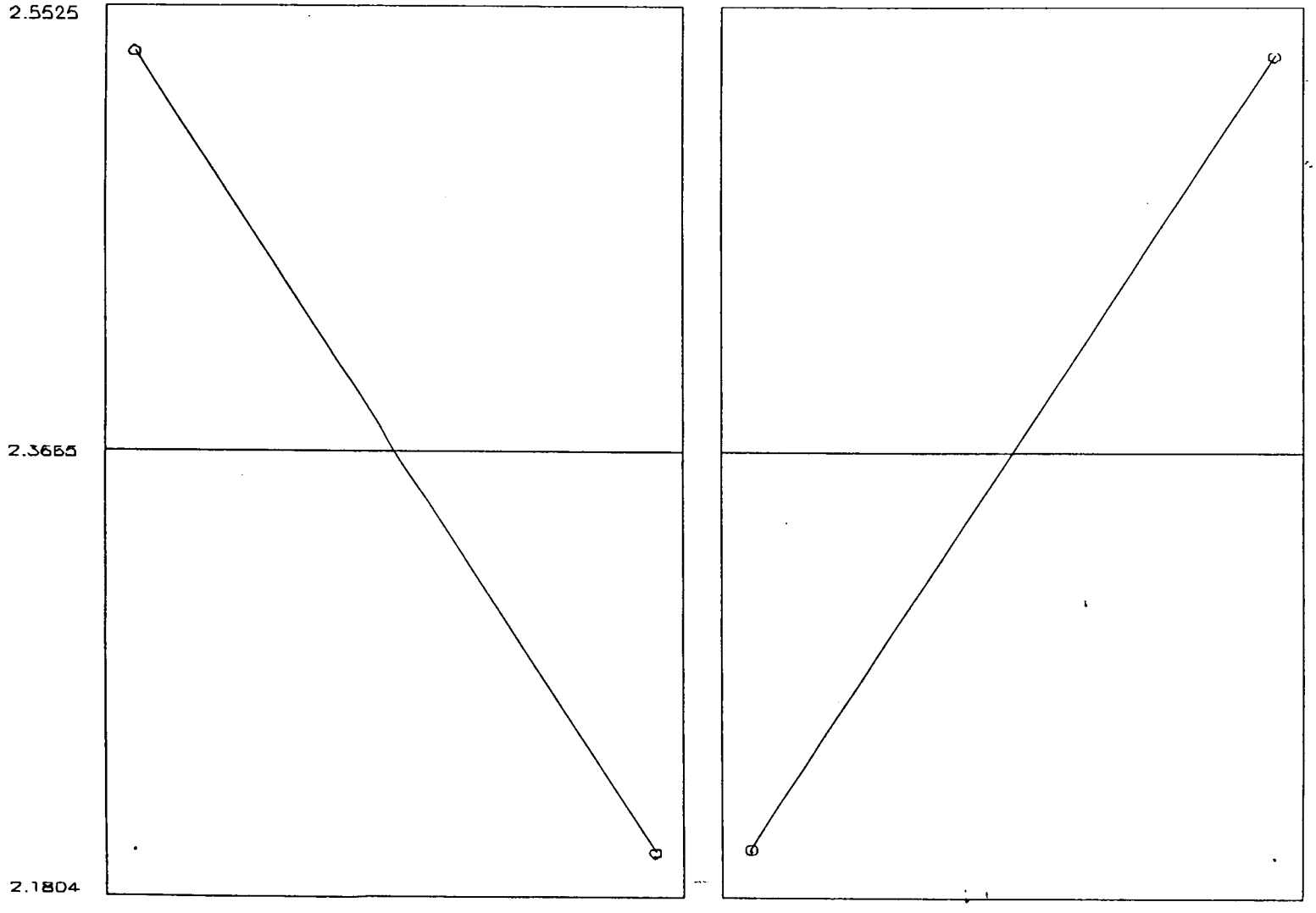

Factors	GAS PRESS	GAS TYPE
Level Names	100 800	N2 HE

Figure 12

Output

Title. Solid State Flow Sensor Screening Test
Comment: Identification of Interactions
Response: Flow & Err
Design: [L4] Treatments: [4] Replicates: [1] Full Factorial: 2^(2)
Global Value Auto Scaling In Effect For Response (Main Effect) Plots

File: FLOW3_D.DAT
Date: 03-14-1996
Time: 16:06:02

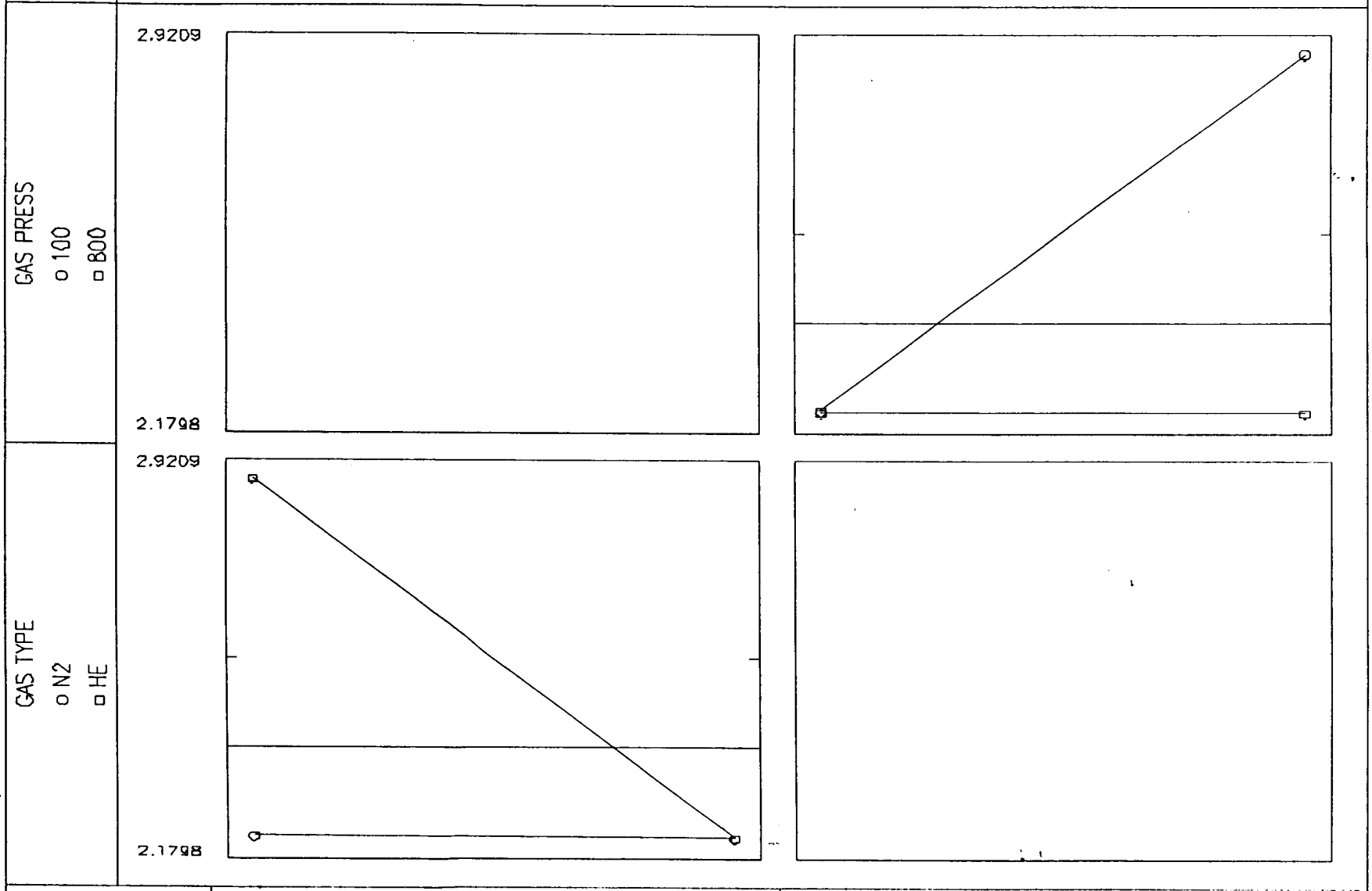

Factors	GAS PRESS	GAS TYPE
Level Names	100 800	N2 HE

Figure 13

File: FLOW3_E .DAT
Title: Solid State Flow Sensor Screening Test
Comment: Identification of Interactions
Response: Flow & Err

Analysis Of Variance (ANOVA) Table

#	Factor	DOF	SOS	Percent	Mean-Sqr	Fcalc	Fcrit	Effect
1	GAS TEMP	1	.000902	0.16	.0009022	2.021	161.4	-.030050
	Ln	1	.000903	0.16		2.023		
2	GAS TYPE	1	.574484	99.77	.5744839	1287.	161.4	.757950
	Ln	1	.574488	99.77		1287.		
	Residual	1	.000446	0.08	.0004463			
	Replicate	0	.000000	0.00	.0000000			
	Pooled	1	.000446	0.08	.0004463			
	Total	3	.575832	100.00				

SOS Grand Total: 26.9435
SOS Mean (CF) : 26.3677
SOS Total : .575832

Table 20

Output

Title. Solid State Flow Sensor Screening Test
Comment: Identification of Interactions
Response: Flow & Err
Design: [L4] Treatments: [4] Replicates: [1] Full Factorial: 2^(2)
Level Average Auto Scaling In Effect For Response (Main Effect) Plots

File: FLOW3_E.DAT
Date: 03-14-1996
Time: 16:07:32

Main Effects

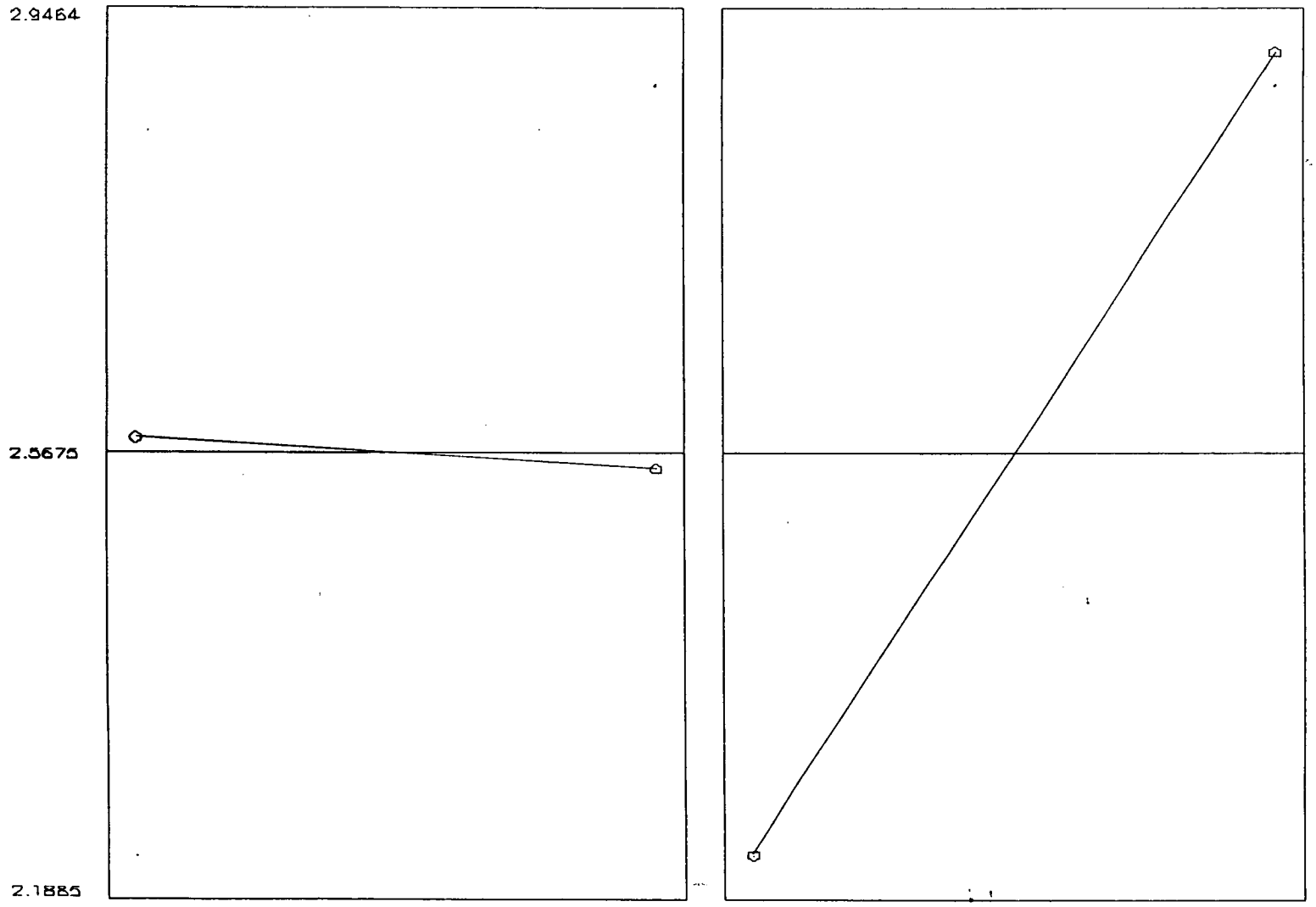

Factors	GAS TEMP	GAS TYPE
Level Names	40 165	N2 HE

Figure 14

Output

Title. Solid State Flow Sensor Screening Test
Comment: Identification of Interactions
Response: Flow & Err
Design: [L4] Treatments: [4] Replicates: [1] Full Factorial: 2^(2)
Global Value Auto Scaling In Effect For Response (Main Effect) Plots

File: FLOW3_E.DAT
Date: 03-14-1996
Time: 16:07:51

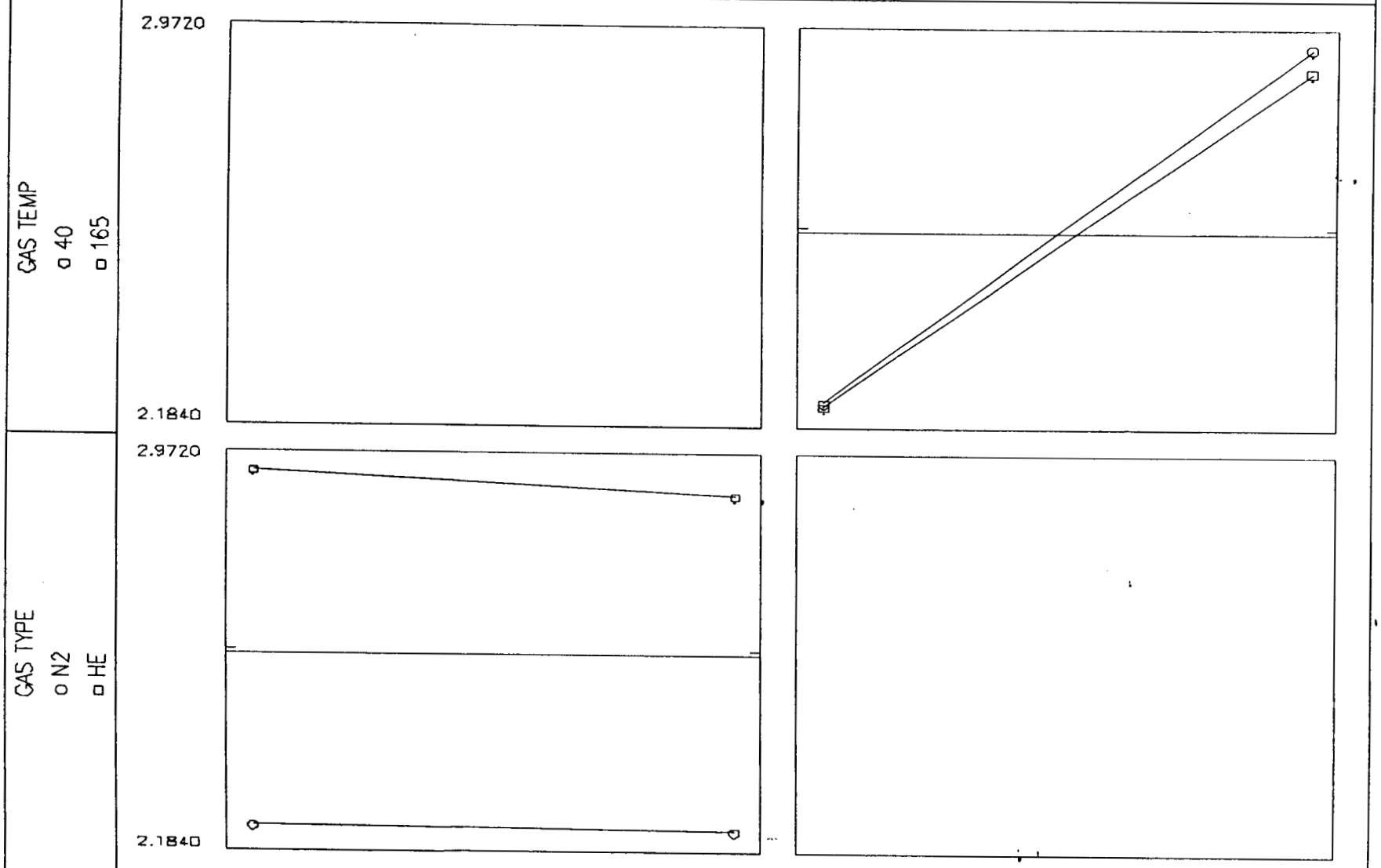

Factors	GAS TEMP	GAS TYPE
Level Names	40 165	N2 HE

Figure 15

UNIT 1 DOE 3D REPEAT

RUN NUMBER	GAS PRESS	GAS TYPE	FLOW ACTUAL	FLOW RS232	CORR RS232	ERROR % READING	FLOW ANALOG	CORR ANALOG	ERROR % READING
1	100	N2	5.017	5.607	5.5880	11.76	5.639	5.6199	12.40
2	850	N2	5.051	5.578	5.5217	10.43	5.598	5.5415	10.83
3	100	He	0.5027	0.5298	5.2695	5.39	0.5317	5.2884	5.77
4	850	He	0.4978	0.5145	5.1677	3.35	0.5154	5.1768	3.54

Table 21

File: FLOW3_D .DAT
Title: Solid State Flow Sensor Screening Test
Comment: Identification of Interactions
Response: Flow & Err

Analysis Of Variance (ANOVA) Table

#	Factor	DOF	SOS	Percent	Mean-Sqr	Fcalc	Fcrit	Effect
1	GAS PRESS	1	.007065	5.87	.0070648	21.53	161.4	-.084050
	Ln	1	.007064	5.87		21.53		
2	GAS TYPE	1	.113052	93.86	.1130524	344.6	161.4	-.336250
	Ln	1	.113064	93.87		344.6		
	Residual	1	.000328	0.27	.0003281			
	Replicate	0	.000000	0.00	.0000000			
	Pooled	1	.000328	0.27	.0003281			
	Total	3	.120445	100.00				

SOS Grand Total: 116.188
SOS Mean (CF) : 116.067
SOS Total : .120445

Table 22

Output

Title. Solid State Flow Sensor Screening Test
Comment: Identification of Interactions
Response: Flow & Err
Design: [L4] Treatments: [4] Replicates: [1] Full Factorial: 2^(2)
Level Average Auto Scaling In Effect For Response (Main Effect) Plots

File; FLOW3_D.DAT
Date: 03-15-1996
Time: 13:25:15

Main Effects

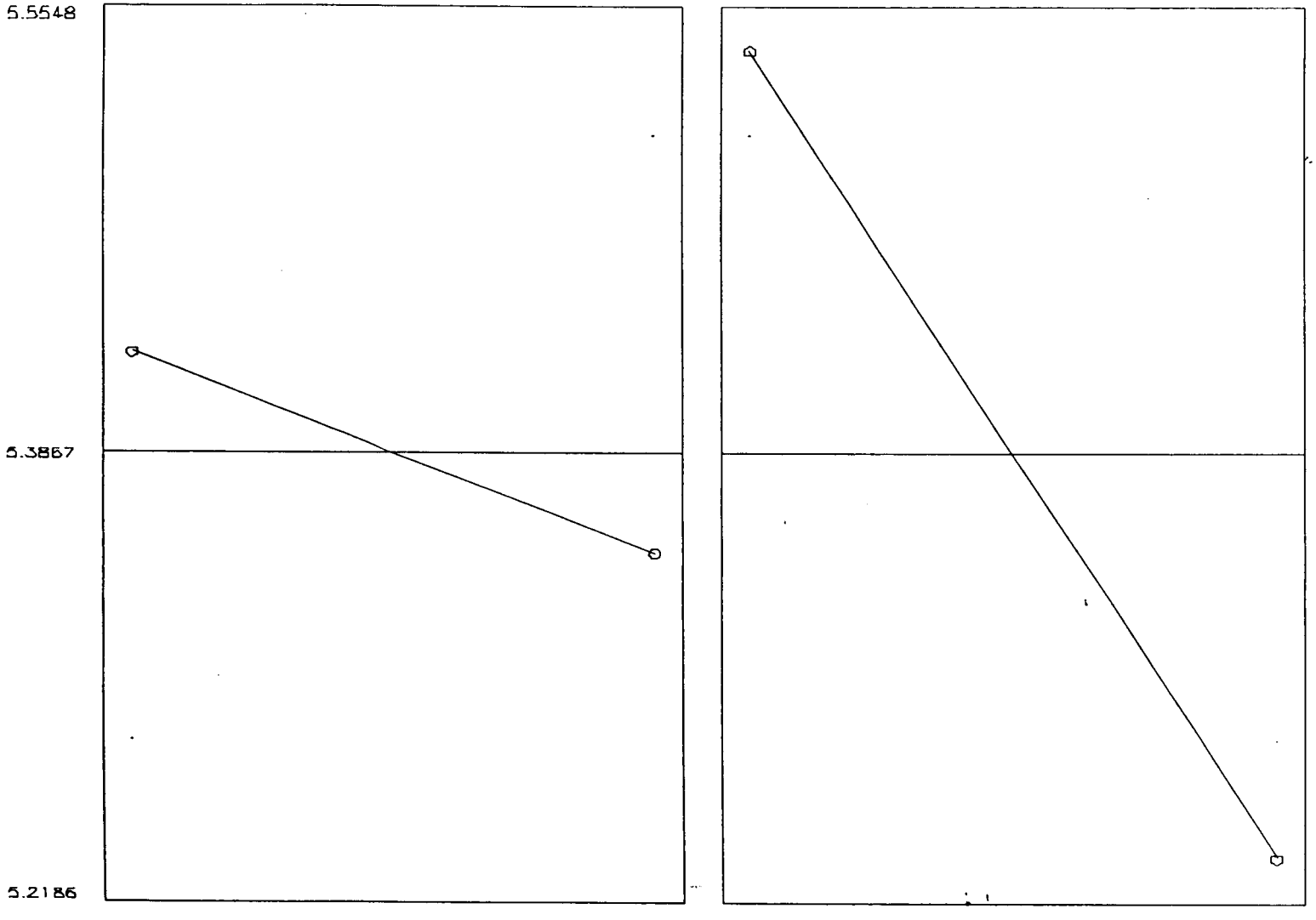

Factors	GAS PRESS	GAS TYPE
Level Names	100 800	N2 HE

Figure 16

Output

Title. Solid State Flow Sensor Screening Test
Comment: Identification of Interactions
Response: Flow & Err
Design: [L4] Treatments: [4] Replicates: [1] Full Factorial: 2^(2)
Global Value Auto Scaling In Effect For Response (Main Effect) Plots

File: FLOW3_D.DAT
Date: 03-15-1996
Time: 13:26:14

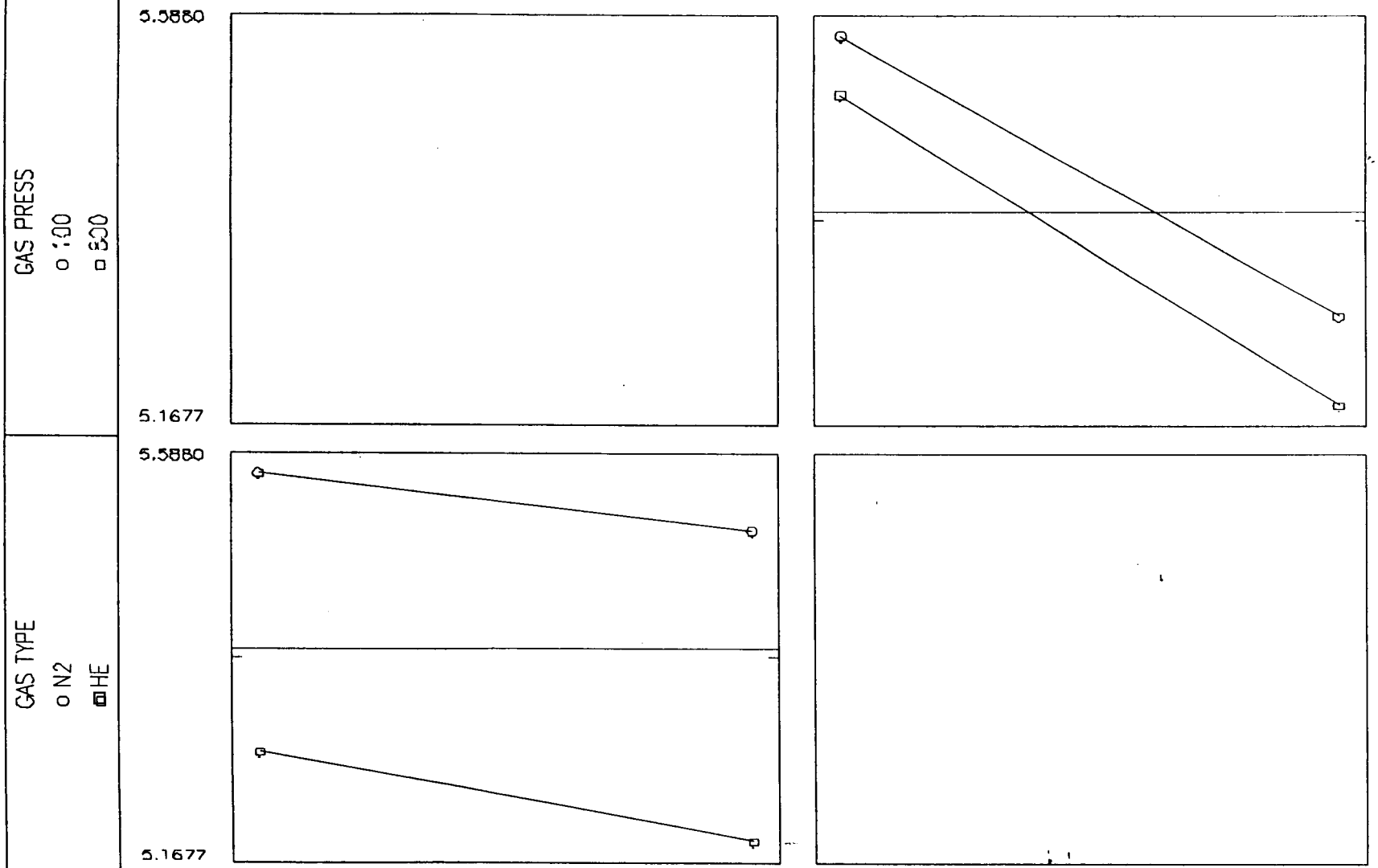

Factors	GAS PRESS	GAS TYPE
Level Names	100 800	N2 HE

Figure 17

HONEYWELL FLOW SENSOR UNIT 1

GAS	PRESS	TEMP	ERROR (0.33 TO 8 LB/HR)			
			AVERAGE	STD DEV	MAX	MIN
He	900	30	8.6	7.15	48.1	-14.2
He	100	30	8.1	6.61	76.2	-5.9
He	900	180	8	4.94	40.1	-7.3
He	100	180	8.8	5.68	74	-9.7
N2	900	30	11.1	3.37	40.1	-8
N2	100	30	10.5	3.94	59.8	-0.5
N2	900	180	9.4	5.3	39.1	-16.8
N2	100	180	10.9	3.41	34.6	-2.4
O2	900	30	13.1	3.3	35.9	1.5
O2	100	30	9.5	5.06	36.3	-24.2
O2	900	180	8.3	4.78	32.8	-17.4
O2	100	180	9.8	4.67	25.3	-15.5

Table 23

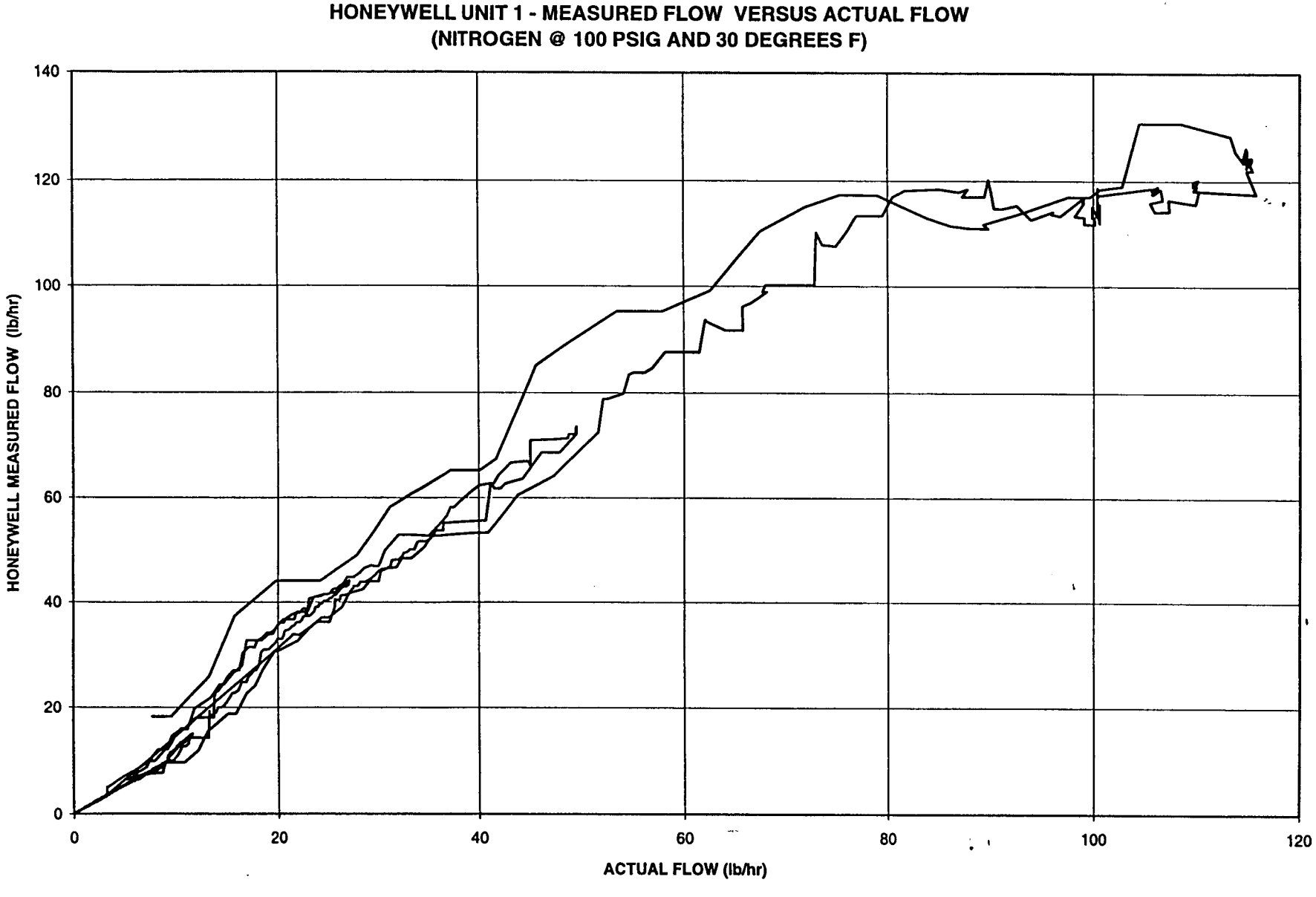
HONEYWELL UNIT 1 - MEASURED FLOW VERSUS ACTUAL FLOW
(NITROGEN @ 100 PSIG AND 30 DEGREES F)
HONEYWELL MEASURED FLOW (lb/hr)
ACTUAL FLOW (lb/hr)
0
20
40
60
80
100
120
140

Figure 18

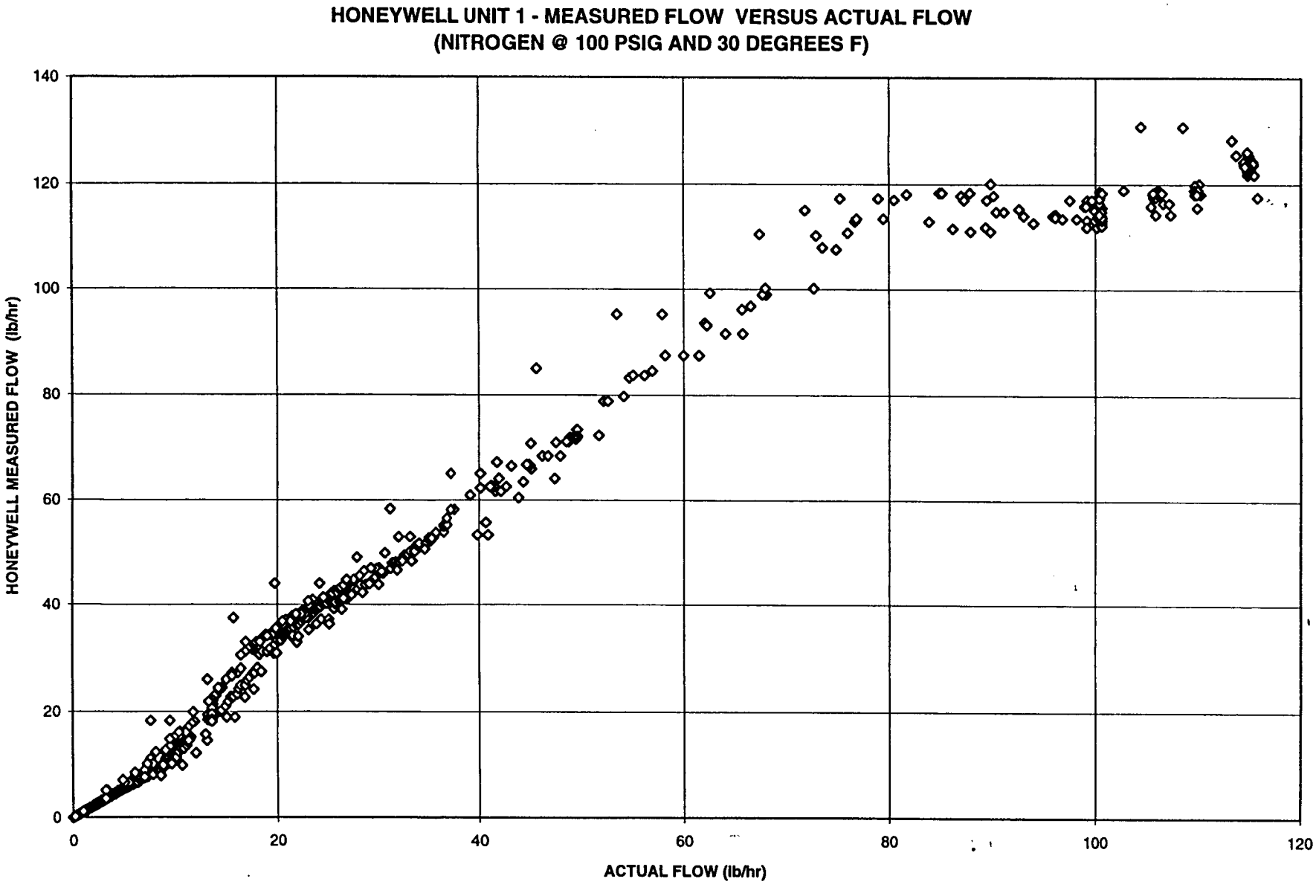
HONEYWELL UNIT 1 - MEASURED FLOW VERSUS ACTUAL FLOW
(NITROGEN @ 100 PSIG AND 30 DEGREES F)
HONEYWELL MEASURED FLOW (lb/hr)
ACTUAL FLOW (lb/hr)
0
20
40
60
80
100
120
140

Figure 19

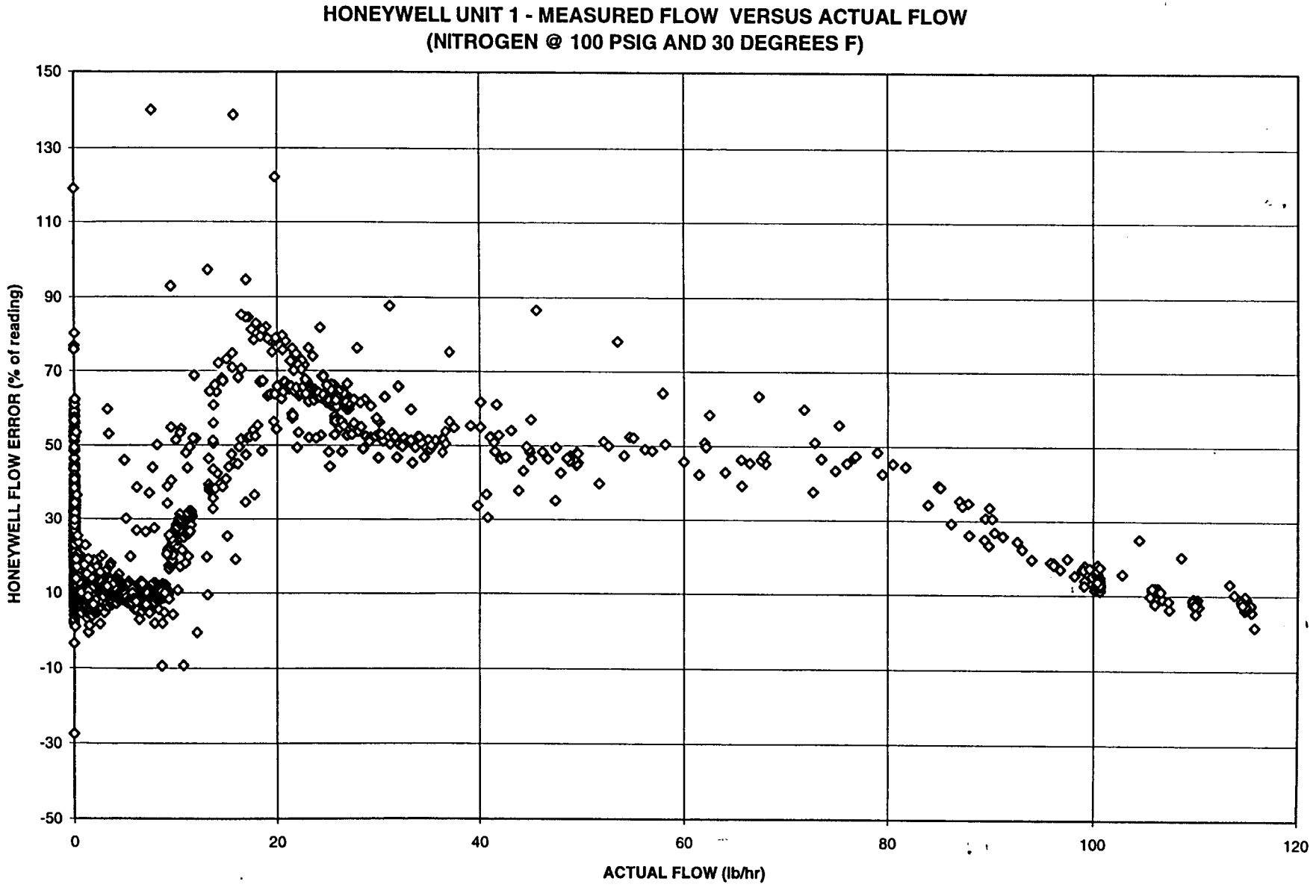
HONEYWELL UNIT 1 - MEASURED FLOW VERSUS ACTUAL FLOW
(NITROGEN @ 100 PSIG AND 30 DEGREES F)
HONEYWELL FLOW ERROR (% of reading)
150
130
110
90
70
50
30
10
-10
-30
-50
0
20
40
60
80
100
120
ACTUAL FLOW (lb/hr)

Figure 20

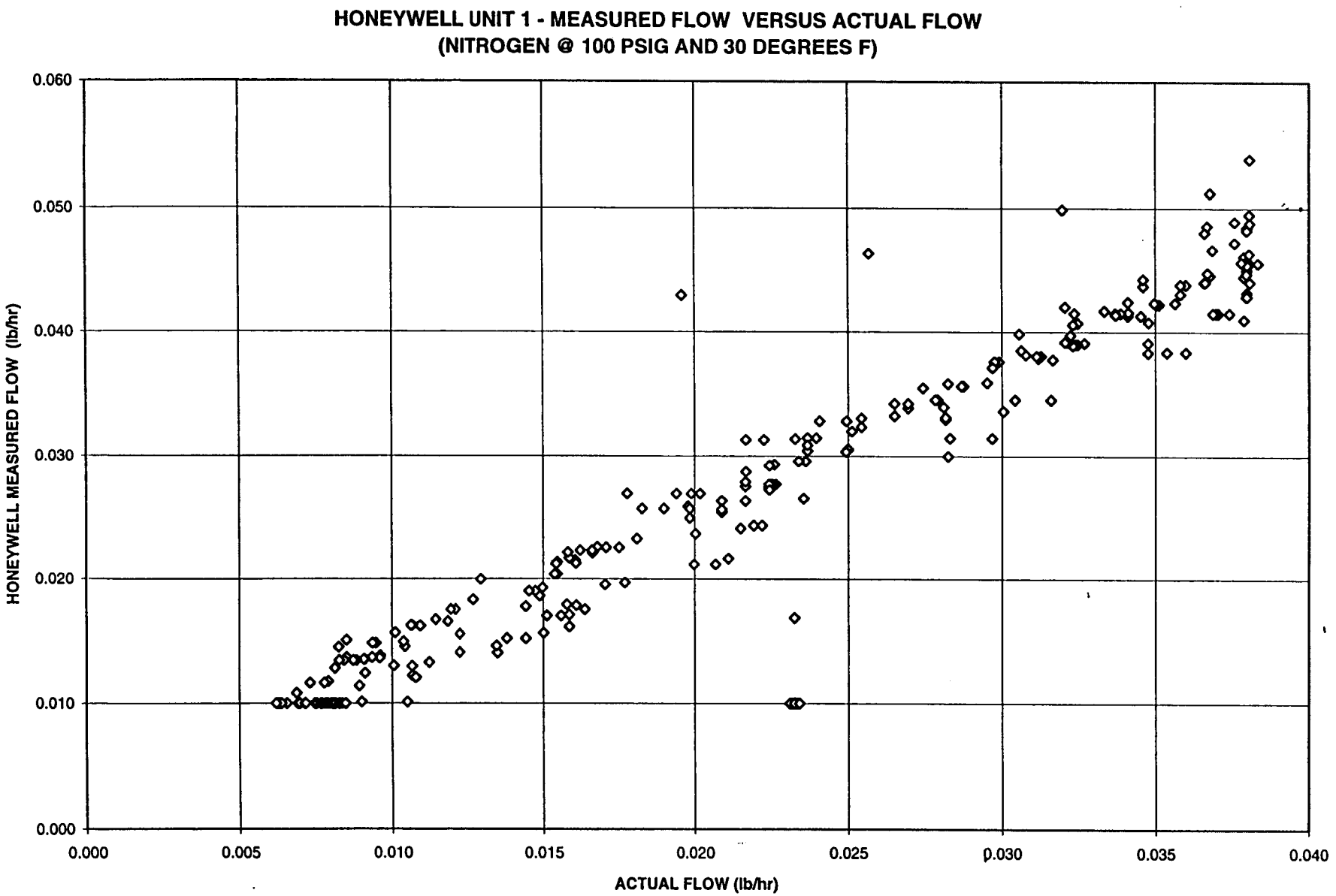
HONEYWELL UNIT 1 - MEASURED FLOW VERSUS ACTUAL FLOW
(NITROGEN @ 100 PSIG AND 30 DEGREES F)
HONEYWELL MEASURED FLOW (lb/hr)
0.060
0.050
0.040
0.030
0.020
0.010
0.000
0.000
0.005
0.010
0.015
0.020
0.025
0.030
0.035
0.040
ACTUAL FLOW (lb/hr)

Figure 21

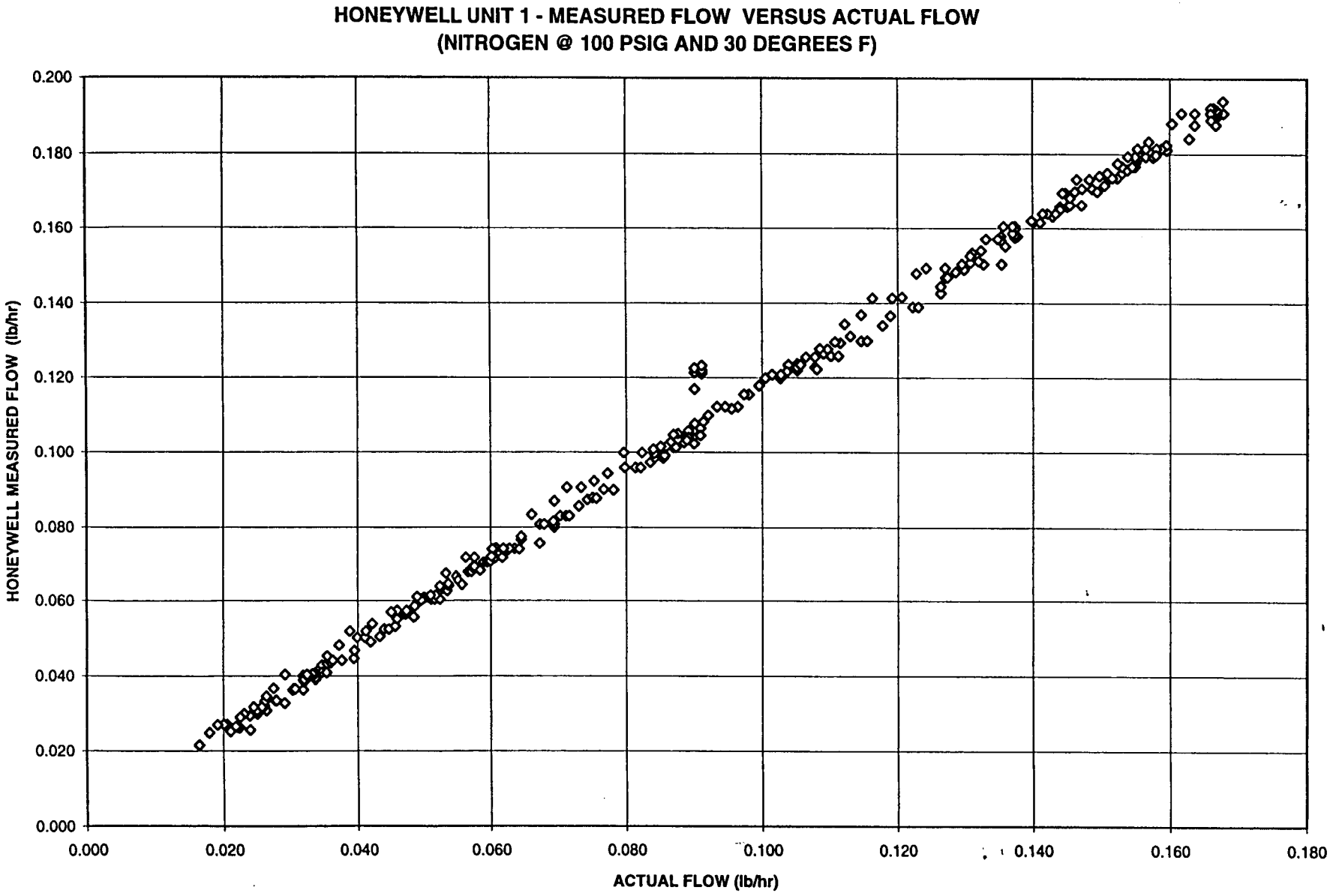
HONEYWELL UNIT 1 - MEASURED FLOW VERSUS ACTUAL FLOW
(NITROGEN @ 100 PSIG AND 30 DEGREES F)
HONEYWELL MEASURED FLOW (lb/hr)
0.200
0.180
0.160
0.140
0.120
0.100
0.080
0.060
0.040
0.020
0.000
0.000
0.020
0.040
0.060
0.080
0.100
0.120
0.140
0.160
0.180
ACTUAL FLOW (lb/hr)

Figure 22

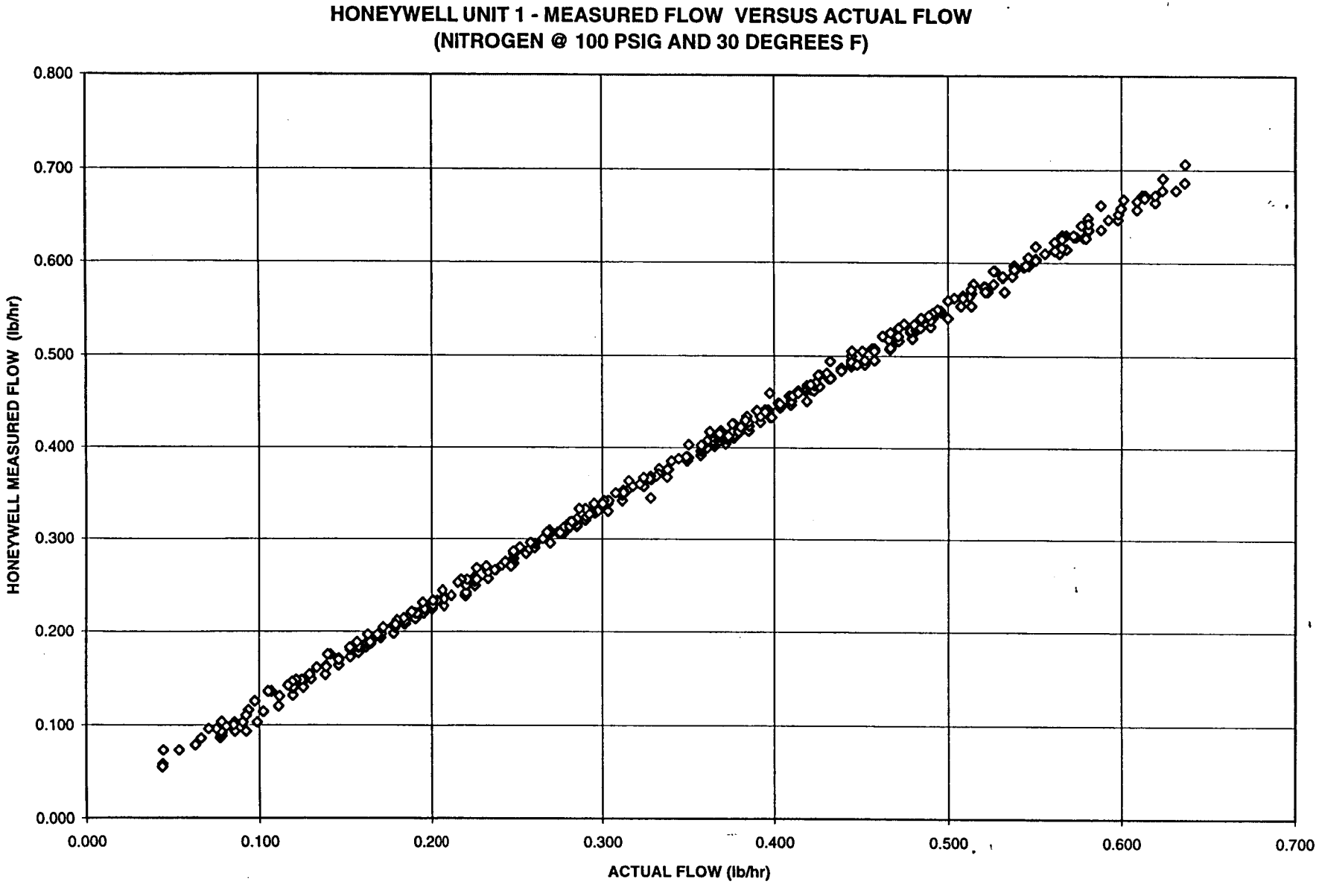
HONEYWELL UNIT 1 - MEASURED FLOW VERSUS ACTUAL FLOW
(NITROGEN @ 100 PSIG AND 30 DEGREES F)
HONEYWELL MEASURED FLOW (lb/hr)
0.800
0.700
0.600
0.500
0.400
0.300
0.200
0.100
0.000
0.000
0.100
0.200
0.300
0.400
0.500
0.600
0.700
ACTUAL FLOW (lb/hr)

Figure 23

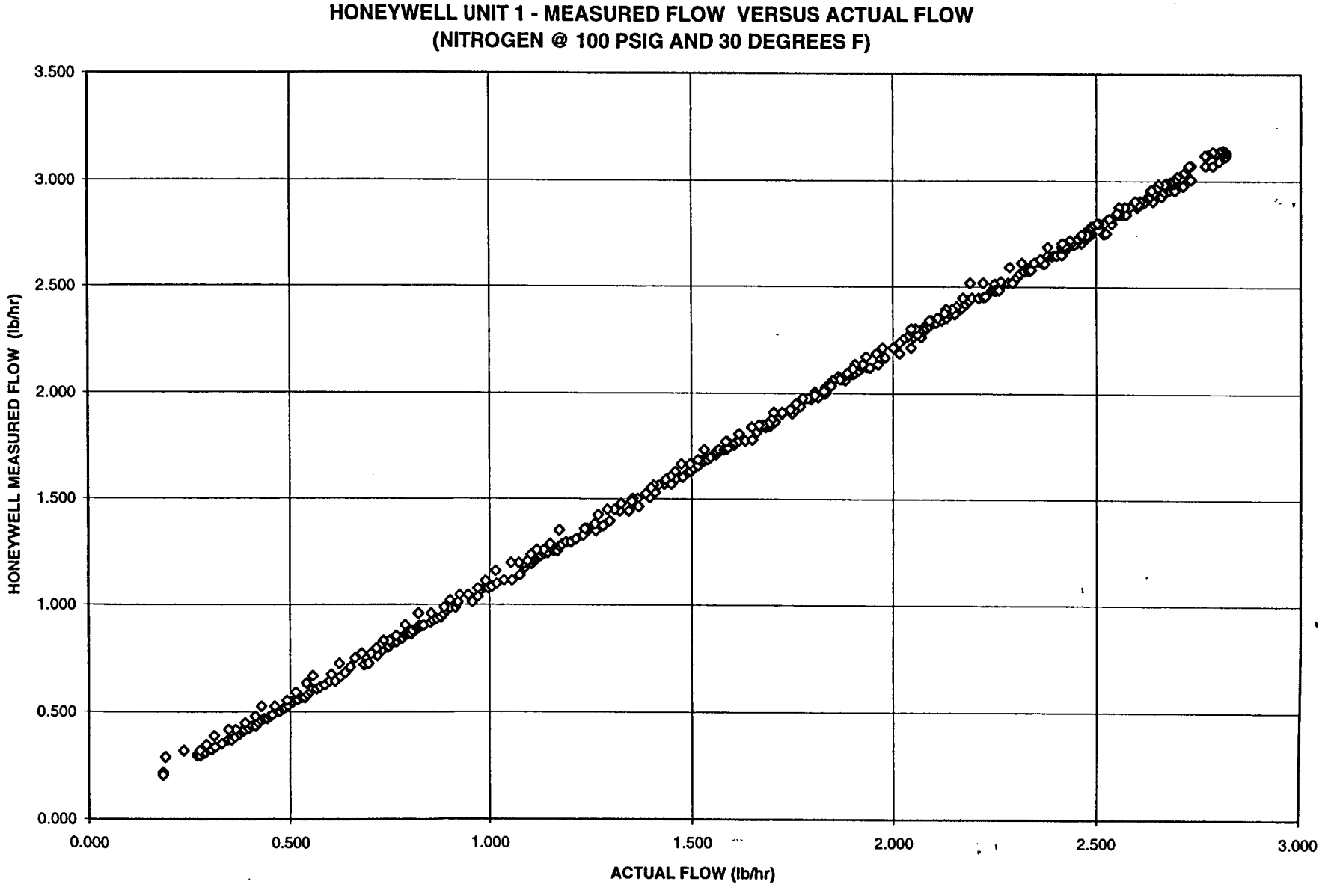
HONEYWELL UNIT 1 - MEASURED FLOW VERSUS ACTUAL FLOW
(NITROGEN @ 100 PSIG AND 30 DEGREES F)
HONEYWELL MEASURED FLOW (lb/hr)
3.500
3.000
2.500
2.000
1.500
1.000
0.500
0.000
0.000
0.500
1.000
1.500
2.000
2.500
3.000
ACTUAL FLOW (lb/hr)

Figure 24

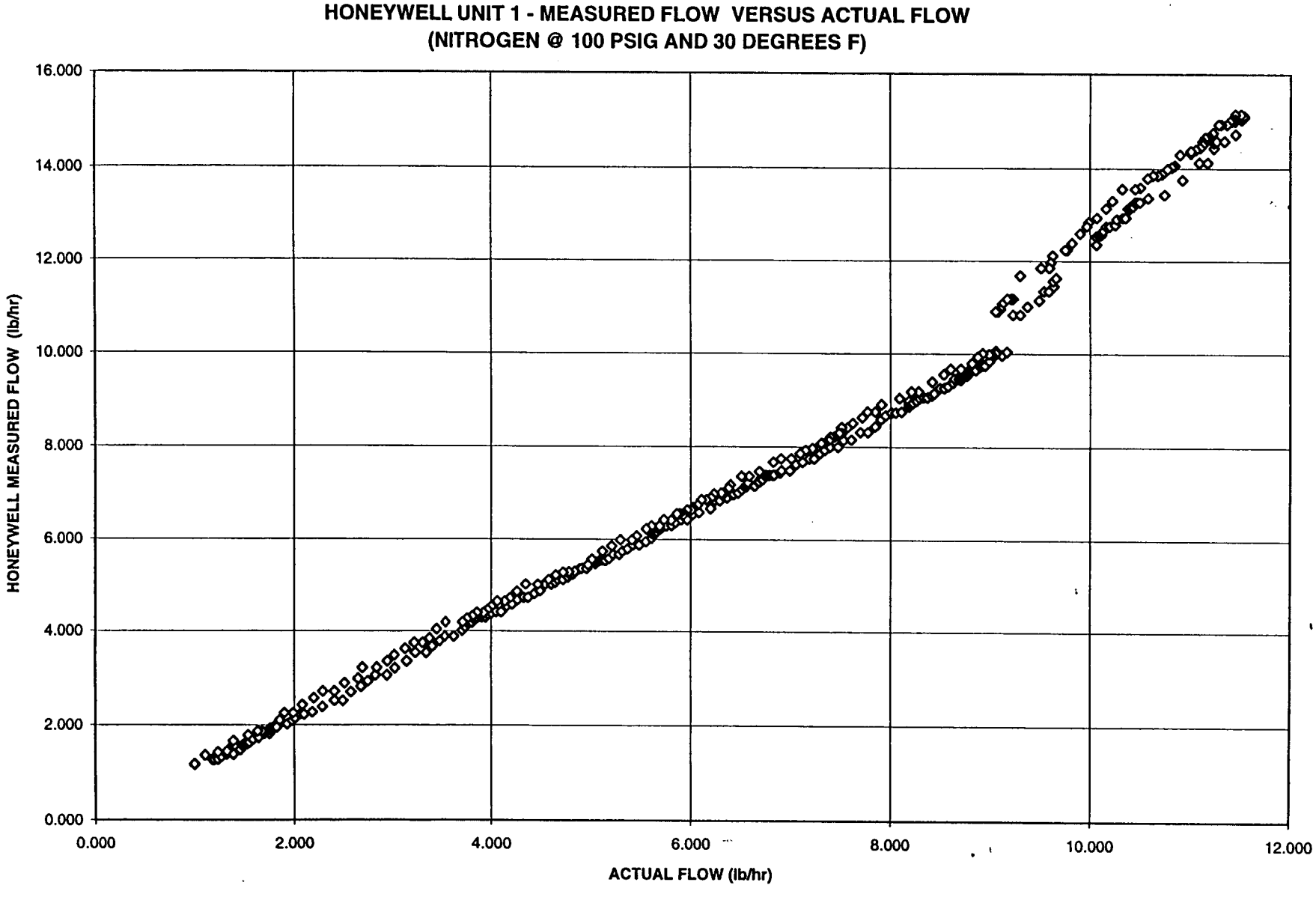
HONEYWELL UNIT 1 - MEASURED FLOW VERSUS ACTUAL FLOW
(NITROGEN @ 100 PSIG AND 30 DEGREES F)
HONEYWELL MEASURED FLOW (lb/hr)
16.000
14.000
12.000
10.000
8.000
6.000
4.000
2.000
0.000
0.000
2.000
4.000
6.000
8.000
10.000
12.000
ACTUAL FLOW (lb/hr)

Figure 25

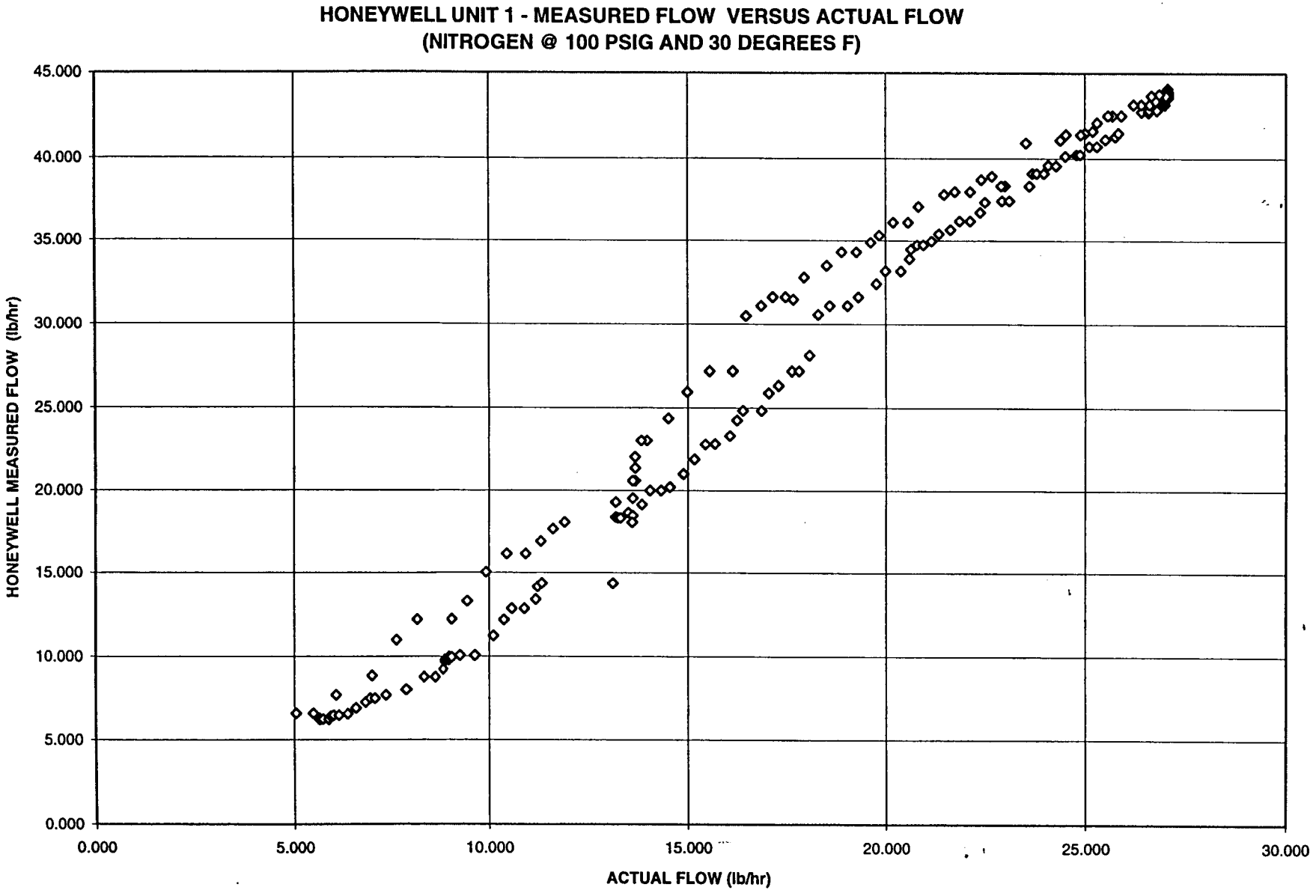
HONEYWELL UNIT 1 - MEASURED FLOW VERSUS ACTUAL FLOW
(NITROGEN @ 100 PSIG AND 30 DEGREES F)
HONEYWELL MEASURED FLOW (lb/hr)
45.000
40.000
35.000
30.000
25.000
20.000
15.000
10.000
5.000
0.000
0.000
5.000
10.000
15.000
20.000
25.000
30.000
ACTUAL FLOW (lb/hr)

Figure 26

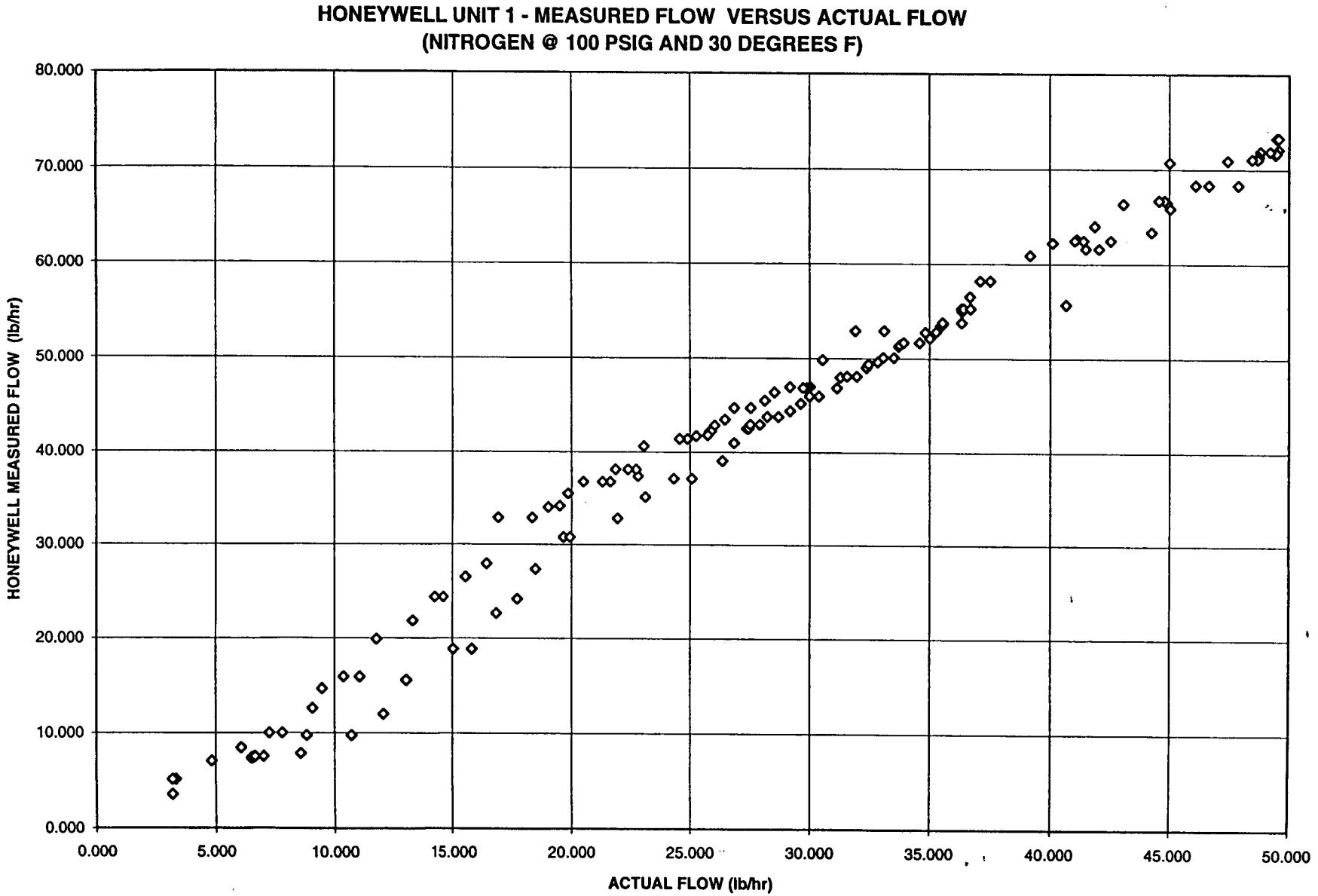
HONEYWELL UNIT 1 - MEASURED FLOW VERSUS ACTUAL FLOW
(NITROGEN @ 100 PSIG AND 30 DEGREES F)
HONEYWELL MEASURED FLOW (lb/hr)
80.000
70.000
60.000
50.000
40.000
30.000
20.000
10.000
0.000
0.000
5.000
10.000
15.000
20.000
25.000
30.000
35.000
40.000
45.000
50.000
ACTUAL FLOW (lb/hr)

Figure 27

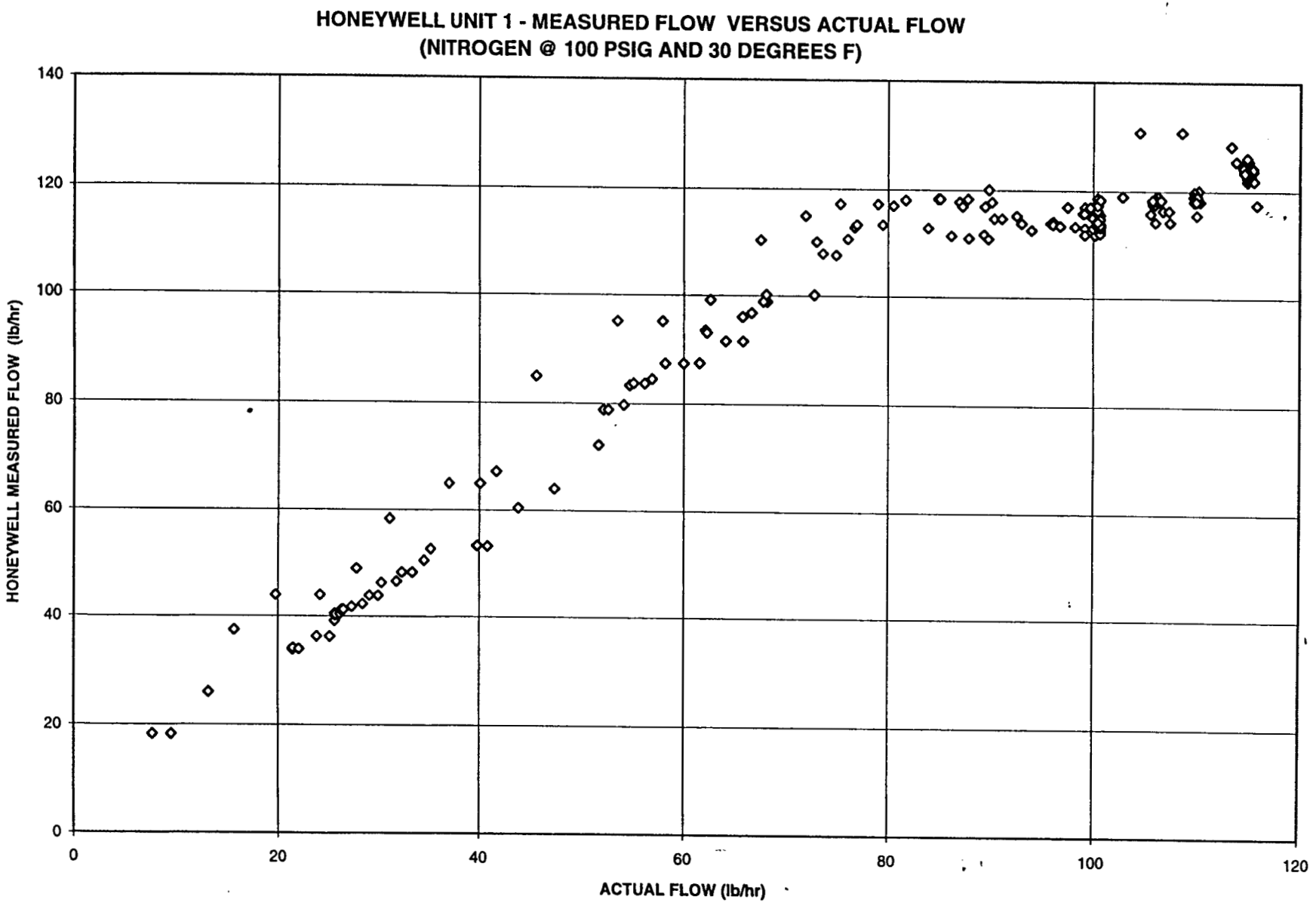
HONEYWELL UNIT 1 - MEASURED FLOW VERSUS ACTUAL FLOW
(NITROGEN @ 100 PSIG AND 30 DEGREES F)
HONEYWELL MEASURED FLOW (lb/hr)
ACTUAL FLOW (lb/hr)
0
20
40
60
80
100
120
140

Figure 28

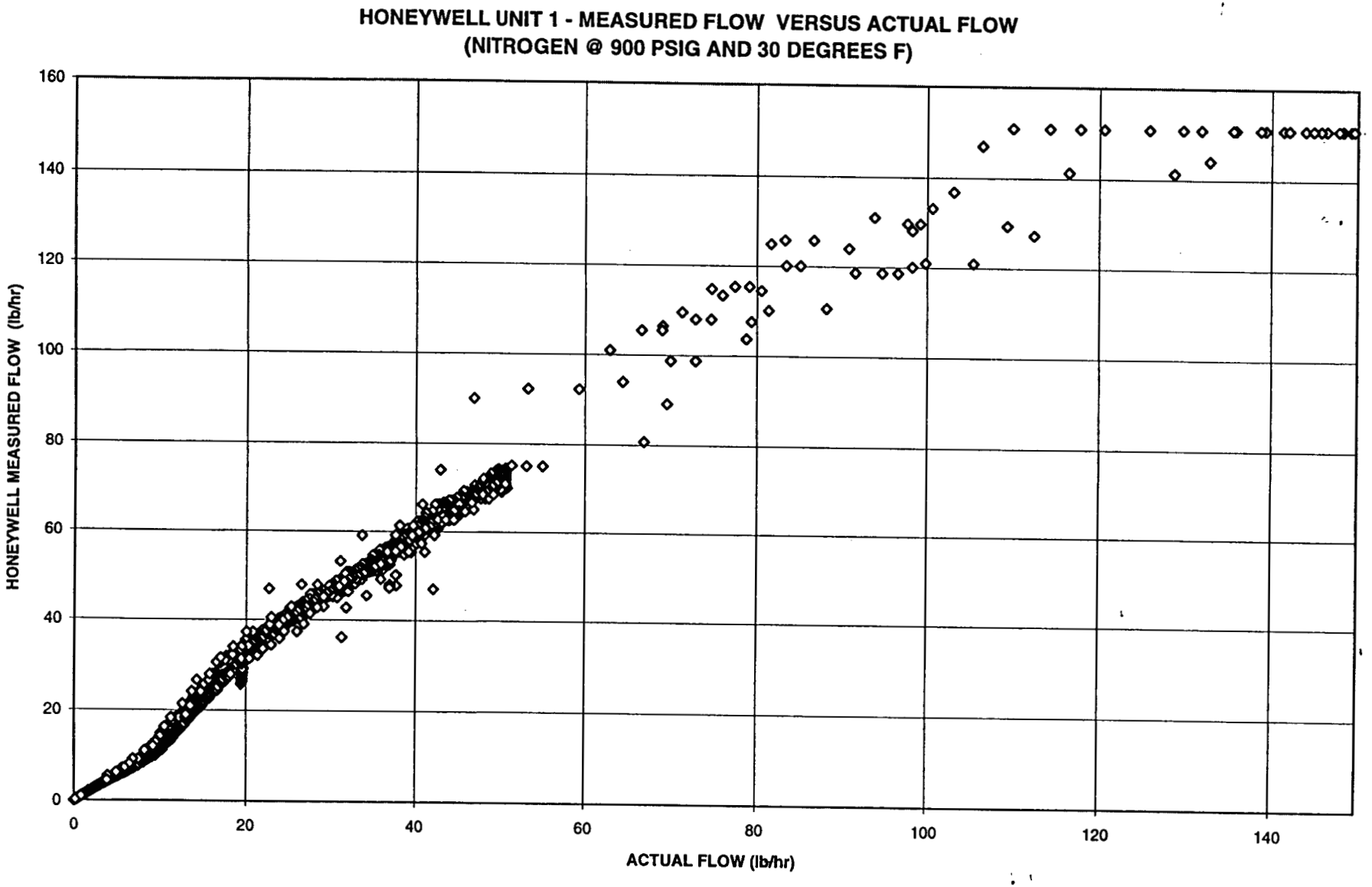
HONEYWELL UNIT 1 - MEASURED FLOW VERSUS ACTUAL FLOW
(NITROGEN @ 900 PSIG AND 30 DEGREES F)
HONEYWELL MEASURED FLOW (lb/hr)
ACTUAL FLOW (lb/hr)
0
20
40
60
80
100
120
140
160

Figure 29

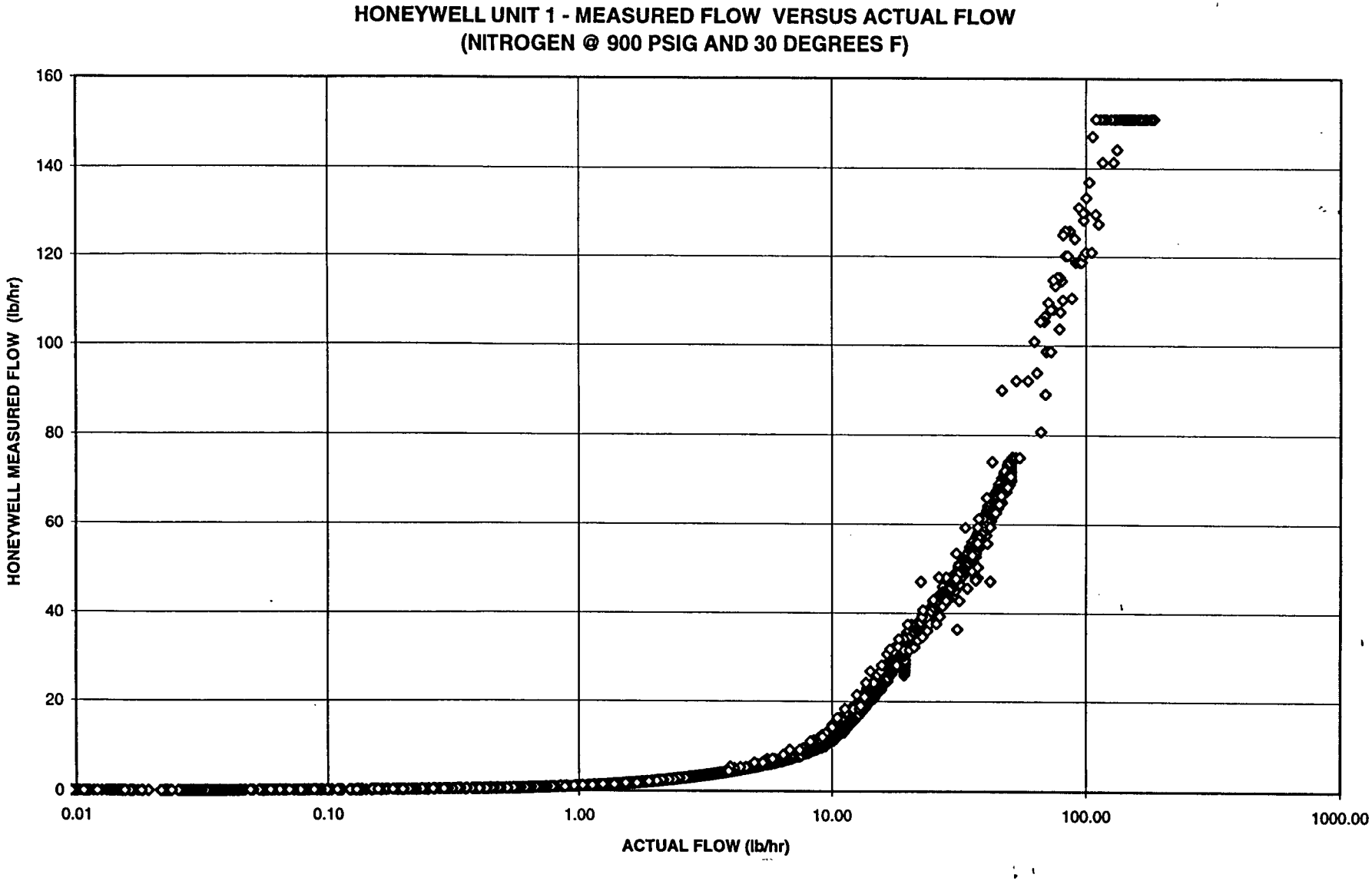
HONEYWELL UNIT 1 - MEASURED FLOW VERSUS ACTUAL FLOW
(NITROGEN @ 900 PSIG AND 30 DEGREES F)
HONEYWELL MEASURED FLOW (lb/hr)
160
140
120
100
80
60
40
20
0
0.01
0.10
1.00
10.00
100.00
1000.00
ACTUAL FLOW (lb/hr)

Figure 30

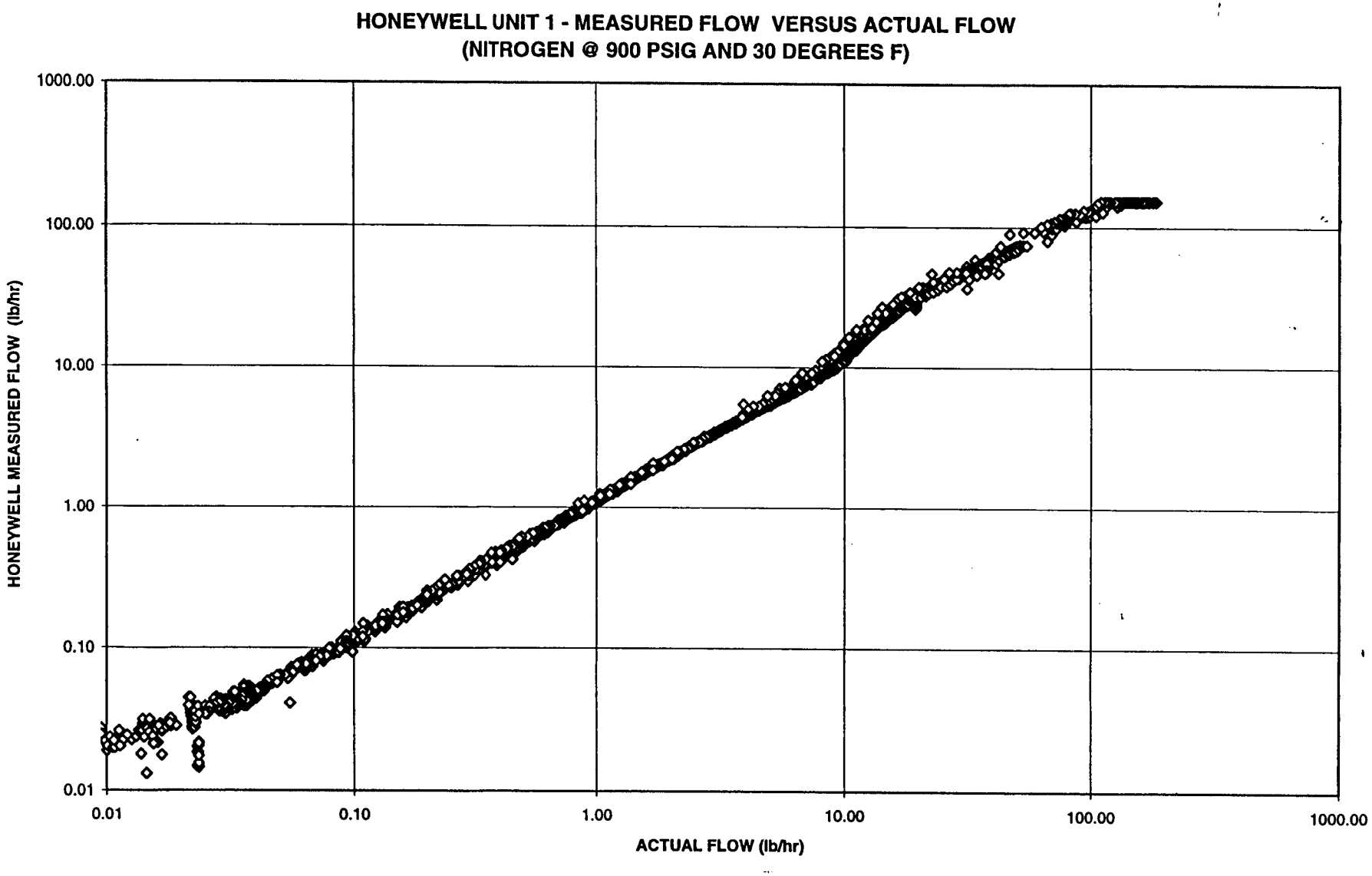
HONEYWELL UNIT 1 - MEASURED FLOW VERSUS ACTUAL FLOW
(NITROGEN @ 900 PSIG AND 30 DEGREES F)
HONEYWELL MEASURED FLOW (lb/hr)
1000.00
100.00
10.00
1.00
0.10
0.01
0.01
0.10
1.00
10.00
100.00
1000.00
ACTUAL FLOW (lb/hr)

Figure 31

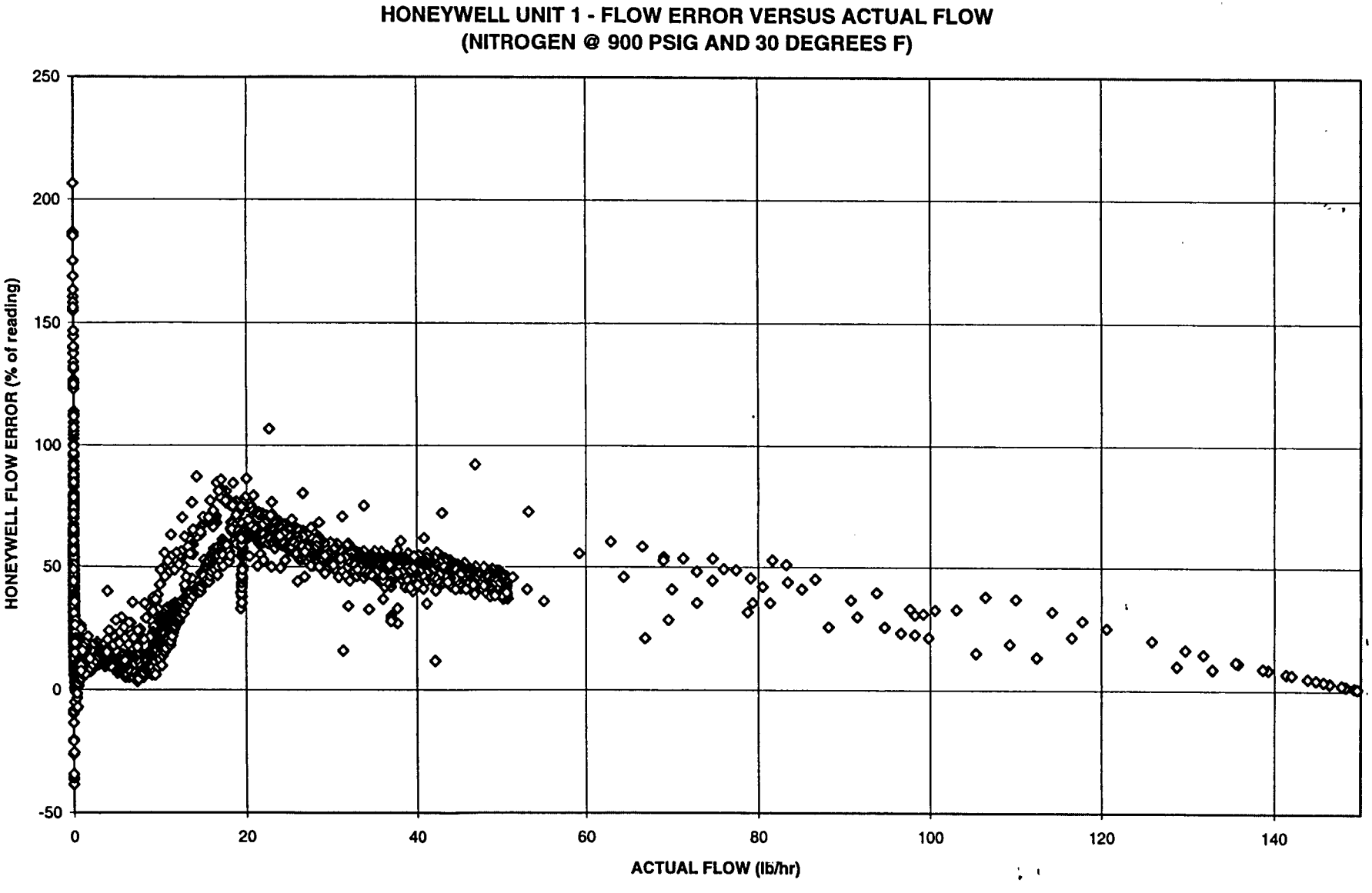
HONEYWELL UNIT 1 - FLOW ERROR VERSUS ACTUAL FLOW
(NITROGEN @ 900 PSIG AND 30 DEGREES F)
HONEYWELL FLOW ERROR (% of reading)
250
200
150
100
50
0
-50
0
20
40
60
80
100
120
140
ACTUAL FLOW (lb/hr)

Figure 32

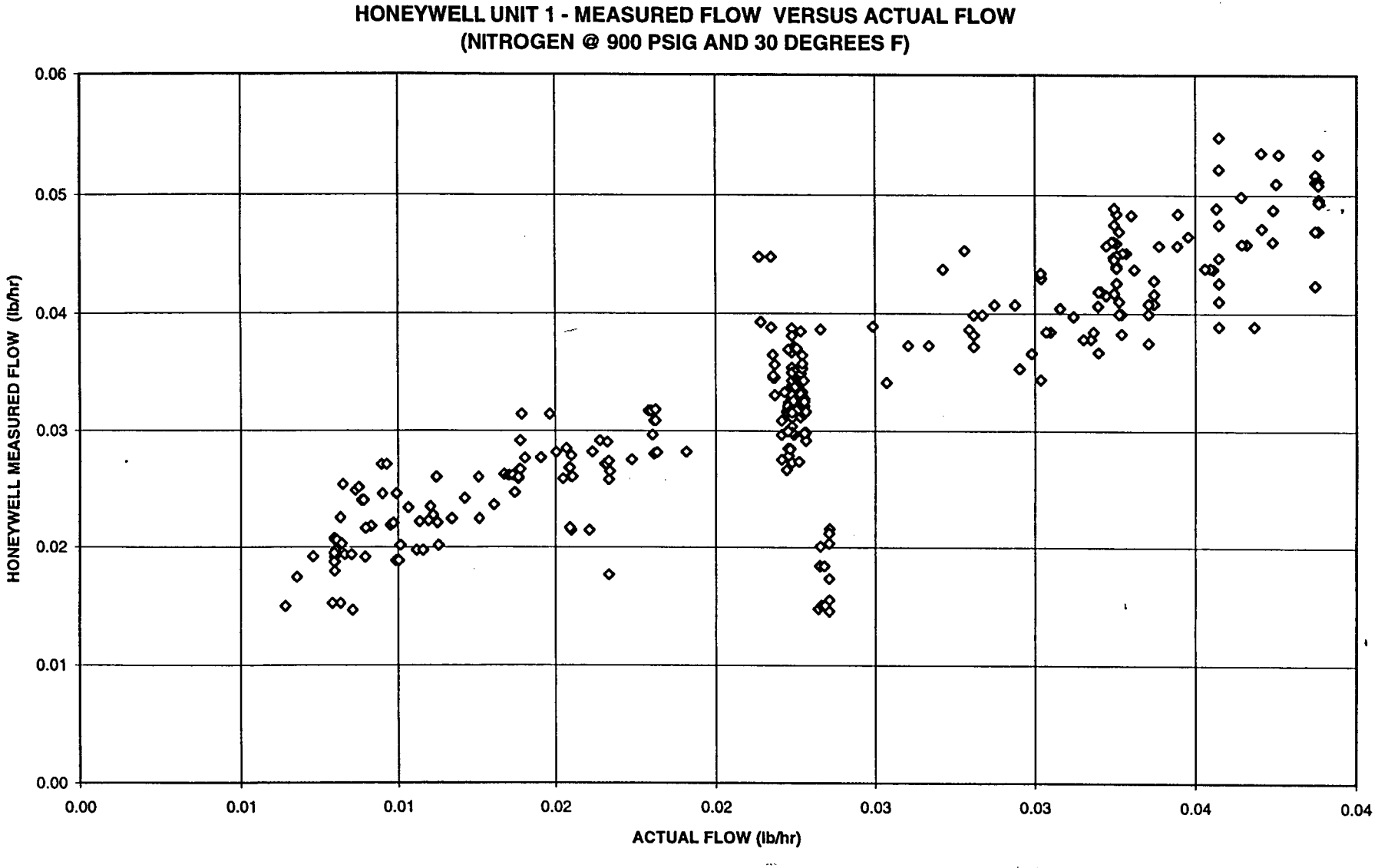
HONEYWELL UNIT 1 - MEASURED FLOW VERSUS ACTUAL FLOW
(NITROGEN @ 900 PSIG AND 30 DEGREES F)
HONEYWELL MEASURED FLOW (lb/hr)
0.06
0.05
0.04
0.03
0.02
0.01
0.00
0.00
0.01
0.01
0.02
0.02
0.03
0.03
0.04
0.04
ACTUAL FLOW (lb/hr)

Figure 33

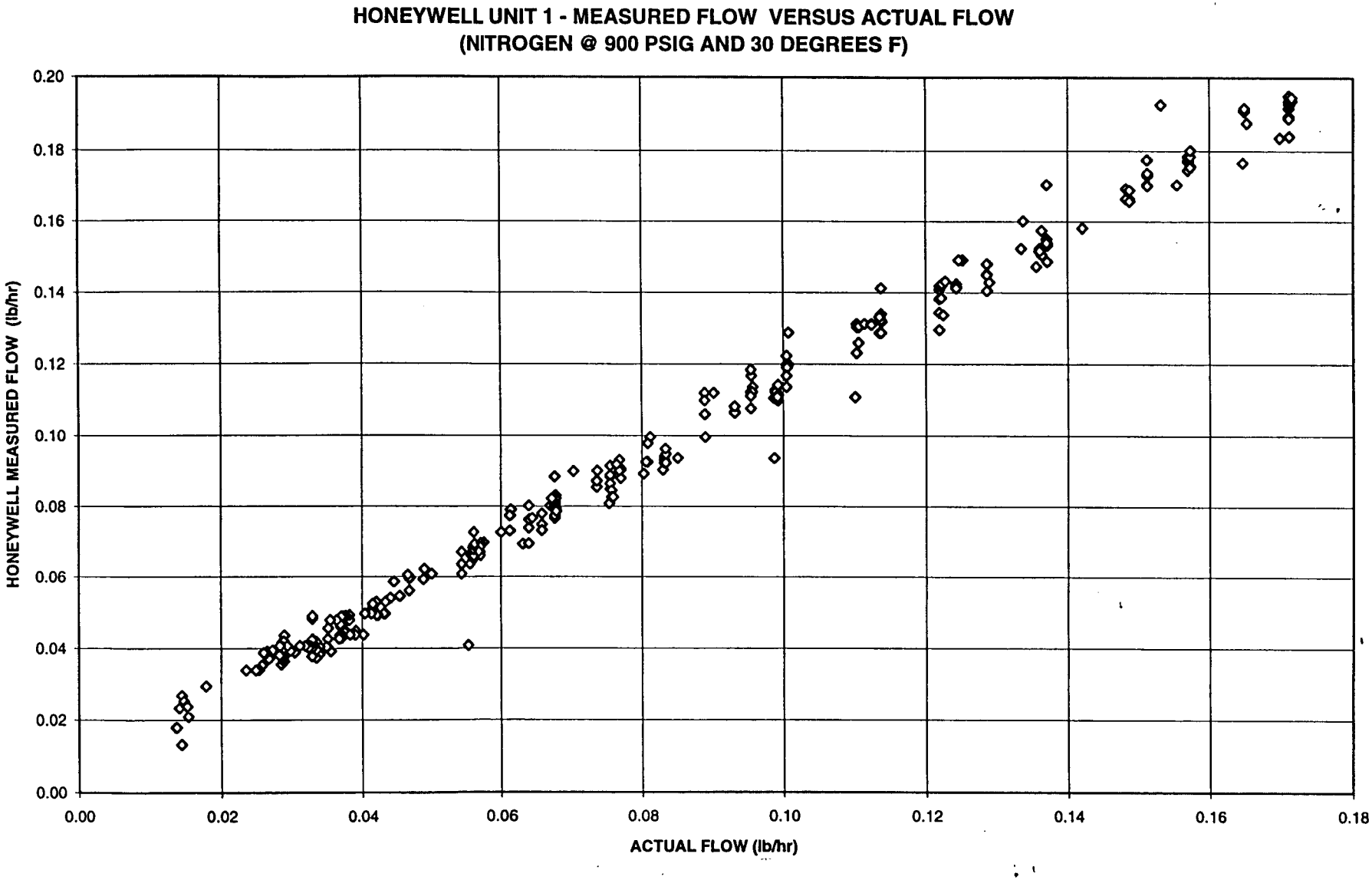
HONEYWELL UNIT 1 - MEASURED FLOW VERSUS ACTUAL FLOW
(NITROGEN @ 900 PSIG AND 30 DEGREES F)
HONEYWELL MEASURED FLOW (lb/hr)
0.20
0.18
0.16
0.14
0.12
0.10
0.08
0.06
0.04
0.02
0.00
0.00
0.02
0.04
0.06
0.08
0.10
0.12
0.14
0.16
0.18
ACTUAL FLOW (lb/hr)

Figure 34

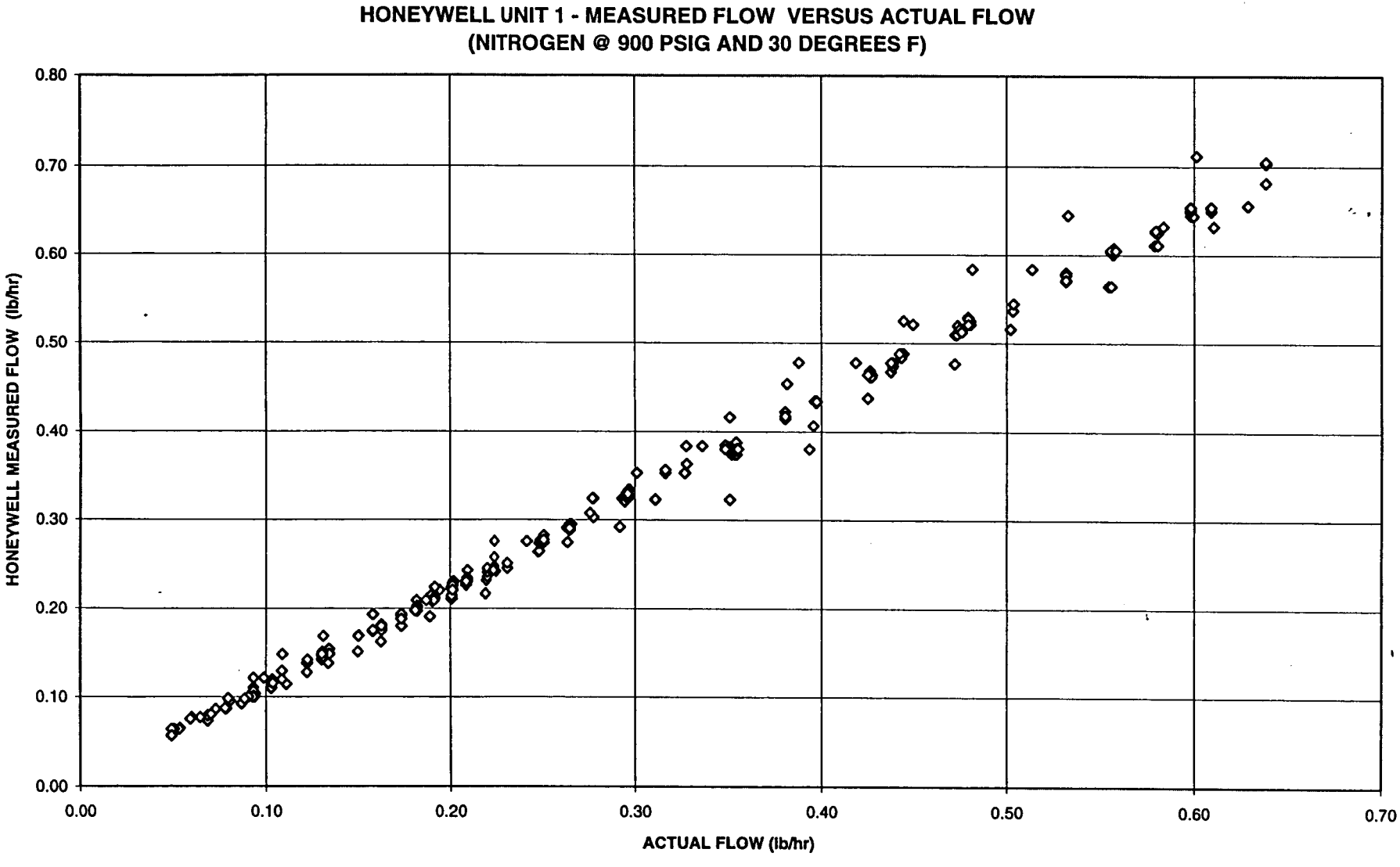
HONEYWELL UNIT 1 - MEASURED FLOW VERSUS ACTUAL FLOW
(NITROGEN @ 900 PSIG AND 30 DEGREES F)
HONEYWELL MEASURED FLOW (lb/hr)
0.80
0.70
0.60
0.50
0.40
0.30
0.20
0.10
0.00
0.00
0.10
0.20
0.30
0.40
0.50
0.60
0.70
ACTUAL FLOW (lb/hr)

Figure 35

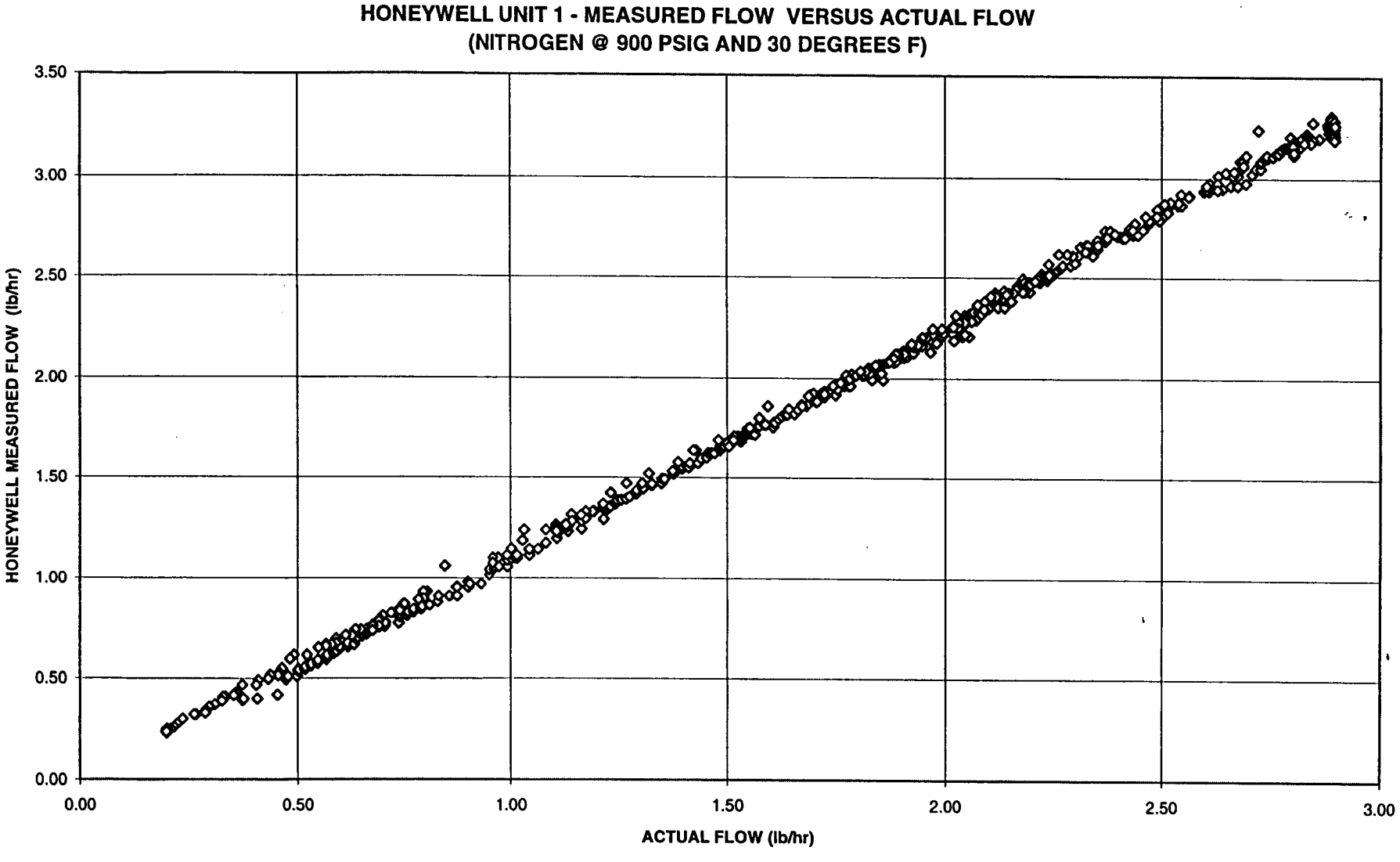
HONEYWELL UNIT 1 - MEASURED FLOW VERSUS ACTUAL FLOW
(NITROGEN @ 900 PSIG AND 30 DEGREES F)
HONEYWELL MEASURED FLOW (lb/hr)
3.50
3.00
2.50
2.00
1.50
1.00
0.50
0.00
0.00
0.50
1.00
1.50
2.00
2.50
3.00
ACTUAL FLOW (lb/hr)

Figure 36

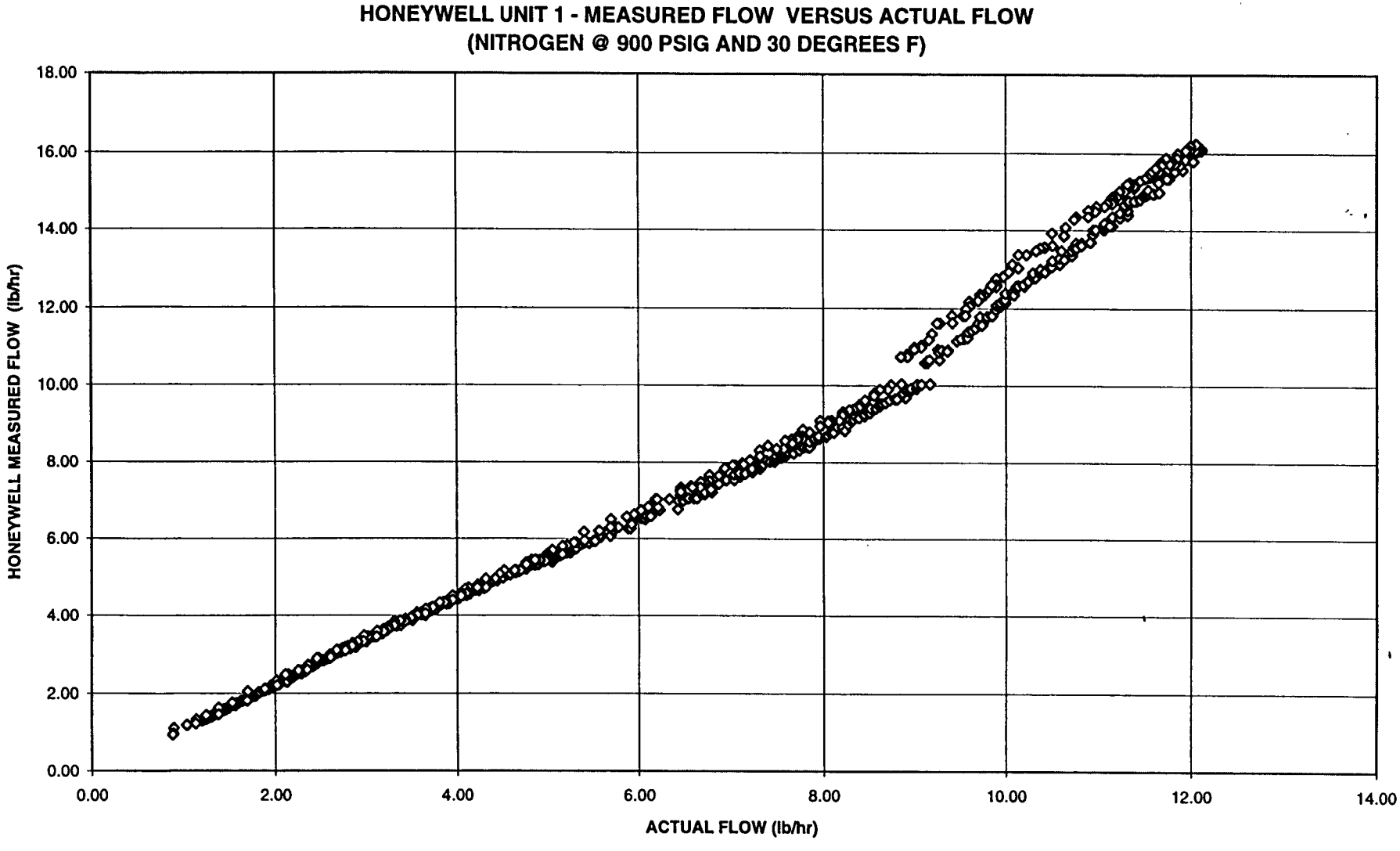
HONEYWELL UNIT 1 - MEASURED FLOW VERSUS ACTUAL FLOW
(NITROGEN @ 900 PSIG AND 30 DEGREES F)
HONEYWELL MEASURED FLOW (lb/hr)
18.00
16.00
14.00
12.00
10.00
8.00
6.00
4.00
2.00
0.00
0.00
2.00
4.00
6.00
8.00
10.00
12.00
14.00
ACTUAL FLOW (lb/hr)

Figure 37

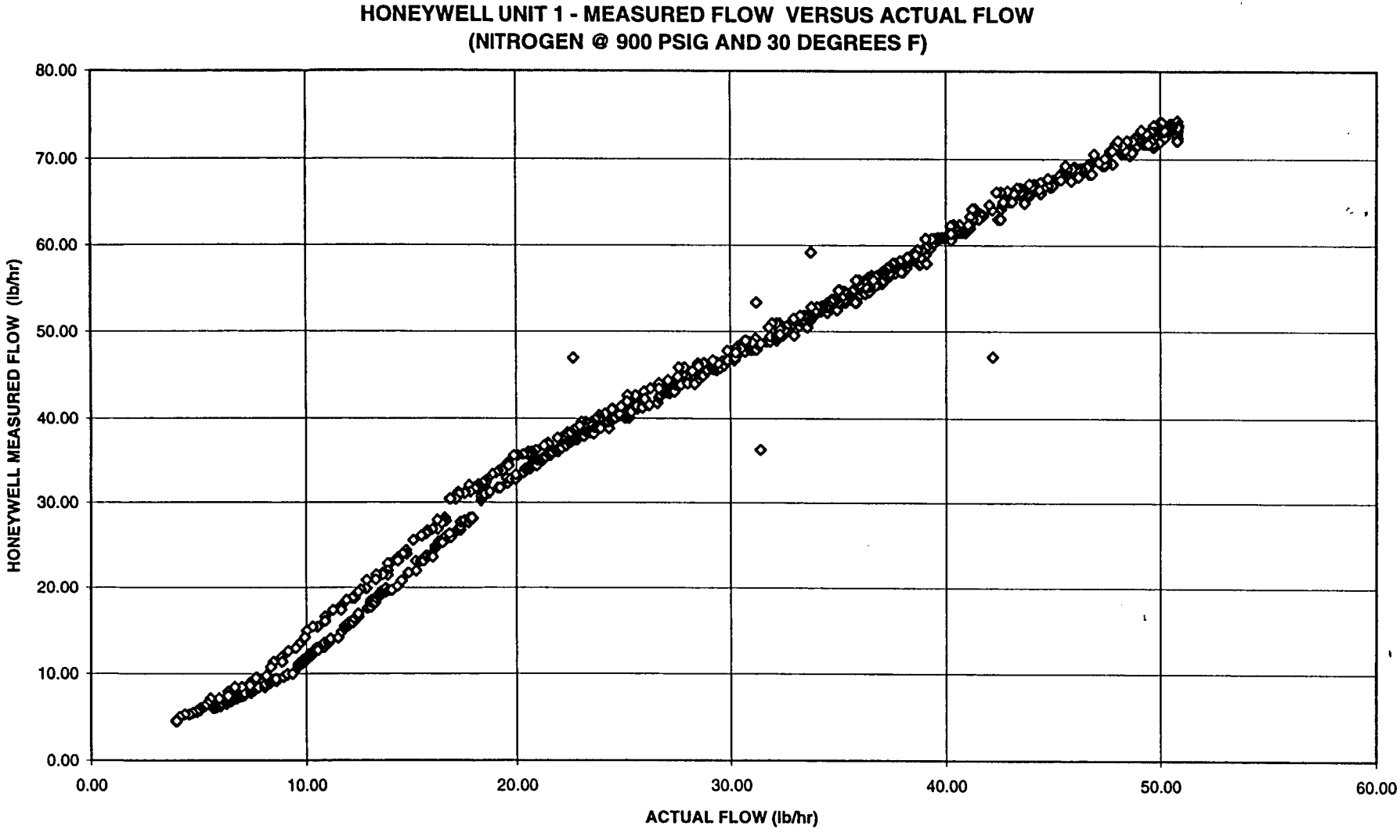
HONEYWELL UNIT 1 - MEASURED FLOW VERSUS ACTUAL FLOW
(NITROGEN @ 900 PSIG AND 30 DEGREES F)
HONEYWELL MEASURED FLOW (lb/hr)
80.00
70.00
60.00
50.00
40.00
30.00
20.00
10.00
0.00
0.00
10.00
20.00
30.00
40.00
50.00
60.00
ACTUAL FLOW (lb/hr)

Figure 38

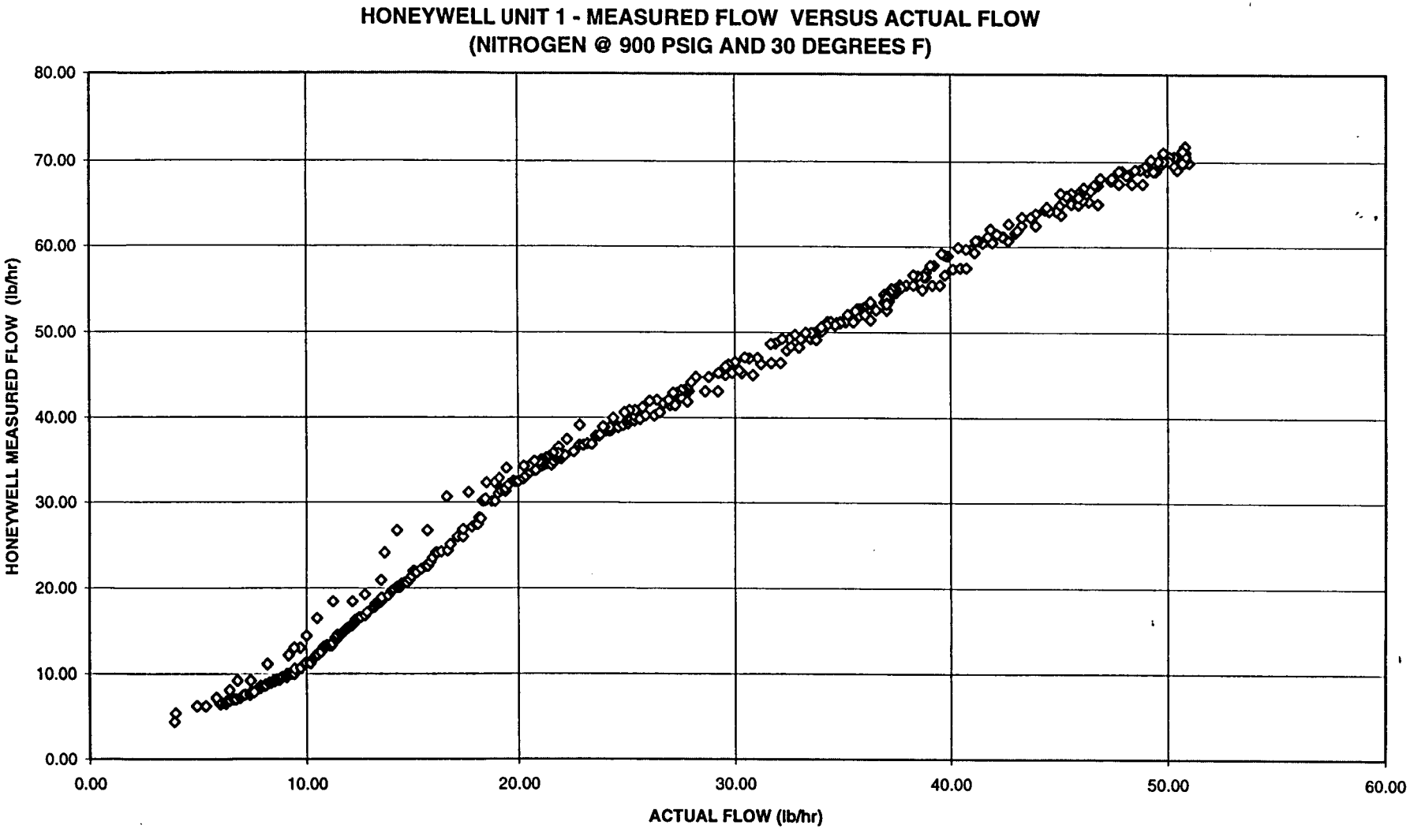
HONEYWELL UNIT 1 - MEASURED FLOW VERSUS ACTUAL FLOW
(NITROGEN @ 900 PSIG AND 30 DEGREES F)
HONEYWELL MEASURED FLOW (lb/hr)
80.00
70.00
60.00
50.00
40.00
30.00
20.00
10.00
0.00
0.00
10.00
20.00
30.00
40.00
50.00
60.00
ACTUAL FLOW (lb/hr)

Figure 39

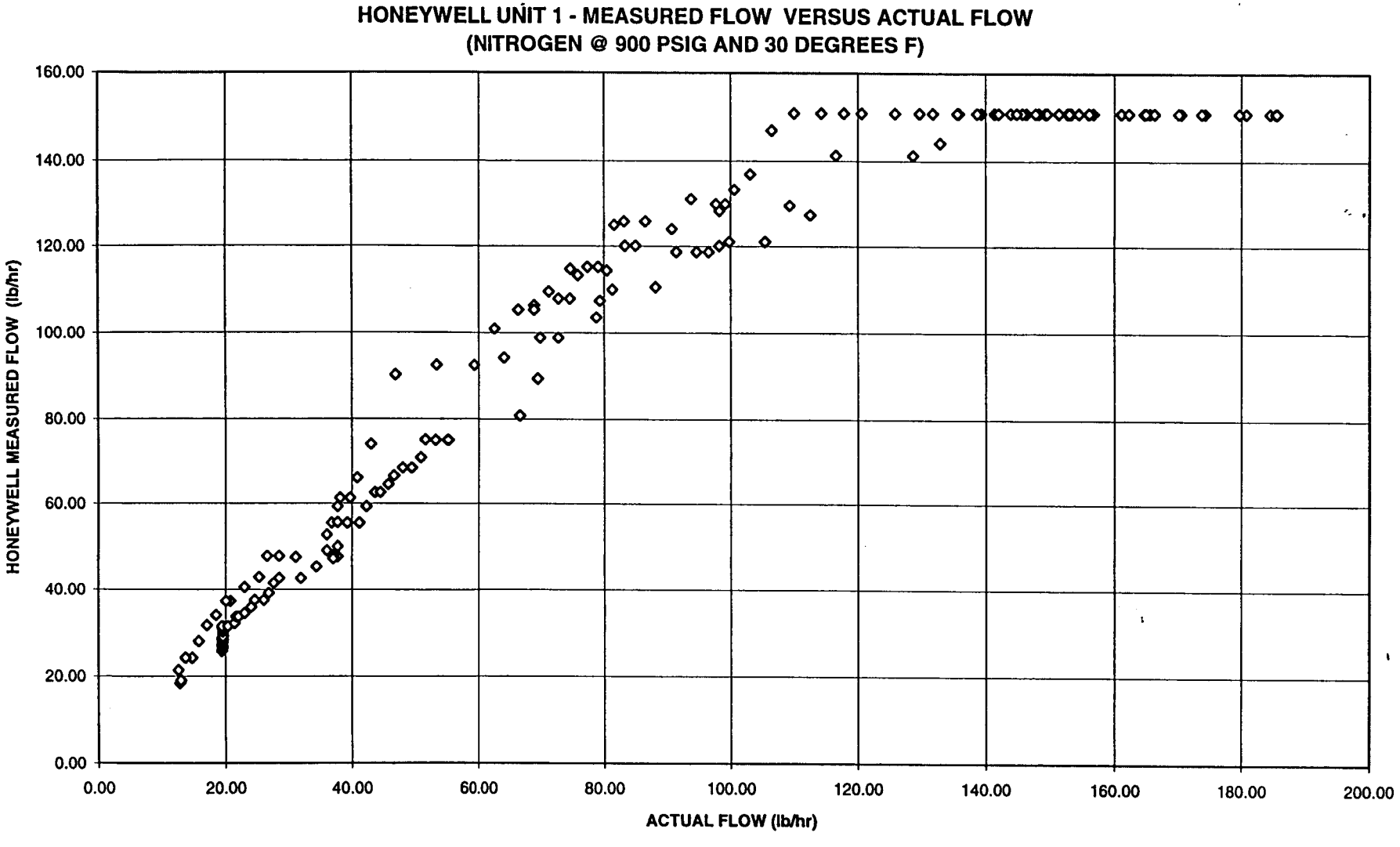
HONEYWELL UNIT 1 - MEASURED FLOW VERSUS ACTUAL FLOW
(NITROGEN @ 900 PSIG AND 30 DEGREES F)
HONEYWELL MEASURED FLOW (lb/hr)
160.00
140.00
120.00
100.00
80.00
60.00
40.00
20.00
0.00
0.00
20.00
40.00
60.00
80.00
100.00
120.00
140.00
160.00
180.00
200.00
ACTUAL FLOW (lb/hr)

Figure 40

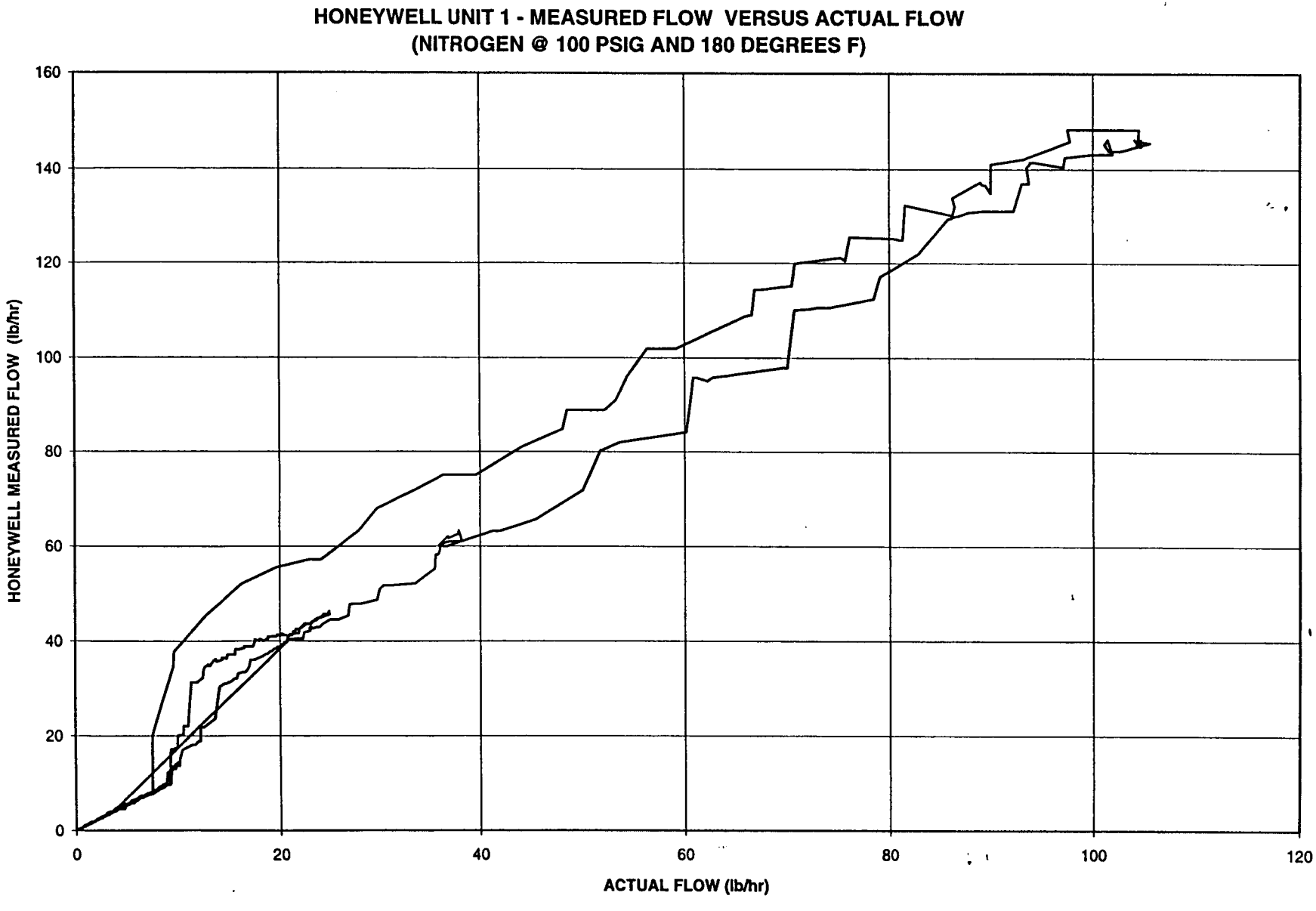
HONEYWELL UNIT 1 - MEASURED FLOW VERSUS ACTUAL FLOW
(NITROGEN @ 100 PSIG AND 180 DEGREES F)
HONEYWELL MEASURED FLOW (lb/hr)
160
140
120
100
80
60
40
20
0
0
20
40
60
80
100
120
ACTUAL FLOW (lb/hr)

Figure 41

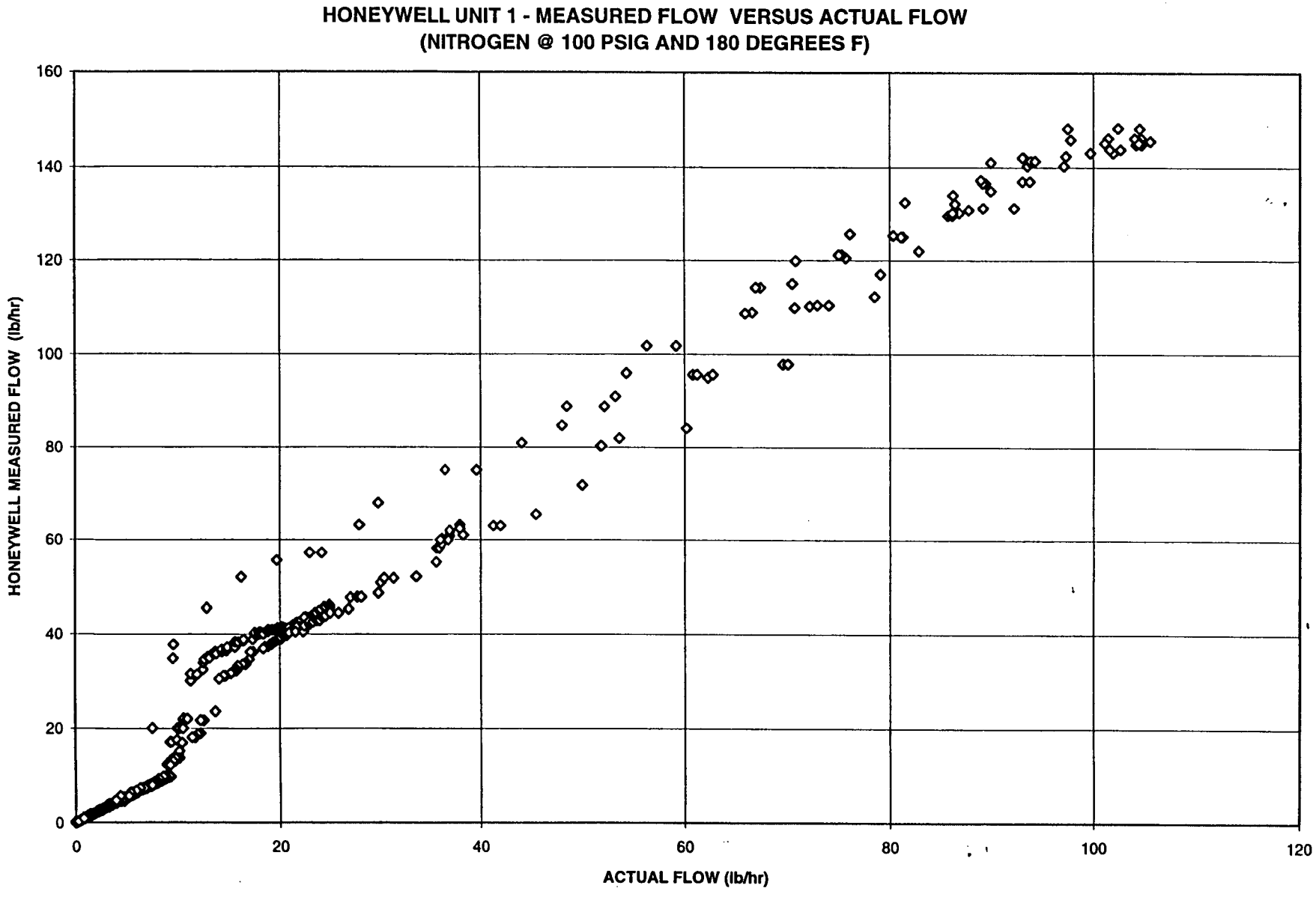
HONEYWELL UNIT 1 - MEASURED FLOW VERSUS ACTUAL FLOW
(NITROGEN @ 100 PSIG AND 180 DEGREES F)
HONEYWELL MEASURED FLOW (lb/hr)
ACTUAL FLOW (lb/hr)
0
20
40
60
80
100
120
140
160

Figure 42

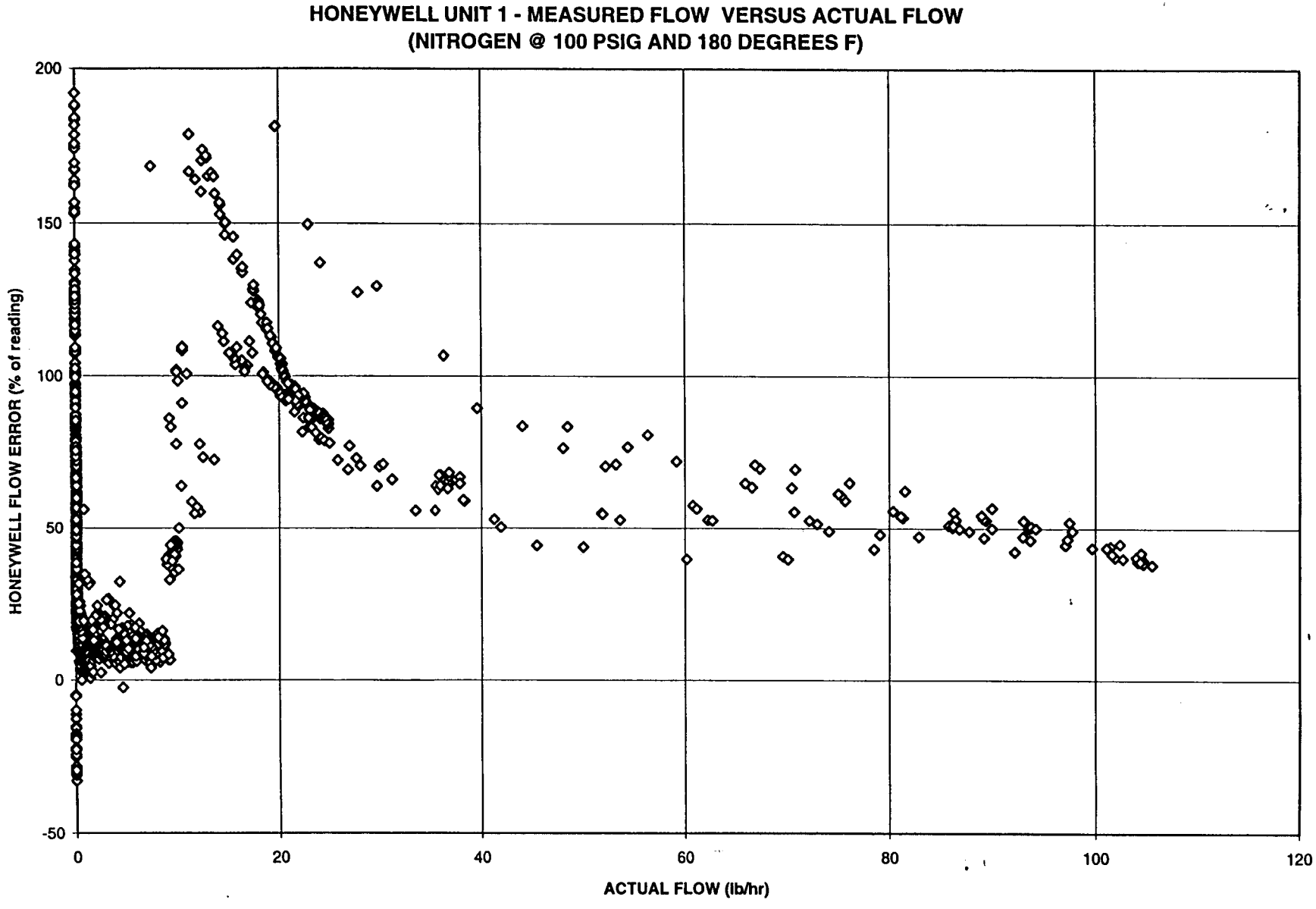
HONEYWELL UNIT 1 - MEASURED FLOW VERSUS ACTUAL FLOW
(NITROGEN @ 100 PSIG AND 180 DEGREES F)
HONEYWELL FLOW ERROR (% of reading)
200
150
100
50
0
-50
0
20
40
60
80
100
120
ACTUAL FLOW (lb/hr)

Figure 43

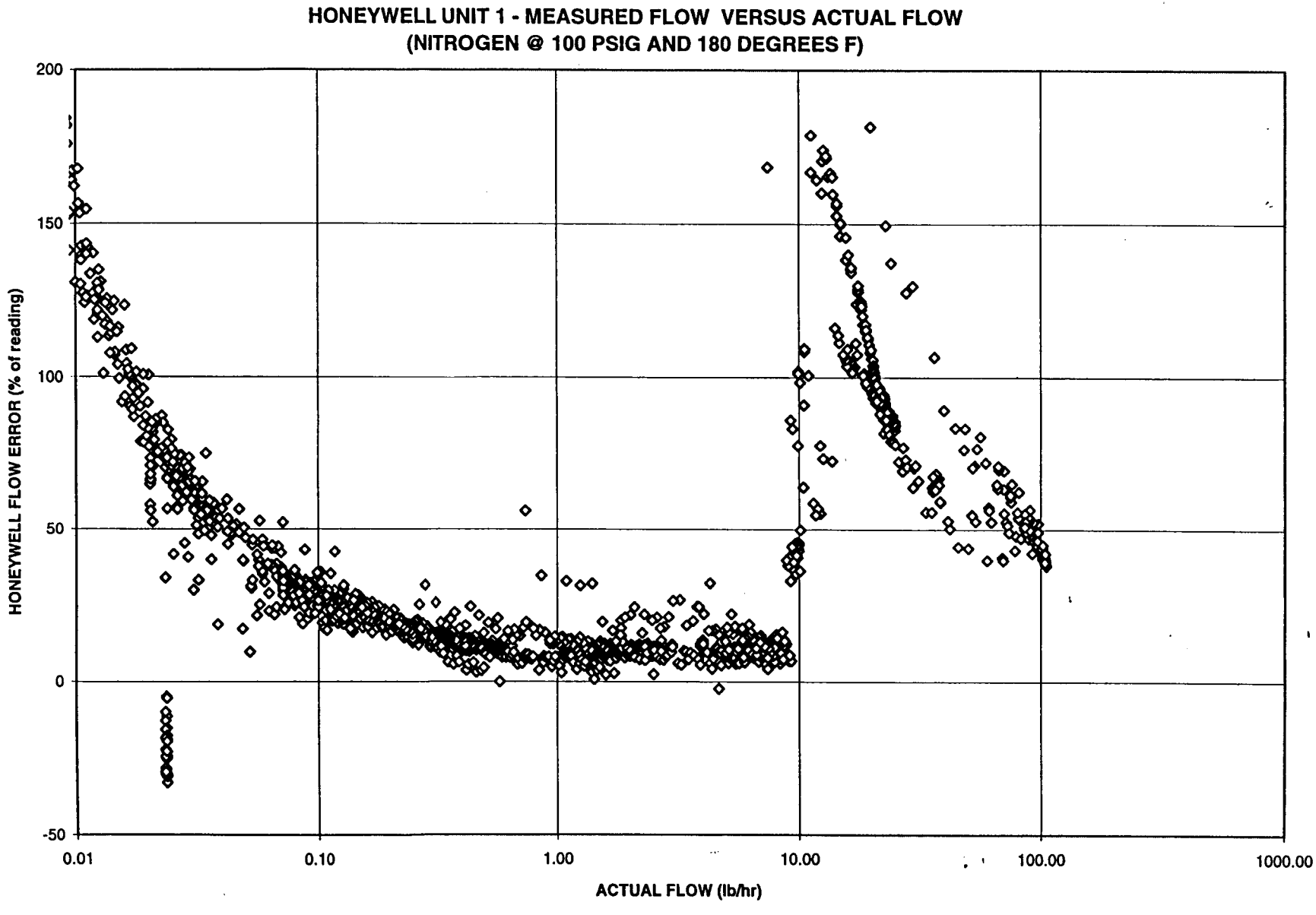
HONEYWELL UNIT 1 - MEASURED FLOW VERSUS ACTUAL FLOW
(NITROGEN @ 100 PSIG AND 180 DEGREES F)
HONEYWELL FLOW ERROR (% of reading)
200
150
100
50
0
-50
0.01
0.10
1.00
10.00
100.00
1000.00
ACTUAL FLOW (lb/hr)

Figure 44

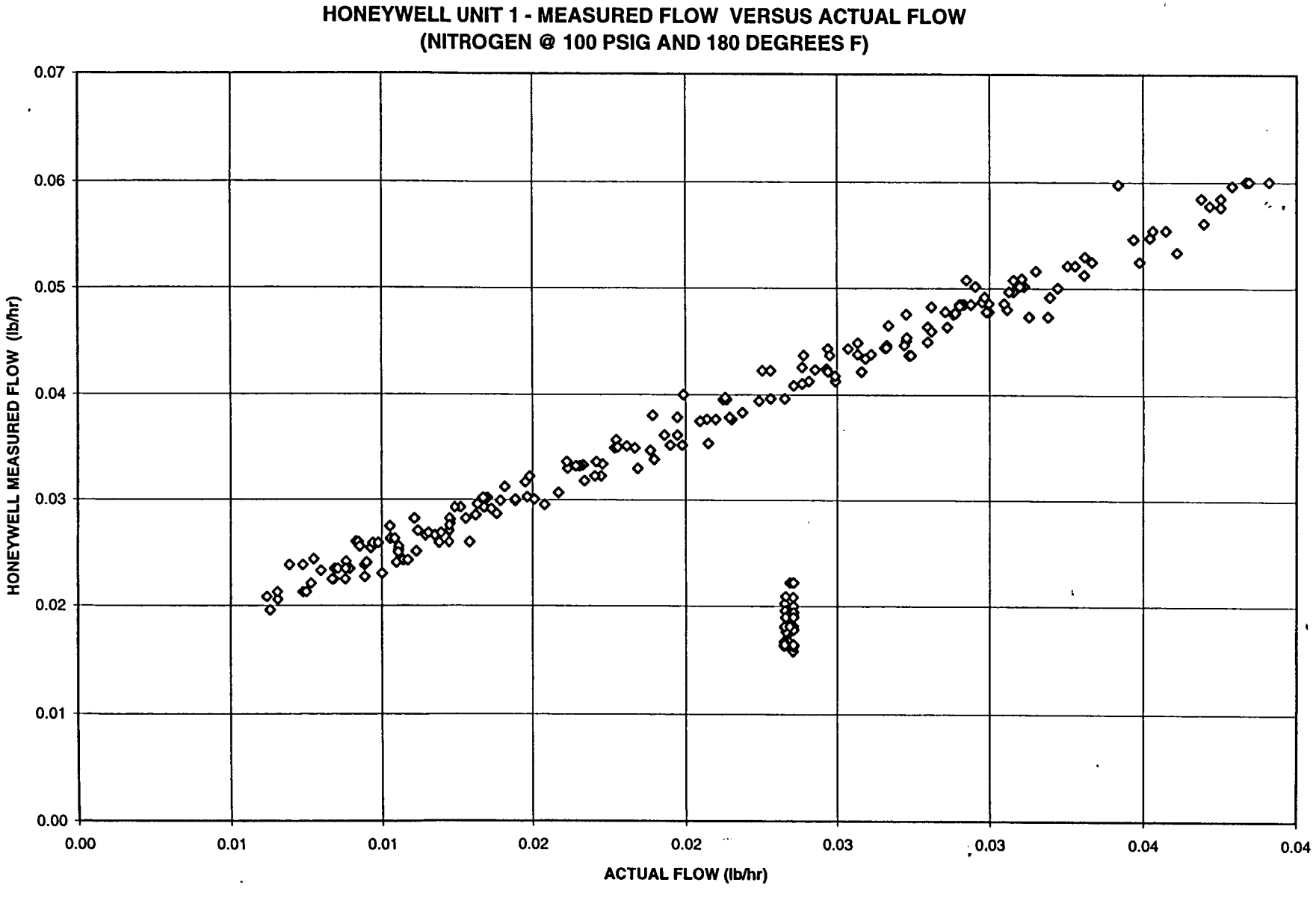
HONEYWELL UNIT 1 - MEASURED FLOW VERSUS ACTUAL FLOW
(NITROGEN @ 100 PSIG AND 180 DEGREES F)
HONEYWELL MEASURED FLOW (lb/hr)
0.07
0.06
0.05
0.04
0.03
0.02
0.01
0.00
0.00
0.01
0.01
0.02
0.02
0.03
0.03
0.04
0.04
ACTUAL FLOW (lb/hr)

Figure 45

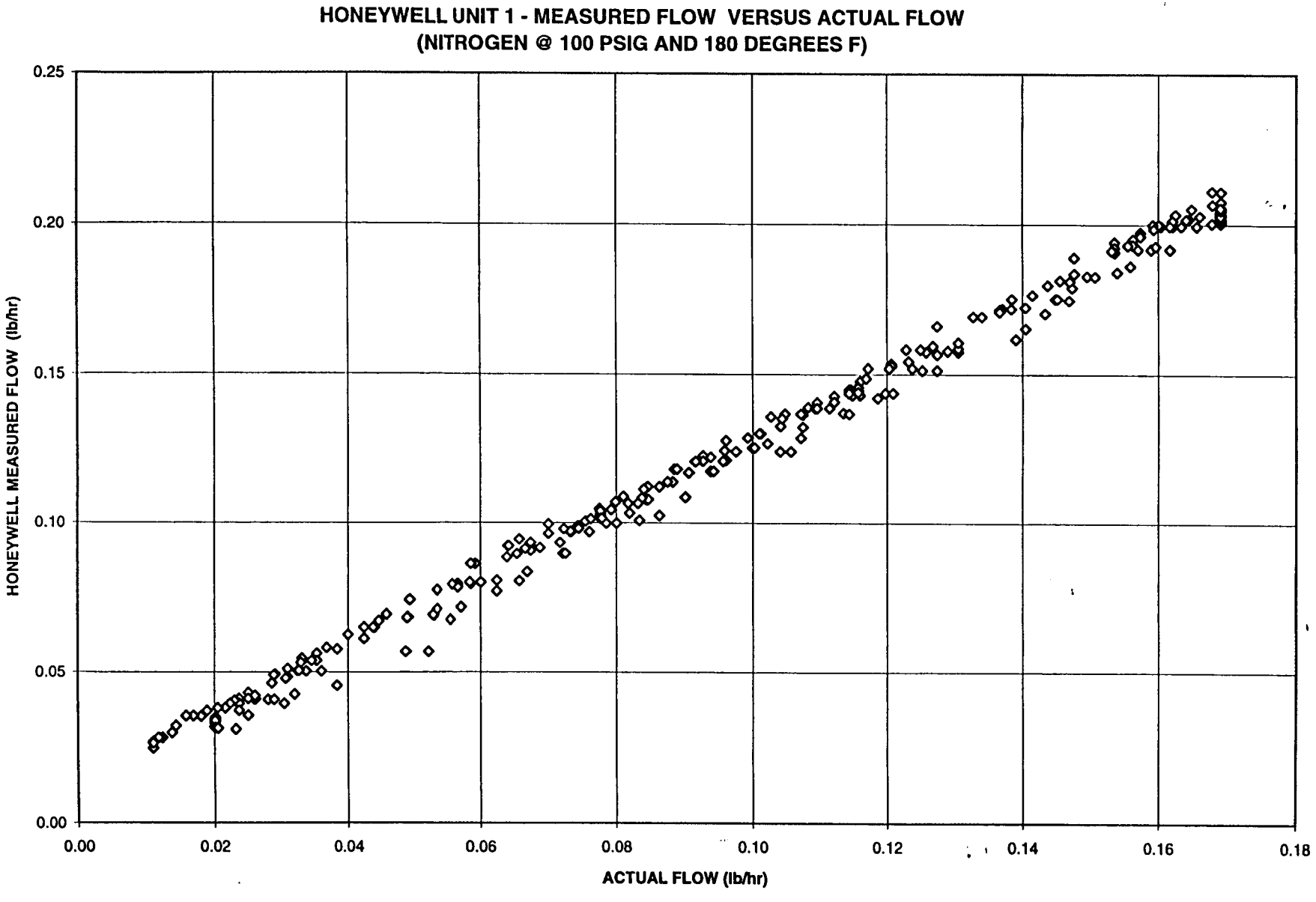
HONEYWELL UNIT 1 - MEASURED FLOW VERSUS ACTUAL FLOW
(NITROGEN @ 100 PSIG AND 180 DEGREES F)
HONEYWELL MEASURED FLOW (lb/hr)
0.25
0.20
0.15
0.10
0.05
0.00
0.00
0.02
0.04
0.06
0.08
0.10
0.12
0.14
0.16
0.18
ACTUAL FLOW (lb/hr)

Figure 46

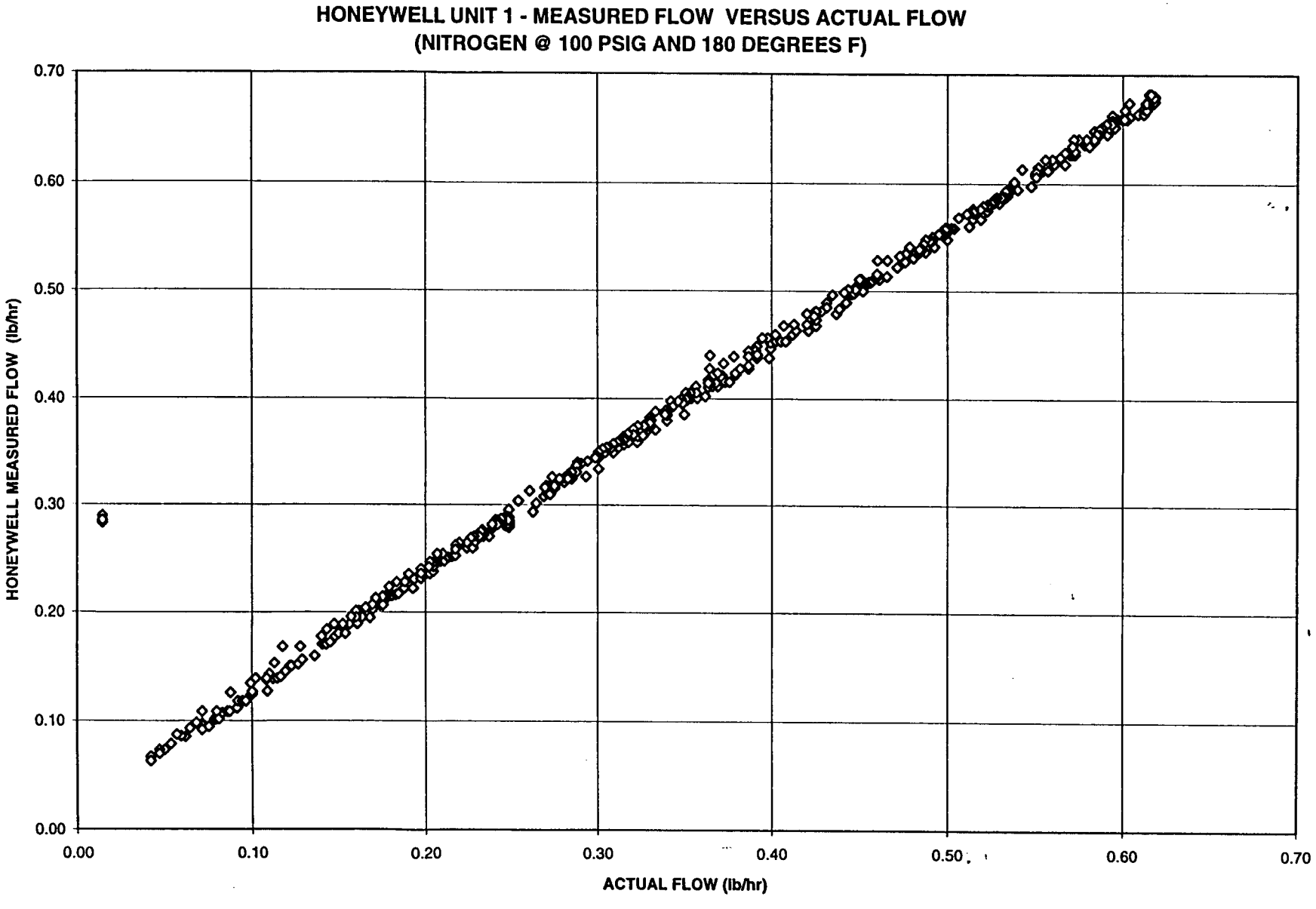
HONEYWELL UNIT 1 - MEASURED FLOW VERSUS ACTUAL FLOW
(NITROGEN @ 100 PSIG AND 180 DEGREES F)
HONEYWELL MEASURED FLOW (lb/hr)
0.70
0.60
0.50
0.40
0.30
0.20
0.10
0.00
0.00
0.10
0.20
0.30
0.40
0.50
0.60
0.70
ACTUAL FLOW (lb/hr)

Figure 47

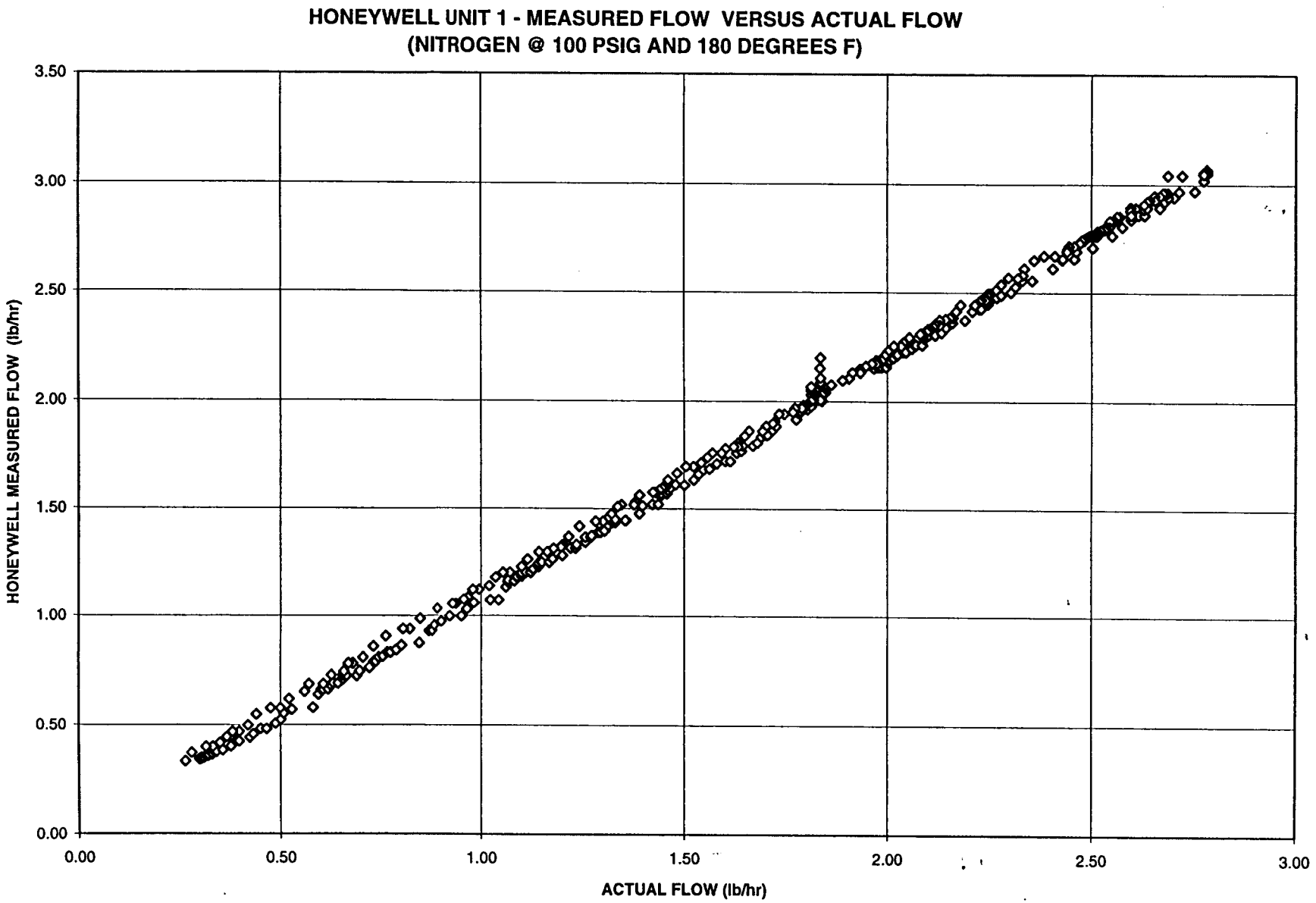
HONEYWELL UNIT 1 - MEASURED FLOW VERSUS ACTUAL FLOW
(NITROGEN @ 100 PSIG AND 180 DEGREES F)
HONEYWELL MEASURED FLOW (lb/hr)
3.50
3.00
2.50
2.00
1.50
1.00
0.50
0.00
0.00
0.50
1.00
1.50
2.00
2.50
3.00
ACTUAL FLOW (lb/hr)

Figure 48

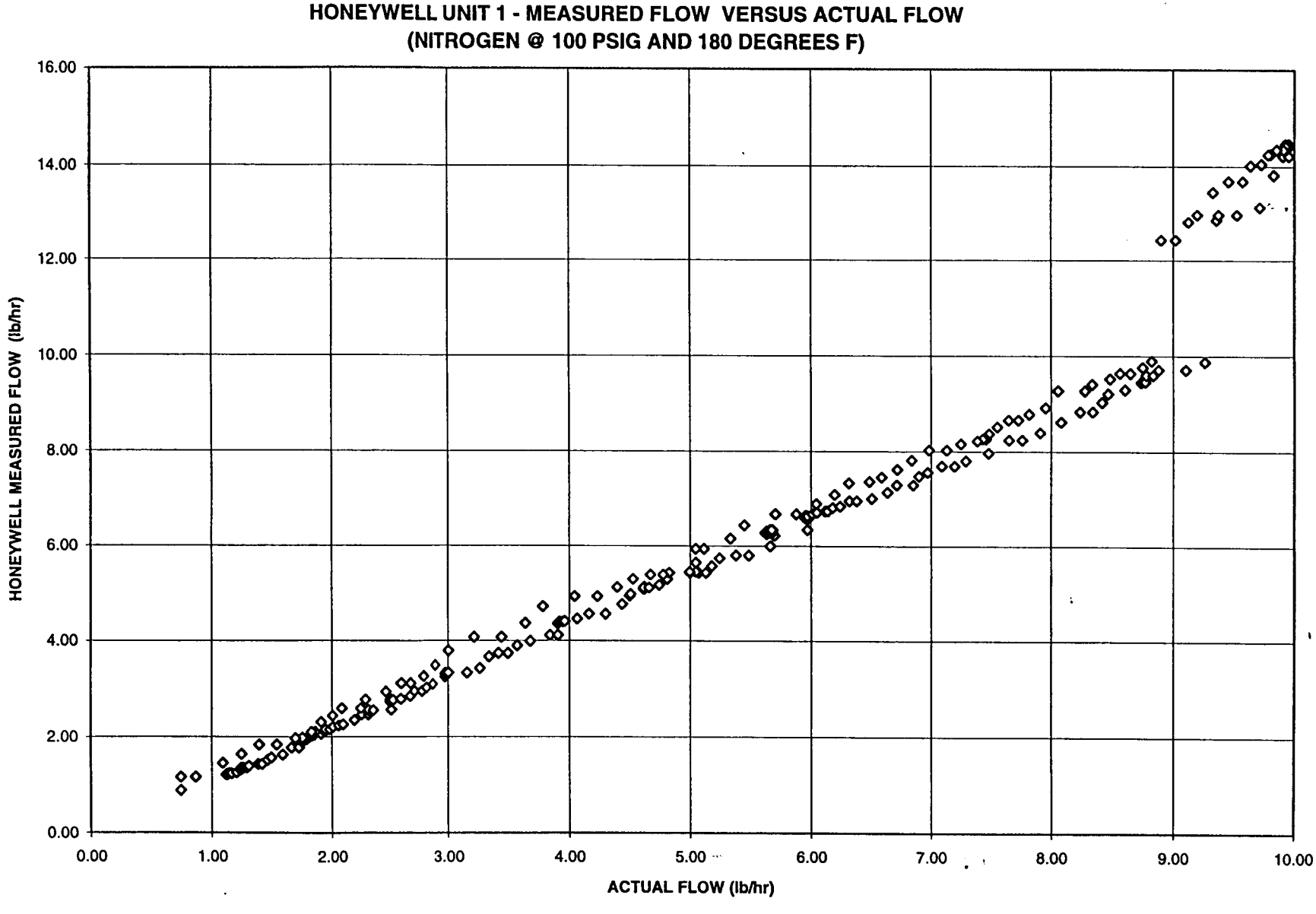
HONEYWELL UNIT 1 - MEASURED FLOW VERSUS ACTUAL FLOW
(NITROGEN @ 100 PSIG AND 180 DEGREES F)
HONEYWELL MEASURED FLOW (lb/hr)
16.00
14.00
12.00
10.00
8.00
6.00
4.00
2.00
0.00
0.00
1.00
2.00
3.00
4.00
5.00
6.00
7.00
8.00
9.00
10.00
ACTUAL FLOW (lb/hr)

Figure 49

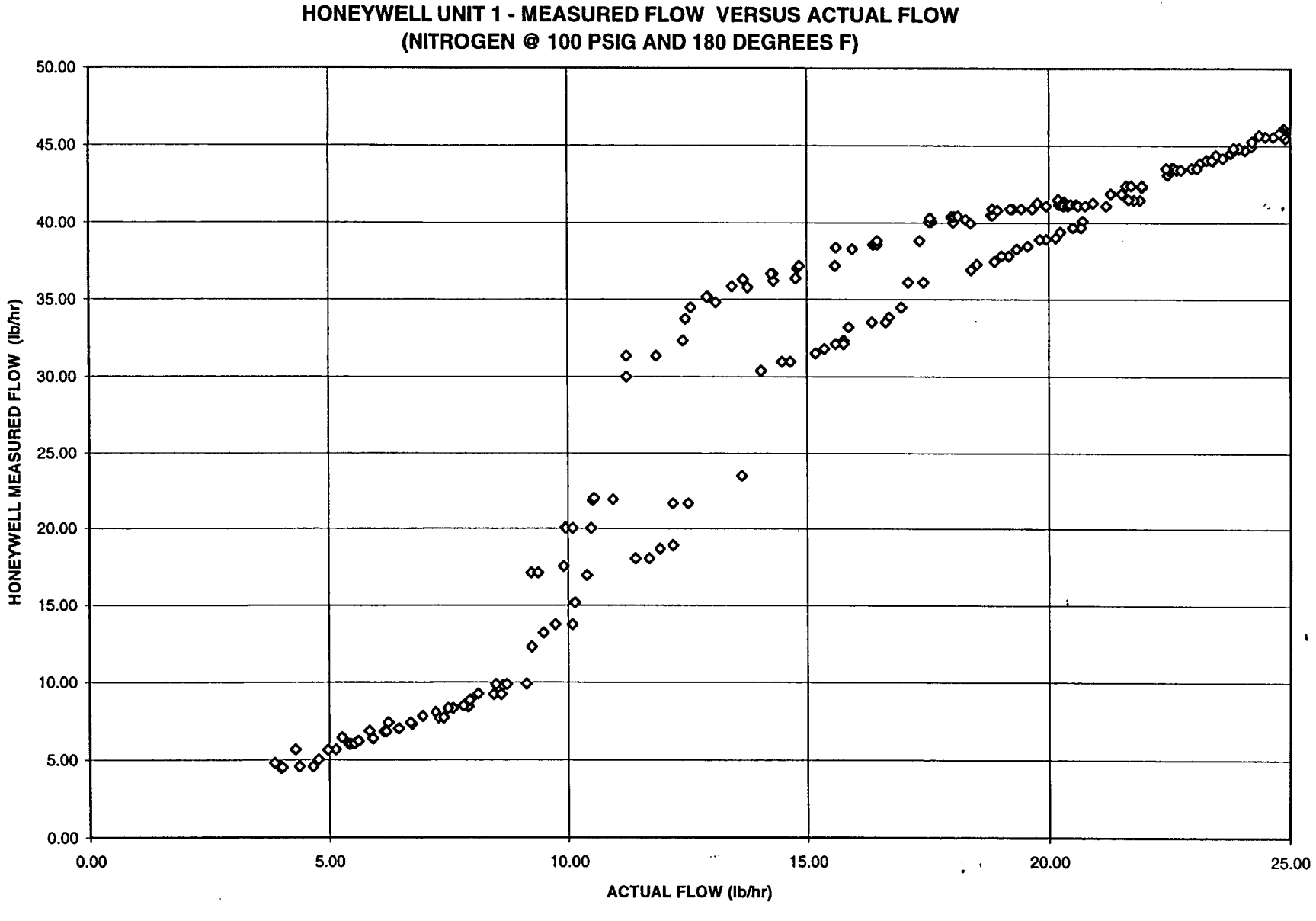
HONEYWELL UNIT 1 - MEASURED FLOW VERSUS ACTUAL FLOW
(NITROGEN @ 100 PSIG AND 180 DEGREES F)
HONEYWELL MEASURED FLOW (lb/hr)
50.00
45.00
40.00
35.00
30.00
25.00
20.00
15.00
10.00
5.00
0.00
0.00
5.00
10.00
15.00
20.00
25.00
ACTUAL FLOW (lb/hr)

Figure 50

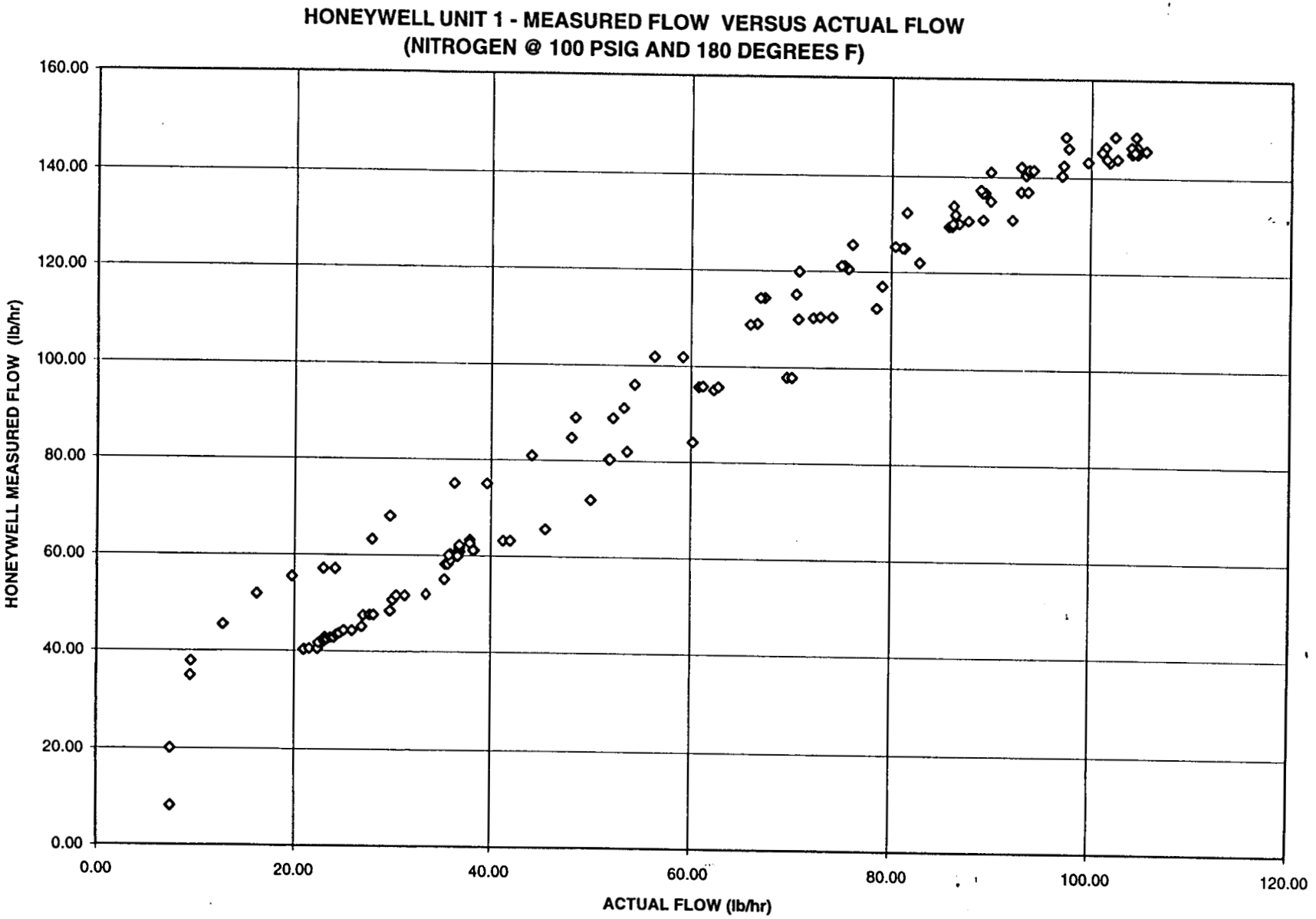
HONEYWELL UNIT 1 - MEASURED FLOW VERSUS ACTUAL FLOW
(NITROGEN @ 100 PSIG AND 180 DEGREES F)
HONEYWELL MEASURED FLOW (lb/hr)
160.00
140.00
120.00
100.00
80.00
60.00
40.00
20.00
0.00
0.00
20.00
40.00
60.00
80.00
100.00
120.00
ACTUAL FLOW (lb/hr)

Figure 51

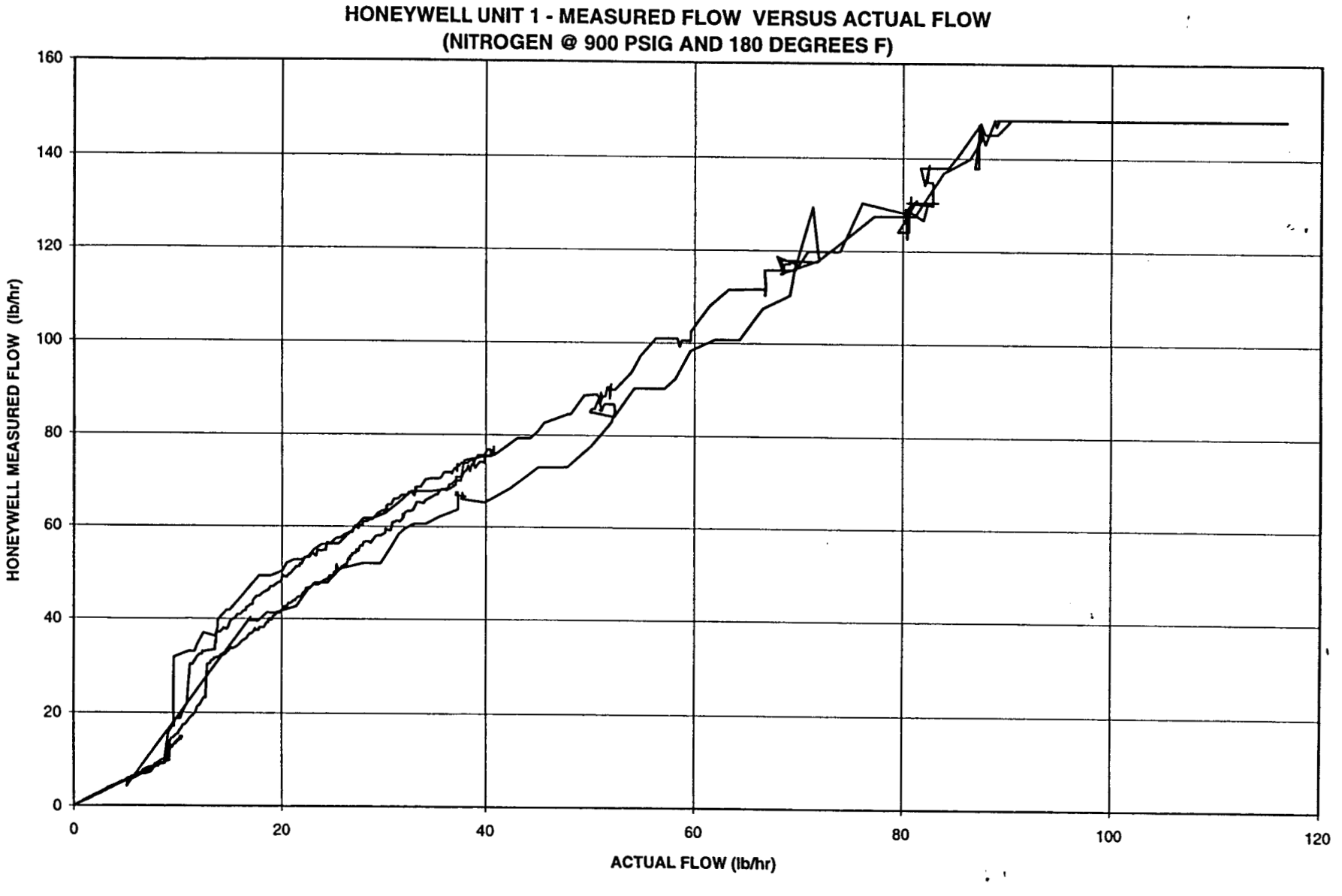
HONEYWELL UNIT 1 - MEASURED FLOW VERSUS ACTUAL FLOW
(NITROGEN @ 900 PSIG AND 180 DEGREES F)
HONEYWELL MEASURED FLOW (lb/hr)
160
140
120
100
80
60
40
20
0
0
20
40
60
80
100
120
ACTUAL FLOW (lb/hr)

Figure 52

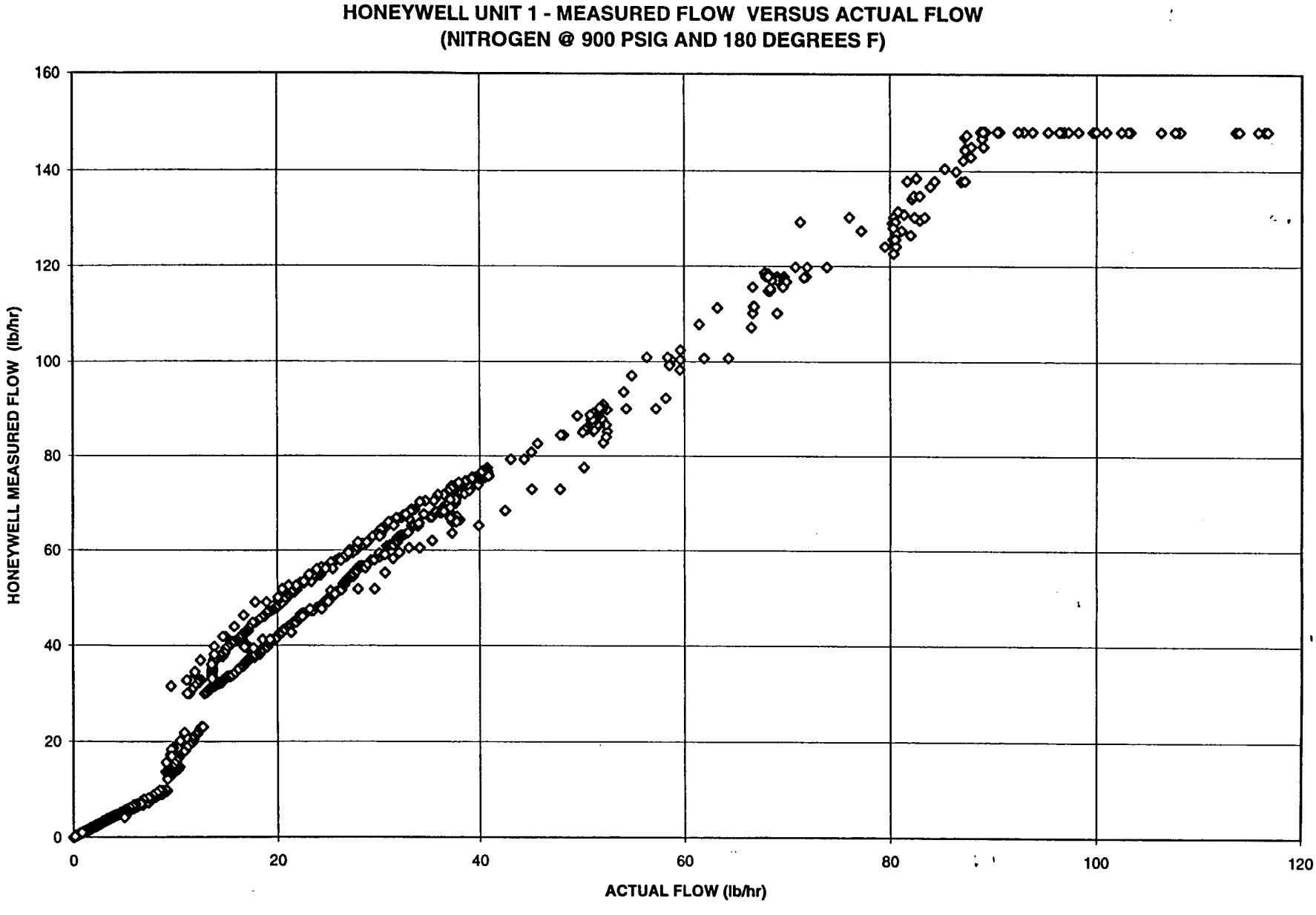
HONEYWELL UNIT 1 - MEASURED FLOW VERSUS ACTUAL FLOW
(NITROGEN @ 900 PSIG AND 180 DEGREES F)
HONEYWELL MEASURED FLOW (lb/hr)
ACTUAL FLOW (lb/hr)
0
20
40
60
80
100
120
140
160

Figure 53

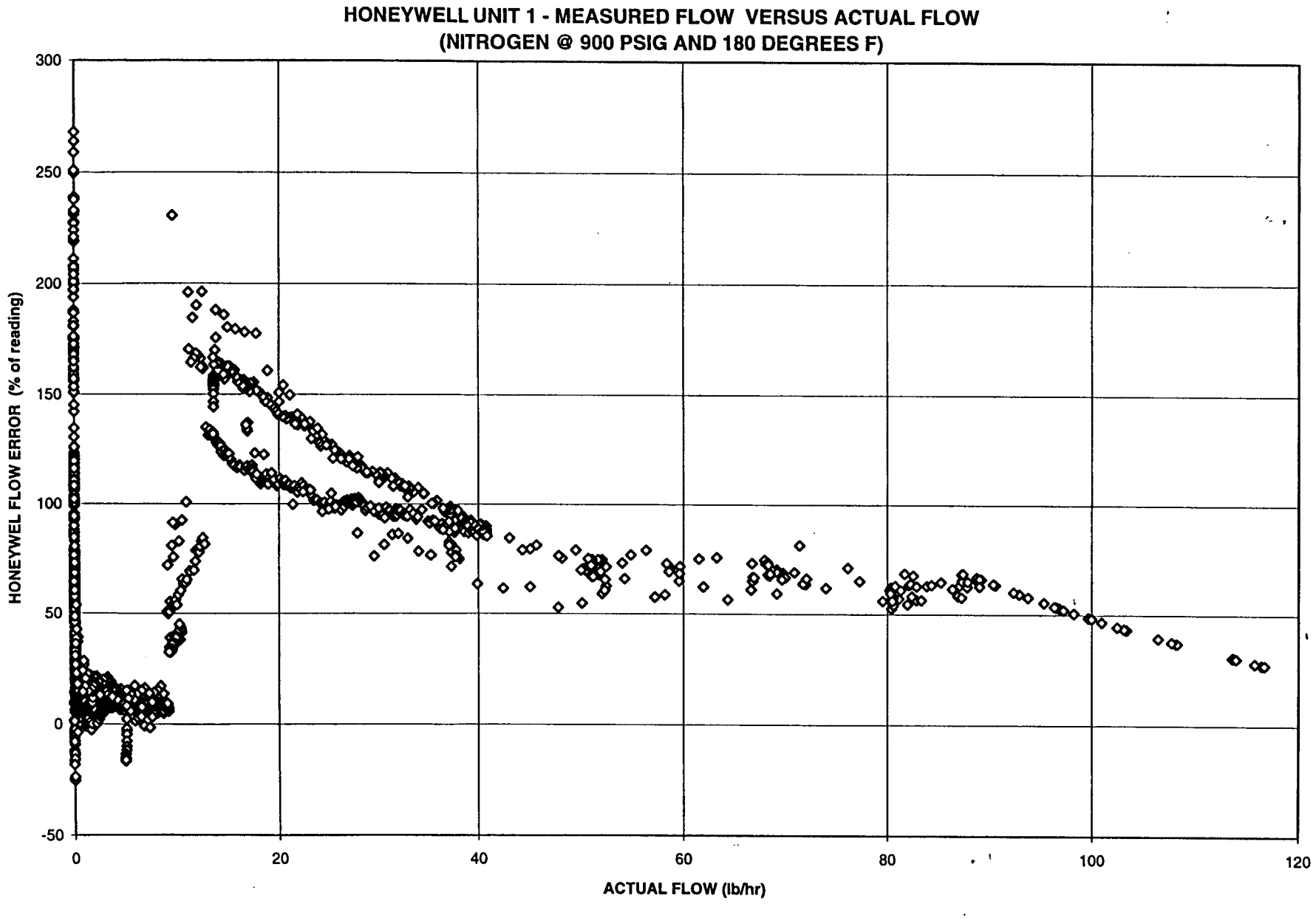
HONEYWELL UNIT 1 - MEASURED FLOW VERSUS ACTUAL FLOW
(NITROGEN @ 900 PSIG AND 180 DEGREES F)
HONEYWEL FLOW ERROR (% of reading)
300
250
200
150
100
50
0
-50
0
20
40
60
80
100
120
ACTUAL FLOW (lb/hr)

Figure 54

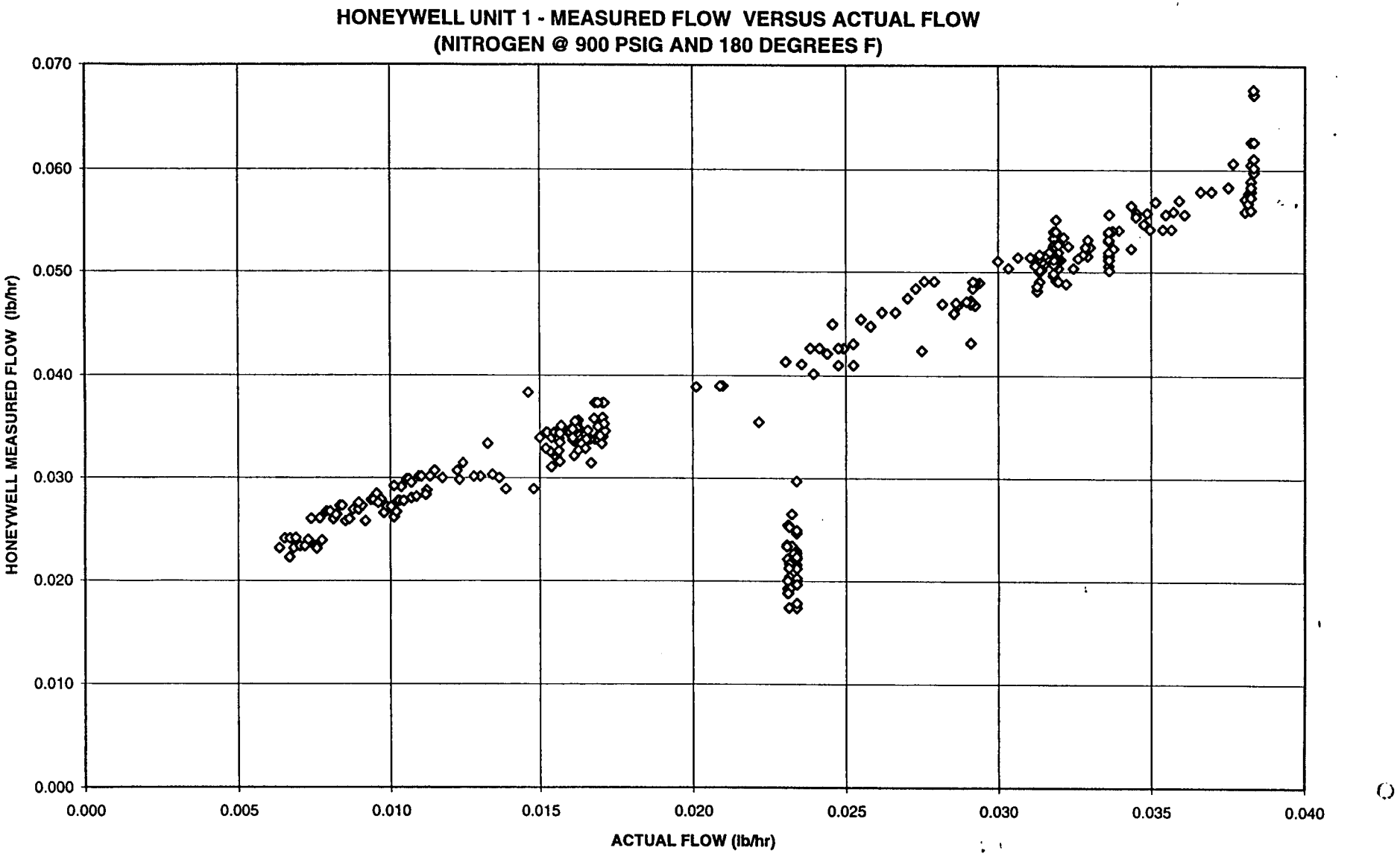
HONEYWELL UNIT 1 - MEASURED FLOW VERSUS ACTUAL FLOW
(NITROGEN @ 900 PSIG AND 180 DEGREES F)
HONEYWELL MEASURED FLOW (lb/hr)
0.070
0.060
0.050
0.040
0.030
0.020
0.010
0.000
0.000
0.005
0.010
0.015
0.020
0.025
0.030
0.035
0.040
ACTUAL FLOW (lb/hr)

Figure 55

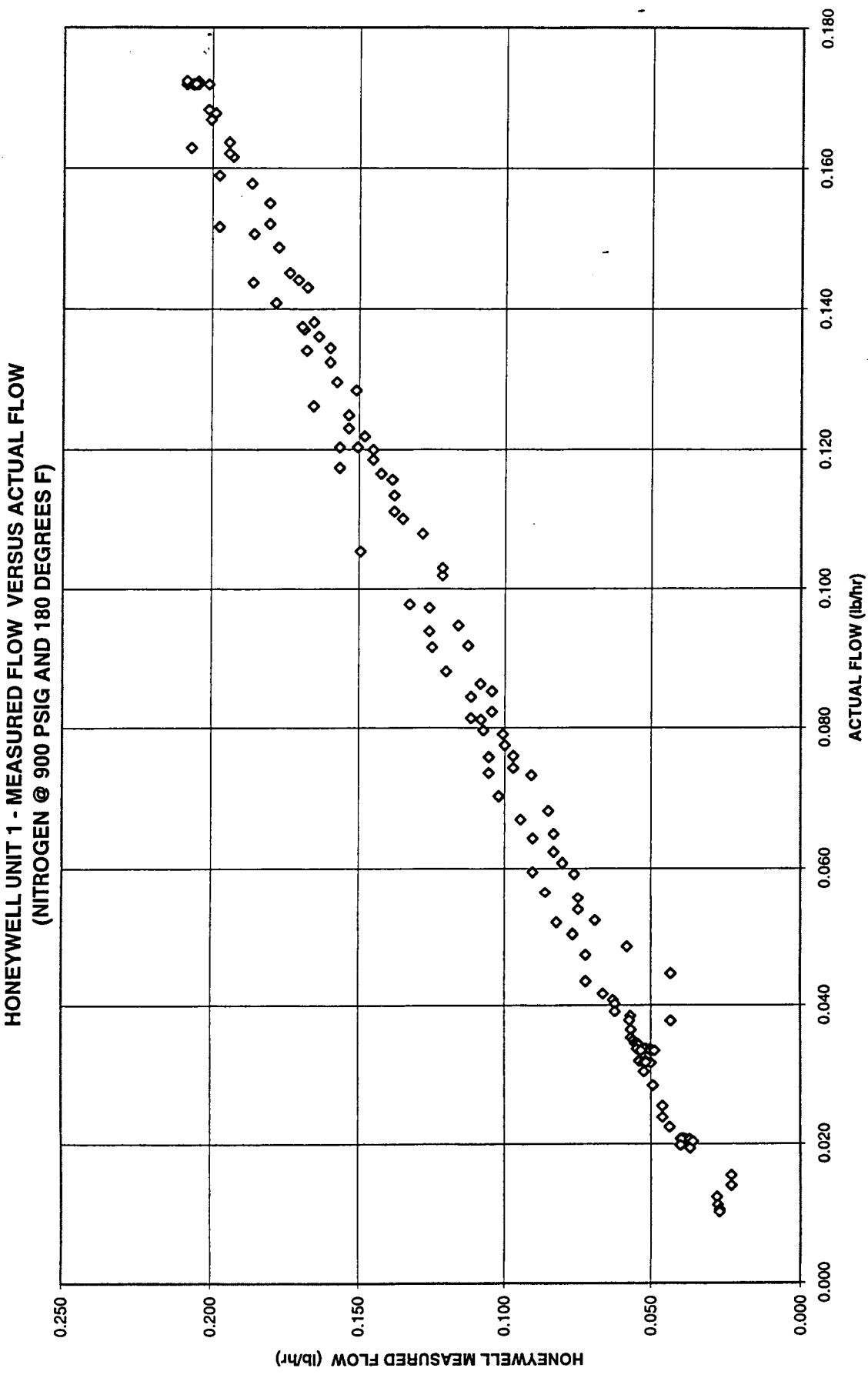
HONEYWELL UNIT 1 - MEASURED FLOW VERSUS ACTUAL FLOW
(NITROGEN @ 900 PSIG AND 180 DEGREES F)
HONEYWELL MEASURED FLOW (lb/hr)
0.250
0.200
0.150
0.100
0.050
0.000
ACTUAL FLOW (lb/hr)
0.000
0.020
0.040
0.060
0.080
0.100
0.120
0.140
0.160
0.180

Figure 56

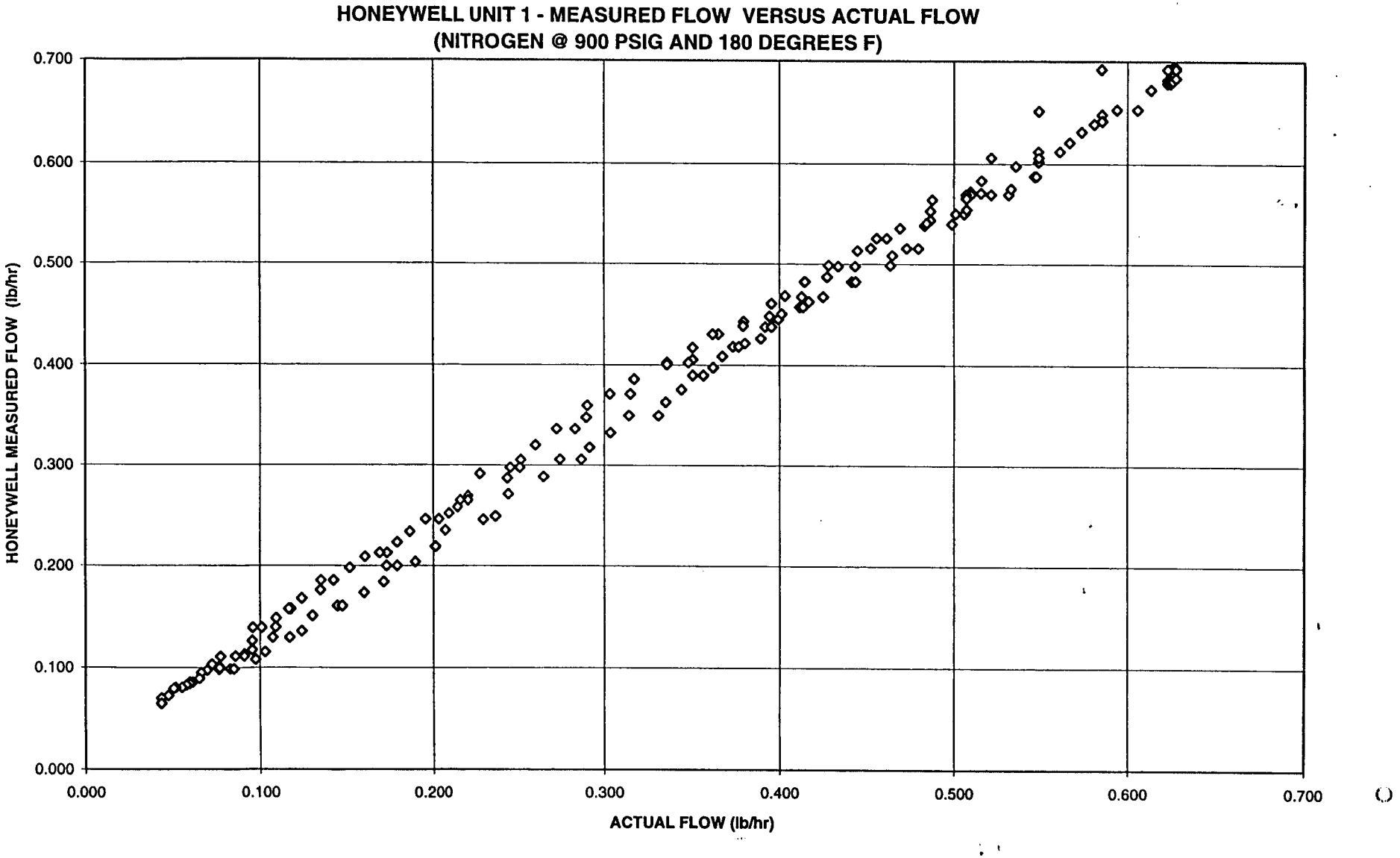
HONEYWELL UNIT 1 - MEASURED FLOW VERSUS ACTUAL FLOW
(NITROGEN @ 900 PSIG AND 180 DEGREES F)
HONEYWELL MEASURED FLOW (lb/hr)
0.700
0.600
0.500
0.400
0.300
0.200
0.100
0.000
0.000
0.100
0.200
0.300
0.400
0.500
0.600
0.700
ACTUAL FLOW (lb/hr)

Figure 57

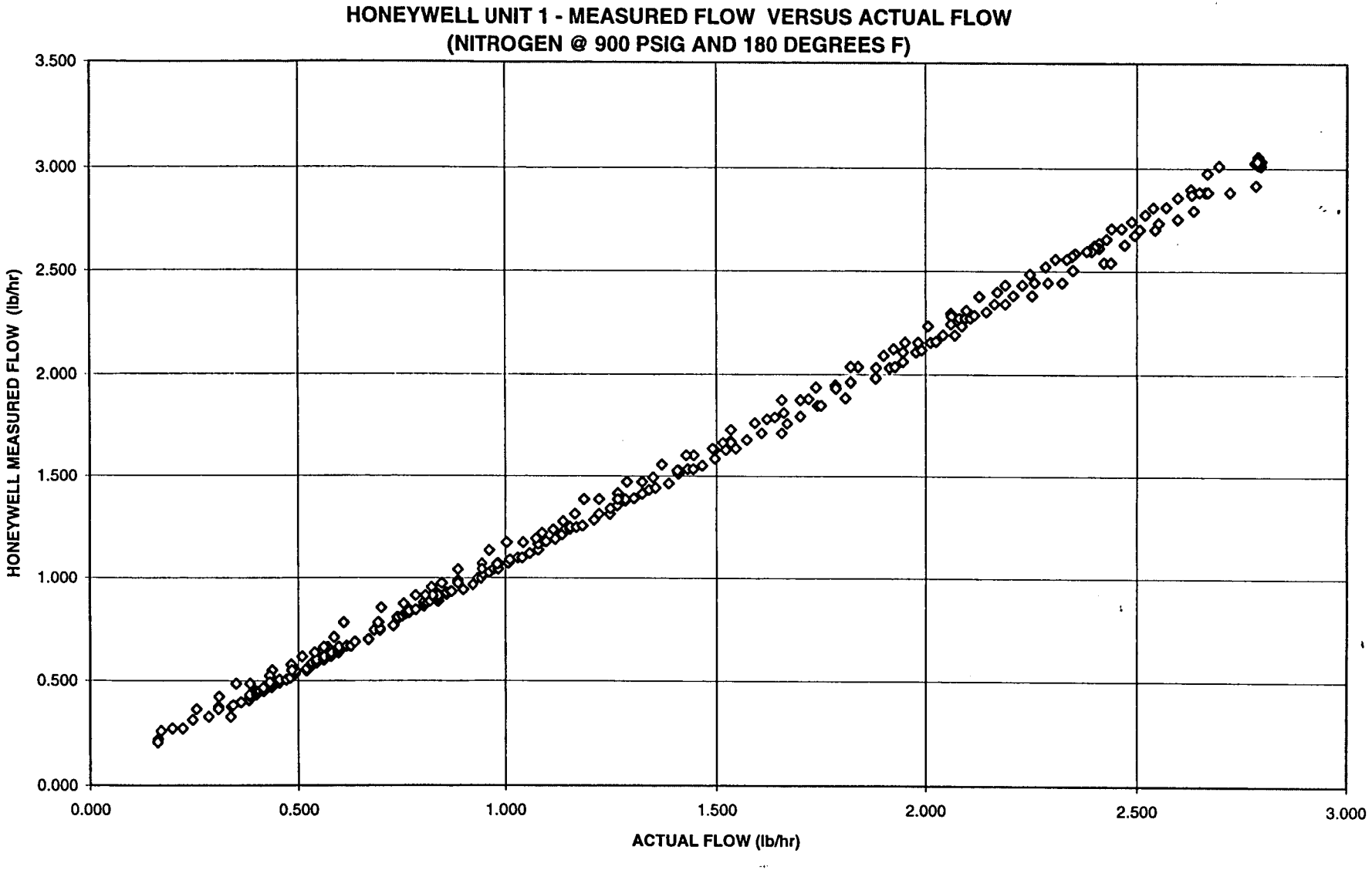
HONEYWELL UNIT 1 - MEASURED FLOW VERSUS ACTUAL FLOW
(NITROGEN @ 900 PSIG AND 180 DEGREES F)
HONEYWELL MEASURED FLOW (lb/hr)
3.500
3.000
2.500
2.000
1.500
1.000
0.500
0.000
0.000
0.500
1.000
1.500
2.000
2.500
3.000
ACTUAL FLOW (lb/hr)

Figure 58

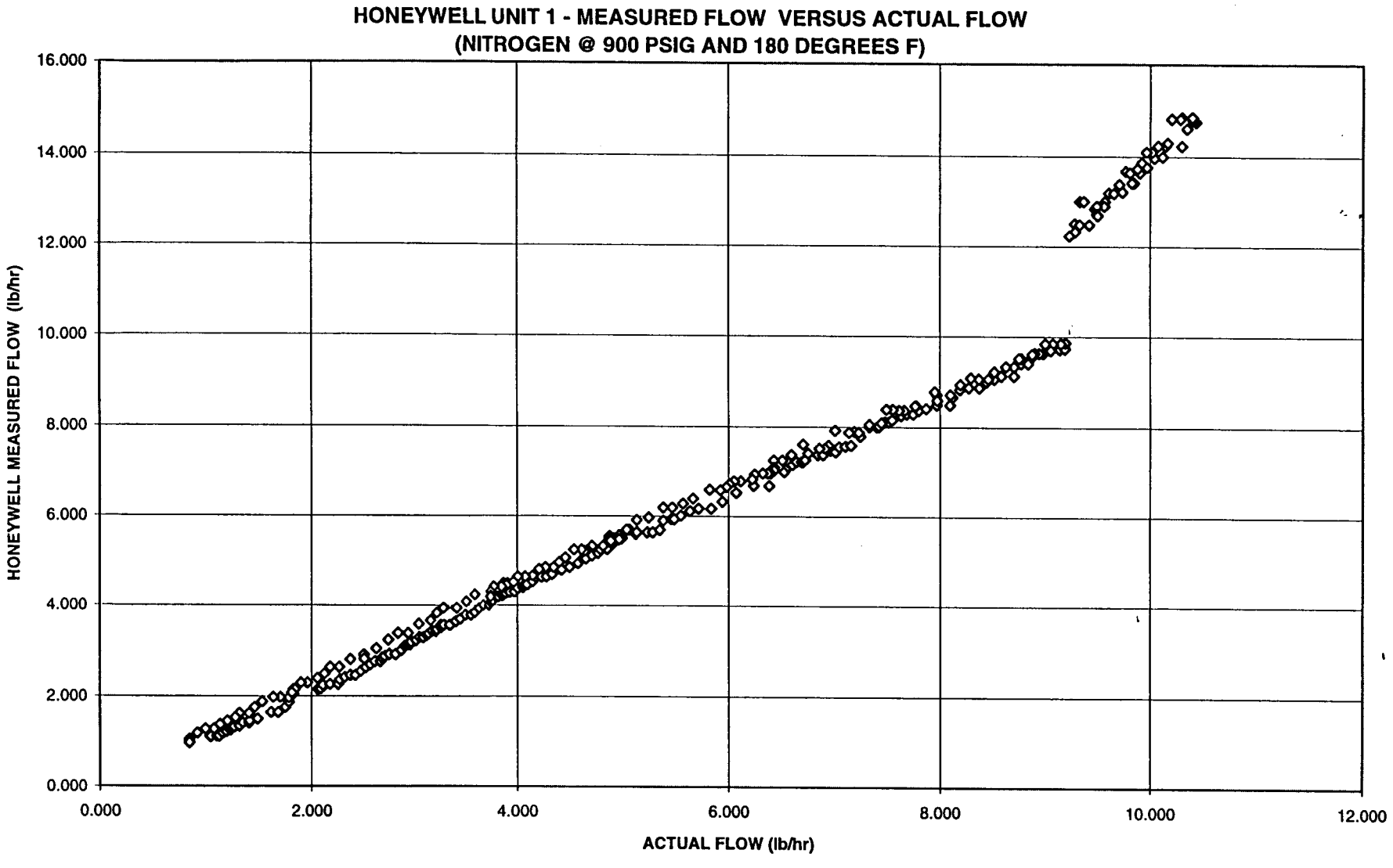
HONEYWELL UNIT 1 - MEASURED FLOW VERSUS ACTUAL FLOW
(NITROGEN @ 900 PSIG AND 180 DEGREES F)
HONEYWELL MEASURED FLOW (lb/hr)
16.000
14.000
12.000
10.000
8.000
6.000
4.000
2.000
0.000
0.000
2.000
4.000
6.000
8.000
10.000
12.000
ACTUAL FLOW (lb/hr)

Figure 59

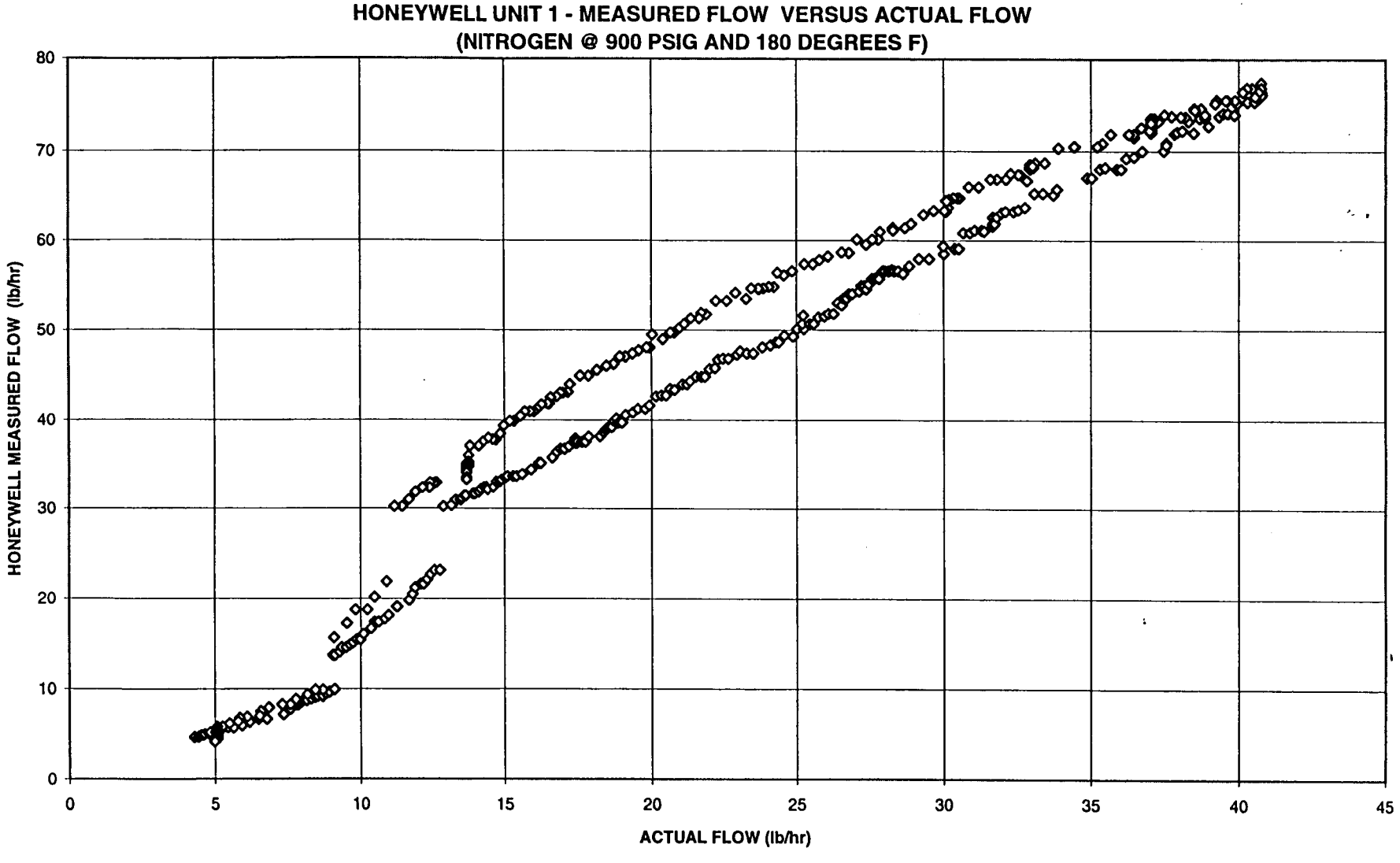
HONEYWELL UNIT 1 - MEASURED FLOW VERSUS ACTUAL FLOW
(NITROGEN @ 900 PSIG AND 180 DEGREES F)
HONEYWELL MEASURED FLOW (lb/hr)
ACTUAL FLOW (lb/hr)
0
10
20
30
40
50
60
70
80
0
5
10
15
20
25
30
35
40
45

Figure 60

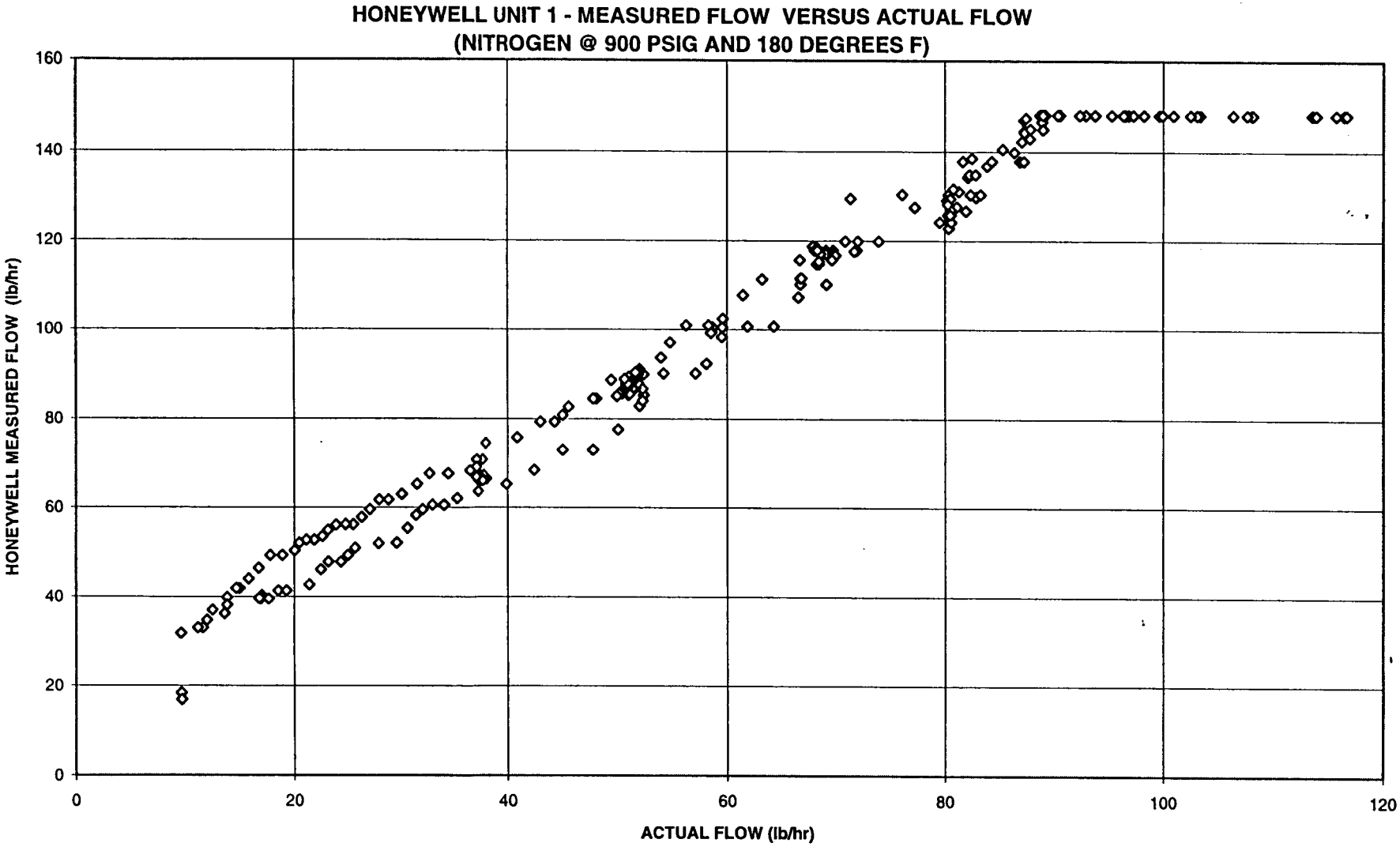
HONEYWELL UNIT 1 - MEASURED FLOW VERSUS ACTUAL FLOW
(NITROGEN @ 900 PSIG AND 180 DEGREES F)
HONEYWELL MEASURED FLOW (lb/hr)
ACTUAL FLOW (lb/hr)
0
20
40
60
80
100
120
140
160

Figure 61

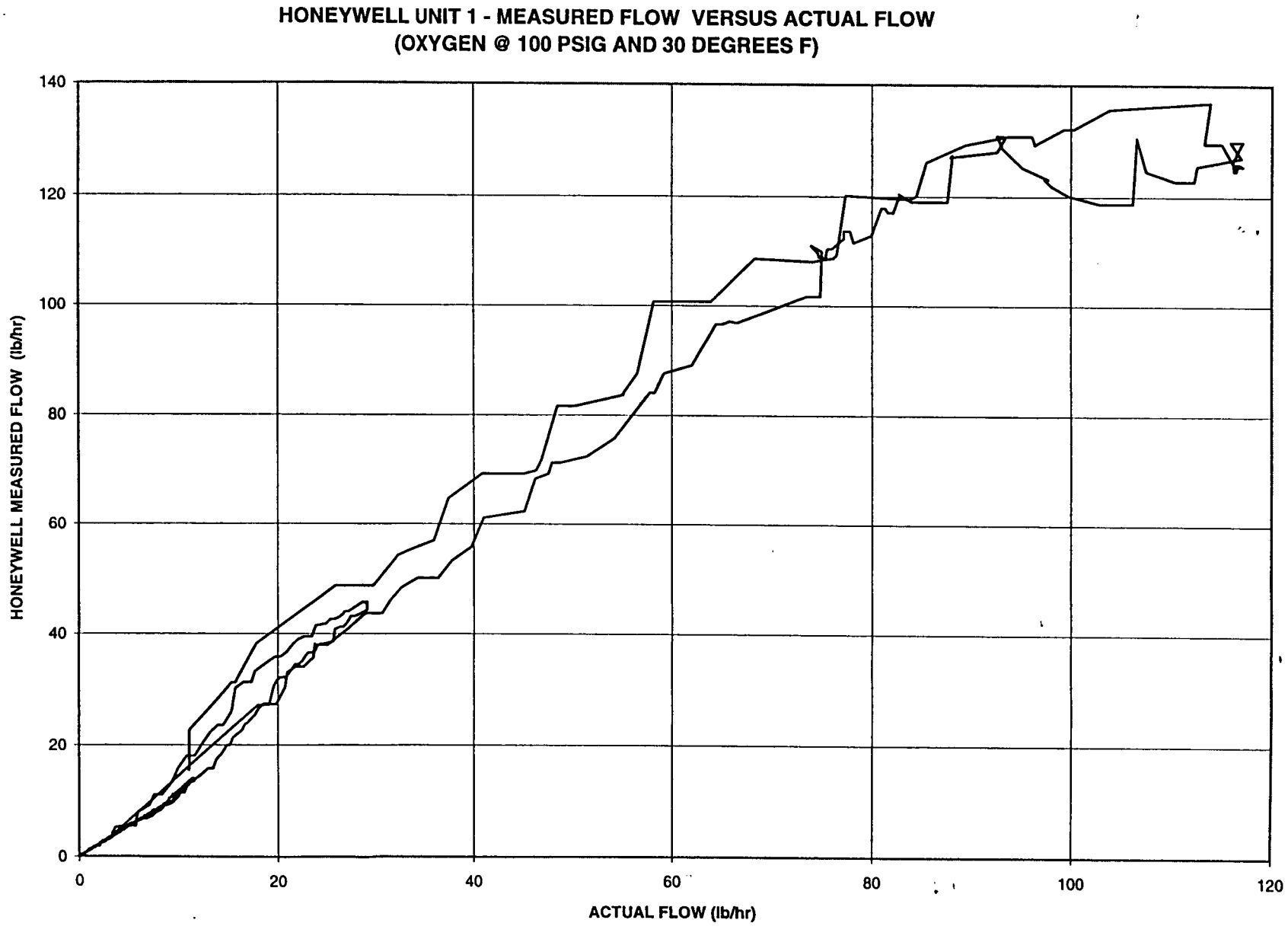
HONEYWELL UNIT 1 - MEASURED FLOW VERSUS ACTUAL FLOW
(OXYGEN @ 100 PSIG AND 30 DEGREES F)
HONEYWELL MEASURED FLOW (lb/hr)
ACTUAL FLOW (lb/hr)
0
20
40
60
80
100
120
140

Figure 62

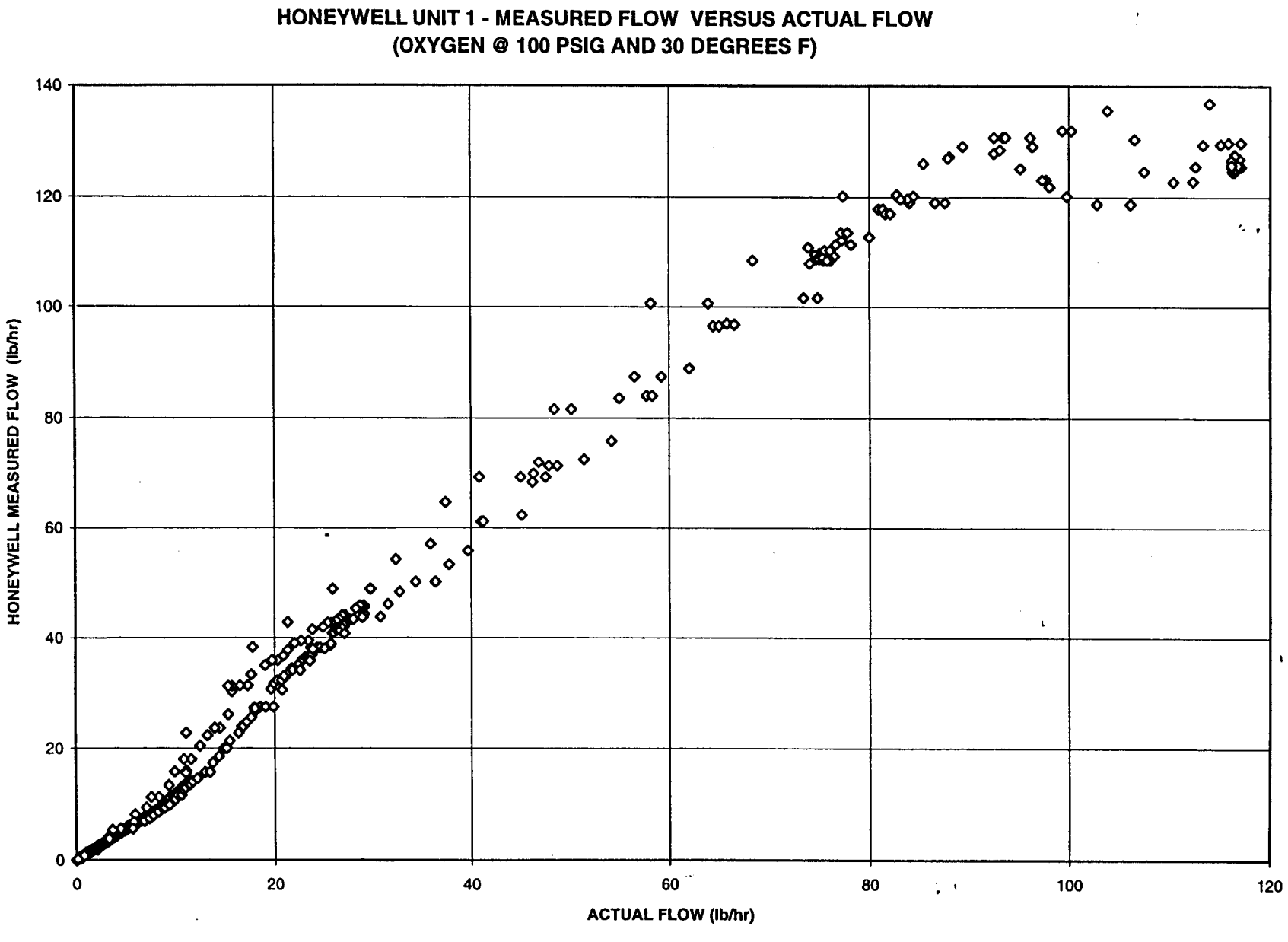
HONEYWELL UNIT 1 - MEASURED FLOW VERSUS ACTUAL FLOW
(OXYGEN @ 100 PSIG AND 30 DEGREES F)
HONEYWELL MEASURED FLOW (lb/hr)
ACTUAL FLOW (lb/hr)
0
20
40
60
80
100
120
140

Figure 63

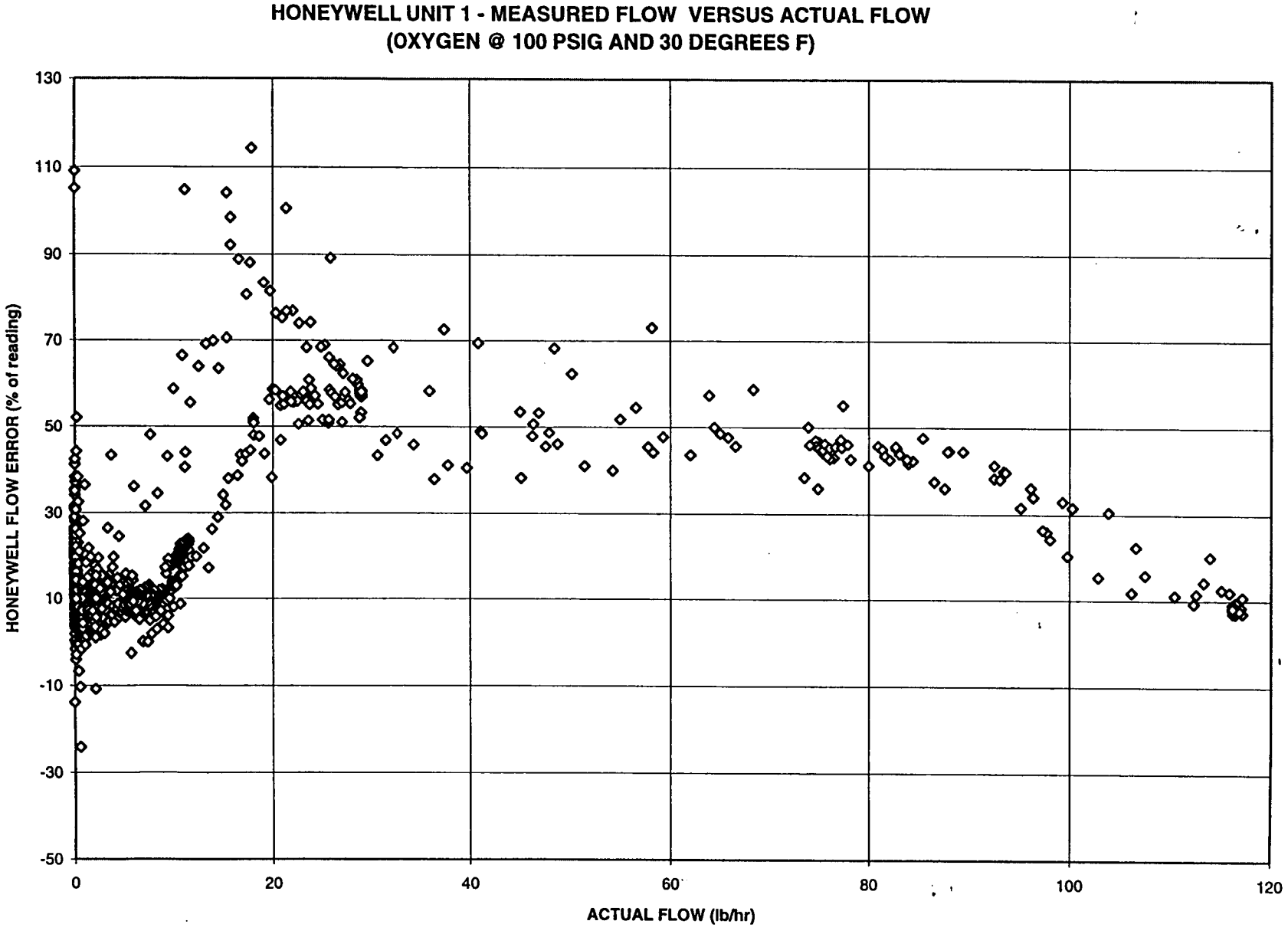
HONEYWELL UNIT 1 - MEASURED FLOW VERSUS ACTUAL FLOW
(OXYGEN @ 100 PSIG AND 30 DEGREES F)
HONEYWELL FLOW ERROR (% of reading)
130
110
90
70
50
30
10
-10
-30
-50
0
20
40
60
80
100
120
ACTUAL FLOW (lb/hr)

Figure 64

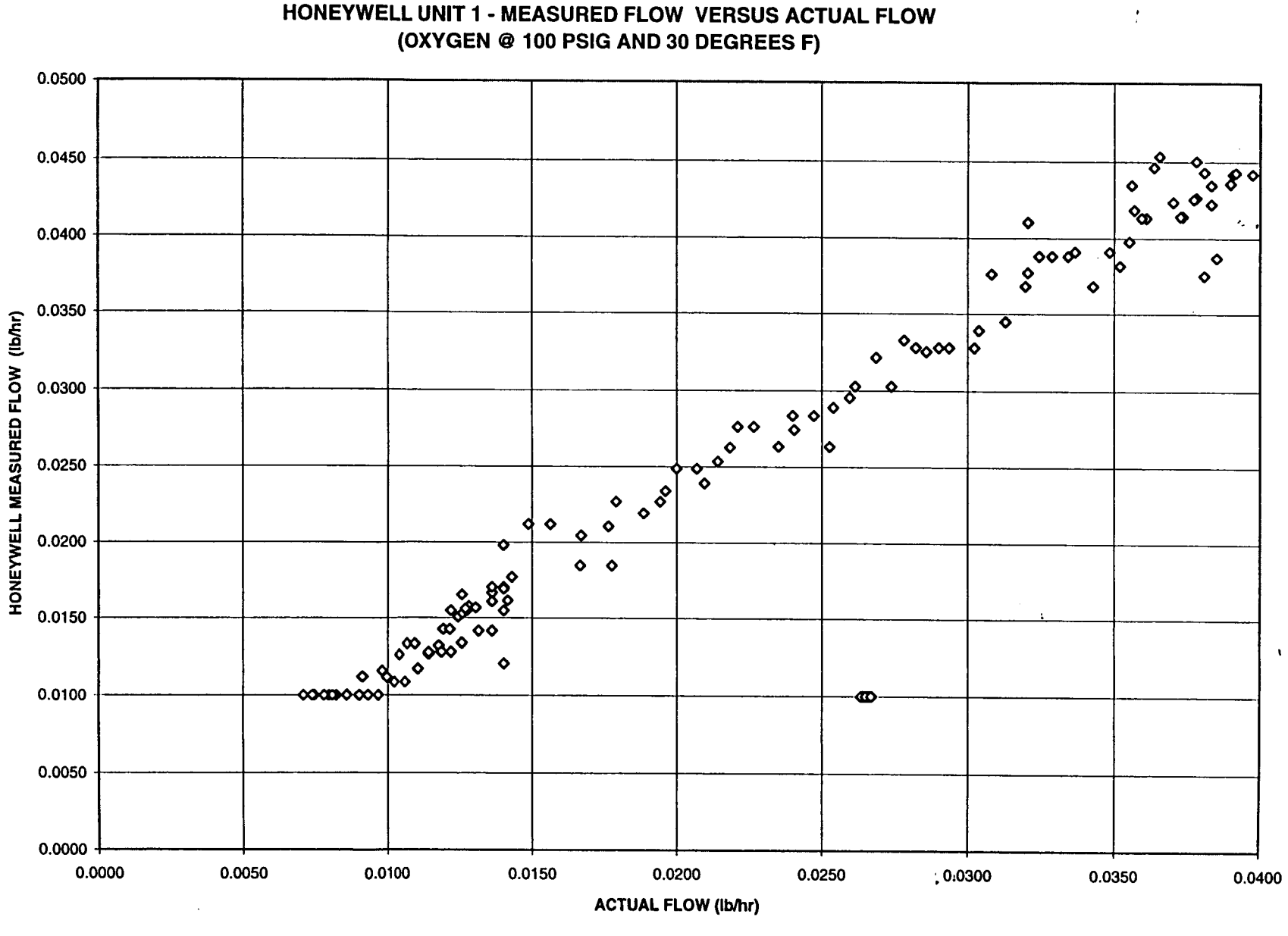
HONEYWELL UNIT 1 - MEASURED FLOW VERSUS ACTUAL FLOW
(OXYGEN @ 100 PSIG AND 30 DEGREES F)
HONEYWELL MEASURED FLOW (lb/hr)
0.0500
0.0450
0.0400
0.0350
0.0300
0.0250
0.0200
0.0150
0.0100
0.0050
0.0000
0.0000
0.0050
0.0100
0.0150
0.0200
0.0250
0.0300
0.0350
0.0400
ACTUAL FLOW (lb/hr)

Figure 65

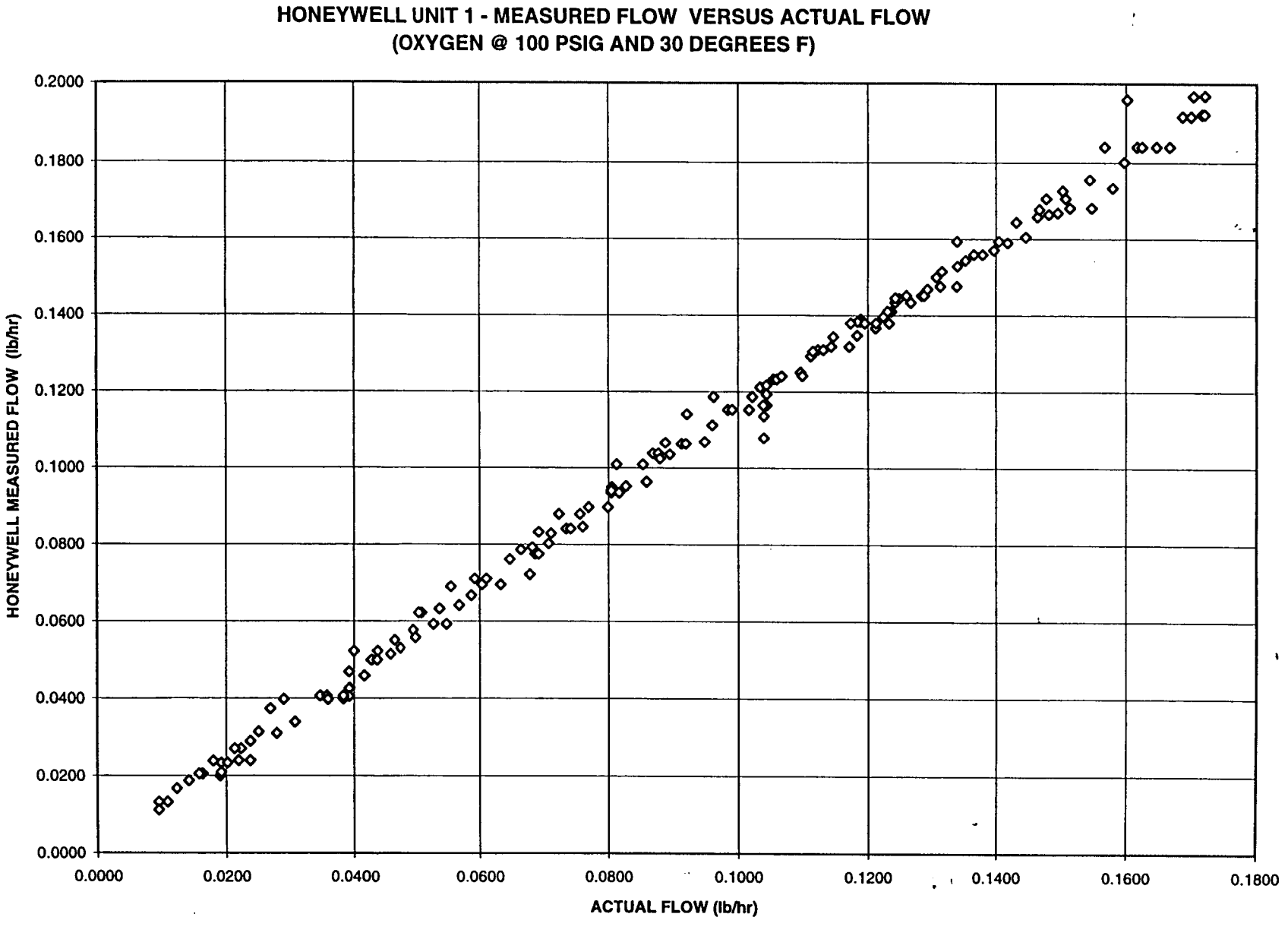
HONEYWELL UNIT 1 - MEASURED FLOW VERSUS ACTUAL FLOW
(OXYGEN @ 100 PSIG AND 30 DEGREES F)
HONEYWELL MEASURED FLOW (lb/hr)
0.2000
0.1800
0.1600
0.1400
0.1200
0.1000
0.0800
0.0600
0.0400
0.0200
0.0000
0.0000
0.0200
0.0400
0.0600
0.0800
0.1000
0.1200
0.1400
0.1600
0.1800
ACTUAL FLOW (lb/hr)

Figure 66

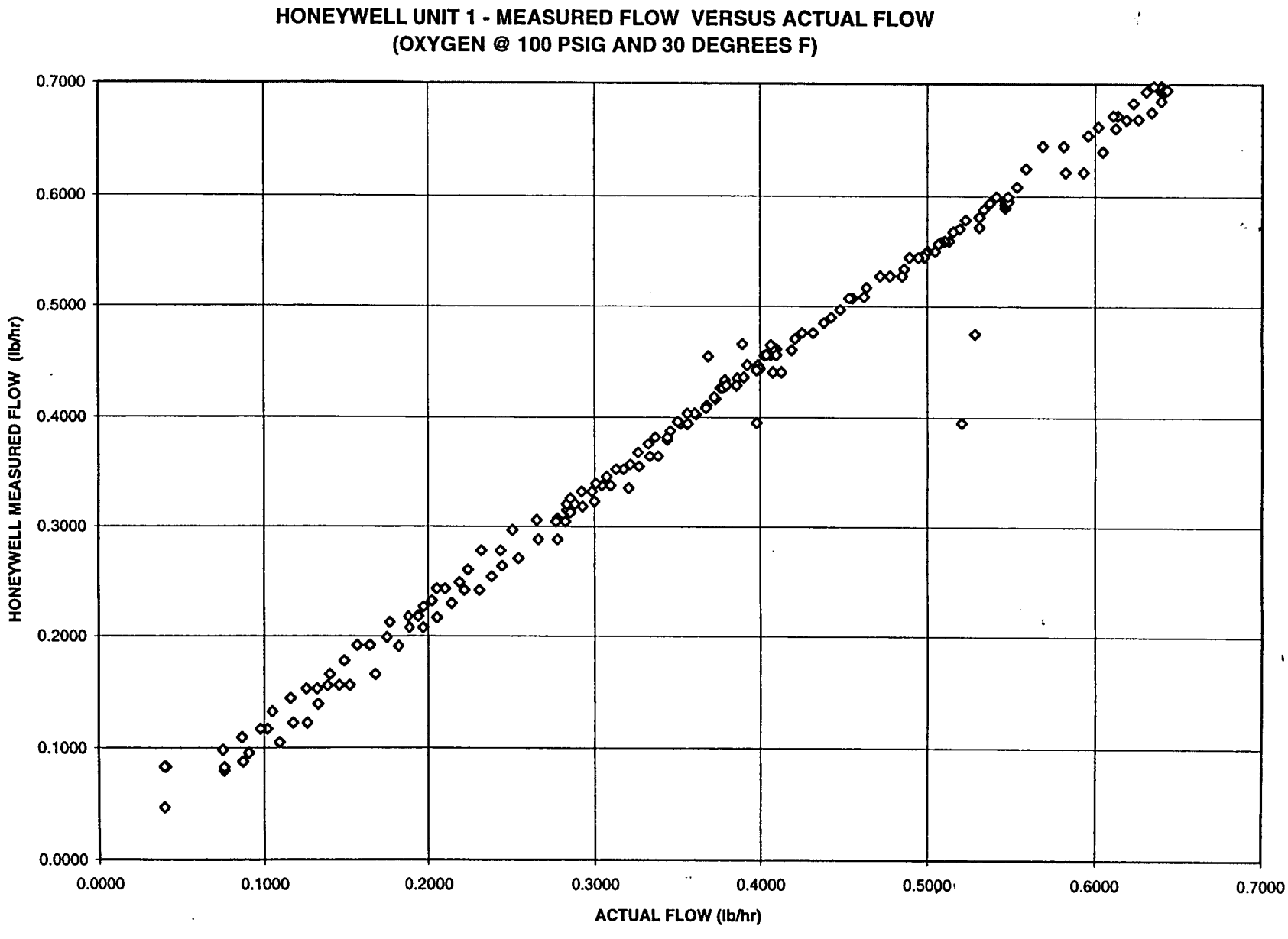
HONEYWELL UNIT 1 - MEASURED FLOW VERSUS ACTUAL FLOW
(OXYGEN @ 100 PSIG AND 30 DEGREES F)
HONEYWELL MEASURED FLOW (lb/hr)
0.7000
0.6000
0.5000
0.4000
0.3000
0.2000
0.1000
0.0000
0.0000
0.1000
0.2000
0.3000
0.4000
0.5000
0.6000
0.7000
ACTUAL FLOW (lb/hr)

Figure 67

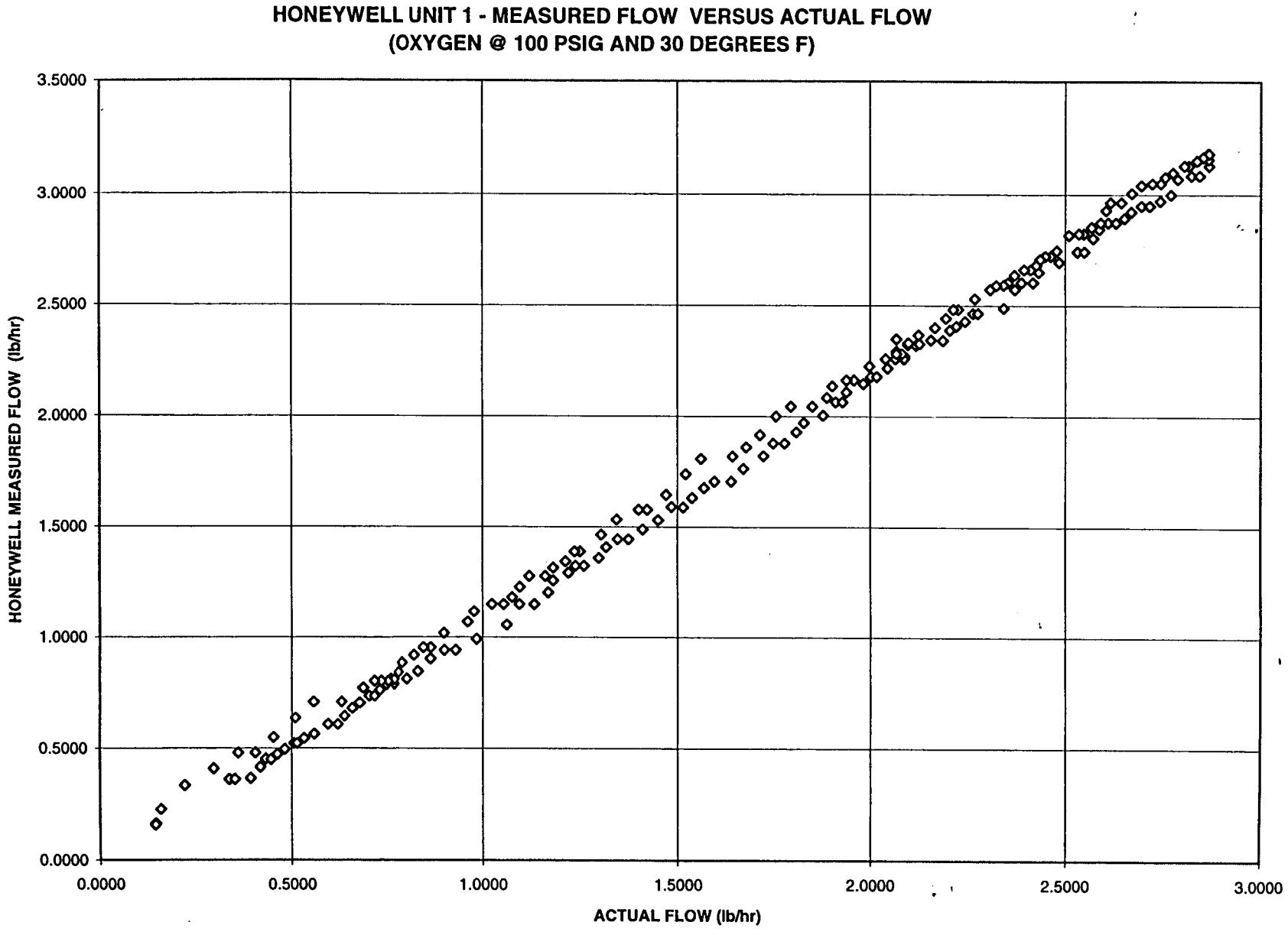
HONEYWELL UNIT 1 - MEASURED FLOW VERSUS ACTUAL FLOW
(OXYGEN @ 100 PSIG AND 30 DEGREES F)
HONEYWELL MEASURED FLOW (lb/hr)
3.5000
3.0000
2.5000
2.0000
1.5000
1.0000
0.5000
0.0000
0.0000
0.5000
1.0000
1.5000
2.0000
2.5000
3.0000
ACTUAL FLOW (lb/hr)

Figure 68

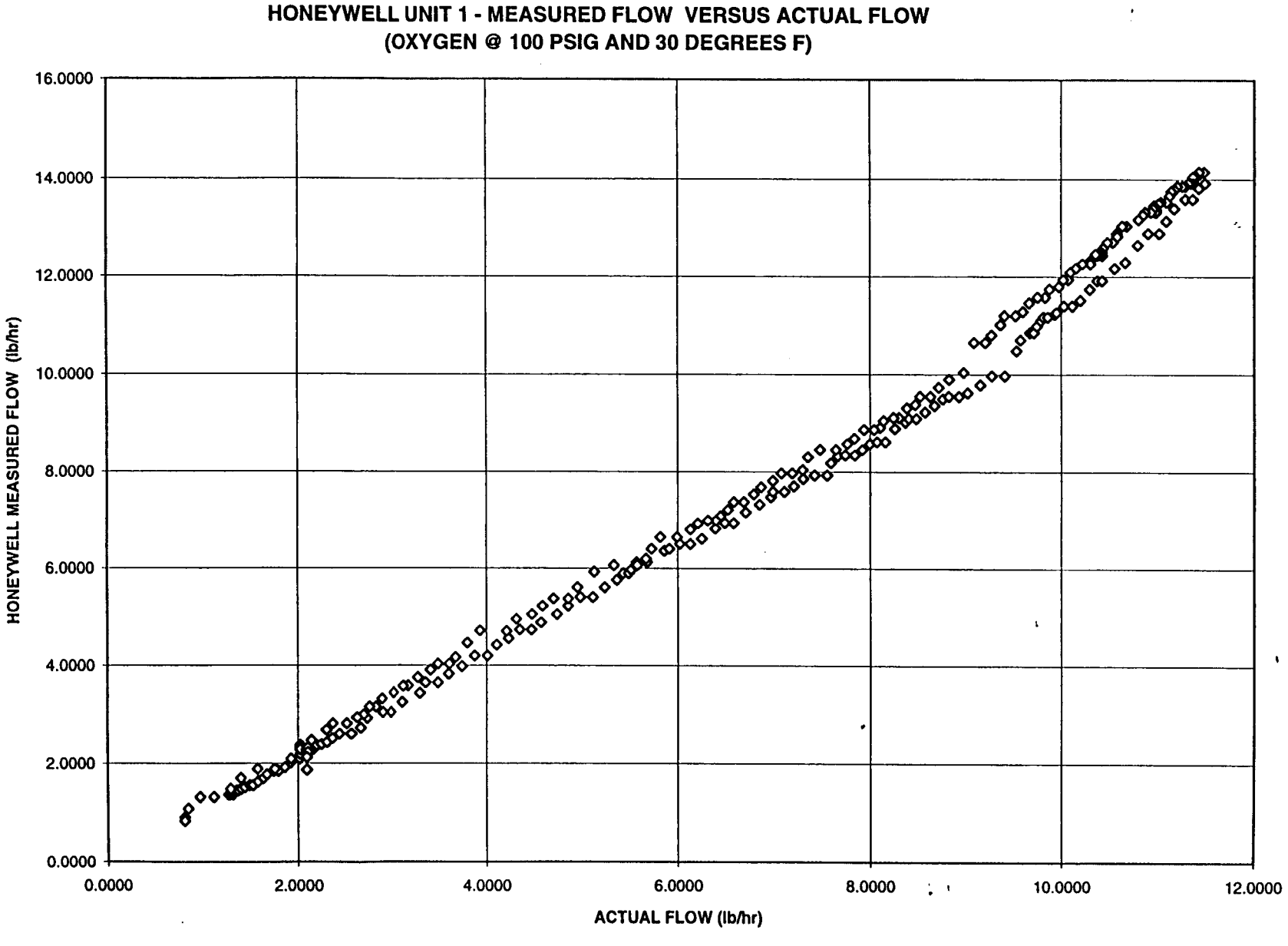
HONEYWELL UNIT 1 - MEASURED FLOW VERSUS ACTUAL FLOW
(OXYGEN @ 100 PSIG AND 30 DEGREES F)
HONEYWELL MEASURED FLOW (lb/hr)
16.0000
14.0000
12.0000
10.0000
8.0000
6.0000
4.0000
2.0000
0.0000
0.0000
2.0000
4.0000
6.0000
8.0000
10.0000
12.0000
ACTUAL FLOW (lb/hr)

Figure 69

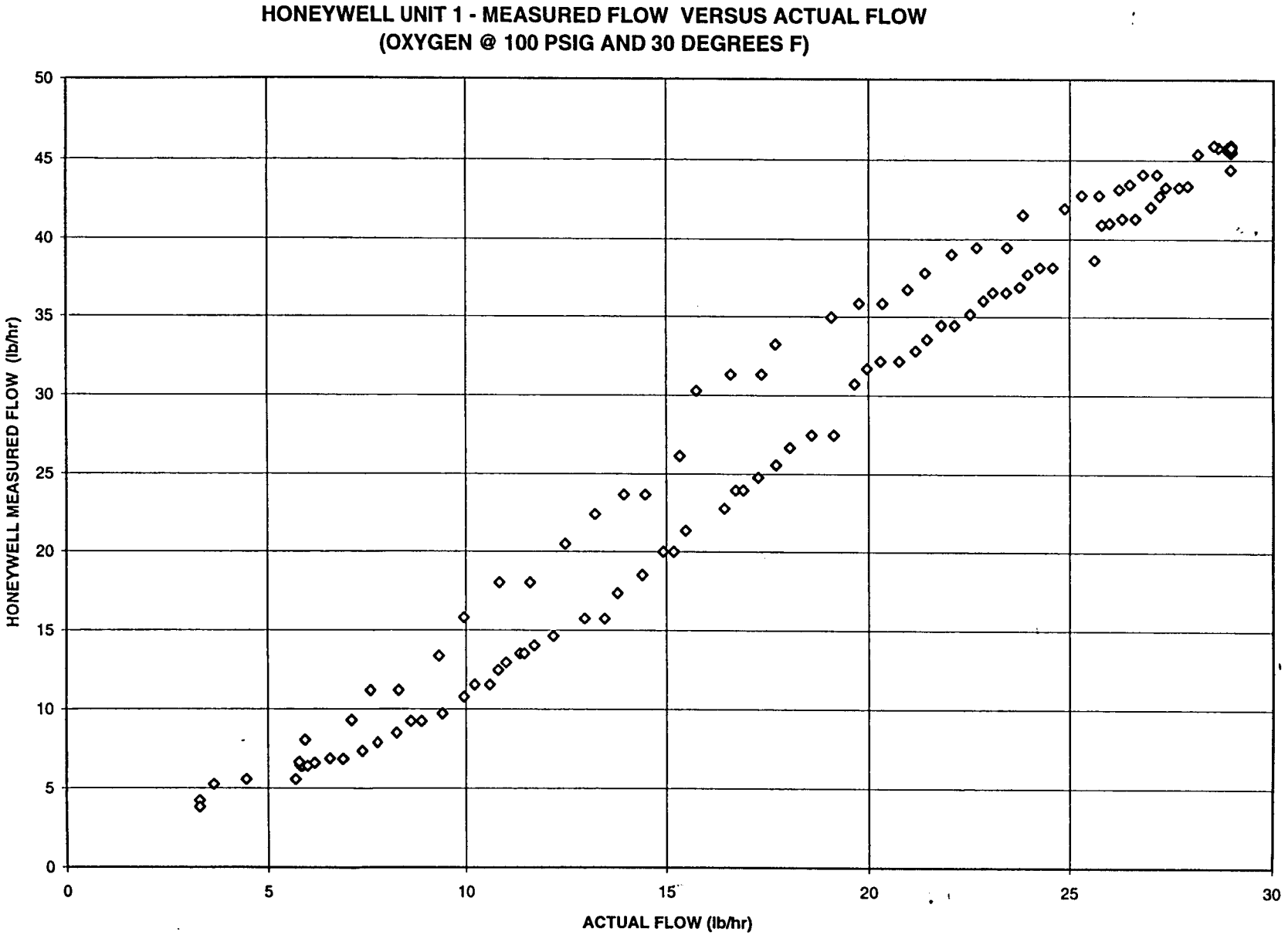
HONEYWELL UNIT 1 - MEASURED FLOW VERSUS ACTUAL FLOW
(OXYGEN @ 100 PSIG AND 30 DEGREES F)
HONEYWELL MEASURED FLOW (lb/hr)
ACTUAL FLOW (lb/hr)
0
5
10
15
20
25
30
35
40
45
50

Figure 70

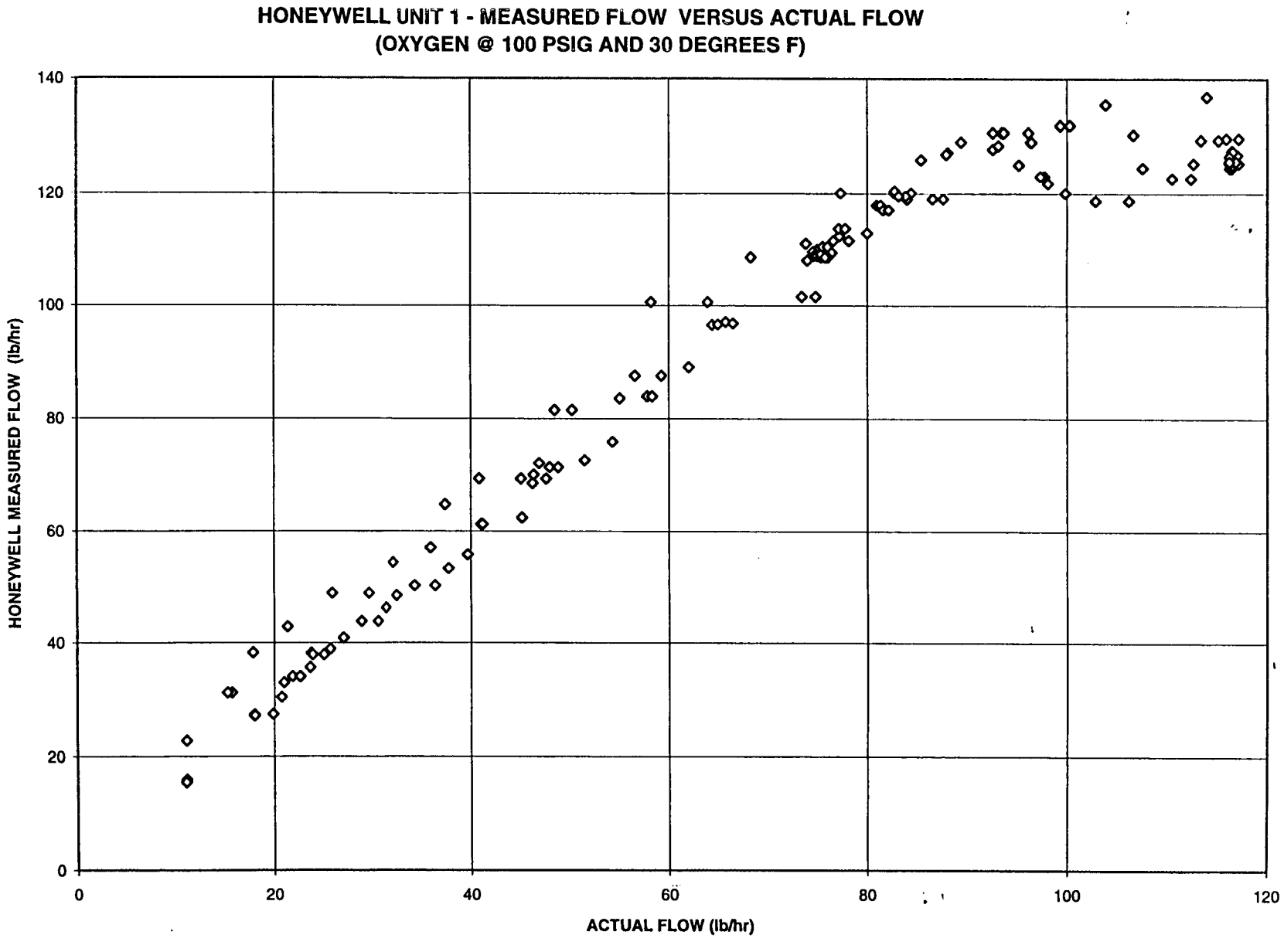
HONEYWELL UNIT 1 - MEASURED FLOW VERSUS ACTUAL FLOW
(OXYGEN @ 100 PSIG AND 30 DEGREES F)
HONEYWELL MEASURED FLOW (lb/hr)
ACTUAL FLOW (lb/hr)
0
20
40
60
80
100
120
140

Figure 71

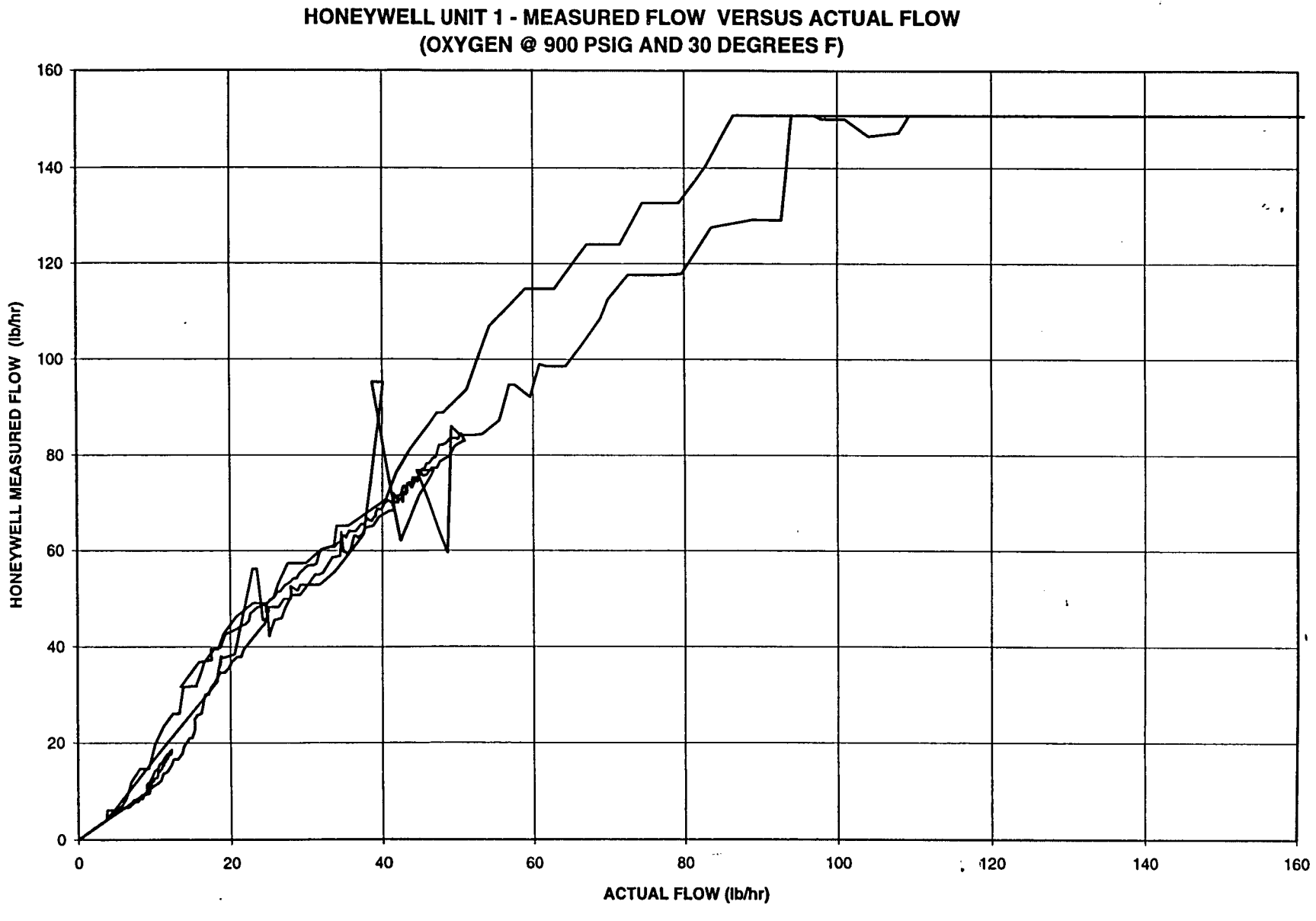
HONEYWELL UNIT 1 - MEASURED FLOW VERSUS ACTUAL FLOW
(OXYGEN @ 900 PSIG AND 30 DEGREES F)
HONEYWELL MEASURED FLOW (lb/hr)
ACTUAL FLOW (lb/hr)
0
20
40
60
80
100
120
140
160

Figure 72

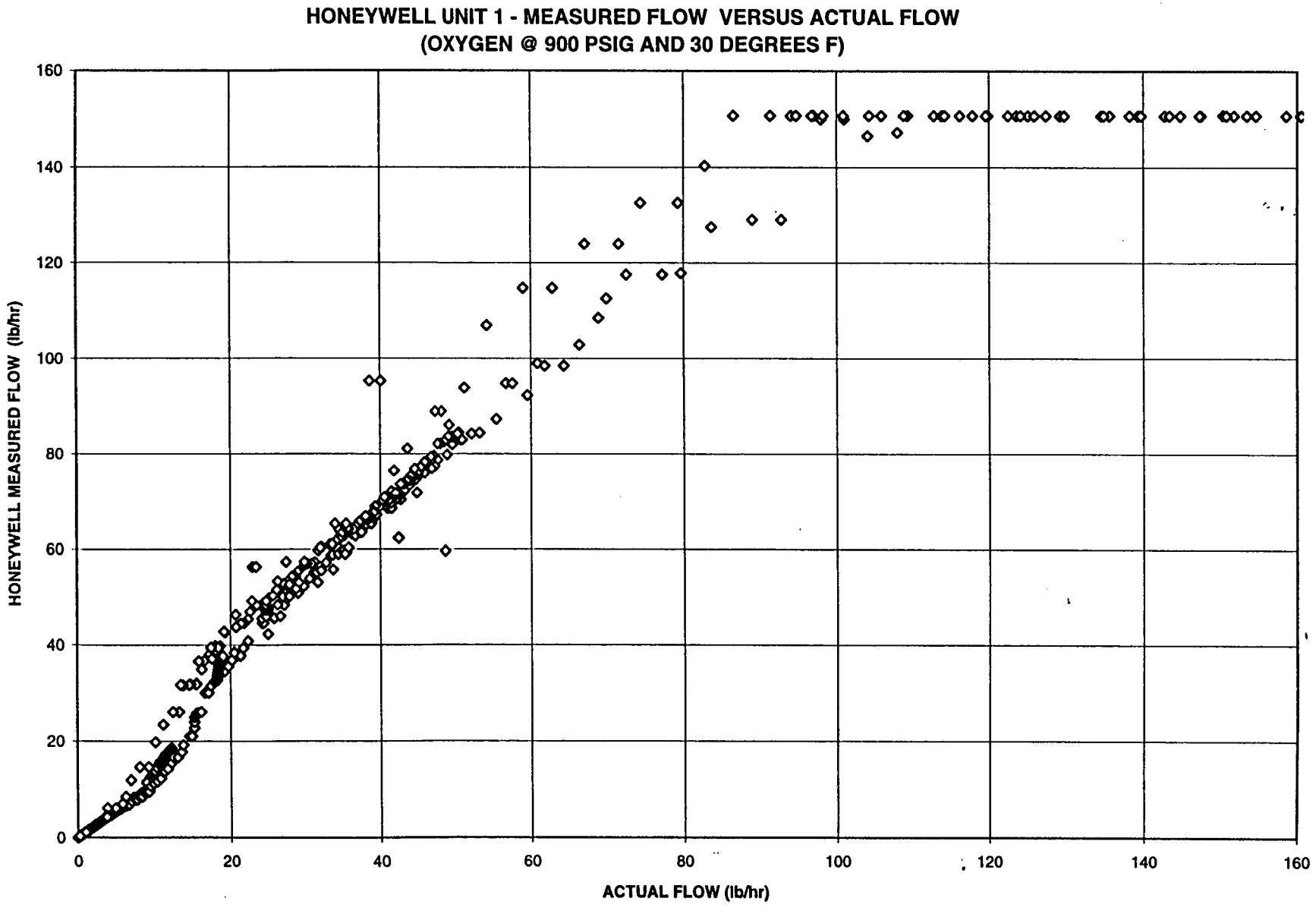
HONEYWELL UNIT 1 - MEASURED FLOW VERSUS ACTUAL FLOW
(OXYGEN @ 900 PSIG AND 30 DEGREES F)
HONEYWELL MEASURED FLOW (lb/hr)
ACTUAL FLOW (lb/hr)
0
20
40
60
80
100
120
140
160

Figure 73

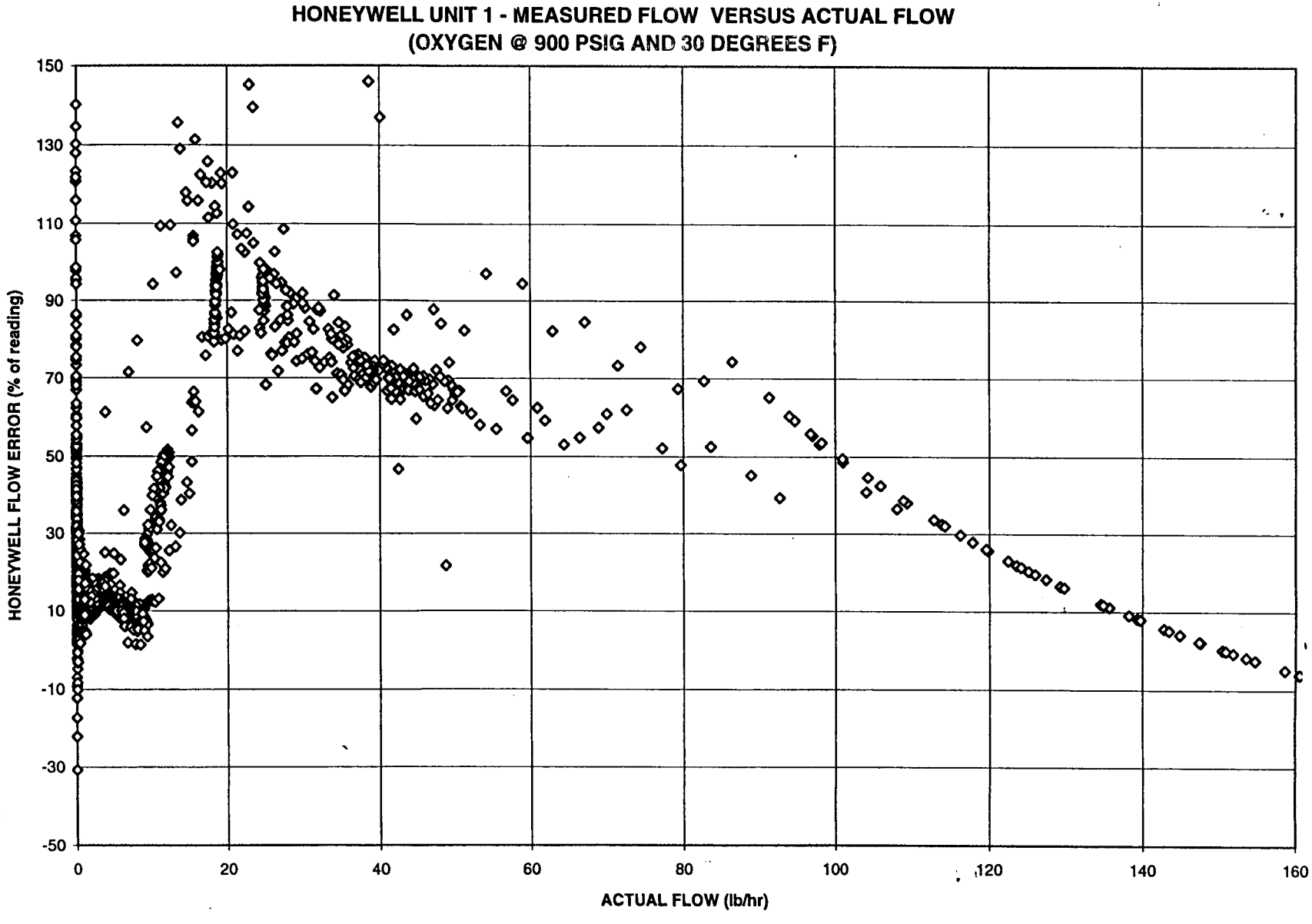
HONEYWELL UNIT 1 - MEASURED FLOW VERSUS ACTUAL FLOW
(OXYGEN @ 900 PSIG AND 30 DEGREES F)
HONEYWELL FLOW ERROR (% of reading)
150
130
110
90
70
50
30
10
-10
-30
-50
0
20
40
60
80
100
120
140
160
ACTUAL FLOW (lb/hr)

Figure 74

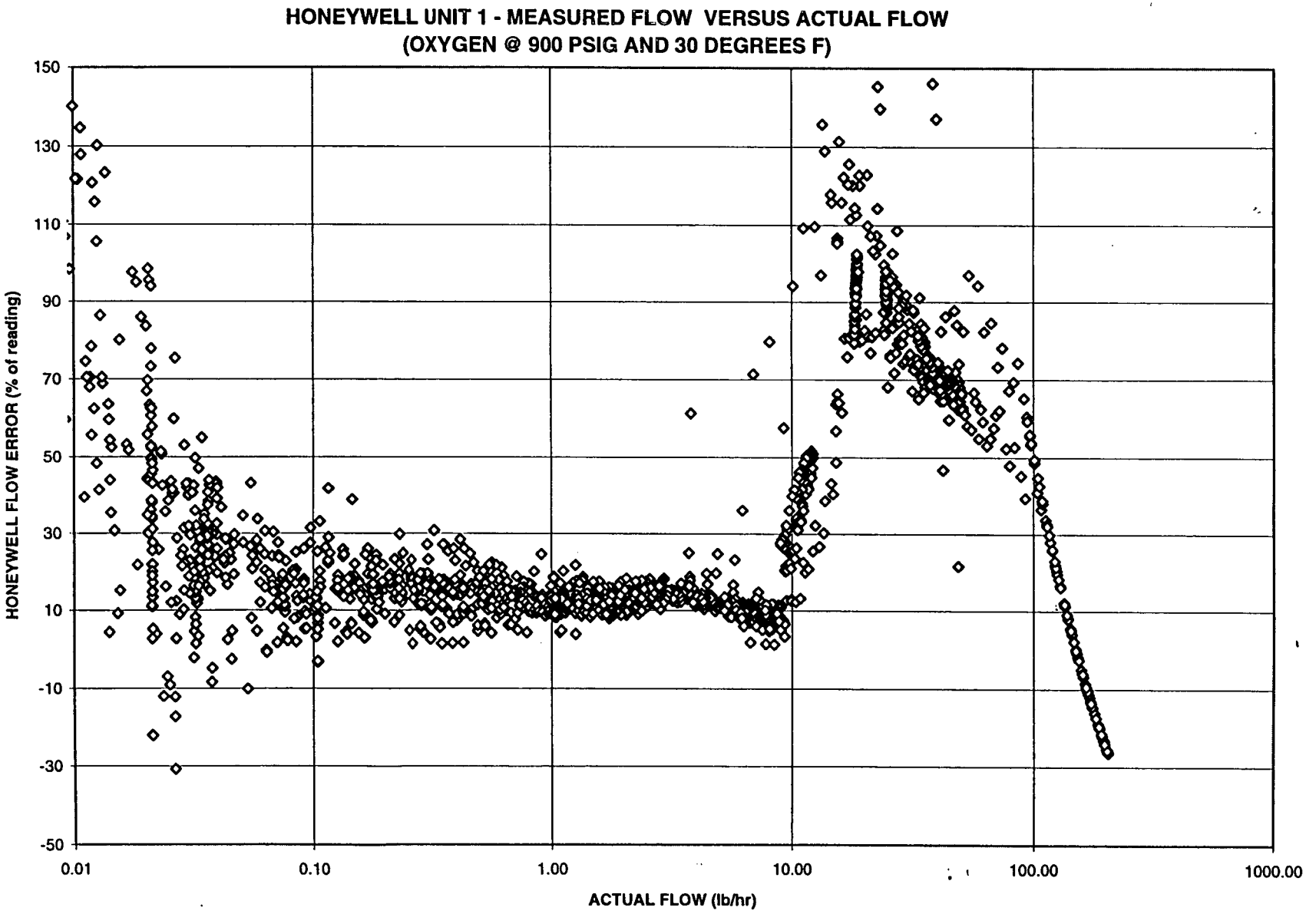
HONEYWELL UNIT 1 - MEASURED FLOW VERSUS ACTUAL FLOW
(OXYGEN @ 900 PSIG AND 30 DEGREES F)
HONEYWELL FLOW ERROR (% of reading)
150
130
110
90
70
50
30
10
-10
-30
-50
0.01
0.10
1.00
10.00
100.00
1000.00
ACTUAL FLOW (lb/hr)

Figure 75

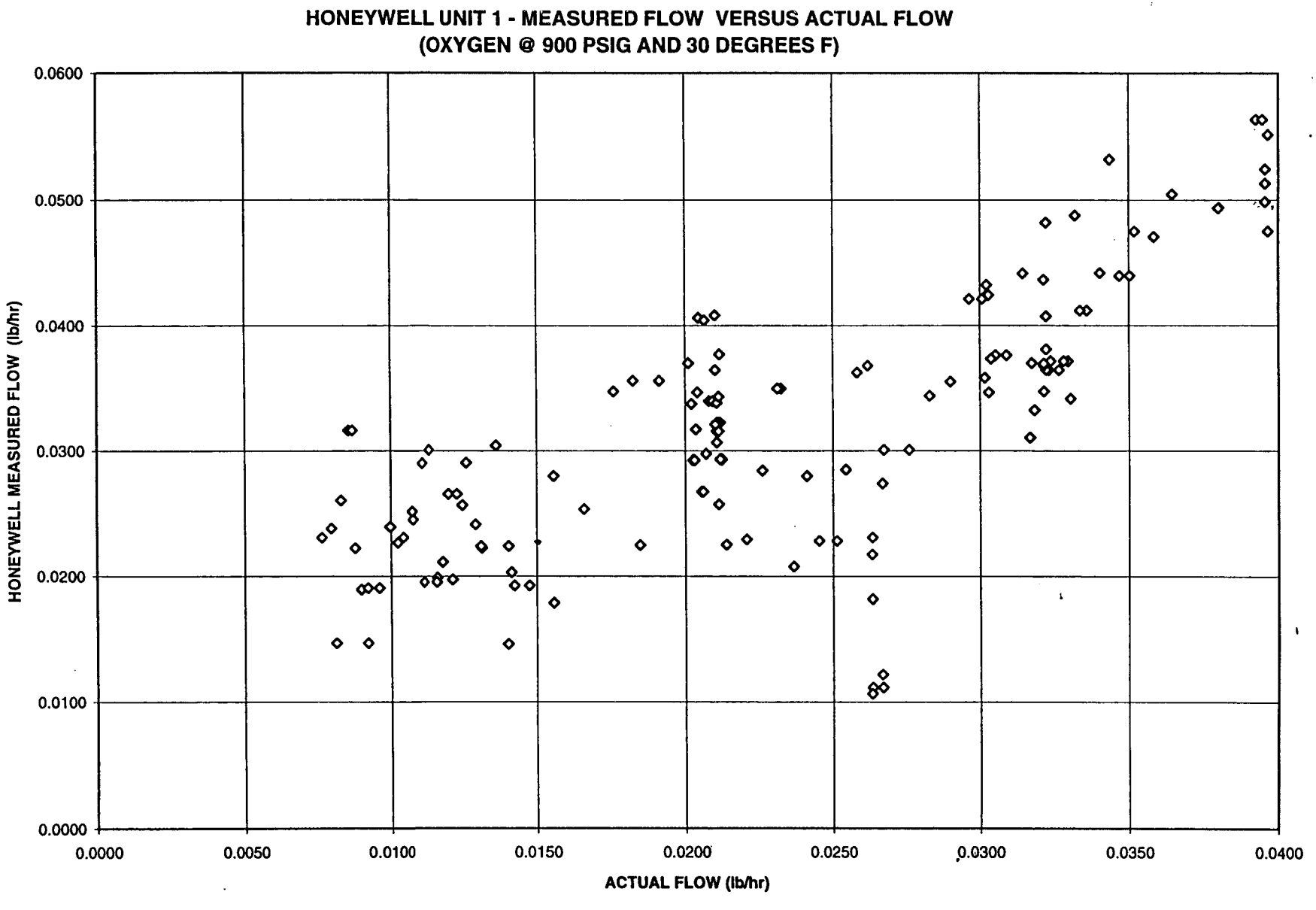
HONEYWELL UNIT 1 - MEASURED FLOW VERSUS ACTUAL FLOW
(OXYGEN @ 900 PSIG AND 30 DEGREES F)
HONEYWELL MEASURED FLOW (lb/hr)
0.0600
0.0500
0.0400
0.0300
0.0200
0.0100
0.0000
0.0000
0.0050
0.0100
0.0150
0.0200
0.0250
0.0300
0.0350
0.0400
ACTUAL FLOW (lb/hr)

Figure 76

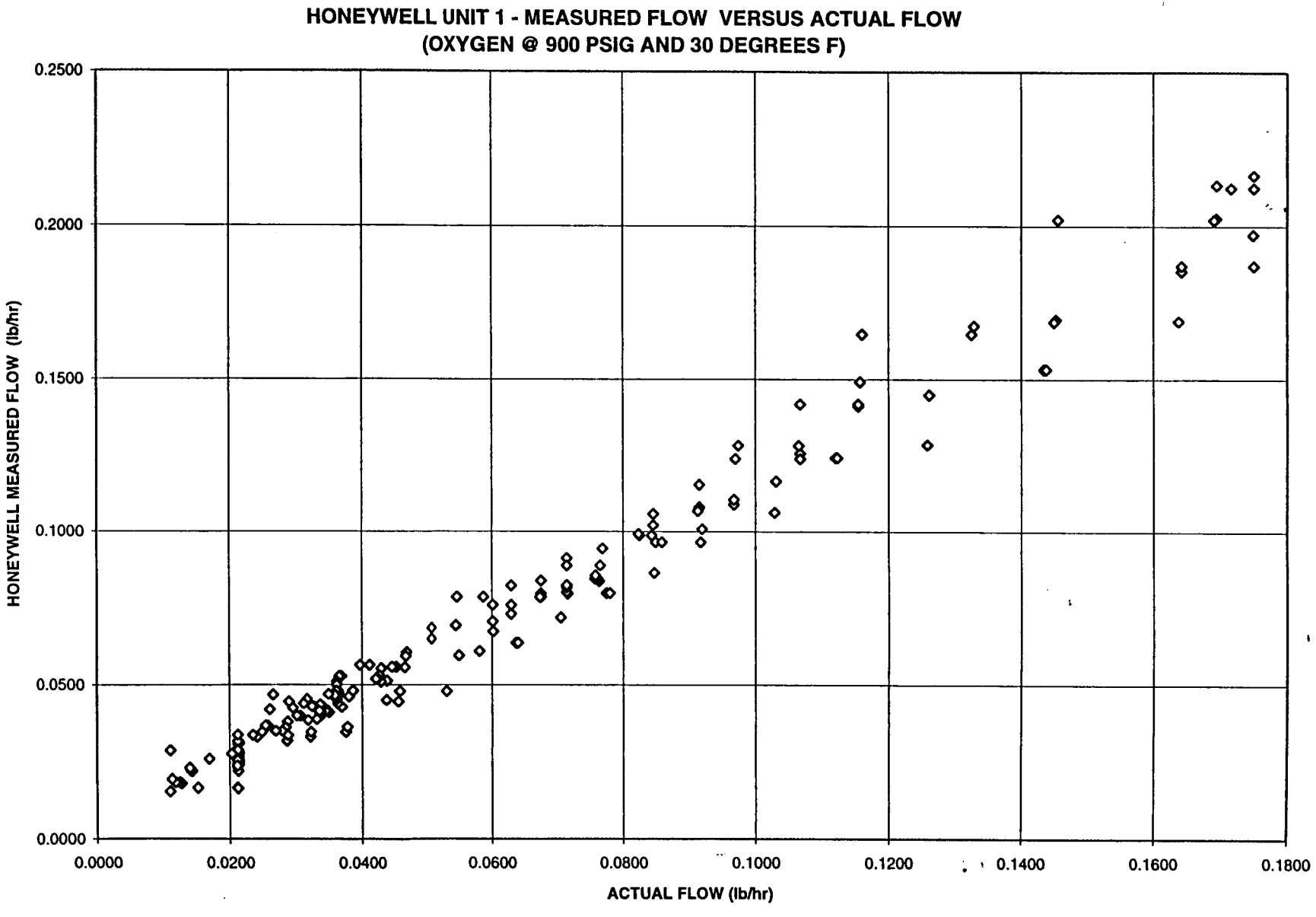
HONEYWELL UNIT 1 - MEASURED FLOW VERSUS ACTUAL FLOW
(OXYGEN @ 900 PSIG AND 30 DEGREES F)
HONEYWELL MEASURED FLOW (lb/hr)
0.2500
0.2000
0.1500
0.1000
0.0500
0.0000
0.0000
0.0200
0.0400
0.0600
0.0800
0.1000
0.1200
0.1400
0.1600
0.1800
ACTUAL FLOW (lb/hr)

Figure 77

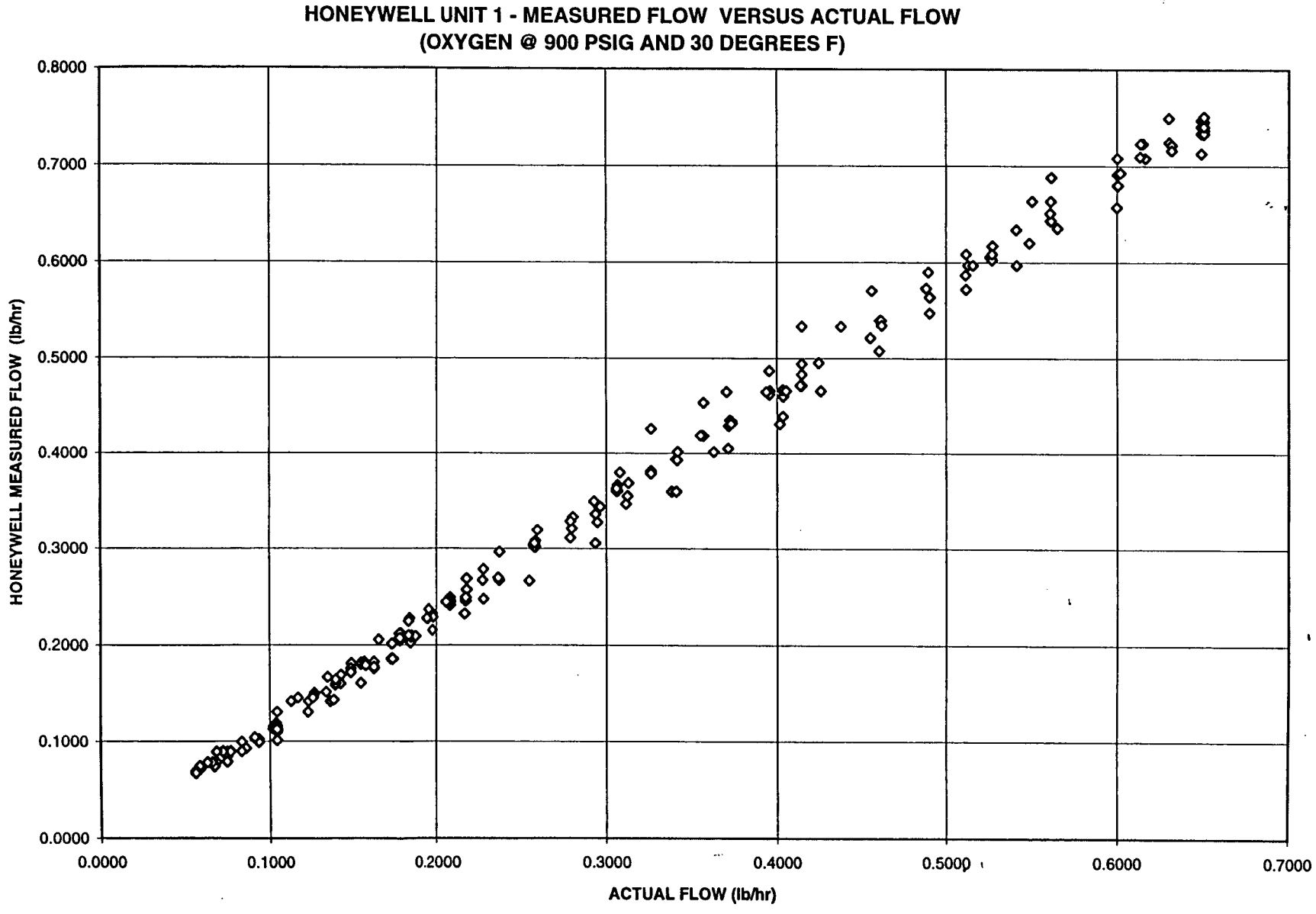
HONEYWELL UNIT 1 - MEASURED FLOW VERSUS ACTUAL FLOW
(OXYGEN @ 900 PSIG AND 30 DEGREES F)
HONEYWELL MEASURED FLOW (lb/hr)
0.8000
0.7000
0.6000
0.5000
0.4000
0.3000
0.2000
0.1000
0.0000
0.0000
0.1000
0.2000
0.3000
0.4000
0.5000
0.6000
0.7000
ACTUAL FLOW (lb/hr)

Figure 78

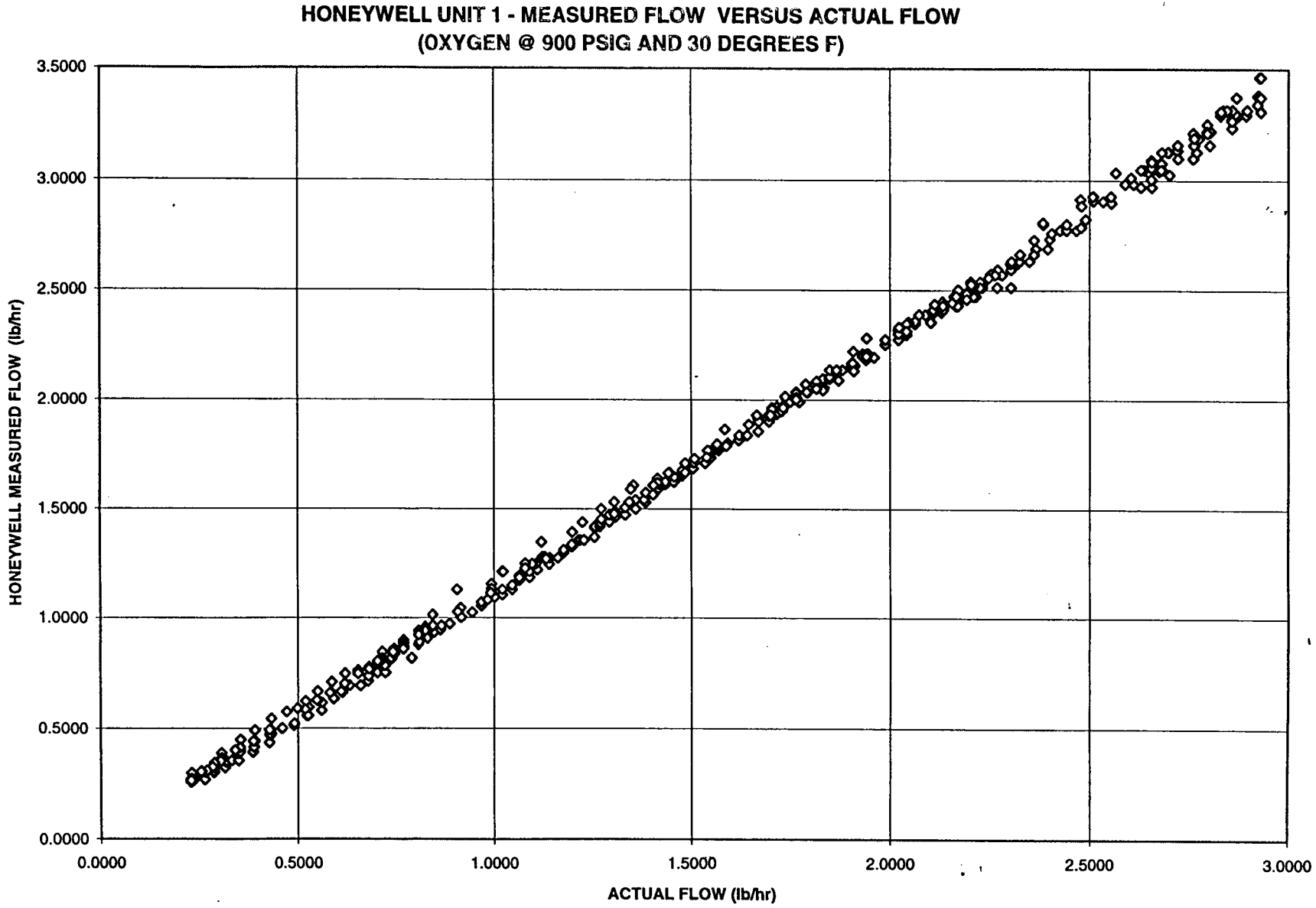
HONEYWELL UNIT 1 - MEASURED FLOW VERSUS ACTUAL FLOW
(OXYGEN @ 900 PSIG AND 30 DEGREES F)
HONEYWELL MEASURED FLOW (lb/hr)
3.5000
3.0000
2.5000
2.0000
1.5000
1.0000
0.5000
0.0000
0.0000
0.5000
1.0000
1.5000
2.0000
2.5000
3.0000
ACTUAL FLOW (lb/hr)

Figure 79

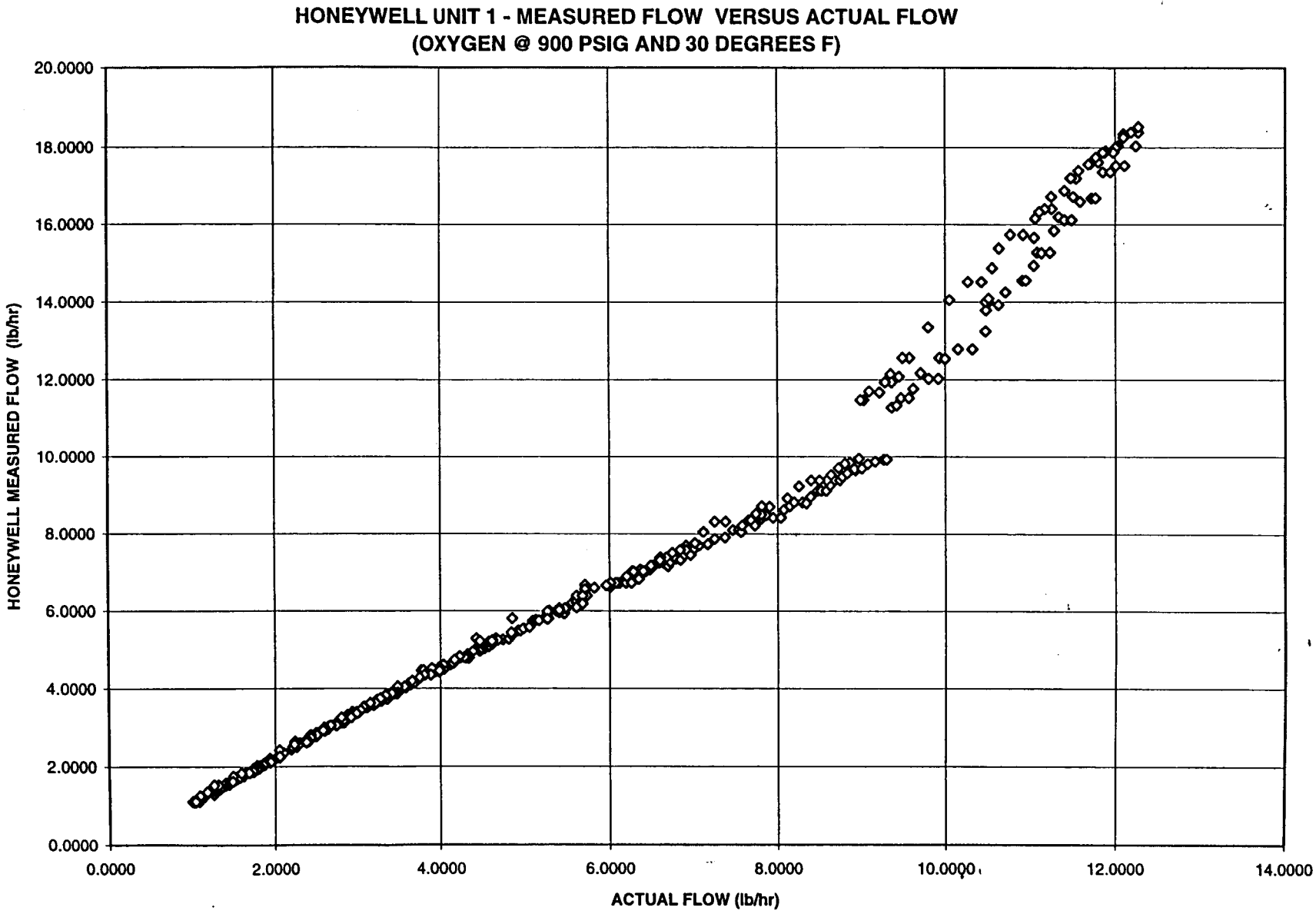
HONEYWELL UNIT 1 - MEASURED FLOW VERSUS ACTUAL FLOW
(OXYGEN @ 900 PSIG AND 30 DEGREES F)
HONEYWELL MEASURED FLOW (lb/hr)
20.0000
18.0000
16.0000
14.0000
12.0000
10.0000
8.0000
6.0000
4.0000
2.0000
0.0000
0.0000
2.0000
4.0000
6.0000
8.0000
10.0000
12.0000
14.0000
ACTUAL FLOW (lb/hr)

Figure 80

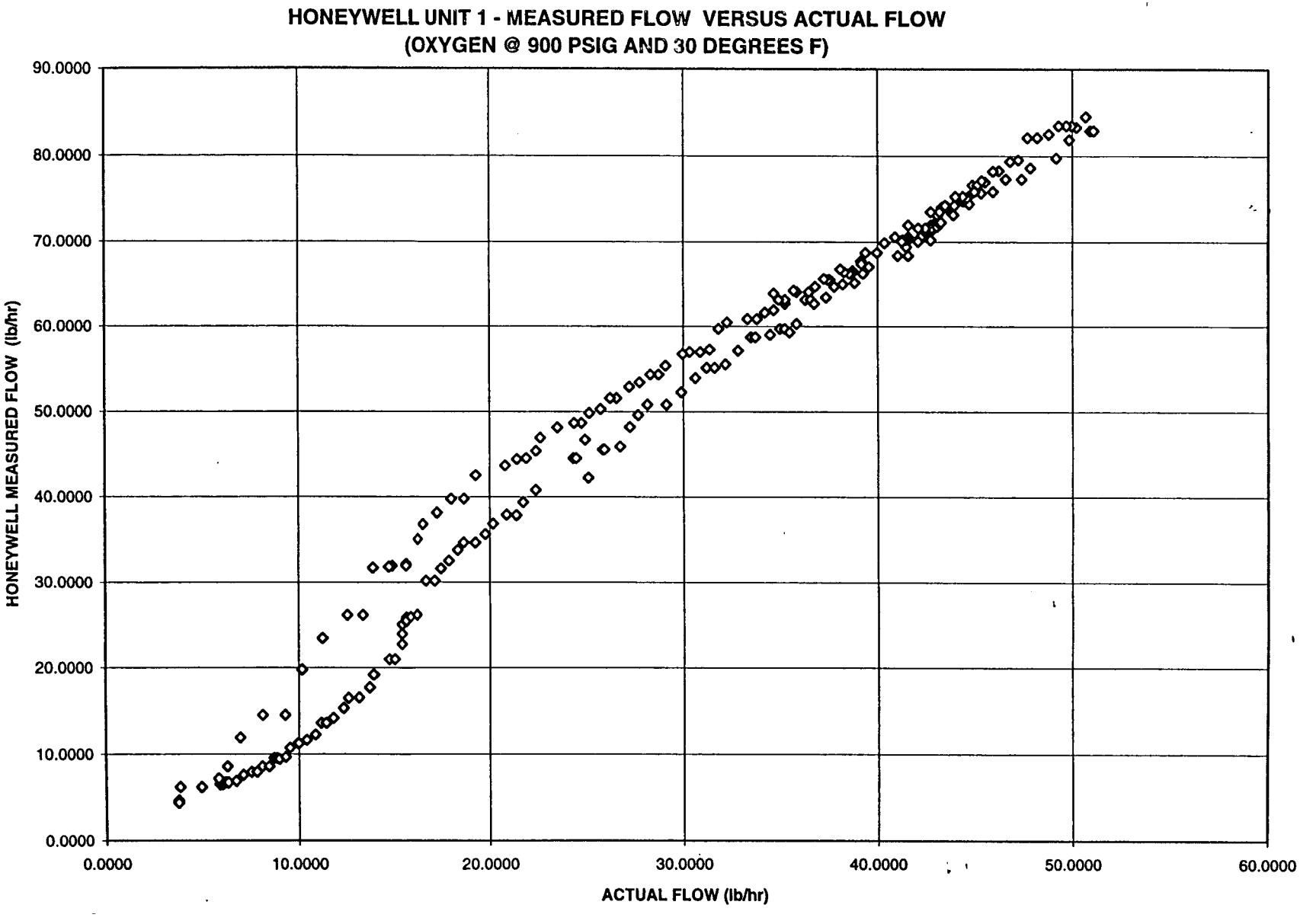
HONEYWELL UNIT 1 - MEASURED FLOW VERSUS ACTUAL FLOW
(OXYGEN @ 900 PSIG AND 30 DEGREES F)
HONEYWELL MEASURED FLOW (lb/hr)
90.0000
80.0000
70.0000
60.0000
50.0000
40.0000
30.0000
20.0000
10.0000
0.0000
0.0000
10.0000
20.0000
30.0000
40.0000
50.0000
60.0000
ACTUAL FLOW (lb/hr)

Figure 81

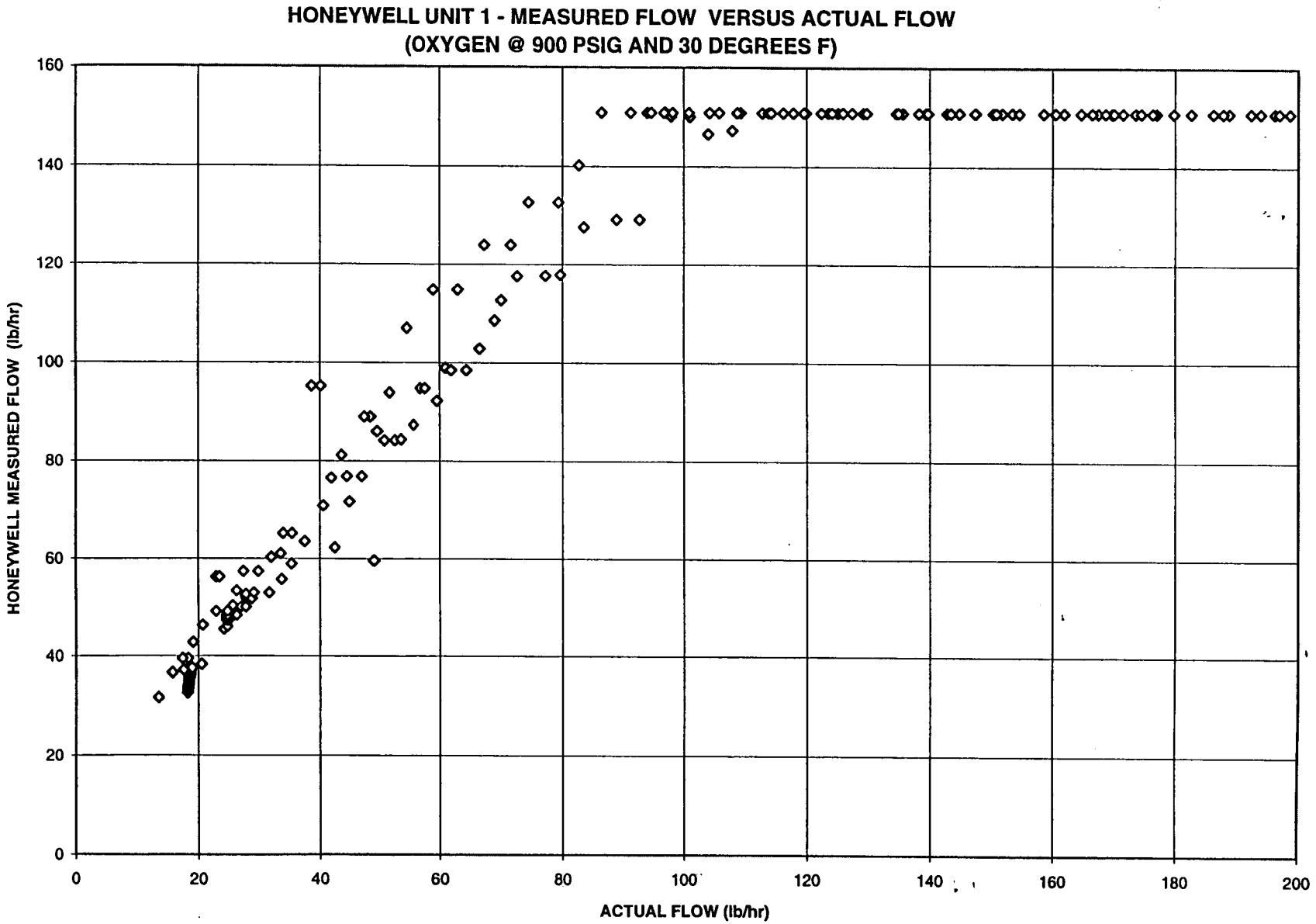
HONEYWELL UNIT 1 - MEASURED FLOW VERSUS ACTUAL FLOW
(OXYGEN @ 900 PSIG AND 30 DEGREES F)
HONEYWELL MEASURED FLOW (lb/hr)
ACTUAL FLOW (lb/hr)
0
20
40
60
80
100
120
140
160
180
200

Figure 82

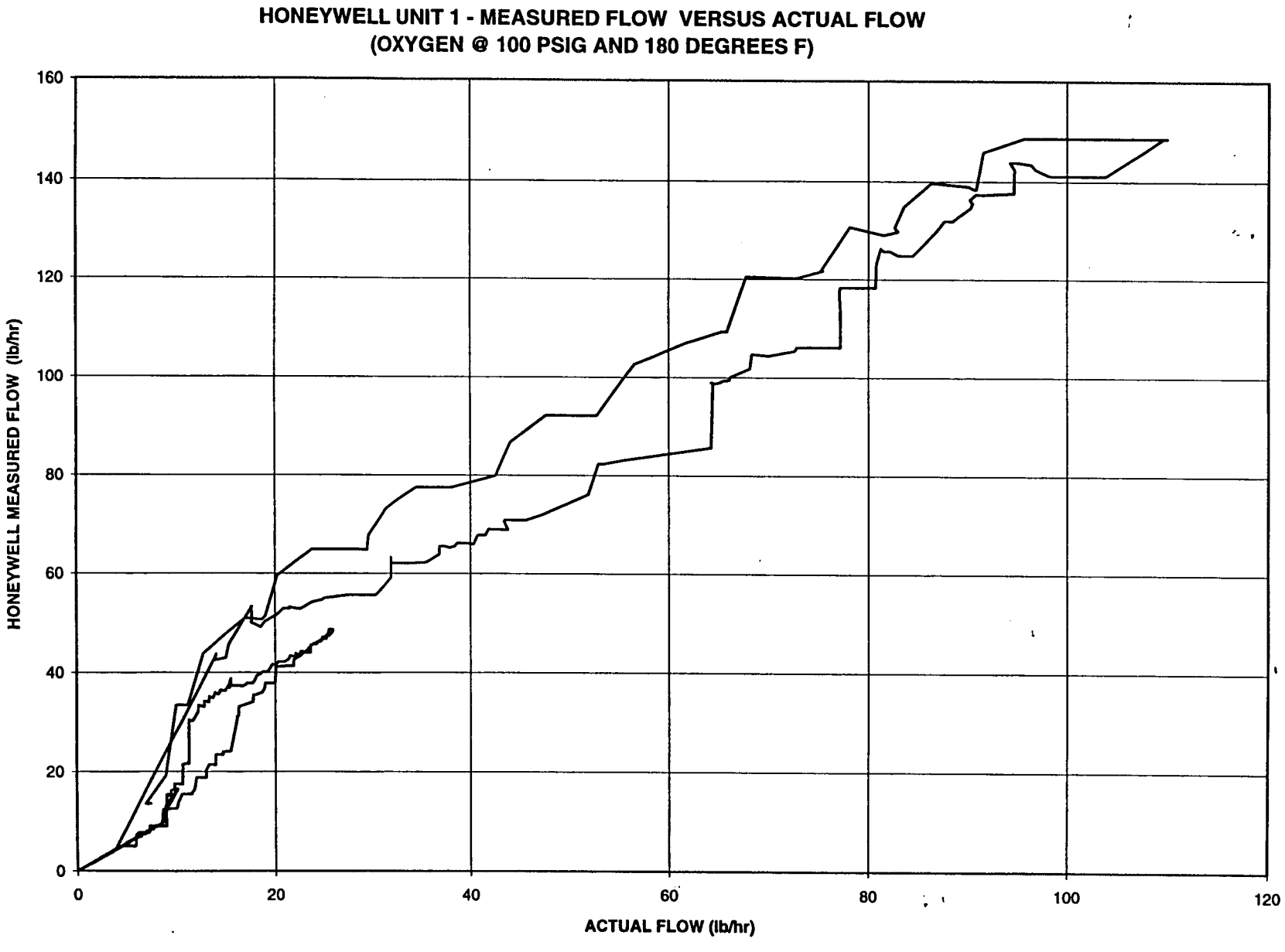
HONEYWELL UNIT 1 - MEASURED FLOW VERSUS ACTUAL FLOW
(OXYGEN @ 100 PSIG AND 180 DEGREES F)
HONEYWELL MEASURED FLOW (lb/hr)
160
140
120
100
80
60
40
20
0
0
20
40
60
80
100
120
ACTUAL FLOW (lb/hr)

Figure 83

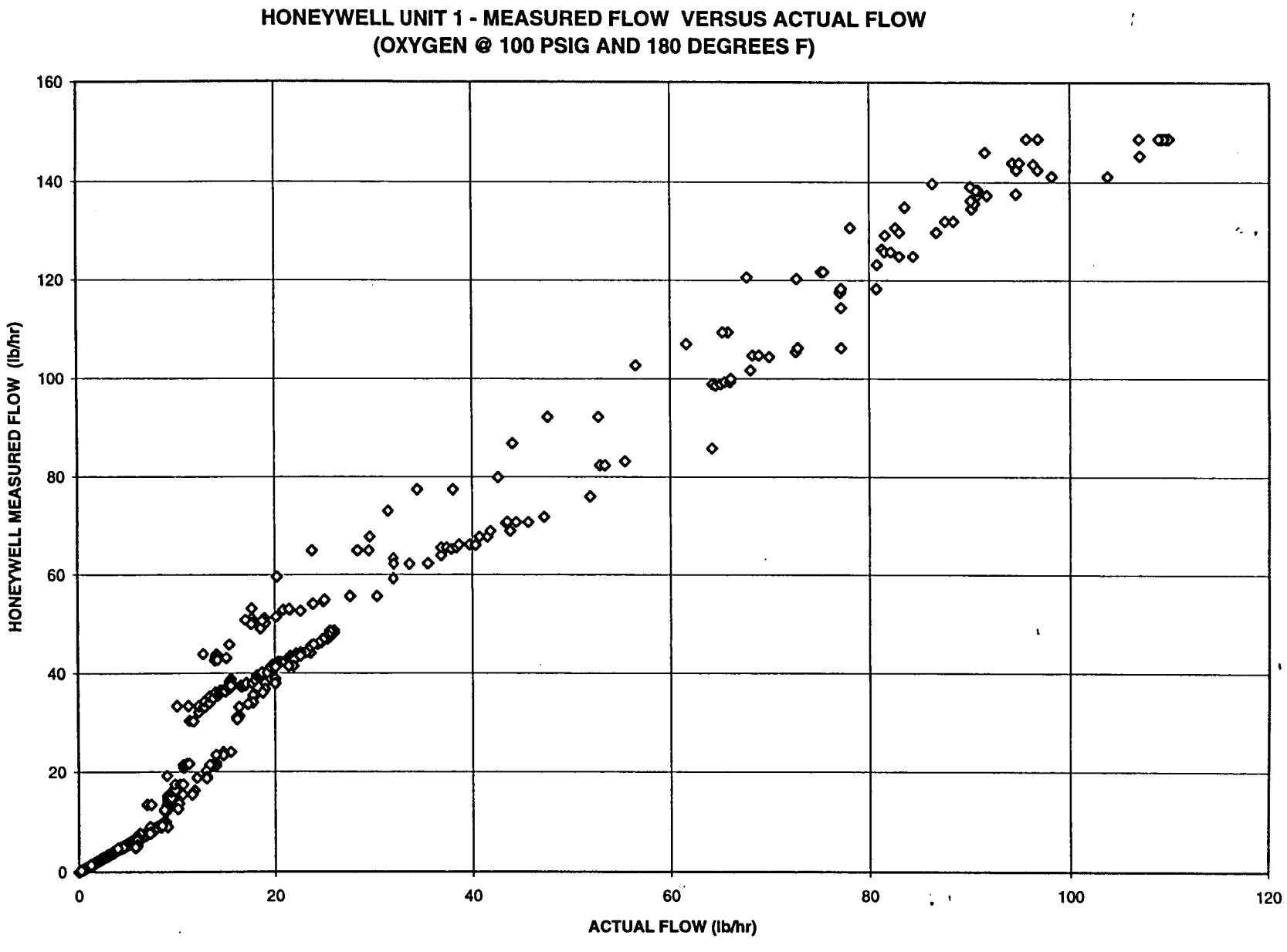
HONEYWELL UNIT 1 - MEASURED FLOW VERSUS ACTUAL FLOW
(OXYGEN @ 100 PSIG AND 180 DEGREES F)
HONEYWELL MEASURED FLOW (lb/hr)
ACTUAL FLOW (lb/hr)
0
20
40
60
80
100
120
140
160

Figure 84

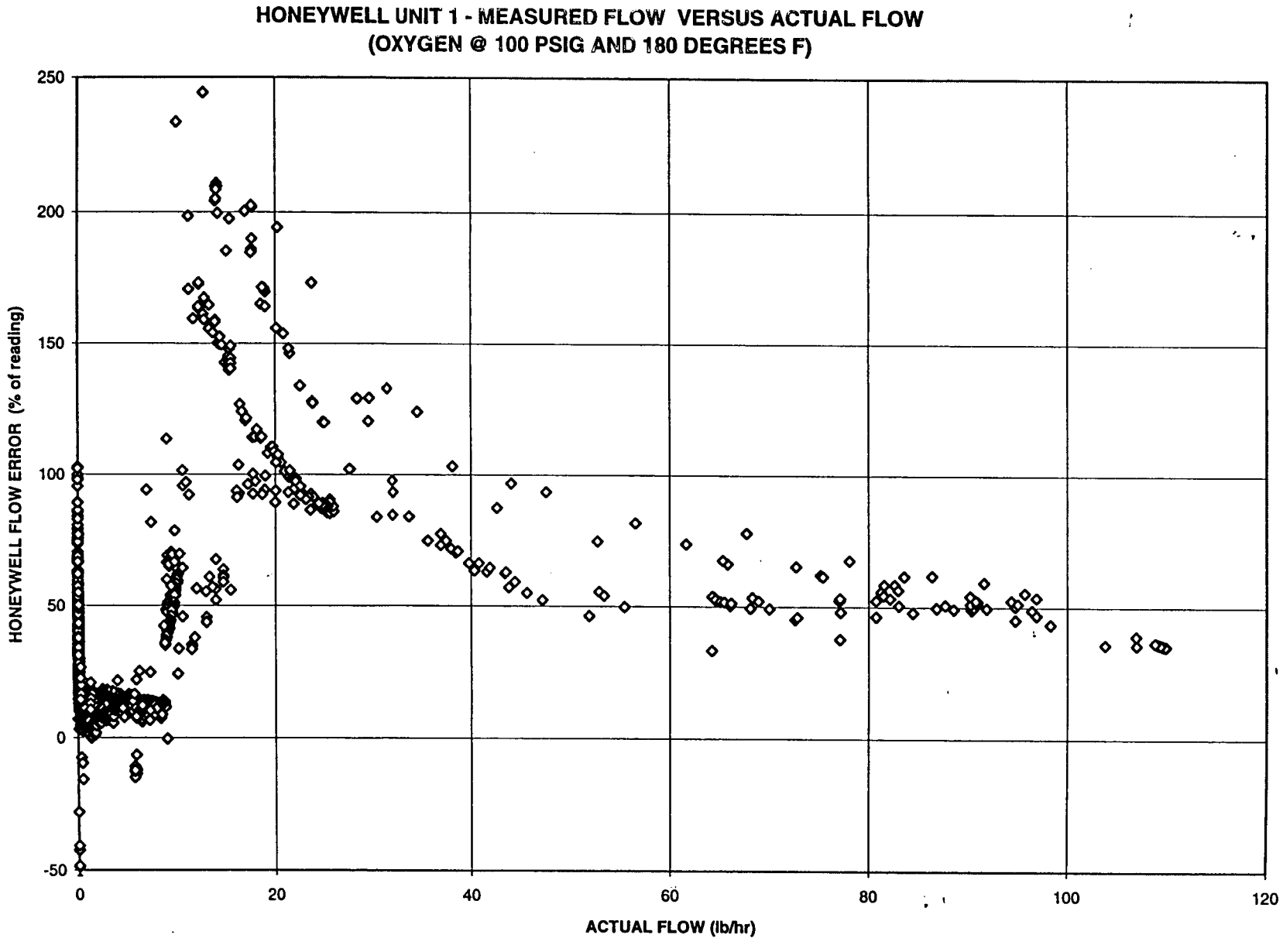
HONEYWELL UNIT 1 - MEASURED FLOW VERSUS ACTUAL FLOW
(OXYGEN @ 100 PSIG AND 180 DEGREES F)
HONEYWELL FLOW ERROR (% of reading)
250
200
150
100
50
0
-50
0
20
40
60
80
100
120
ACTUAL FLOW (lb/hr)

Figure 85

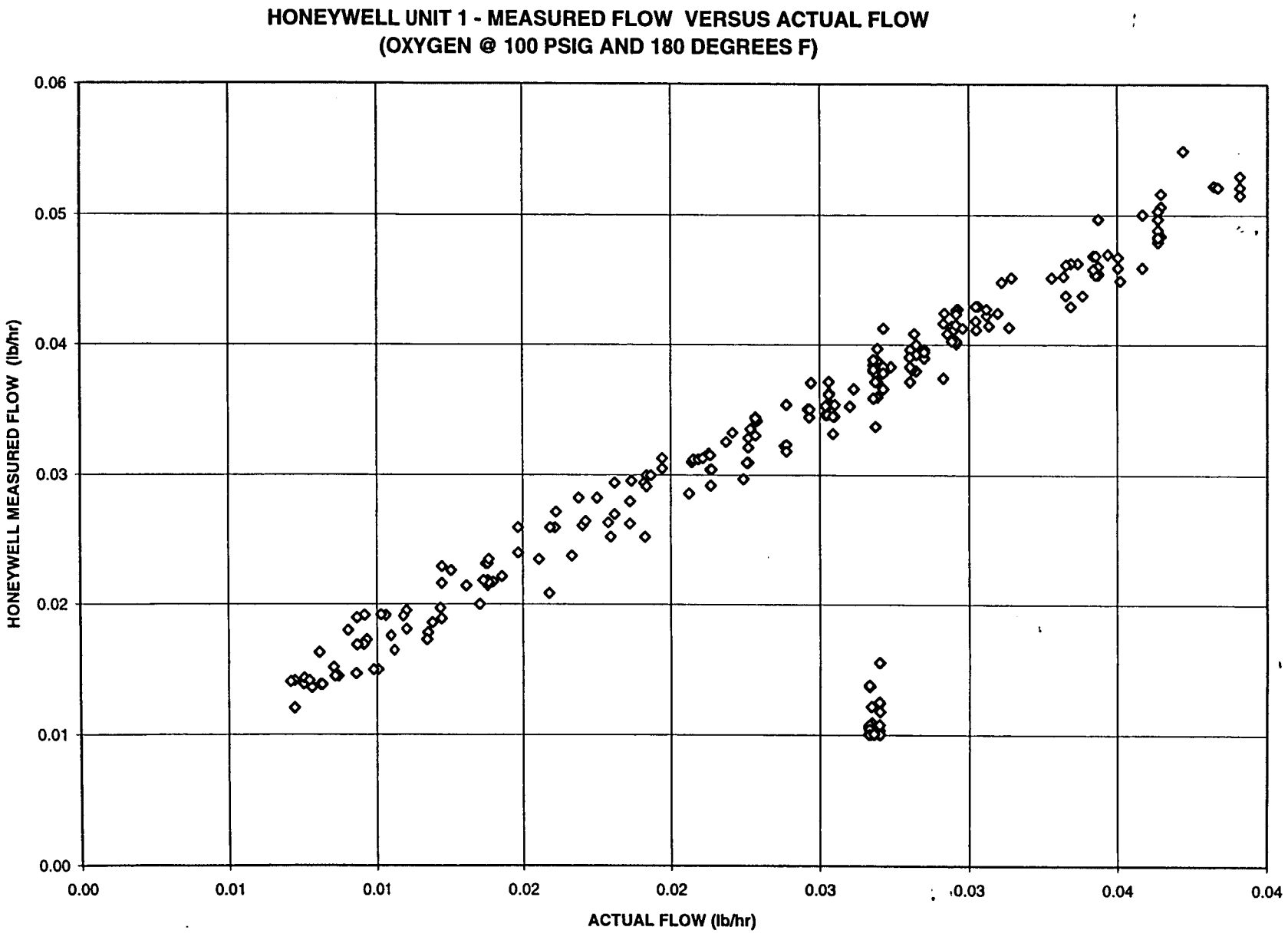
HONEYWELL UNIT 1 - MEASURED FLOW VERSUS ACTUAL FLOW
(OXYGEN @ 100 PSIG AND 180 DEGREES F)
HONEYWELL MEASURED FLOW (lb/hr)
0.06
0.05
0.04
0.03
0.02
0.01
0.00
0.00
0.01
0.01
0.02
0.02
0.03
0.03
0.04
0.04
ACTUAL FLOW (lb/hr)

Figure 86

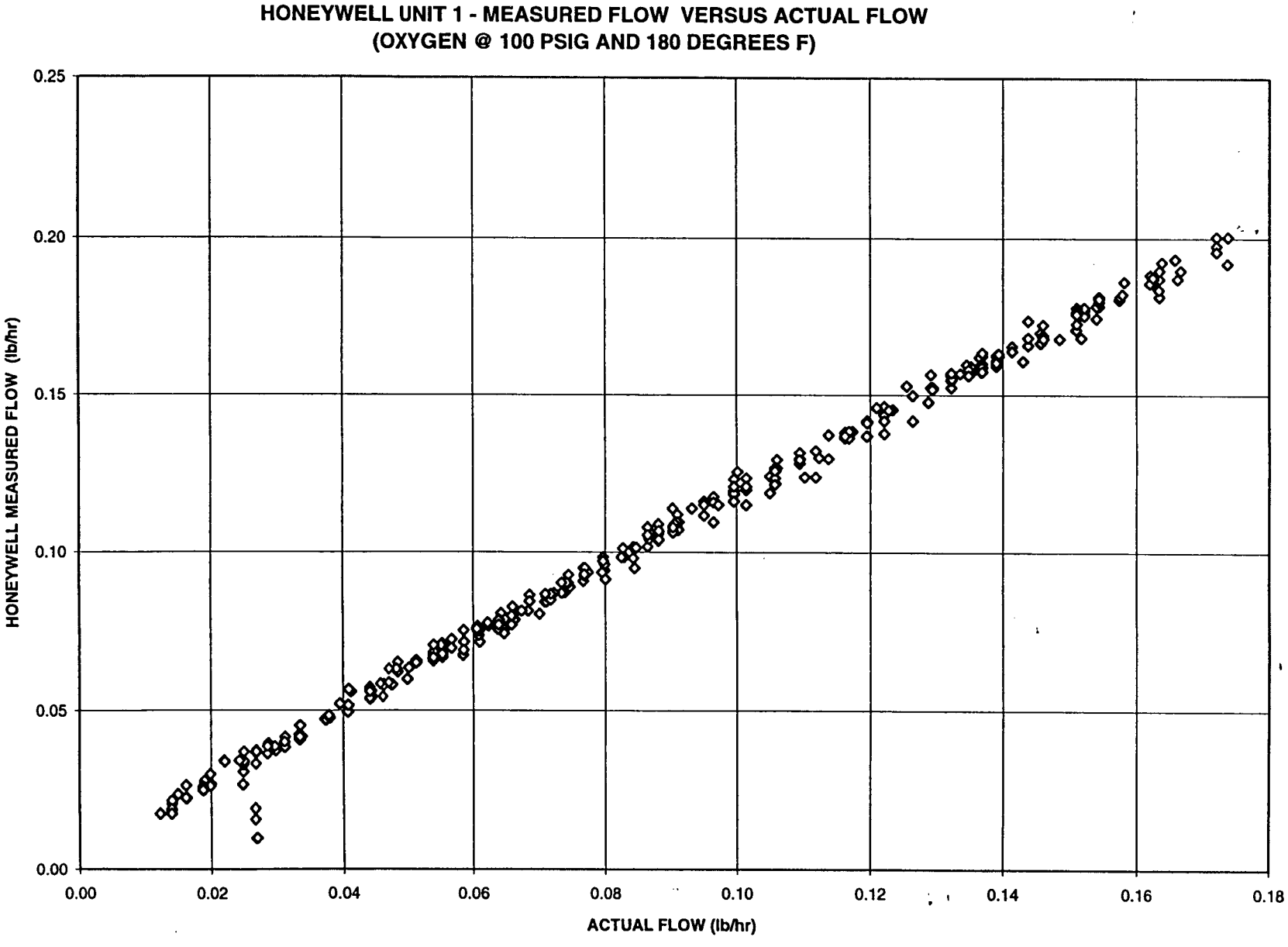
HONEYWELL UNIT 1 - MEASURED FLOW VERSUS ACTUAL FLOW
(OXYGEN @ 100 PSIG AND 180 DEGREES F)
HONEYWELL MEASURED FLOW (lb/hr)
0.25
0.20
0.15
0.10
0.05
0.00
0.00
0.02
0.04
0.06
0.08
0.10
0.12
0.14
0.16
0.18
ACTUAL FLOW (lb/hr)

Figure 87

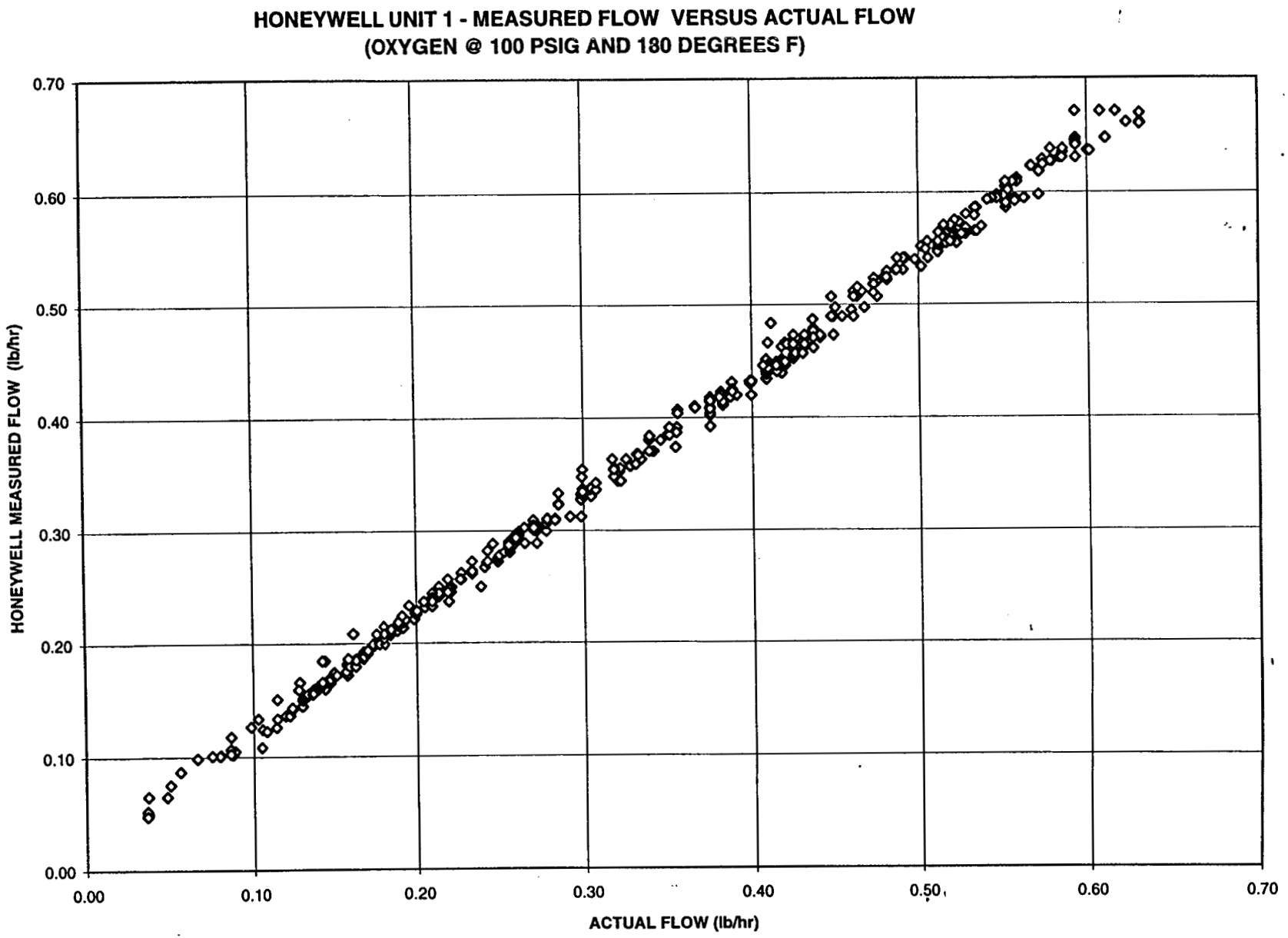
HONEYWELL UNIT 1 - MEASURED FLOW VERSUS ACTUAL FLOW
(OXYGEN @ 100 PSIG AND 180 DEGREES F)
HONEYWELL MEASURED FLOW (lb/hr)
0.70
0.60
0.50
0.40
0.30
0.20
0.10
0.00
0.00
0.10
0.20
0.30
0.40
0.50
0.60
0.70
ACTUAL FLOW (lb/hr)

Figure 88

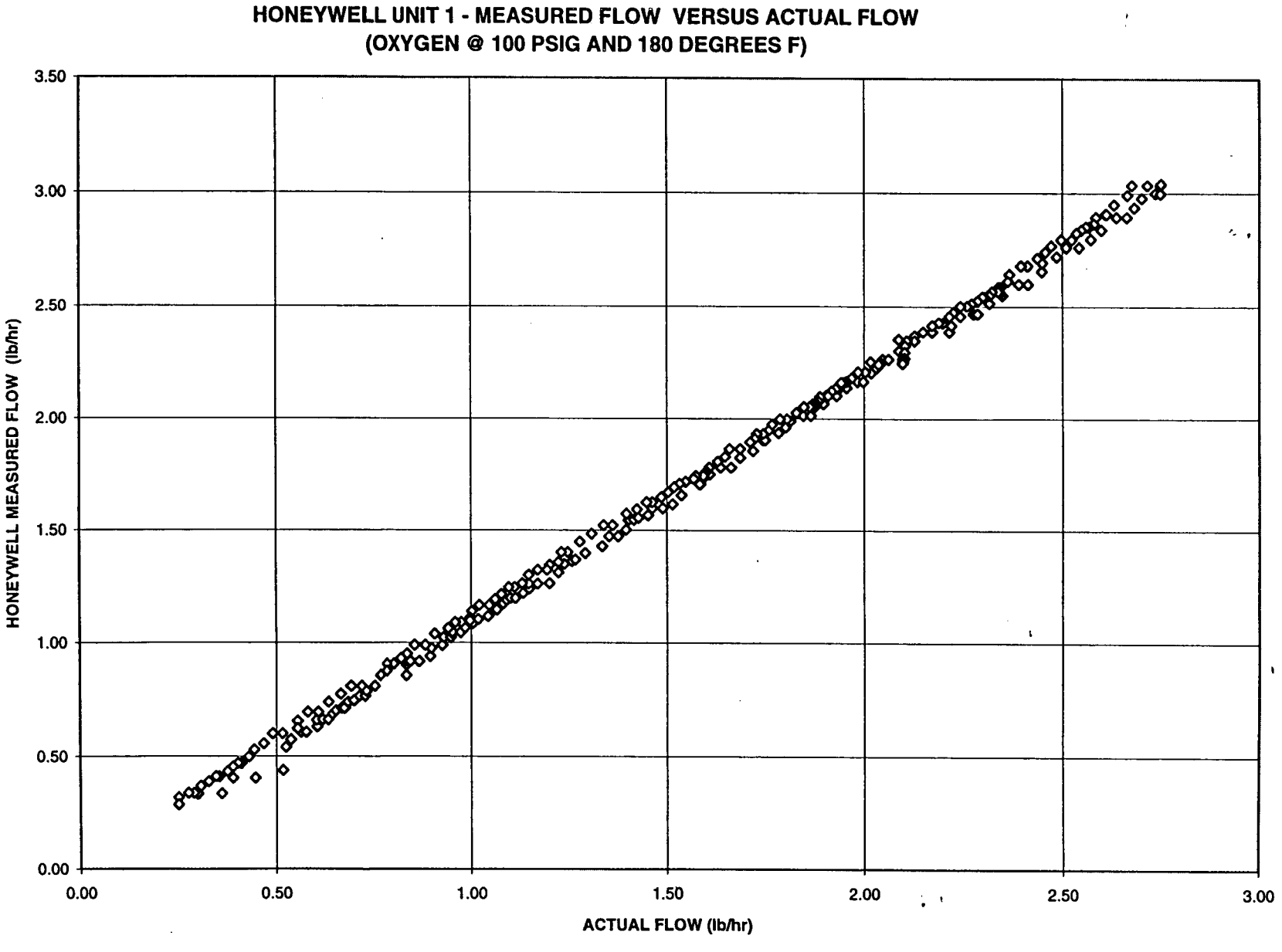
HONEYWELL UNIT 1 - MEASURED FLOW VERSUS ACTUAL FLOW
(OXYGEN @ 100 PSIG AND 180 DEGREES F)
HONEYWELL MEASURED FLOW (lb/hr)
3.50
3.00
2.50
2.00
1.50
1.00
0.50
0.00
0.00
0.50
1.00
1.50
2.00
2.50
3.00
ACTUAL FLOW (lb/hr)

Figure 89

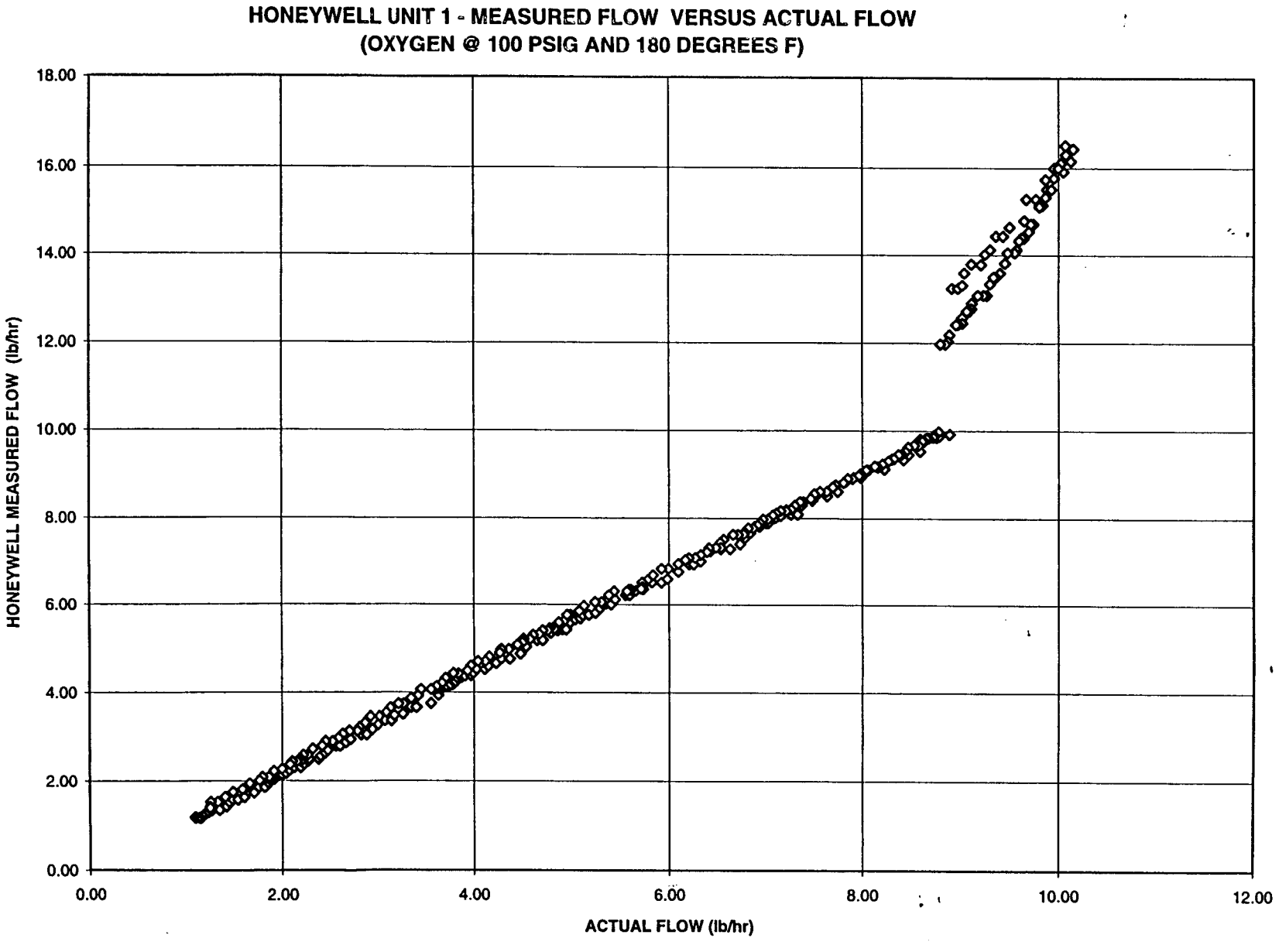
HONEYWELL UNIT 1 - MEASURED FLOW VERSUS ACTUAL FLOW
(OXYGEN @ 100 PSIG AND 180 DEGREES F)
HONEYWELL MEASURED FLOW (lb/hr)
18.00
16.00
14.00
12.00
10.00
8.00
6.00
4.00
2.00
0.00
0.00
2.00
4.00
6.00
8.00
10.00
12.00
ACTUAL FLOW (lb/hr)

Figure 90

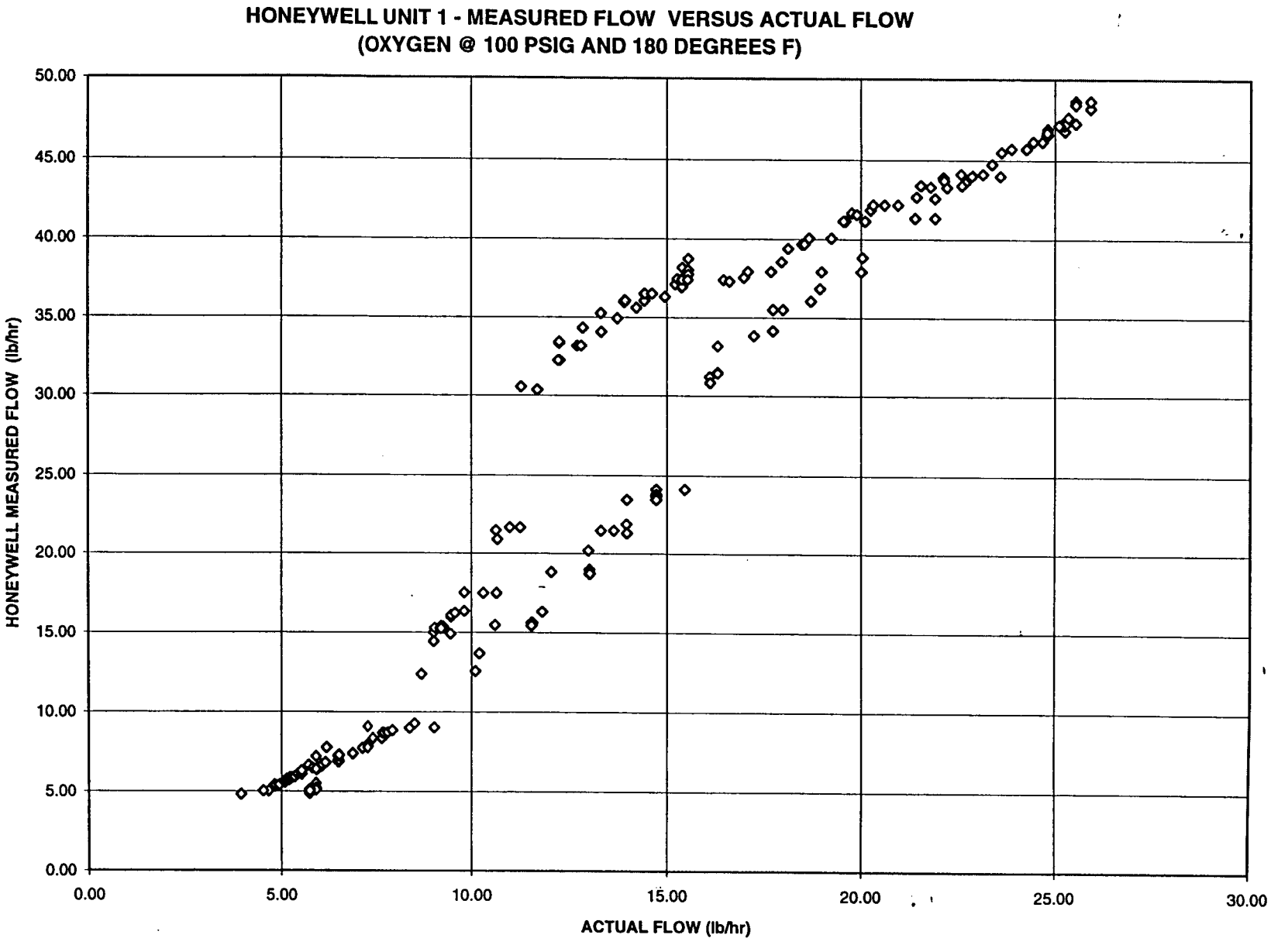
HONEYWELL UNIT 1 - MEASURED FLOW VERSUS ACTUAL FLOW
(OXYGEN @ 100 PSIG AND 180 DEGREES F)
HONEYWELL MEASURED FLOW (lb/hr)
50.00
45.00
40.00
35.00
30.00
25.00
20.00
15.00
10.00
5.00
0.00
0.00
5.00
10.00
15.00
20.00
25.00
30.00
ACTUAL FLOW (lb/hr)

Figure 91

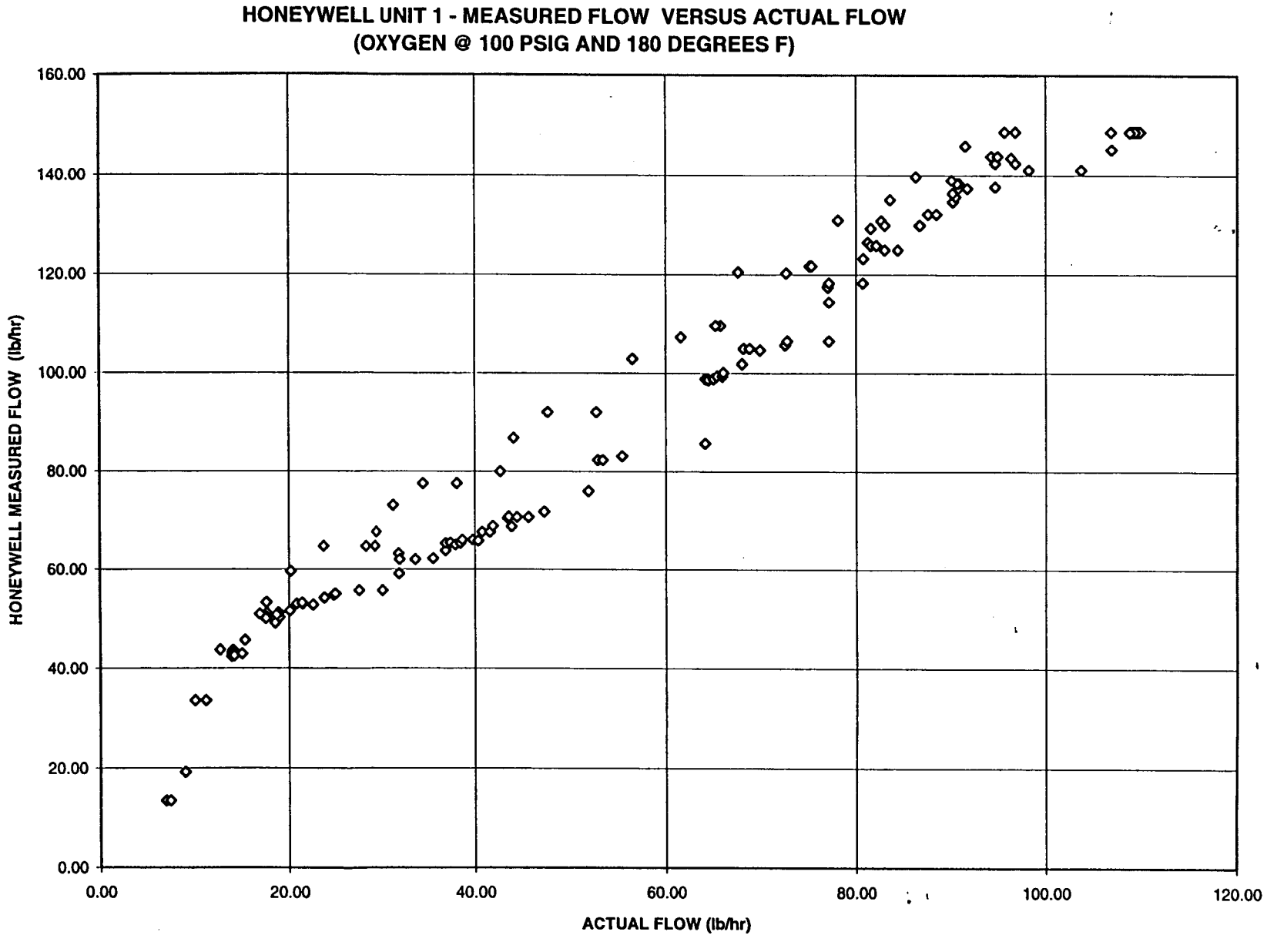
HONEYWELL UNIT 1 - MEASURED FLOW VERSUS ACTUAL FLOW
(OXYGEN @ 100 PSIG AND 180 DEGREES F)
HONEYWELL MEASURED FLOW (lb/hr)
160.00
140.00
120.00
100.00
80.00
60.00
40.00
20.00
0.00
0.00
20.00
40.00
60.00
80.00
100.00
120.00
ACTUAL FLOW (lb/hr)

Figure 92

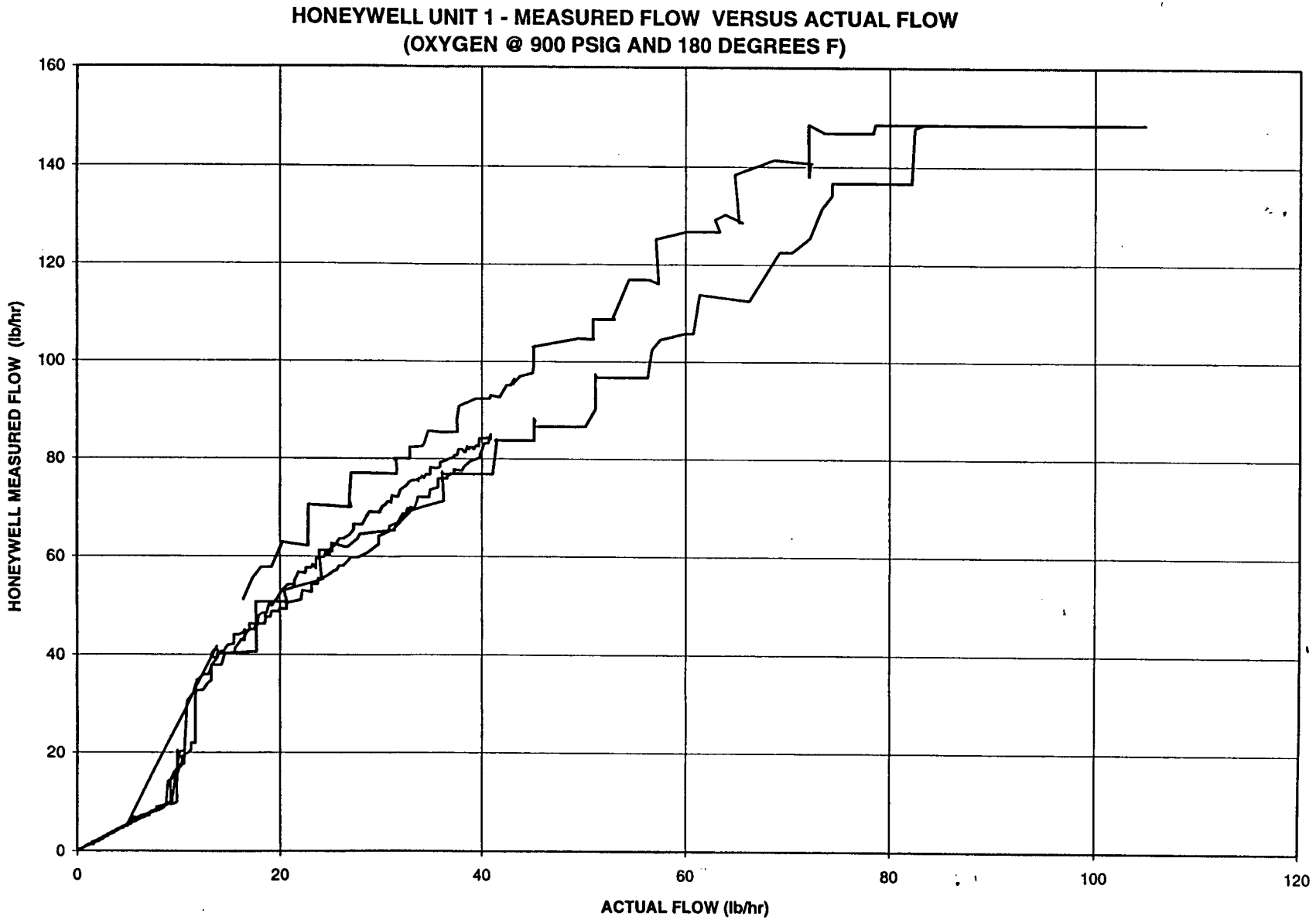
HONEYWELL UNIT 1 - MEASURED FLOW VERSUS ACTUAL FLOW
(OXYGEN @ 900 PSIG AND 180 DEGREES F)
HONEYWELL MEASURED FLOW (lb/hr)
160
140
120
100
80
60
40
20
0
0
20
40
60
80
100
120
ACTUAL FLOW (lb/hr)

Figure 93

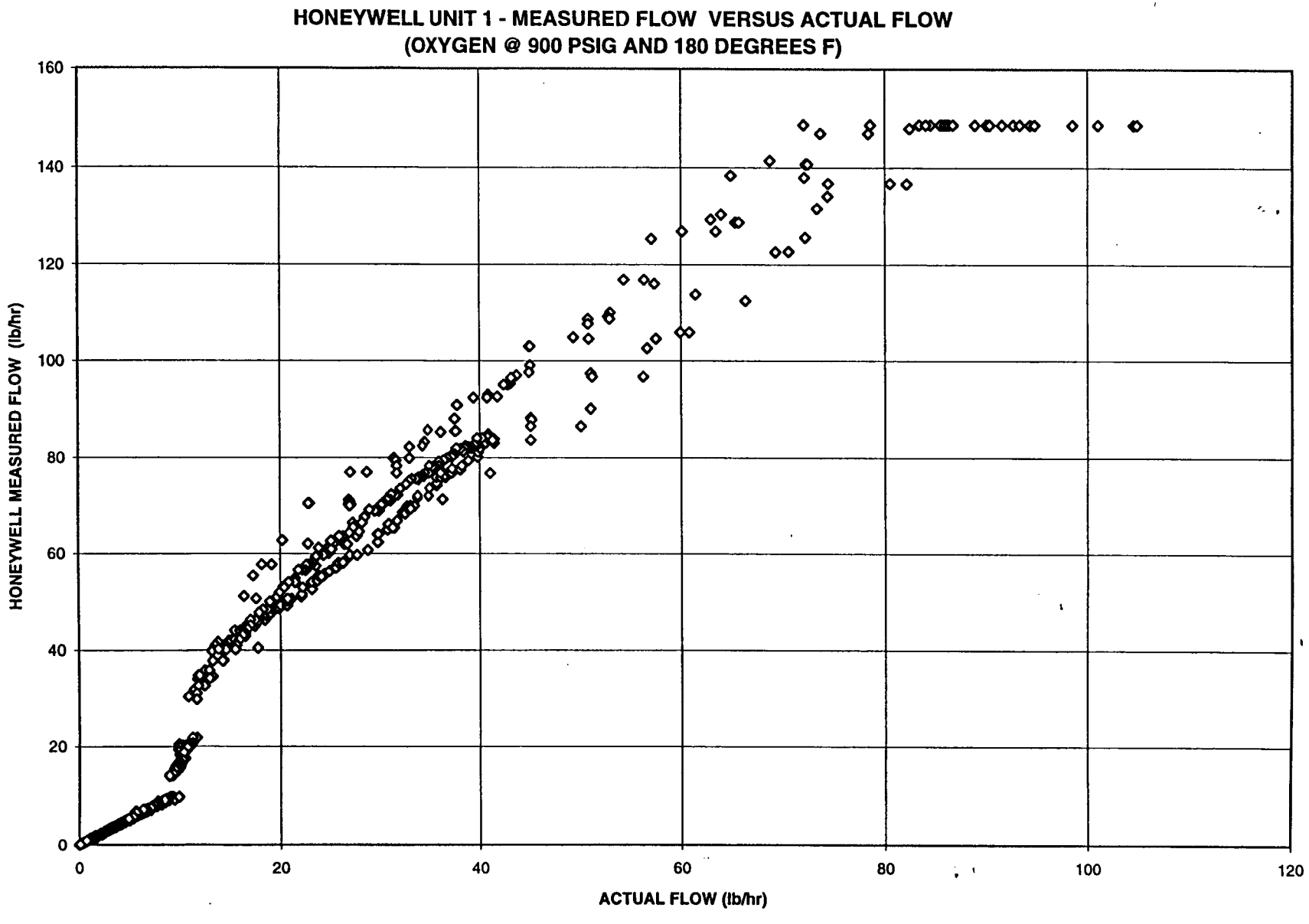
HONEYWELL UNIT 1 - MEASURED FLOW VERSUS ACTUAL FLOW
(OXYGEN @ 900 PSIG AND 180 DEGREES F)
HONEYWELL MEASURED FLOW (lb/hr)
ACTUAL FLOW (lb/hr)
0
20
40
60
80
100
120
140
160

Figure 94

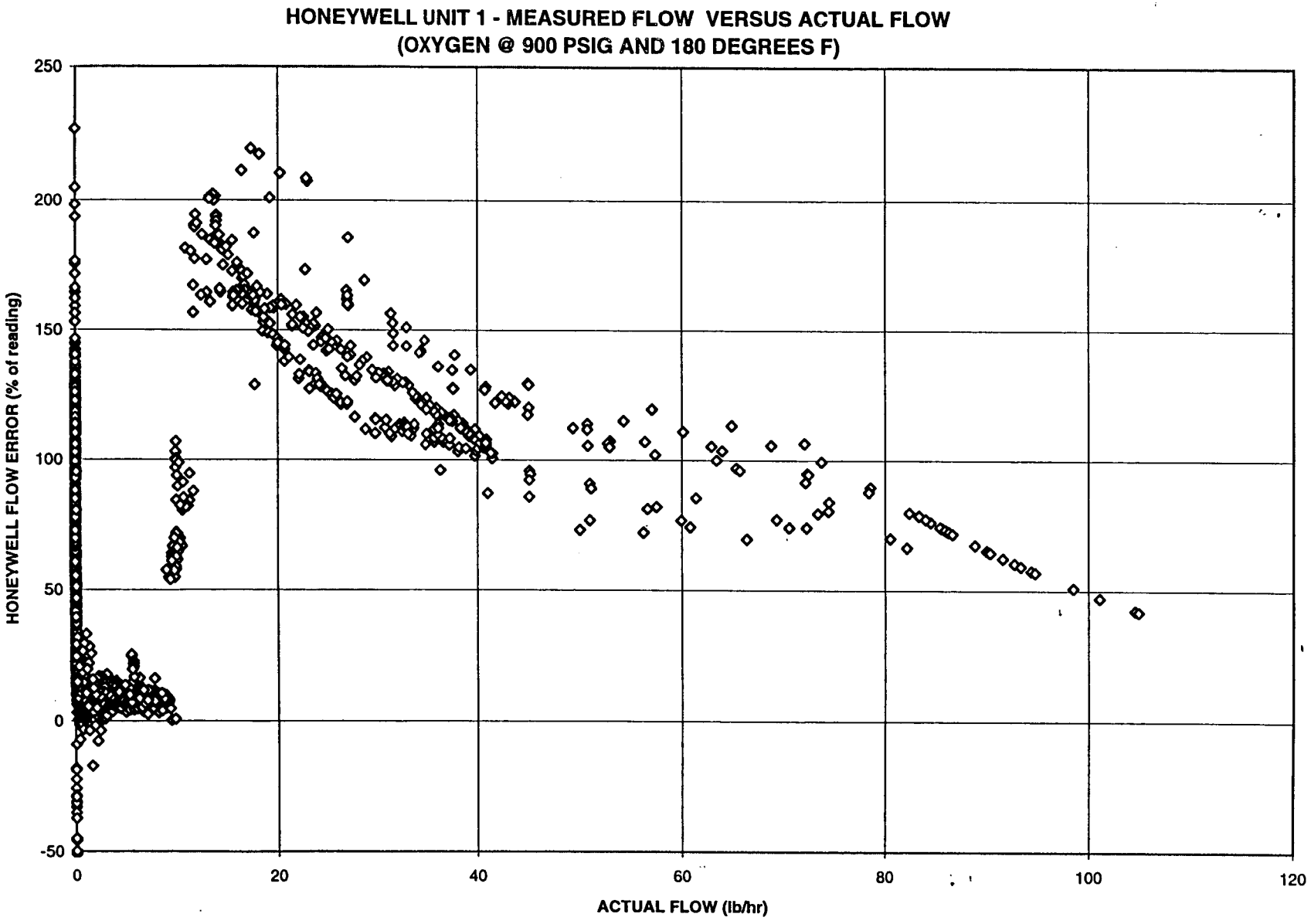
HONEYWELL UNIT 1 - MEASURED FLOW VERSUS ACTUAL FLOW
(OXYGEN @ 900 PSIG AND 180 DEGREES F)
HONEYWELL FLOW ERROR (% of reading)
250
200
150
100
50
0
-50
0
20
40
60
80
100
120
ACTUAL FLOW (lb/hr)

Figure 95

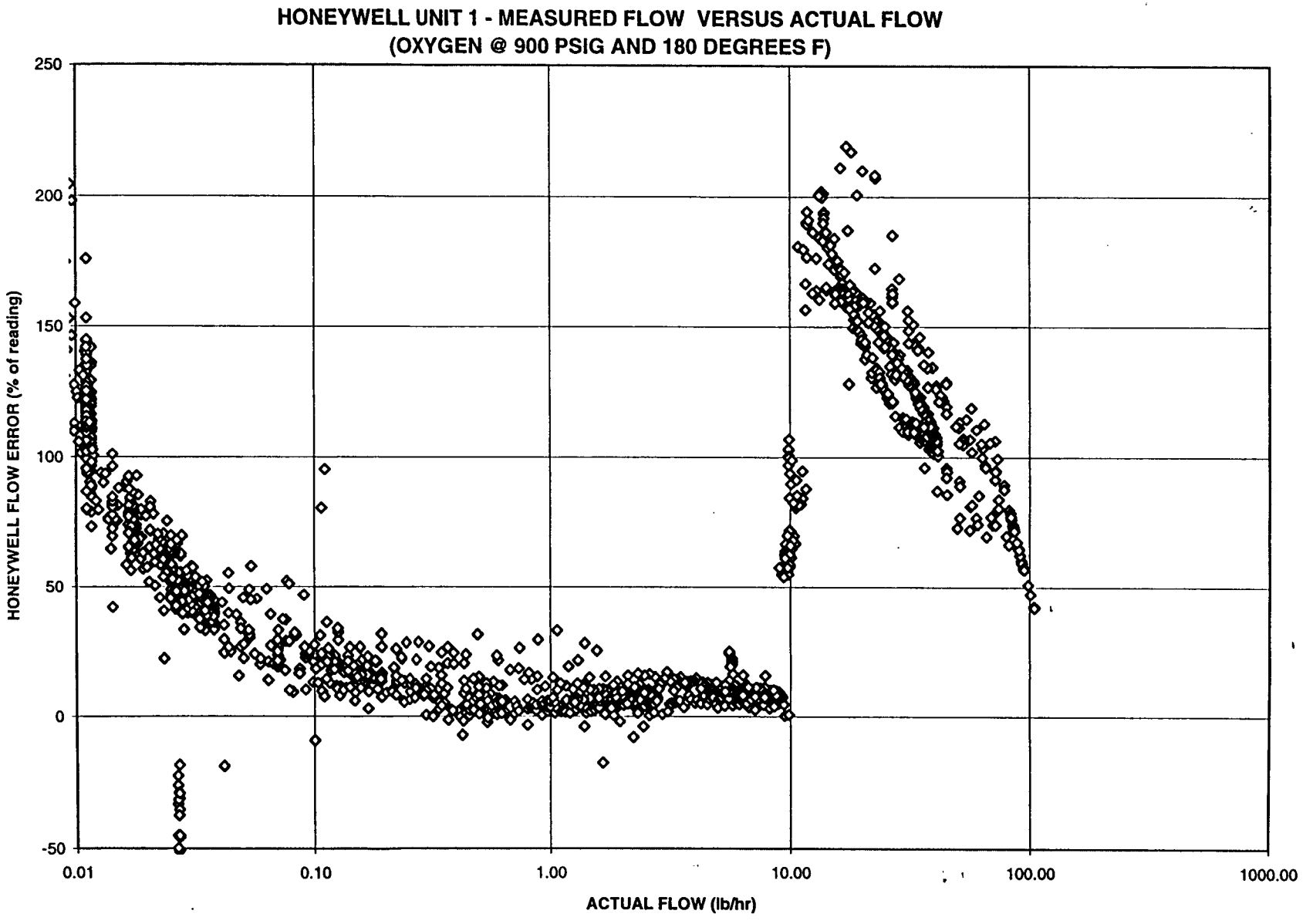
HONEYWELL UNIT 1 - MEASURED FLOW VERSUS ACTUAL FLOW
(OXYGEN @ 900 PSIG AND 180 DEGREES F)
HONEYWELL FLOW ERROR (% of reading)
250
200
150
100
50
0
-50
0.01
0.10
1.00
10.00
100.00
1000.00
ACTUAL FLOW (lb/hr)

Figure 96

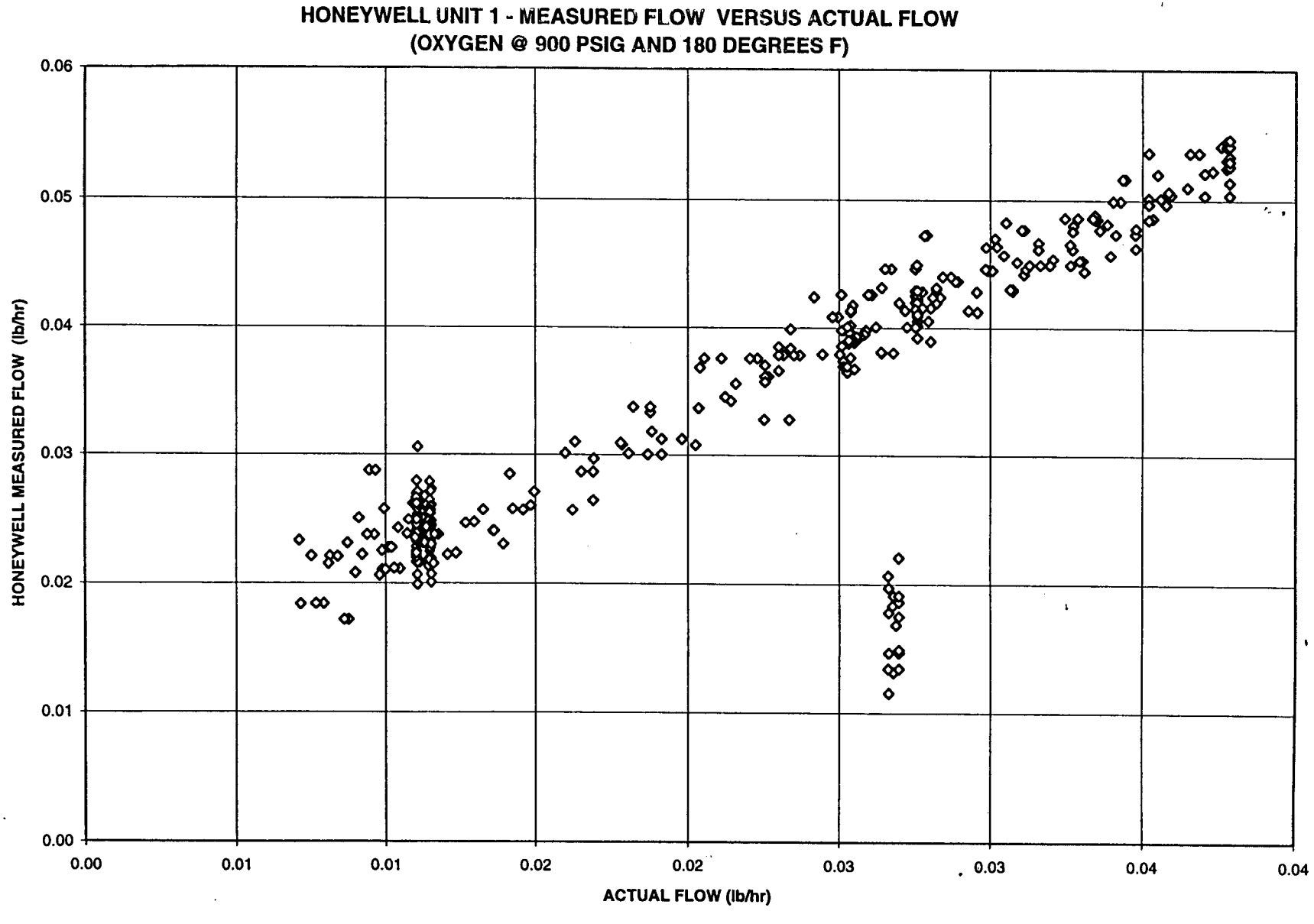
HONEYWELL UNIT 1 - MEASURED FLOW VERSUS ACTUAL FLOW
(OXYGEN @ 900 PSIG AND 180 DEGREES F)
HONEYWELL MEASURED FLOW (lb/hr)
0.06
0.05
0.04
0.03
0.02
0.01
0.00
0.00
0.01
0.01
0.02
0.02
0.03
0.03
0.04
0.04
ACTUAL FLOW (lb/hr)

Figure 97

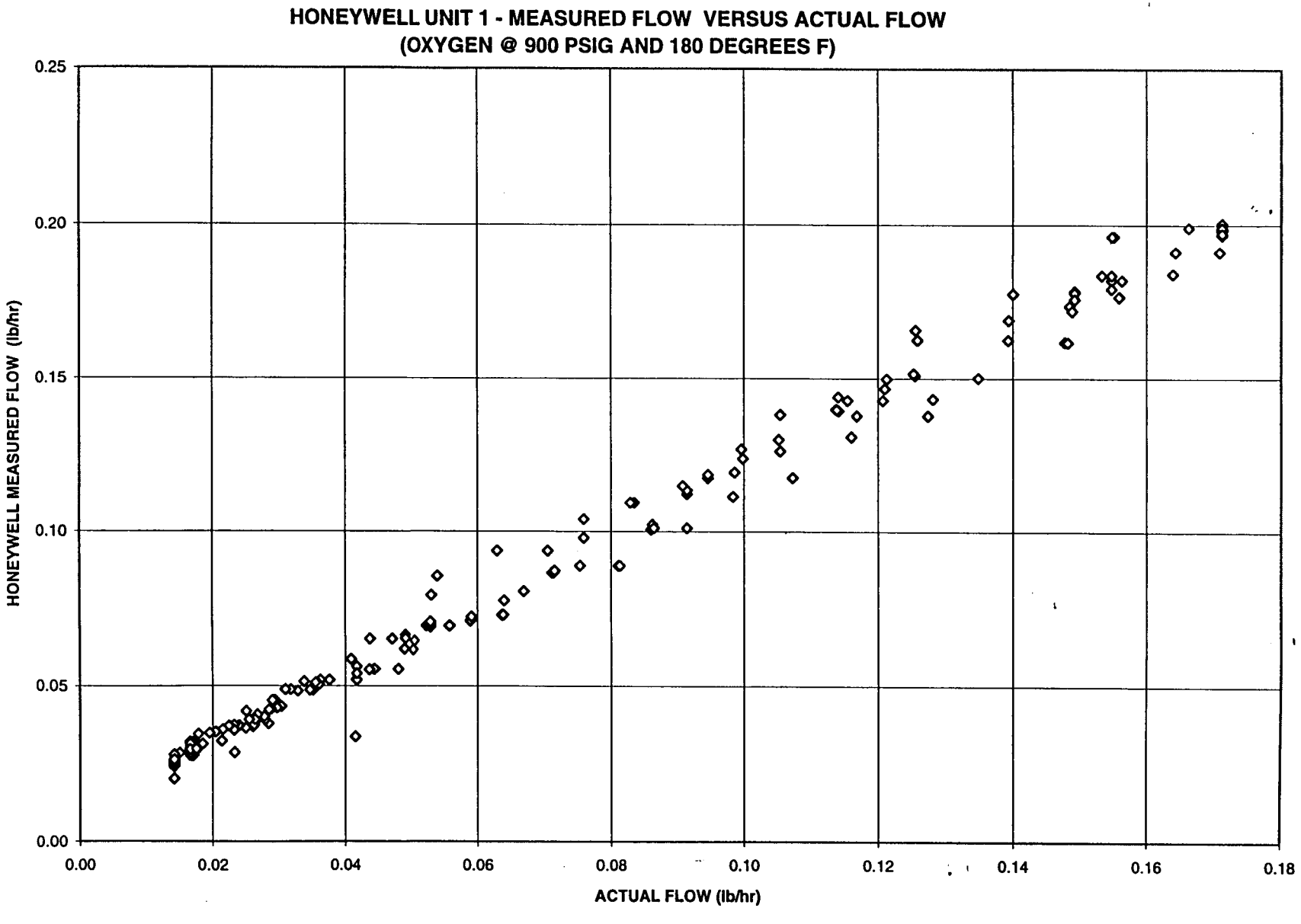
HONEYWELL UNIT 1 - MEASURED FLOW VERSUS ACTUAL FLOW
(OXYGEN @ 900 PSIG AND 180 DEGREES F)
HONEYWELL MEASURED FLOW (lb/hr)
0.25
0.20
0.15
0.10
0.05
0.00
0.00
0.02
0.04
0.06
0.08
0.10
0.12
0.14
0.16
0.18
ACTUAL FLOW (lb/hr)

Figure 98

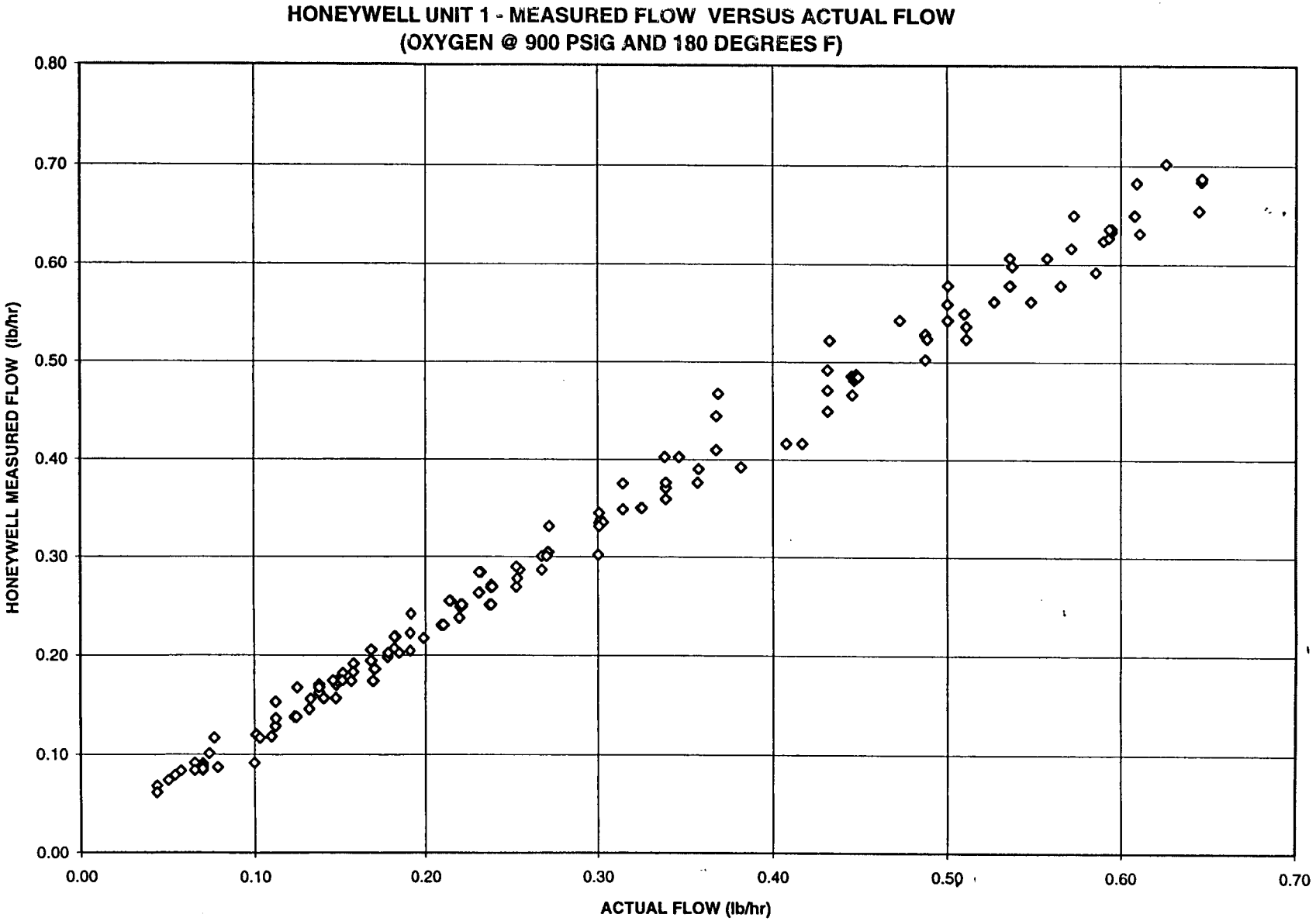
HONEYWELL UNIT 1 - MEASURED FLOW VERSUS ACTUAL FLOW
(OXYGEN @ 900 PSIG AND 180 DEGREES F)
HONEYWELL MEASURED FLOW (lb/hr)
0.80
0.70
0.60
0.50
0.40
0.30
0.20
0.10
0.00
0.00
0.10
0.20
0.30
0.40
0.50
0.60
0.70
ACTUAL FLOW (lb/hr)

Figure 99

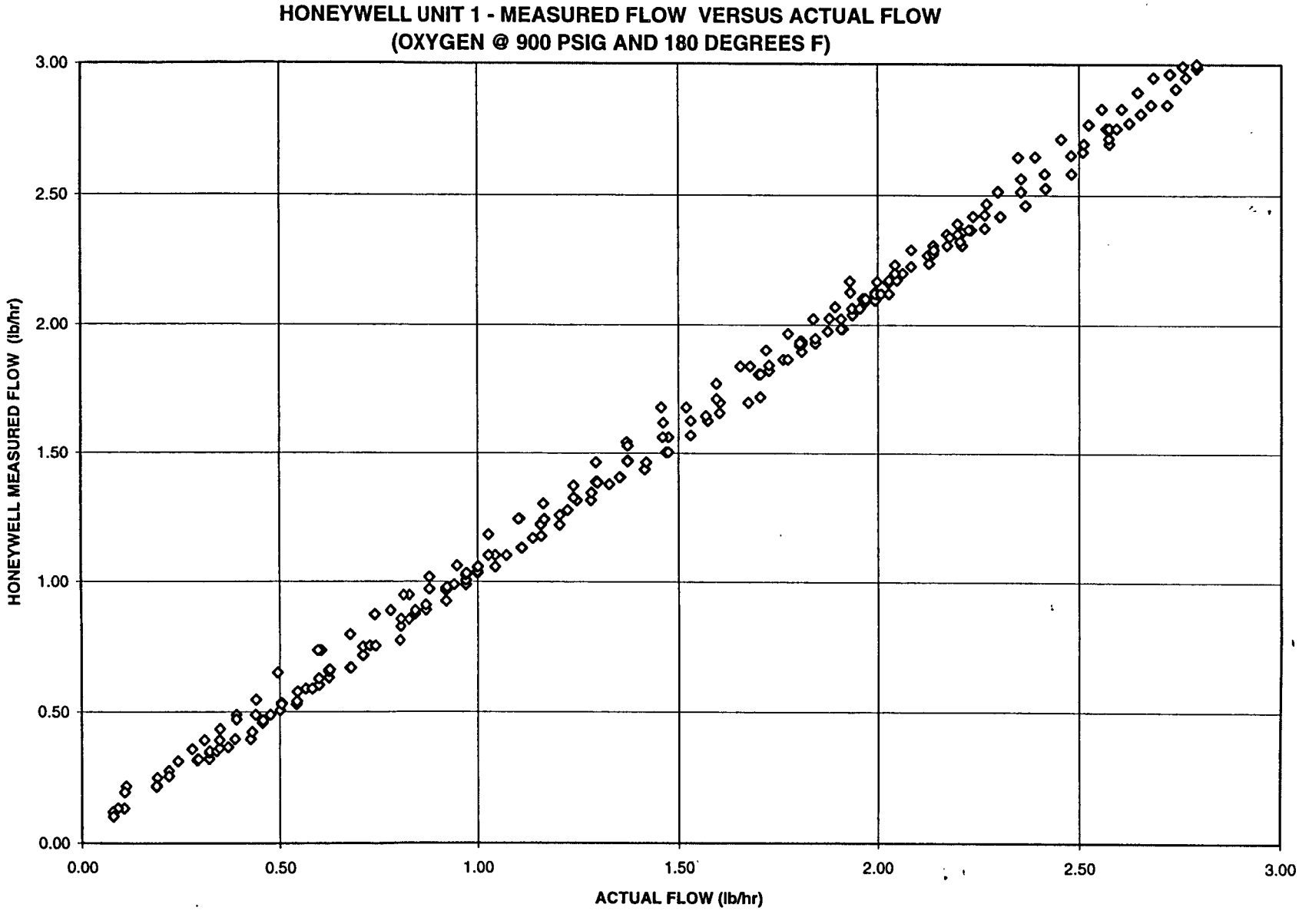
HONEYWELL UNIT 1 - MEASURED FLOW VERSUS ACTUAL FLOW
(OXYGEN @ 900 PSIG AND 180 DEGREES F)
HONEYWELL MEASURED FLOW (lb/hr)
3.00
2.50
2.00
1.50
1.00
0.50
0.00
0.00
0.50
1.00
1.50
2.00
2.50
3.00
ACTUAL FLOW (lb/hr)

Figure 100

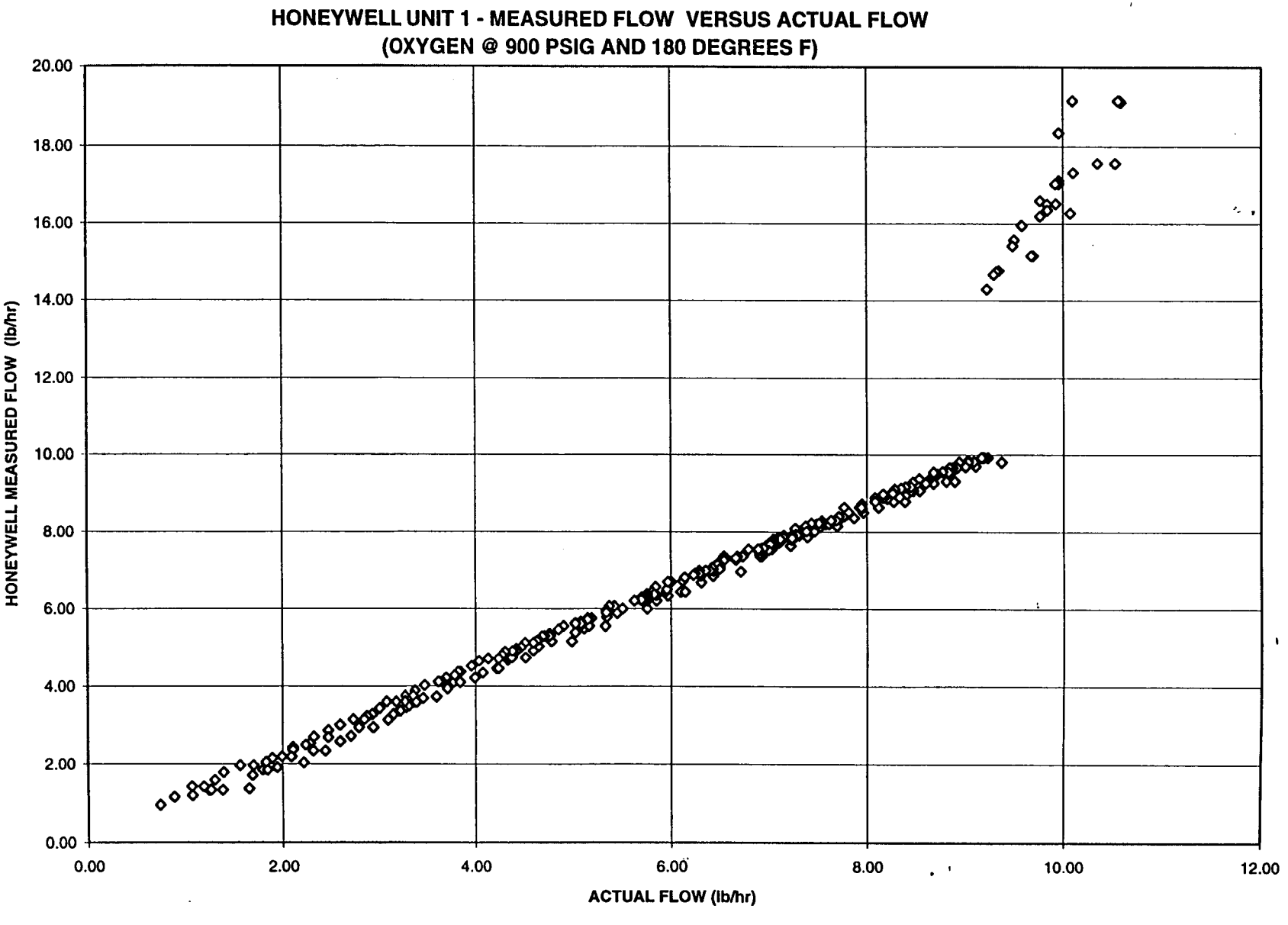
HONEYWELL UNIT 1 - MEASURED FLOW VERSUS ACTUAL FLOW
(OXYGEN @ 900 PSIG AND 180 DEGREES F)
HONEYWELL MEASURED FLOW (lb/hr)
20.00
18.00
16.00
14.00
12.00
10.00
8.00
6.00
4.00
2.00
0.00
0.00
2.00
4.00
6.00
8.00
10.00
12.00
ACTUAL FLOW (lb/hr)

Figure 101

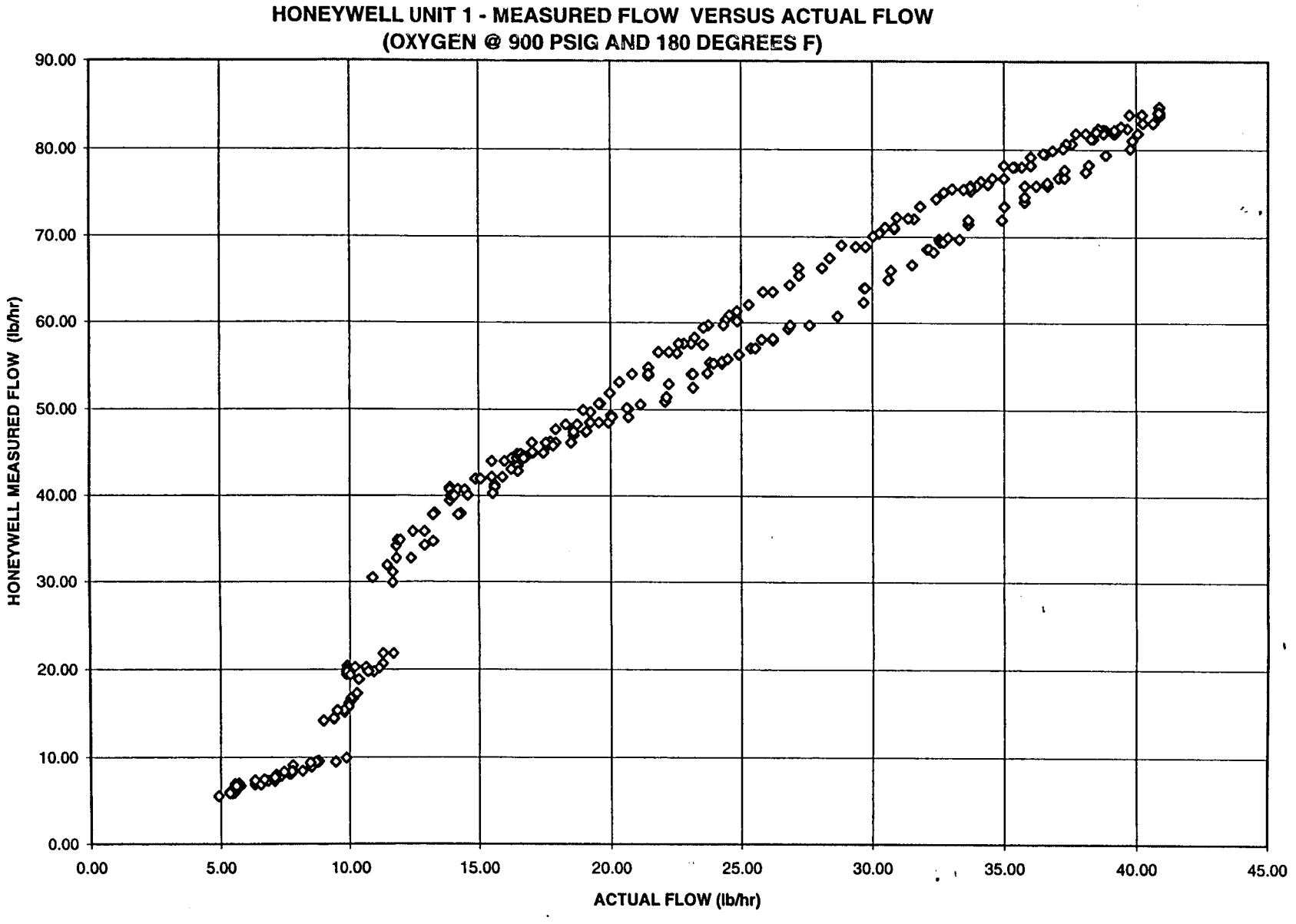
HONEYWELL UNIT 1 - MEASURED FLOW VERSUS ACTUAL FLOW
(OXYGEN @ 900 PSIG AND 180 DEGREES F)
HONEYWELL MEASURED FLOW (lb/hr)
90.00
80.00
70.00
60.00
50.00
40.00
30.00
20.00
10.00
0.00
0.00
5.00
10.00
15.00
20.00
25.00
30.00
35.00
40.00
45.00
ACTUAL FLOW (lb/hr)

Figure 102

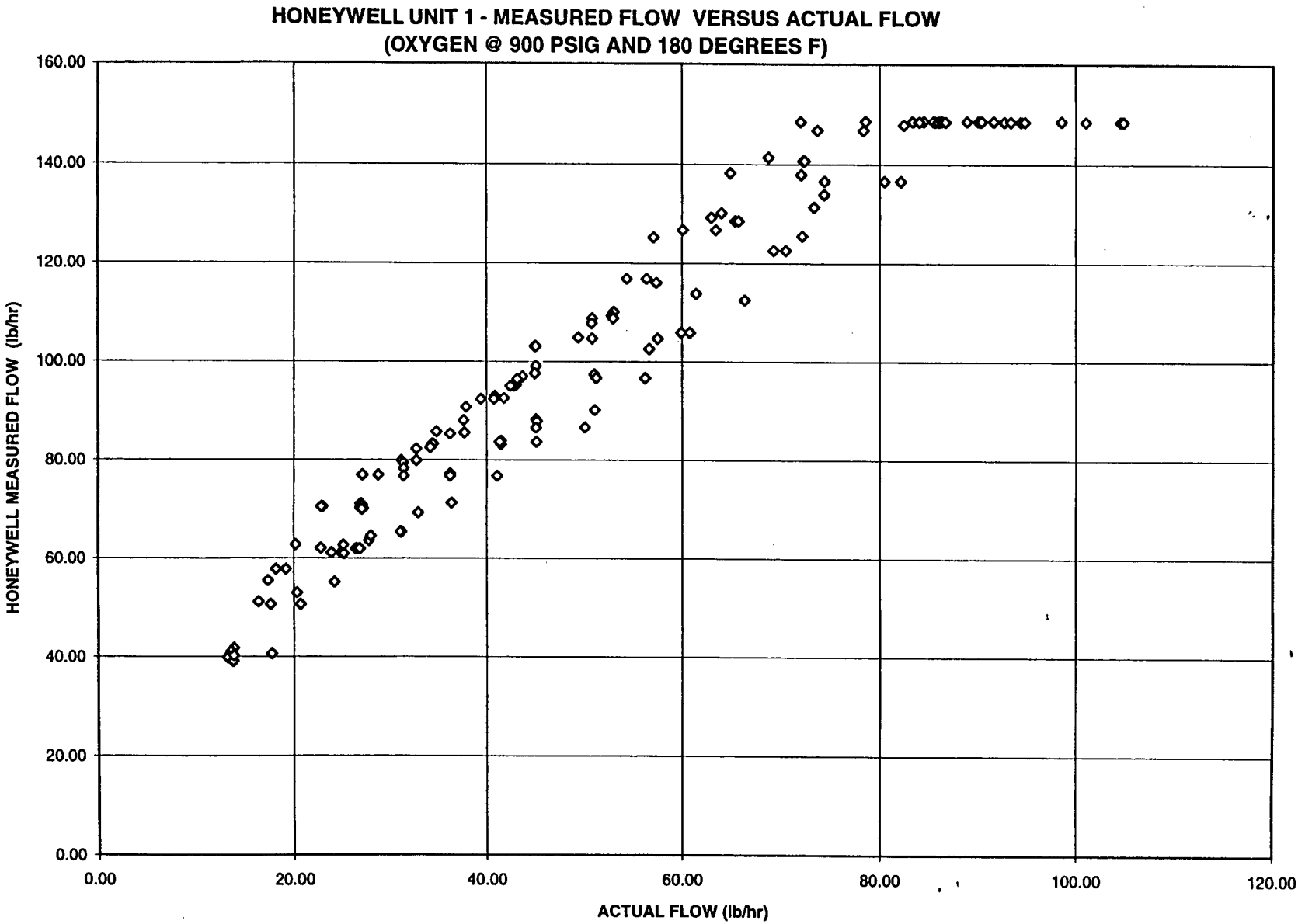
HONEYWELL UNIT 1 - MEASURED FLOW VERSUS ACTUAL FLOW
(OXYGEN @ 900 PSIG AND 180 DEGREES F)
HONEYWELL MEASURED FLOW (lb/hr)
160.00
140.00
120.00
100.00
80.00
60.00
40.00
20.00
0.00
0.00
20.00
40.00
60.00
80.00
100.00
120.00
ACTUAL FLOW (lb/hr)

Figure 103

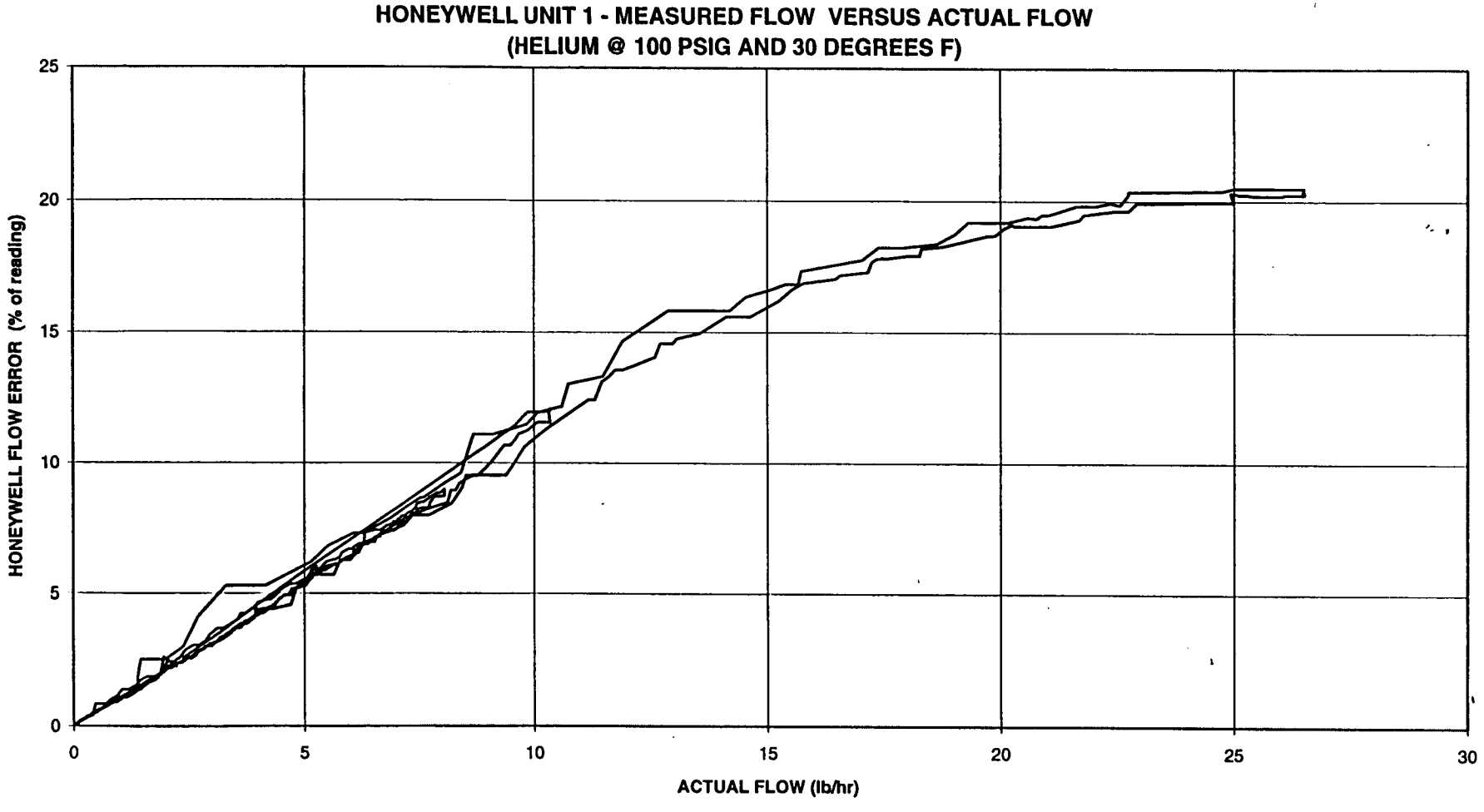
HONEYWELL UNIT 1 - MEASURED FLOW VERSUS ACTUAL FLOW
(HELIUM @ 100 PSIG AND 30 DEGREES F)
HONEYWELL FLOW ERROR (% of reading)
25
20
15
10
5
0
0
5
10
15
20
25
30
ACTUAL FLOW (lb/hr)

Figure 104

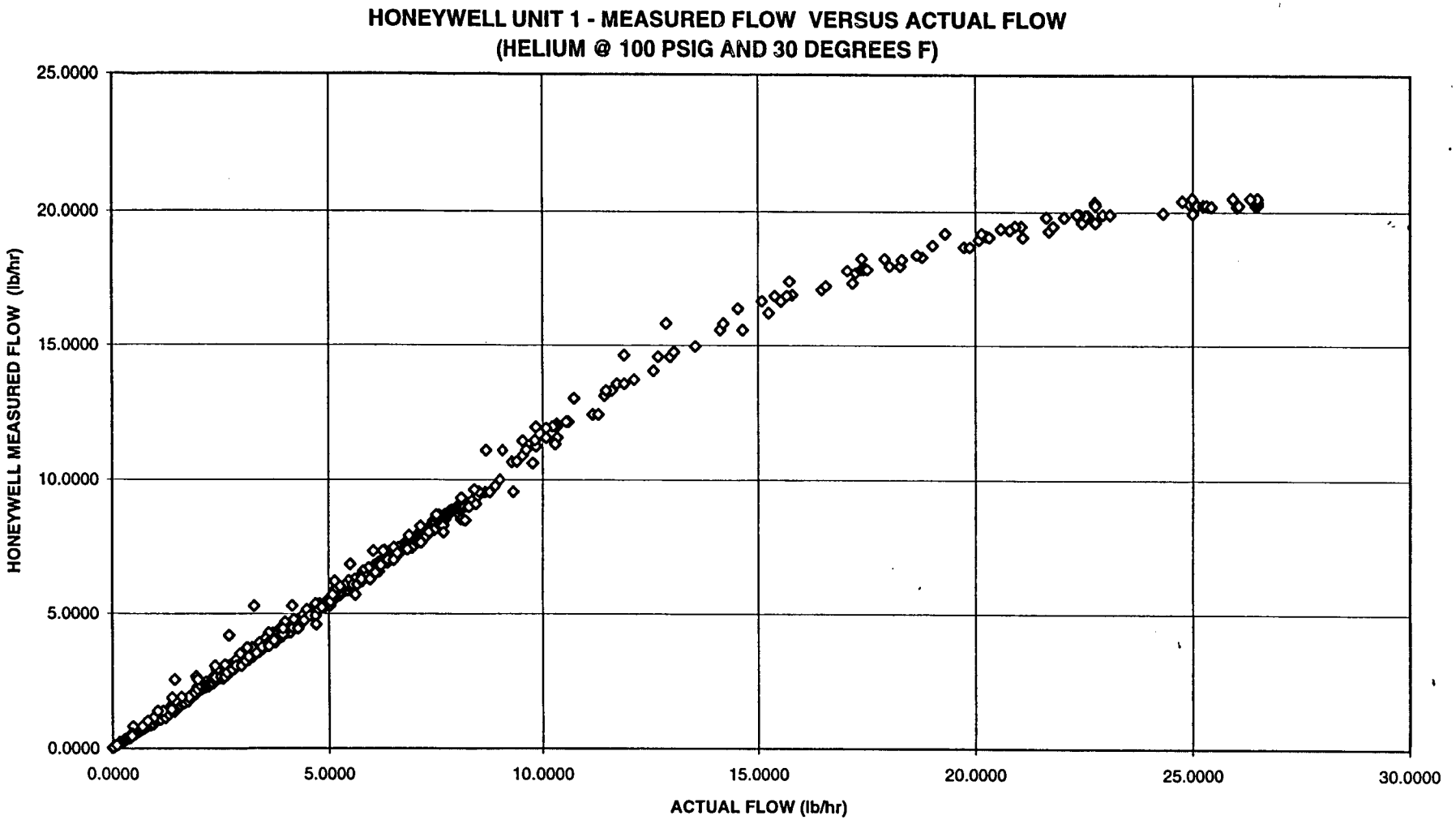
HONEYWELL UNIT 1 - MEASURED FLOW VERSUS ACTUAL FLOW
(HELIUM @ 100 PSIG AND 30 DEGREES F)
HONEYWELL MEASURED FLOW (lb/hr)
25.0000
20.0000
15.0000
10.0000
5.0000
0.0000
0.0000
5.0000
10.0000
15.0000
20.0000
25.0000
30.0000
ACTUAL FLOW (lb/hr)

Figure 105

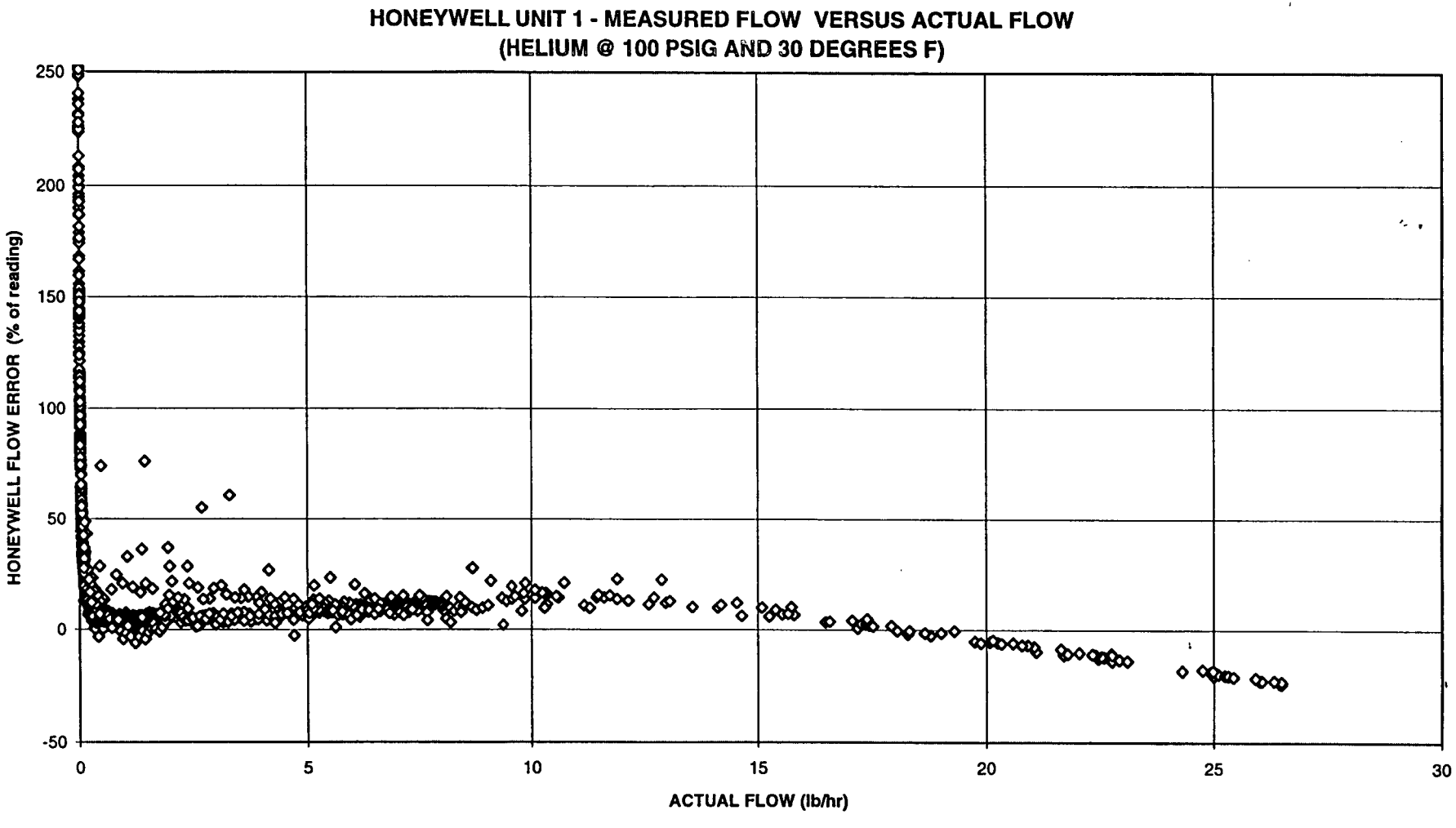
HONEYWELL UNIT 1 - MEASURED FLOW VERSUS ACTUAL FLOW
(HELIUM @ 100 PSIG AND 30 DEGREES F)
HONEYWELL FLOW ERROR (% of reading)
250
200
150
100
50
0
-50
0
5
10
15
20
25
30
ACTUAL FLOW (lb/hr)

Figure 106

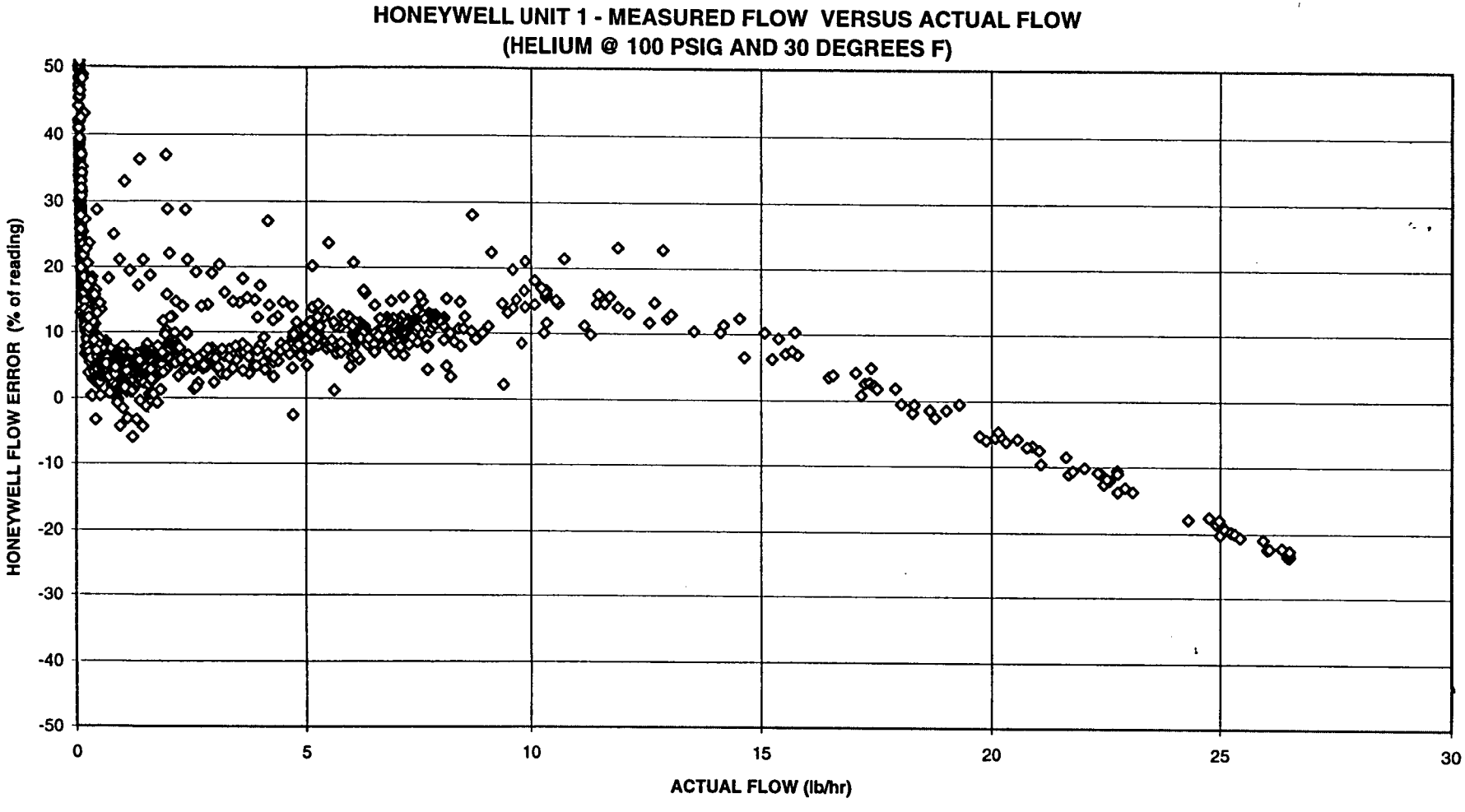
HONEYWELL UNIT 1 - MEASURED FLOW VERSUS ACTUAL FLOW
(HELIUM @ 100 PSIG AND 30 DEGREES F)
HONEYWELL FLOW ERROR (% of reading)
50
40
30
20
10
0
-10
-20
-30
-40
-50
0
5
10
15
20
25
30
ACTUAL FLOW (lb/hr)

Figure 107

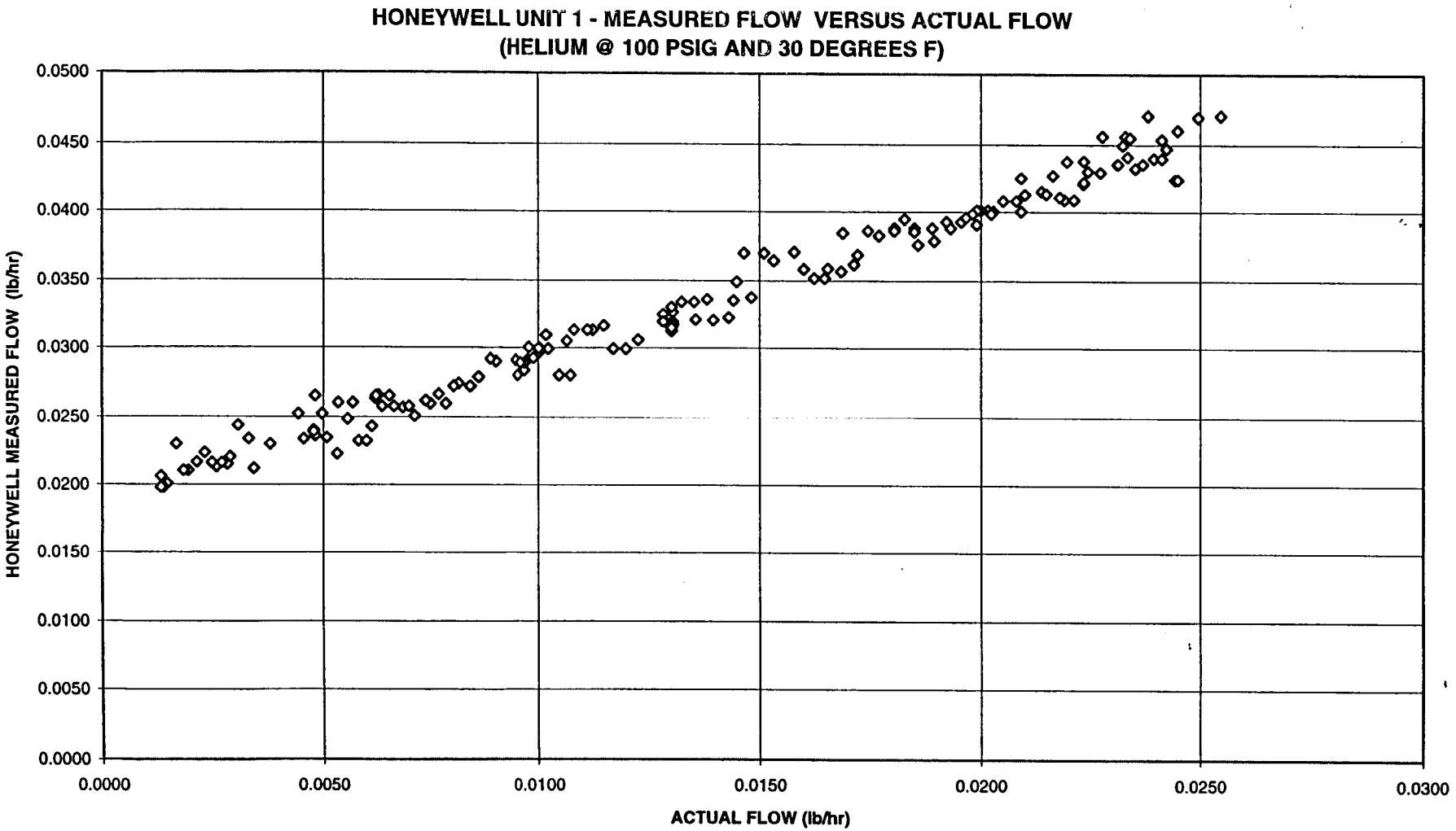
HONEYWELL UNIT 1 - MEASURED FLOW VERSUS ACTUAL FLOW
(HELIUM @ 100 PSIG AND 30 DEGREES F)
HONEYWELL MEASURED FLOW (lb/hr)
0.0500
0.0450
0.0400
0.0350
0.0300
0.0250
0.0200
0.0150
0.0100
0.0050
0.0000
0.0000
0.0050
0.0100
0.0150
0.0200
0.0250
0.0300
ACTUAL FLOW (lb/hr)

Figure 108

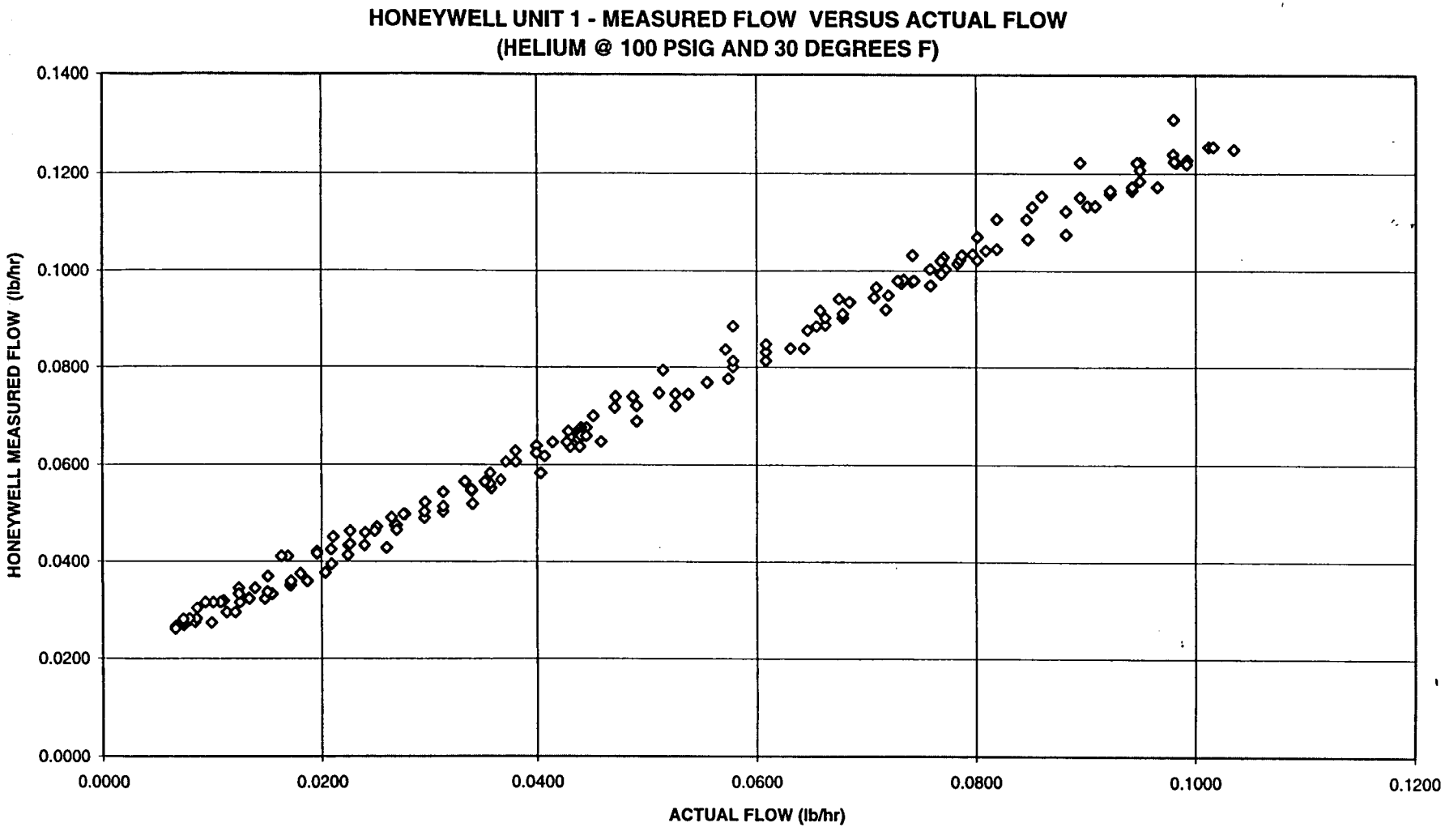
HONEYWELL UNIT 1 - MEASURED FLOW VERSUS ACTUAL FLOW
(HELIUM @ 100 PSIG AND 30 DEGREES F)
HONEYWELL MEASURED FLOW (lb/hr)
0.1400
0.1200
0.1000
0.0800
0.0600
0.0400
0.0200
0.0000
0.0000
0.0200
0.0400
0.0600
0.0800
0.1000
0.1200
ACTUAL FLOW (lb/hr)

Figure 109

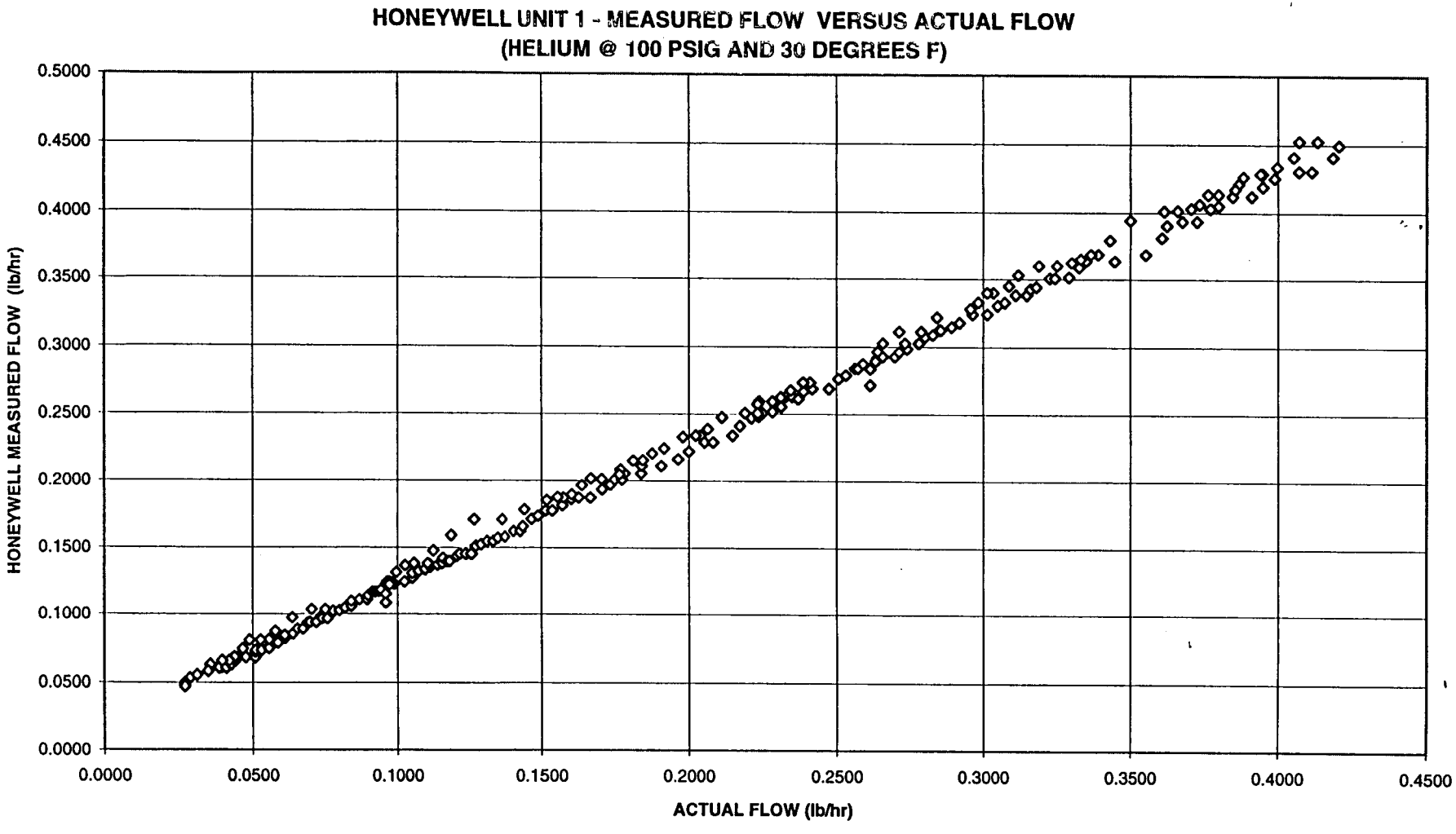
HONEYWELL UNIT 1 - MEASURED FLOW VERSUS ACTUAL FLOW
(HELIUM @ 100 PSIG AND 30 DEGREES F)
HONEYWELL MEASURED FLOW (lb/hr)
0.5000
0.4500
0.4000
0.3500
0.3000
0.2500
0.2000
0.1500
0.1000
0.0500
0.0000
0.0000
0.0500
0.1000
0.1500
0.2000
0.2500
0.3000
0.3500
0.4000
0.4500
ACTUAL FLOW (lb/hr)

Figure 110

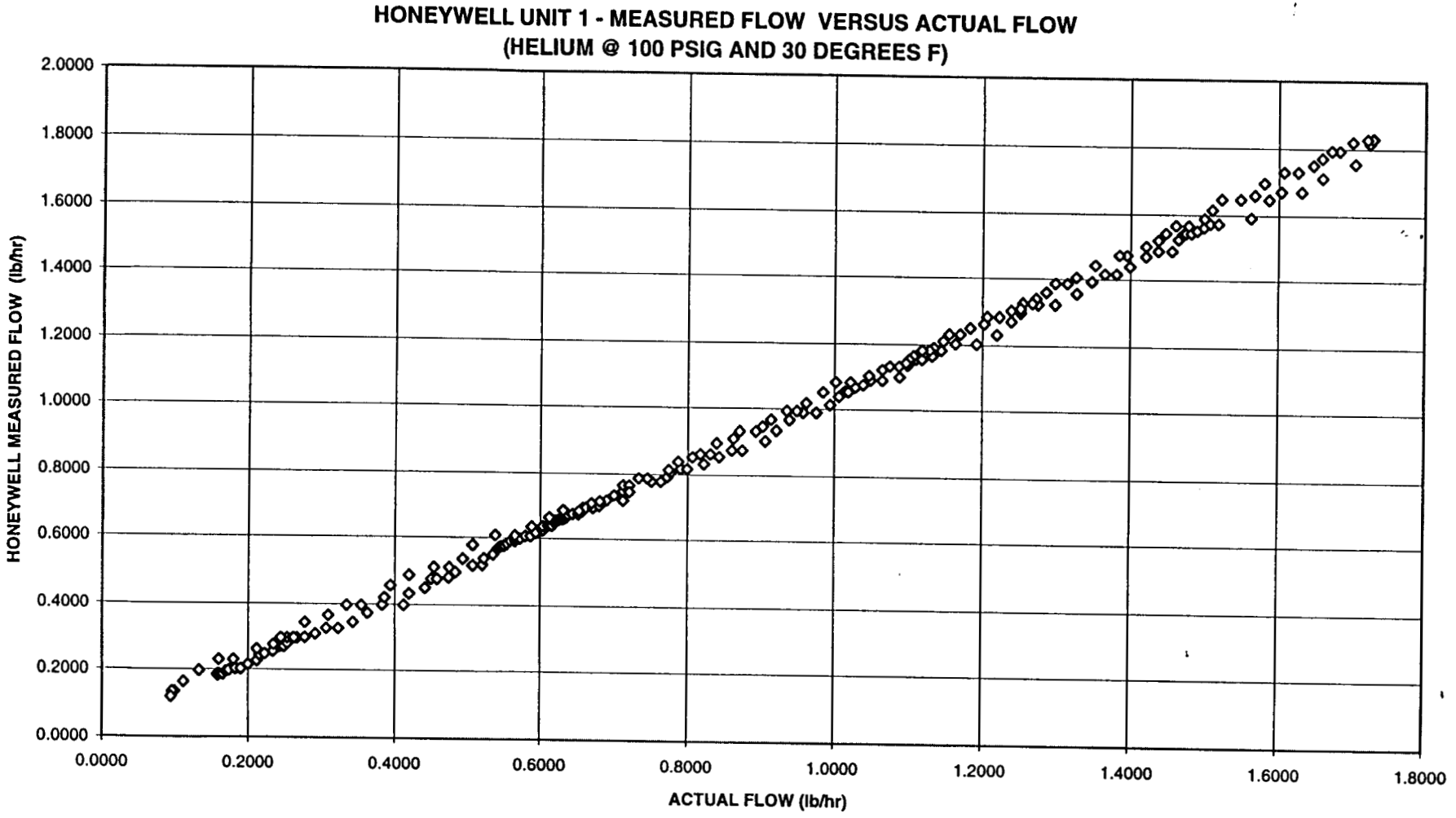
HONEYWELL UNIT 1 - MEASURED FLOW VERSUS ACTUAL FLOW
(HELIUM @ 100 PSIG AND 30 DEGREES F)
HONEYWELL MEASURED FLOW (lb/hr)
2.0000
1.8000
1.6000
1.4000
1.2000
1.0000
0.8000
0.6000
0.4000
0.2000
0.0000
0.0000
0.2000
0.4000
0.6000
0.8000
1.0000
1.2000
1.4000
1.6000
1.8000
ACTUAL FLOW (lb/hr)

Figure 111

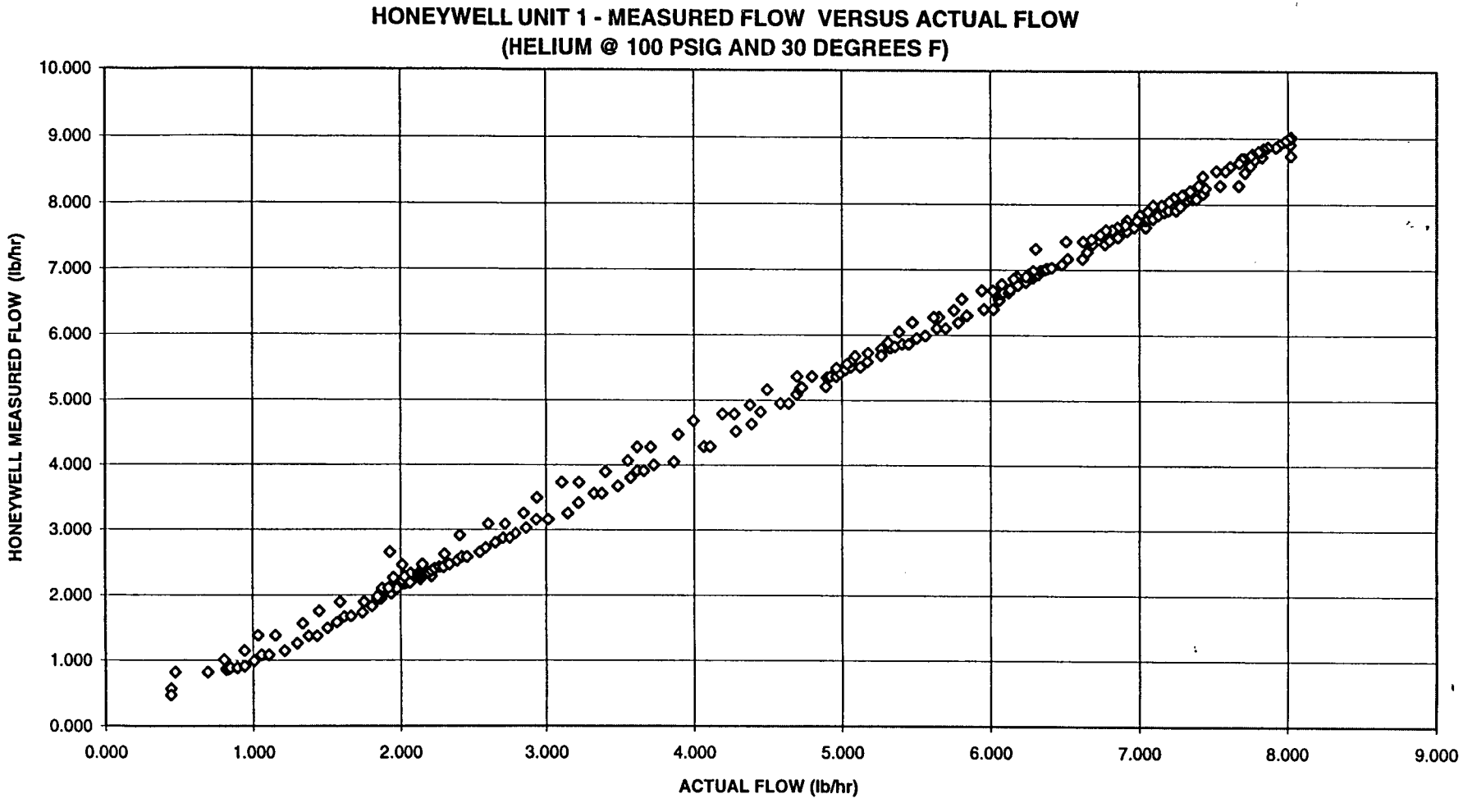
HONEYWELL UNIT 1 - MEASURED FLOW VERSUS ACTUAL FLOW
(HELIUM @ 100 PSIG AND 30 DEGREES F)
HONEYWELL MEASURED FLOW (lb/hr)
10.000
9.000
8.000
7.000
6.000
5.000
4.000
3.000
2.000
1.000
0.000
0.000
1.000
2.000
3.000
4.000
5.000
6.000
7.000
8.000
9.000
ACTUAL FLOW (lb/hr)

Figure 112

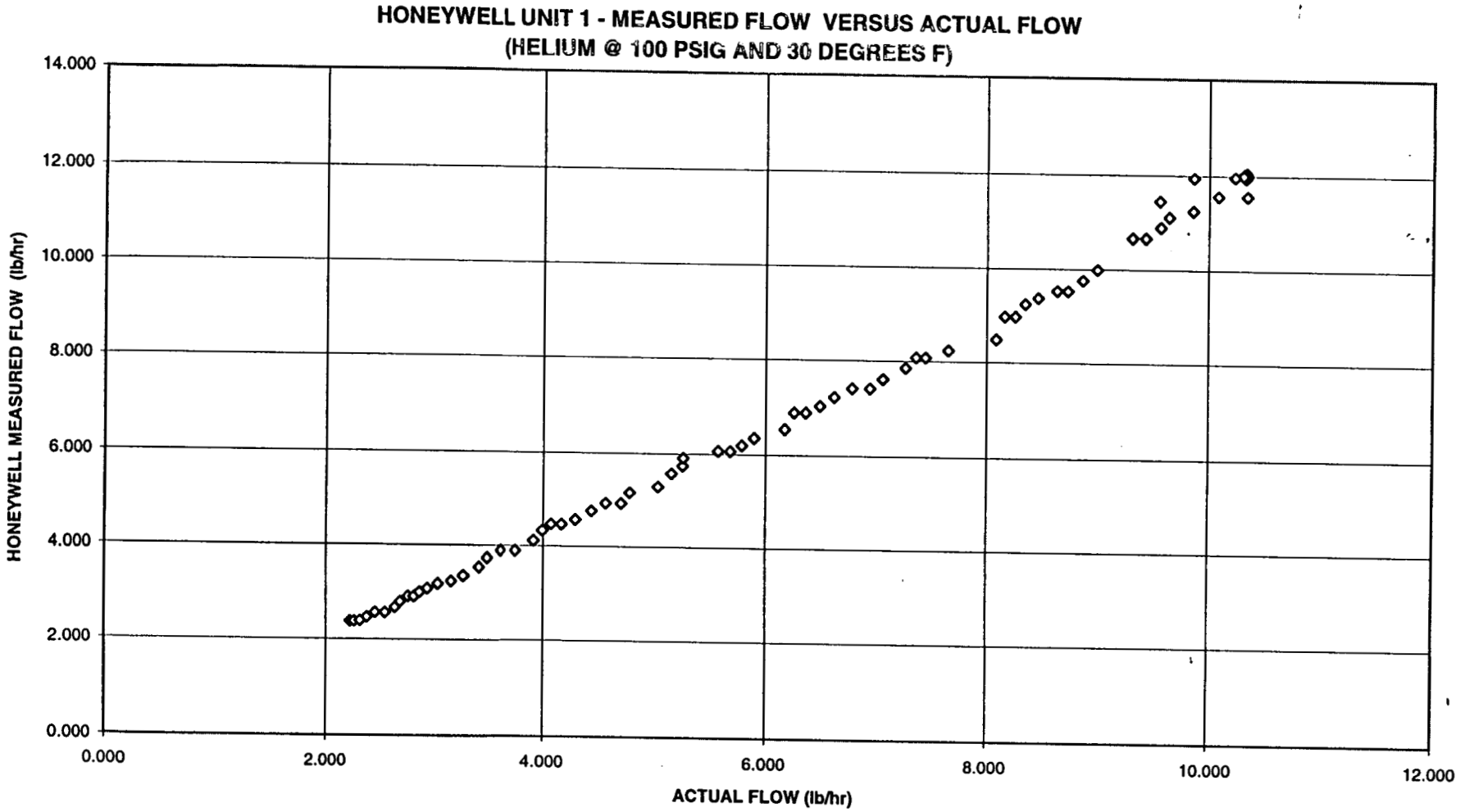
HONEYWELL UNIT 1 - MEASURED FLOW VERSUS ACTUAL FLOW
(HELIUM @ 100 PSIG AND 30 DEGREES F)
HONEYWELL MEASURED FLOW (lb/hr)
14.000
12.000
10.000
8.000
6.000
4.000
2.000
0.000
0.000
2.000
4.000
6.000
8.000
10.000
12.000
ACTUAL FLOW (lb/hr)

Figure 113

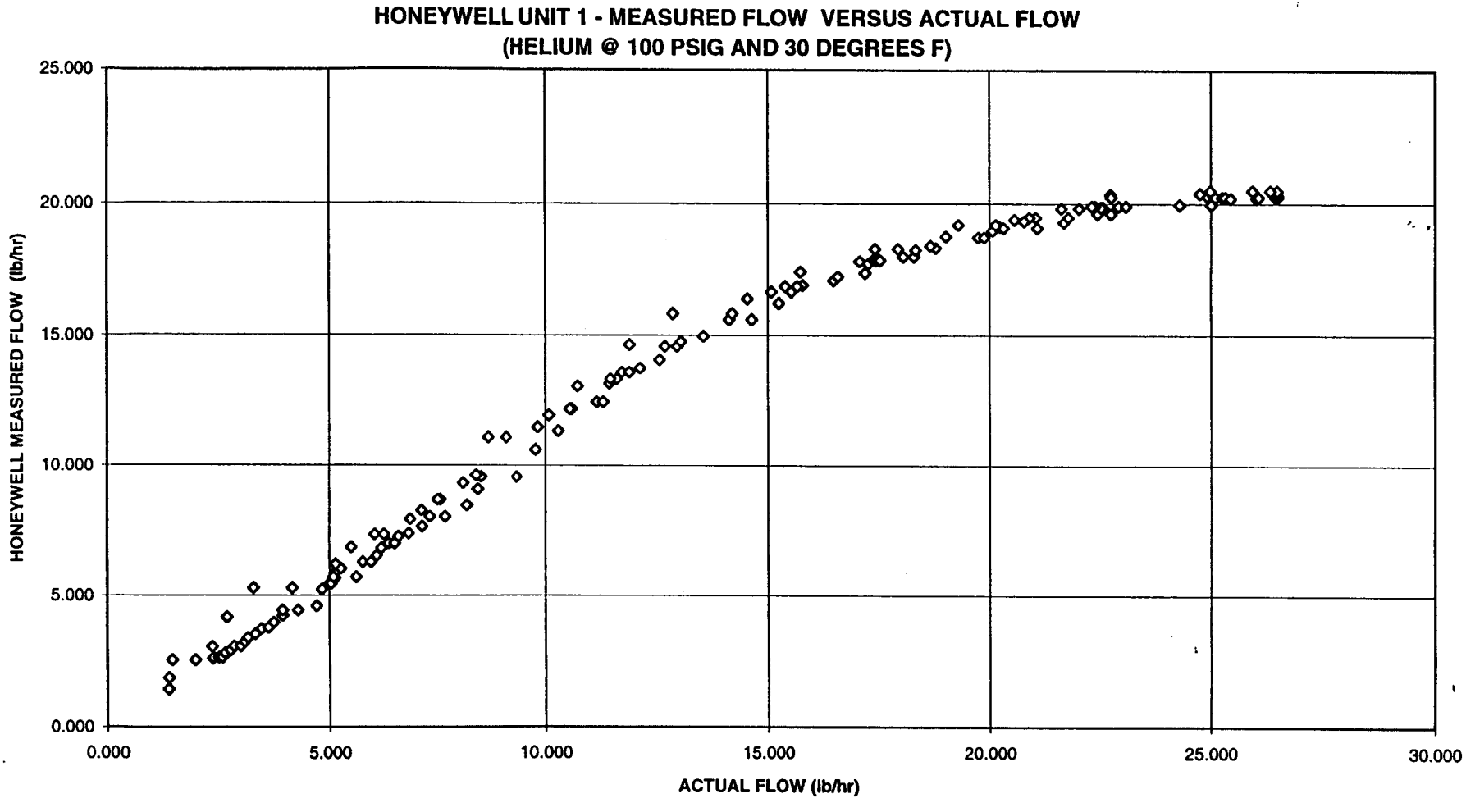
HONEYWELL UNIT 1 - MEASURED FLOW VERSUS ACTUAL FLOW
(HELIUM @ 100 PSIG AND 30 DEGREES F)
HONEYWELL MEASURED FLOW (lb/hr)
25.000
20.000
15.000
10.000
5.000
0.000
0.000
5.000
10.000
15.000
20.000
25.000
30.000
ACTUAL FLOW (lb/hr)

Figure 114

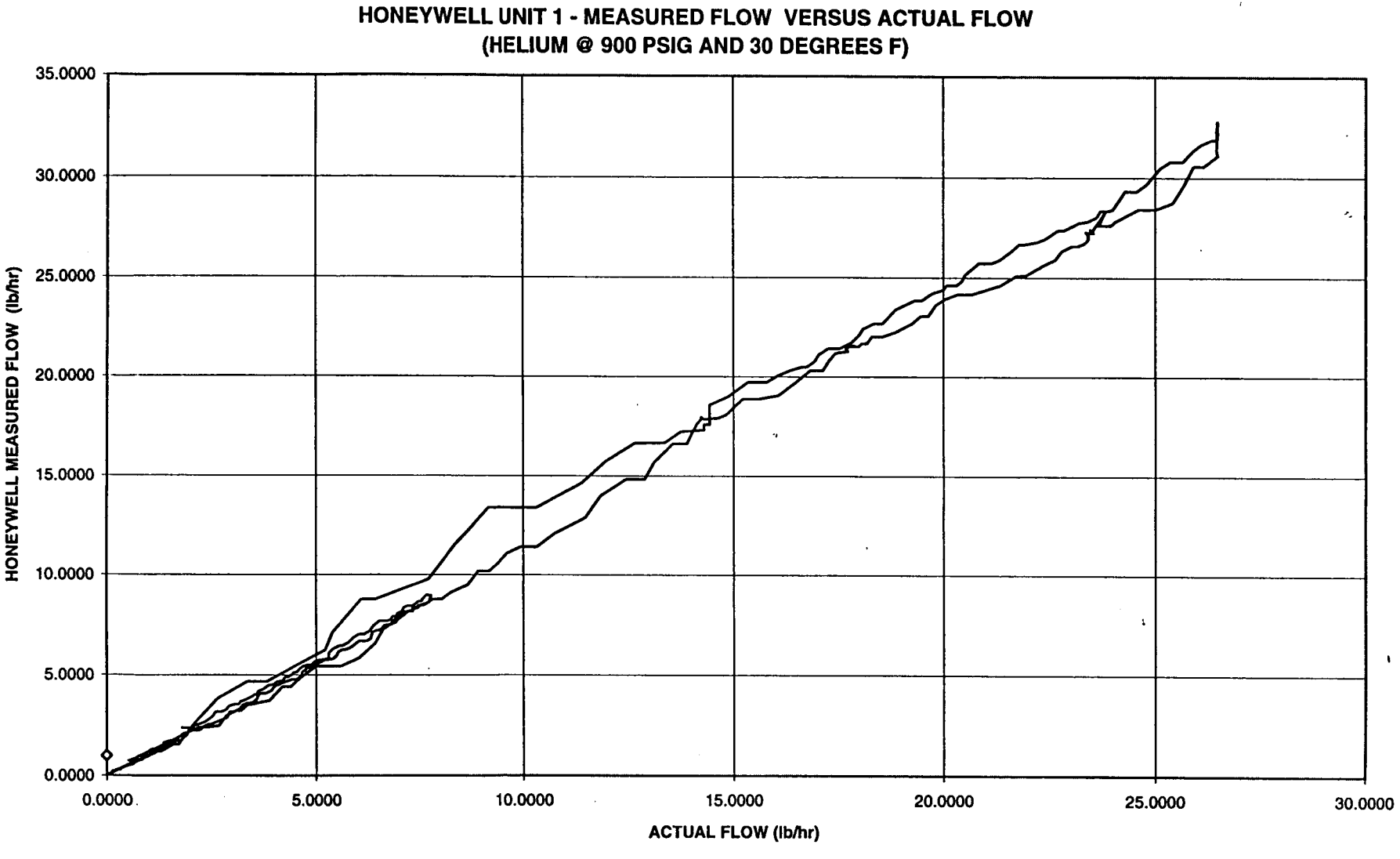
HONEYWELL UNIT 1 - MEASURED FLOW VERSUS ACTUAL FLOW
(HELIUM @ 900 PSIG AND 30 DEGREES F)
HONEYWELL MEASURED FLOW (lb/hr)
35.0000
30.0000
25.0000
20.0000
15.0000
10.0000
5.0000
0.0000
0.0000
5.0000
10.0000
15.0000
20.0000
25.0000
30.0000
ACTUAL FLOW (lb/hr)

Figure 115

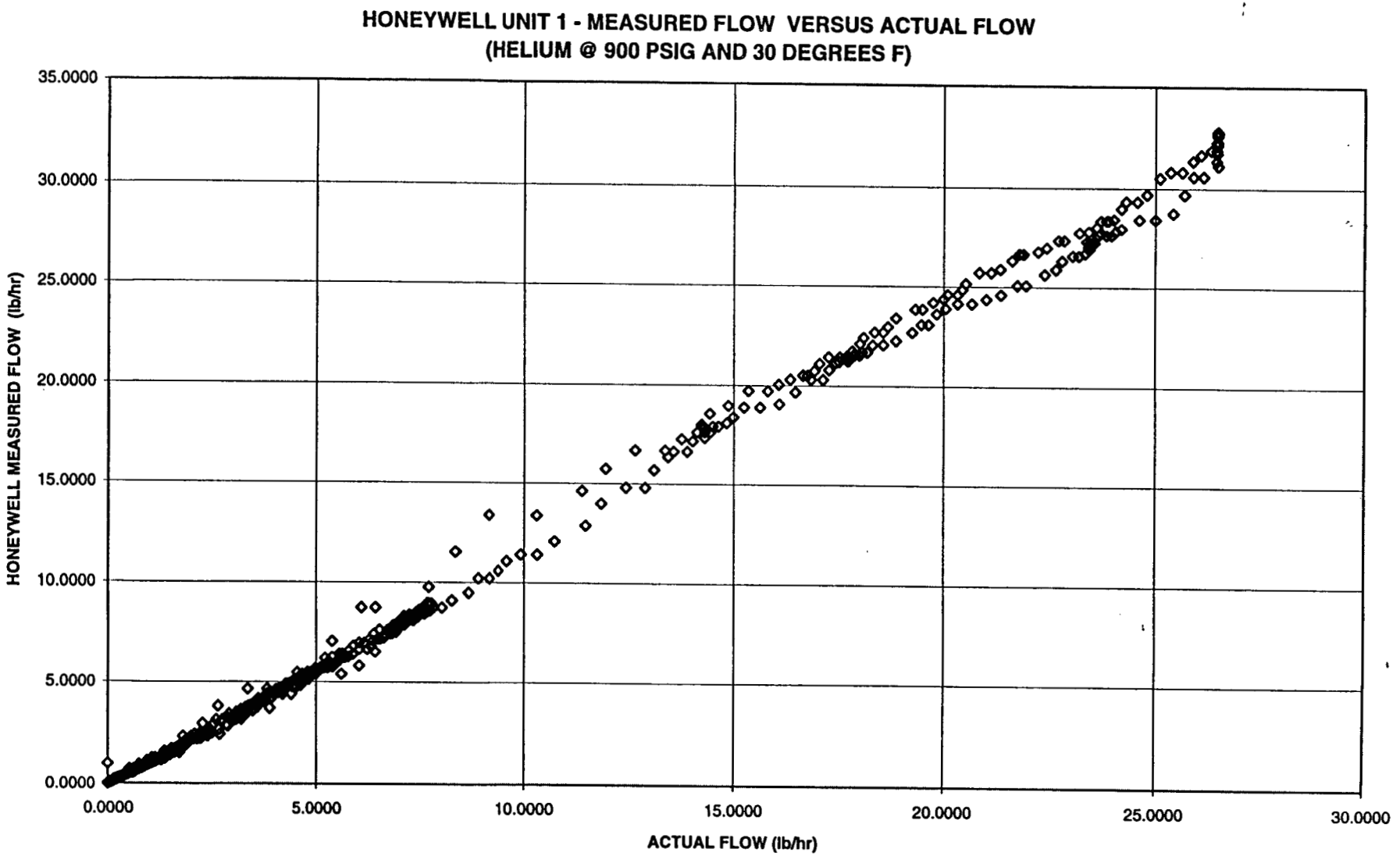
HONEYWELL UNIT 1 - MEASURED FLOW VERSUS ACTUAL FLOW
(HELIUM @ 900 PSIG AND 30 DEGREES F)
HONEYWELL MEASURED FLOW (lb/hr)
35.0000
30.0000
25.0000
20.0000
15.0000
10.0000
5.0000
0.0000
0.0000
5.0000
10.0000
15.0000
20.0000
25.0000
30.0000
ACTUAL FLOW (lb/hr)

Figure 116

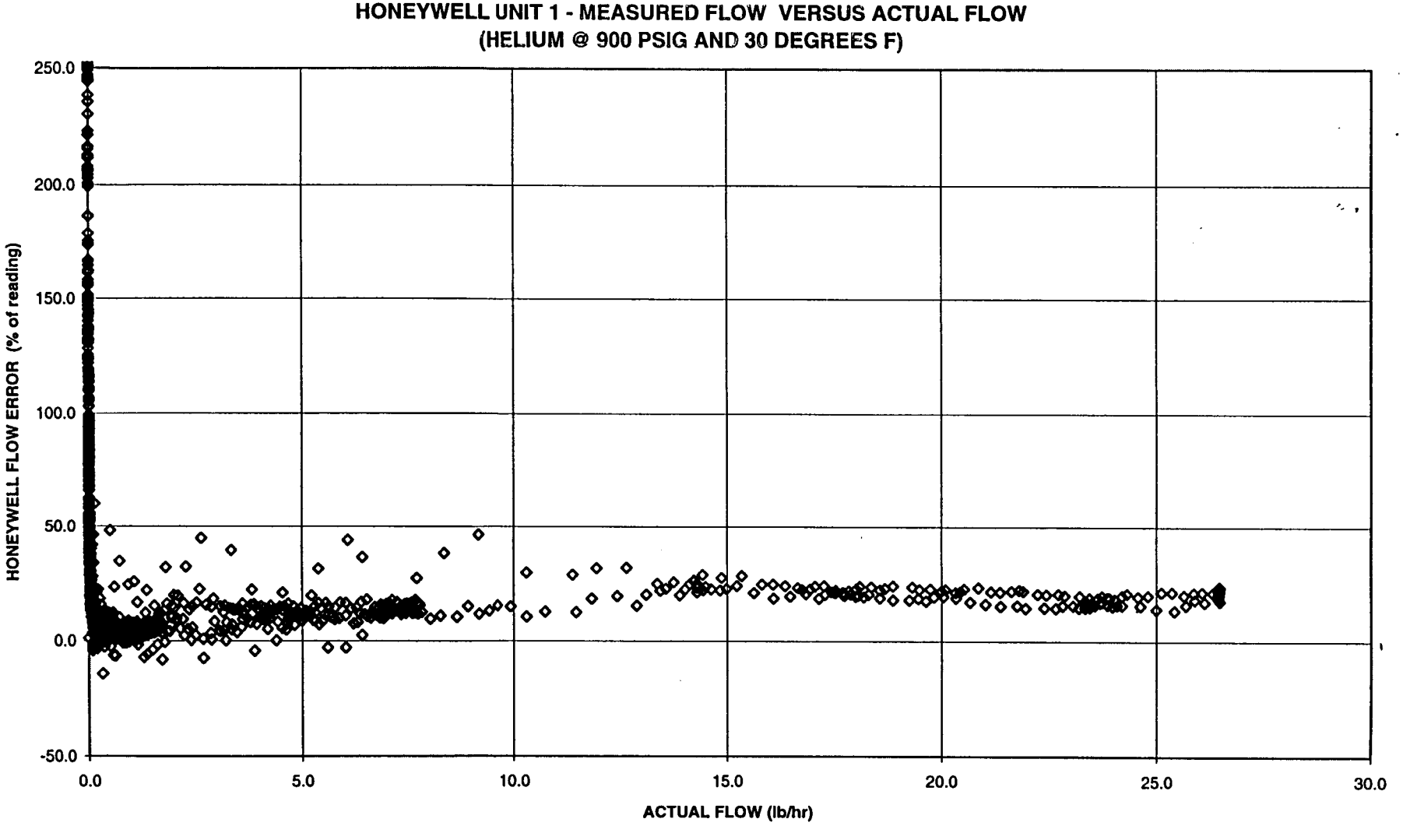
HONEYWELL UNIT 1 - MEASURED FLOW VERSUS ACTUAL FLOW
(HELIUM @ 900 PSIG AND 30 DEGREES F)
HONEYWELL FLOW ERROR (% of reading)
250.0
200.0
150.0
100.0
50.0
0.0
-50.0
0.0
5.0
10.0
15.0
20.0
25.0
30.0
ACTUAL FLOW (lb/hr)

Figure 117

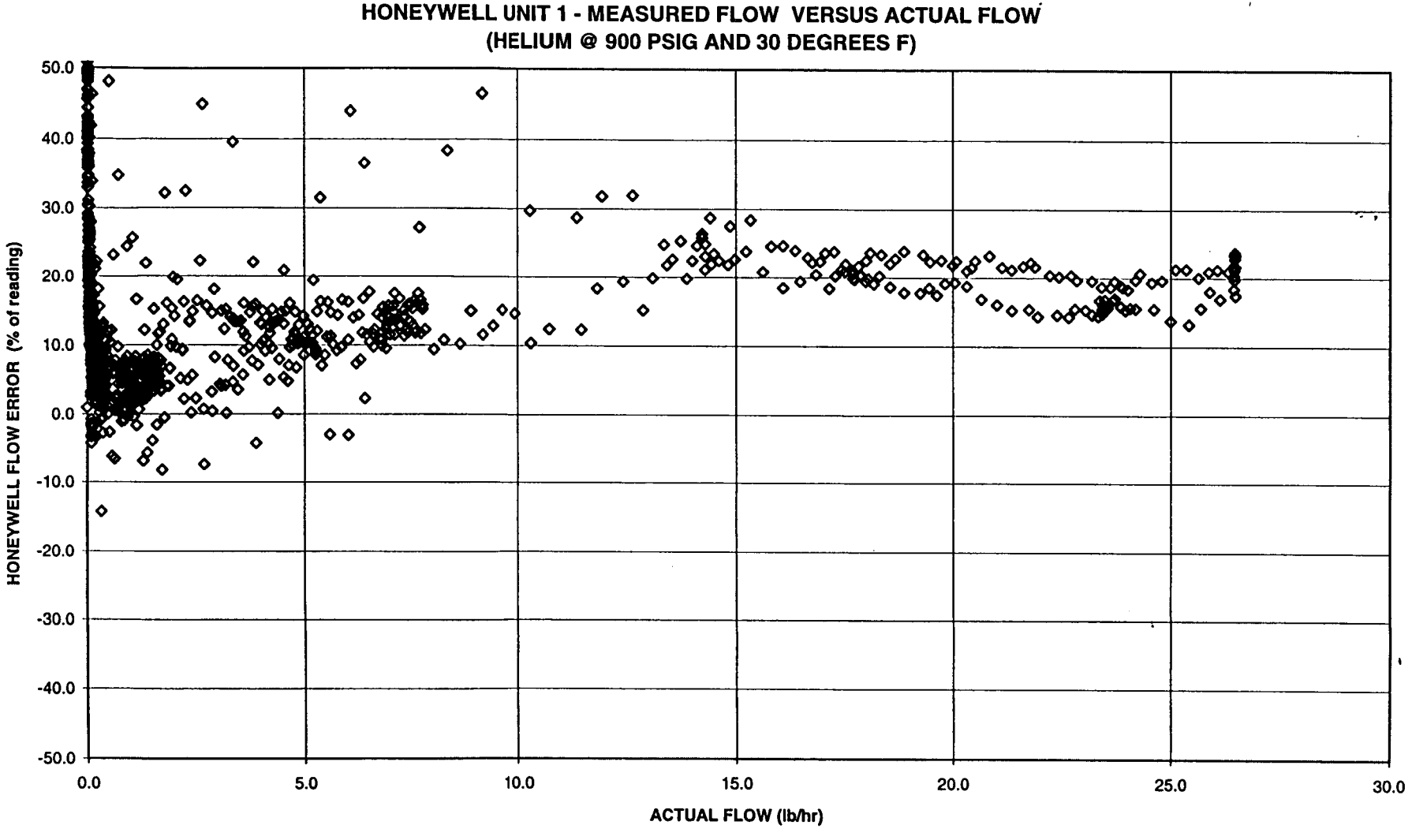
HONEYWELL UNIT 1 - MEASURED FLOW VERSUS ACTUAL FLOW
(HELIUM @ 900 PSIG AND 30 DEGREES F)
HONEYWELL FLOW ERROR (% of reading)
50.0
40.0
30.0
20.0
10.0
0.0
-10.0
-20.0
-30.0
-40.0
-50.0
0.0
5.0
10.0
15.0
20.0
25.0
30.0
ACTUAL FLOW (lb/hr)

Figure 118

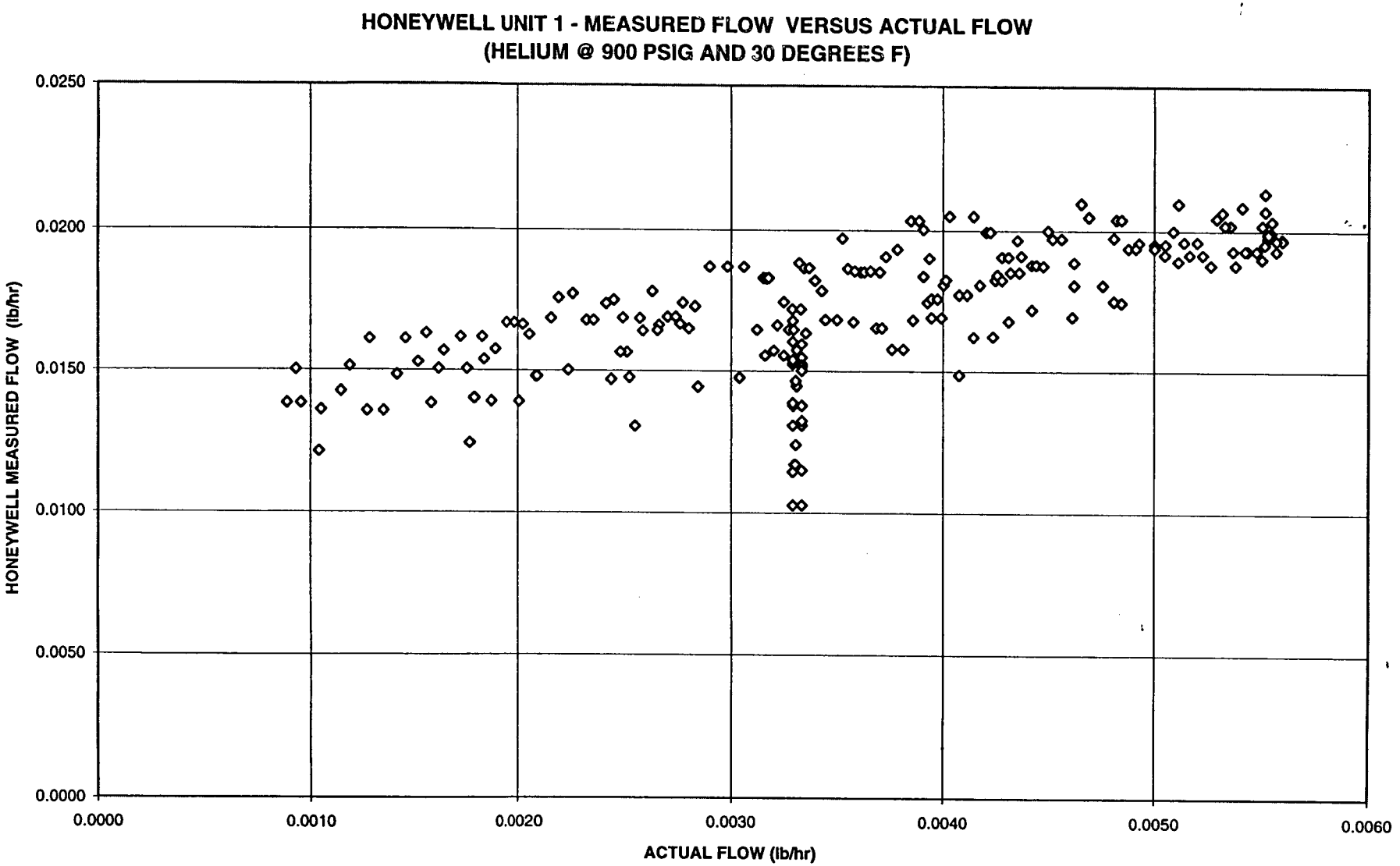
HONEYWELL UNIT 1 - MEASURED FLOW VERSUS ACTUAL FLOW
(HELIUM @ 900 PSIG AND 30 DEGREES F)
HONEYWELL MEASURED FLOW (lb/hr)
0.0250
0.0200
0.0150
0.0100
0.0050
0.0000
0.0000
0.0010
0.0020
0.0030
0.0040
0.0050
0.0060
ACTUAL FLOW (lb/hr)

Figure 119

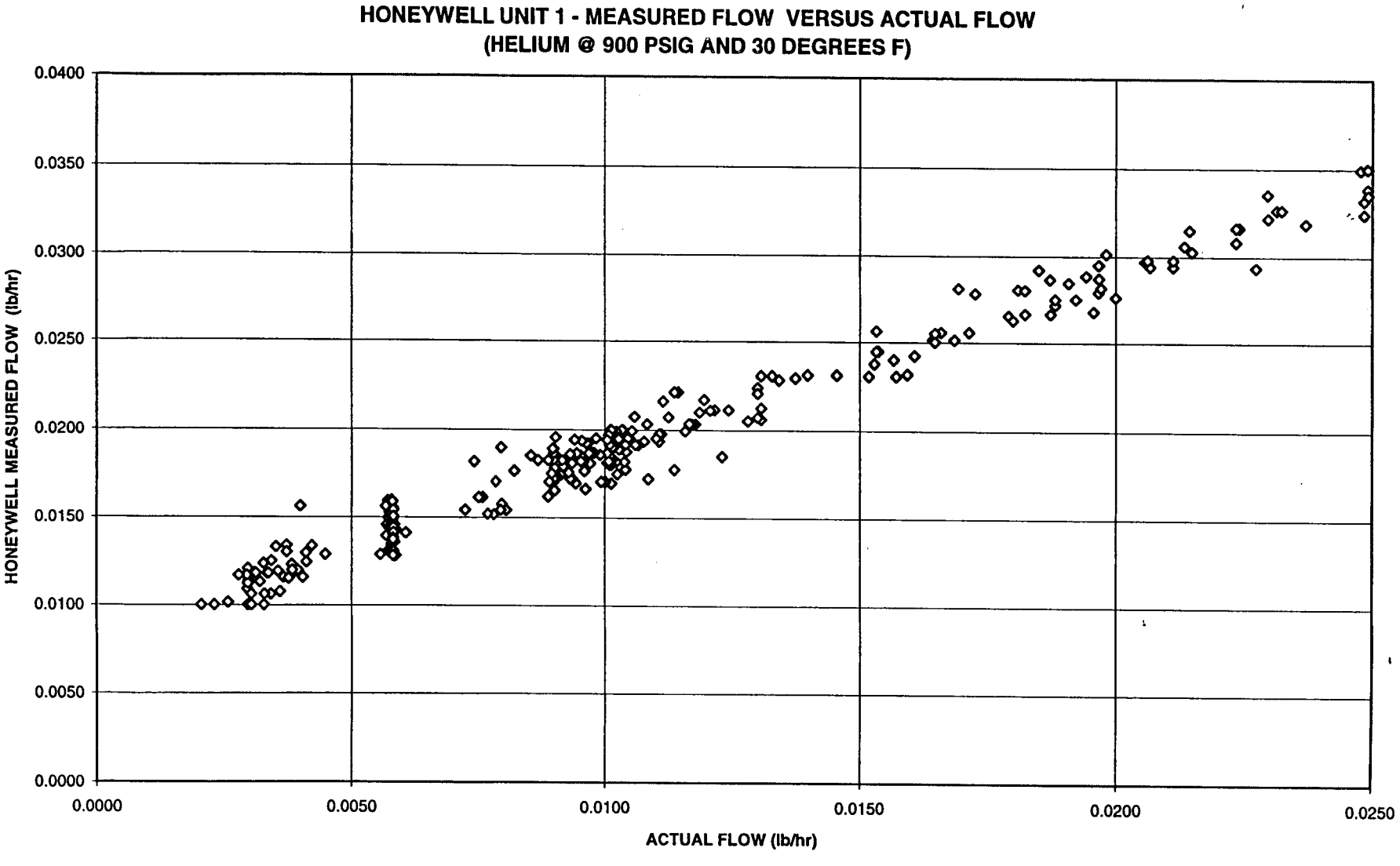
HONEYWELL UNIT 1 - MEASURED FLOW VERSUS ACTUAL FLOW
(HELIUM @ 900 PSIG AND 30 DEGREES F)
HONEYWELL MEASURED FLOW (lb/hr)
0.0400
0.0350
0.0300
0.0250
0.0200
0.0150
0.0100
0.0050
0.0000
0.0000
0.0050
0.0100
0.0150
0.0200
0.0250
ACTUAL FLOW (lb/hr)

Figure 120

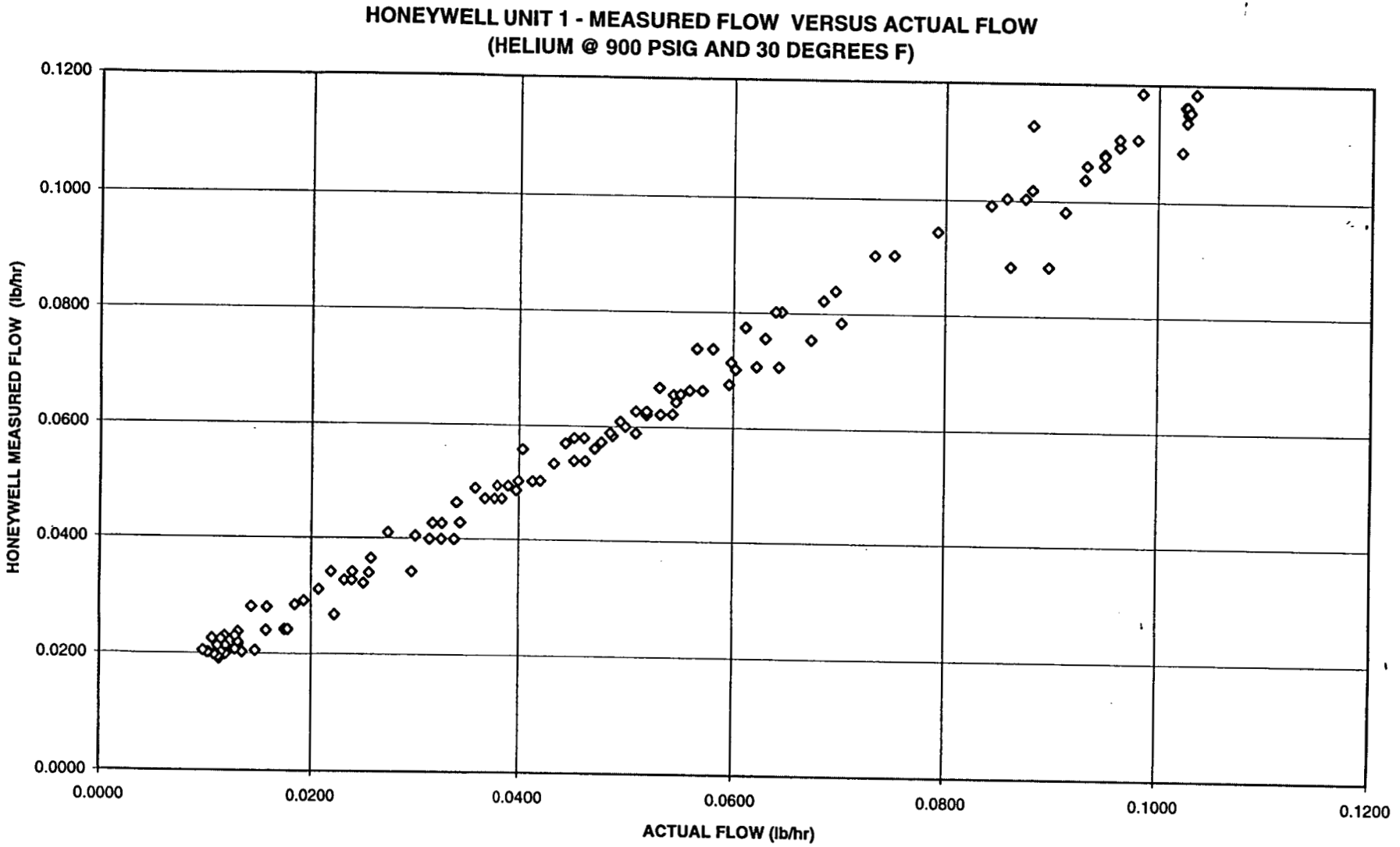
HONEYWELL UNIT 1 - MEASURED FLOW VERSUS ACTUAL FLOW
(HELIUM @ 900 PSIG AND 30 DEGREES F)
HONEYWELL MEASURED FLOW (lb/hr)
0.1200
0.1000
0.0800
0.0600
0.0400
0.0200
0.0000
0.0000
0.0200
0.0400
0.0600
0.0800
0.1000
0.1200
ACTUAL FLOW (lb/hr)

Figure 121

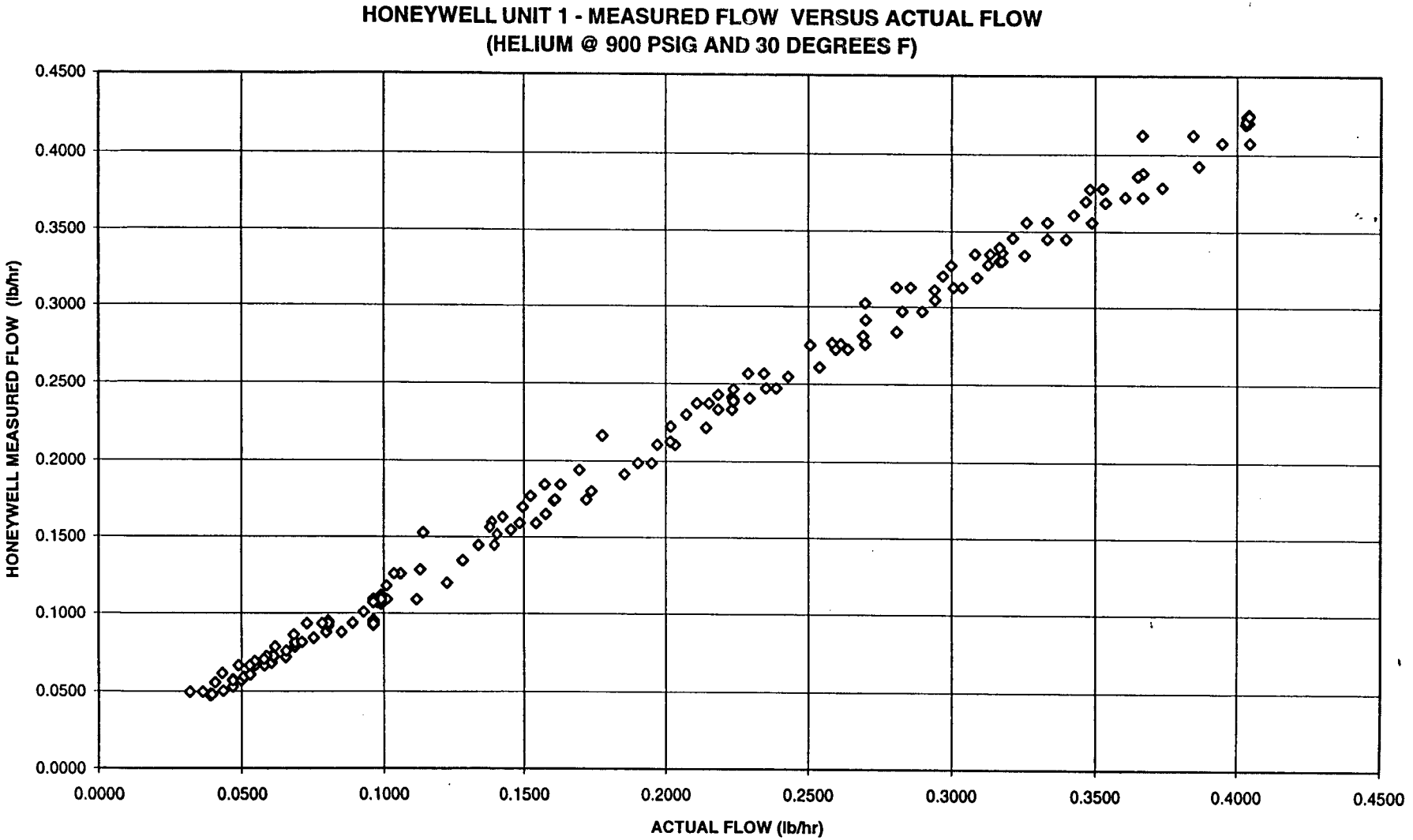
HONEYWELL UNIT 1 - MEASURED FLOW VERSUS ACTUAL FLOW
(HELIUM @ 900 PSIG AND 30 DEGREES F)
HONEYWELL MEASURED FLOW (lb/hr)
0.4500
0.4000
0.3500
0.3000
0.2500
0.2000
0.1500
0.1000
0.0500
0.0000
0.0000
0.0500
0.1000
0.1500
0.2000
0.2500
0.3000
0.3500
0.4000
0.4500
ACTUAL FLOW (lb/hr)

Figure 122

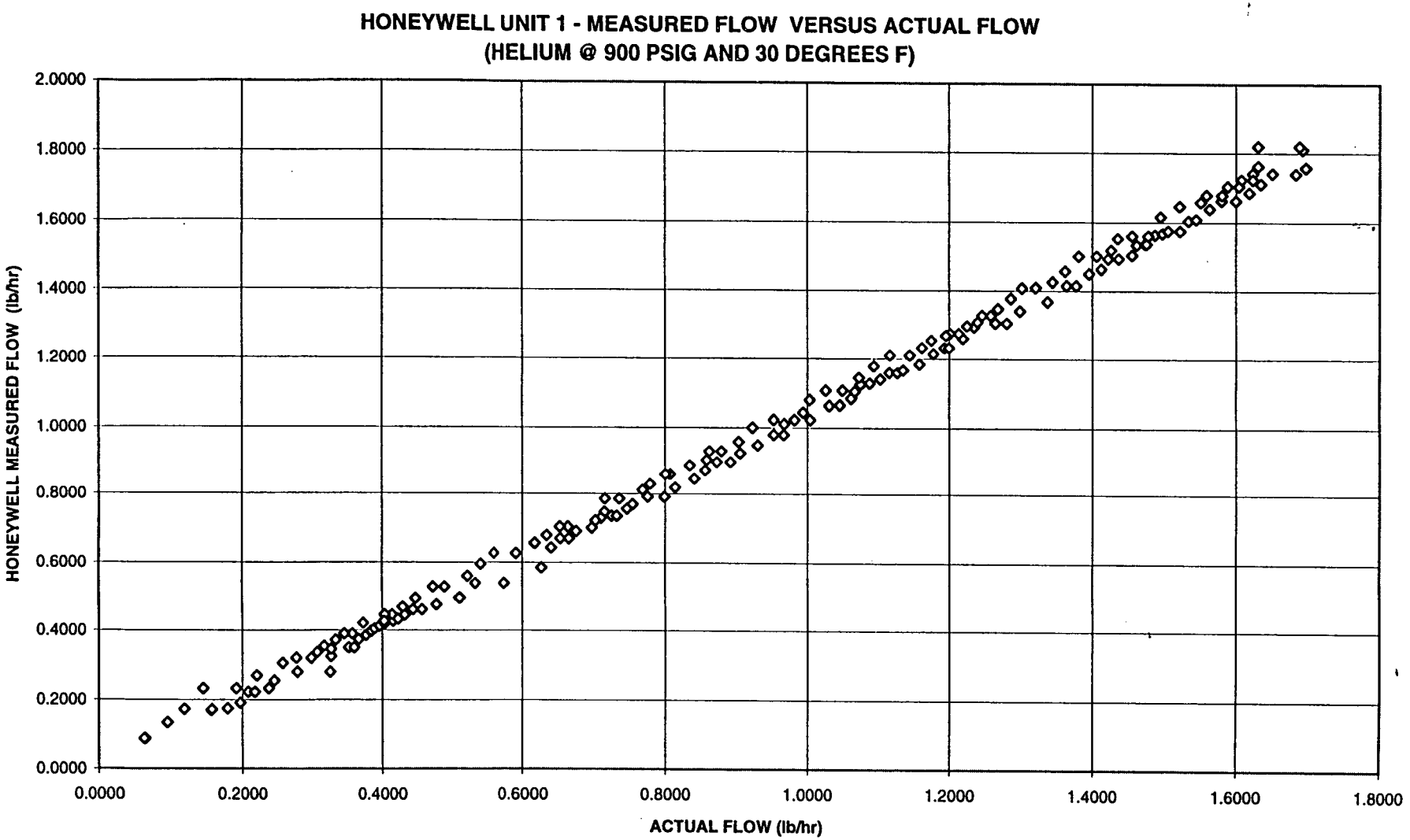
HONEYWELL UNIT 1 - MEASURED FLOW VERSUS ACTUAL FLOW
(HELIUM @ 900 PSIG AND 30 DEGREES F)
HONEYWELL MEASURED FLOW (lb/hr)
2.0000
1.8000
1.6000
1.4000
1.2000
1.0000
0.8000
0.6000
0.4000
0.2000
0.0000
0.0000
0.2000
0.4000
0.6000
0.8000
1.0000
1.2000
1.4000
1.6000
1.8000
ACTUAL FLOW (lb/hr)

Figure 123

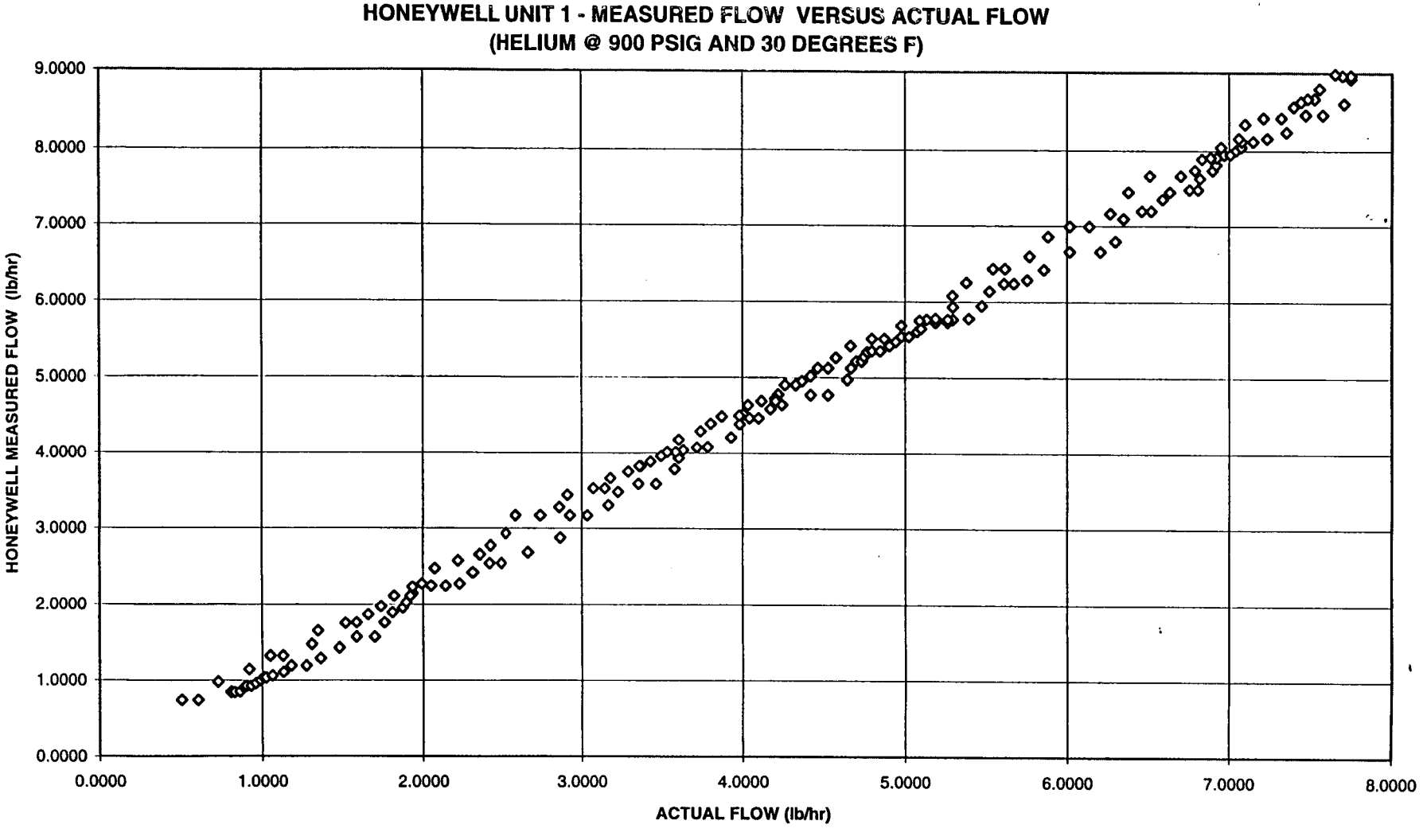
HONEYWELL UNIT 1 - MEASURED FLOW VERSUS ACTUAL FLOW
(HELIUM @ 900 PSIG AND 30 DEGREES F)
HONEYWELL MEASURED FLOW (lb/hr)
9.0000
8.0000
7.0000
6.0000
5.0000
4.0000
3.0000
2.0000
1.0000
0.0000
0.0000
1.0000
2.0000
3.0000
4.0000
5.0000
6.0000
7.0000
8.0000
ACTUAL FLOW (lb/hr)

Figure 124

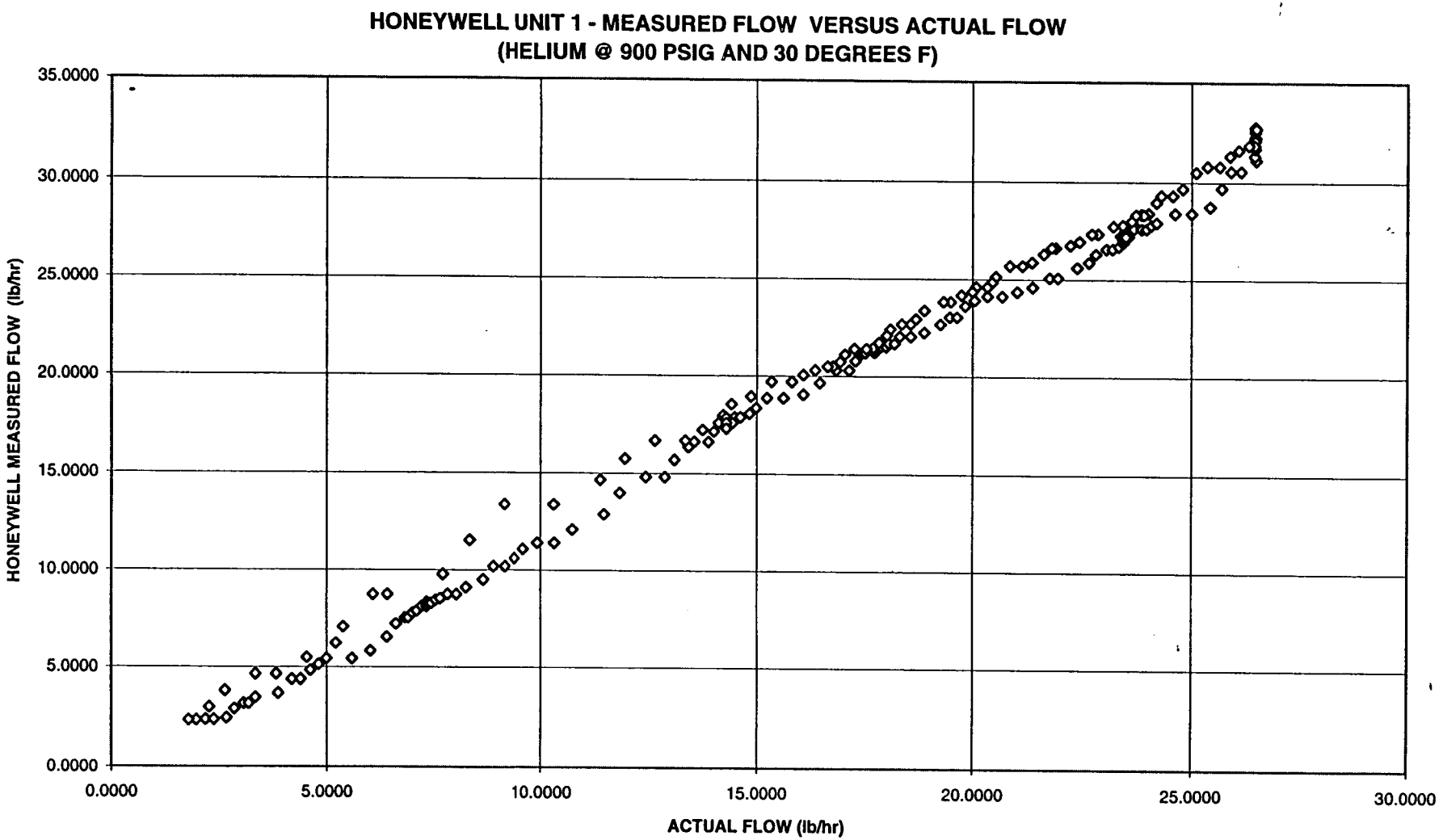
HONEYWELL UNIT 1 - MEASURED FLOW VERSUS ACTUAL FLOW
(HELIUM @ 900 PSIG AND 30 DEGREES F)
HONEYWELL MEASURED FLOW (lb/hr)
35.0000
30.0000
25.0000
20.0000
15.0000
10.0000
5.0000
0.0000
0.0000
5.0000
10.0000
15.0000
20.0000
25.0000
30.0000
ACTUAL FLOW (lb/hr)

Figure 125

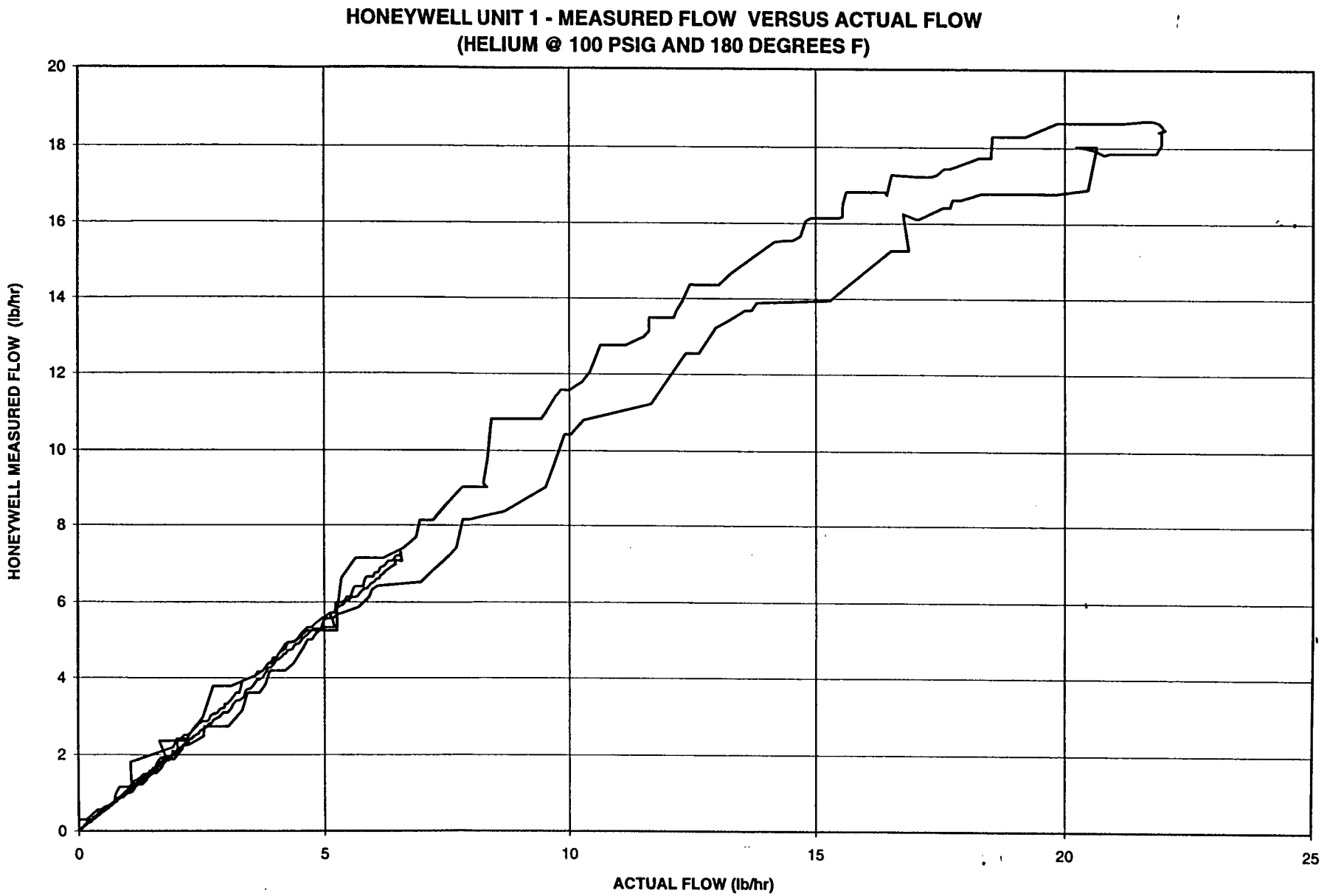
HONEYWELL UNIT 1 - MEASURED FLOW VERSUS ACTUAL FLOW
(HELIUM @ 100 PSIG AND 180 DEGREES F)
HONEYWELL MEASURED FLOW (lb/hr)
ACTUAL FLOW (lb/hr)
0
2
4
6
8
10
12
14
16
18
20
0
5
10
15
20
25

Figure 126

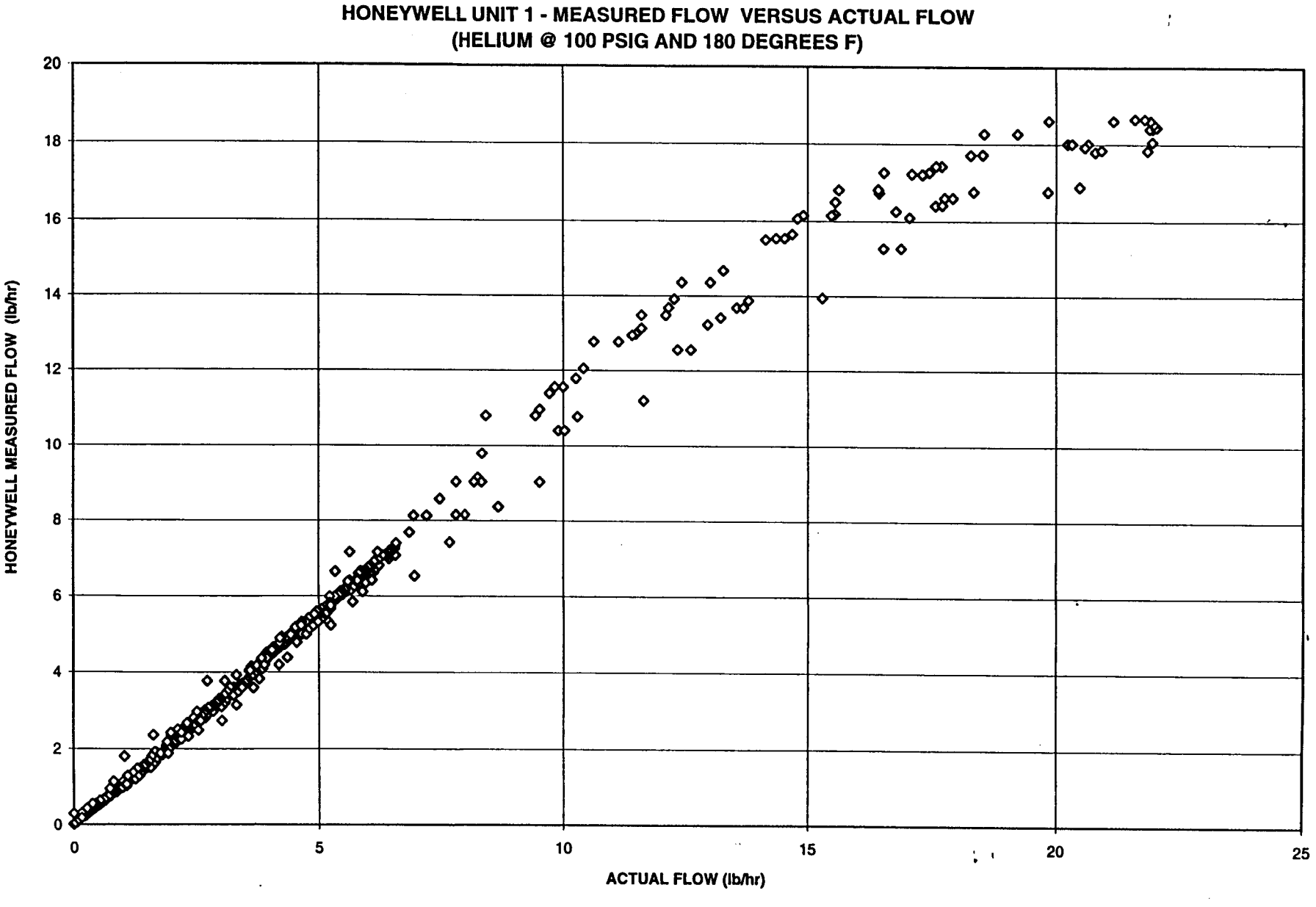
HONEYWELL UNIT 1 - MEASURED FLOW VERSUS ACTUAL FLOW
(HELIUM @ 100 PSIG AND 180 DEGREES F)
HONEYWELL MEASURED FLOW (lb/hr)
ACTUAL FLOW (lb/hr)
0
2
4
6
8
10
12
14
16
18
20
0
5
10
15
20
25

Figure 127

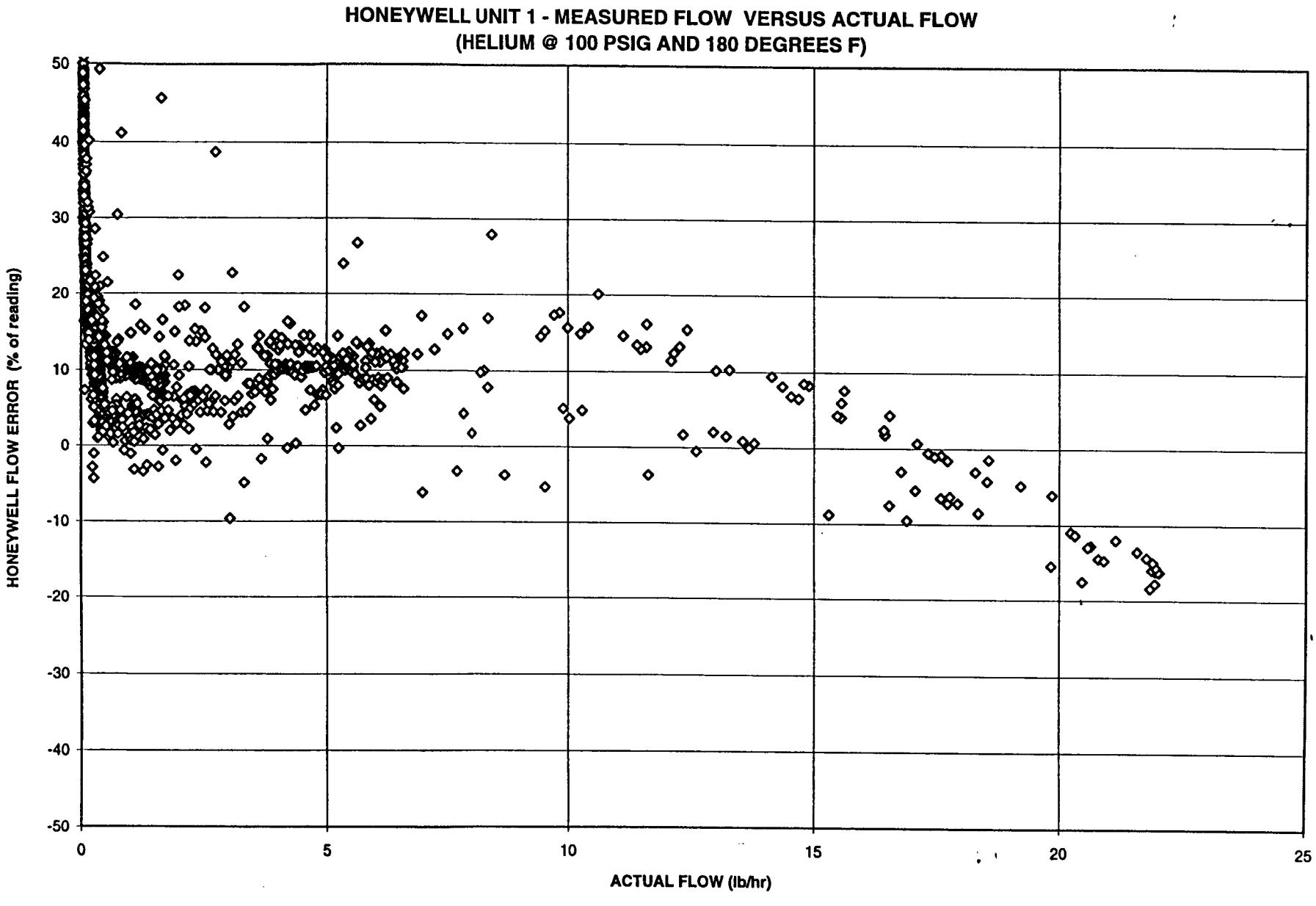
HONEYWELL UNIT 1 - MEASURED FLOW VERSUS ACTUAL FLOW
(HELIUM @ 100 PSIG AND 180 DEGREES F)
HONEYWELL FLOW ERROR (% of reading)
50
40
30
20
10
0
-10
-20
-30
-40
-50
0
5
10
15
20
25
ACTUAL FLOW (lb/hr)

Figure 128

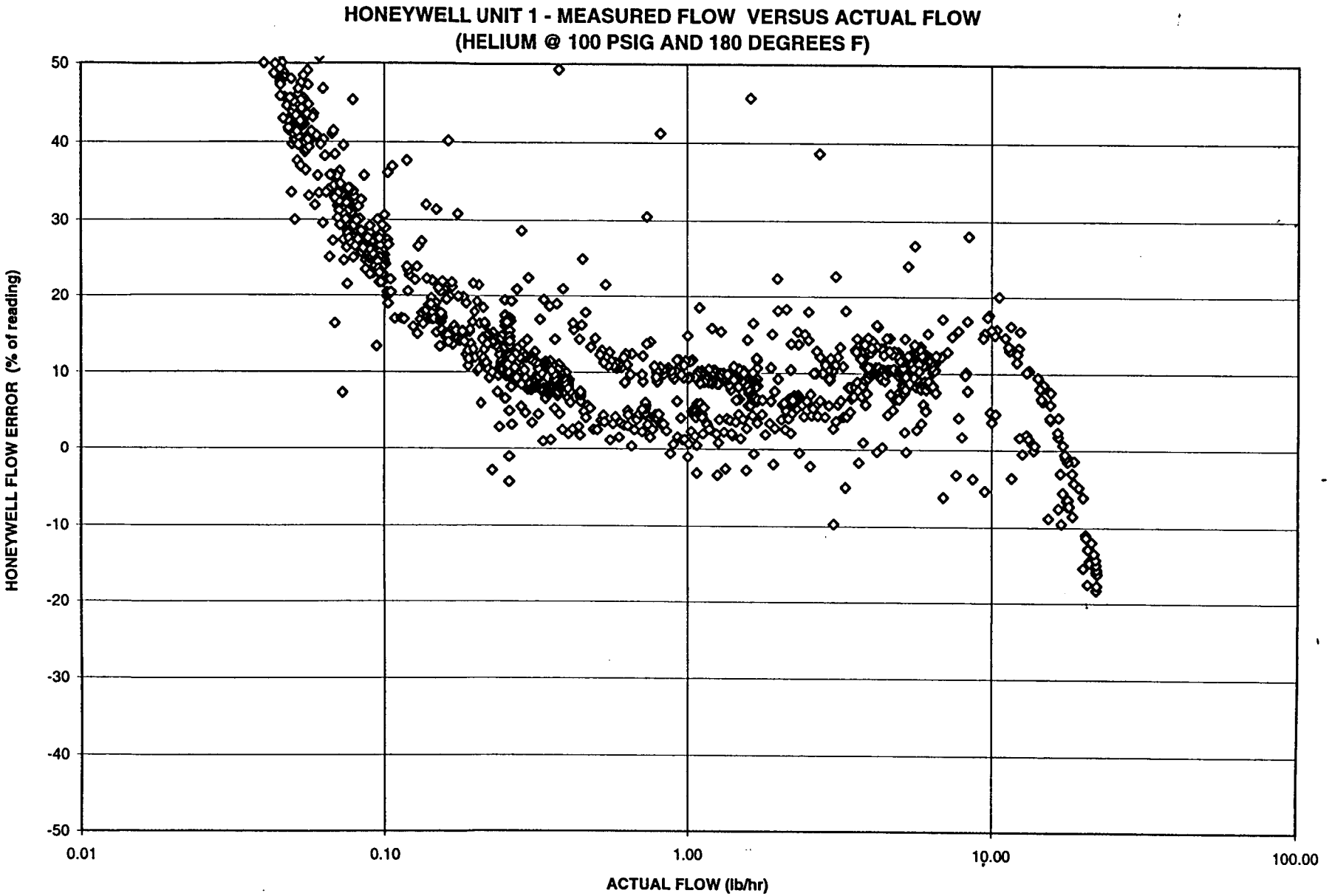
HONEYWELL UNIT 1 - MEASURED FLOW VERSUS ACTUAL FLOW
(HELIUM @ 100 PSIG AND 180 DEGREES F)
HONEYWELL FLOW ERROR (% of reading)
50
40
30
20
10
0
-10
-20
-30
-40
-50
0.01
0.10
1.00
10.00
100.00
ACTUAL FLOW (lb/hr)

Figure 129

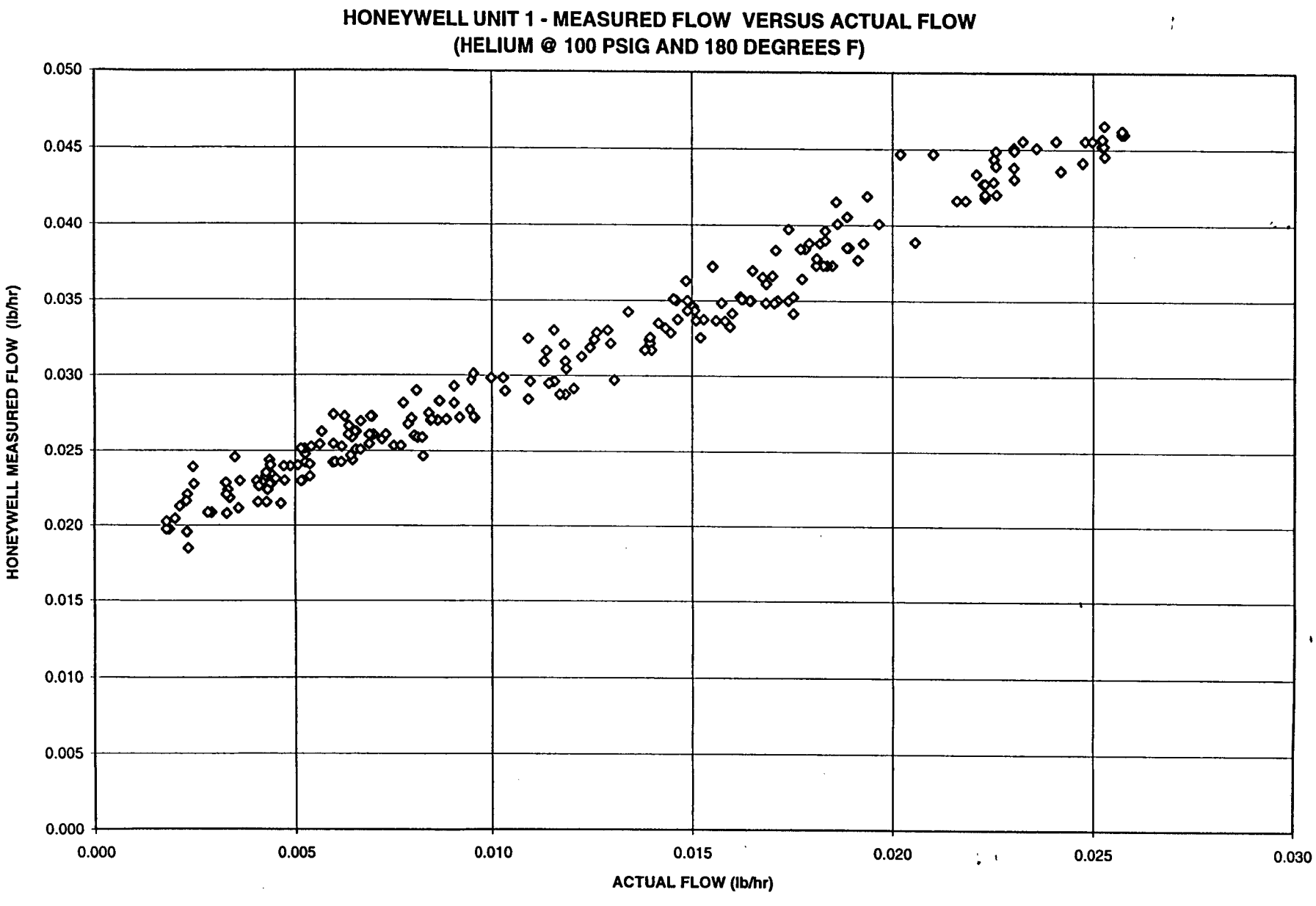
HONEYWELL UNIT 1 - MEASURED FLOW VERSUS ACTUAL FLOW
(HELIUM @ 100 PSIG AND 180 DEGREES F)
HONEYWELL MEASURED FLOW (lb/hr)
0.050
0.045
0.040
0.035
0.030
0.025
0.020
0.015
0.010
0.005
0.000
0.000
0.005
0.010
0.015
0.020
0.025
0.030
ACTUAL FLOW (lb/hr)

Figure 130

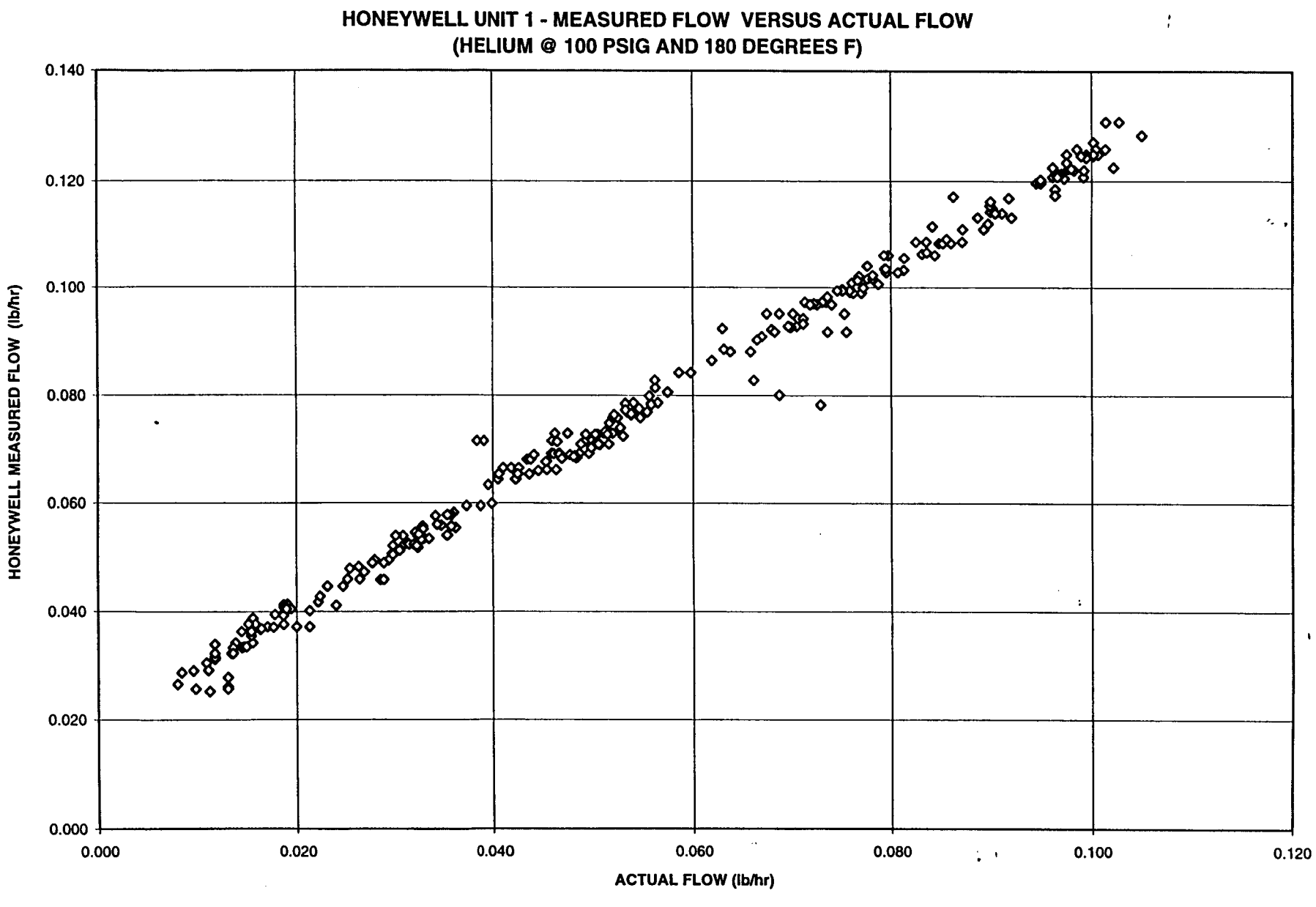
HONEYWELL UNIT 1 - MEASURED FLOW VERSUS ACTUAL FLOW
(HELIUM @ 100 PSIG AND 180 DEGREES F)
HONEYWELL MEASURED FLOW (lb/hr)
0.140
0.120
0.100
0.080
0.060
0.040
0.020
0.000
0.000
0.020
0.040
0.060
0.080
0.100
0.120
ACTUAL FLOW (lb/hr)

Figure 131

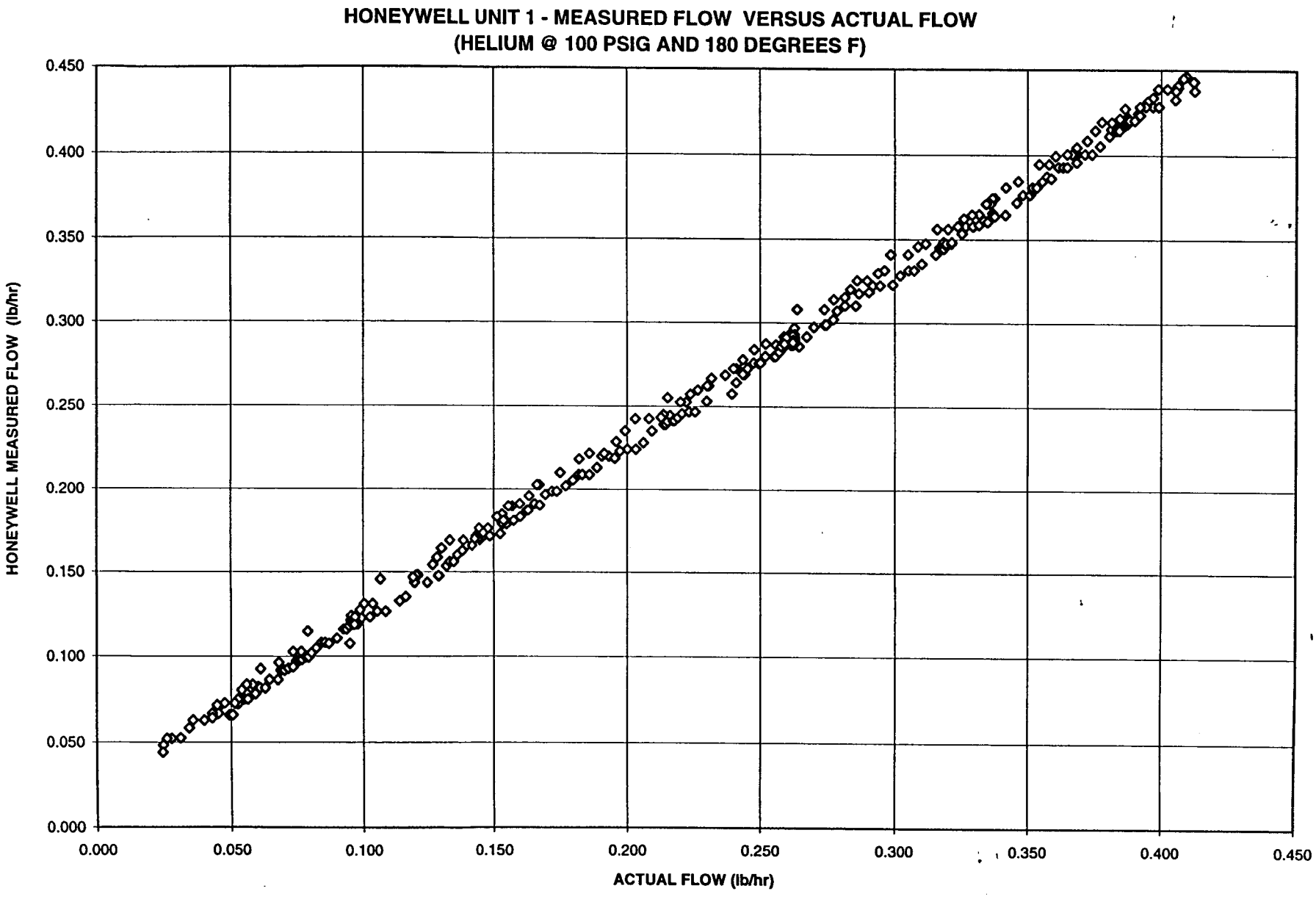
HONEYWELL UNIT 1 - MEASURED FLOW VERSUS ACTUAL FLOW
(HELIUM @ 100 PSIG AND 180 DEGREES F)
HONEYWELL MEASURED FLOW (lb/hr)
0.450
0.400
0.350
0.300
0.250
0.200
0.150
0.100
0.050
0.000
0.000
0.050
0.100
0.150
0.200
0.250
0.300
0.350
0.400
0.450
ACTUAL FLOW (lb/hr)

Figure 132

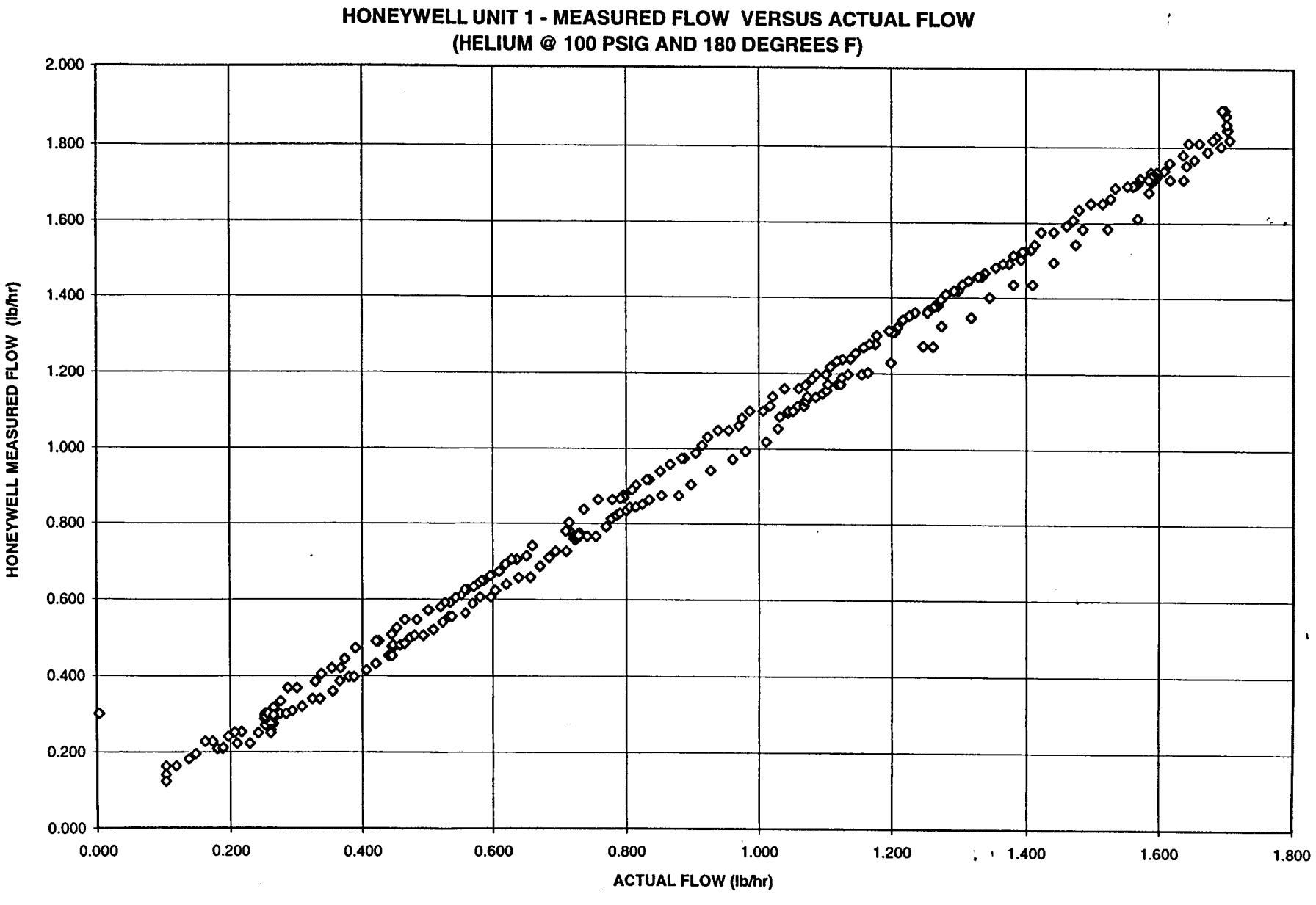
HONEYWELL UNIT 1 - MEASURED FLOW VERSUS ACTUAL FLOW
(HELIUM @ 100 PSIG AND 180 DEGREES F)
HONEYWELL MEASURED FLOW (lb/hr)
2.000
1.800
1.600
1.400
1.200
1.000
0.800
0.600
0.400
0.200
0.000
0.000
0.200
0.400
0.600
0.800
1.000
1.200
1.400
1.600
1.800
ACTUAL FLOW (lb/hr)

Figure 133

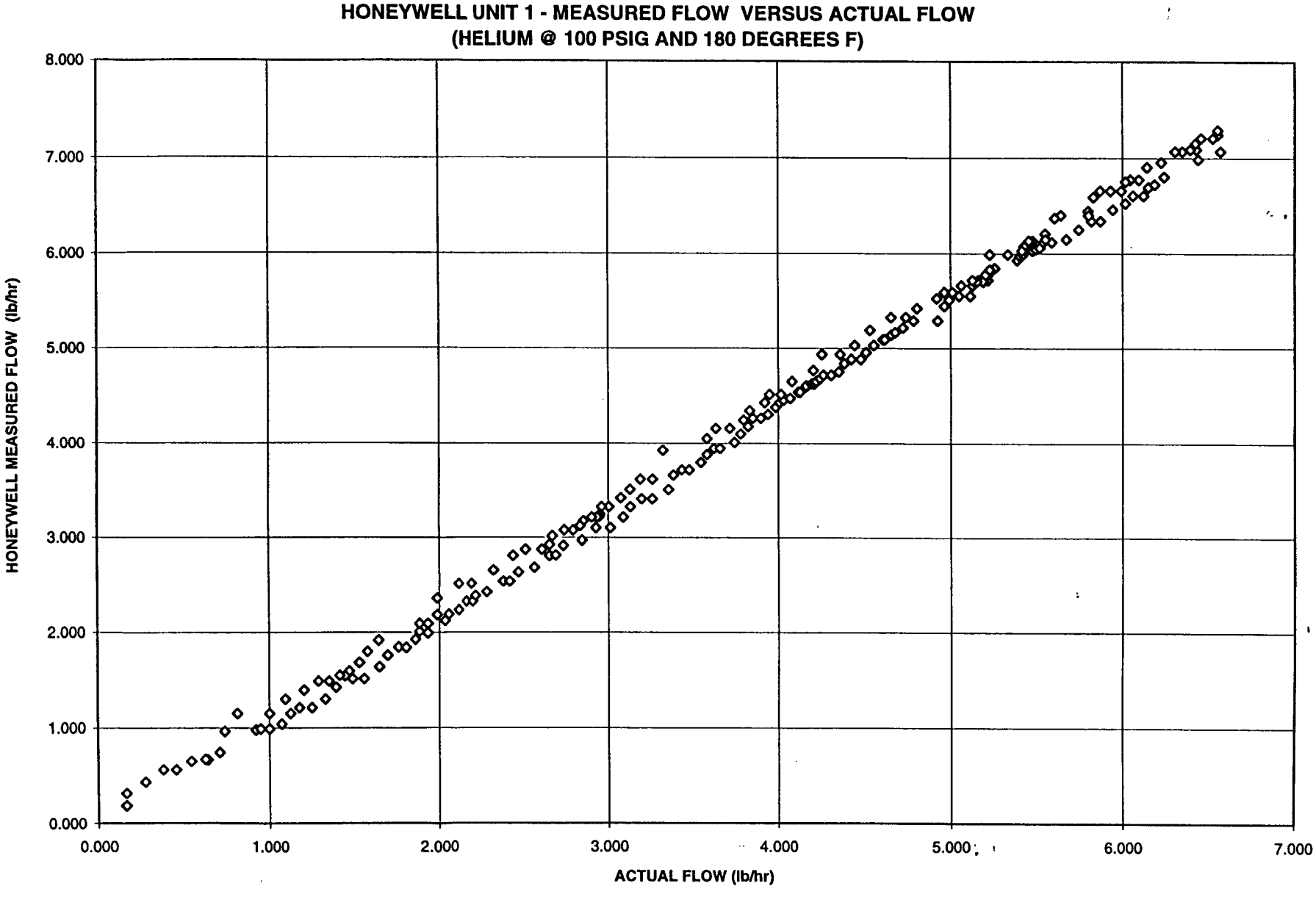
HONEYWELL UNIT 1 - MEASURED FLOW VERSUS ACTUAL FLOW
(HELIUM @ 100 PSIG AND 180 DEGREES F)
HONEYWELL MEASURED FLOW (lb/hr)
8.000
7.000
6.000
5.000
4.000
3.000
2.000
1.000
0.000
0.000
1.000
2.000
3.000
4.000
5.000
6.000
7.000
ACTUAL FLOW (lb/hr)

Figure 134

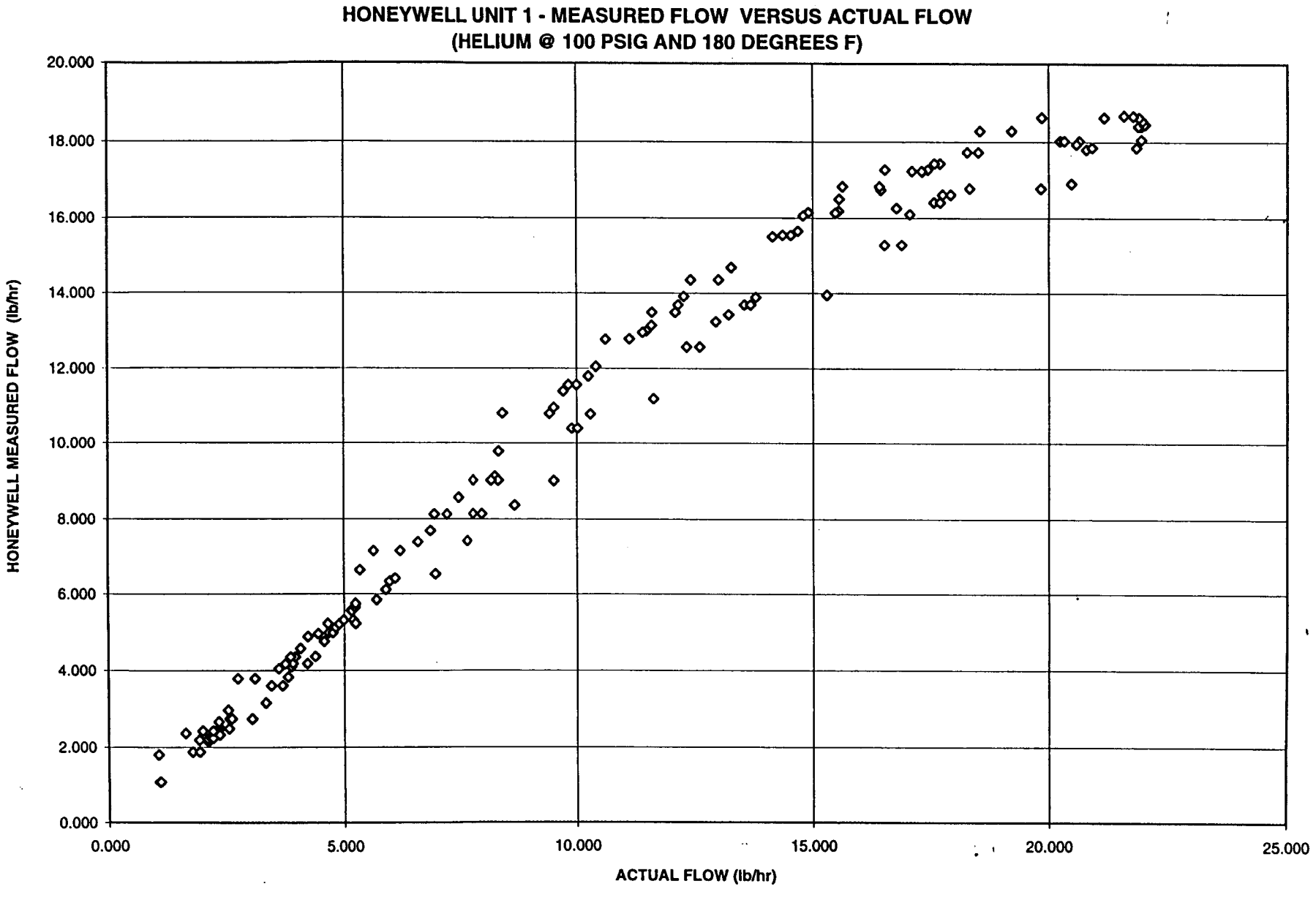
HONEYWELL UNIT 1 - MEASURED FLOW VERSUS ACTUAL FLOW
(HELIUM @ 100 PSIG AND 180 DEGREES F)
HONEYWELL MEASURED FLOW (lb/hr)
20.000
18.000
16.000
14.000
12.000
10.000
8.000
6.000
4.000
2.000
0.000
0.000
5.000
10.000
15.000
20.000
25.000
ACTUAL FLOW (lb/hr)

Figure 135

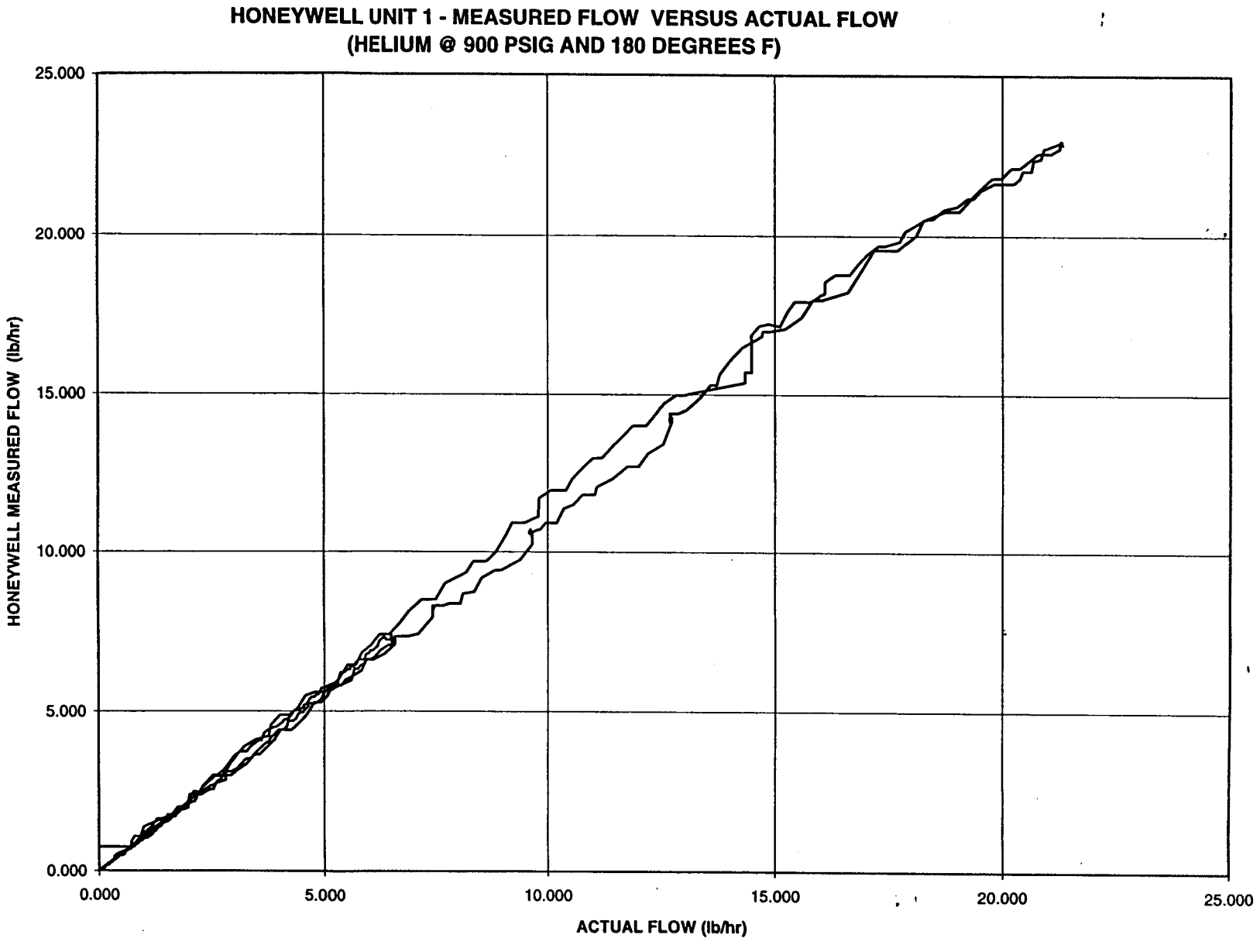
HONEYWELL UNIT 1 - MEASURED FLOW VERSUS ACTUAL FLOW
(HELIUM @ 900 PSIG AND 180 DEGREES F)
HONEYWELL MEASURED FLOW (lb/hr)
25.000
20.000
15.000
10.000
5.000
0.000
0.000
5.000
10.000
15.000
20.000
25.000
ACTUAL FLOW (lb/hr)

Figure 136

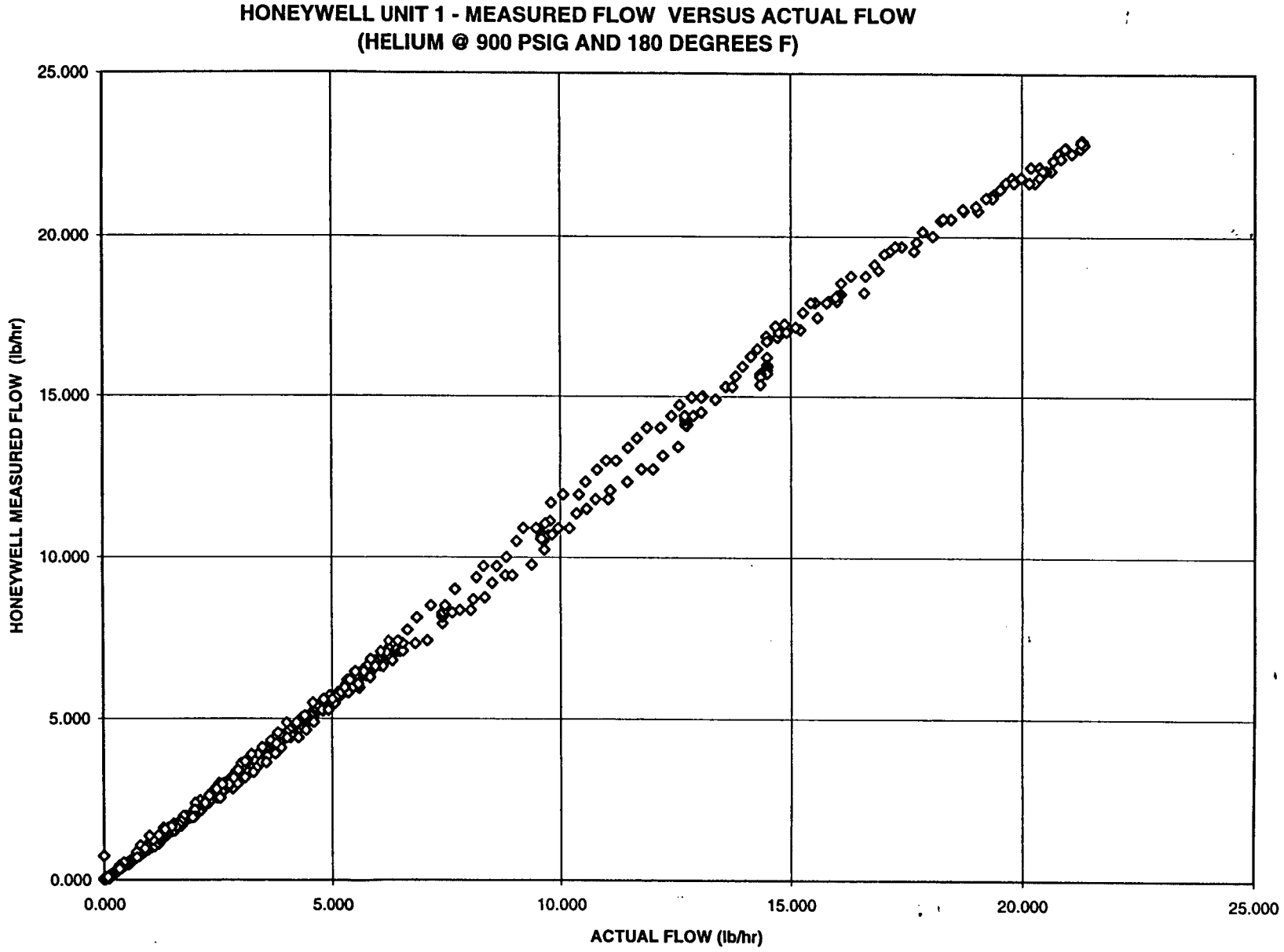
HONEYWELL UNIT 1 - MEASURED FLOW VERSUS ACTUAL FLOW
(HELIUM @ 900 PSIG AND 180 DEGREES F)
HONEYWELL MEASURED FLOW (lb/hr)
25.000
20.000
15.000
10.000
5.000
0.000
0.000
5.000
10.000
15.000
20.000
25.000
ACTUAL FLOW (lb/hr)

Figure 137

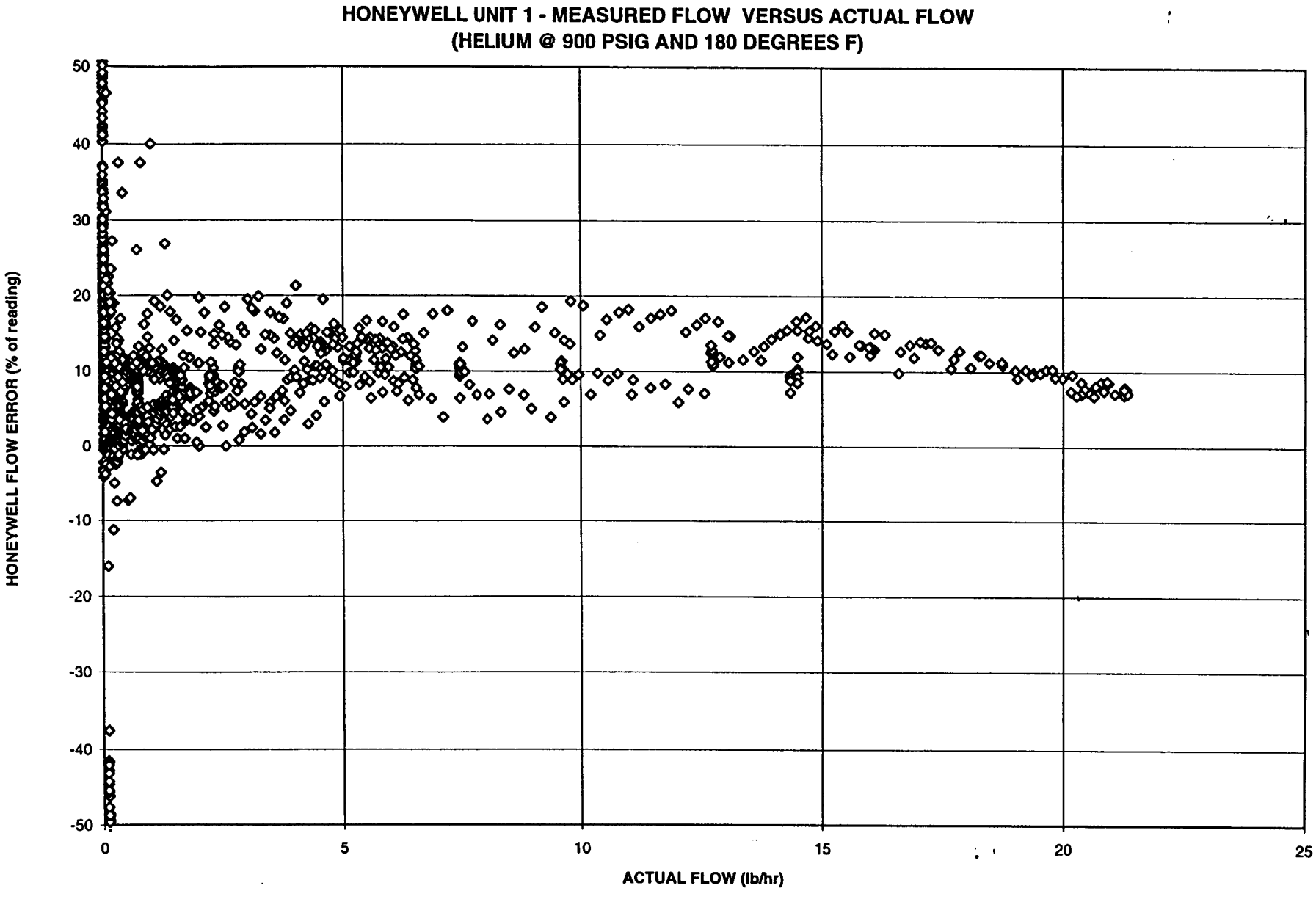
HONEYWELL UNIT 1 - MEASURED FLOW VERSUS ACTUAL FLOW
(HELIUM @ 900 PSIG AND 180 DEGREES F)
HONEYWELL FLOW ERROR (% of reading)
50
40
30
20
10
0
-10
-20
-30
-40
-50
0
5
10
15
20
25
ACTUAL FLOW (lb/hr)

Figure 138

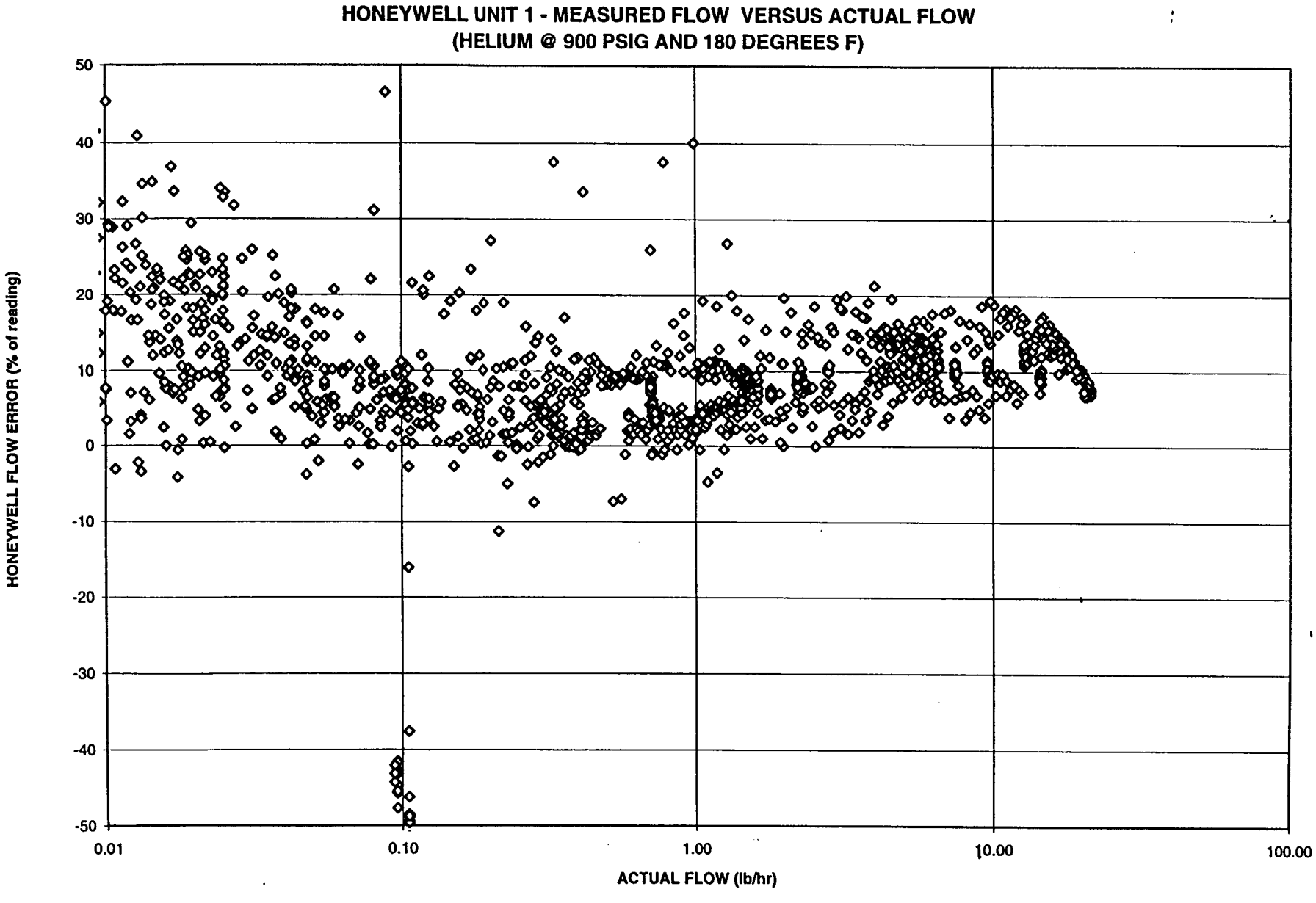
HONEYWELL UNIT 1 - MEASURED FLOW VERSUS ACTUAL FLOW
(HELIUM @ 900 PSIG AND 180 DEGREES F)
HONEYWELL FLOW ERROR (% of reading)
50
40
30
20
10
0
-10
-20
-30
-40
-50
0.01
0.10
1.00
10.00
100.00
ACTUAL FLOW (lb/hr)

Figure 139

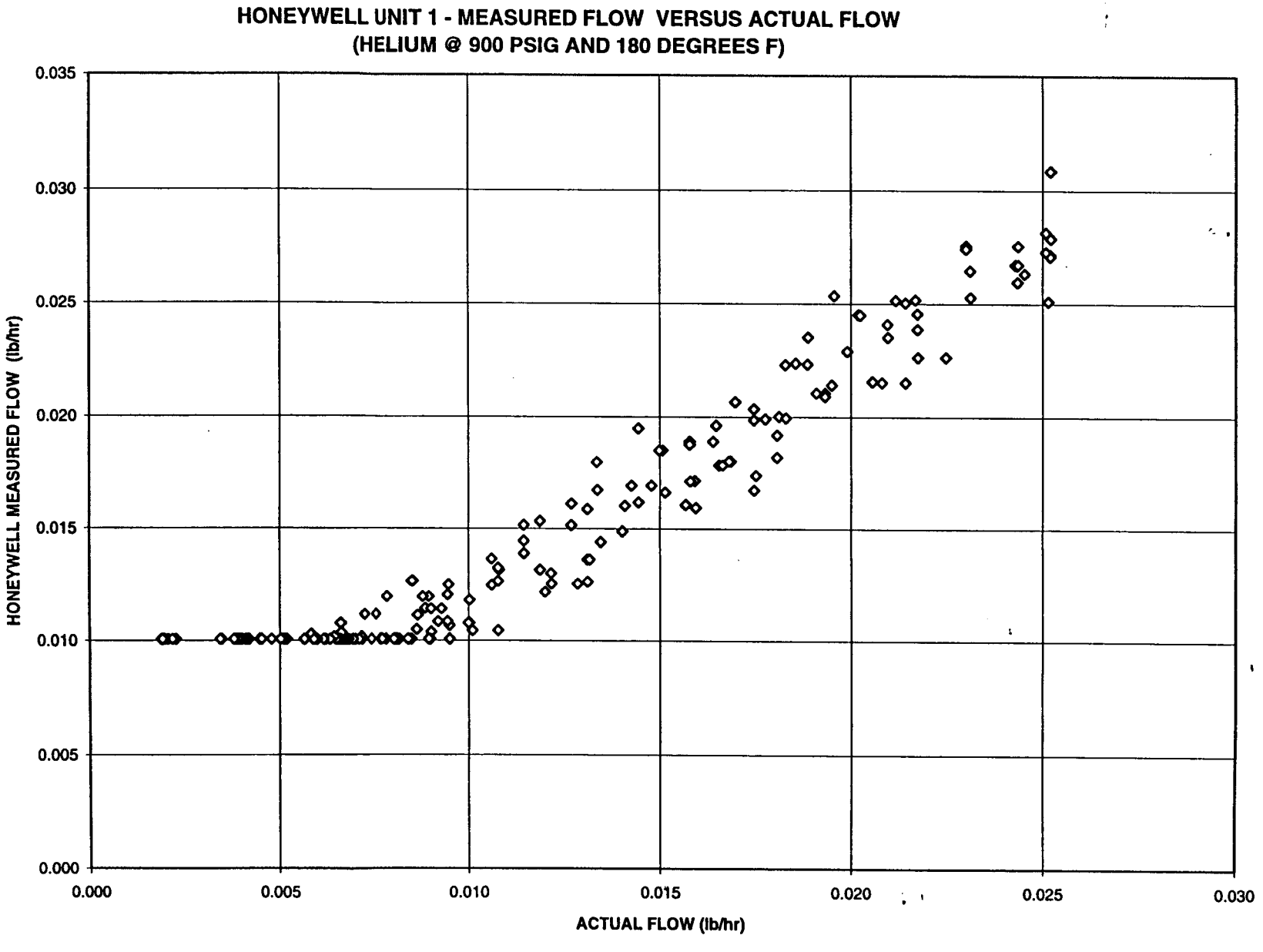
HONEYWELL UNIT 1 - MEASURED FLOW VERSUS ACTUAL FLOW
(HELIUM @ 900 PSIG AND 180 DEGREES F)
HONEYWELL MEASURED FLOW (lb/hr)
0.035
0.030
0.025
0.020
0.015
0.010
0.005
0.000
0.000
0.005
0.010
0.015
0.020
0.025
0.030
ACTUAL FLOW (lb/hr)

Figure 140

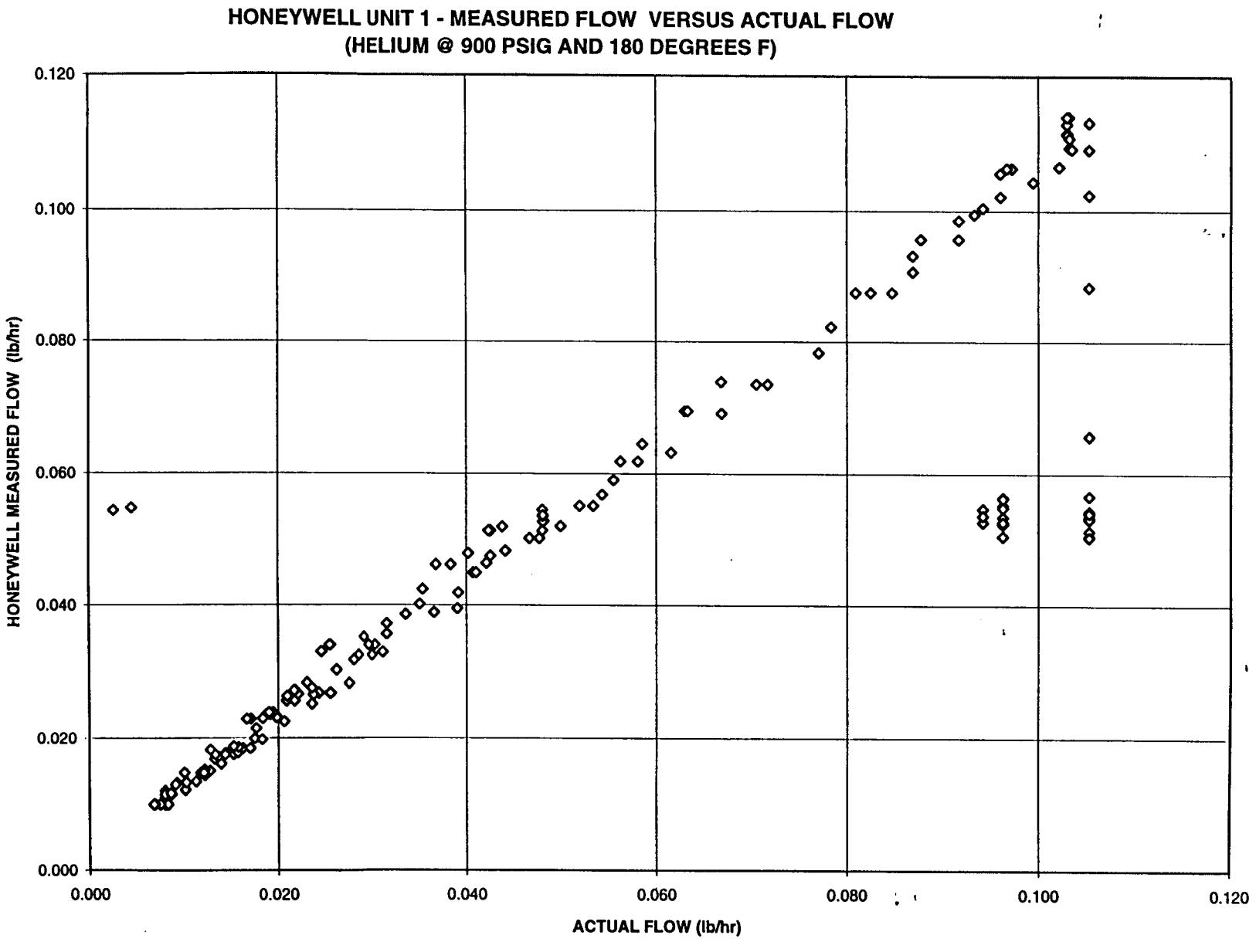
HONEYWELL UNIT 1 - MEASURED FLOW VERSUS ACTUAL FLOW
(HELIUM @ 900 PSIG AND 180 DEGREES F)
HONEYWELL MEASURED FLOW (lb/hr)
0.120
0.100
0.080
0.060
0.040
0.020
0.000
0.000
0.020
0.040
0.060
0.080
0.100
0.120
ACTUAL FLOW (lb/hr)

Figure 141

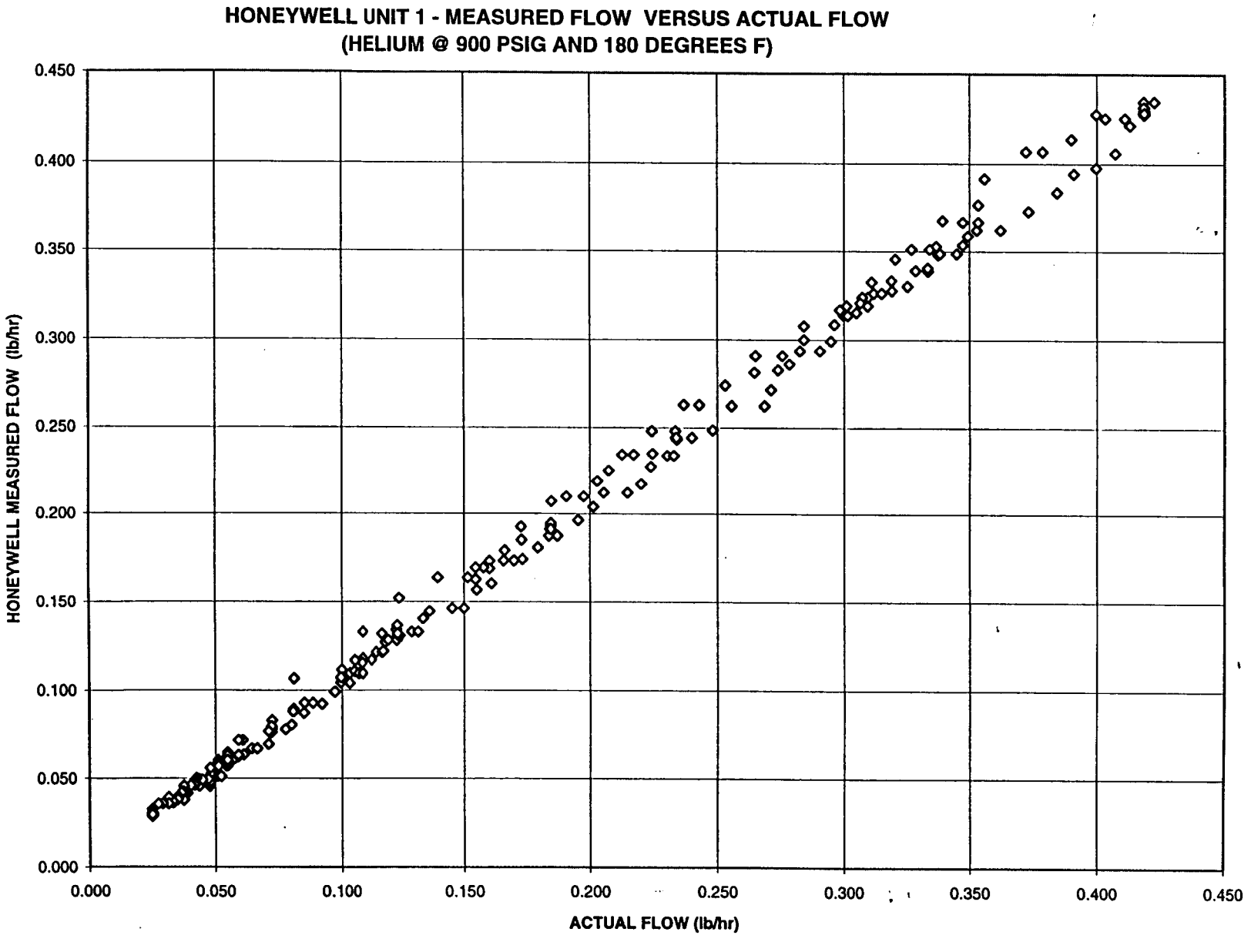
HONEYWELL UNIT 1 - MEASURED FLOW VERSUS ACTUAL FLOW
(HELIUM @ 900 PSIG AND 180 DEGREES F)
HONEYWELL MEASURED FLOW (lb/hr)
0.450
0.400
0.350
0.300
0.250
0.200
0.150
0.100
0.050
0.000
0.000
0.050
0.100
0.150
0.200
0.250
0.300
0.350
0.400
0.450
ACTUAL FLOW (lb/hr)

Figure 142

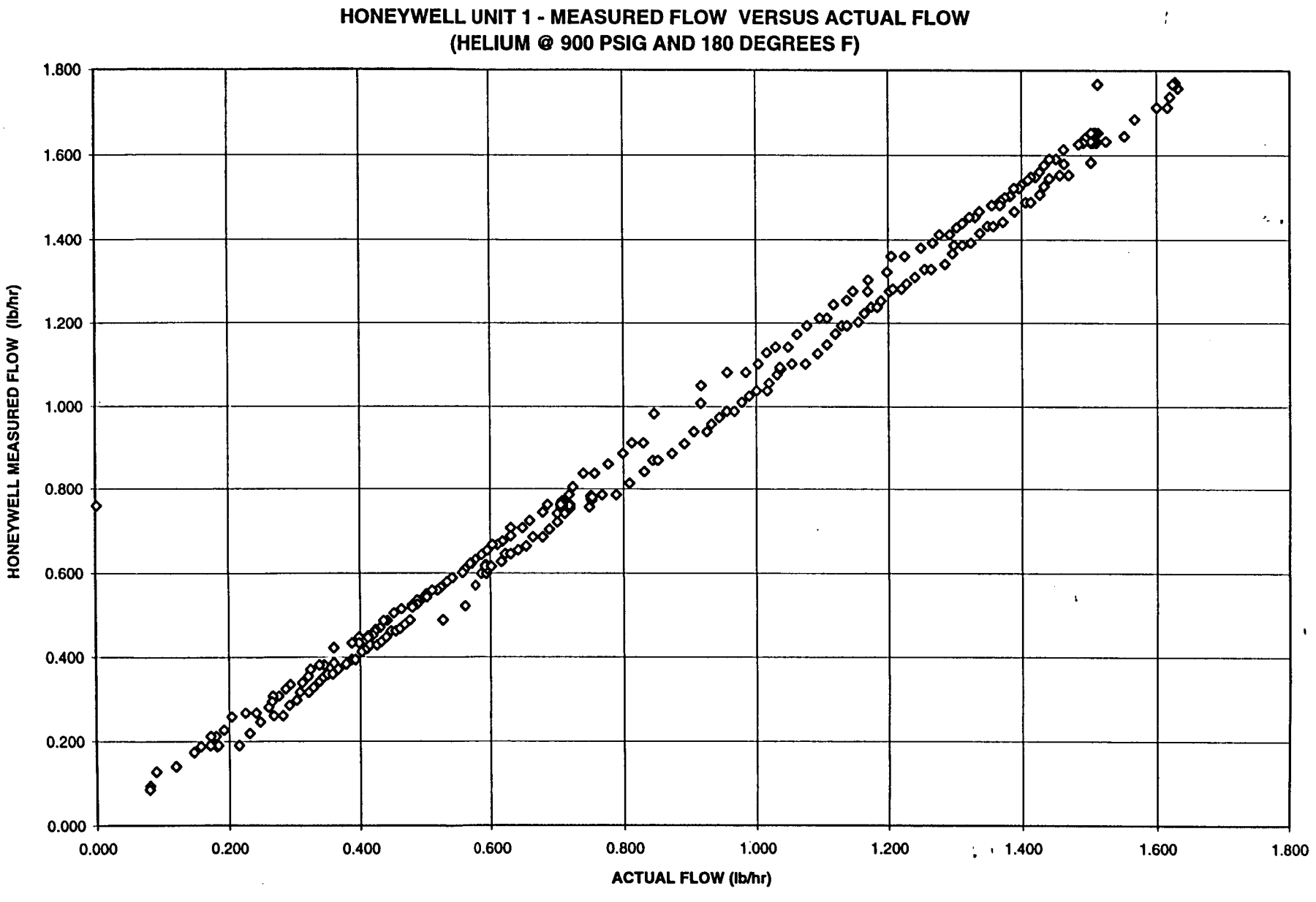
HONEYWELL UNIT 1 - MEASURED FLOW VERSUS ACTUAL FLOW
(HELIUM @ 900 PSIG AND 180 DEGREES F)
HONEYWELL MEASURED FLOW (lb/hr)
1.800
1.600
1.400
1.200
1.000
0.800
0.600
0.400
0.200
0.000
0.000
0.200
0.400
0.600
0.800
1.000
1.200
1.400
1.600
1.800
ACTUAL FLOW (lb/hr)

Figure 143

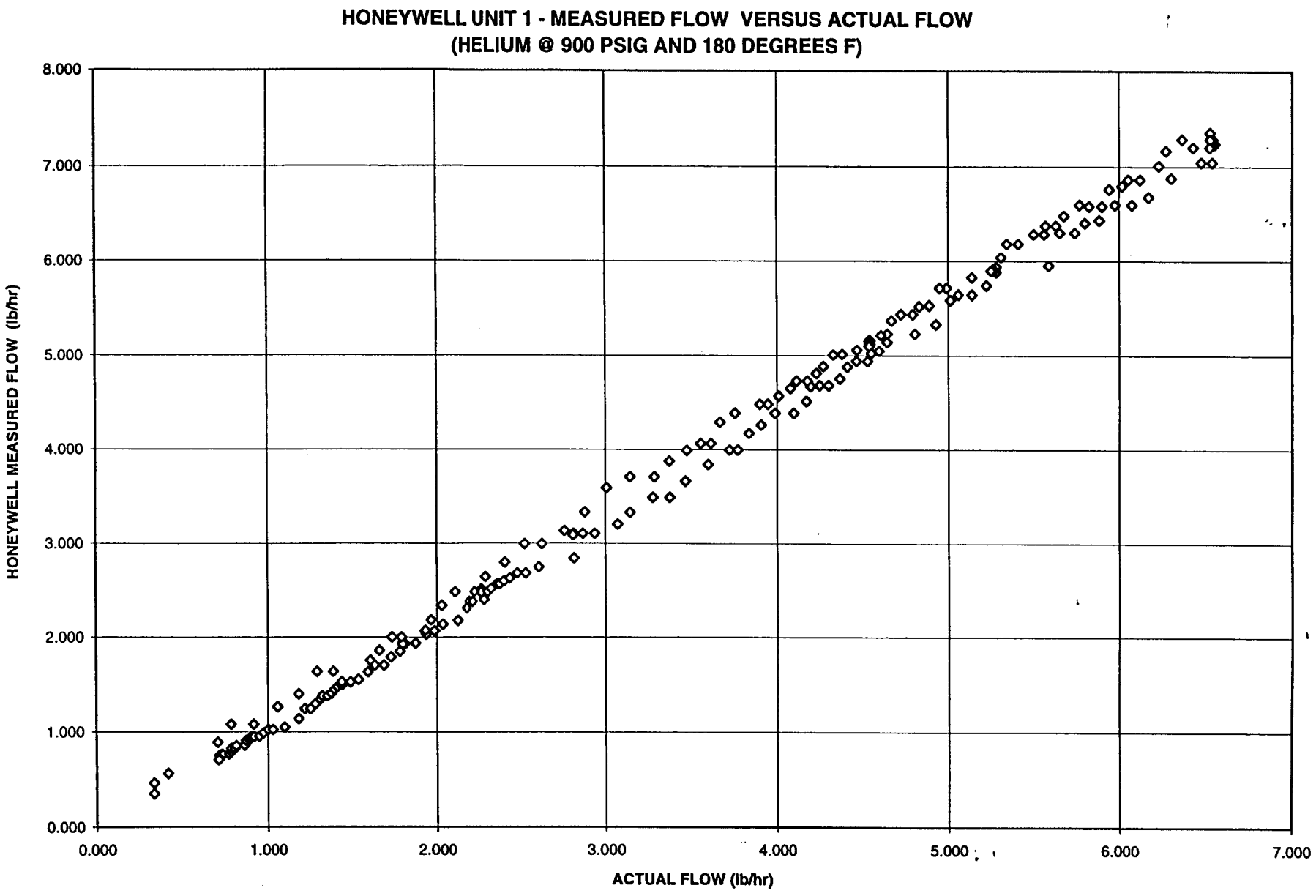
HONEYWELL UNIT 1 - MEASURED FLOW VERSUS ACTUAL FLOW
(HELIUM @ 900 PSIG AND 180 DEGREES F)
HONEYWELL MEASURED FLOW (lb/hr)
8.000
7.000
6.000
5.000
4.000
3.000
2.000
1.000
0.000
0.000
1.000
2.000
3.000
4.000
5.000
6.000
7.000
ACTUAL FLOW (lb/hr)

Figure 144

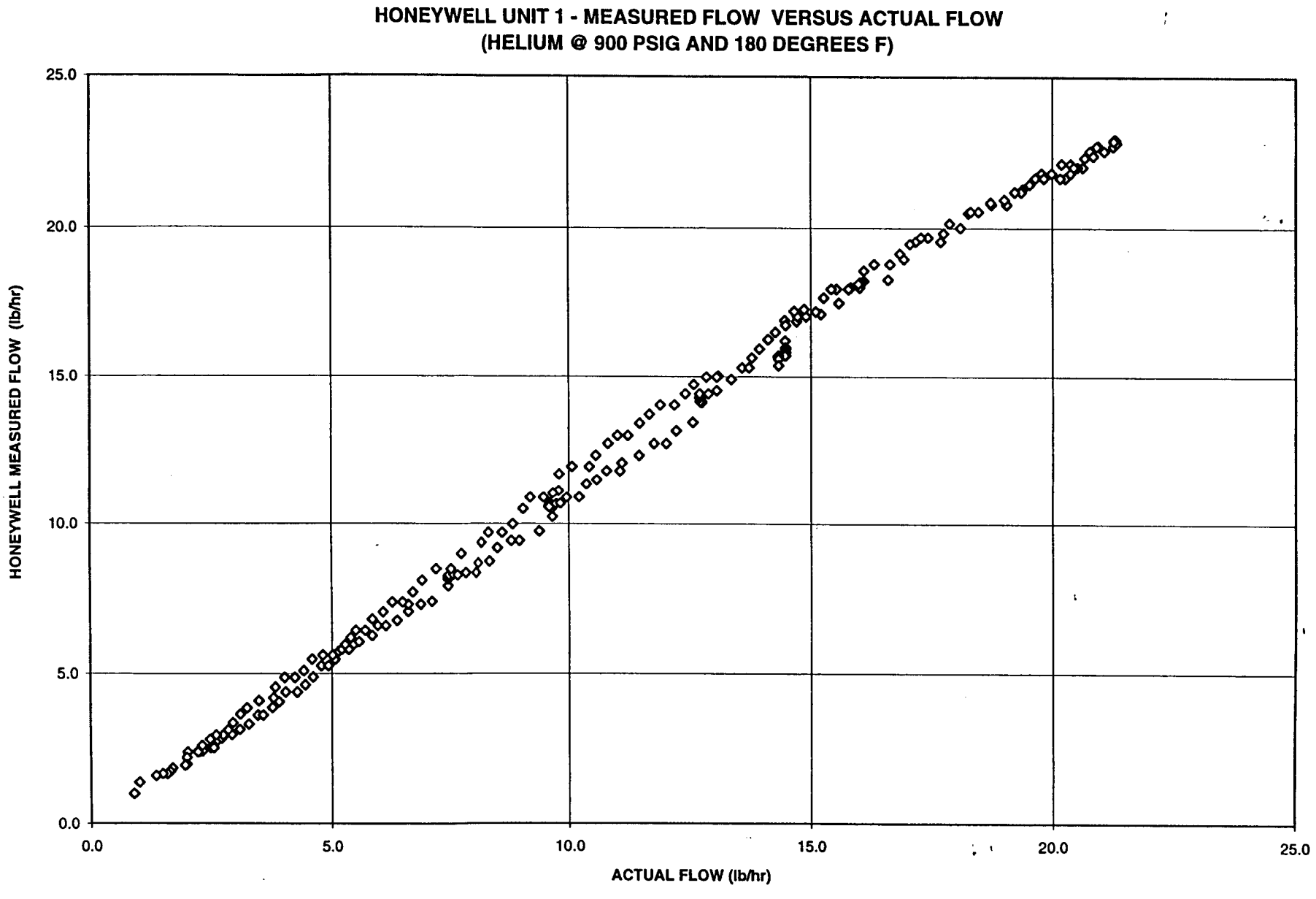
HONEYWELL UNIT 1 - MEASURED FLOW VERSUS ACTUAL FLOW
(HELIUM @ 900 PSIG AND 180 DEGREES F)
HONEYWELL MEASURED FLOW (lb/hr)
25.0
20.0
15.0
10.0
5.0
0.0
0.0
5.0
10.0
15.0
20.0
25.0
ACTUAL FLOW (lb/hr)

Figure 145

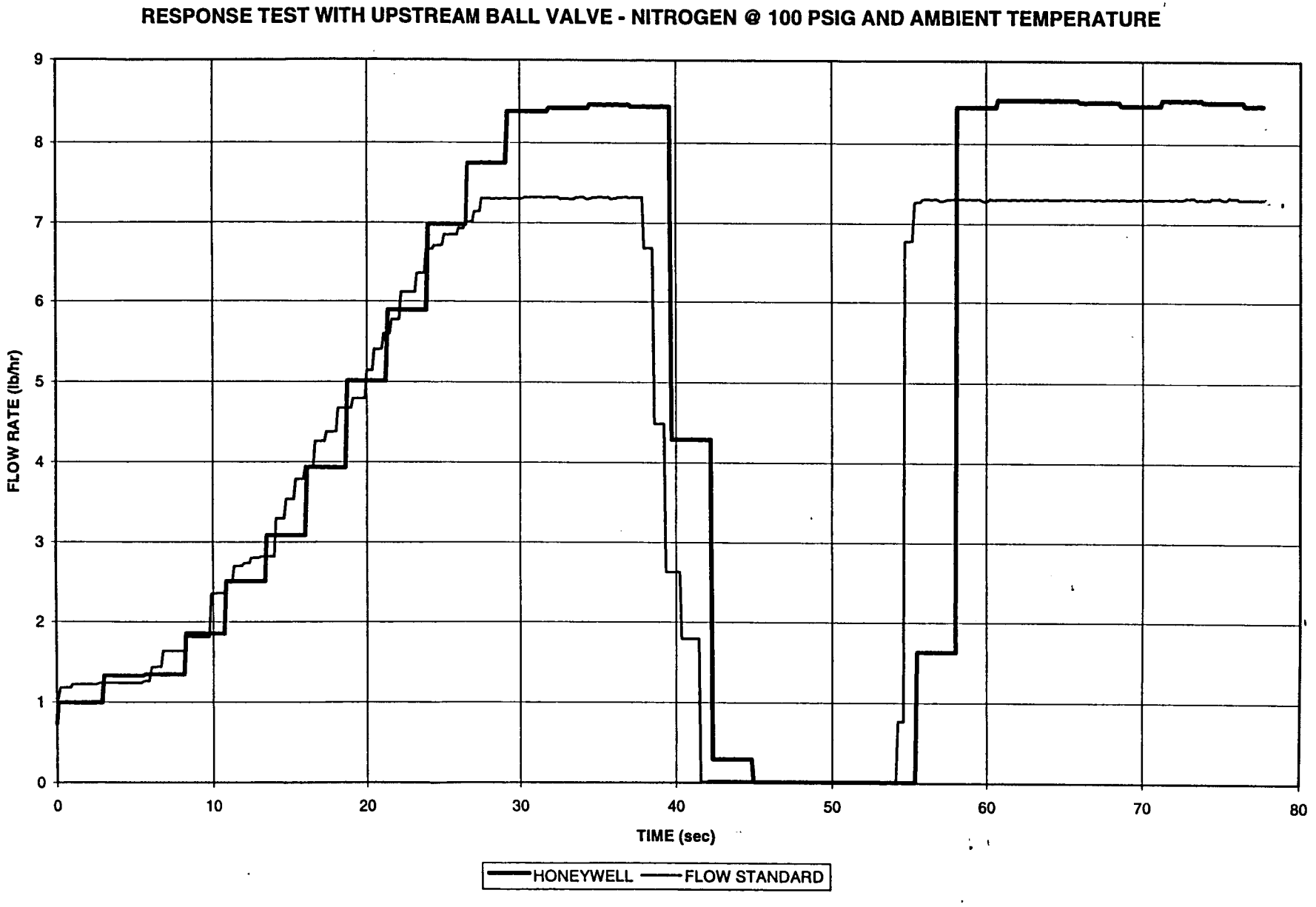
RESPONSE TEST WITH UPSTREAM BALL VALVE - NITROGEN @ 100 PSIG AND AMBIENT TEMPERATURE
FLOW RATE (lb/hr)
0
1
2
3
4
5
6
7
8
9
0
10
20
30
40
50
60
70
80
TIME (sec)
HONEYWELL
FLOW STANDARD

Figure 146

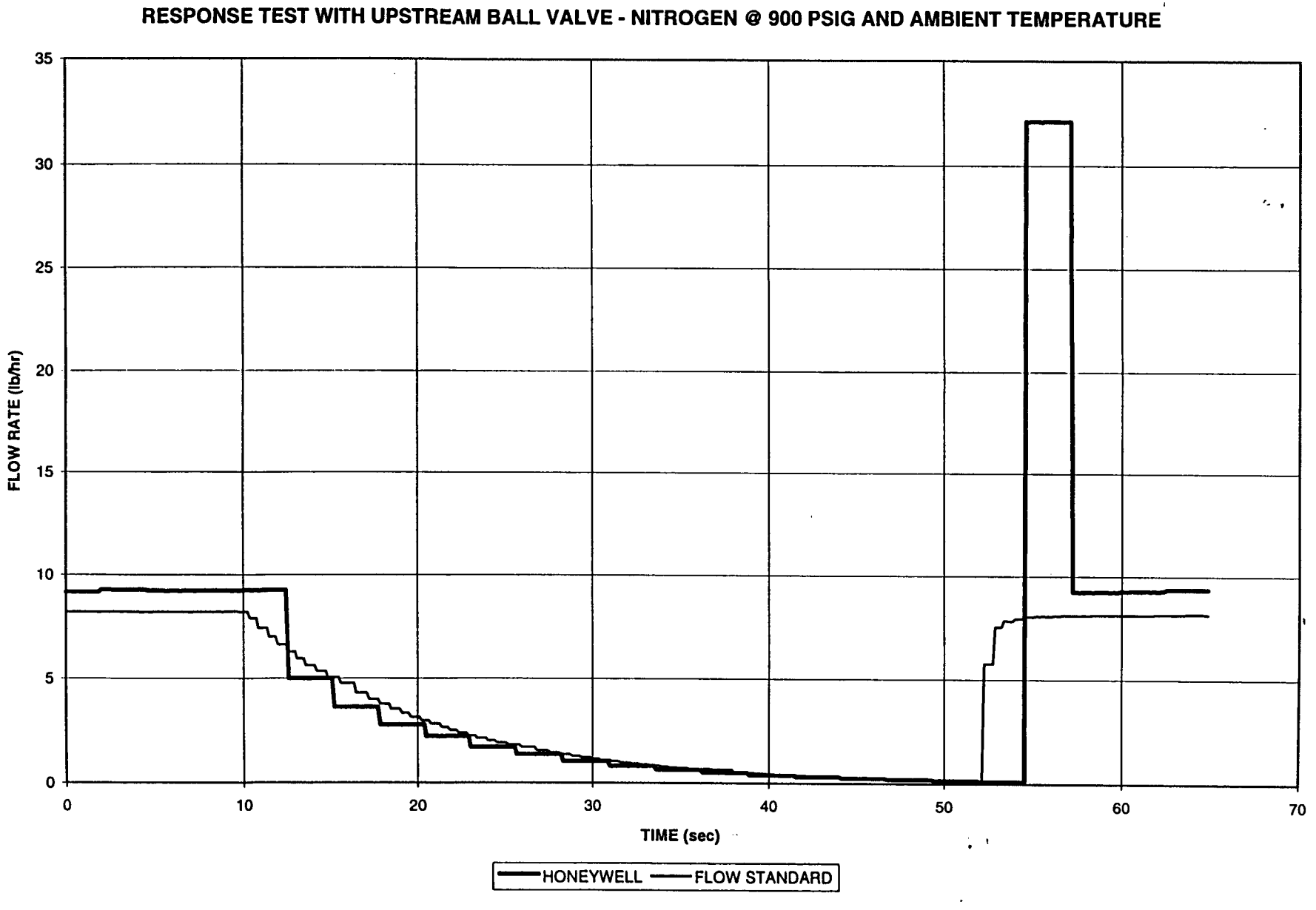
RESPONSE TEST WITH UPSTREAM BALL VALVE - NITROGEN @ 900 PSIG AND AMBIENT TEMPERATURE
FLOW RATE (lb/hr)
35
30
25
20
15
10
5
0
0
10
20
30
40
50
60
70
TIME (sec)
HONEYWELL
FLOW STANDARD

Figure 147

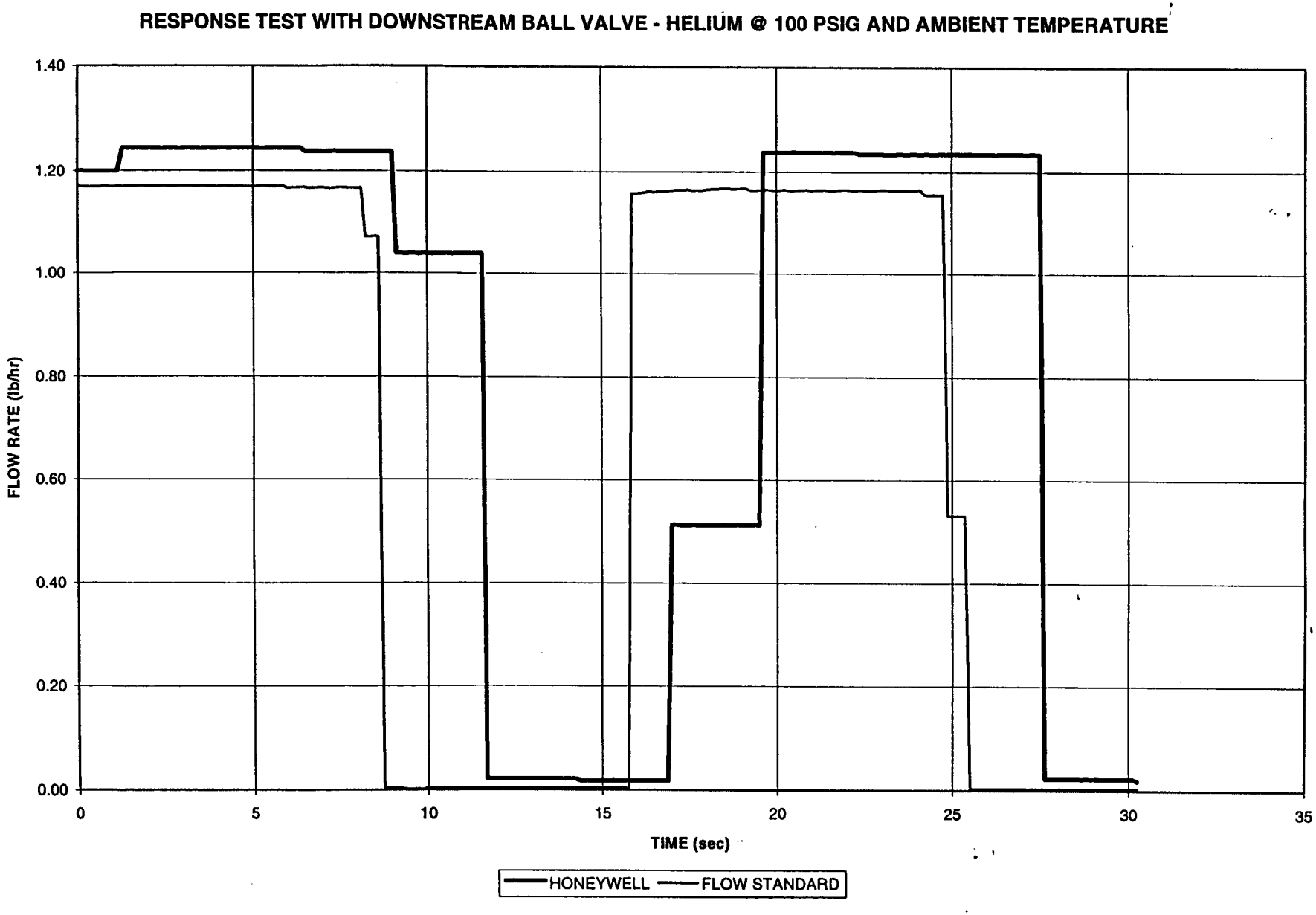
RESPONSE TEST WITH DOWNSTREAM BALL VALVE - HELIUM @ 100 PSIG AND AMBIENT TEMPERATURE
FLOW RATE (lb/hr)
1.40
1.20
1.00
0.80
0.60
0.40
0.20
0.00
0
5
10
15
20
25
30
35
TIME (sec)
HONEYWELL
FLOW STANDARD

Figure 148

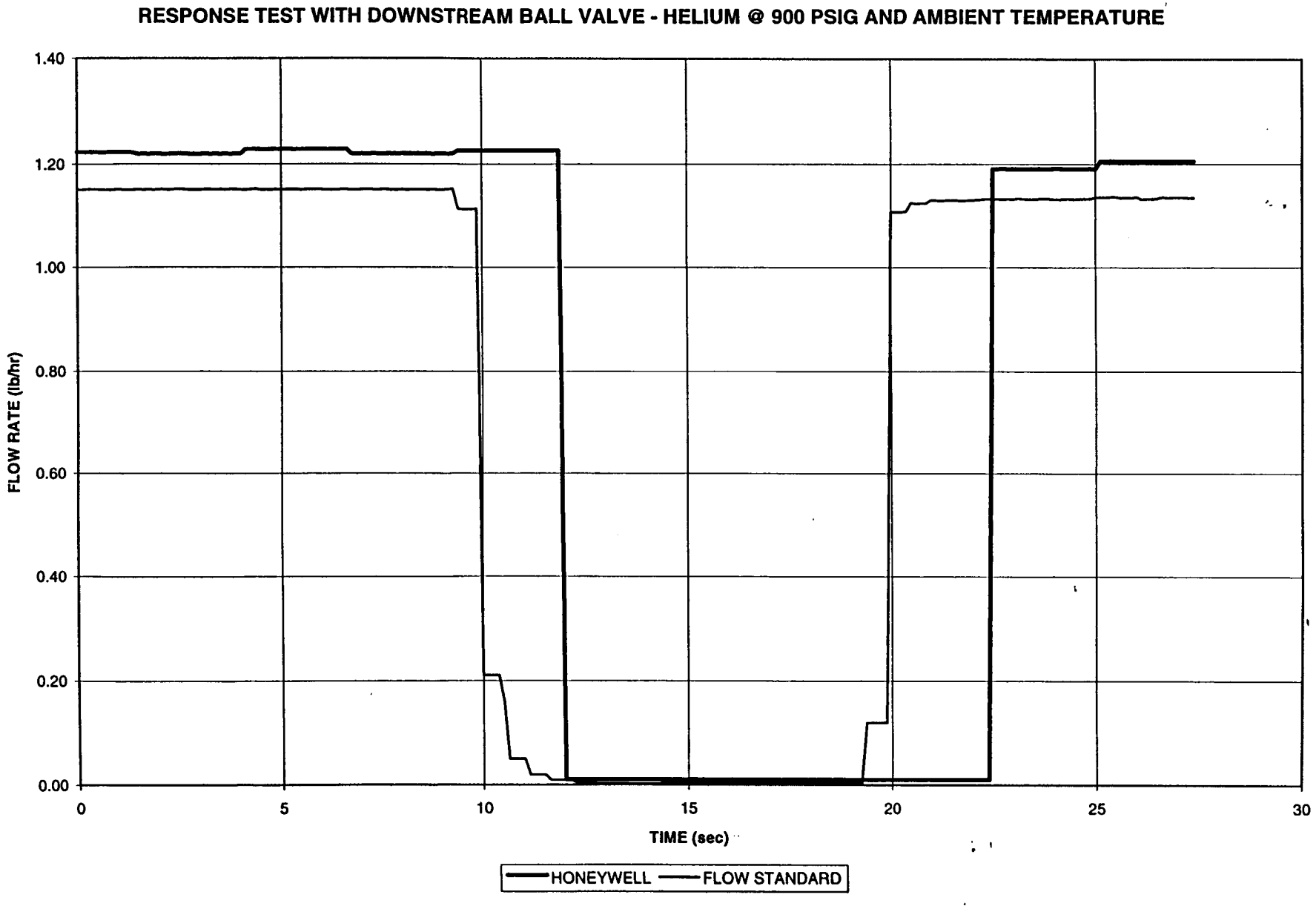
RESPONSE TEST WITH DOWNSTREAM BALL VALVE - HELIUM @ 900 PSIG AND AMBIENT TEMPERATURE
FLOW RATE (lb/hr)
1.40
1.20
1.00
0.80
0.60
0.40
0.20
0.00
0
5
10
15
20
25
30
TIME (sec)
HONEYWELL
FLOW STANDARD

Figure 149

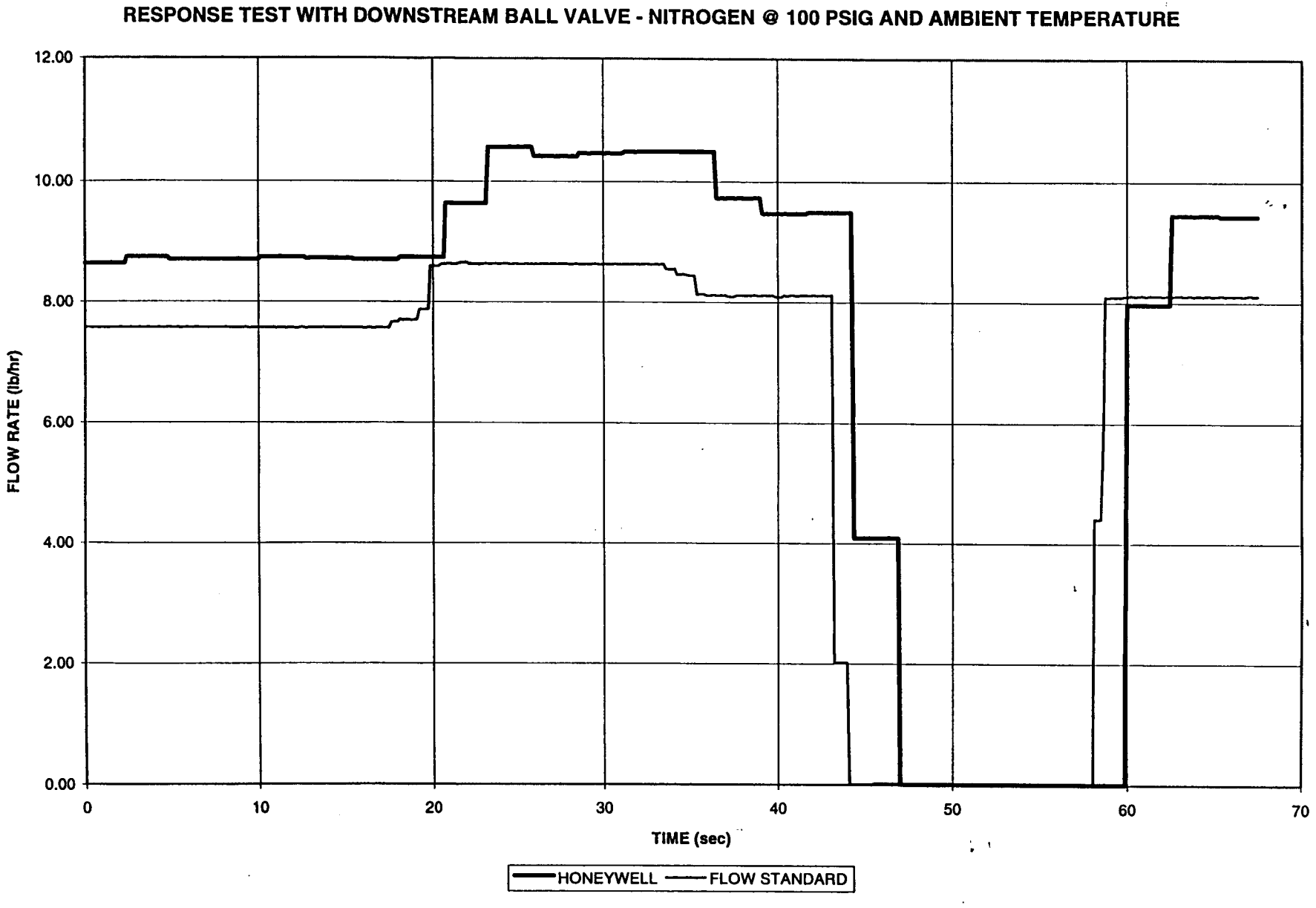
RESPONSE TEST WITH DOWNSTREAM BALL VALVE - NITROGEN @ 100 PSIG AND AMBIENT TEMPERATURE
12.00
10.00
8.00
6.00
4.00
2.00
0.00
FLOW RATE (lb/hr)
0
10
20
30
40
50
60
70
TIME (sec)
HONEYWELL
FLOW STANDARD

Figure 150

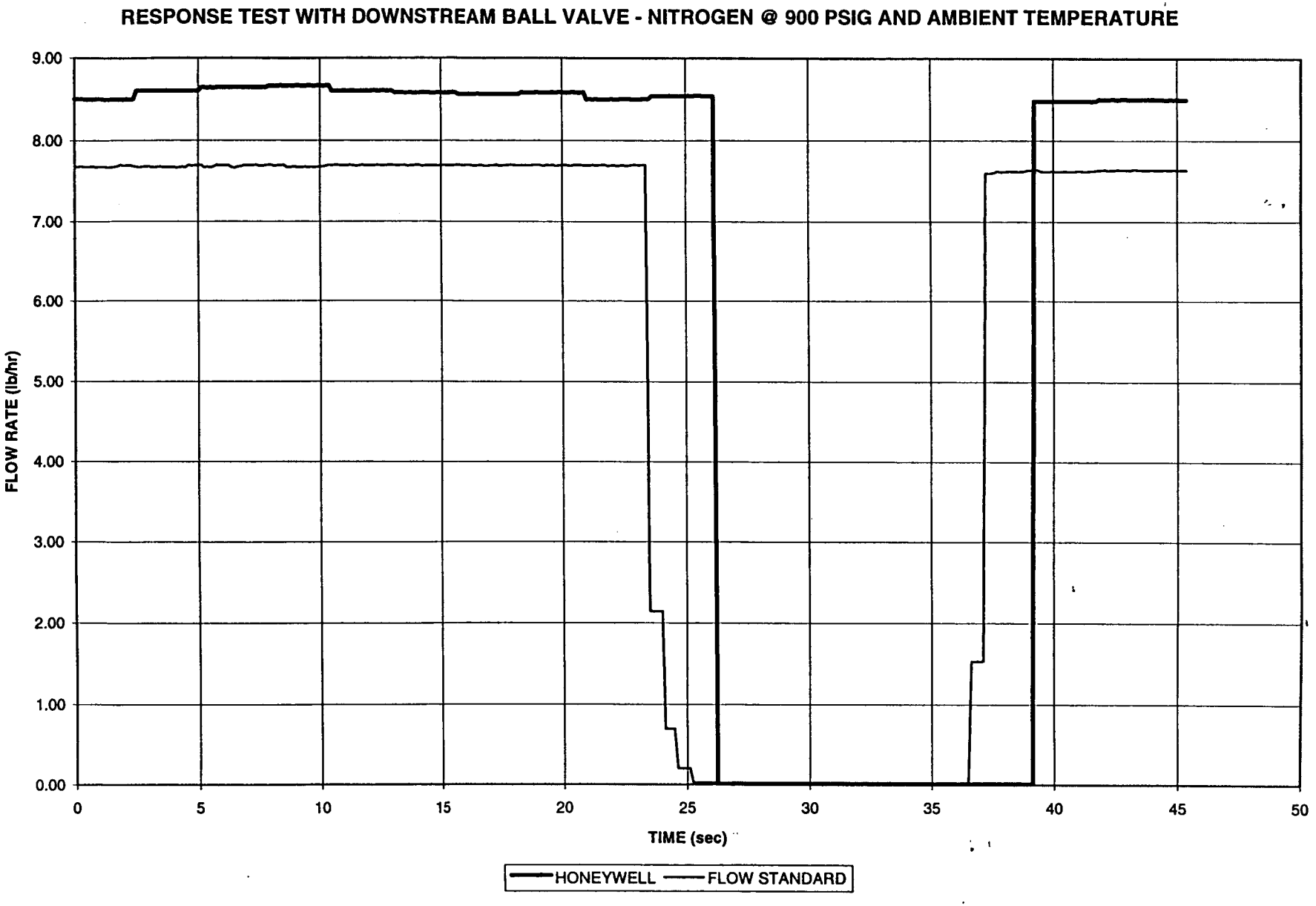
RESPONSE TEST WITH DOWNSTREAM BALL VALVE - NITROGEN @ 900 PSIG AND AMBIENT TEMPERATURE
FLOW RATE (lb/hr)
9.00
8.00
7.00
6.00
5.00
4.00
3.00
2.00
1.00
0.00
0
5
10
15
20
25
30
35
40
45
50
TIME (sec)
HONEYWELL
FLOW STANDARD

Figure 151

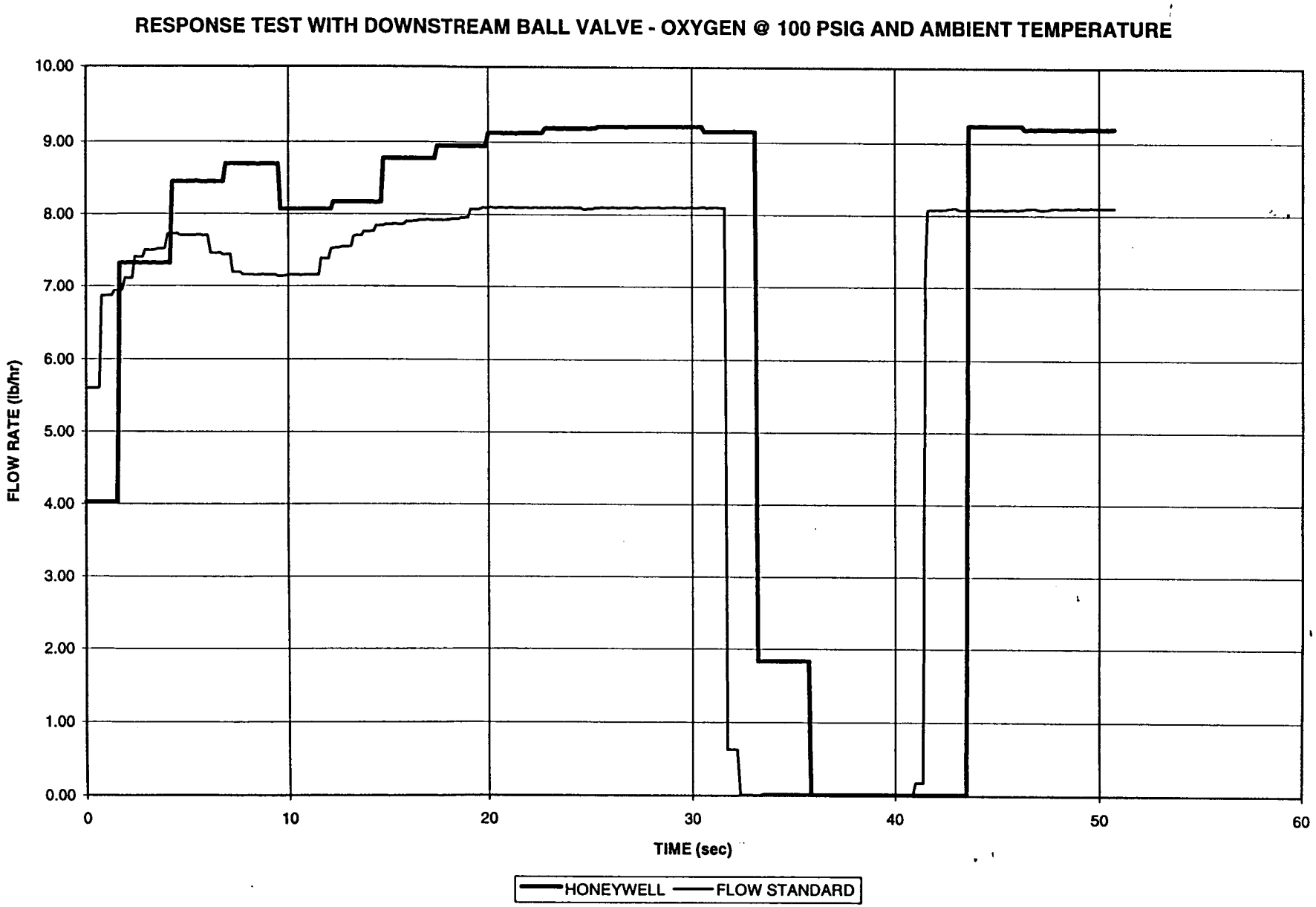
RESPONSE TEST WITH DOWNSTREAM BALL VALVE - OXYGEN @ 100 PSIG AND AMBIENT TEMPERATURE
FLOW RATE (lb/hr)
10.00
9.00
8.00
7.00
6.00
5.00
4.00
3.00
2.00
1.00
0.00
0
10
20
30
40
50
60
TIME (sec)
HONEYWELL
FLOW STANDARD

Figure 152

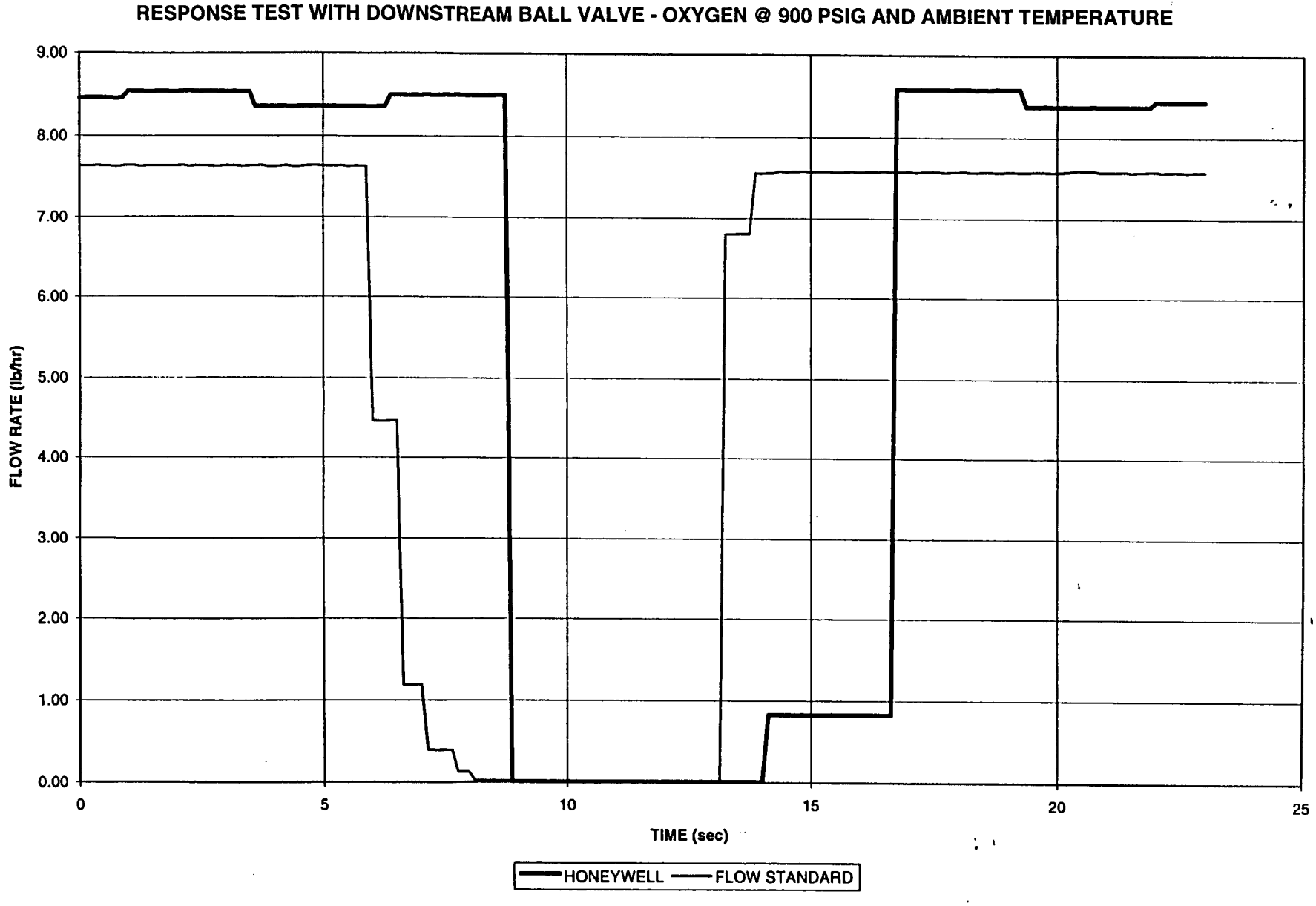
RESPONSE TEST WITH DOWNSTREAM BALL VALVE - OXYGEN @ 900 PSIG AND AMBIENT TEMPERATURE
9.00
8.00
7.00
6.00
5.00
4.00
3.00
2.00
1.00
0.00
FLOW RATE (lb/hr)
0
5
10
15
20
25
TIME (sec)
HONEYWELL
FLOW STANDARD

Figure 153

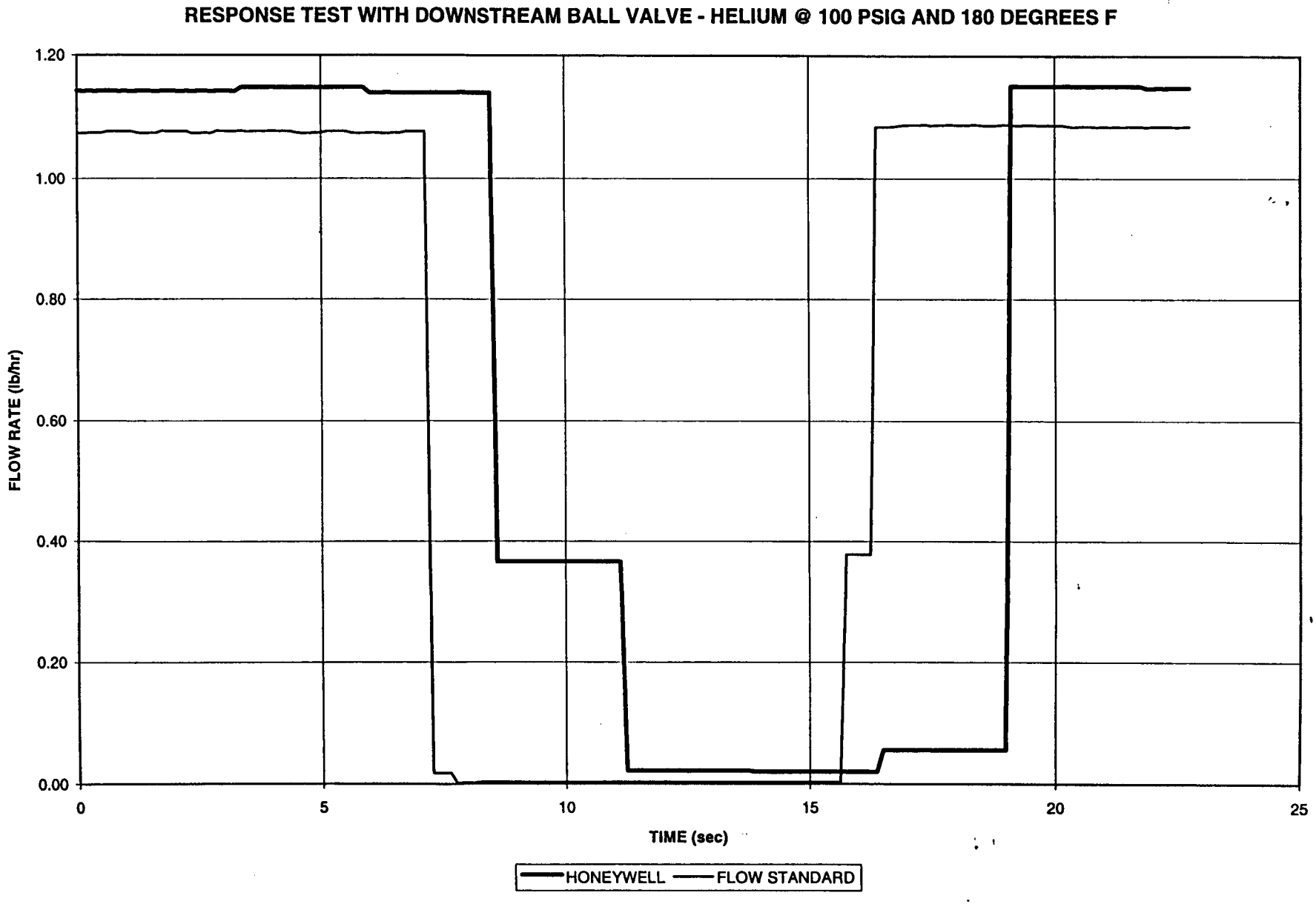
RESPONSE TEST WITH DOWNSTREAM BALL VALVE - HELIUM @ 100 PSIG AND 180 DEGREES F
1.20
1.00
0.80
0.60
0.40
0.20
0.00
FLOW RATE (lb/hr)
0
5
10
15
20
25
TIME (sec)
HONEYWELL
FLOW STANDARD

Figure 154

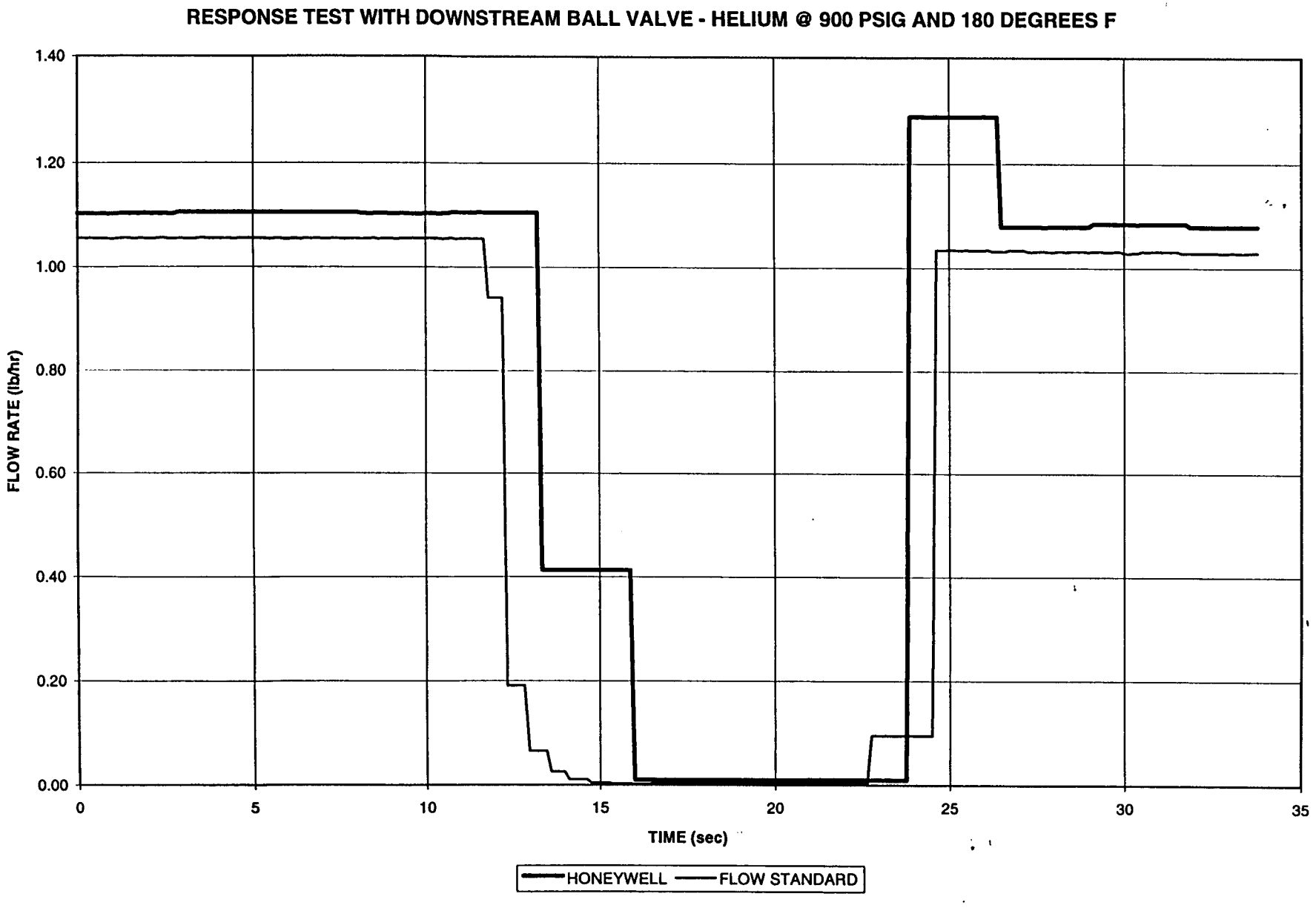
RESPONSE TEST WITH DOWNSTREAM BALL VALVE - HELIUM @ 900 PSIG AND 180 DEGREES F
FLOW RATE (lb/hr)
1.40
1.20
1.00
0.80
0.60
0.40
0.20
0.00
0
5
10
15
20
25
30
35
TIME (sec)
HONEYWELL
FLOW STANDARD

Figure 155

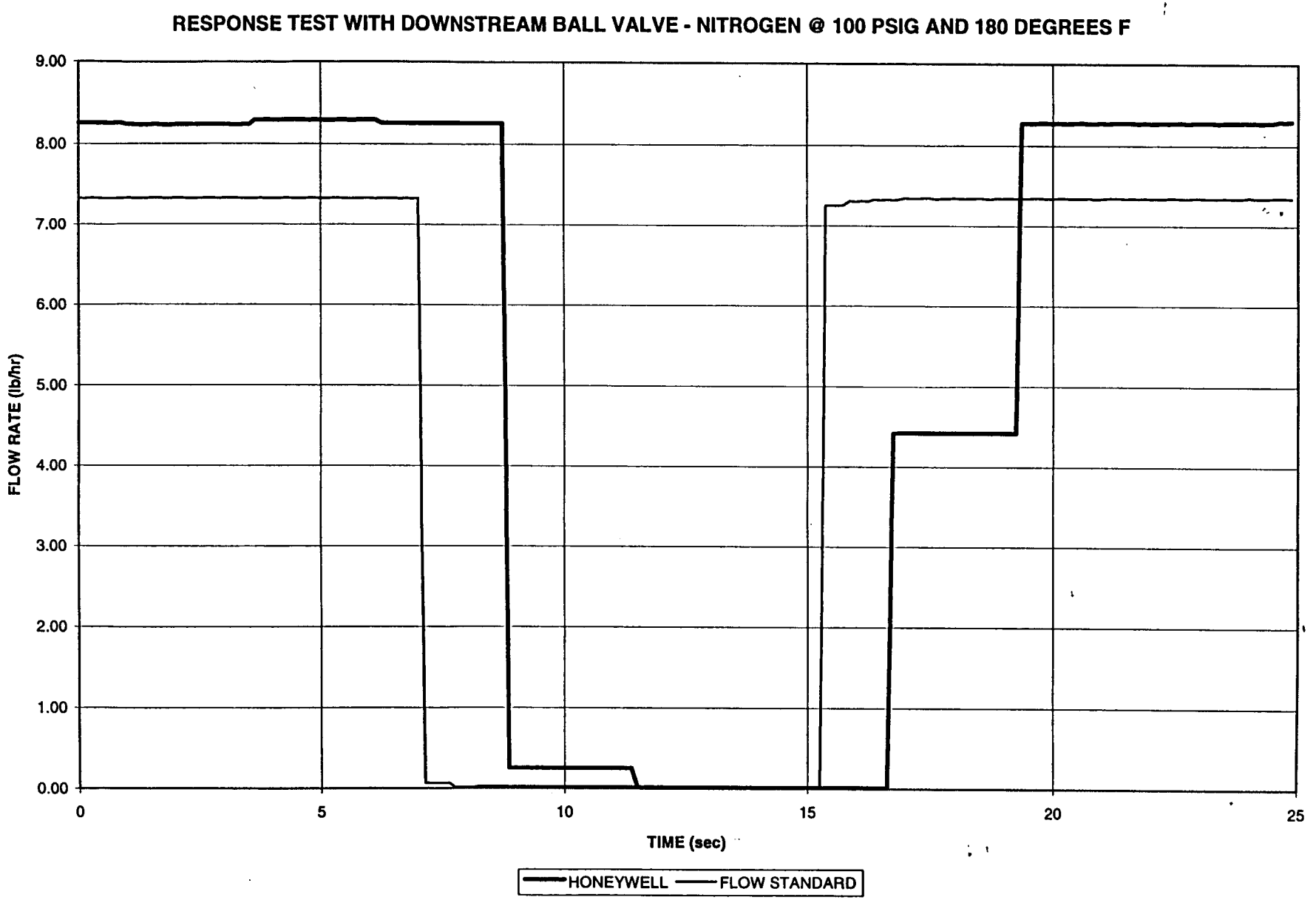
RESPONSE TEST WITH DOWNSTREAM BALL VALVE - NITROGEN @ 100 PSIG AND 180 DEGREES F
FLOW RATE (lb/hr)
9.00
8.00
7.00
6.00
5.00
4.00
3.00
2.00
1.00
0.00
0
5
10
15
20
25
TIME (sec)
HONEYWELL
FLOW STANDARD

Figure 156

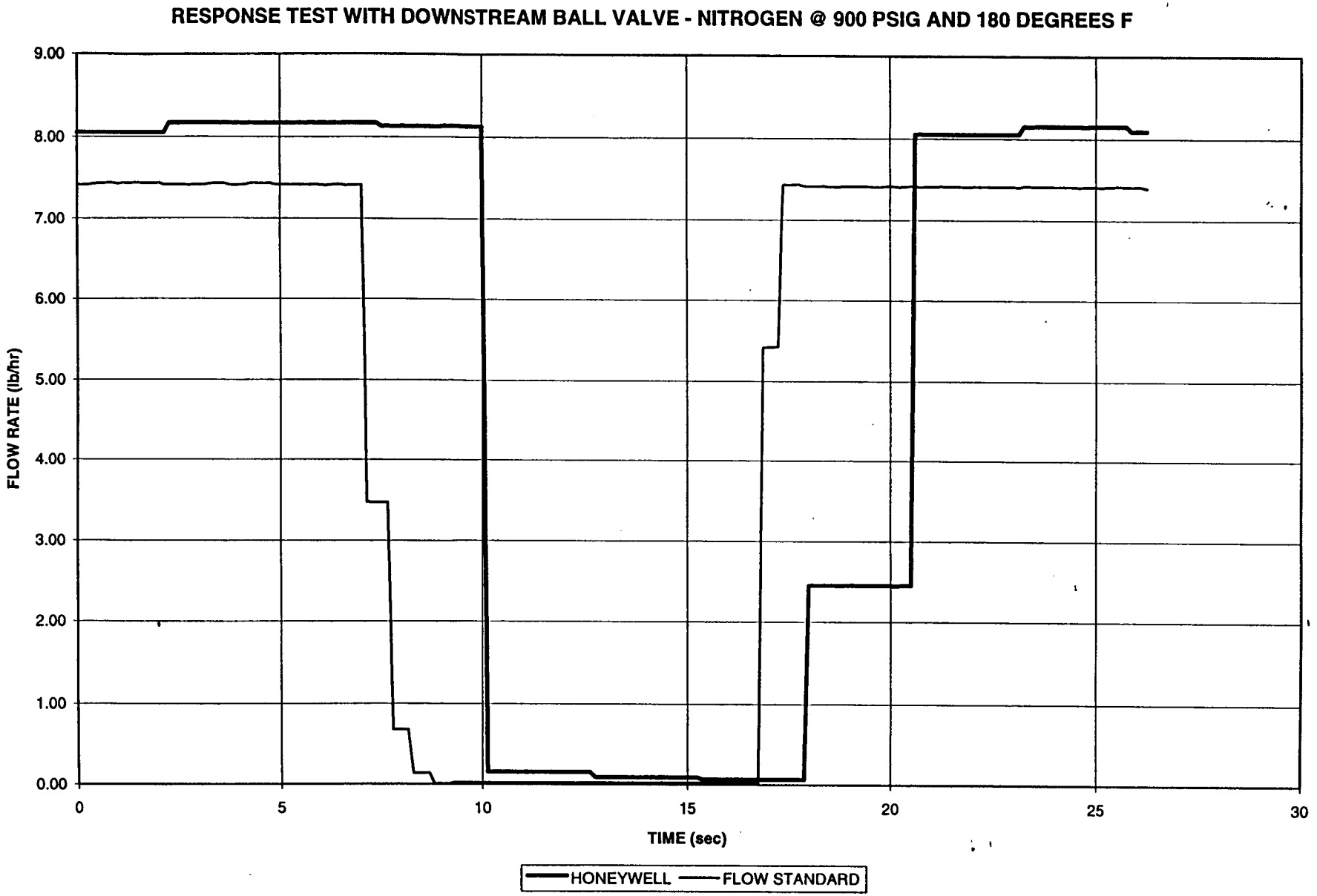
RESPONSE TEST WITH DOWNSTREAM BALL VALVE - NITROGEN @ 900 PSIG AND 180 DEGREES F
FLOW RATE (lb/hr)
9.00
8.00
7.00
6.00
5.00
4.00
3.00
2.00
1.00
0.00
0
5
10
15
20
25
30
TIME (sec)
HONEYWELL
FLOW STANDARD

Figure 157

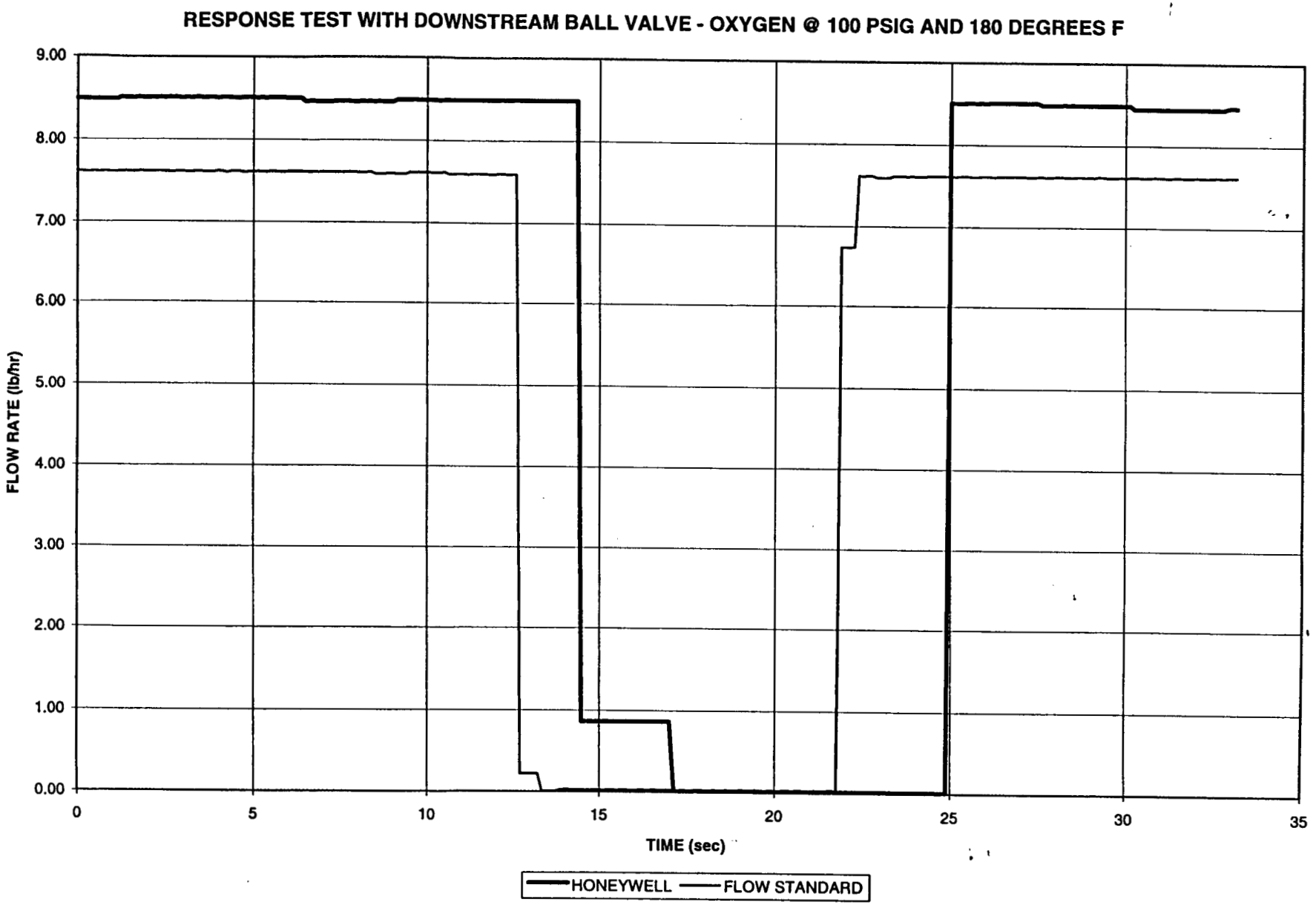
RESPONSE TEST WITH DOWNSTREAM BALL VALVE - OXYGEN @ 100 PSIG AND 180 DEGREES F
FLOW RATE (lb/hr)
9.00
8.00
7.00
6.00
5.00
4.00
3.00
2.00
1.00
0.00
0
5
10
15
20
25
30
35
TIME (sec)
HONEYWELL
FLOW STANDARD

Figure 158

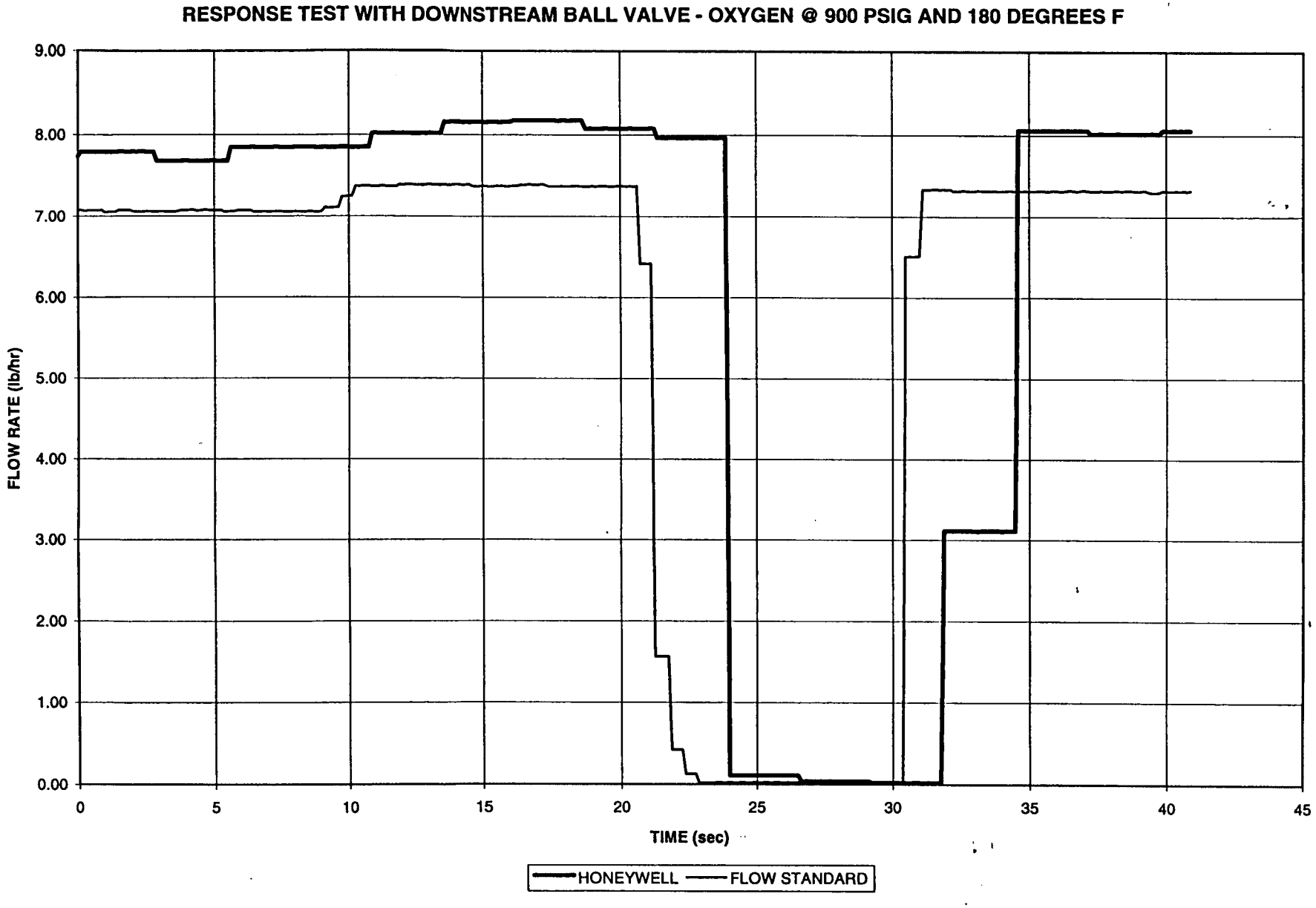
RESPONSE TEST WITH DOWNSTREAM BALL VALVE - OXYGEN @ 900 PSIG AND 180 DEGREES F
FLOW RATE (lb/hr)
9.00
8.00
7.00
6.00
5.00
4.00
3.00
2.00
1.00
0.00
0
5
10
15
20
25
30
35
40
45
TIME (sec)
HONEYWELL
FLOW STANDARD

Figure 159

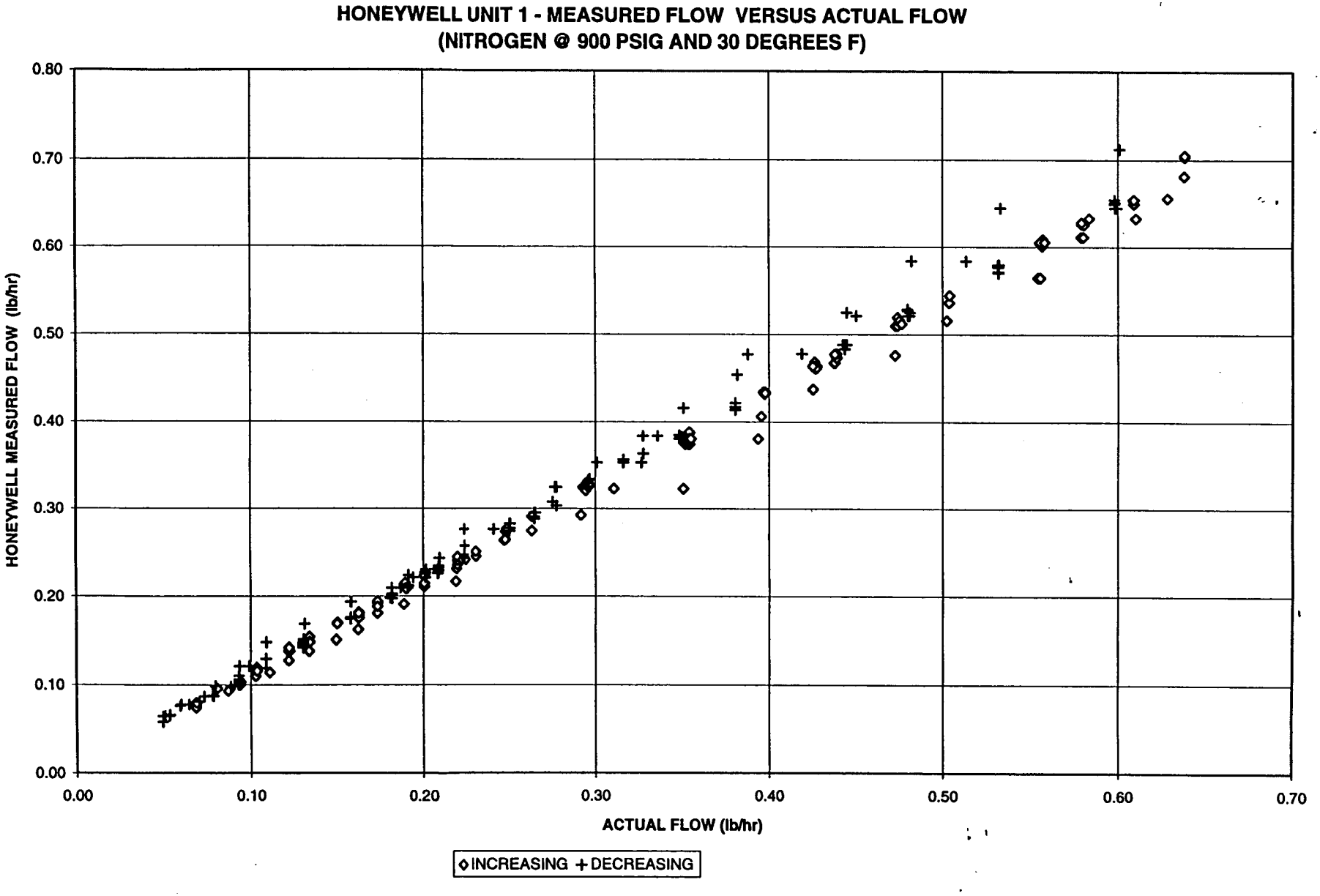
HONEYWELL UNIT 1 - MEASURED FLOW VERSUS ACTUAL FLOW
(NITROGEN @ 900 PSIG AND 30 DEGREES F)
HONEYWELL MEASURED FLOW (lb/hr)
0.80
0.70
0.60
0.50
0.40
0.30
0.20
0.10
0.00
0.00
0.10
0.20
0.30
0.40
0.50
0.60
0.70
ACTUAL FLOW (lb/hr)
◇INCREASING +DECREASING

Figure 160

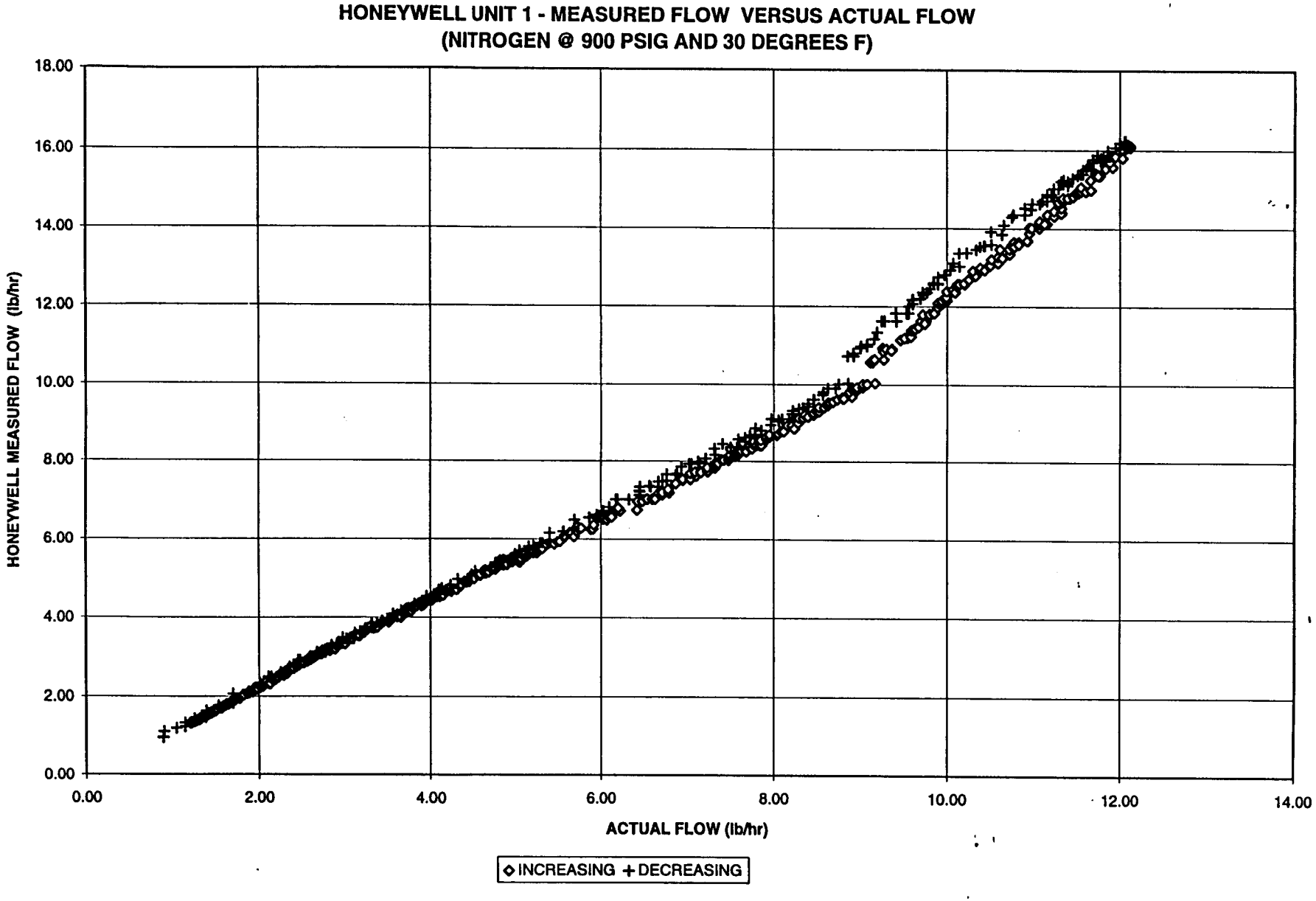
HONEYWELL UNIT 1 - MEASURED FLOW VERSUS ACTUAL FLOW
(NITROGEN @ 900 PSIG AND 30 DEGREES F)
HONEYWELL MEASURED FLOW (lb/hr)
18.00
16.00
14.00
12.00
10.00
8.00
6.00
4.00
2.00
0.00
0.00
2.00
4.00
6.00
8.00
10.00
12.00
14.00
ACTUAL FLOW (lb/hr)
◇ INCREASING + DECREASING

Figure 161

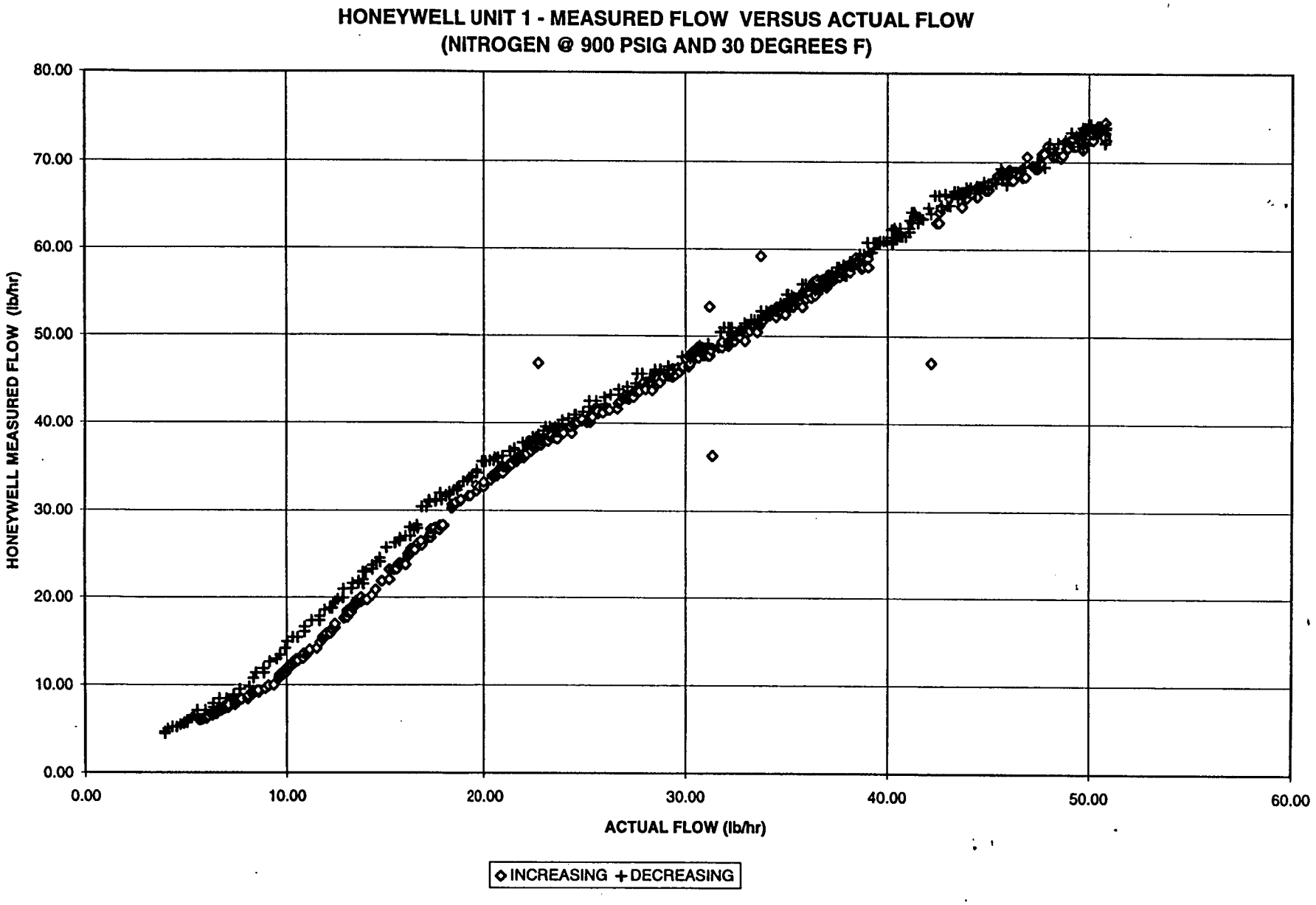
HONEYWELL UNIT 1 - MEASURED FLOW VERSUS ACTUAL FLOW
(NITROGEN @ 900 PSIG AND 30 DEGREES F)
HONEYWELL MEASURED FLOW (lb/hr)
80.00
70.00
60.00
50.00
40.00
30.00
20.00
10.00
0.00
0.00
10.00
20.00
30.00
40.00
50.00
60.00
ACTUAL FLOW (lb/hr)
◇ INCREASING + DECREASING

Figure 162

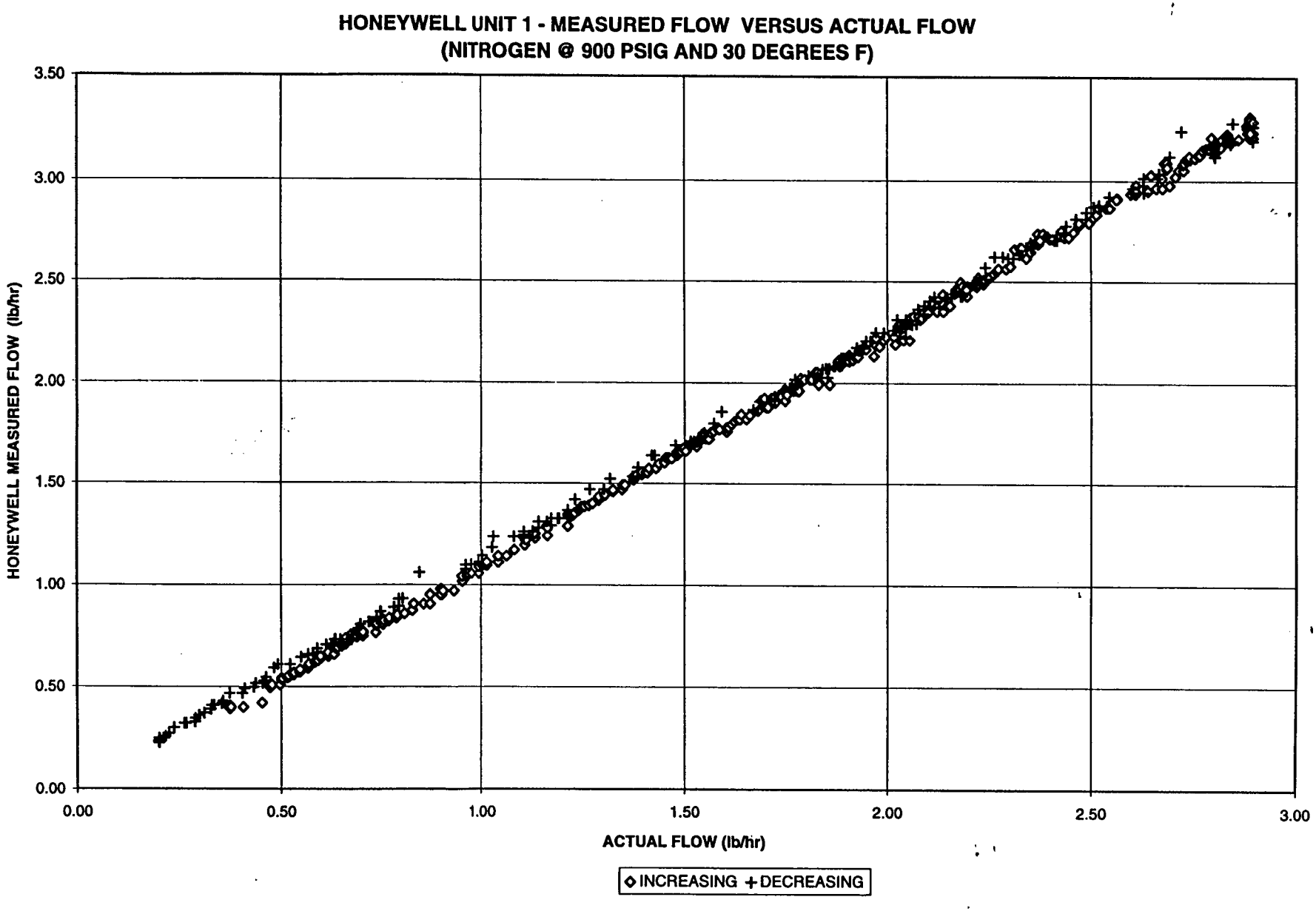
HONEYWELL UNIT 1 - MEASURED FLOW VERSUS ACTUAL FLOW
(NITROGEN @ 900 PSIG AND 30 DEGREES F)
HONEYWELL MEASURED FLOW (lb/hr)
3.50
3.00
2.50
2.00
1.50
1.00
0.50
0.00
0.00
0.50
1.00
1.50
2.00
2.50
3.00
ACTUAL FLOW (lb/hr)
◇ INCREASING + DECREASING

Figure 163

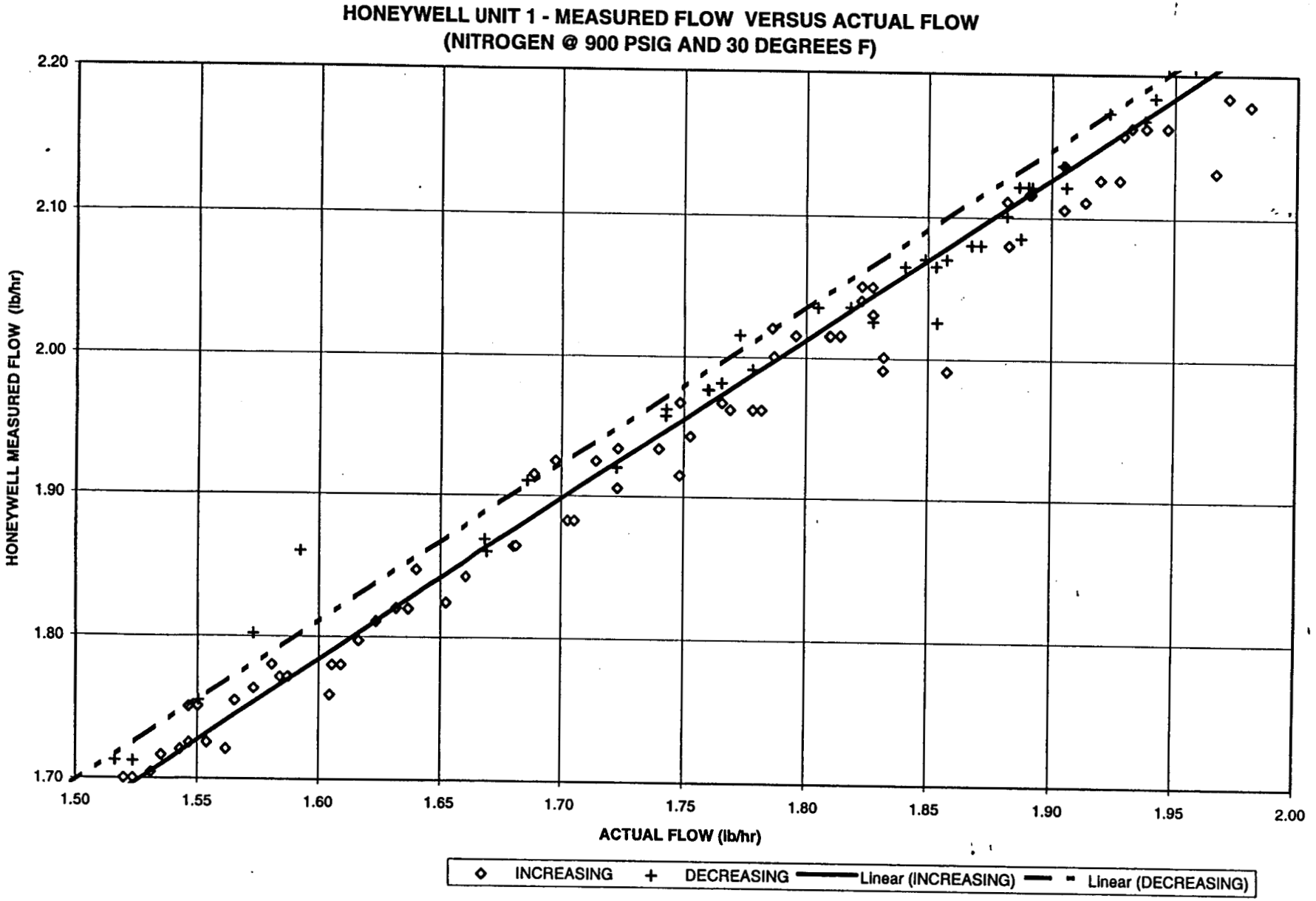
HONEYWELL UNIT 1 - MEASURED FLOW VERSUS ACTUAL FLOW
(NITROGEN @ 900 PSIG AND 30 DEGREES F)
HONEYWELL MEASURED FLOW (lb/hr)
2.20
2.10
2.00
1.90
1.80
1.70
1.50
1.55
1.60
1.65
1.70
1.75
1.80
1.85
1.90
1.95
2.00
ACTUAL FLOW (lb/hr)
INCREASING
DECREASING
Linear (INCREASING)
Linear (DECREASING)

Figure 164

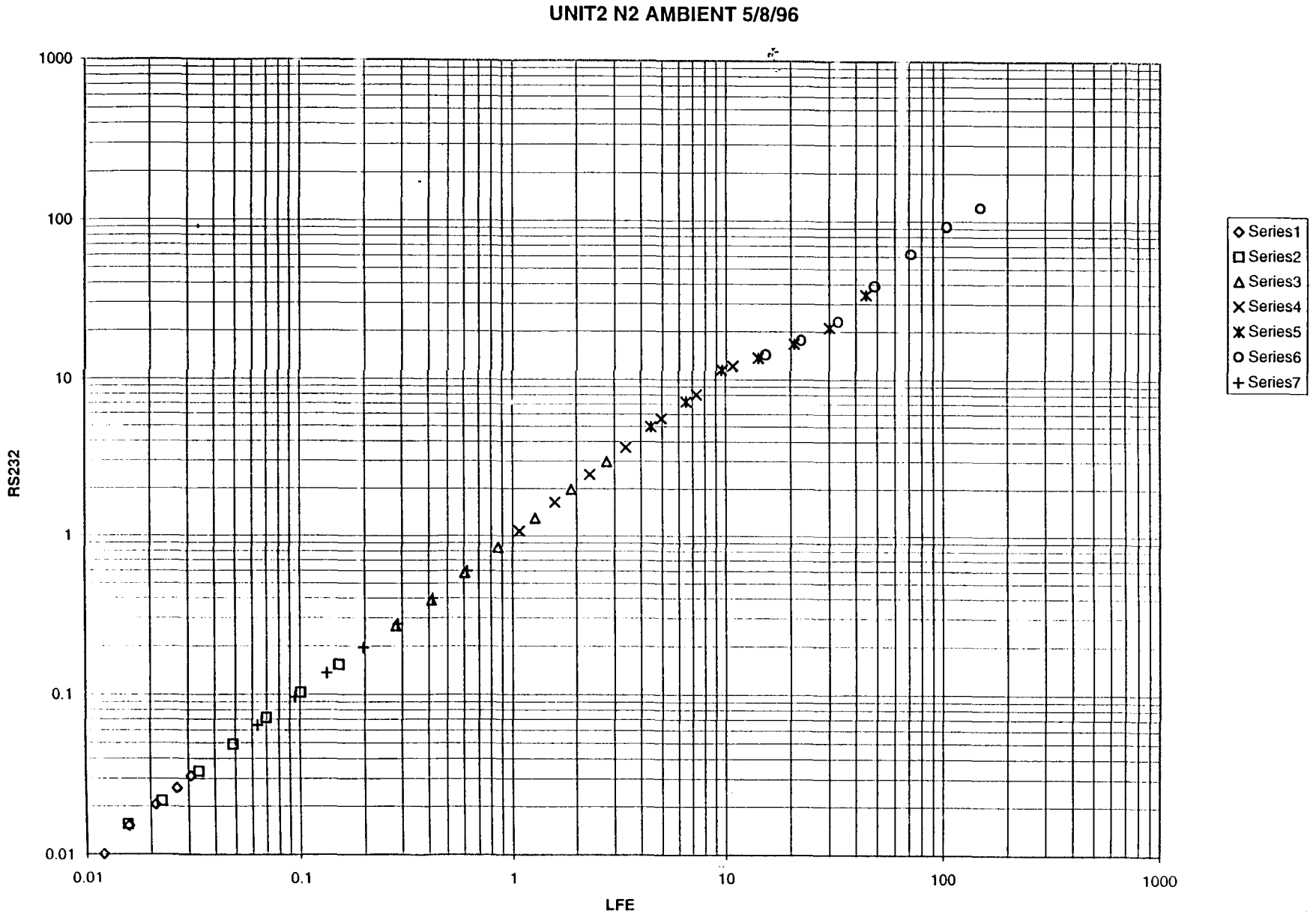
UNIT2 N2 AMBIENT 5/8/96
RS232
LFE
1000
100
10
1
0.1
0.01
0.01
0.1
1
10
100
1000
Series1
Series2
Series3
Series4
Series5
Series6
Series7

Figure 1

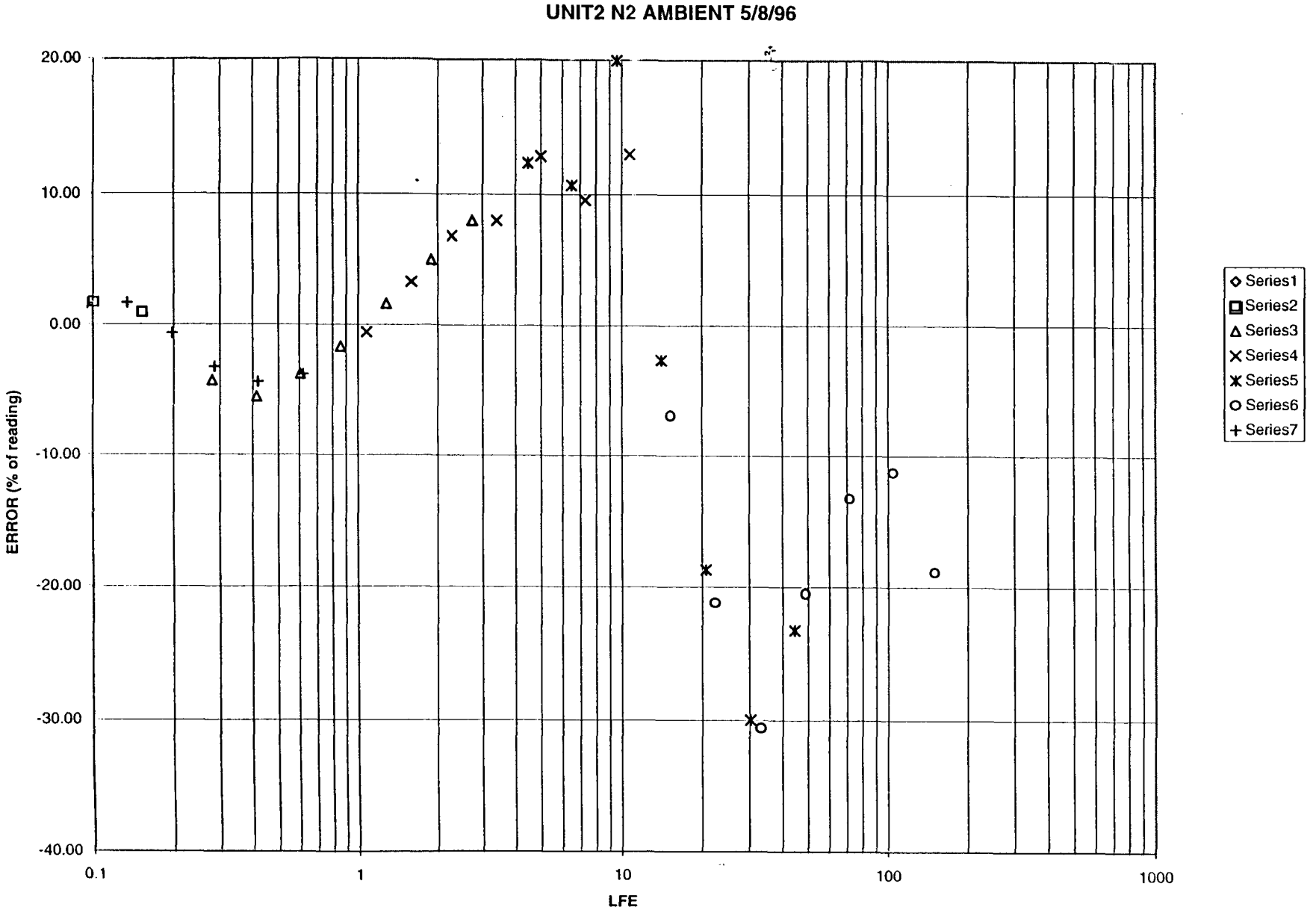
UNIT2 N2 AMBIENT 5/8/96
20.00
10.00
0.00
-10.00
-20.00
-30.00
-40.00
ERROR (% of reading)
0.1
1
10
100
1000
LFE
Series1
Series2
Series3
Series4
Series5
Series6
Series7

Figure 2

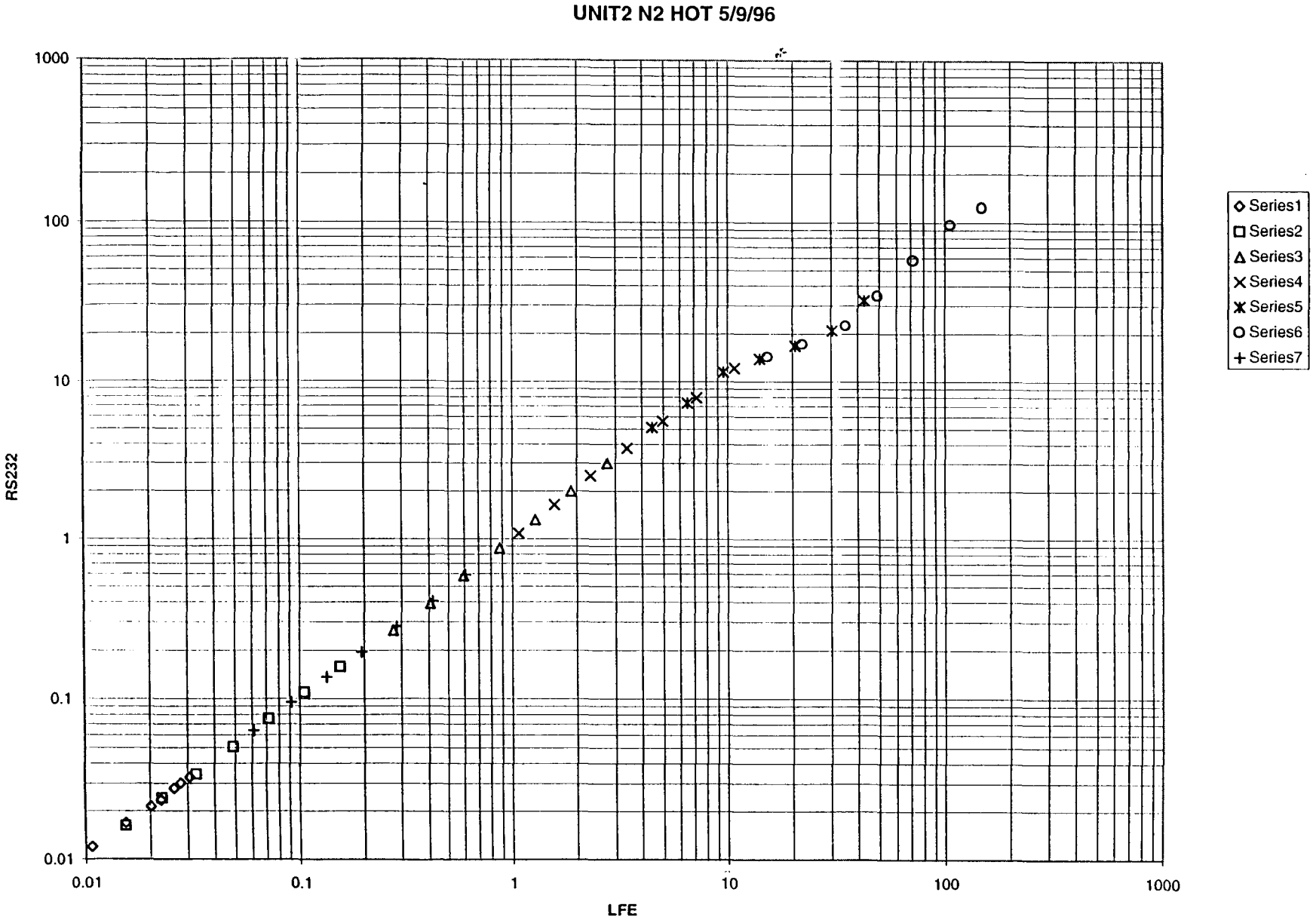
UNIT2 N2 HOT 5/9/96
1000
100
10
1
0.1
0.01
RS232
0.01
0.1
1
10
100
1000
LFE
Series1
Series2
Series3
Series4
Series5
Series6
Series7

Figure 3

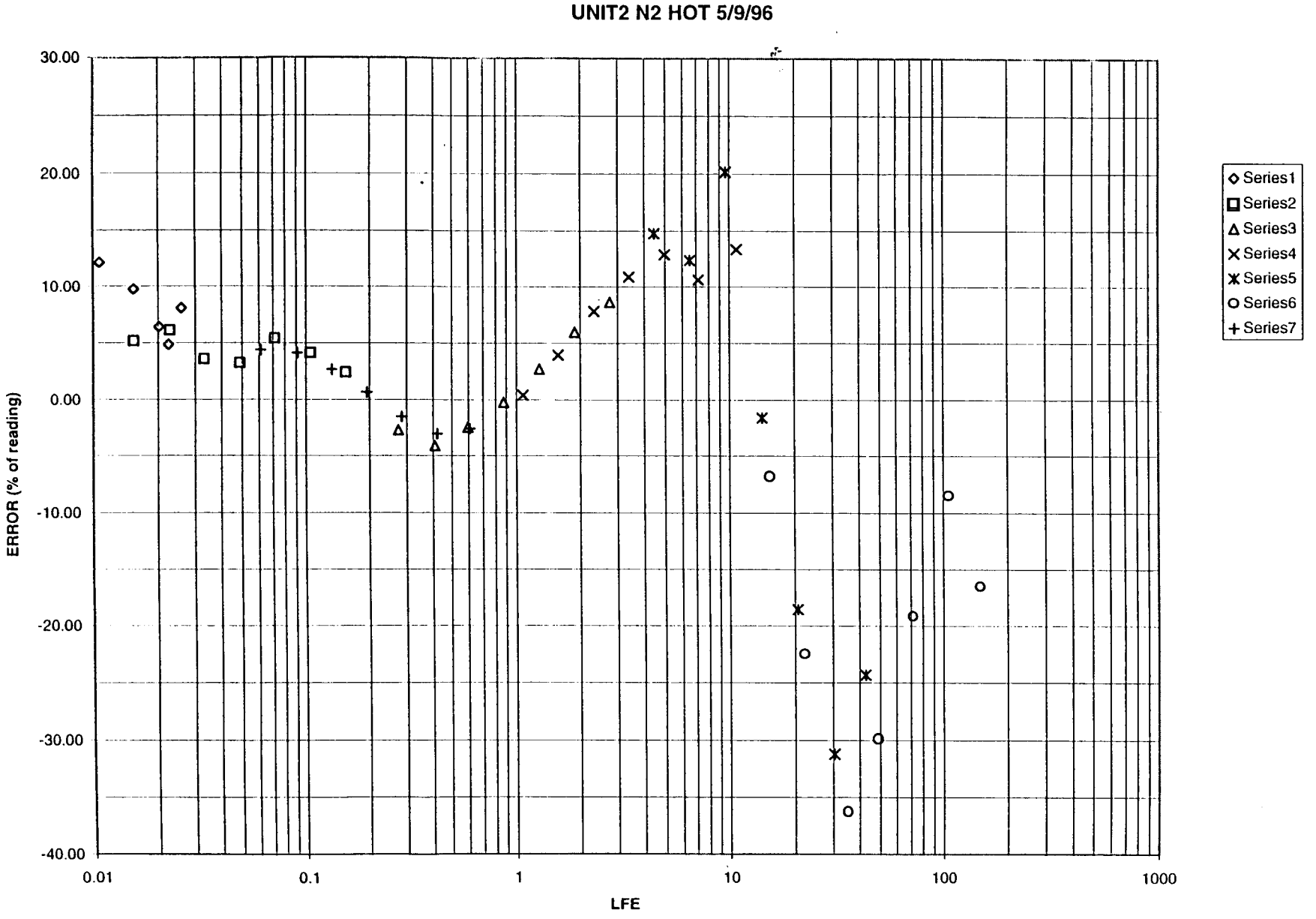
UNIT2 N2 HOT 5/9/96
30.00
20.00
10.00
0.00
-10.00
-20.00
-30.00
-40.00
ERROR (% of reading)
0.01
0.1
1
10
100
1000
LFE
Series1
Series2
Series3
Series4
Series5
Series6
Series7

Figure 4

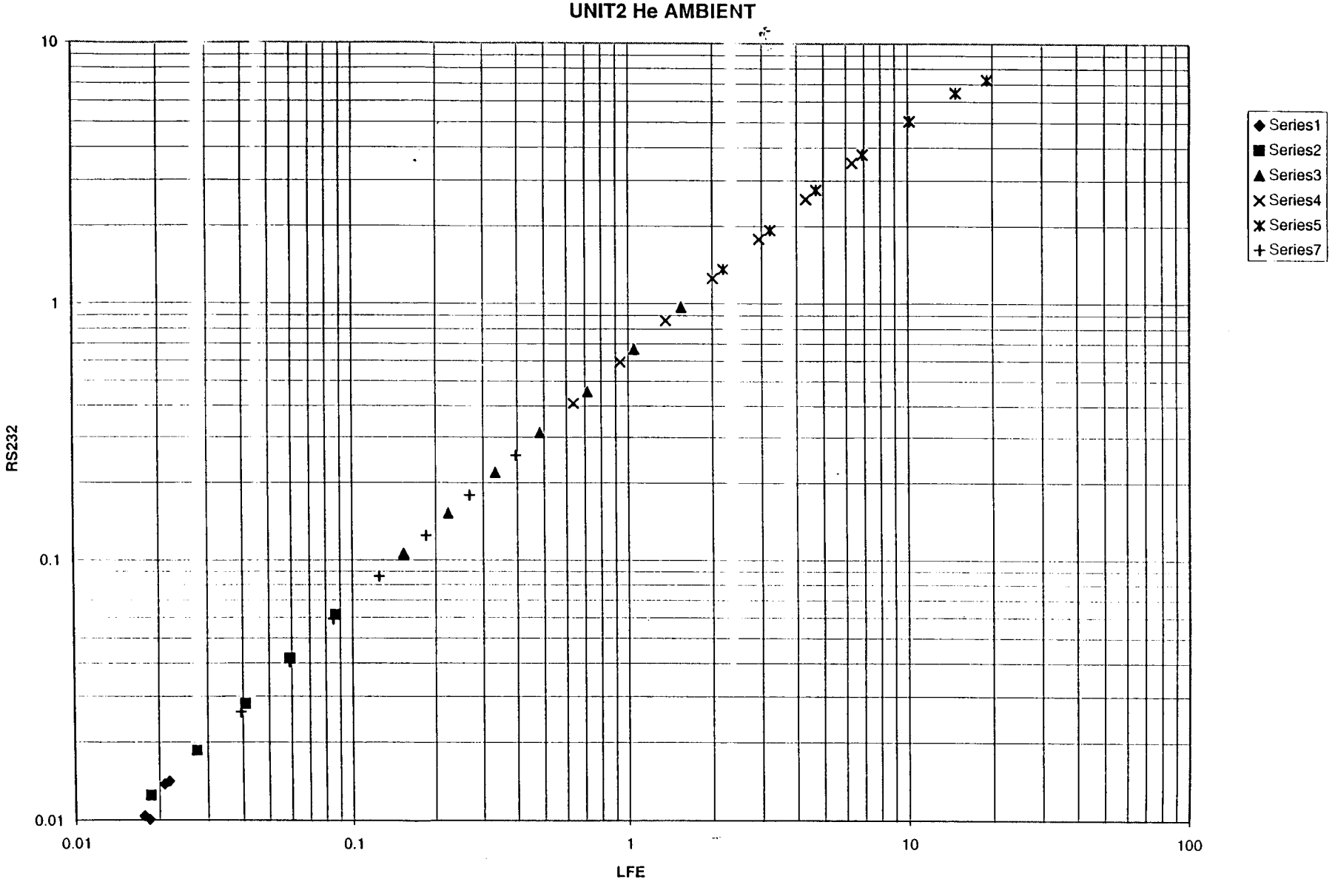
UNIT2 He AMBIENT
10
1
0.1
0.01
RS232
0.01
0.1
1
10
100
LFE
Series1
Series2
Series3
Series4
Series5
Series7

Figure 5

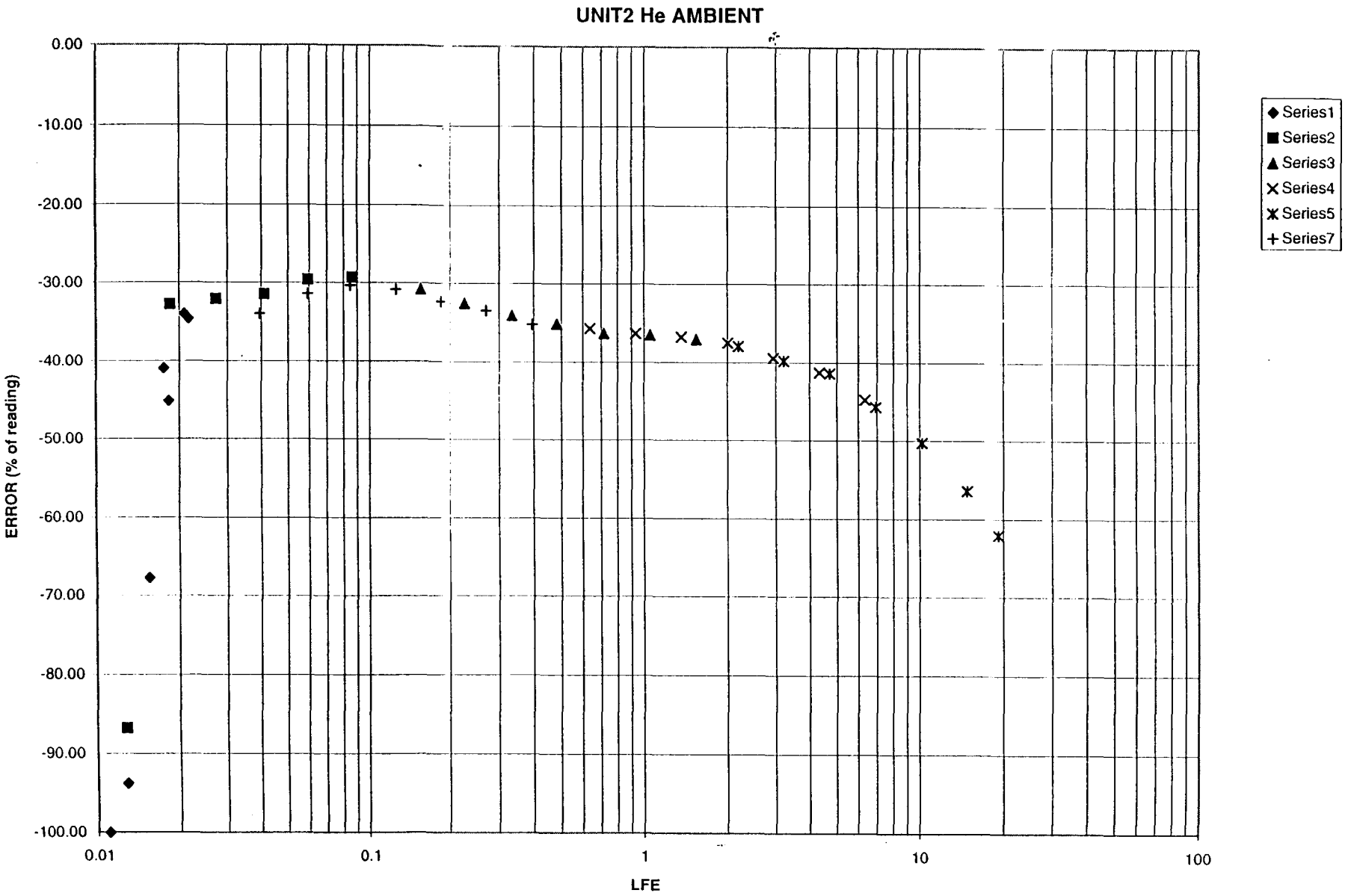
UNIT2 He AMBIENT
0.00
-10.00
-20.00
-30.00
-40.00
-50.00
-60.00
-70.00
-80.00
-90.00
-100.00
ERROR (% of reading)
0.01
0.1
1
10
100
LFE
Series1
Series2
Series3
Series4
Series5
Series7

Figure 6

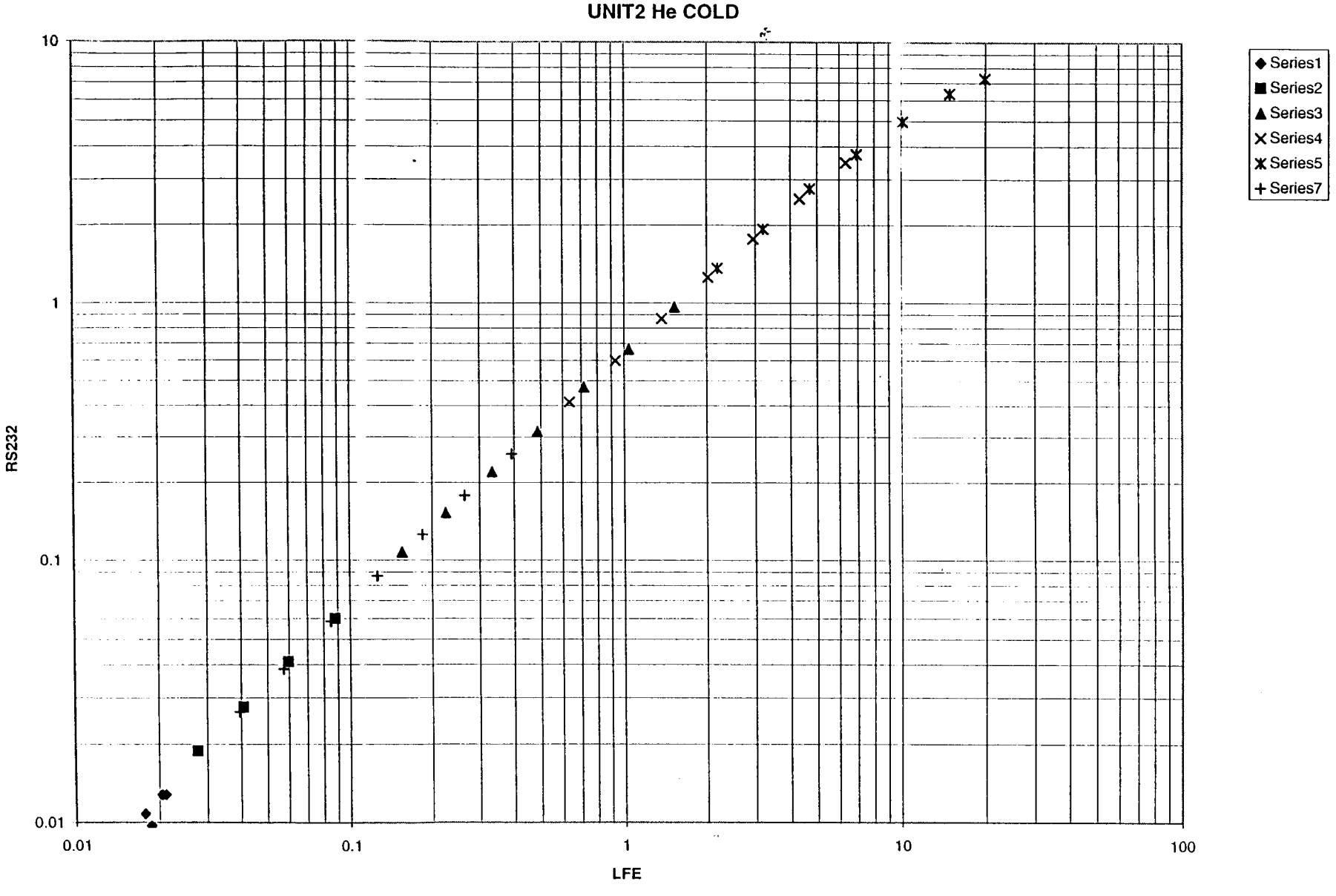
UNIT2 He COLD
10
1
0.1
0.01
RS232
0.01
0.1
1
10
100
LFE
Series1
Series2
Series3
Series4
Series5
Series7

Figure 7

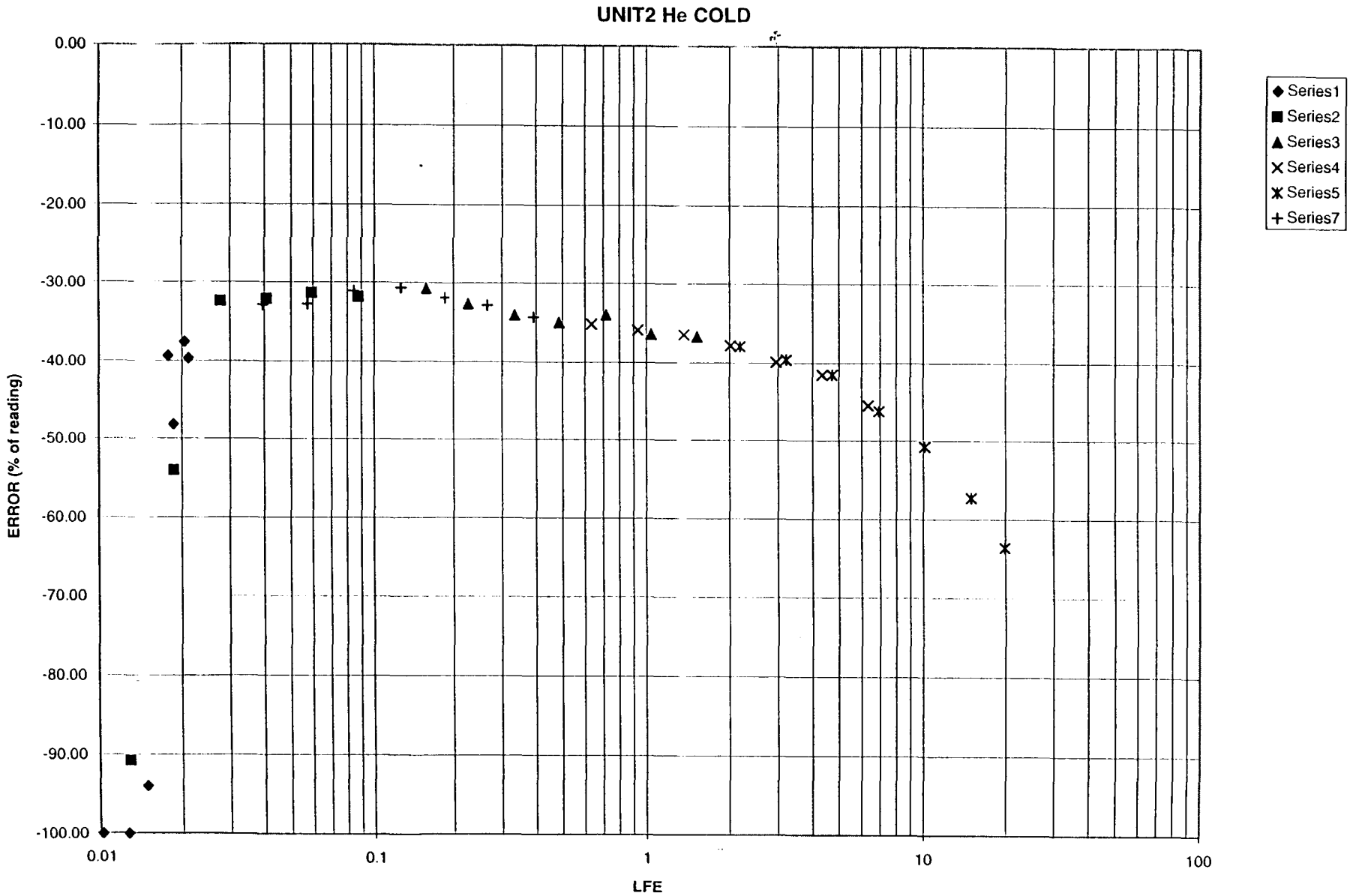
UNIT2 He COLD
0.00
-10.00
-20.00
-30.00
-40.00
-50.00
-60.00
-70.00
-80.00
-90.00
-100.00
ERROR (% of reading)
0.01
0.1
1
10
100
LFE
Series1
Series2
Series3
Series4
Series5
Series7

Figure 8

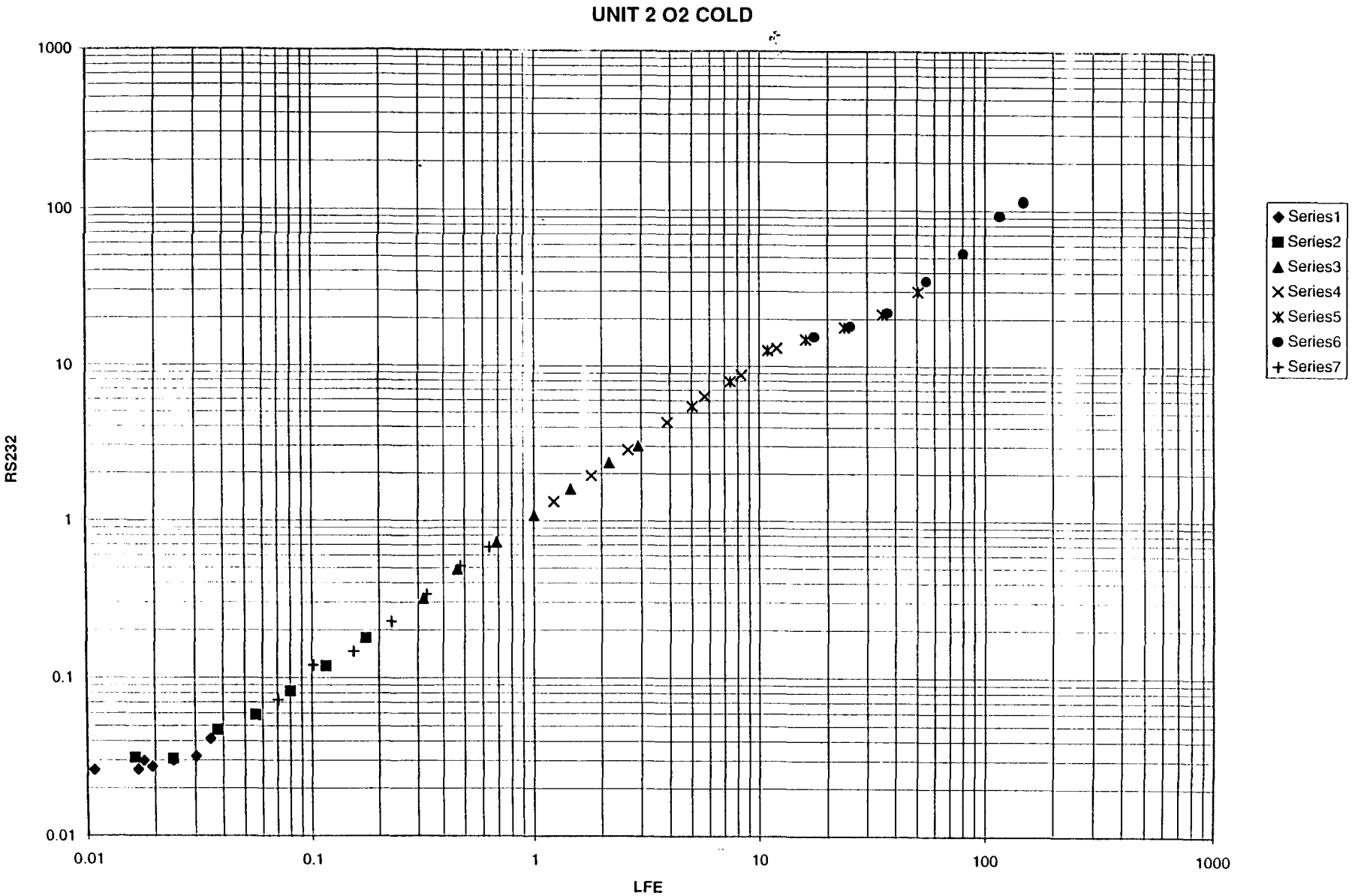
UNIT 2 O2 COLD
RS232
LFE
1000
100
10
1
0.1
0.01
0.01
0.1
1
10
100
1000
Series1
Series2
Series3
Series4
Series5
Series6
Series7

Figure 9

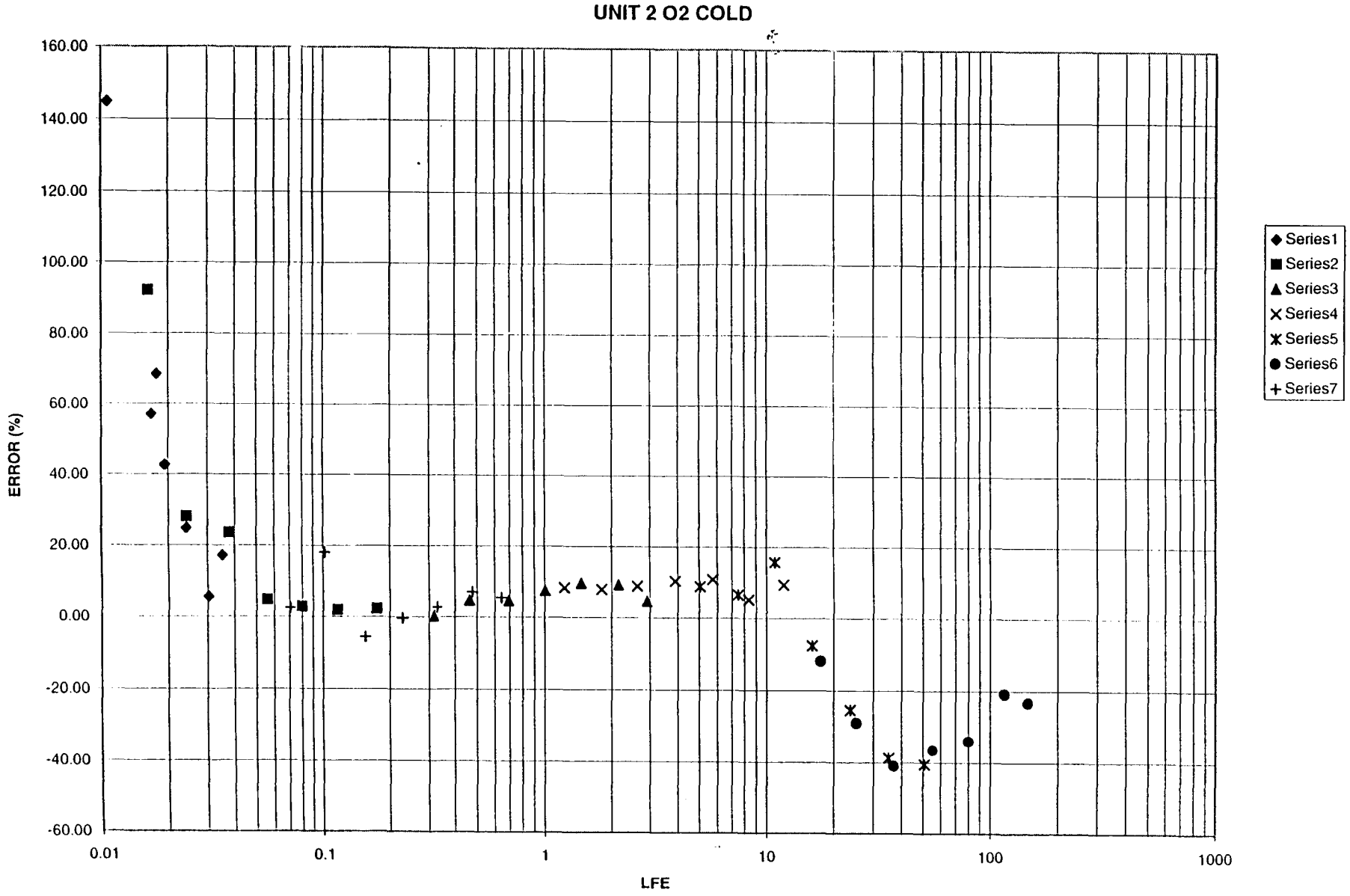
UNIT 2 O2 COLD
160.00
140.00
120.00
100.00
80.00
60.00
40.00
20.00
0.00
-20.00
-40.00
-60.00
ERROR (%)
0.01
0.1
1
10
100
1000
LFE
Series1
Series2
Series3
Series4
Series5
Series6
Series7

Figure 10

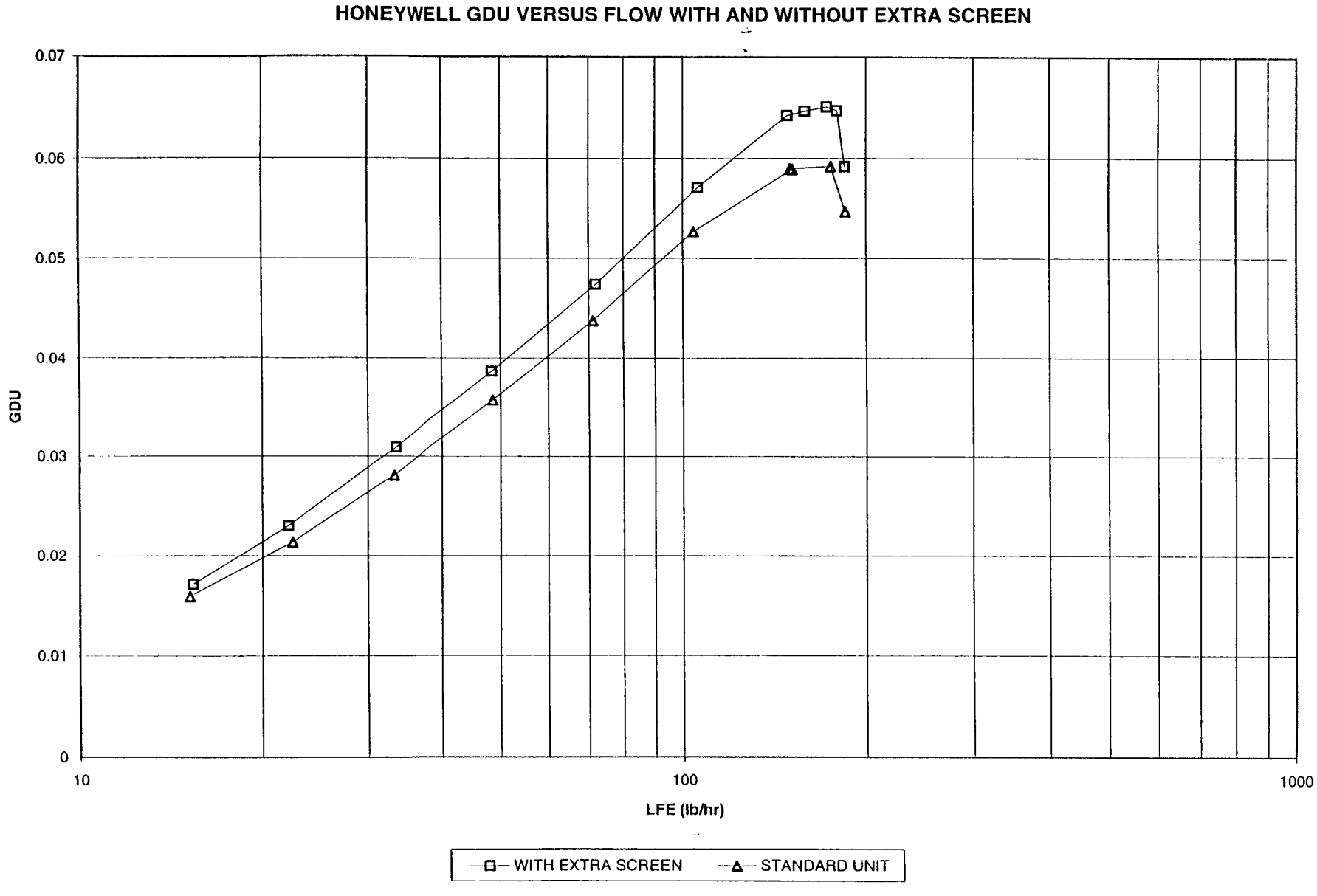
HONEYWELL GDU VERSUS FLOW WITH AND WITHOUT EXTRA SCREEN
0.07
0.06
0.05
0.04
0.03
0.02
0.01
0
GDU
10
100
1000
LFE (lb/hr)
WITH EXTRA SCREEN
STANDARD UNIT

Figure 1

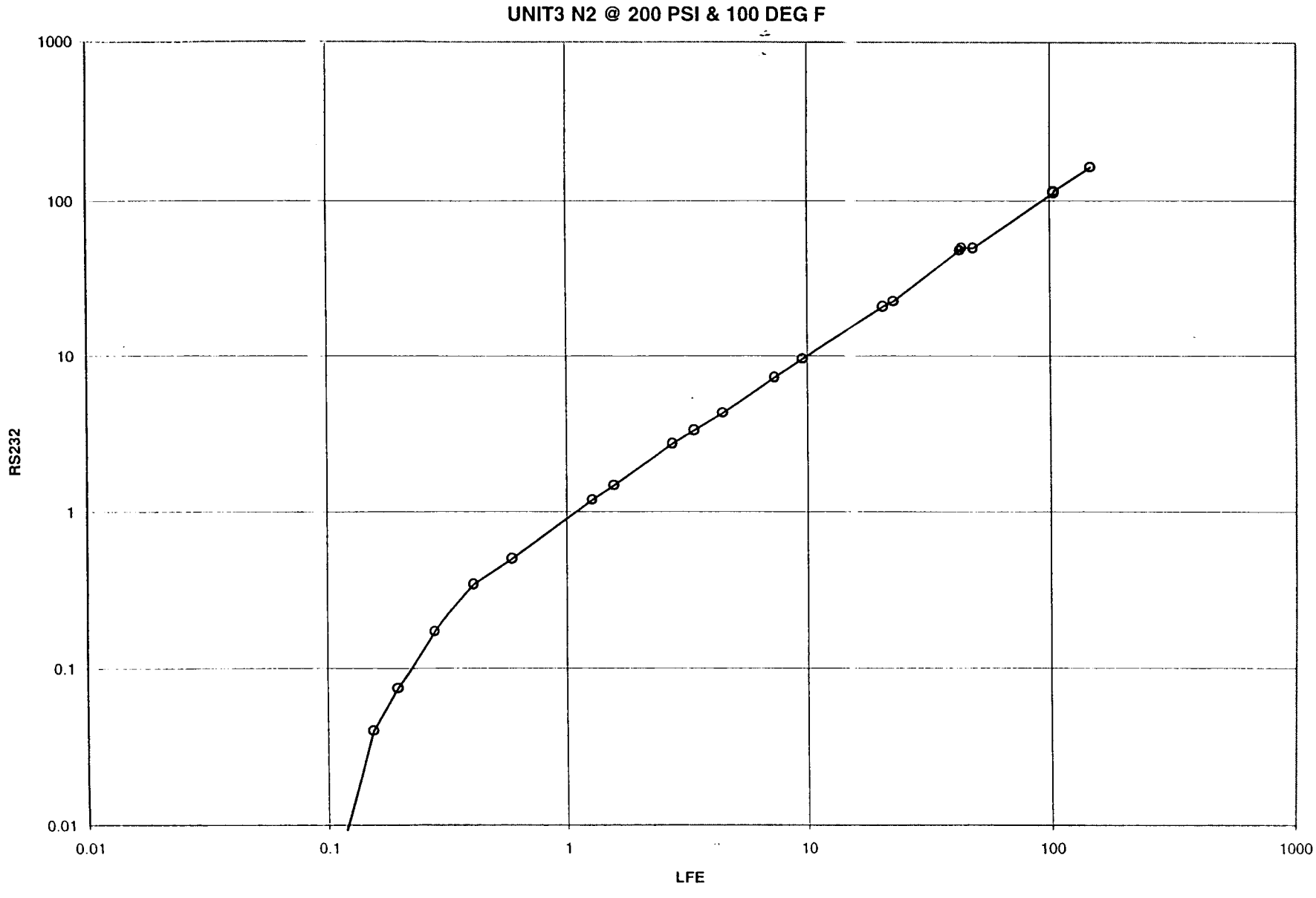
UNIT3 N2 @ 200 PSI & 100 DEG F
1000
100
10
1
0.1
0.01
RS232
0.01
0.1
1
10
100
1000
LFE

Figure 2

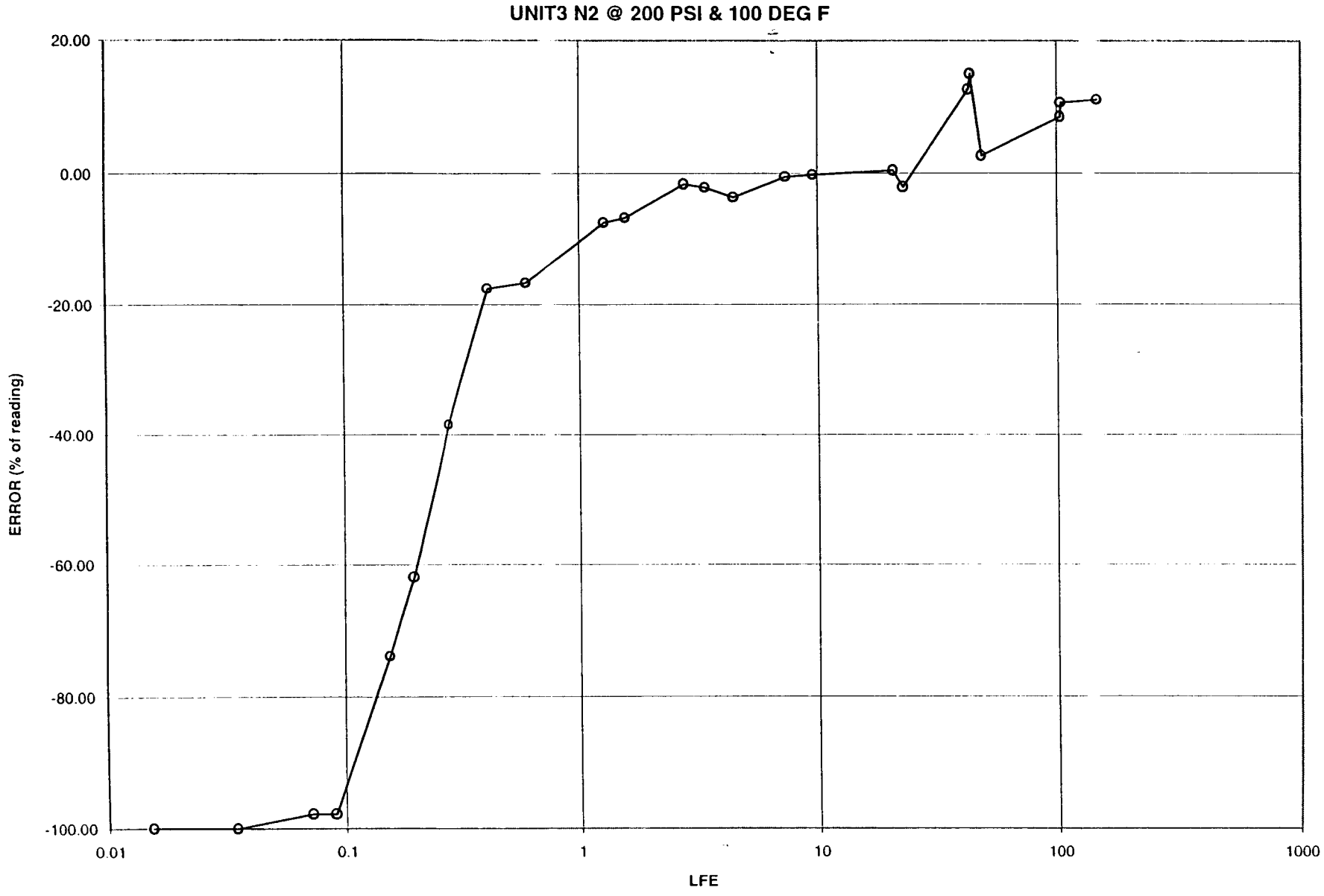
UNIT3 N2 @ 200 PSI & 100 DEG F
20.00
0.00
-20.00
-40.00
-60.00
-80.00
-100.00
ERROR (% of reading)
0.01
0.1
1
10
100
1000
LFE

Figure 3

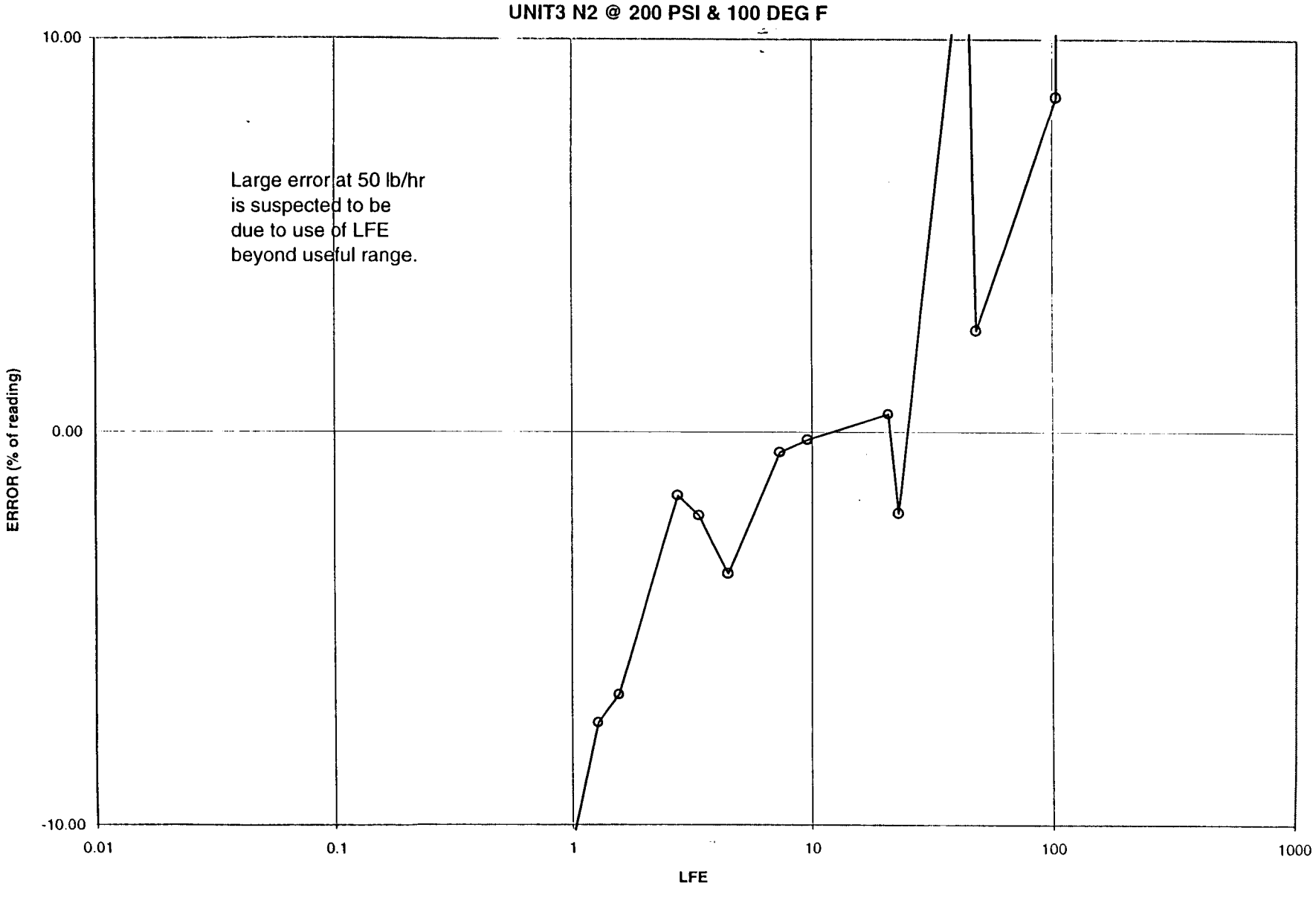
UNIT3 N2 @ 200 PSI & 100 DEG F
Large error at 50 lb/hr is suspected to be due to use of LFE beyond useful range.
10.00
0.00
-10.00
ERROR (% of reading)
0.01
0.1
1
10
100
1000
LFE

Figure 4

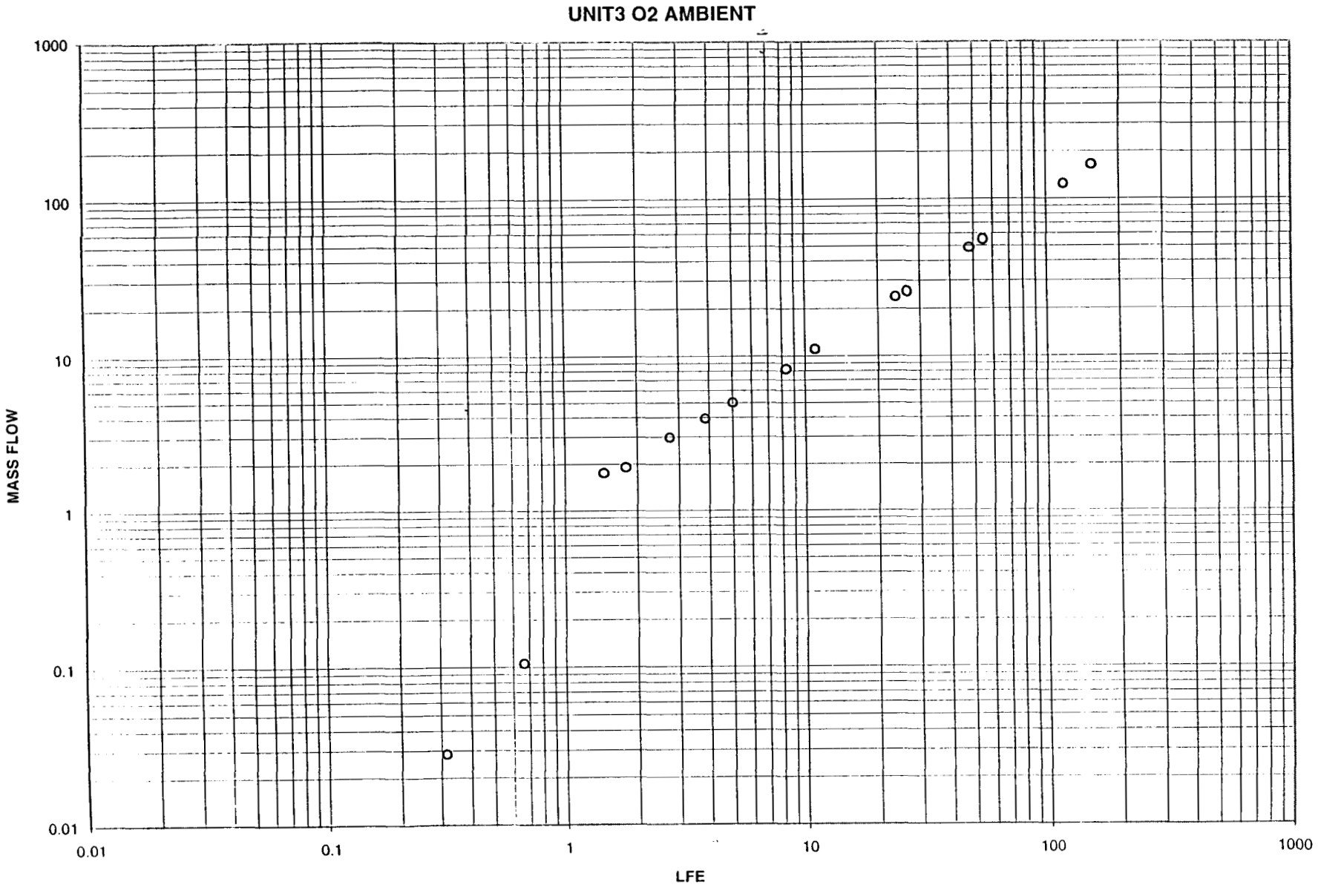
UNIT3 O2 AMBIENT
MASS FLOW
1000
100
10
1
0.1
0.01
0.01
0.1
1
10
100
1000
LFE

Figure 5

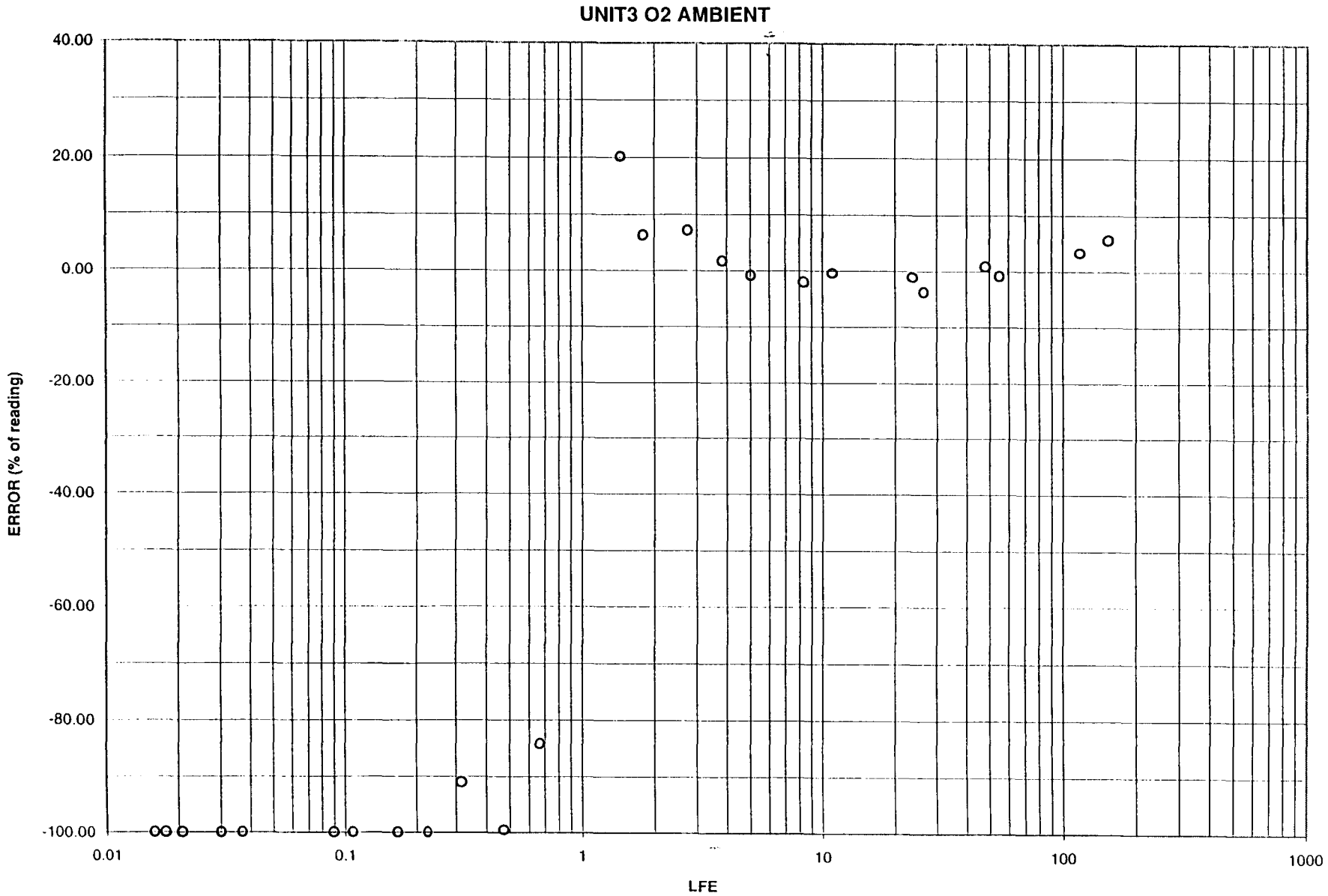
UNIT3 O2 AMBIENT
40.00
20.00
0.00
-20.00
-40.00
-60.00
-80.00
-100.00
ERROR (% of reading)
0.01
0.1
1
10
100
1000
LFE

Figure 6

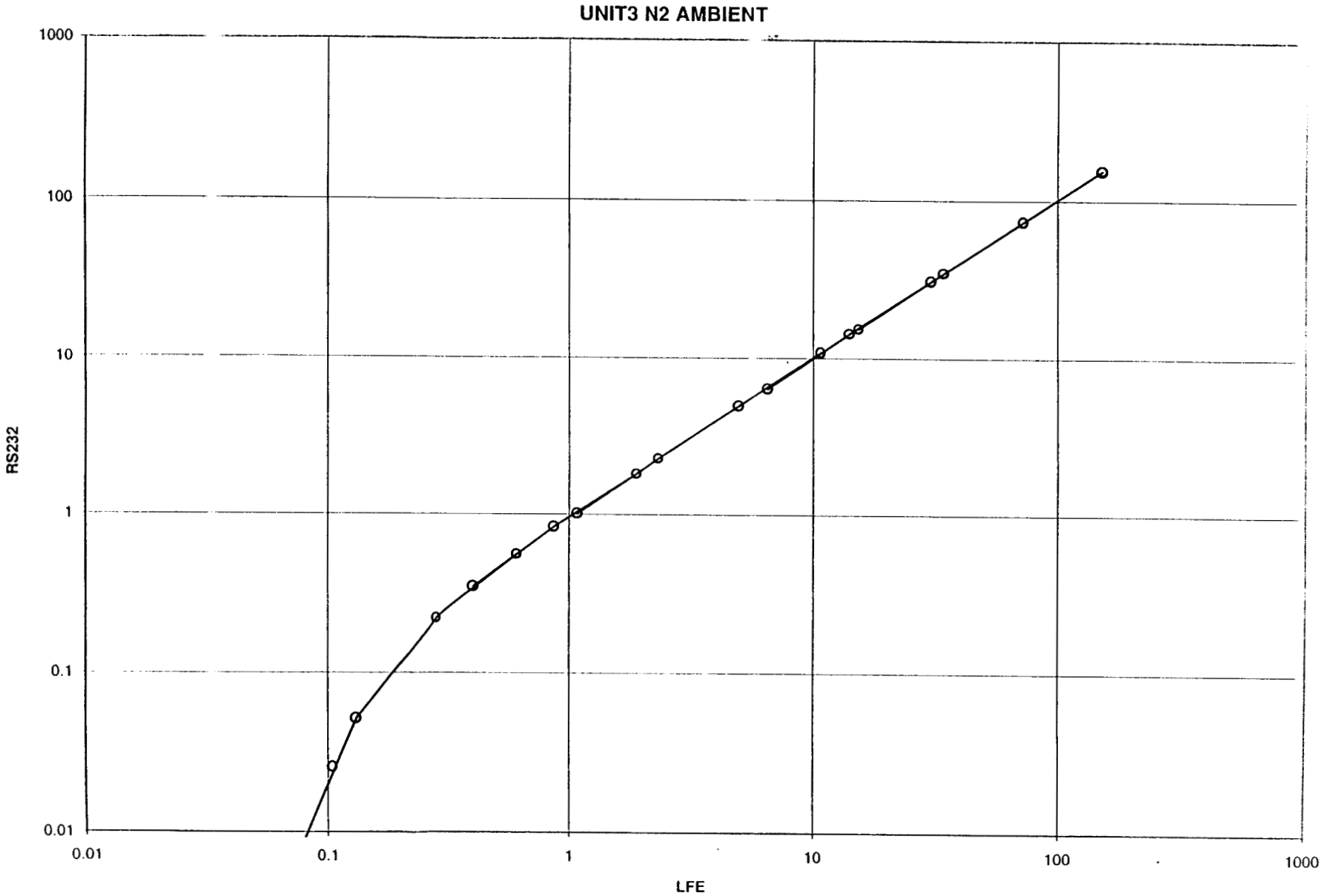
UNIT3 N2 AMBIENT
1000
100
10
1
0.1
0.01
RS232
0.01
0.1
1
10
100
1000
LFE

Figure 7

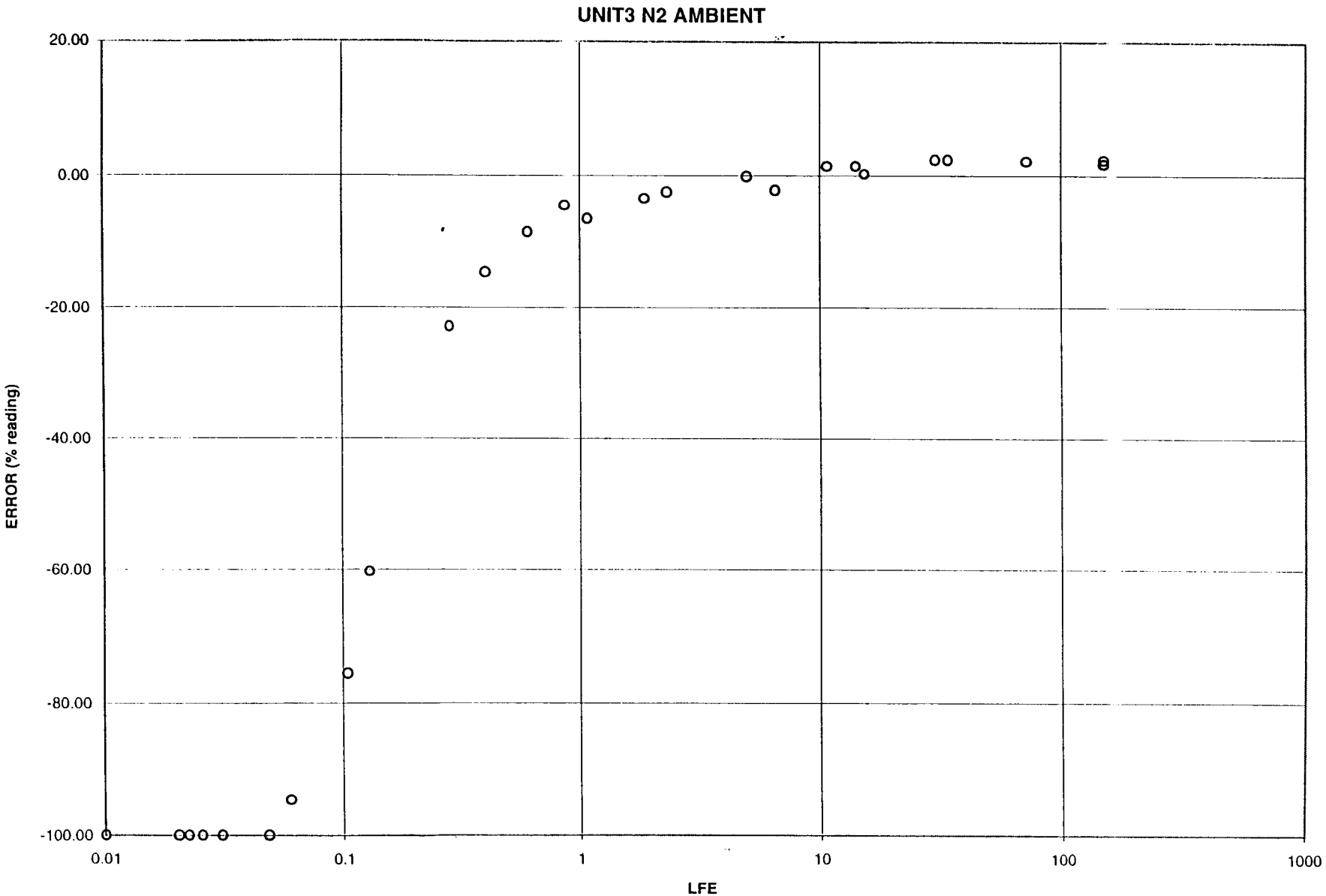
UNIT3 N2 AMBIENT
20.00
0.00
-20.00
-40.00
-60.00
-80.00
-100.00
ERROR (% reading)
0.01
0.1
1
10
100
1000
LFE

Figure 8

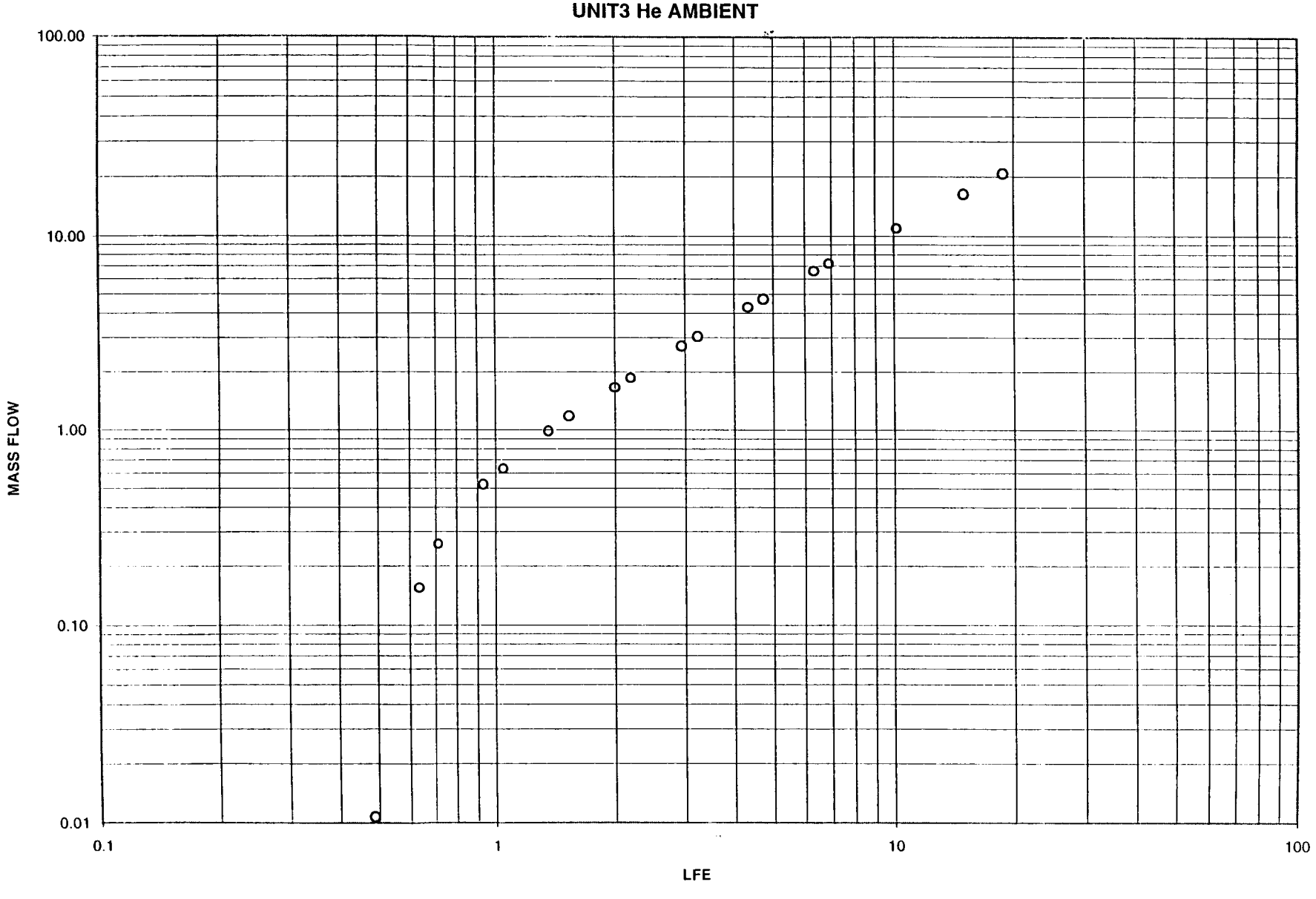
UNIT3 He AMBIENT
100.00
10.00
1.00
0.10
0.01
MASS FLOW
0.1
1
10
100
LFE

Figure 9

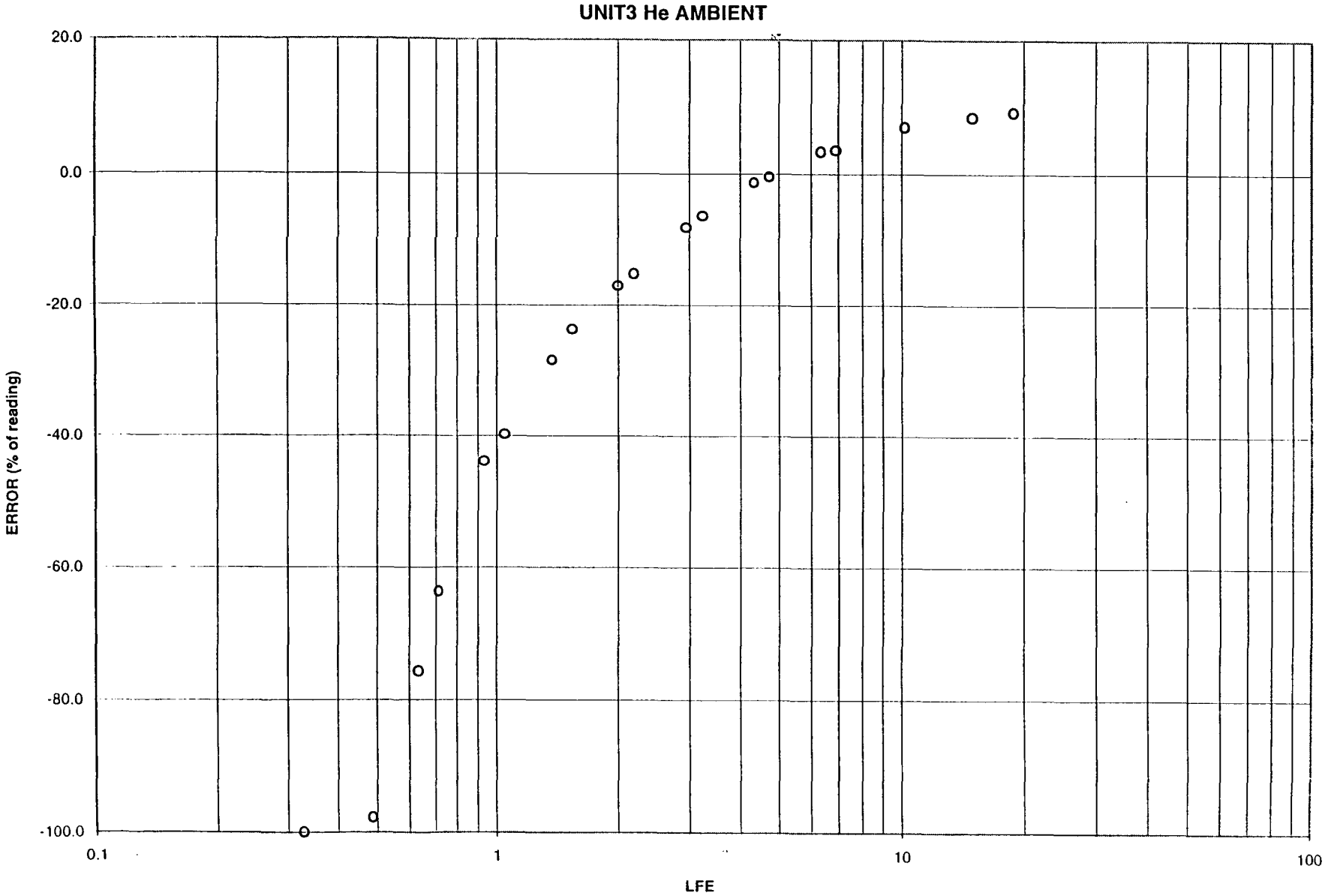
UNIT3 He AMBIENT
20.0
0.0
-20.0
-40.0
-60.0
-80.0
-100.0
ERROR (% of reading)
0.1
1
10
100
LFE

Figure 10

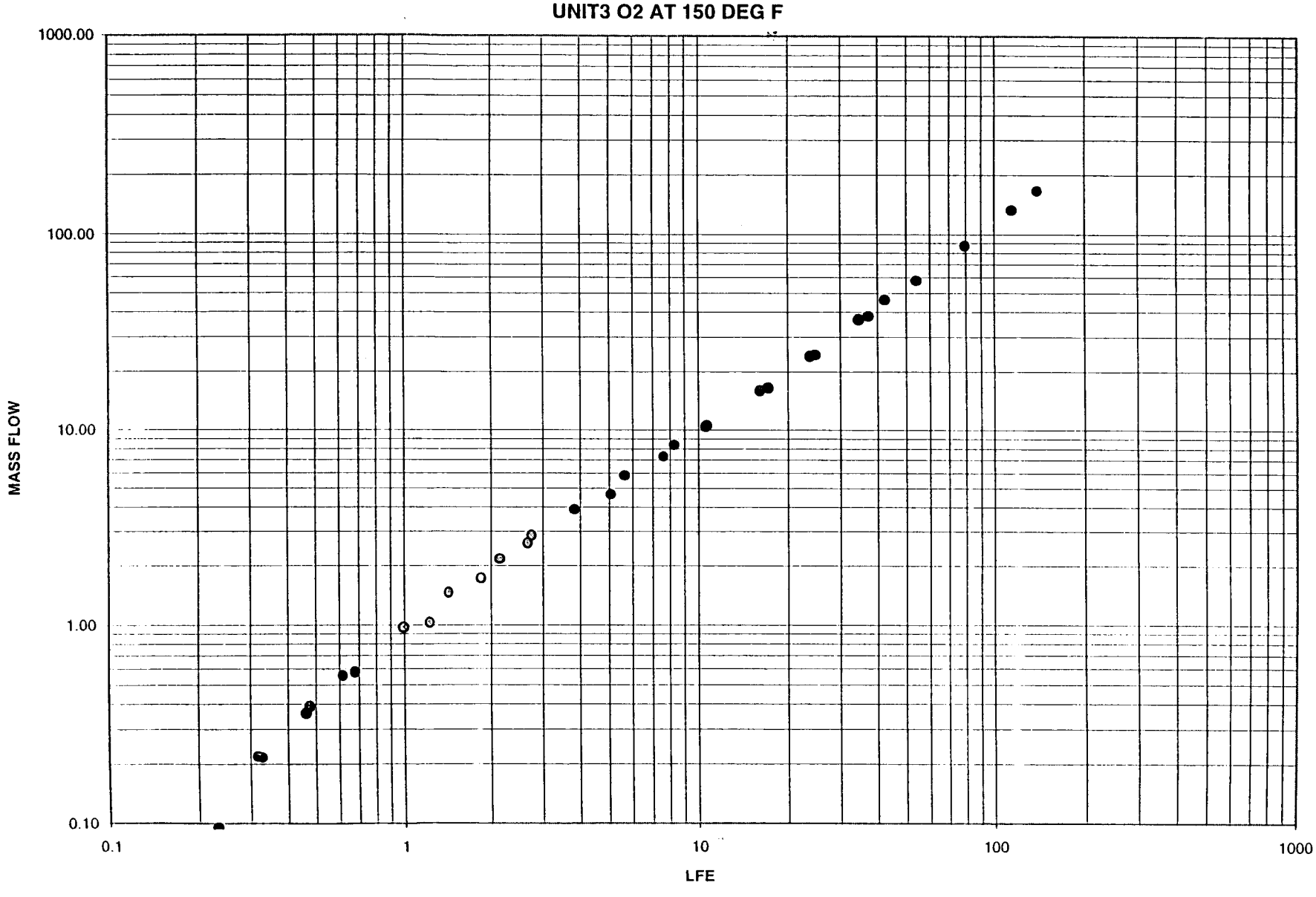
UNIT3 O2 AT 150 DEG F
1000.00
100.00
10.00
1.00
0.10
MASS FLOW
0.1
1
10
100
1000
LFE

Figure 11

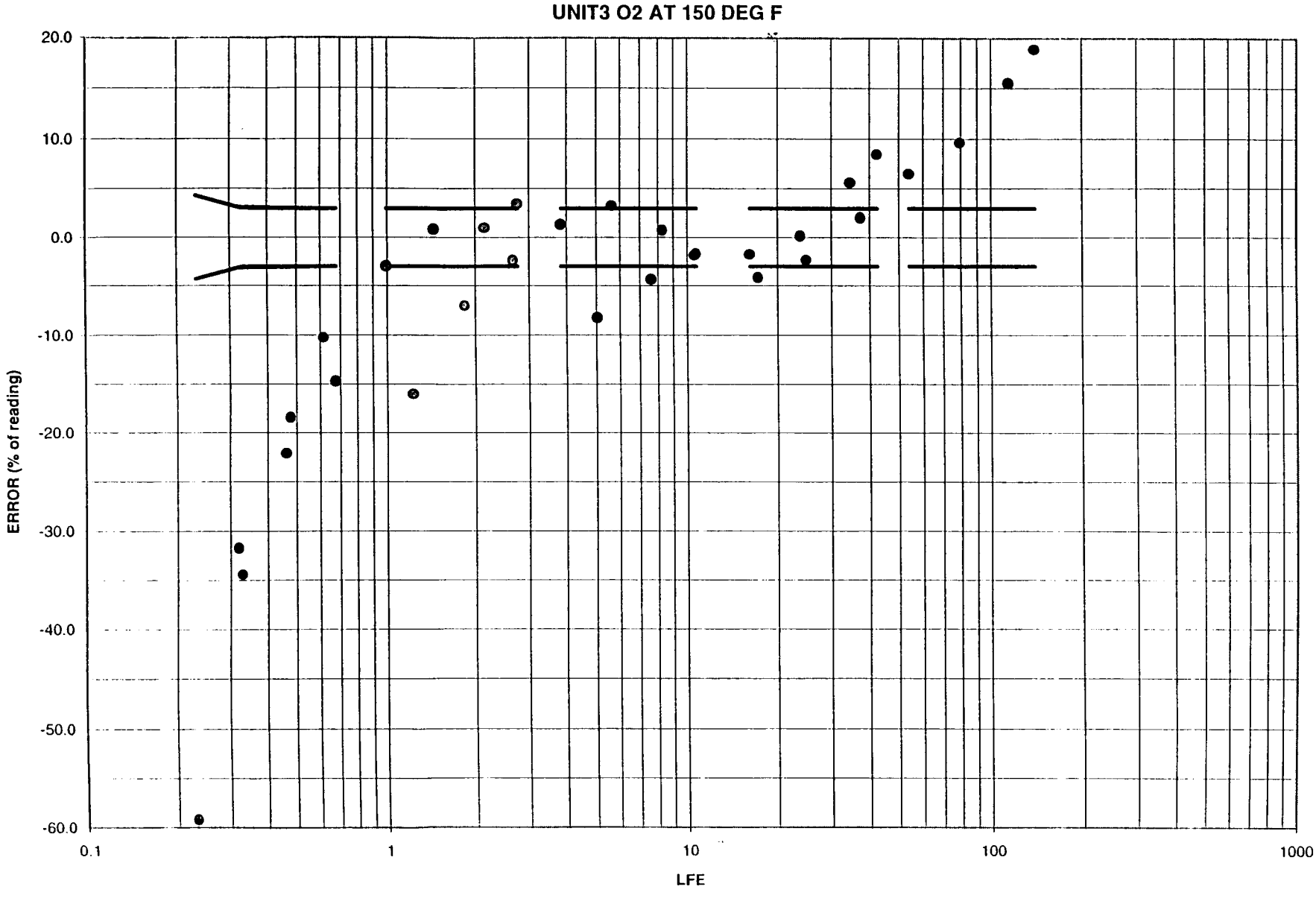
UNIT3 O2 AT 150 DEG F
20.0
10.0
0.0
-10.0
-20.0
-30.0
-40.0
-50.0
-60.0
ERROR (% of reading)
0.1
1
10
100
1000
LFE

Figure 12

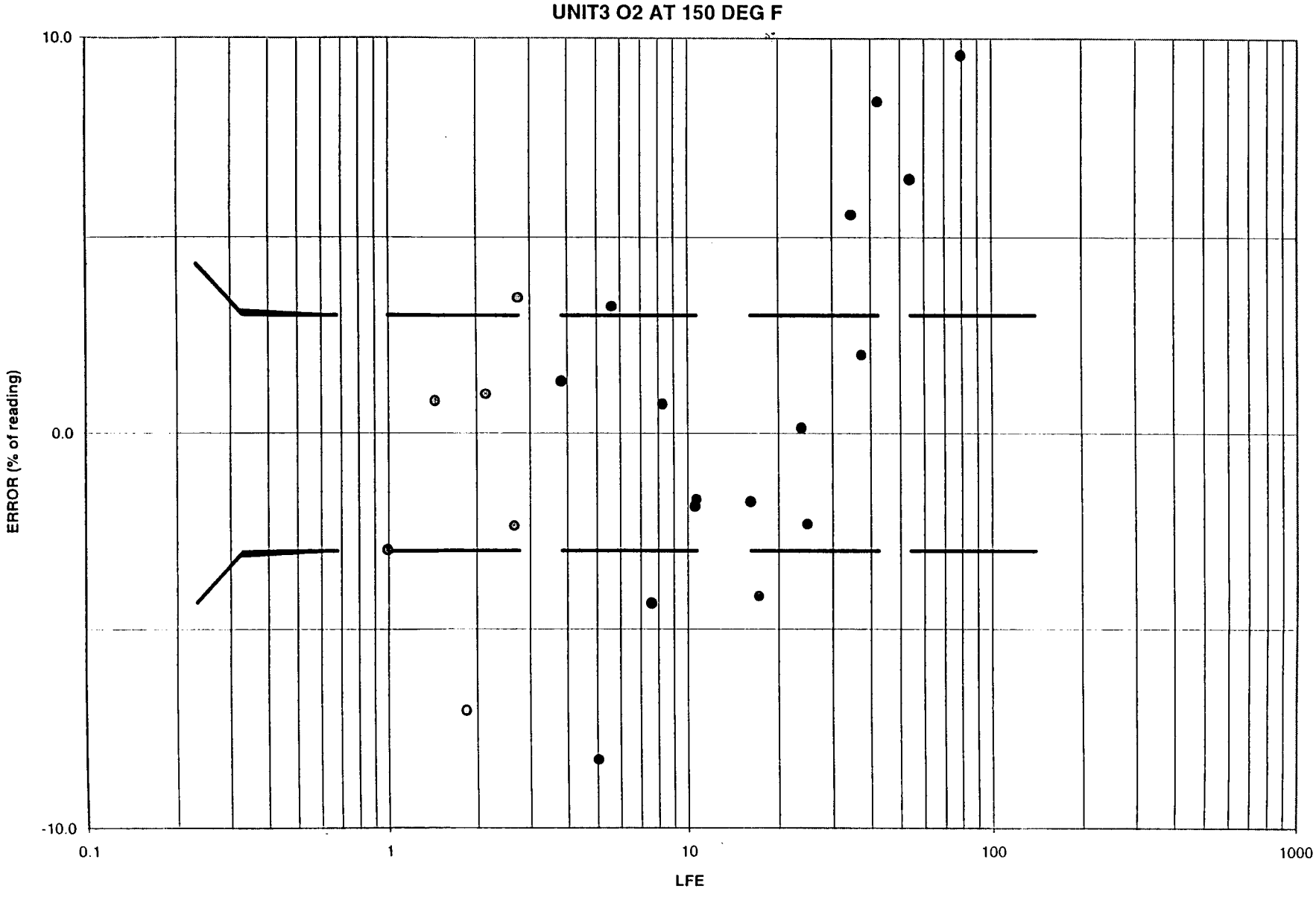
UNIT3 O2 AT 150 DEG F
10.0
0.0
-10.0
ERROR (% of reading)
0.1
1
10
100
1000
LFE

Figure 13

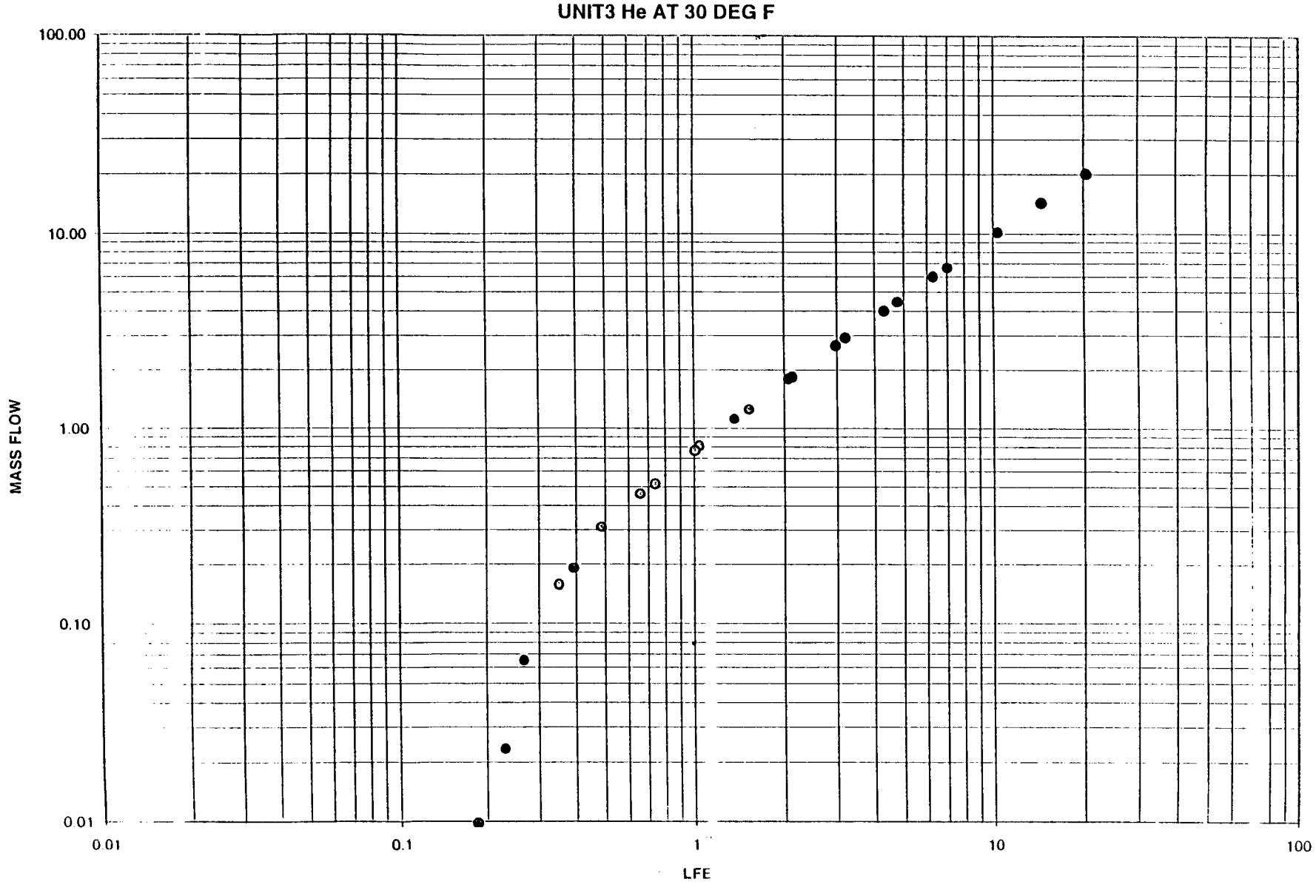
UNIT3 He AT 30 DEG F
100.00
10.00
1.00
0.10
0.01
MASS FLOW
0.01
0.1
1
10
100
LFE

Figure 14

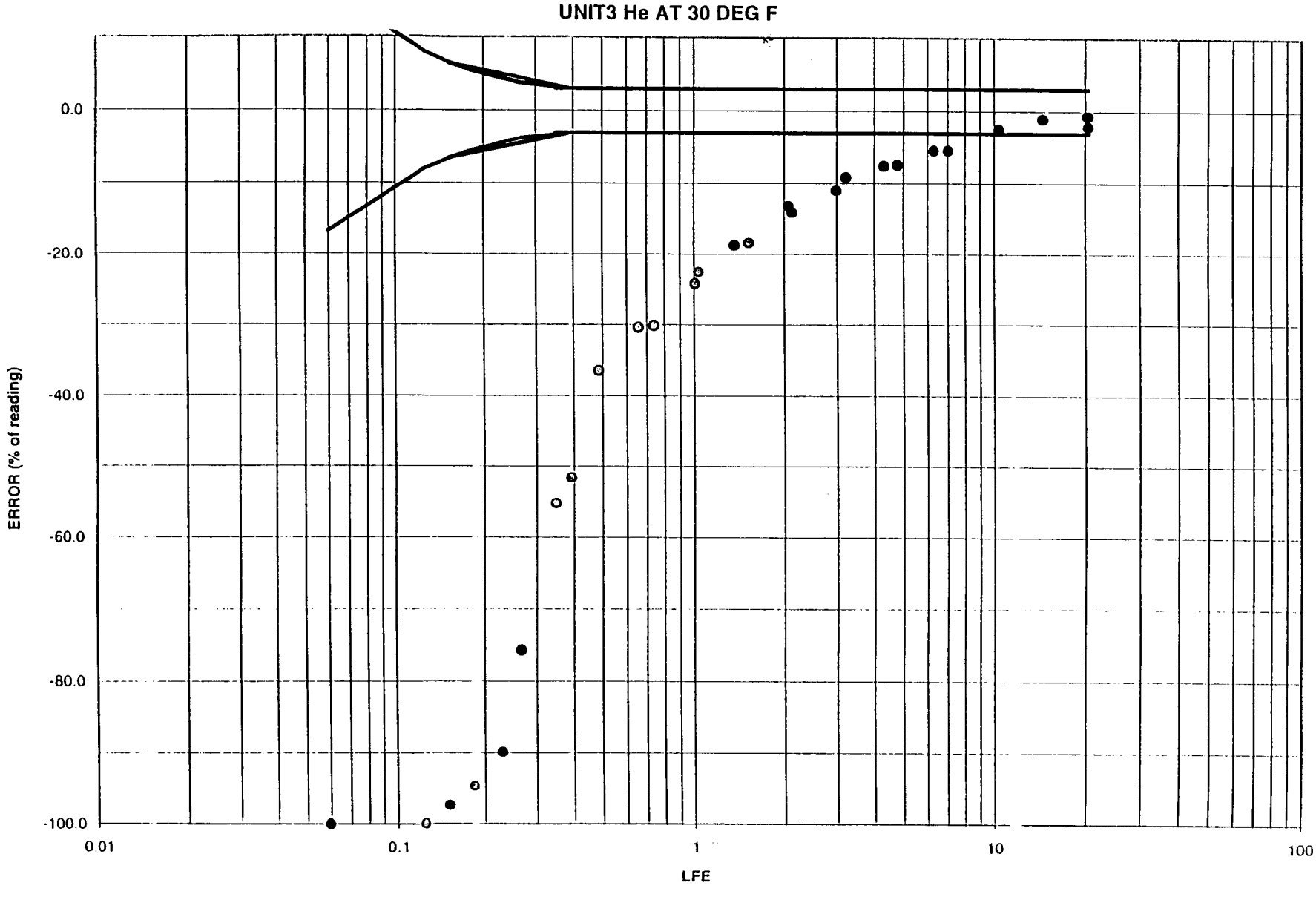
UNIT3 He AT 30 DEG F
0.0
-20.0
-40.0
-60.0
-80.0
-100.0
ERROR (% of reading)
0.01
0.1
1
10
100
LFE

Figure 15

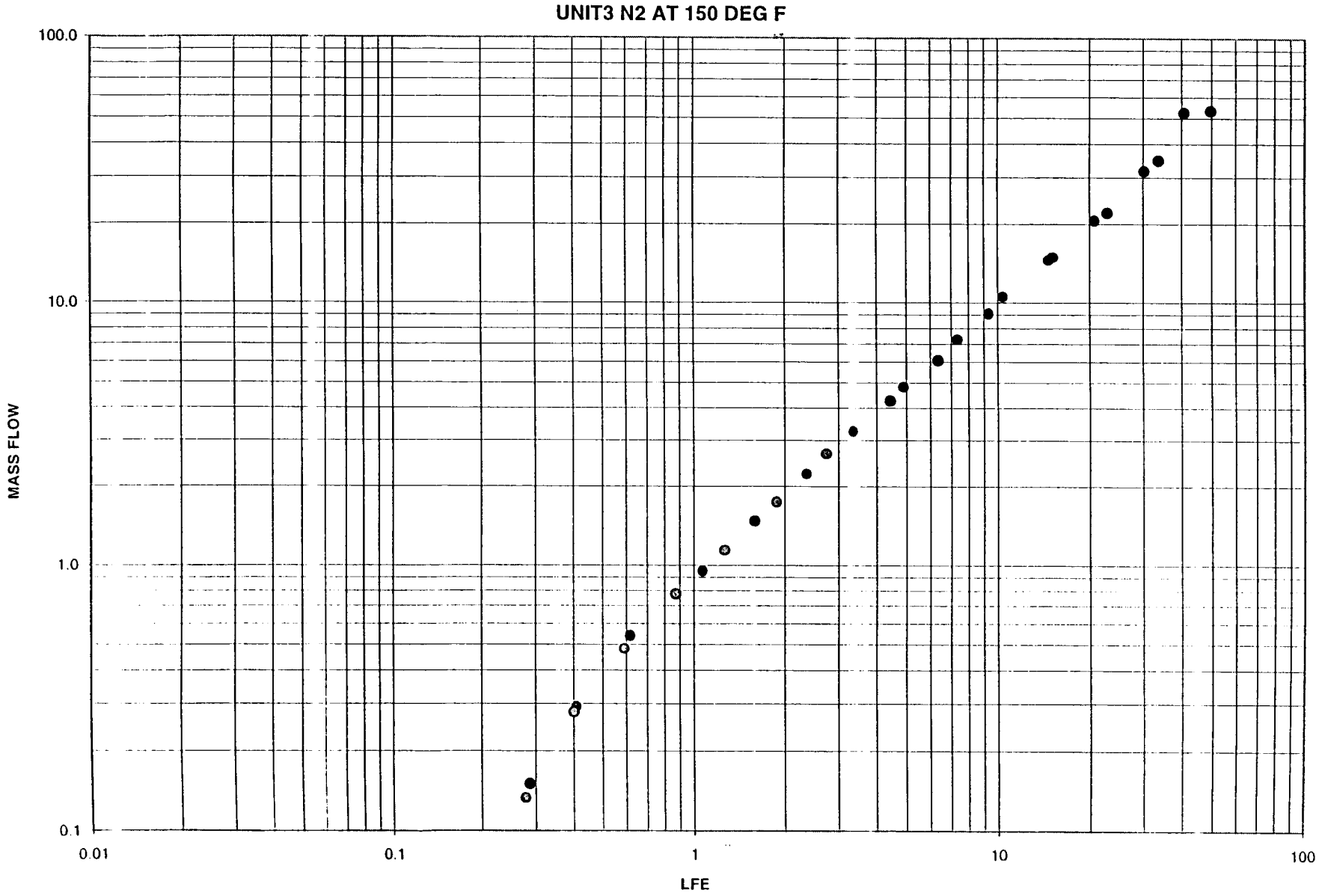

Figure 16

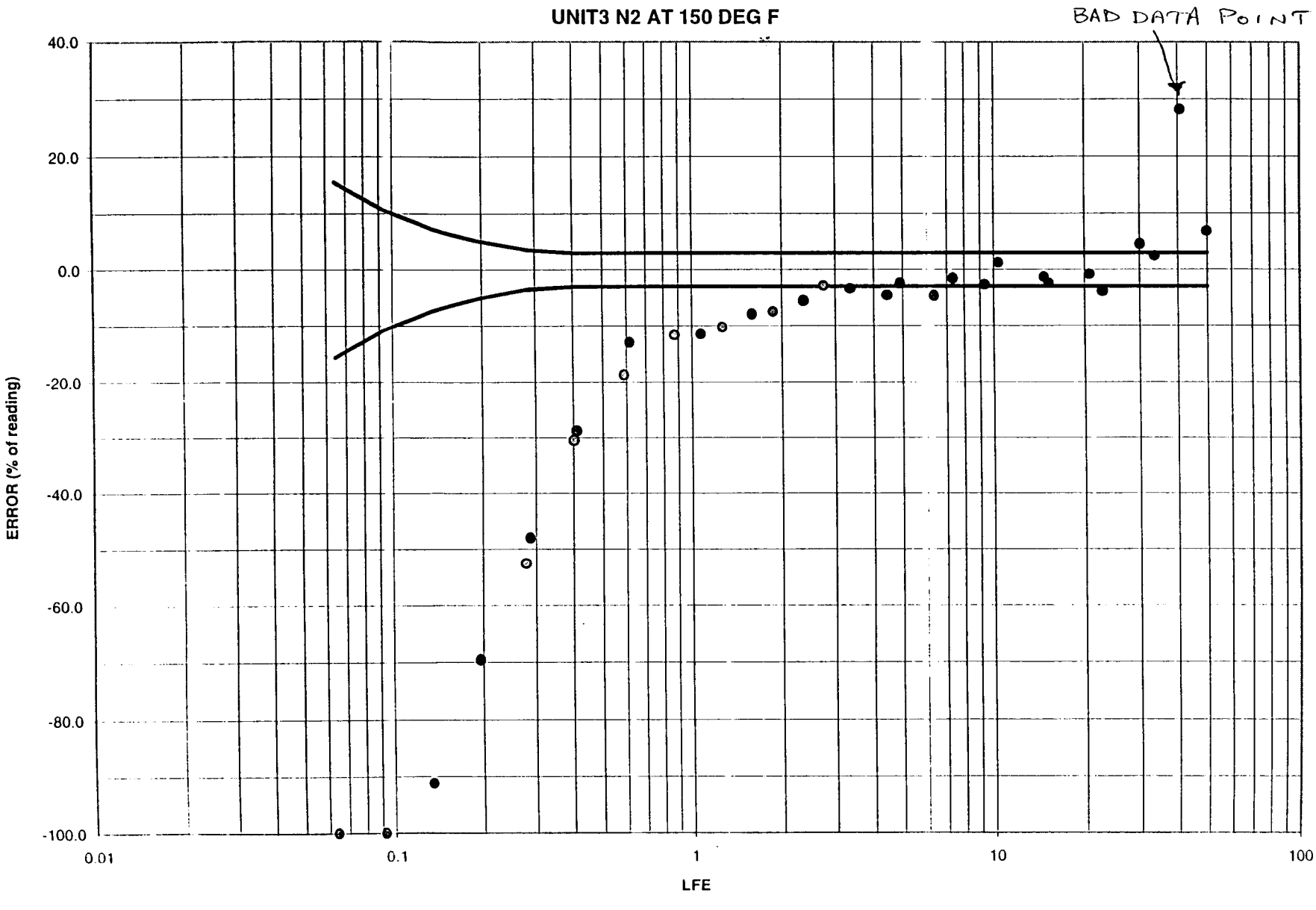
UNIT3 N2 AT 150 DEG F
BAD DATA POINT
40.0
20.0
0.0
-20.0
-40.0
-60.0
-80.0
-100.0
ERROR (% of reading)
0.01
0.1
1
10
100
LFE

Figure 17

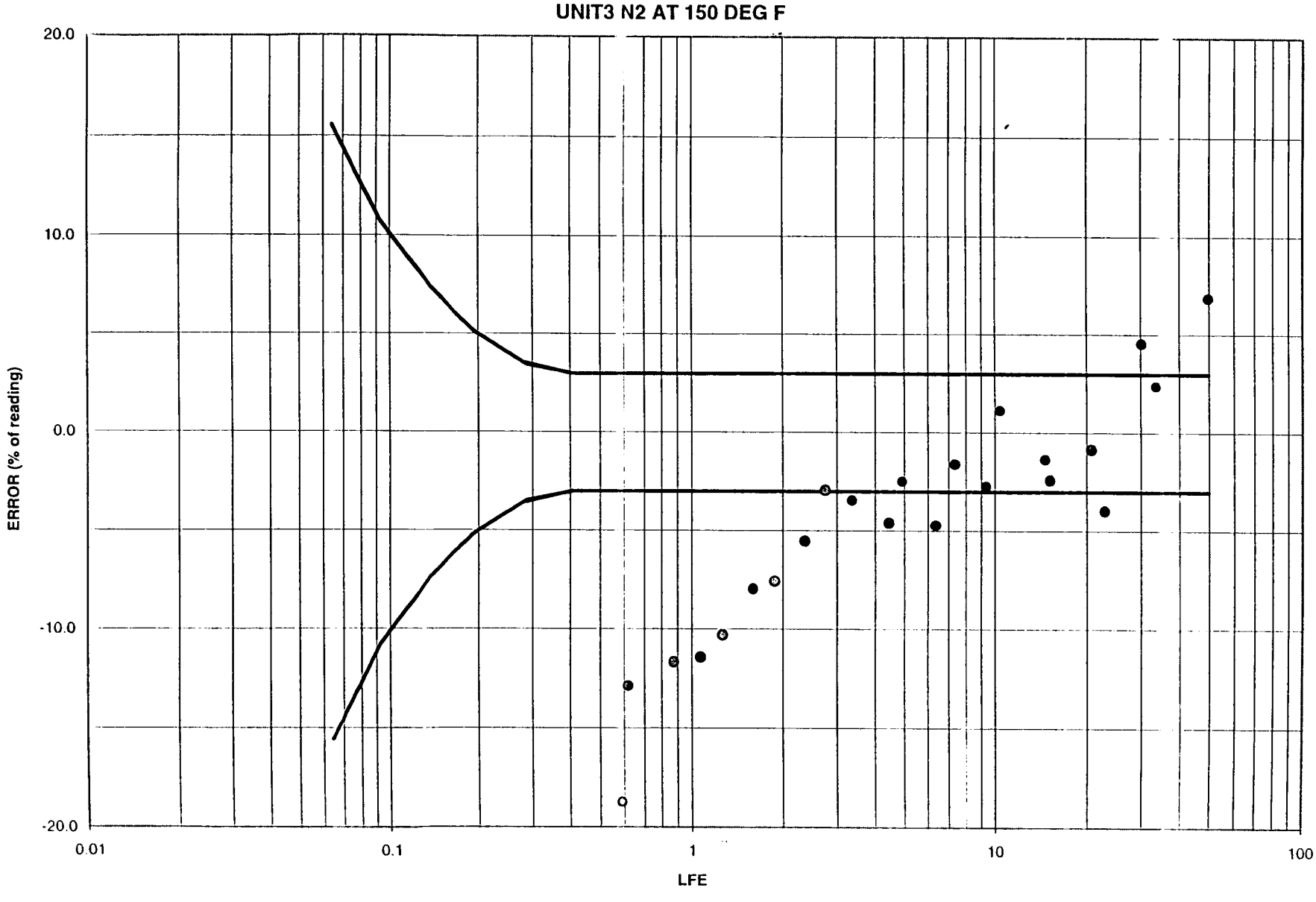
UNIT3 N2 AT 150 DEG F
20.0
10.0
0.0
-10.0
-20.0
ERROR (% of reading)
0.01
0.1
1
10
100
LFE

Figure 18

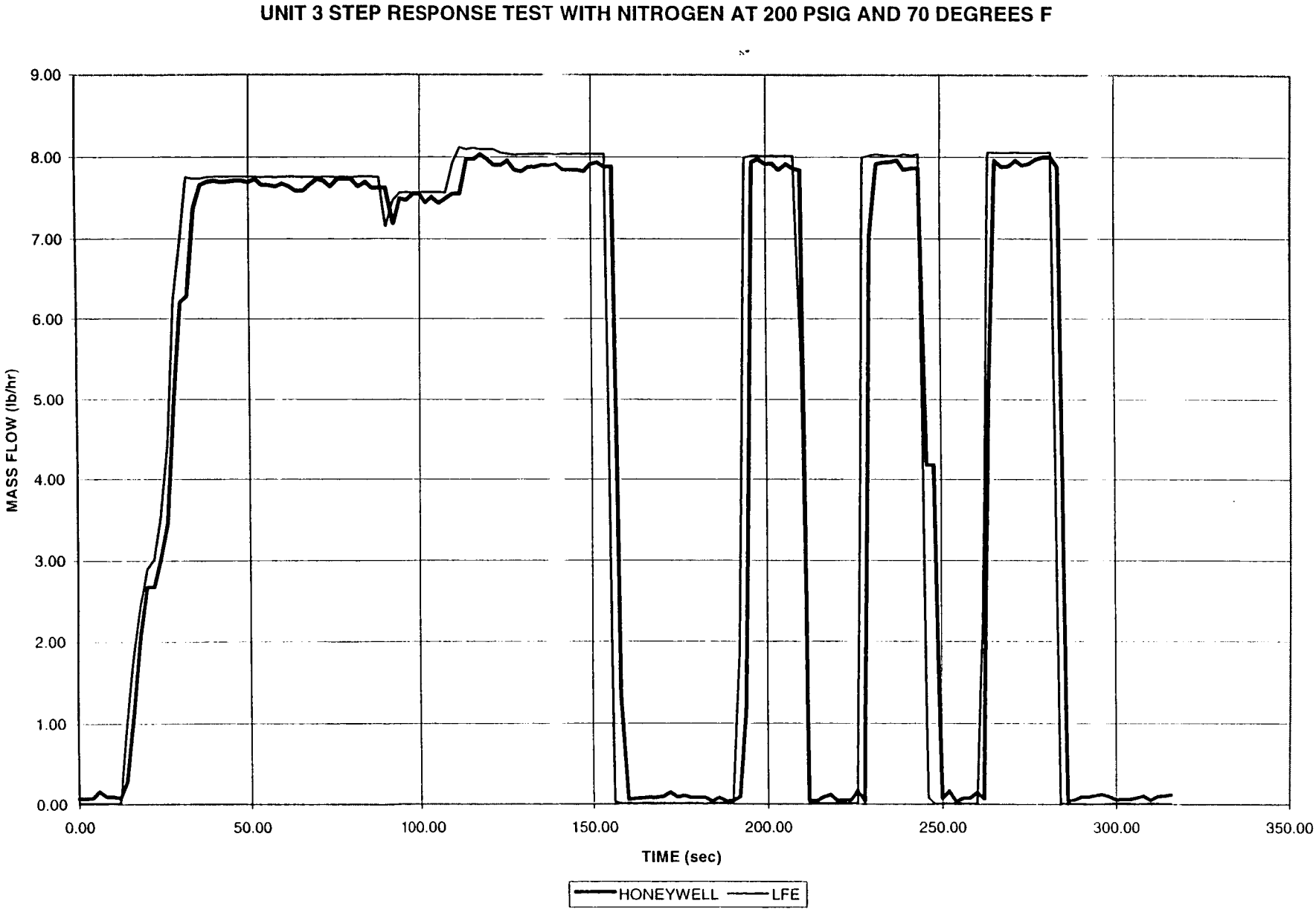
UNIT 3 STEP RESPONSE TEST WITH NITROGEN AT 200 PSIG AND 70 DEGREES F
MASS FLOW (lb/hr)
9.00
8.00
7.00
6.00
5.00
4.00
3.00
2.00
1.00
0.00
0.00
50.00
100.00
150.00
200.00
250.00
300.00
350.00
TIME (sec)
HONEYWELL
LFE

Figure 19

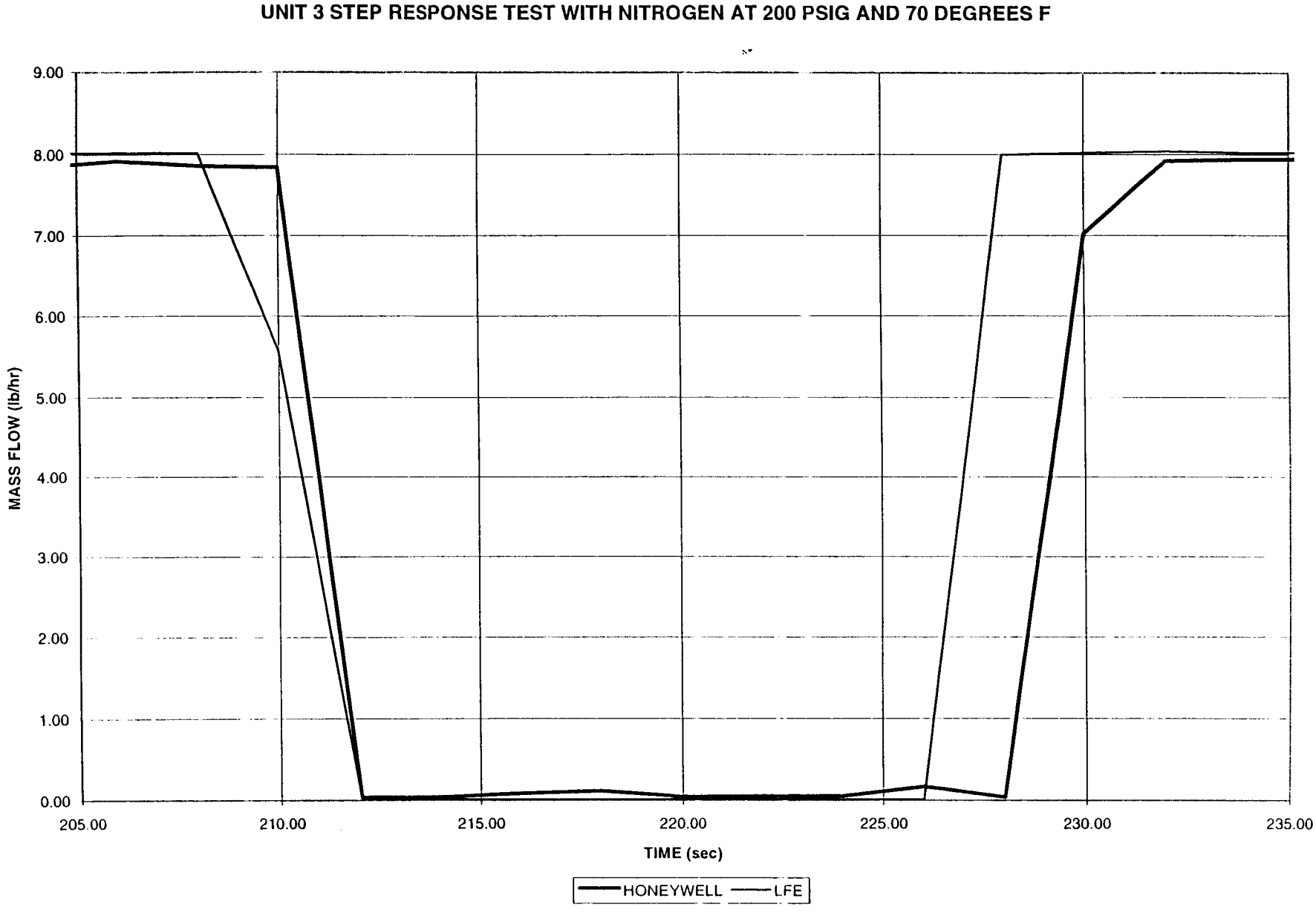
UNIT 3 STEP RESPONSE TEST WITH NITROGEN AT 200 PSIG AND 70 DEGREES F
9.00
8.00
7.00
6.00
5.00
4.00
3.00
2.00
1.00
0.00
MASS FLOW (lb/hr)
205.00
210.00
215.00
220.00
225.00
230.00
235.00
TIME (sec)
HONEYWELL
LFE

Figure 20

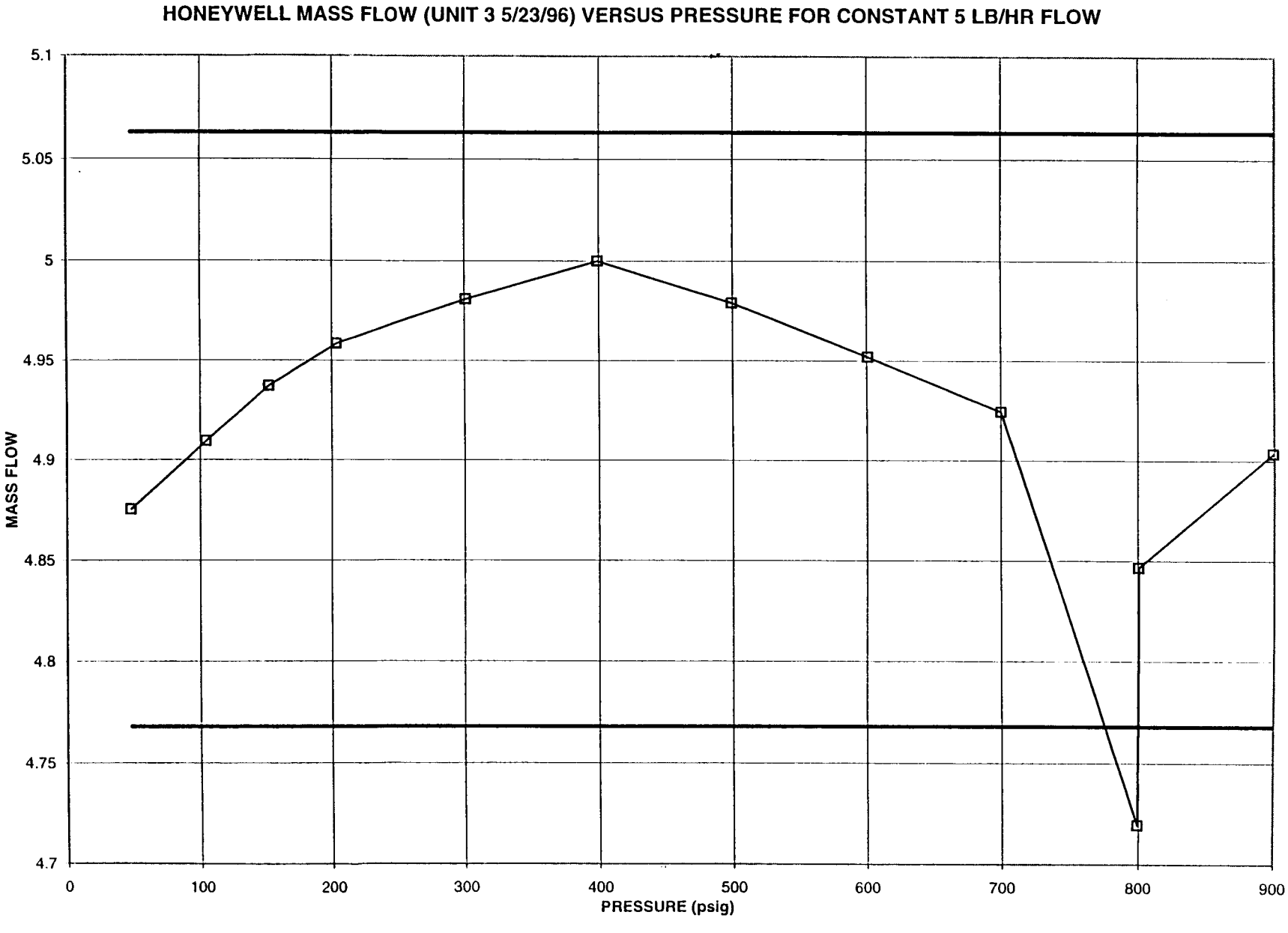
HONEYWELL MASS FLOW (UNIT 3 5/23/96) VERSUS PRESSURE FOR CONSTANT 5 LB/HR FLOW
MASS FLOW
5.1
5.05
5
4.95
4.9
4.85
4.8
4.75
4.7
0
100
200
300
400
500
600
700
800
900
PRESSURE (psig)

Figure 21

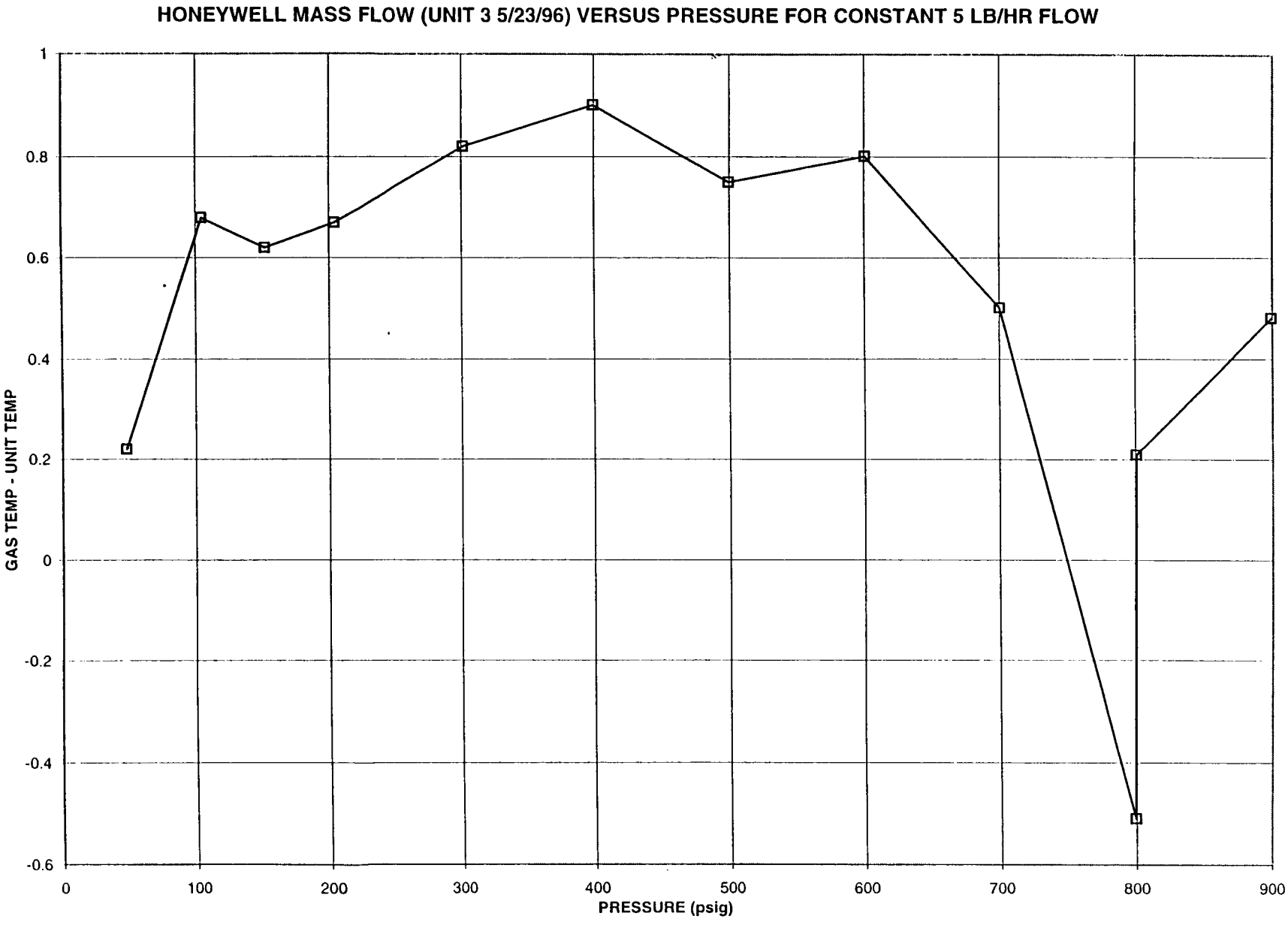
HONEYWELL MASS FLOW (UNIT 3 5/23/96) VERSUS PRESSURE FOR CONSTANT 5 LB/HR FLOW
GAS TEMP - UNIT TEMP
1
0.8
0.6
0.4
0.2
0
-0.2
-0.4
-0.6
0
100
200
300
400
500
600
700
800
900
PRESSURE (psig)

Figure 22

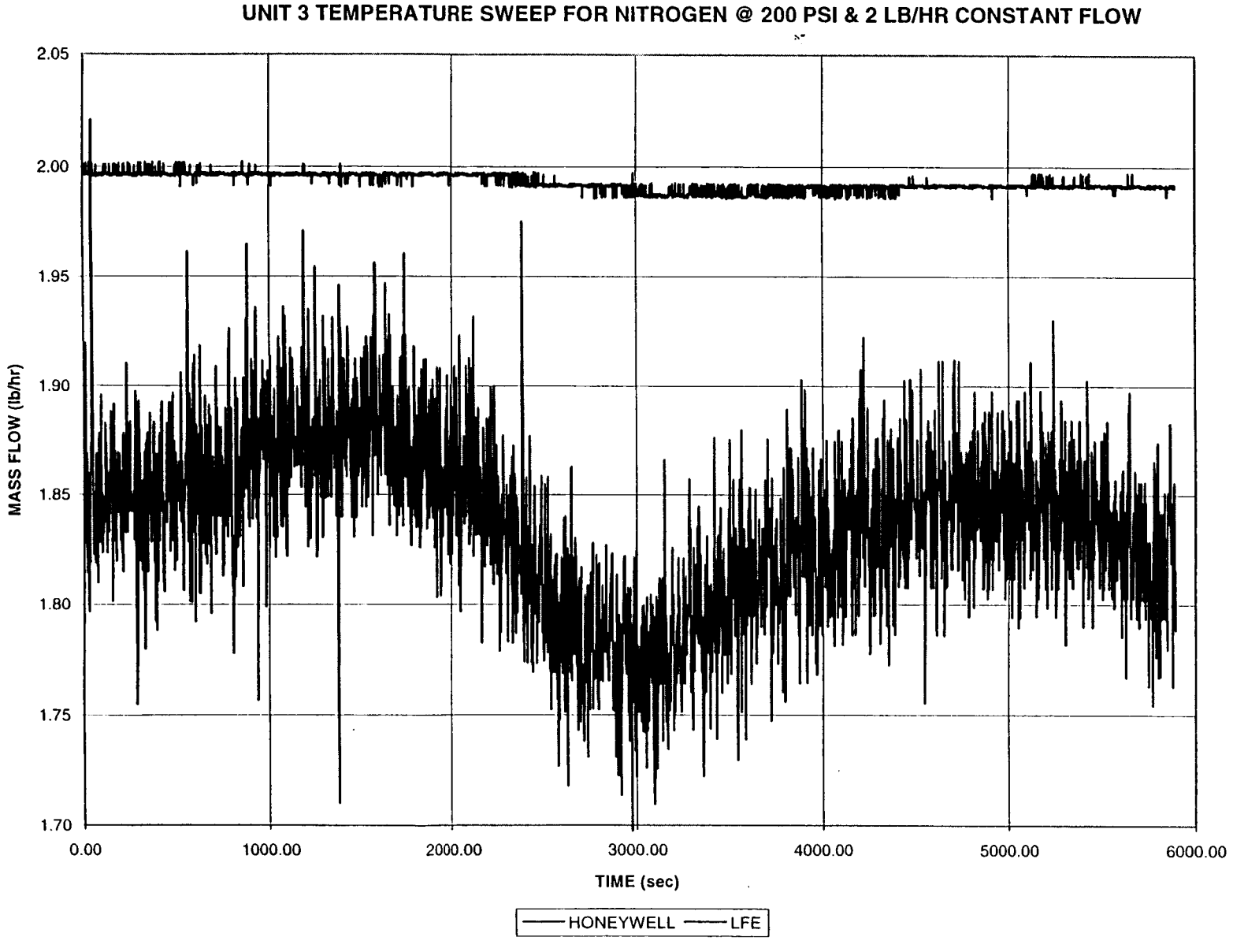
UNIT 3 TEMPERATURE SWEEP FOR NITROGEN @ 200 PSI & 2 LB/HR CONSTANT FLOW
MASS FLOW (lb/hr)
2.05
2.00
1.95
1.90
1.85
1.80
1.75
1.70
0.00
1000.00
2000.00
3000.00
4000.00
5000.00
6000.00
TIME (sec)
HONEYWELL
LFE

Figure 23

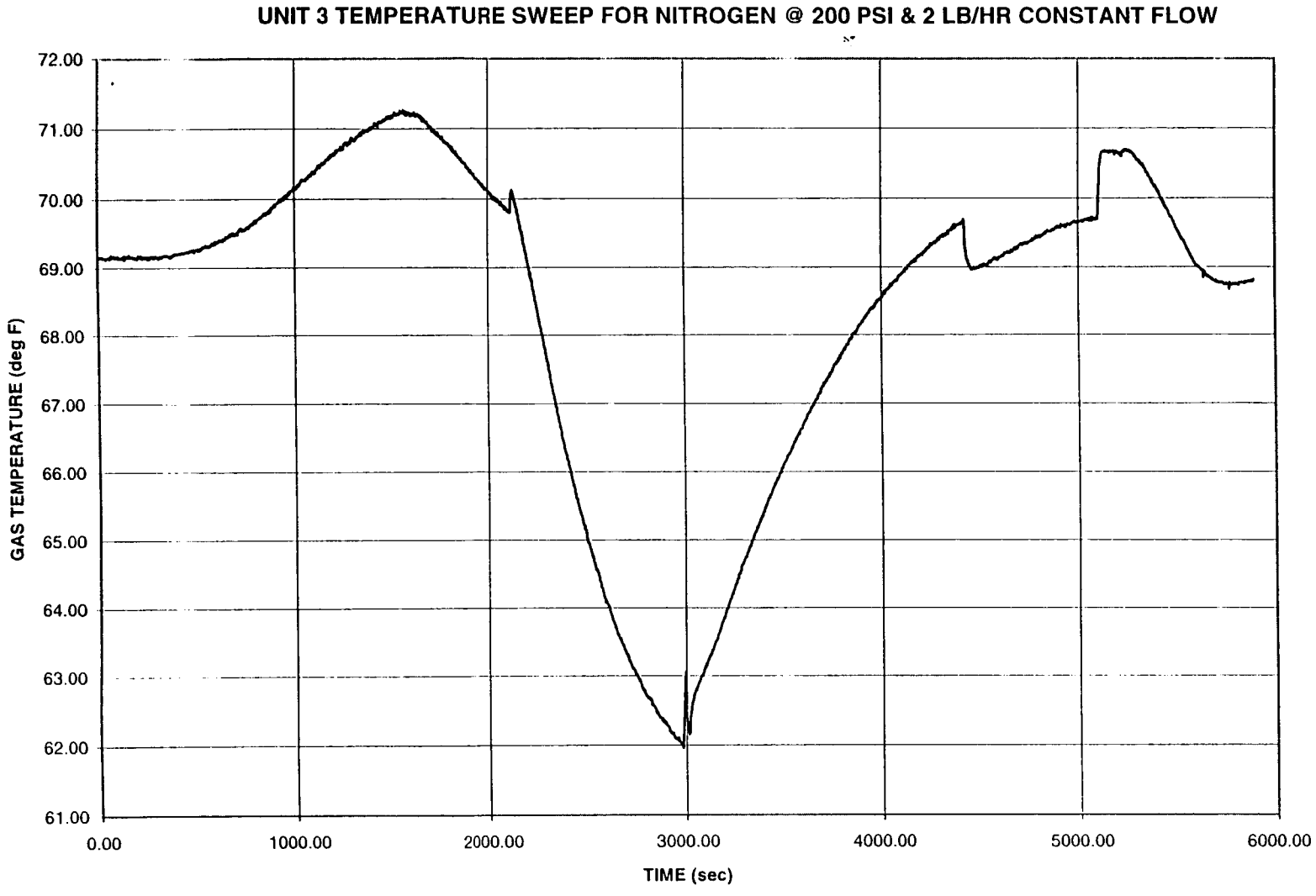
UNIT 3 TEMPERATURE SWEEP FOR NITROGEN @ 200 PSI & 2 LB/HR CONSTANT FLOW
GAS TEMPERATURE (deg F)
72.00
71.00
70.00
69.00
68.00
67.00
66.00
65.00
64.00
63.00
62.00
61.00
0.00
1000.00
2000.00
3000.00
4000.00
5000.00
6000.00
TIME (sec)

Figure 24

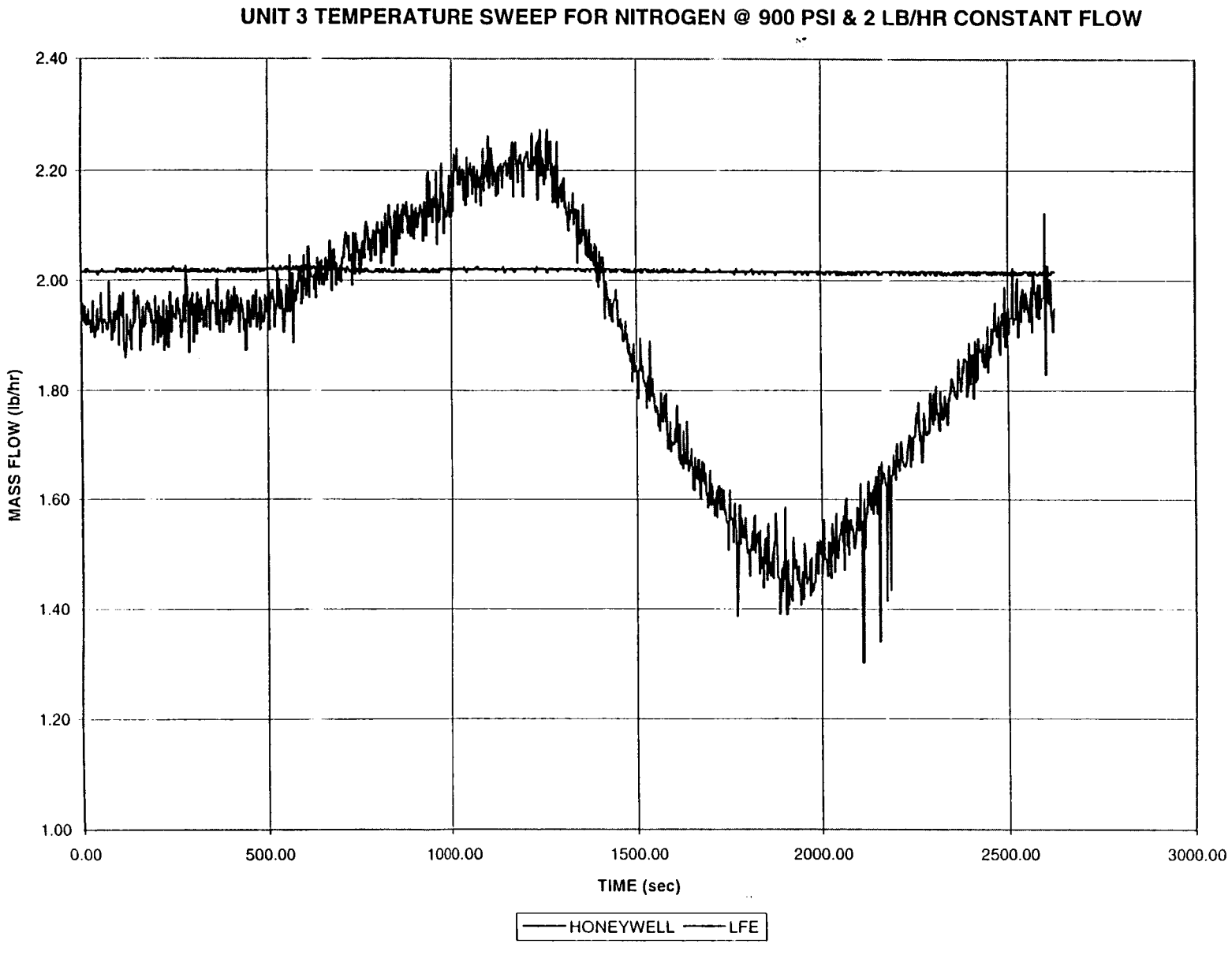
UNIT 3 TEMPERATURE SWEEP FOR NITROGEN @ 900 PSI & 2 LB/HR CONSTANT FLOW
MASS FLOW (lb/hr)
2.40
2.20
2.00
1.80
1.60
1.40
1.20
1.00
0.00
500.00
1000.00
1500.00
2000.00
2500.00
3000.00
TIME (sec)
HONEYWELL
LFE

Figure 25

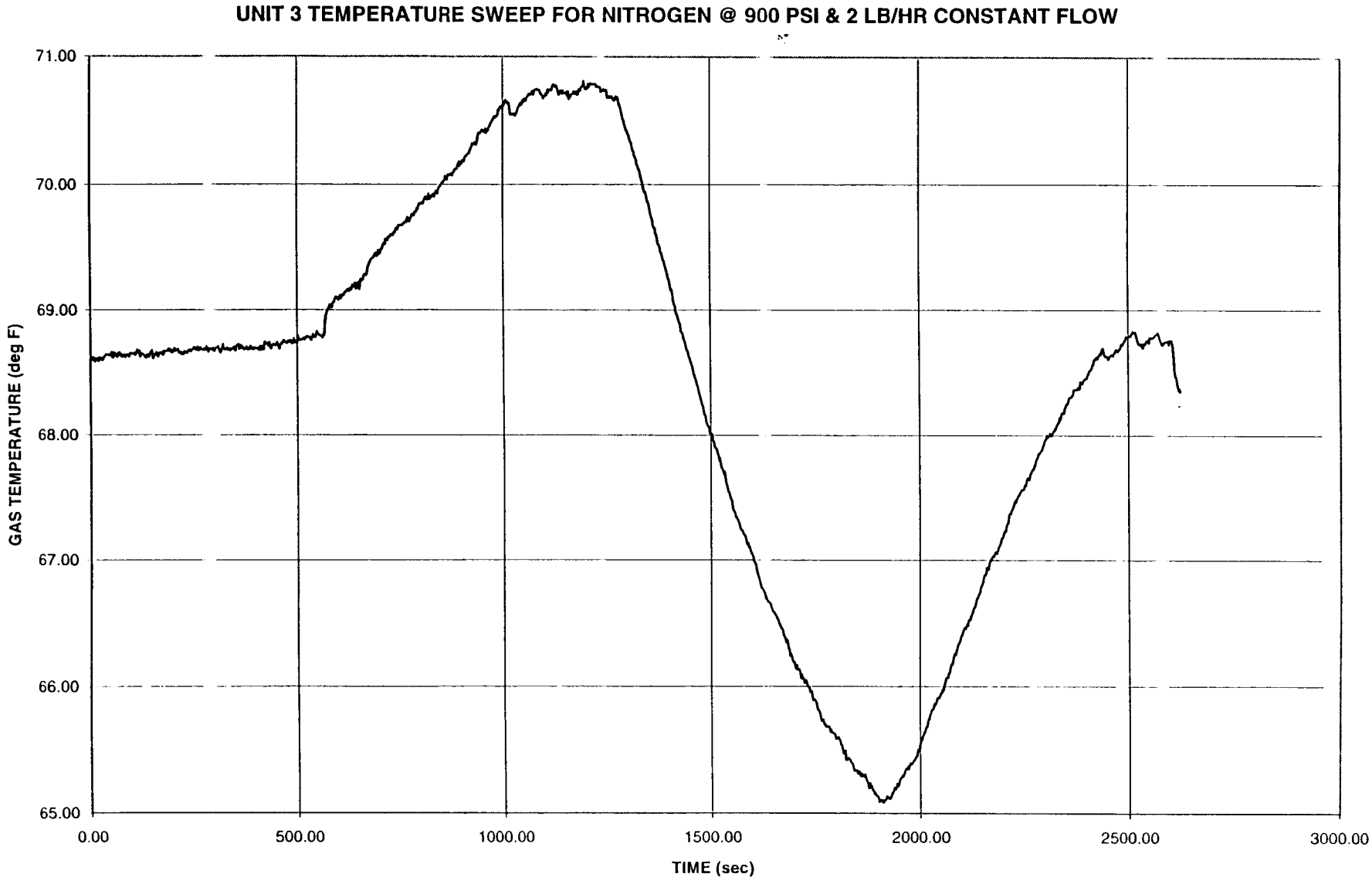
UNIT 3 TEMPERATURE SWEEP FOR NITROGEN @ 900 PSI & 2 LB/HR CONSTANT FLOW
71.00
70.00
69.00
68.00
67.00
66.00
65.00
GAS TEMPERATURE (deg F)
0.00
500.00
1000.00
1500.00
2000.00
2500.00
3000.00
TIME (sec)

Figure 26

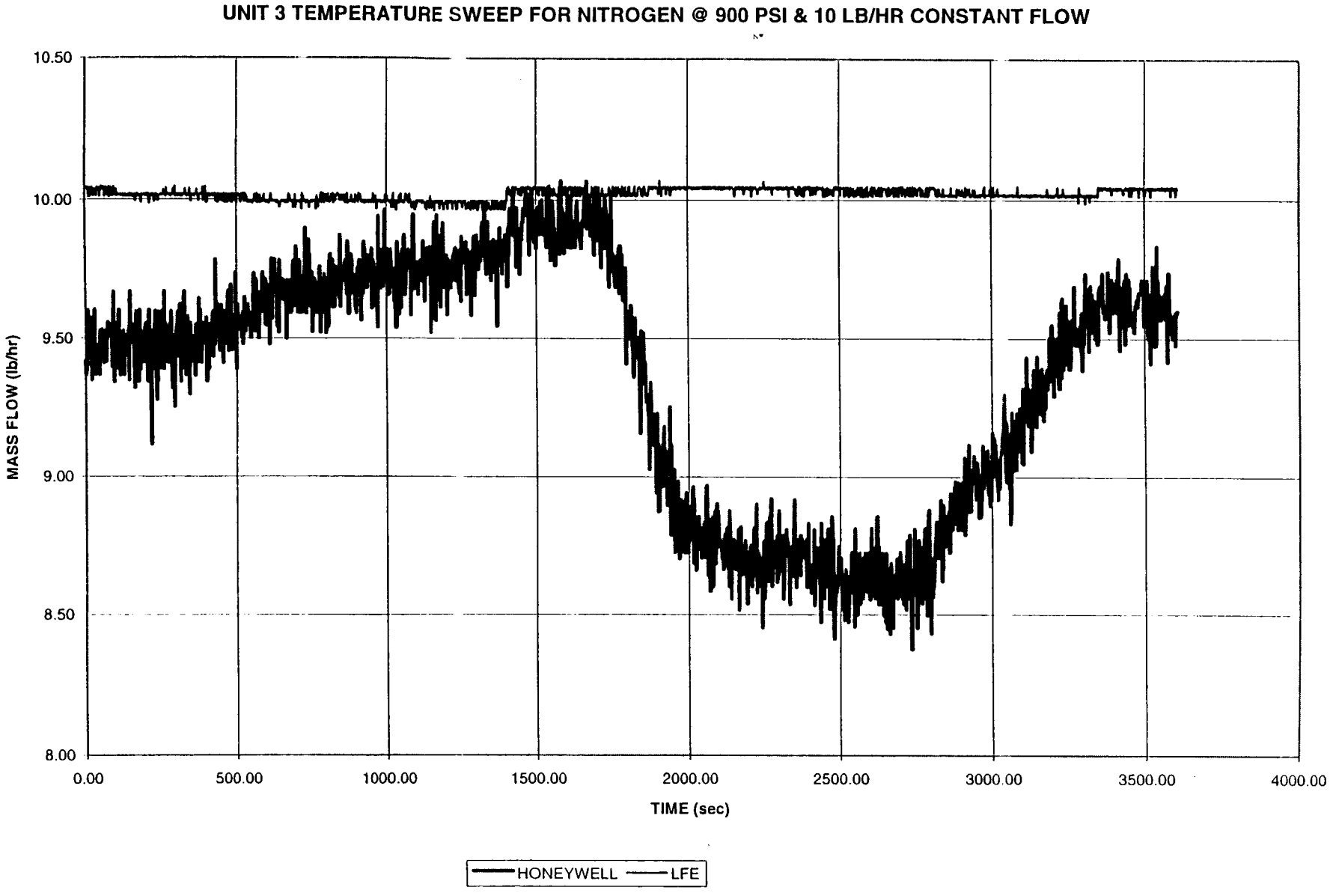
UNIT 3 TEMPERATURE SWEEP FOR NITROGEN @ 900 PSI & 10 LB/HR CONSTANT FLOW
MASS FLOW (lb/hr)
10.50
10.00
9.50
9.00
8.50
8.00
0.00
500.00
1000.00
1500.00
2000.00
2500.00
3000.00
3500.00
4000.00
TIME (sec)
HONEYWELL
LFE

Figure 27

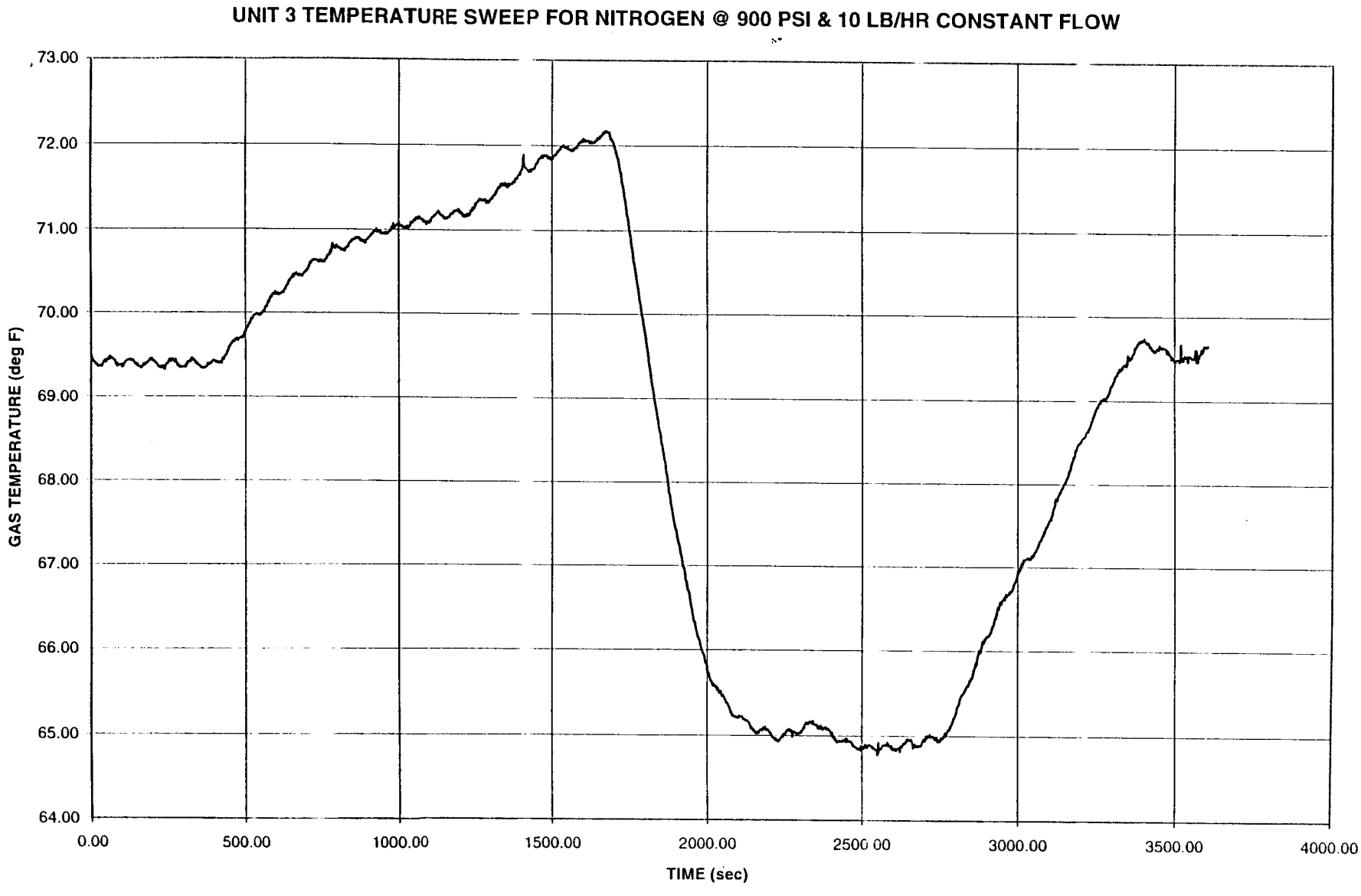
UNIT 3 TEMPERATURE SWEEP FOR NITROGEN @ 900 PSI & 10 LB/HR CONSTANT FLOW
GAS TEMPERATURE (deg F)
73.00
72.00
71.00
70.00
69.00
68.00
67.00
66.00
65.00
64.00
0.00
500.00
1000.00
1500.00
2000.00
2500.00
3000.00
3500.00
4000.00
TIME (sec)

Figure 28

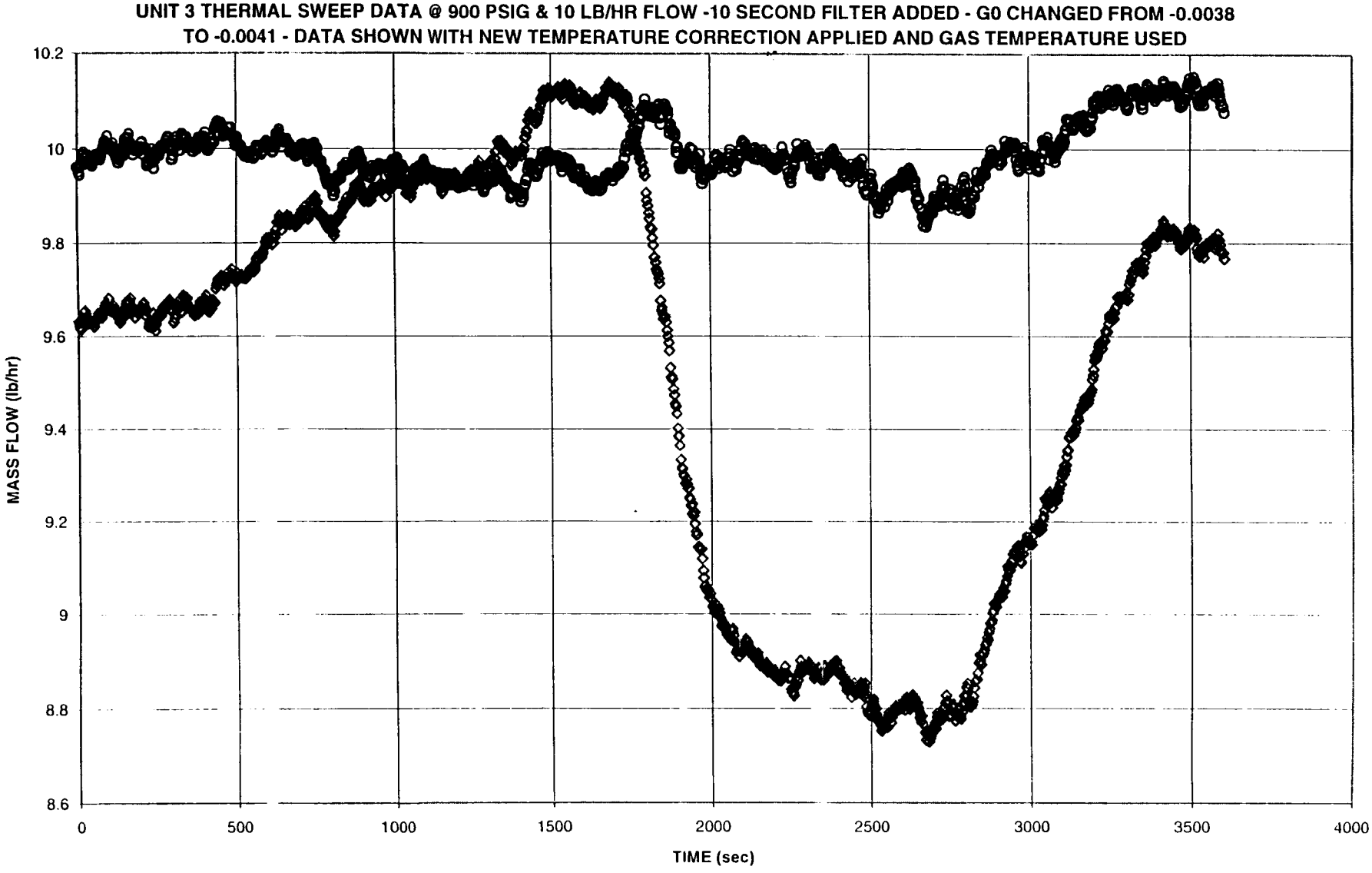
UNIT 3 THERMAL SWEEP DATA @ 900 PSIG & 10 LB/HR FLOW -10 SECOND FILTER ADDED - G0 CHANGED FROM -0.0038 TO -0.0041 - DATA SHOWN WITH NEW TEMPERATURE CORRECTION APPLIED AND GAS TEMPERATURE USED
MASS FLOW (lb/hr)
10.2
10
9.8
9.6
9.4
9.2
9
8.8
8.6
0
500
1000
1500
2000
2500
3000
3500
4000
TIME (sec)

Figure 29

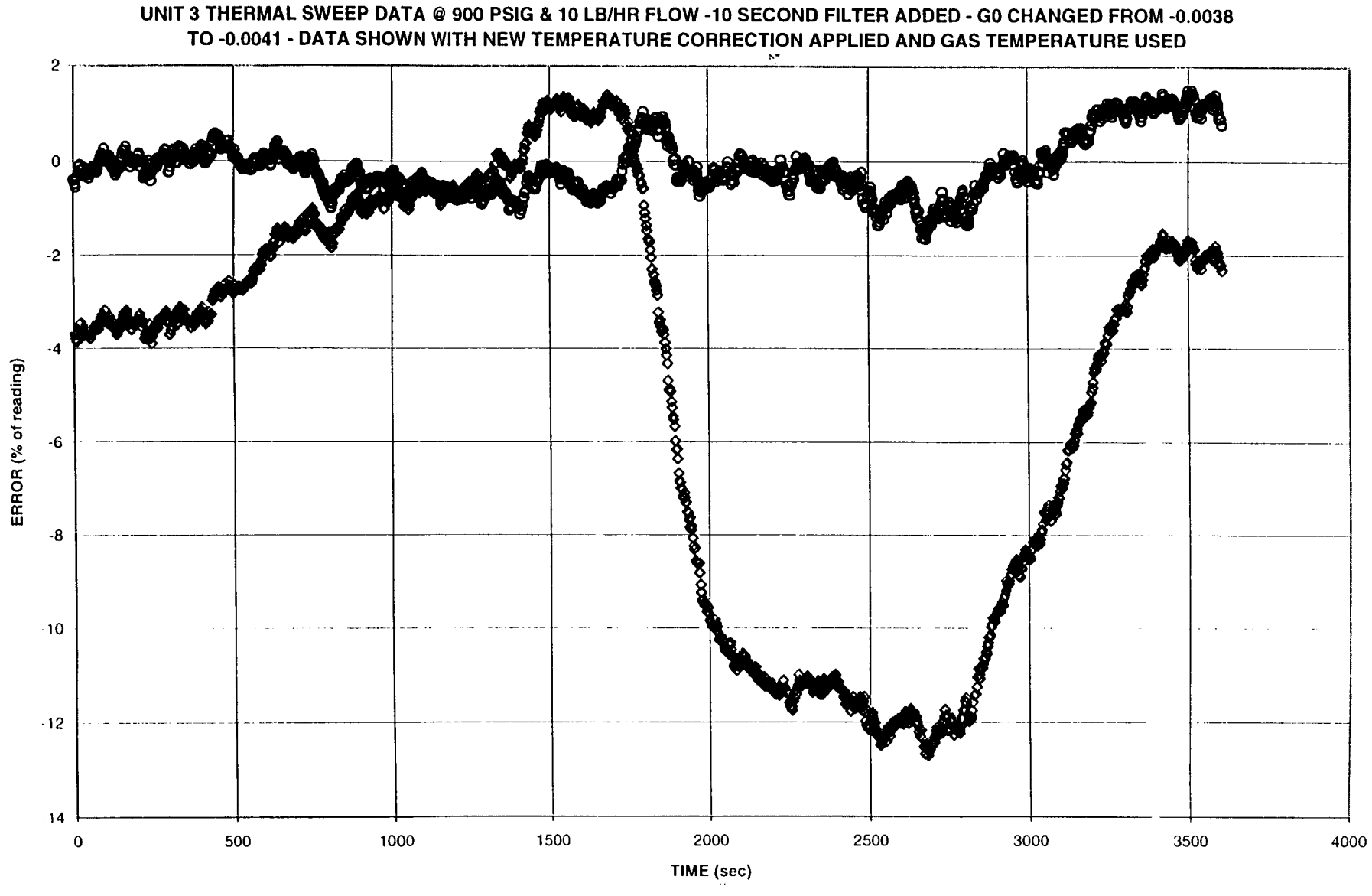
UNIT 3 THERMAL SWEEP DATA @ 900 PSIG & 10 LB/HR FLOW -10 SECOND FILTER ADDED - G0 CHANGED FROM -0.0038 TO -0.0041 - DATA SHOWN WITH NEW TEMPERATURE CORRECTION APPLIED AND GAS TEMPERATURE USED
ERROR (% of reading)
2
0
-2
-4
-6
-8
-10
-12
-14
0
500
1000
1500
2000
2500
3000
3500
4000
TIME (sec)

Figure 30

To: BOB FRAMPTON From : U. BONNE

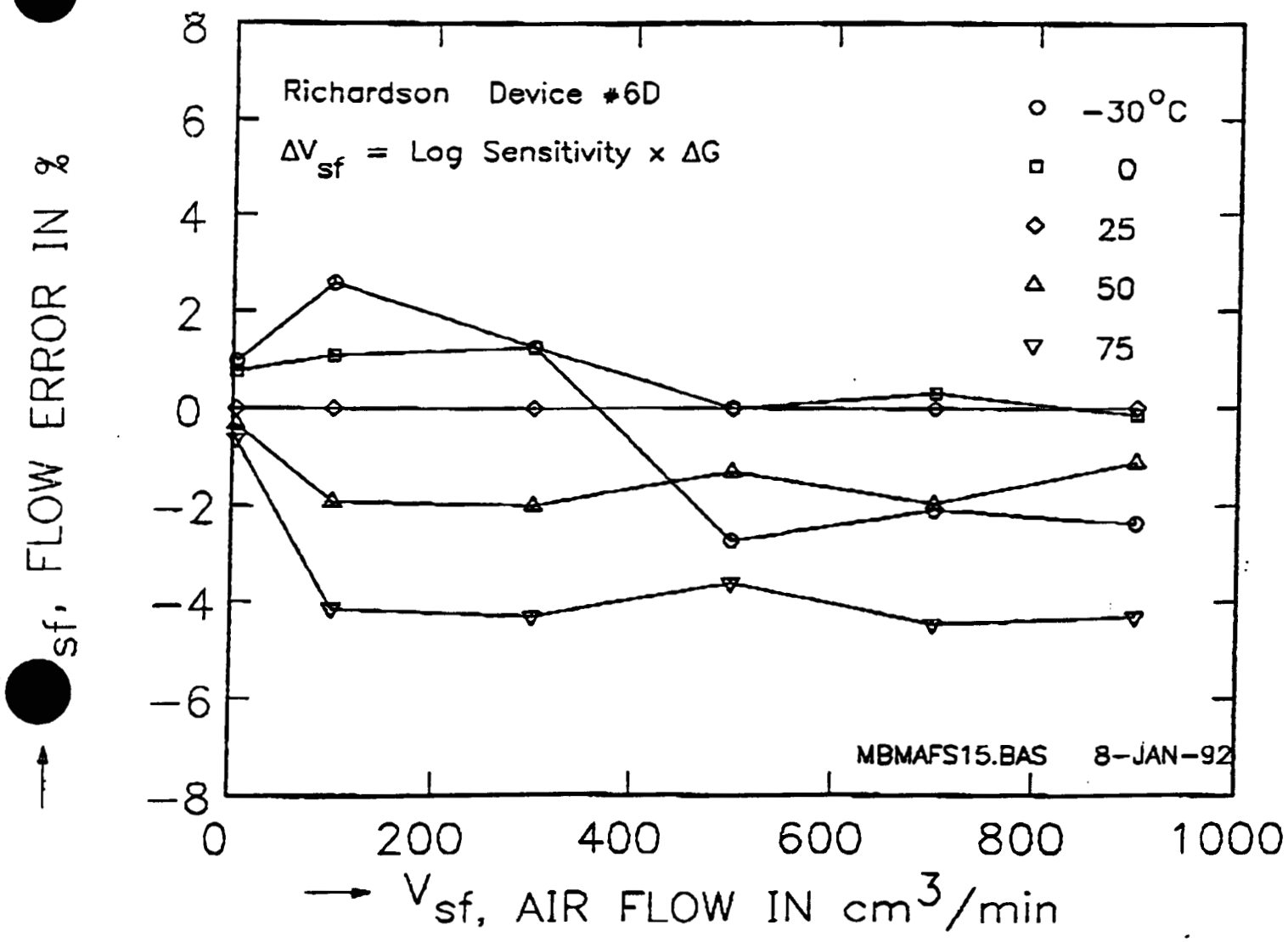

FIG. 3. TEMPERATURE CORRECTION PERFORMANCE OF ANALOG CIRCUIT, REF.TO 25°C DATA. 2.5x0.8mm(0.10x0.03in.) FLOW CHANNEL

Figure 31

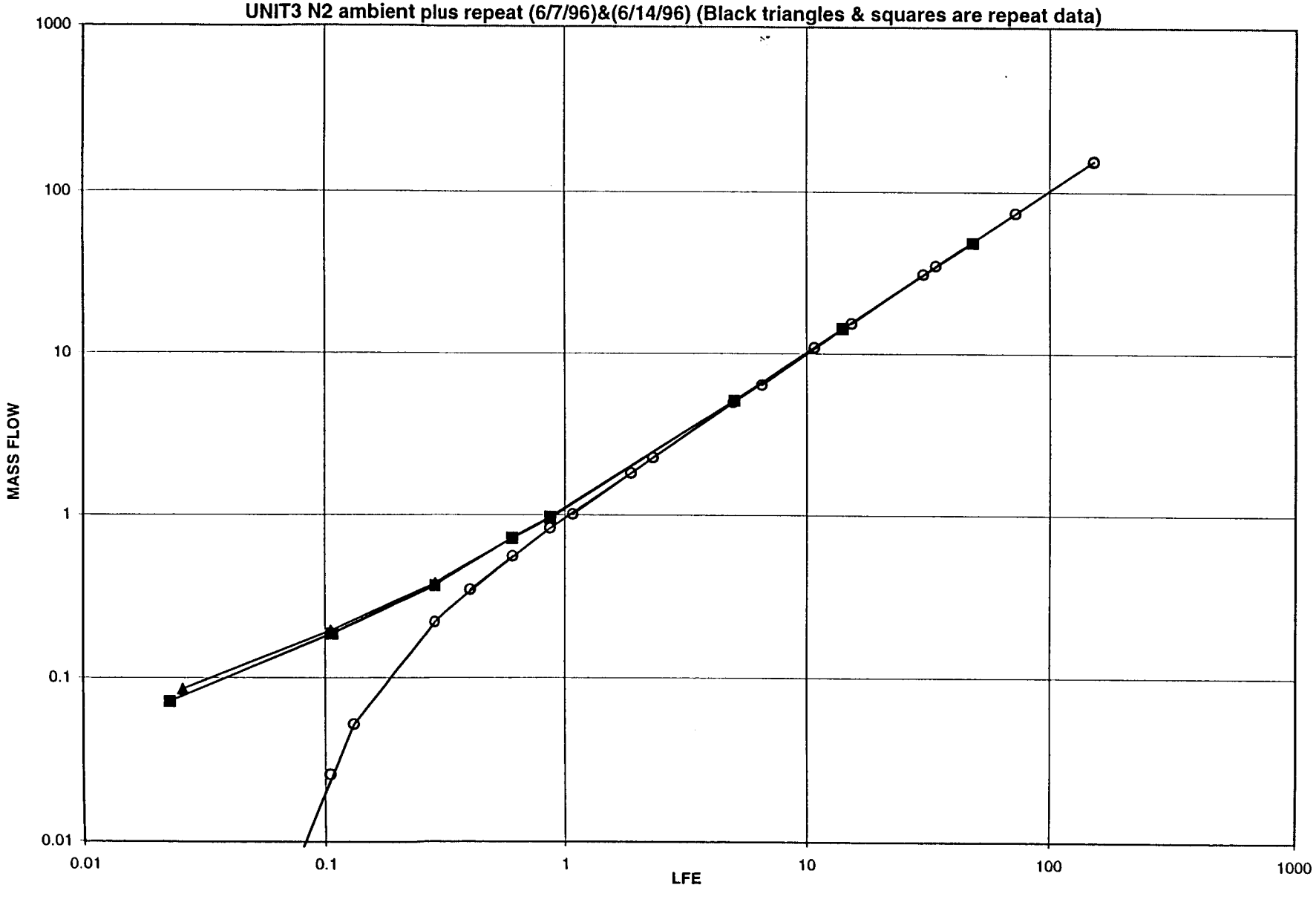
UNIT3 N2 ambient plus repeat (6/7/96)&(6/14/96) (Black triangles & squares are repeat data)
1000
100
10
1
0.1
0.01
MASS FLOW
0.01
0.1
1
10
100
1000
LFE

Figure 32

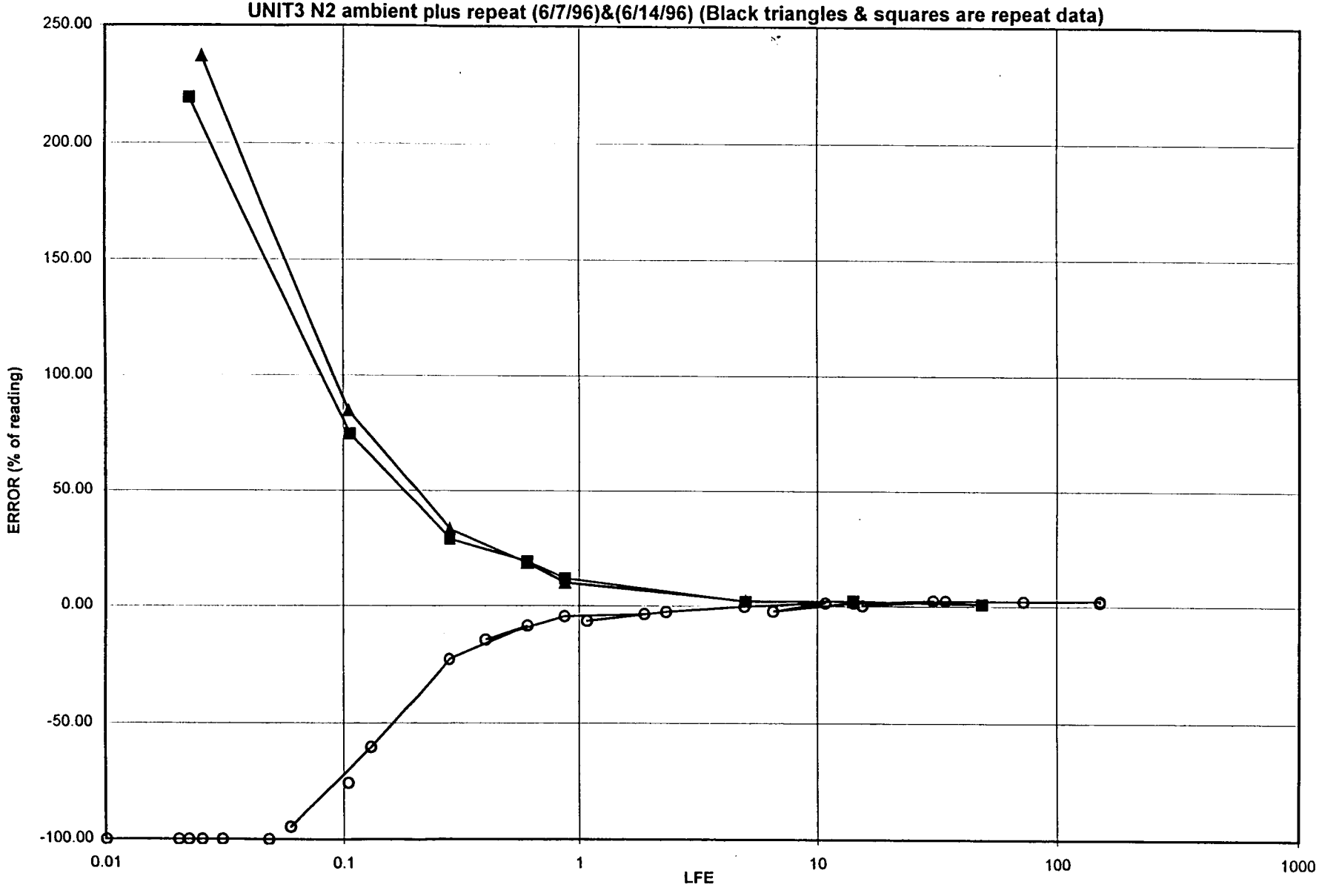
UNIT3 N2 ambient plus repeat (6/7/96)&(6/14/96) (Black triangles & squares are repeat data)
250.00
200.00
150.00
100.00
50.00
0.00
-50.00
-100.00
ERROR (% of reading)
0.01
0.1
1
10
100
1000
LFE

Figure 33

GAS FLOW SENSORS FOR SPACE APPLICATIONS

Phase I. Fabrication of Two Demonstration Units

Final Technical Report

to
Carleton Technologies, Inc.
120 Cobham Drive
Orchard Park, NY 14127-4195

Attn: Jim J. Walleshauser
Phone: 716/662-0006 x 293
Fax: 716/662-0747

by
Honeywell Technology Center
12001 State Highway 55, 4B75
Plymouth, MN 55441-4771

Principal Investigators	Ulrich Bonne	(612) 954-2758
and	David Kubisiak	(612) 954-2795
Section Management	Earl Benser	(612) 954-2789
Business Development	Greg Olson	(612) 954-2731
Contract Administration	Rebecca Kemp	(612) 954-2712

15 March 1996

GAS FLOW SENSORS FOR SPACE APPLICATIONS
Phase I. Fabrication of Two Demonstration Units

1. EXECUTIVE SUMMARY

The purpose of this program was to demonstrate the performance of a thermal flow microsensor. It would be intended for the measurement of flows of helium, nitrogen, oxygen and hydrogen in both the ARPCS (Atmospheric Revitalization Pressure Control Subsystem) and in the FCS (Fuel Cell System), which have been using sensors that experienced high failure rates.

An existing sensor design was adapted for this project. Two sensors were built and tested, and delivered to Carleton for further tests, after improvements were made to overcome interferences by what was recognized as thermal microconvection.

In spite of the improvements, the test results indicate that not all performance attributes materialized, which had been predicted for operation at pressures up to 61 bar (900 psi), based on previous data of flow microsensor performance up to 4 bar (60 psia). The unforeseen factor that increasingly interfered as pressure was increased, was one caused by thermal microconvection currents generated by the sensor's microheaters. These caused both large, signal shifts as well as deterioration of the S/N ratio. Whereas the direct influence of these currents could be reduced significantly via implemented improvements[14], the ability of a single point flow sensor to meet the accuracy specifications over the large 15,000:1 dynamic flow range remained marginal.

Test results of these improved units, while meeting expectations in terms of the response time, power consumption, insensitivity to orientation up to 500 psi, and accuracy at flows below 5 lb/h, were disappointing as far as accuracies achieved with the high flow sensing approach (above 5 lb/h), labour-intensive adjustments of the matching of the high and low flow signals, flow signal errors resulting from the temperature difference between the flowing gas and the sensor block, in which the property and temperature sensors are mounted, the orientation sensitivity at 900 psig and signal noise, and the fact that the remaining orientation sensitivity also prevented us from differentiating between N_2 and O_2.

We therefore recommended that the direct, single-point flow measurement of Units#1 and 2 be replaced by a bypass, multiple-point flow sensing approach. Such recommendation was made on the basis of tests made with two such units, which not only showed predictable gas composition correction behaviour, a possibility to replace the heater power approach used at high flows by the more accurate differential approach over the the full flow range, but also a more linear and predictable output, enhanced S/N and the possibility of further reducing the effect of orientation-dependent, thermal microconvection, due to the beneficial influence of mounting the sensor chip in a well-defined, more constraining microchannel.

TABLE OF CONTENTS

2. INTRODUCTION

The purpose of this program was to adapt an existing design, build, calibrate and test two sensors for the measurement of gas mass flow of helium, nitrogen, oxygen and hydrogen; this single design flow sensor was to serve in multiple applications in both the ARPCS (Atmospheric Revitalization Pressure Control Subsystem) and in the FCS (Fuel Cell System), which have been using sensors that experienced high failure rates. The redesigned sensors were to be able to meet the target specifications listed in Table 1, with the noted exceptions for the demonstration units completed in this phase of the program. Ultimately the redesigned production sensors are to replace those shown in Figs.1a and b.

The main deliverables were to consist of:
- Two testable flow sensors, with all fluid and electrical mating connectors needed to interface with existing NASA equipment, with circuitry to provide a 0-5 V output representing a compensated flow range from 0.1 to 150 lb/h; and
- This final report, documenting all applicable performance and accuracy evaluation test results, in relation to the requirements listed in Table 1.

The Honeywell effort was to include flow testing with He (as a simulant of H_2), O_2 and N_2 at pressures between 200-900 psia, up to mass flows of 15 lb/h, and consulting support on tests at Carleton and at NASA-JSC.

3. TECHNICAL DISCUSSION

3.1. **Original Design and Fabrication Plan:** Honeywell-HTC was to adapt its compensated flow microsensor[1] design, see Fig. 3, to NASA-JSC's application. As agreed with Carleton, both deliverable units were to use the connectors and fittings shown in Figs.1 and 2, to be provided by Carleton. The main features of this plan involved tasks to:
- Use existing gas flow microsensor chips[2];
- Adapt existing analog front-end and digital linearization and compensation circuit designs and printed circuit boards;
- Mate the inlet and outlet fittings to existing flow channel designs, which have been used in developmental, electronic gas meters[1,3] to sense flows ranging from less than 0.01 to over 150 lb/h with one single design;
- Design a sealed housing for the electronics, with provisions to accept the specified connectors and sensor inputs; and
- Use and/or adapt Honeywell's T, p and gas composition correction so that one single gas mass flow sensor design can be used with any of the required gases.
- Calibrate each flow sensor system with N_2, O_2 and He, at atmospheric pressure and covering the specified temperature range, with mass flows from 0.01 to 15 lb/h; and with air up to 150 lb/h.
- Provide consulting help in support of comprehensive tests at Carleton (up to 900 psia) and at NASA with hydrogen.

A typical set of anticipated flow sensor performance data is shown in Fig.4, obtained with a flow channel featuring a Venturi nozzle with a 14 mm ID throat. For optimum performance in terms of mass flow range, low noise and output data accuracy we proposed to use the differential measurement approach at low flows, see e.g. G_{d-u} data in Fig.4, and the heater-power approach for high flows, represented by the Htr.Power data in that same figure. At some intermediate range, e.g. 2-8 lb/h in Fig.2, a weighted average between these two measurement approaches was to be formed for each sensor output. Fig.4 also shows that the flow-induced pressure drop, even at atmospheric pressures (or about 60x below the maximum of 900 psia), is about 3x below the performance goal of 28 psid, see Table 1, or 11x further below that goal if the data had been taken at 200 psig. In view of that, and also to insure having (1) adequate signal level at low flows and (2) enough room to fit this flow channel, we agreed with the sponsors (Carleton and NASA) to reduce its cross section to half of its size, i.e. to reduce the throat diameter of the Venturi from 14 to 10 mm[8]. As shown in Fig.5, this reduction was not going to cause excessive flow velocities even at pressures as low as 40 psia.

At this meeting[8] we also reached tentative agreement about how to format the sensor's output in a way that would be compatible with the existing NASA software but not penalize the achievable accuracy of the new sensor. The agreed solution was to proportion the 0-5 volt output to a logarithmic, 0.001-150 lb/h mass flow range. This provides a graininess of only 1.94%, see Fig.6, which could not be achieved with any of the linear scale options. Fig.6a shows that this graininess is consistent with the available bits (nine) and the desired dynamic range (15,000).

The 14 mm diameter sensor packages had been used before for:
(1) developmental, natural gas metering applications[1] near atmospheric pressure,
(2) up to 60 psia to prove that the mass flow sensor outputs were independent of pressure[2], and
(3) at about 3500 psia in a short field test with compressed natural gas; this verified that the sensor structure was strong enough to operate at such pressures, but also showed that further noise suppression work was needed.

Having built the new, 10 mm ID Venturi, we checked that its performance was comparable to that of the previous 14 mm versions, see Fig.7, by completing and plotting the data obtained at 20 and 50 psig. However, when the pressure was raised above 100 psig, unexpected signal distortions were observed, see Fig.8, which became worse as the pressure was increased towards 900 psi. The output signal would drop in spite of maintaining the mass flow constant. The effects were large enough to dispel any hope of achieving a satisfactory sensor performance without major modifications. We therefore agreed with the sponsors that we needed to get back to fundamentals to fix this problem. Honeywell elected to fund this effort independently, because the solutions are needed also for other, non-space applications.

3.2 Thermal Flow Sensor Fundamentals:

Standard volume or mass flow measurements are realized with two sensors that are positioned as indicated in Fig.3: one measures flow while the

other senses thermal conductivity, specific heat, temperature and pressure. The latter is used to generate the compensation factor, C_V, to obtain a fluid composition- and temperature-compensated standard volume flow, as detailed in refs.(1,11):

$$V = V_u/C_V, \text{ or } m = m_u/C_M, \text{ or } m = m_u\rho/C_V$$

with

$$C_V = (k/k_o)^{n1}(c_p/c_{po})^{n2}(Pr/Pr_o)^{n3}(T/T_o)^{n4} \qquad (1)$$

where $n_1 = -0.8827$ or -0.8904
$n_2 = 1.1110$ or 1.1500
$n_3 = 0$ or 0.3003
$n_4 = 0.7000$ or 0.6495[13].

The temperature exponent would ideally only depend on gas properties; in practice it also is influenced by the temperature dependence of sensor materials and electronics. The use of one or the other set of exponents depends on the desired accuracy, and on whether on-line measurement of only k, c_p and T, or k, c_p, η and T is available. As verified recently[11,13], these expressions for C_V are (1) universal for any type of thermal flow sensor, and (2) independent of pressure, within about ±1%. It follows that for operation with <u>known gases</u> the C_V are known except for their temperature dependence, so that a system optimized for least cost and weight, and for max. reliability (i.e. min. number of parts) would not recompute all properties at every time interval, but rather:

(a) receive an external input code to identify the gas being measured, so that the appropriate value of C_V can be activated from memory. Such a value, $C_V=C_{Vo}$ would be one corresponding to a standard temperature, $T=T_o$, or
(b) reduce the measurements to the minimum number required to identify the gas at hand, which would then be associated with the appropriate C_{Vo} from memory.

The sensor output signal for the low-flow region, ΔG_1, can typically be represented by an equation close to $V_{u1} \cong a_o+a_1\Delta G_1^{0.85}$, with $a_o \cong 0$, see Fig.9a, as long as the sensor signal, $\Delta G_1 \equiv \Delta G_{d-u}$, represents a flow that corresponds to a temperature difference, ΔT_{d-u}, that is smaller than the heater temperature rise above the environmental temperature. At larger flows, the signal eventually saturates since $\Delta T_{d-u} < \Delta T_{htr}$. However, at such high flows, the heater power, G_2, required to maintain the set ΔT_{htr} continues to rise, so that flows may be represented and determined by an expression, see also Figs.4 and 7, of $V_{u2} \cong b_o+b_1G_2^{m1}+b_3G_2^{m2}$, which is equivalent to the classical hot-wire anemometer equation, $G_2 \sim H_{p,u2}-H_{p,u2o}$. The above gas composition correction equations apply to it as well[11].

The performance obtained with a flow channel of less than 70 mm (≤3 in.) in length, simply consisting of two screens and one honeycomb flow straightener upstream of a 14 mm ID Venturi nozzle, is illustrated in Fig.9, where Fig.9a shows the overall output signal shape of the

uncompensated signal, for three gases, including N_2, at flows below 15 lb/h, down to ≤5 g/h, i.e. ≤0.01 lb/h, and up to about 10 lb/h, before this differential measurement method saturates. Fig.9b shows that the flow error after compensation for gas type and temperature is less than ±3% of reading.
In Fig.4 the signal V_{d-u} saturates at about 25 lb/h; however, flows greater than 15 lb/h and even beyond 150 lb/h can be measured with the same flow channel, without undue flow noise, by sensing the power required by the sensor heating element to maintain its temperature at a constant temperature rise above ambient (~100°C); while these measurements were taken at atmospheric pressure, no increase in flow noise is expected with flows at 1000 psia since the Reynolds number is pressure independent at constant mass flow. Fig.4 also shows that the pressure drop at 150 lb/h air flow, (circle points), was less than 3 psid.
Fig.10 shows that gas composition or "type of gas" compensation can well be provided within the ±3% error margin for gases differing in properties as much as H_2, He, N_2, air and Ar-CH_4 mixtures; this set of measurements was obtained with a commercial AWM2100V type of Honeywell sensor, but could have been obtained with the above flow channel as well.

The composition and temperature correction is performed by processing the outputs of the flow sensor and those of the property sensor, as described in ref.(1), with an Intel 87C51 microcontroller; Fig.2e graphically illustrates how thermal conductivity and specific heat are measured. Flow measurements of up to 4 bar (60 psia) had indicated that pressure changes do not influence the flow sensor output, as would be the case for a true mass flow sensor. However, at pressures of up to 1000 psia, real gas changes in compressibility factor, thermal conductivity and specific heat (which for ideal gases are pressure-independent) may require that pressure be measured and entered in a compensation scheme. Should that be necessary, the property sensor's built-in Pirany-type pressure sensor will be called into service, as described before[1,7]; its location on the chip is pointed out in the microphotographs of Fig.11[7]. We have used this inherently burst-proof pressure sensor for pressure measurements of up to 2000 psia[7]. Thermal conductivity and specific heat measurements have been routinely carried out to 60 psig, and more recently to 600 psia in our automated calibration system.

The weights and volumes of the demonstration units were estimated by adding the contributions of the housing, which is assumed to be made of aluminum (density of 2.702 g/cm^3) for two single-sided circuit boards of 75 x 150 mm and those of the flow channel of 3.6 mm OD. By subtracting the inner volumes, the weight of the demonstration unit is 0.75 lb, thus leaving 0.6 lb for electronics, fittings, connectors, sensors and flow streighteners; the outer volume computed to 29.95 in.^{3}.
The weight and volume of the mass flow sensor units for the effort in subsequent Phases was estimated as follows: Assuming the worst case that none of the sensors used in this demonstration phase can be eliminated (realistically, the sensing of pressure and specific heat may no longer be needed), the printed circuit boards may be reduced to about 75 x 75 mm in size by a more efficient layout and by using two-sided circuit boards. With dimensions in mm, the estimated contributions of the

housing and flow channel to volume and weight then are: 83 x 83 x 40 - 75 x 75 x 30 + $(38^2 - 22^2)\pi/4$ x 80, which is equivalent to 22.35 $in.^3$ outer volume and 0.995 lb, respectively. The presently used circuits weigh less than 0.25 lb.

The measured power consumption of compensated flow sensors built by Honeywell previously was 1.3 watts, when both flow and property sensors are operated continuously. The measured response time of the flow sensor is about 3 ms, corresponding to a T90 value of 10 ms. A 10-fold flow noise reduction benefit may be taken advantage of by letting the T90 value increase to 1 s. That would leave up to two seconds to perform any linearization, temperature and/or pressure corrections; the composition correction may not need to be used but once after start-up, or very infrequently, depending on the amount of the required correction.

With over 10 years' experience in the use of such temperature-compensated flow microsensors and with over one million of these sensors installed, we can look back on a remarkably successful record of reliability. In addition,

1) accelerated life tests indicated that drift rates extrapolated to normal operating temperatures and to 10 years of service life would amount to less than 0.1%[1],
2) direct exposure of the sensor in the proposed flow channel to particulate mass loadings of 30 g up to sizes of 300 µm in diameter and at mass flows of up to 15 lb/h did not damage the sensor nor change its calibration significantly; and
3) operation and testing of one fully compensated gas meter for 10 months only altered its flow signal by less than ±1% of reading[1].

The above assumes that thermal microconvection effects between the sensor elements are negligible, as determined earlier under near-atmospheric pressure conditions[12]. However, as the pressure increases, the ratio of buoyant/inertial forces, R_{BI}, increase as well and may become large enough to have the associated, thermally-driven flows interfere with flow measurement, especially at low flows. The ratio $R_{BI} = (\Delta T/T)gL/v^2 = (\Delta T/T)gL(p/p_o)^2/v_o^2$,* shows that this interference is proportional to ΔT, p^2 and L, and inversely proportional to v_o^2.

---

* It may be useful to recap some relevant force groups and their dimensionless ratios, to envision the origins of R_{bi}; see Nomenclature for symbols, except as noted:

- Gravity force, GF = mg, with m = mass
- Buoyancy force, BF = $mg\Delta T/T$
- Inertial force, IF = mv^2/L,
- Surface tension f., SF = $m\sigma/(L^2\rho)$ and
- Viscous force, VF = $mvv/L^2 = m(\eta/\rho)v/L^2$.

From these follow, for example:

- The Reynolds No., Re = $L\rho v/\eta$, (=IF/VF),
- The Froude No., Fr = $v^2/(gL)$, (=IF/GF) or
- The Weber No., We = $v^2\rho L/\sigma$, (=IF/SF).
- The Grashof No., Gr = $L^3\rho^2 g\eta^{-2}T^{-3}\Delta T$, (=Re BF/VF) is a hybrid.

3.3 **Actual Design and Fabrication:** At the kick-off meeting[8] or shortly thereafter it was agreed that:

- We would use the existing 3x4" PCBs for the demo units, in spite of exceeding the dimensional limitations of the hardware we plan to replace. This concession may not apply for future production units.
- The output for all gases would be one and the same $\log_{10}$(lb/h), whereby the specified 0-5 V output will correspond to the mass flow range from 0.01 to 150 lb/h, for a 15,000:1 dynamic range.
- The sensor output would provide a digital resolution for NASA's 9-bit (2^9=512) A/D converter of $15{,}000^{1/500}$ = 1.0194, which is equivalent to a resolution of 1.94%, which is still lower than the sensor p-p error spec of 6 %, listed as ±3 % in the performance goals of Table 1.
- We would reduce our Venturi throat area by a factor of 2, so that we can meet the external size of the presently used flow channel. This will shift the data of Fig.4[10] by a factor of 2x to the left.
- We would achieve this by combining the flow microsensor's <u>differential</u> output from 0.01 to 8 lb/h, and its <u>heater-only</u> power output from 4 to 150 lb/h, see Fig.4 or 7, which show data obtained with a flow channel with Venturi throats of 14 and 10 mm ID, respectively.

To meet the performance goals with the 10 mm ID flow channel, we reduced the size of the flow sensor header from a TO5 to a TO18, or from a mesa diameter of 0.300" to 0.168", to make it compatible with the reduced nozzle diameter, see Figs.12-14. Under an independently funded effort[14], the parasitic thermal microflows were reduced by a factor of ≥870 by a combination of sensor chip design and operation[14], and improvements in the flow channel, which consisted of addition of a flow straightener and reduction in the chip head space. Table 2 lists the used construction materials.

The electronics, see Figs.15 and 15a consisted of an analog front end, which controlled the sensor heaters to a temperature rise of about 30°C, and amplified the sensor element outputs of the flow, temperature and thermal conductivity sensor (heater voltage and current). These were then digitized. The thermal conductivity sensor identified the gas being used, so that the stored composition correction could be made without requiring any of the usual pressure or specific heat measurements[1]. The communication protocol set up to interface with Carleton is shown in Fig.15b and is self explanatory.

A photograph of one of the two sensors shipped to Carleton in August of 1995 is shown in Fig.16.

Test results of these units, while meeting expectations in terms of the response time, power consumption, insensitivity to orientation up to 200 psi, and accuracy at flows below 5 lb/h, were disappointing as far as accuracies achieved with the high flow sensing approach (above 5 lb/h), labour-intensive adjustments of the matching of the high and low flow signals, flow signal errors resulting from the temperature difference between the flowing gas and the sensor block, in which the property and temperature sensors are mounted, the orientation sensitivity at 900 psig and signal noise, and the fact that the remaining orientation sensitivity also prevented us from differentiating between N_2 and O_2.

These problems were resolved, or recommended that they be resolved as follows:

(1) O_2 and N_2 Differentiation: Output a logarithmic value of volumetric flow, so that the differentiation between O_2 and N_2 mass flows (which

carries a potential error penalty of 14.2%) is eliminated, except for a residual error of less than 0.4%, resulting from the use of identical values of C_V in eq.(1) for both O_2 and N_2.

(2) S/N Ratio and Output Stability: Upgrade the electronics by taking advantage of as many measurements and as much signal averaging as possible, which still meets the 3 sec response time; and by introducing chopper stabilized amplifiers at the front end, to minimize electronic offset drift as possible,

(3) S/N Ratio, Signal Predictability and Orientation Sensitivity: Provide additional averaging by switching to a bypass flow sensing approach, see Fig.17, to enable multiple flow stream pressure taps; the implemented design shown in Fig.17 uses 8 sampling holes for each of the two Δp taps and the one property sensor tap. Having the flow sensor chip mounted in a well defined microchannel allowed further reductions in the orientation sensitivity. In addition, there was strong evidence that the heater power sensing mode used at high flows could be eliminated, because of the greater range of the more accurate, differential mode in the bypass design.

(4) Reduce the thermal mass to the point where the sensor block follows changes in gas stream temperature with a shorter time constant; thermally isolate both sensors from the sensor housing block; and/or incorporate an additional sensor into the flow sensor to enable implementation of a more effective temperature compensation.

Under the same independently funded effort mentioned above[14], such a flow sensor was built and made available to this project for test purposes. It featured all the improvements listed above except for item (4).

4. SAFETY AND QUALITY ASSURANCE

By way of documenting this sensor's fire safety aspects, derived in-house before the recent approval for use of this sensor in combustible gas environments[5], we attach ref.(4) in the Appendix.

The accuracy of our flow calibrator pistons was determined to be within a 0.46% standard error margin. This determination included uncertainties introduced by dimensions of the glass cylinders, distance between optical switches, absolute pressure and temperature measurements, and uncertainty in the molar volumes.

5. LAB TEST RESULTS

After fabrication and before testing, the sensors were calibrated in a process that consisted of a three-step process:
Determined first were the thermal coefficients of resistance of the sensor elements to be used, and the coefficients of the thermal conductivity sensor, by operating it over a three-dimensional matrix of gases (N_2, He (or H_2) and Ar), pressures (1-30 bar, limited by our pressure sensor) and temperatures (-4 to 60°C); then the coefficients for the flow sensor were determined in a preliminary fashion at HTC by measuring volumetric flows with piston calibrators up to about 15 lb/h, at temperatures from about 0 to 50°C, and at pressures up to 900 psi, before conditioning the gas down to the ambient levels required by the calibrators; these were loaded into the corresponding microcomputer and verified. Finally, the units were calibrated throughout the whole range,

up to 150 lb/h at Carleton, and an updated set of coefficients was determined, reloaded into the microcomputer and verified.

Fig.18a illustrates such a verification of Unit#2 calibration for thermal conductivity, k. The standard and maximum errors were ±0.28 and ±0.97%, respectively, with a relative sensitivity of k to errors in temperature and heater power of only 1.62, i.e. a worst combination of ±1% errors would only lead to a ±1.62% error in k. A verification with H_2, He and N_2 is shown in Fig.18. In both figures, the curves represent the true values of k for 3 and 35 bar (45 and 500 psia). As shown, curves for O_2 and N_2 overlap, as shown more clearly in Fig.19. The consequences of this and suggested solutions were already discussed in the previous Section. As part of additional sensor checkout, we quantified the change in sensor output after a cold start, see Figs.20 and 20a, for Units#1 and #2, respectively. As shown, the electronics takes about 20 min to stabilize; after that time, the readout values of temperature-corrected k values has stabilized, as shown, in spite of continued increases in temperature. The k values outputs increased by 2 and 1%, respectively, during warm-up.

Figs.7 and 8 presented plots of data to verify the preliminary flow calibrations performed before the efforts to eliminate the orientation effect was undertaken[14]. Fig.21 shows the degree of success of those efforts, indicating that the orientation effect has been eliminated to within pressures of 500 psig, but is still noticeable at 900 psig.

The data in the error-plot of Fig.22 correspond to Unit#1, after final coefficients were derived and implemented, for the indicated gases, pressures and temperatures. As shown, the data fall within the dotted, maximum allowed error lines at low flows, but not all do at higher flows. Large size points were obtained by the heater-power method, while the small-sized points represent those obtained by the differential method. The data shown in the lower part of Fig.22 represent error values (right-hand y-axis) of thermal conductivity, Δk in %.

Flows of He measured with Unit#2 exhibited some unexpectedly high output readings, by about a factor of two, even after replacing the flow straightener in the flow channel, see Figs.23 and 24. This cast some doubt on our ability to predict its performance with H_2. Such errant behaviour had not been observed with the same sensors when operated with microsensors, factory assembled into microchannels, see Fig.10, or with the bypass-based units, see Figs.25 and 26[14].

6. CONCLUSIONS AND RECOMMENDATIONS

The above results indicate that not all performance attributes materialized, which had been predicted for operation at pressures up to 61 bar (900 psi), based on previous data of flow microsensor performance up to 4 bar (60 psia). The unforeseen factor that increasingly interfered as pressure was increased, was one caused by thermal microconvection currents generated by the sensor's microheaters. These caused both large, signal shifts as well as deterioration of the S/N ratio. Whereas the direct influence of these currents could be reduced significantly via implemented improvements[14], the ability of a single point flow sensor to meet the accuracy specifications over the large 15,000:1 dynamic flow range remained marginal.

Test results of these improved units, while meeting expectations in terms of the response time, power consumption, insensitivity to orientation up to 500 psi, and accuracy at flows below 5 lb/h, were disappointing as far as accuracies achieved with the high flow sensing approach (above 5 lb/h), labour-intensive adjustments of the matching of the high and low flow signals, flow signal errors resulting from the temperature difference between the flowing gas and the sensor block, in which the property and temperature sensors are mounted, the orientation sensitivity at 900 psig and signal noise, and the fact that the remaining orientation sensitivity also prevented us from differentiating between N_2 and O_2.

We therefore recommended that the direct, single-point flow measurement of Units#1 and 2 be replaced by a bypass, multiple-point flow sensing approach. Such recommendation was made on the basis of tests made with two such units, which not only showed predictable gas composition correction behaviour, a possibility to replace the heater power approach used at high flows by the more accurate differential approach over the the full flow range, but also a more linear and predictable output, enhanced S/N and the possibility of further reducing the effect of orientation-dependent, thermal microconvection, due to the beneficial influence of mounting the sensor chip in a well-defined, more constraining microchannel.

7. REFERENCES:

1. U.Bonne, "Fully Compensated Flow Microsensor for Electronic Gas Metering," Intl. Gas Research Conference, Orlando, FL, November 16-19, 1992, Proceedings, Vol.III, p.859

2. These chips are a "low particle impact" version of a chip that has been in production since 1987 at Honeywell for mass air flow sensing in space conditioning applications

3. U.Bonne, "Compact Gas Flow Meter Using Electronic Microsensors," U.S.Pat. 5,220,830, assigned to Honeywell, 22 Jun.'93

4. U.Bonne, T.Stratton and R.Horning, "Fire Safety Aspects of Si3N4-Pt-Based Microbridge Flow Sensors," Honeywell Technology Center, Bloomington, MN, 29 May 1994

5. DMT-Gesellschaft für Forschung und Prüfung mbH, Berbau-Versuchsstrecke, Dortmund, Germany, Approval #BVS 94.C.7001 U, for Honeywell Flow Sensor AWM2*** Series, issued 15 July 1994

6. Micro Switch, Div. of Honeywell, Product Sheet for "Microbridge Mass Air Flow Sensor, AWM3000 Series, Signal Conditioned, 1-5 VDC Output", Freeport, IL, (1984)

7. U.Bonne and D.Kubisiak, "Overpressure-Proof, Thermal Pressure Sensor for Gases," Solid-State Sensor and Actuator Workshop, Hilton Head Is., SC, 13-16 June 1994, Tech.Digest, p.76

8. "Redesigned Gas Mass Flow Sensor" Project Kick-Off Meeting at Carleton Tech.Inc., Buffalo, NY, 19-20 Jan.1995

9. D.Kubisiak et al, "Microanemometer-Based Flow Sensing," IGT Symposium on "Nat.Gas Quality Measurement," Chicago, IL, 16-18 July 1990, Proceedings

10. U.Bonne and D.Kubisiak et al, "Redesigned Gas Mass Flow Sensors for Space Applications," Proposal to Carleton Technologies Inc., HTC-Plymouth, MN, 8 Sep.'94

11. U.Bonne, "Gas Composition Correction for Hot Element Flow Microsensors," 6th IGT Symposium on "Natural Gas Quality Measurement", Chicago, IL, 10-12 June 1991

12. U.Bonne and G.Havey, "Versatile Microbridge Flow control Sensor Structure and Applications," 22nd Int'l.Conf.Env.Syst., Seattle, WA, 13-16 Ju.'92, SAE Paper# 921175, Fig.9

13. U.Bonne, V.Vesovic and W.A.Wakeham, "Sensing Thermophysical and Transport Properties of Natural Gas with Thermal Microsensors," Int'l.Gas Research Conference, Cannes, France, 6-9 Nov.1995, Proceedings, Paper#070, Proceedings Vol.III p.152

14. U.Bonne, D.Kubisiak, E.Satren and L.Hilton, "Design, Fabrication abd Testing of a Flow Sensor with Bypass," HTC-Plymouth, 15 Mar.'96

8. NOMENCLATURE

c_p	Specific heat in cal/mol
C_M	Composition correction factor for mass flow, dimensionless
C_V	Composition correction factor for vol.flow, dimensionless
d	Flow channel Venturi throat diameter in mm
D_t	Thermal diffusivity in cm^2/s
g	Acceleration of gravity, in cm/s^2
G	Gauge/sensor output signal, typically in V or mV
k	Thermal conductivity in µcal/(cmKs)
H	Nulled heater power of flow sensor in W
He	Helium gas, gas #2
H_P	Heater power of flow sensor in mW
H_2	Hydrogen gas, gas #3
J	Nulled flow sensor signal in V
L	Characteristic dimension, in cm or in.
m	Mass flow rate in g/s or lb/h
M	Molecular weight in g/mol
N_2	Nitrogen gas, gas #1
O_2	Oxygen gas, gas #4
p	Pressure in bar (=10^5 Pa) or psia
Pr	Prandtl number, $Pr = \nu/D_t = \eta c_p/(kM)$, dimensionless
Re	Reynolds No., $Re = Lv\rho/\eta$, dimensionless
T	Temperature in °C
ΔT	Temperature difference or rise, in °C
T_R	Resistance of temperature sensor
U_1	Heater potential of property sensor in V
U_2	Bridge potential of property sensor in volts
v	Velocity in cm/s
V	Volumetric flow rate in L/h or ft^3/h
η	Dynamic viscosity in microPoises, i.e. µg/(s cm)
ν	Kinematic viscosity in cm^2/s
ρ	Density in Stokes, i.e. g/cm3
σ	Surface tension

Subscripts

c	corrected
d	downstream
H	related to heater power
R	related to up- downstream resistance difference
u	uncorrected or upstream

PBCarl95.W04'14Aug/NASA

TABLE 1. Flow Sensor Requirement Goals*. Rev.: 3 Aug. 1995

Parameter	Requirement
Operating Fluids	Nitrogen/Oxygen/Hydrogen/(He)
Flow Range, All Gases (lb/h)	0.01 to 150
Pressure (psia)	100 to 1000
Max Pressure Drop (psid)	O_2 - 0.5 @ 900 psig & 15 lb/h 2.0 @ 900 psig & 75 lb/h N_2 - 0.5 @ 200 psig & 15 lb/h 2.0 @ 200 psig & 75 lb/h 28.0 @ 200 psig & 150 lb/h He or H_2 - 0.5 @ 200 psig & 15 lb/h
Gas Temperature (°F)	35 to 175 (1.7 to 80°C) **N**
Ambient Temperature (°F)	40 to 90 (4.4 to 31°C)
Ambient Pressure (psia)	0 to 15
Acceleration, vertical/down (g)	≤4.4**
lateral (g)	≤3.3±1.5 or ≤4.8**
EMI	**
Accuracy, including linearity, thermal, pressure and composition compensation, and long term stability, (%)	±3 of actual flow @ ≥0.33 lb/h
Zero Flow Offset or Error (lb/h)	≤±0.01 @ ≤0.33 lb/h
Volume ($in.^3$)	30**
Weight (lb)	1.35**
Power (W @ 28 VDC)	1.5 max **N**
Output (VDC ~~Linear~~ Logarithmic)	0 to 5
Response Time, T90 (s)	<3
Particle Impact Sensitivity	Minimal
Self-Check Feature	Very desirable
Service Life (years)	10, w/o maintenance or recal.

* Reflecting NASA-JSC's RFO# 9-BE2-11-4-45 req'ts.of 29 Jul.'94 and those of its Amendment dated 1 Sep.'94

** Demo Unit not to be tested on this item;

N Power will be provided via a 110VAC transformer; the sensor electronic components will be rated to 70°C (good commercial grade); it will implement flow corrections based either on sense gas type on-line or receive gas type input via the RS232.

TABLE 2. FLOW SENSOR CONSTRUCTION MATERIALS EXPOSED TO FLUID MEDIA. Rev. 14 Aug.1995

MATERIALS*	FUNCTION
Aluminum 6061, anodized	Housing
Aluminum honeycomb, .001" Stainless steel mesh, 30-50/in.	Flow streighteners
Glass	Insulation of header posts
Gold plated on Ni, on Kovar	TO-5 and TO-18 headers
Gold wires, 0.001" diameter	Connection to sensor chip
Rubber (Viton), 0.01-0.03" diameter	O-ring seals for the TO headers
Silicon	Sensor chip
Silicon nitride	0.5 to 1 μm thick passivation layer over Pt films
Silicon nitride	Sensor heater support membrane, 1 μm thick
Superglue (Loctitte Superbonder 495)	Attachment of Si die to header

* All at gas temperature, except the ≤20 mW sensor heater elements of passivated Pt, heated to ≤30°C above gas temperature, which was specified to be ≤80°C. Max. power only during max. flow of ≤150 lb/h of N_2.

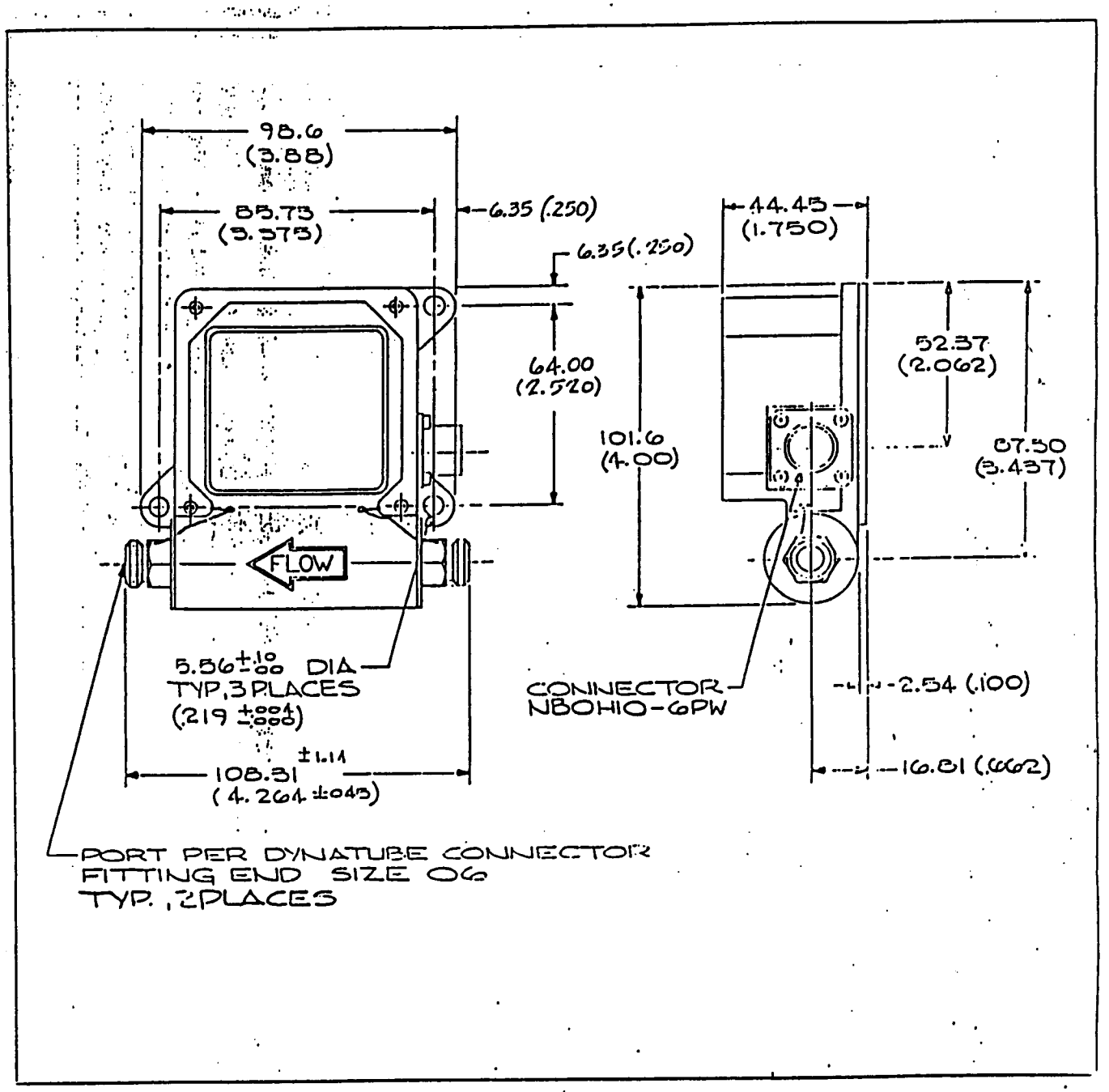

FIG. 1. PRESENTLY USED ATMOSPHERIC REVITALIZATION PRESSURE CONTROL SYSTEM (ARPCS) GAS MASS FLOW SENSOR
Reproduced from Attm't in NASA-JSC RFO# 9-BE2-11-4-45, 29 Jul.'94

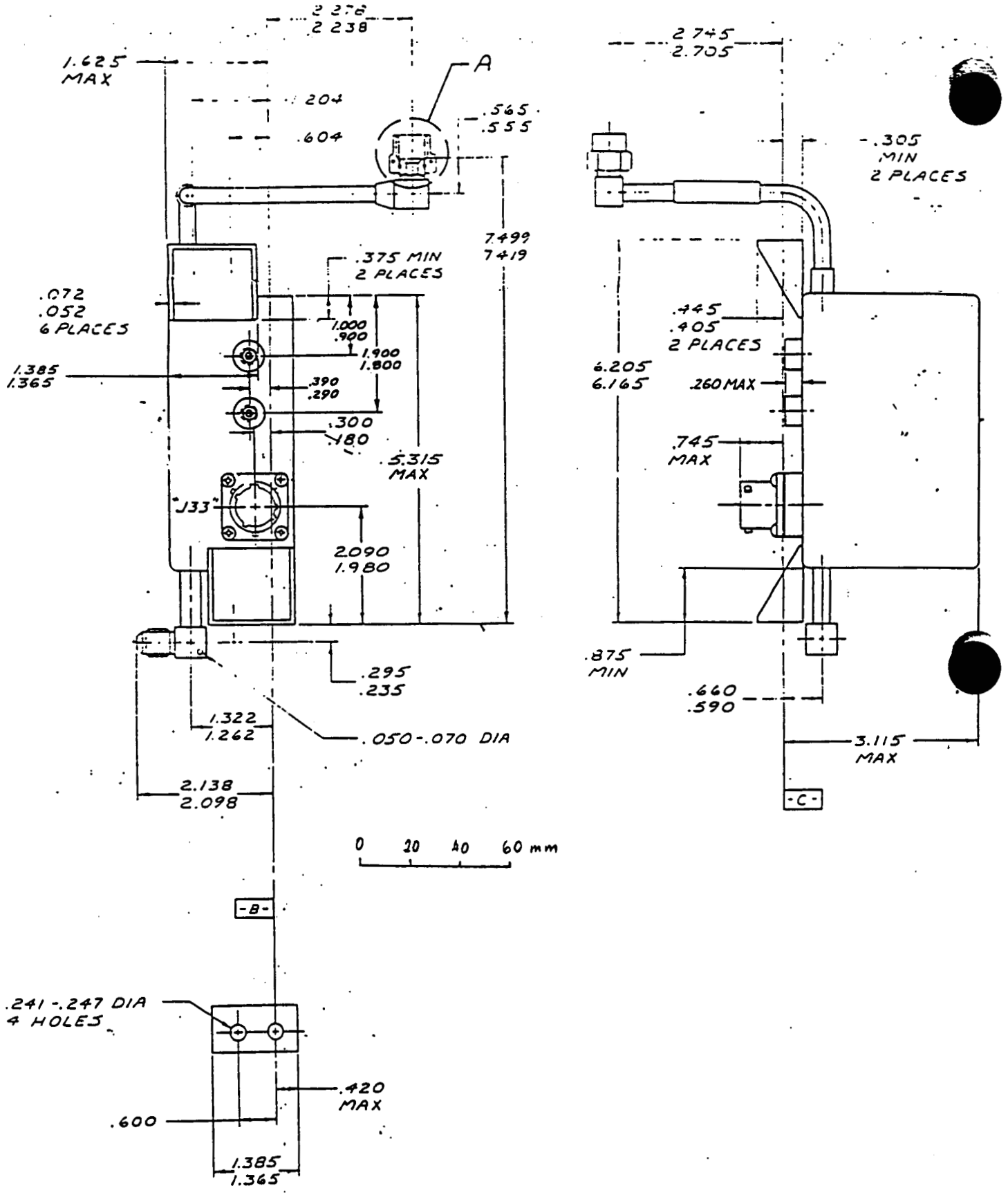

FIG. 2. PRESENTLY USED FUEL CELL SYSTEM GAS MASS FLOW SENSOR
Reproduced from Attm't in NASA-JSC RFO# 9-BE2-11-4-45, 29 Jul.'94

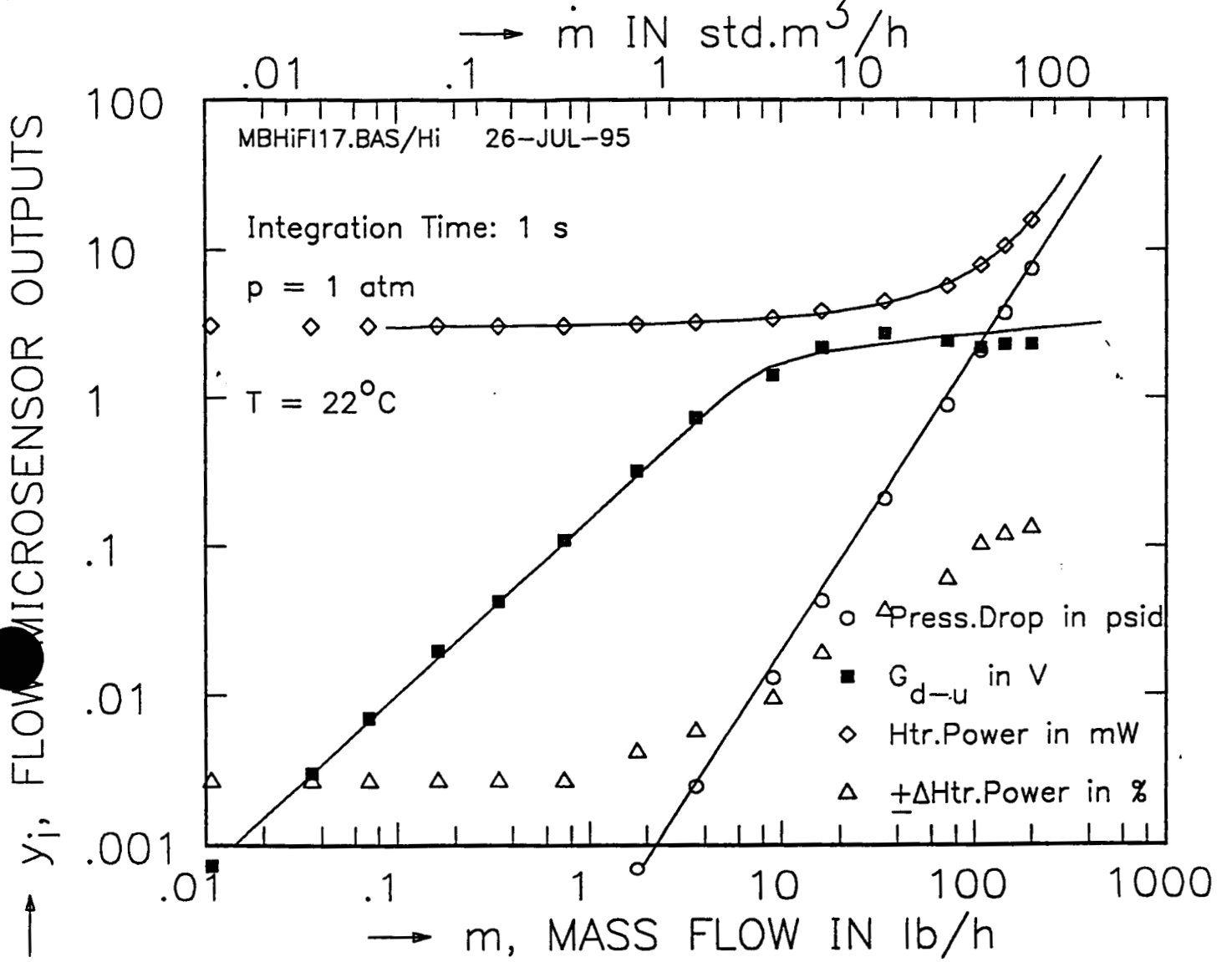

4

FIG. 2. MICROSENSOR OUTPUTS AND FLOW CHANNEL PRESSURE DROP VS. AIR MASS FLOW. NOZZLE THROAT, d=1.4 mm ID. WINDTUNNEL AIR AT AMBIENT CONDITIONS.

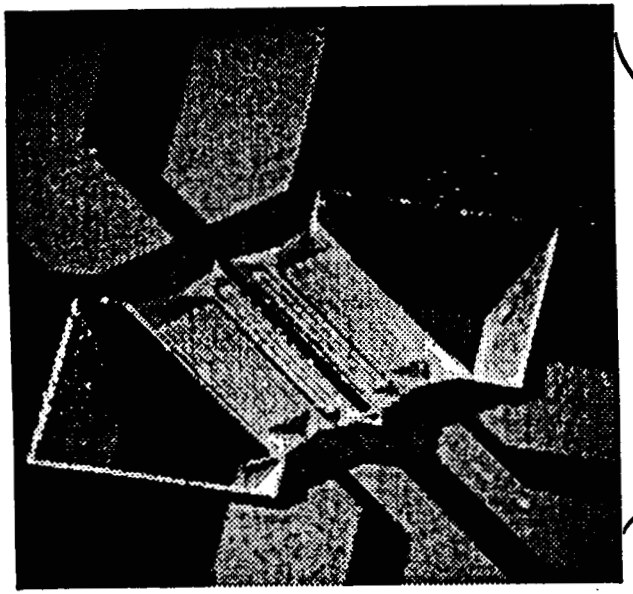

SEM Micrograph

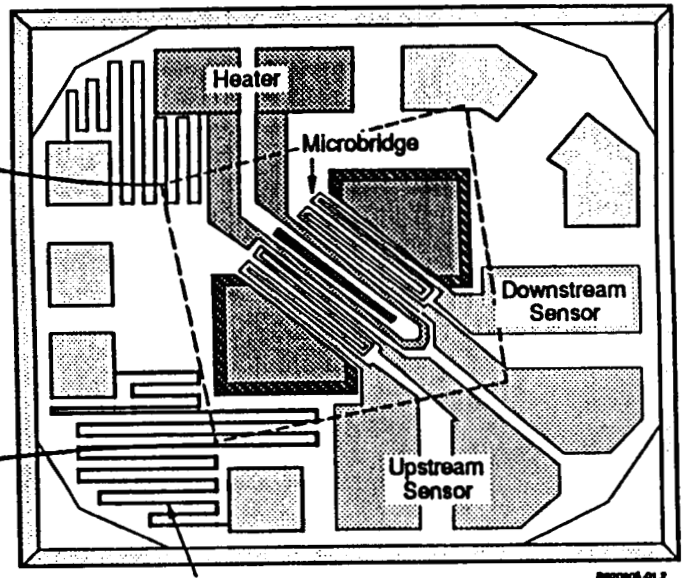

Chip Layout

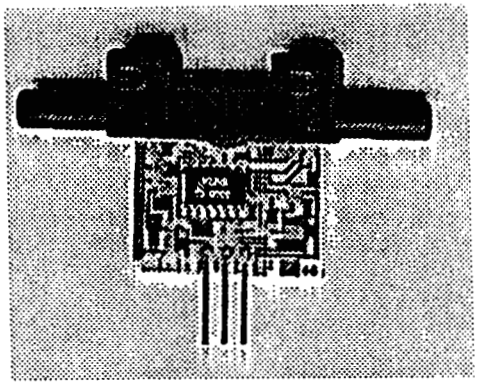

AWM 3100 Sensor Package

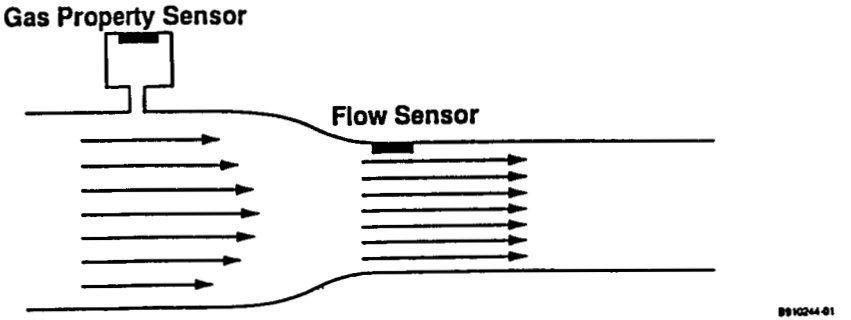

Microbridge Flow Sensor Placement in Metering Flow Channels (not to scale)

Honeywell

FIG. 3. HONEYWELL'S STANDARD COMMERCIAL GAS MASS FLOW MICROSENSOR CHIP

B940087-04

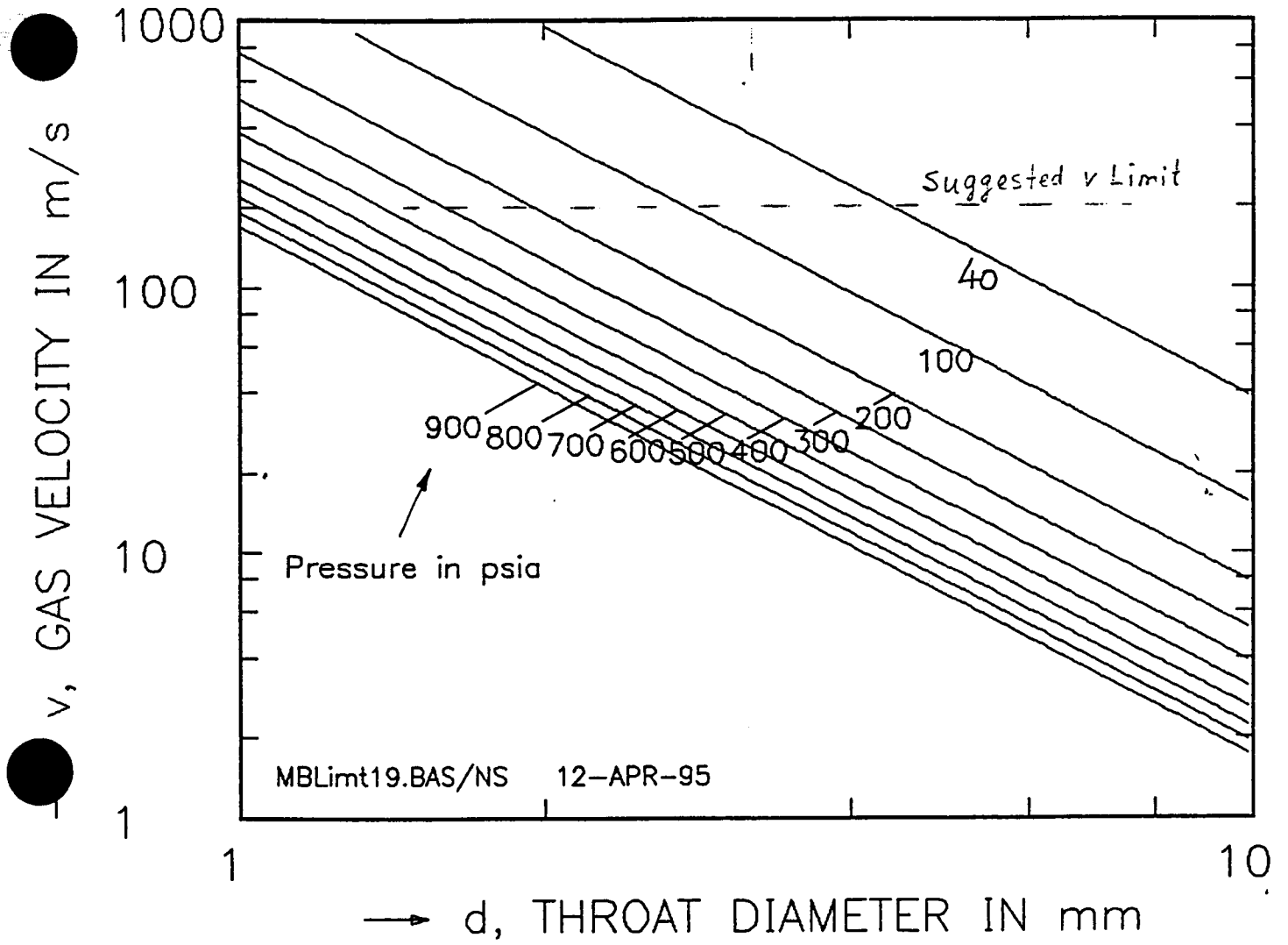

FIG. 1. FLOW VELOCITIES IN THE VENTURI THROAT AT 75 lb/h OF N_2, VS. THROAT DIAM.

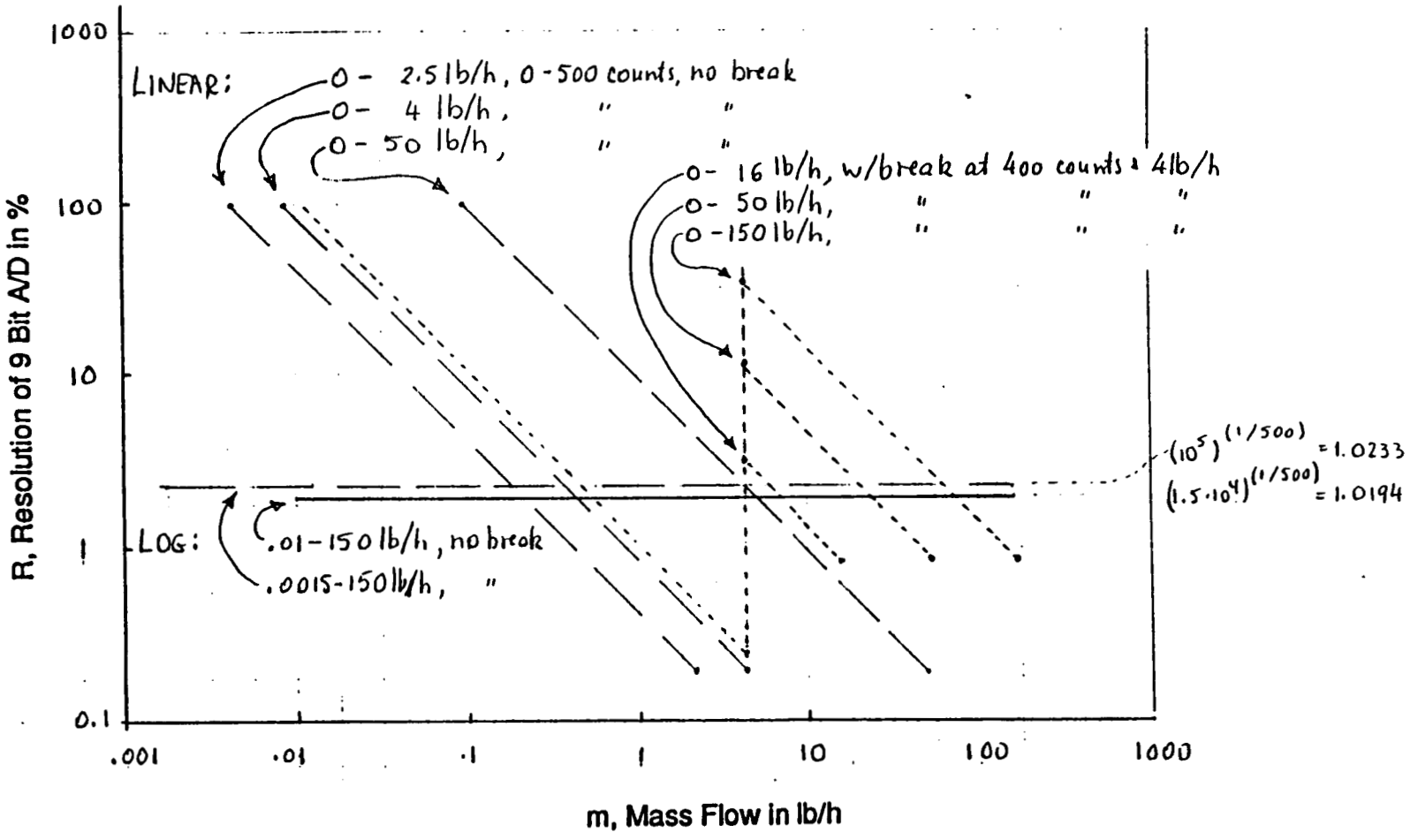

6

FIG. 2a. RESOLUTION OR GRAININESS OF A 9-BIT A/D PROCESSOR VS. MASS FLOW, DEPENDING ON LINEAR OR LOG SENSOR SIGNAL OUTPUT. THE CHOSEN LOG OUTPUT FOR THE RANGE FROM 0.01 TO 150 lb/h PROVIDES A FLOW-INDEPENDENT RESOLUTION OF ±1.94%.

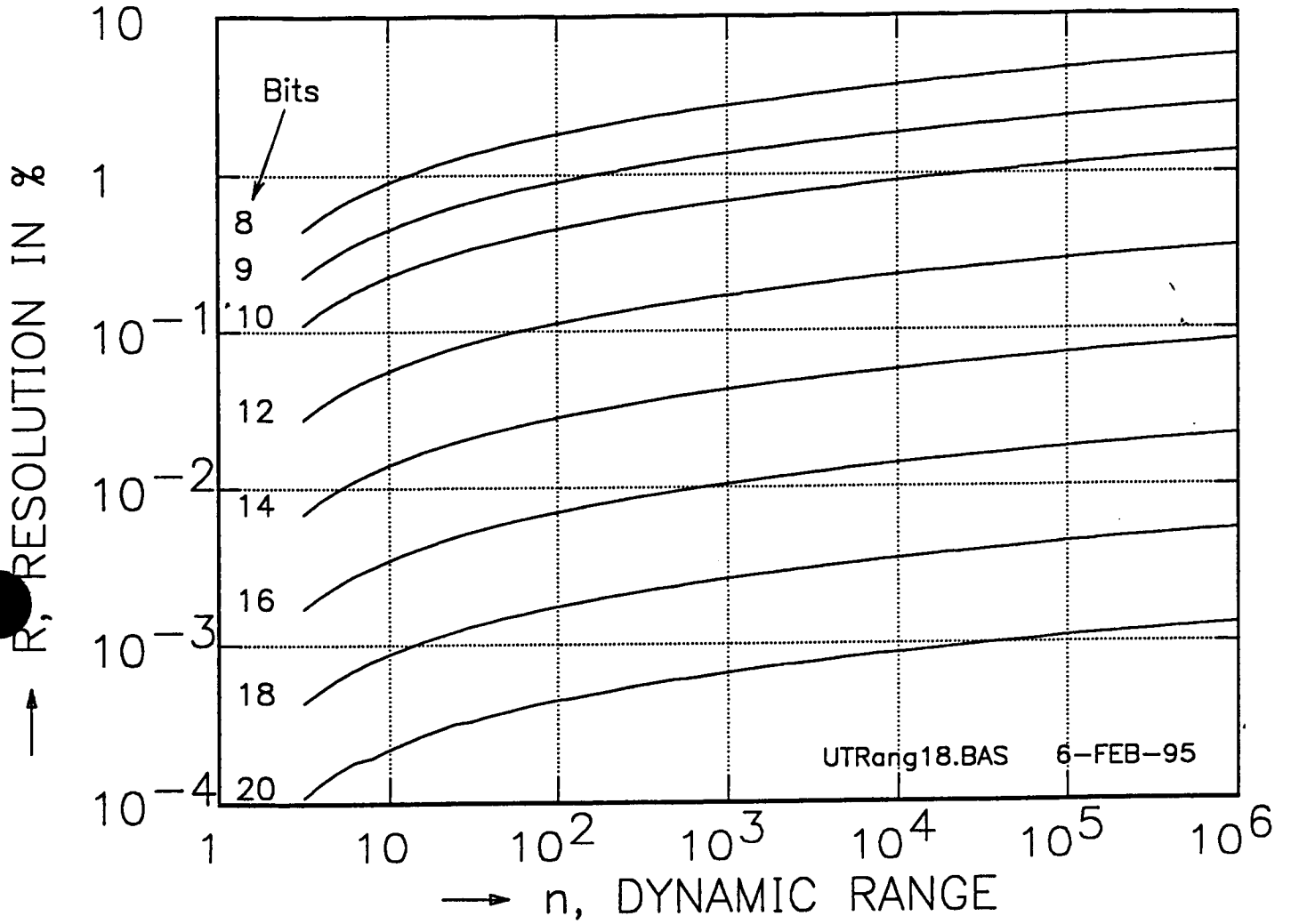

FIG. 1. RESOLUTION OF A DIGITAL PROCESSOR AS A FUNCTION OF ITS WORD SIZE IN BITS AND THE DESIRED DYNAMIC RANGE

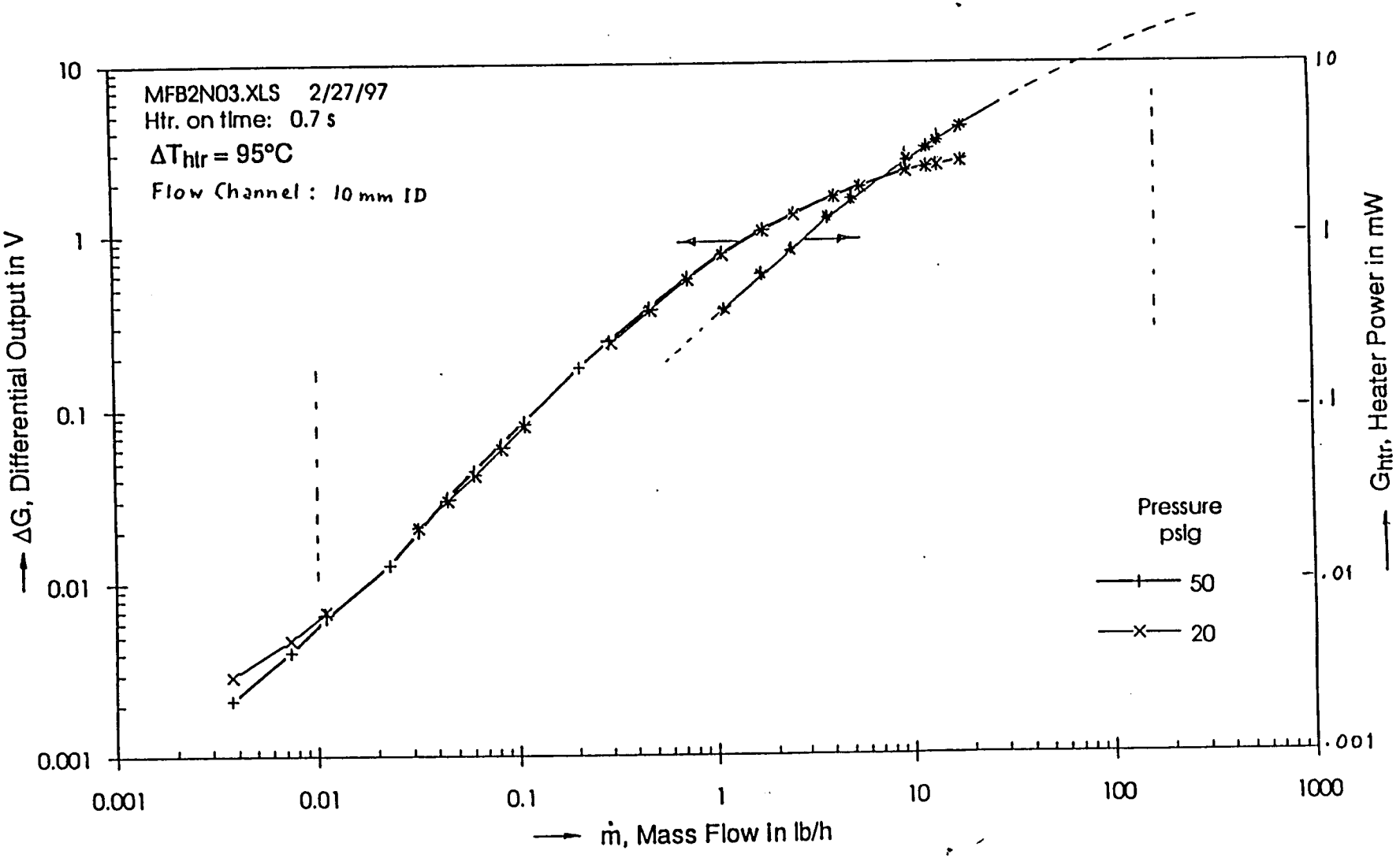

FIG. 4. FLOW SENSOR OUTPUTS VS. MASS FLOW OF N_2, FOR 20 AND 50 psig.
LEFT SCALE: DIFFERENTIAL OUTPUT; RIGHT: HEATER INPUT POWER.

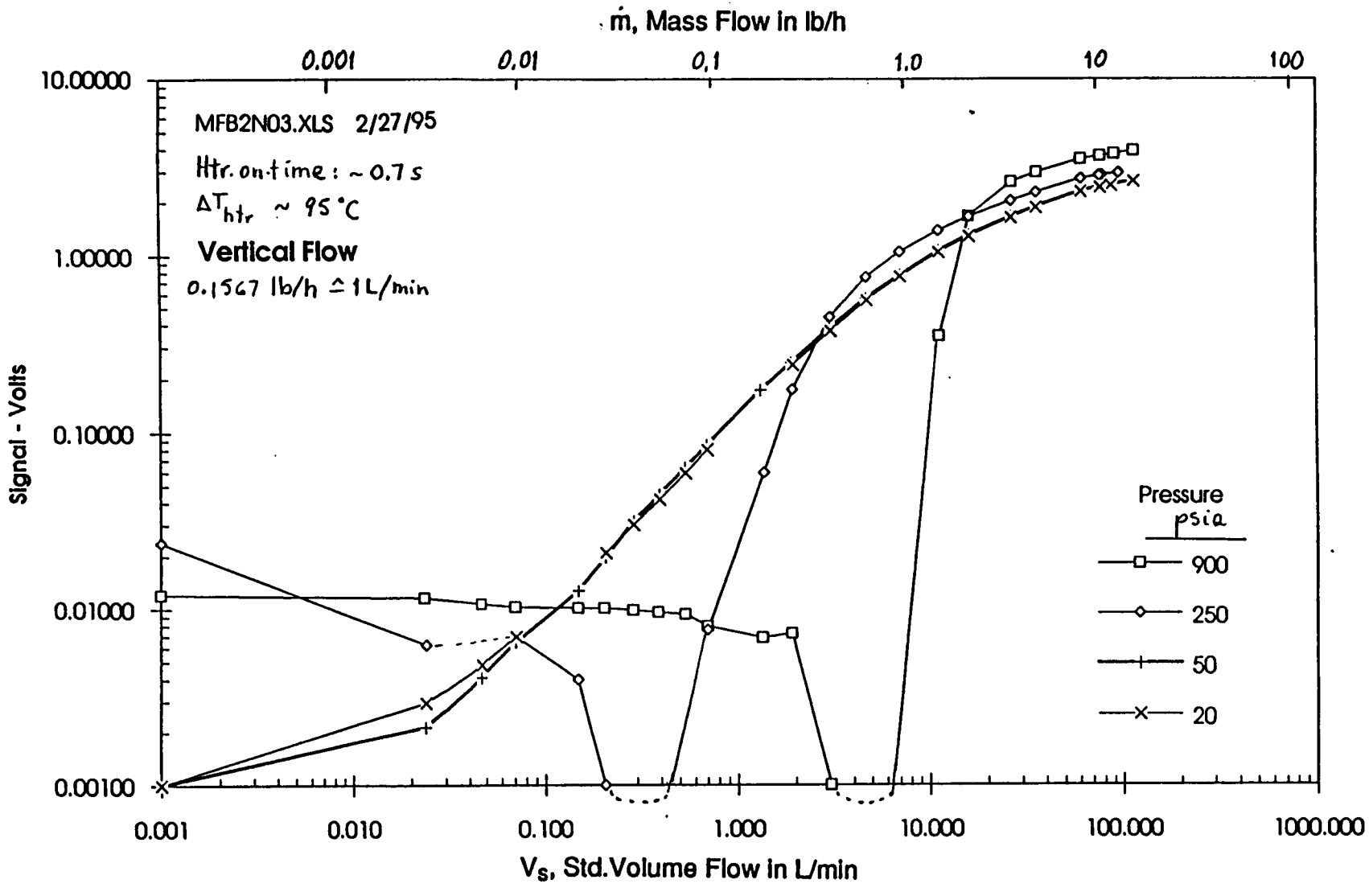

FIG. 9. FLOW MICROSENSOR DIFFERENTIAL OUTPUT VS. FLOW AT VARIOUS PRESSURES, SHOWING AN INCREASING NATURAL CONVECTION EFFECT WITH PRESSURE.

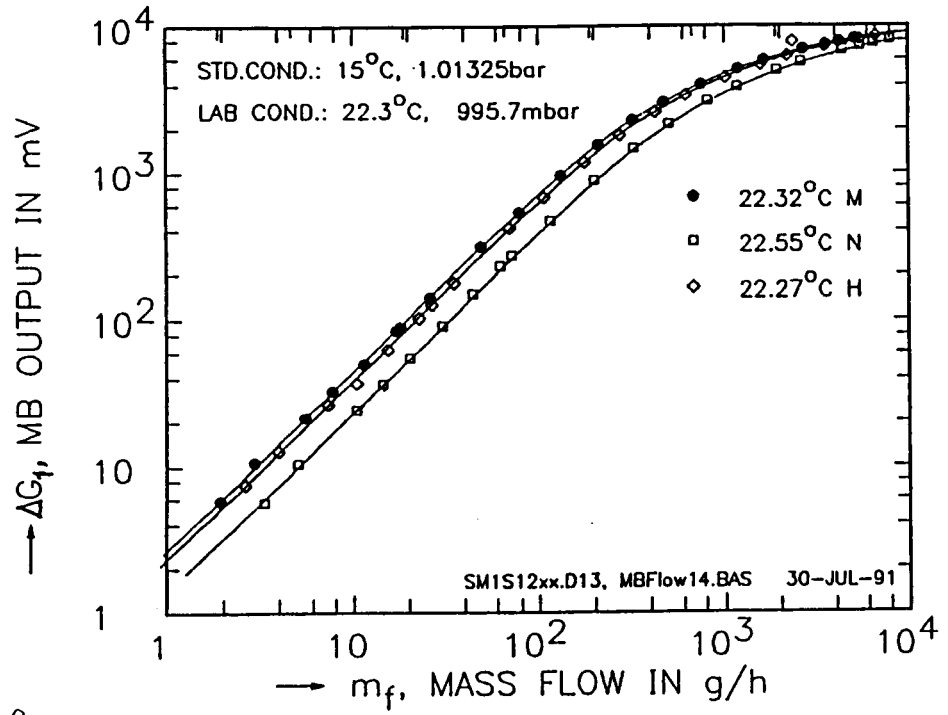

FIG. 5a. UNCOMPENSATED GAS MASS FLOW MICROSENSOR OUTPUT, FOR THREE GASES, WITH A 14 mm OD FLOW NOZZLE.
M=Methane, N=Nitroge, and H=High Viscosity Natural Gas

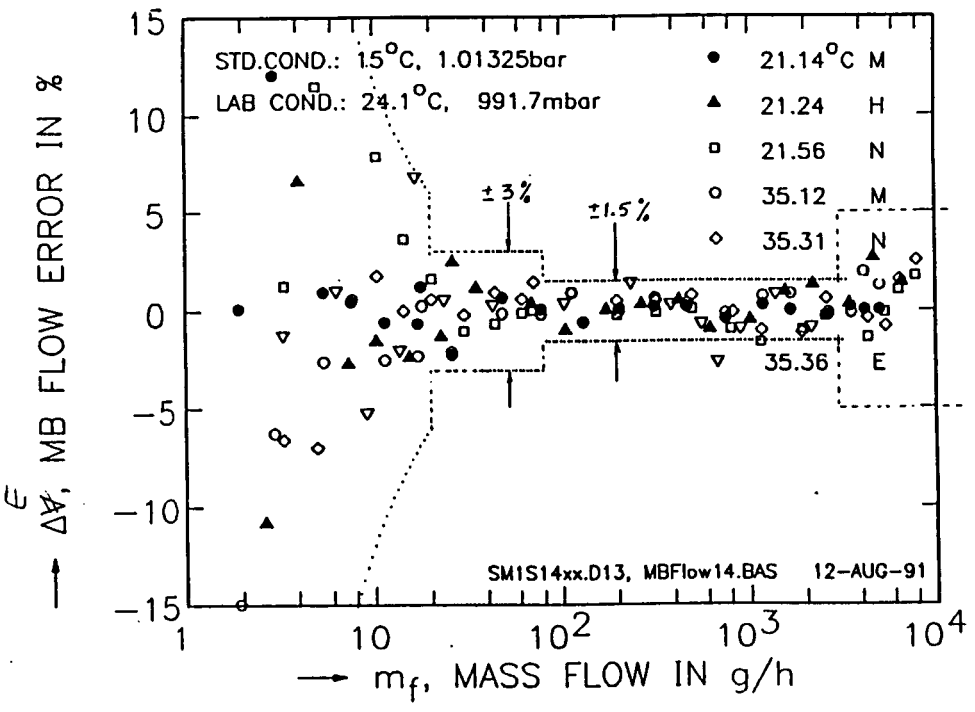

FIG. 5b. COMPENSATED GAS MASS FLOW MICROSENSOR OUTPUT ERROR, FOR FOUR GASES, WITH A 14 mm OD FLOW NOZZLE.
M=Methane, N=Nitroge, and H=High Viscosity Natural Gas
E= Ethane

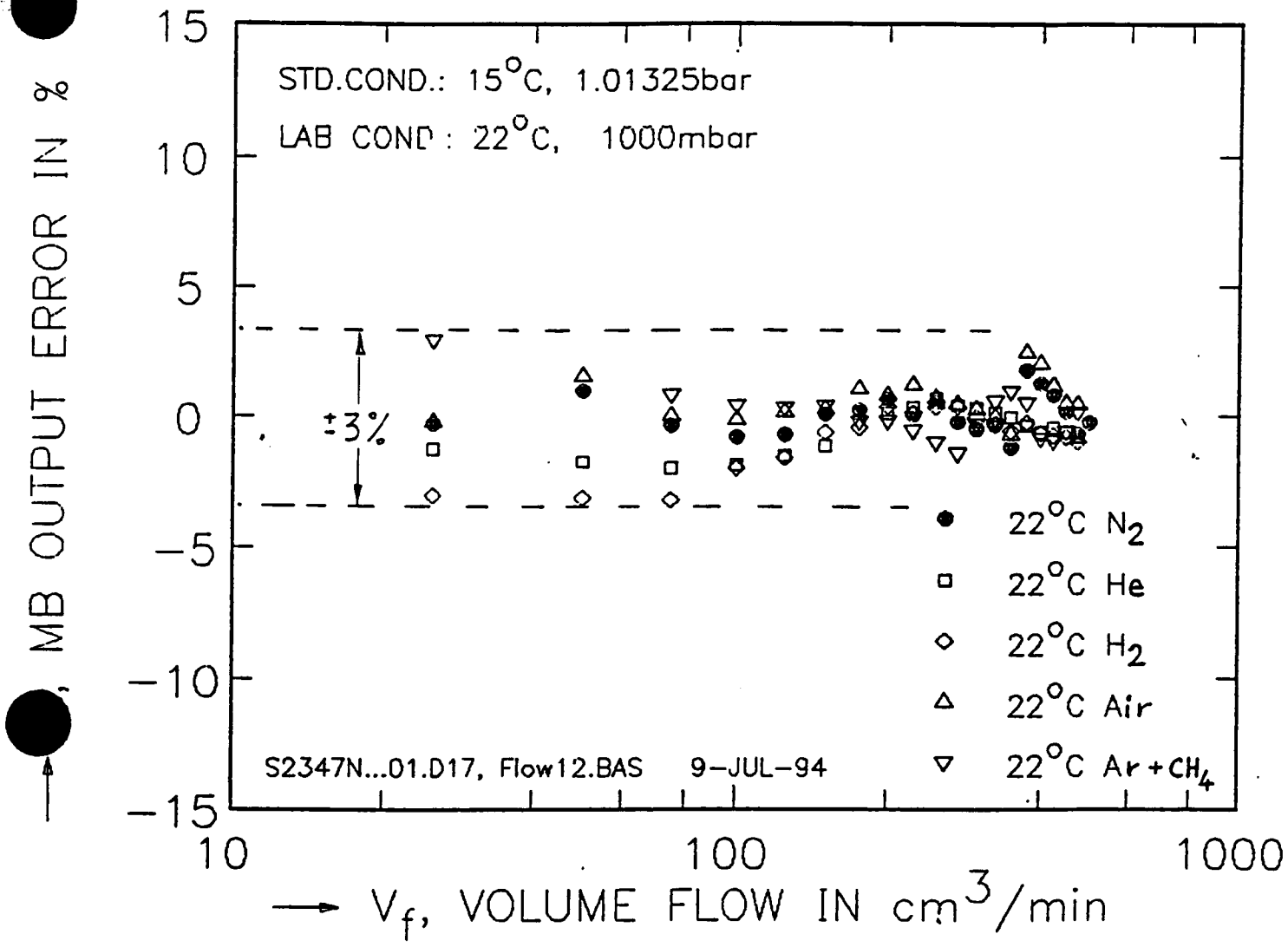

10

FIG. 5d. MBRIDGE SENSOR OUTPUT CORRECTED FLOW ERROR FOR SENSOR NO.: #2347, USING CORRECTION DERIVED FOR SENSOR #2348

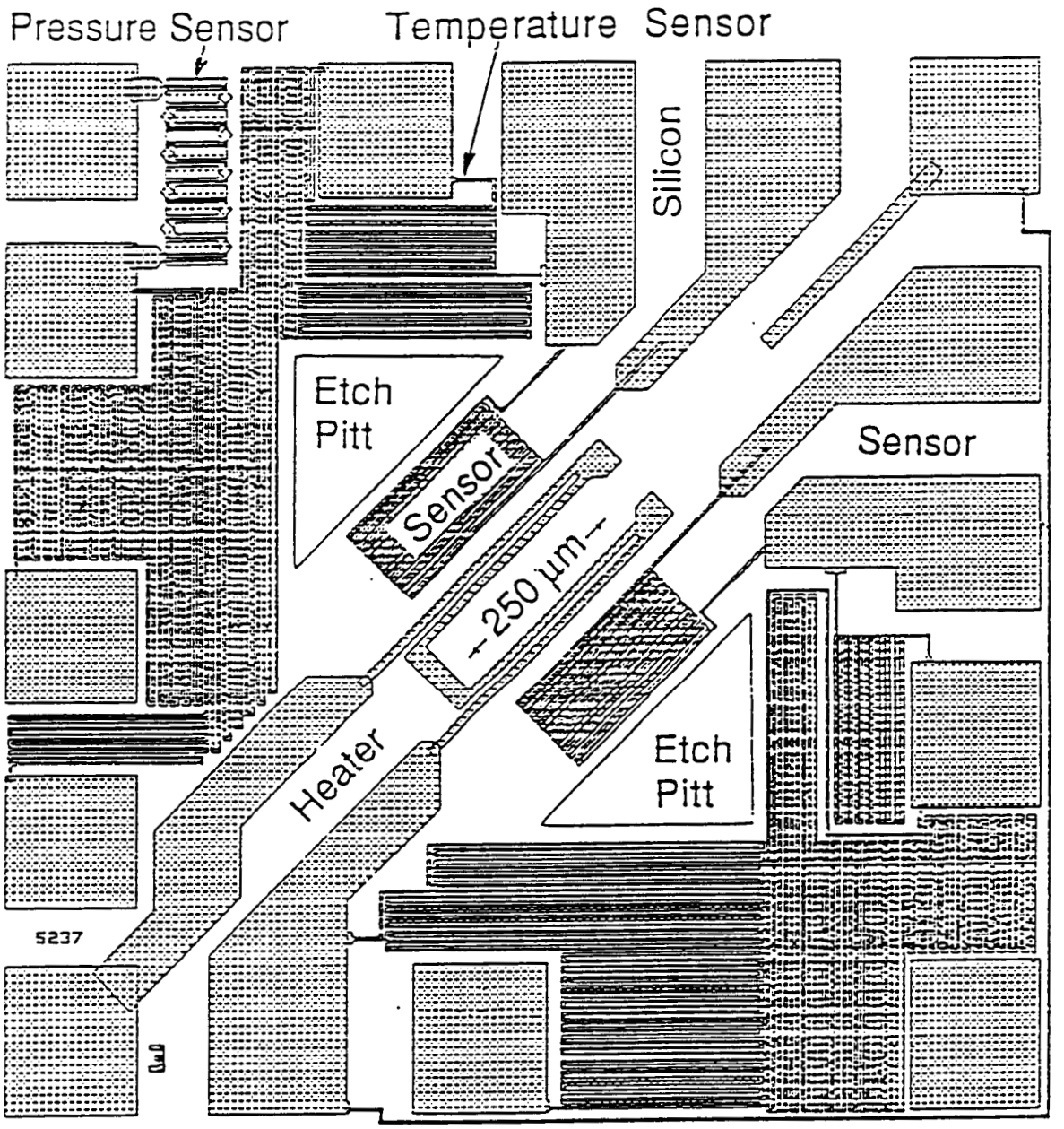

FIG. 1. MICROSENSOR CHIP LAYOUT, SHOWING SEVERAL OF ITS FUNCTIONAL ELEMENTS.

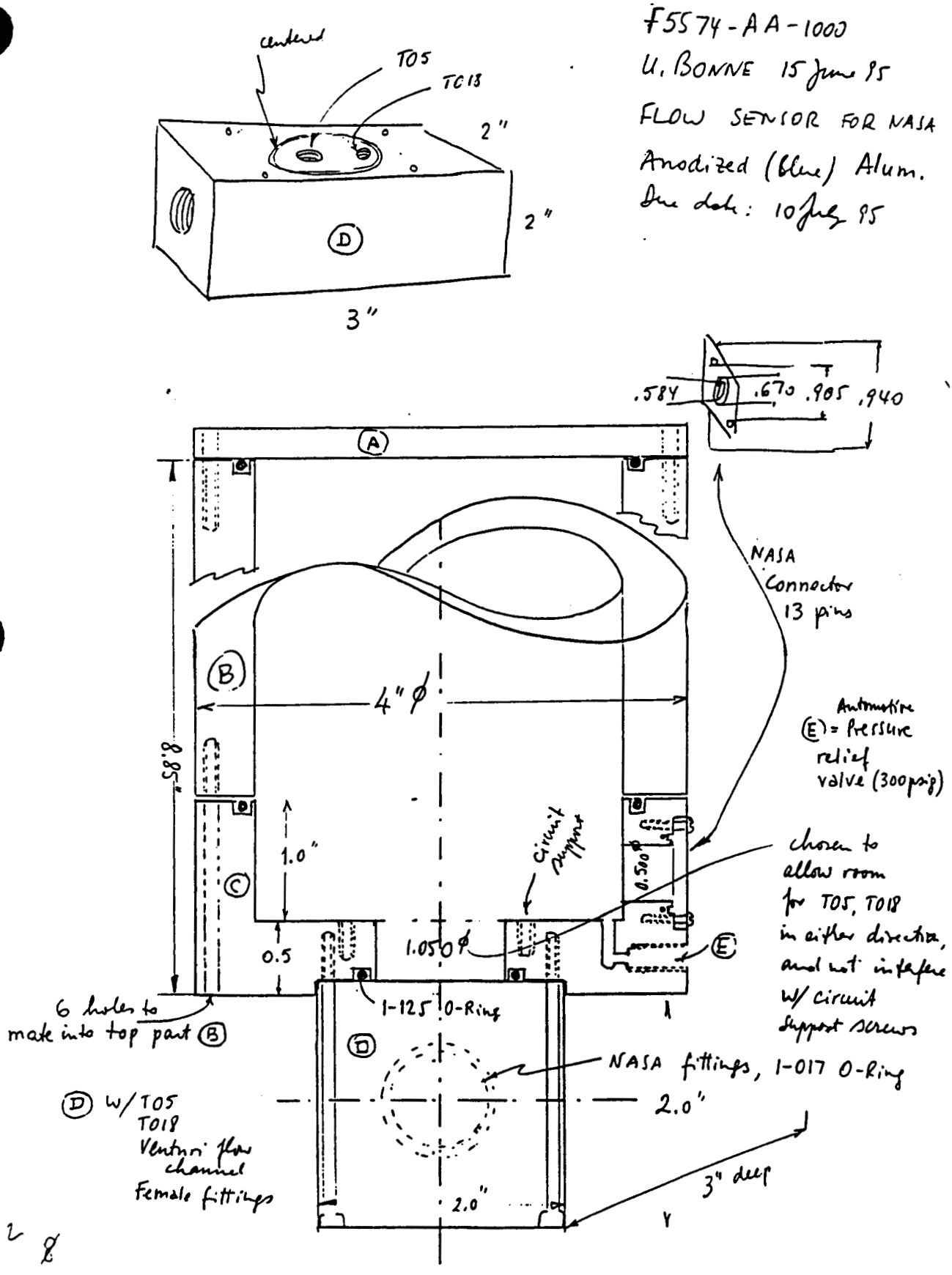

FIG. 6a. FLOW SENSOR HOUSING (A+B+C) AND FLOW CHANNEL (C).

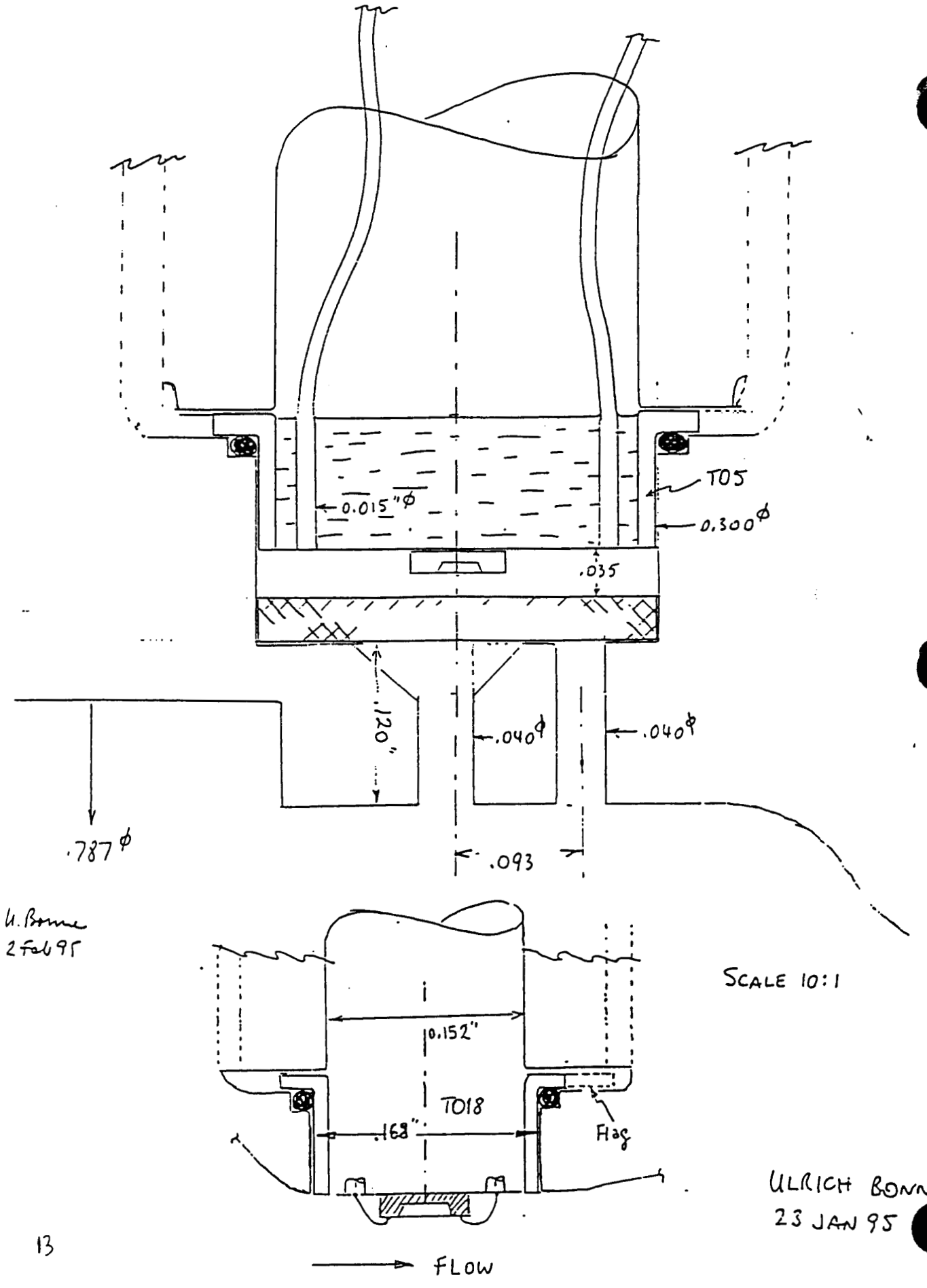

FIG. 2. CROSS SECTION OF CHIP-SUPPORTING HEADERS, TO5 (TOP) and TO18

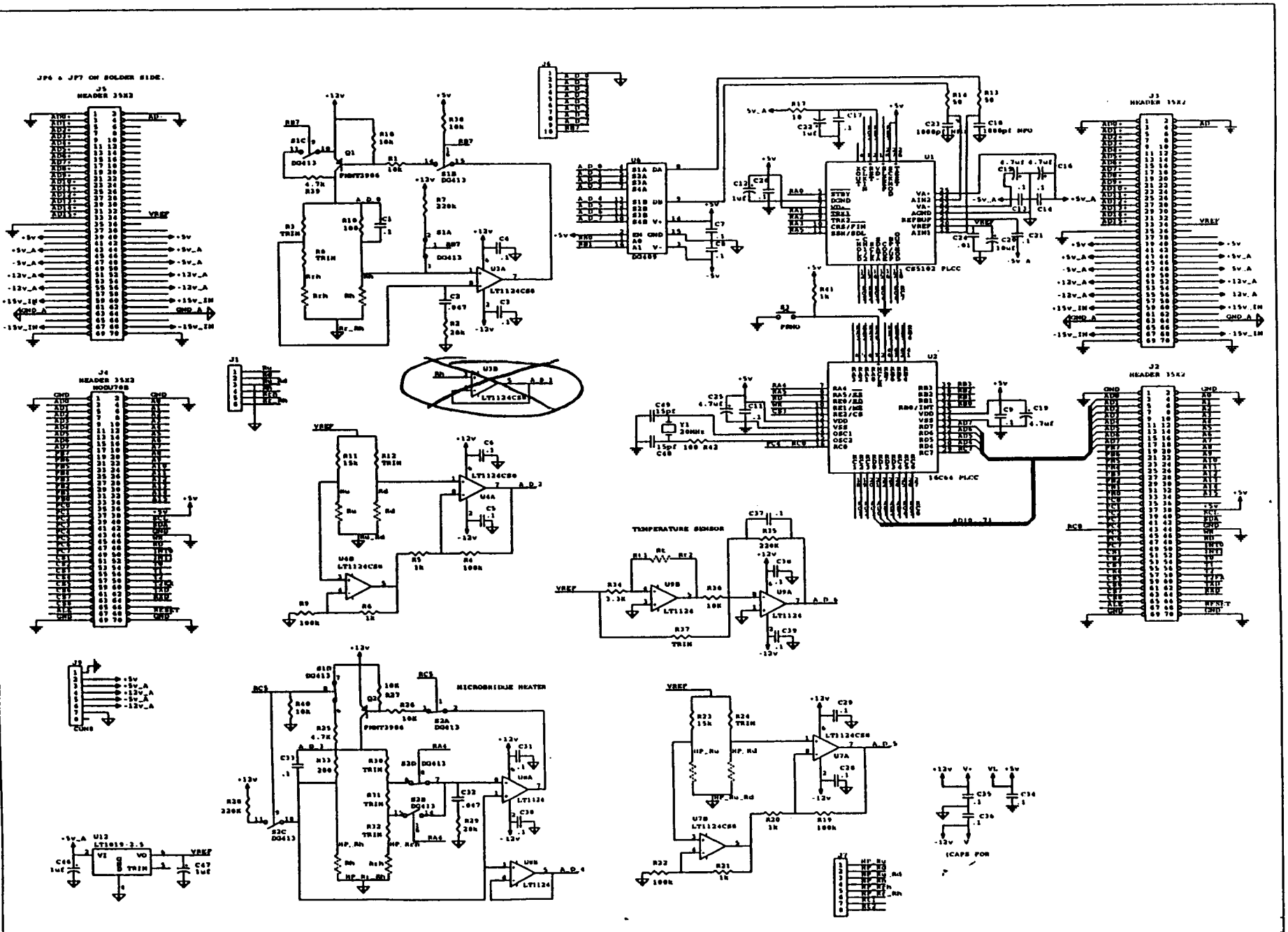

FIG. 15. FLOW SENSOR CIRCUIT: ANALOG FRONT-END FOR k, T and V.

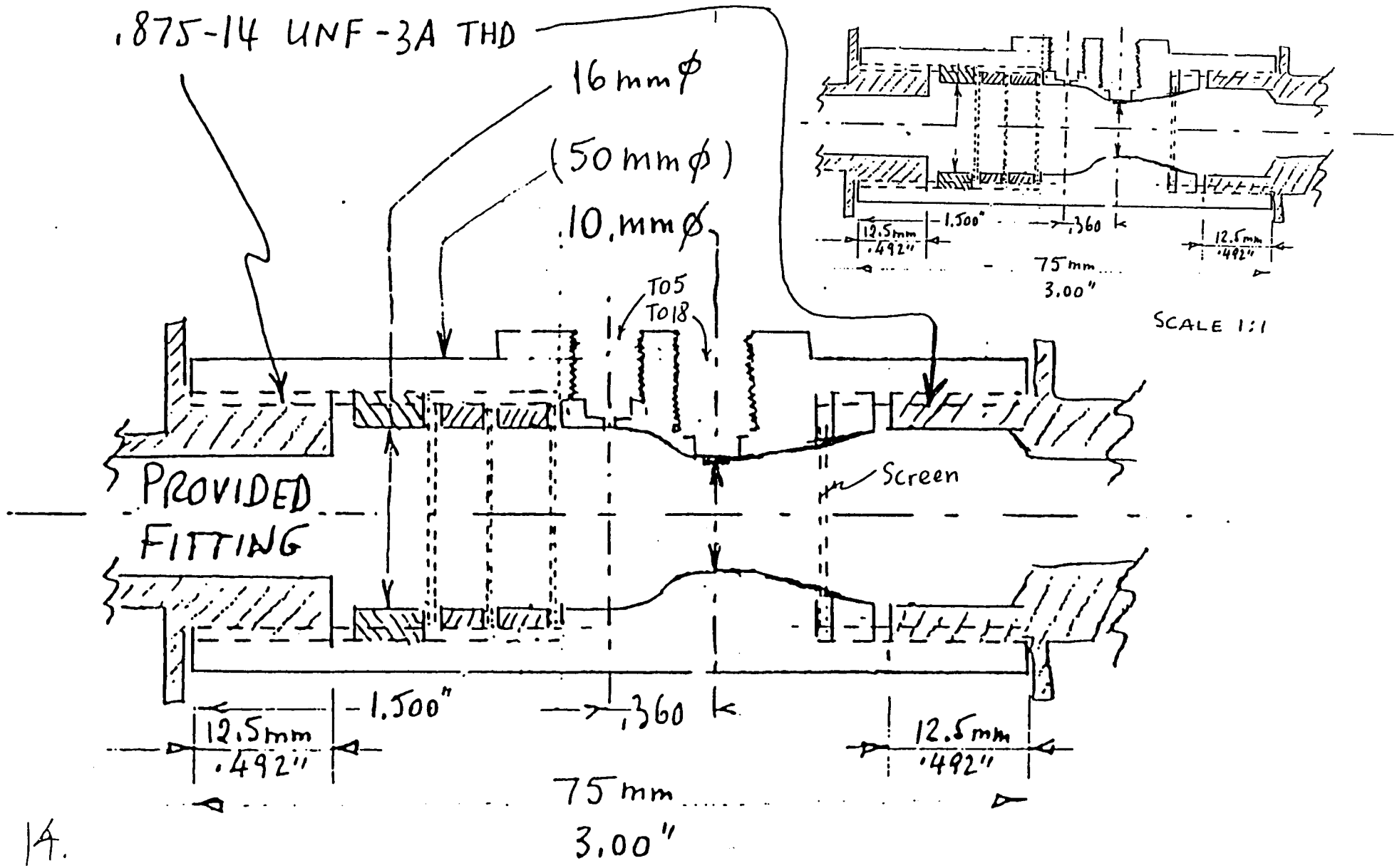

14.

FIG. 6b. SIDE VIEW/CROSS SECTION OF FLOW SENSOR CHANNEL WITH 10 mm VENTURI THROAT, PROVIDED FITTINGS, HEADER SOCKETS AND FLOW-STREIGHTENING SCREENS

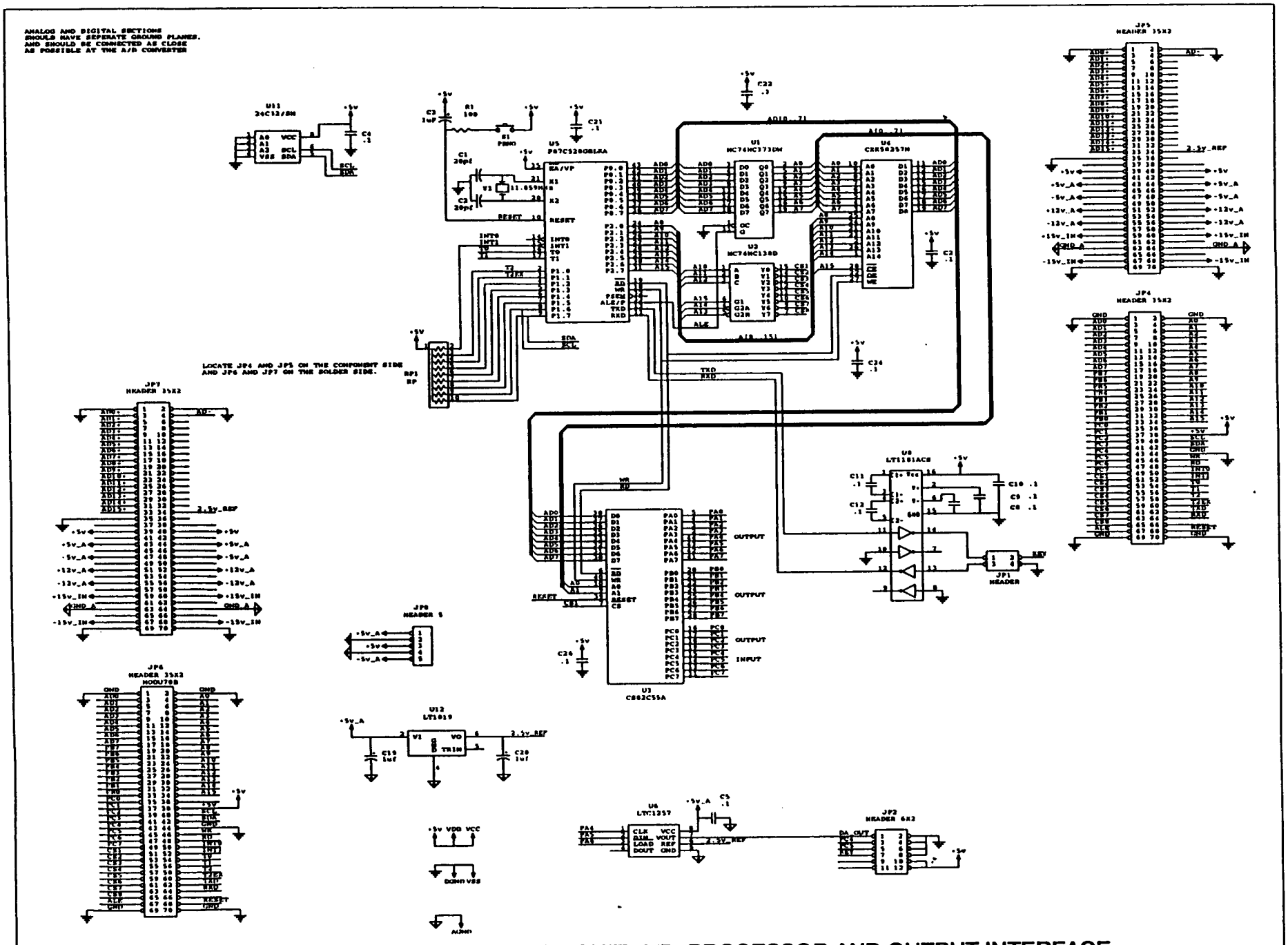

FIG. 15a.FLOW SENSOR CIRCUIT: A/D, PROCESSOR AND OUTPUT INTERFACE

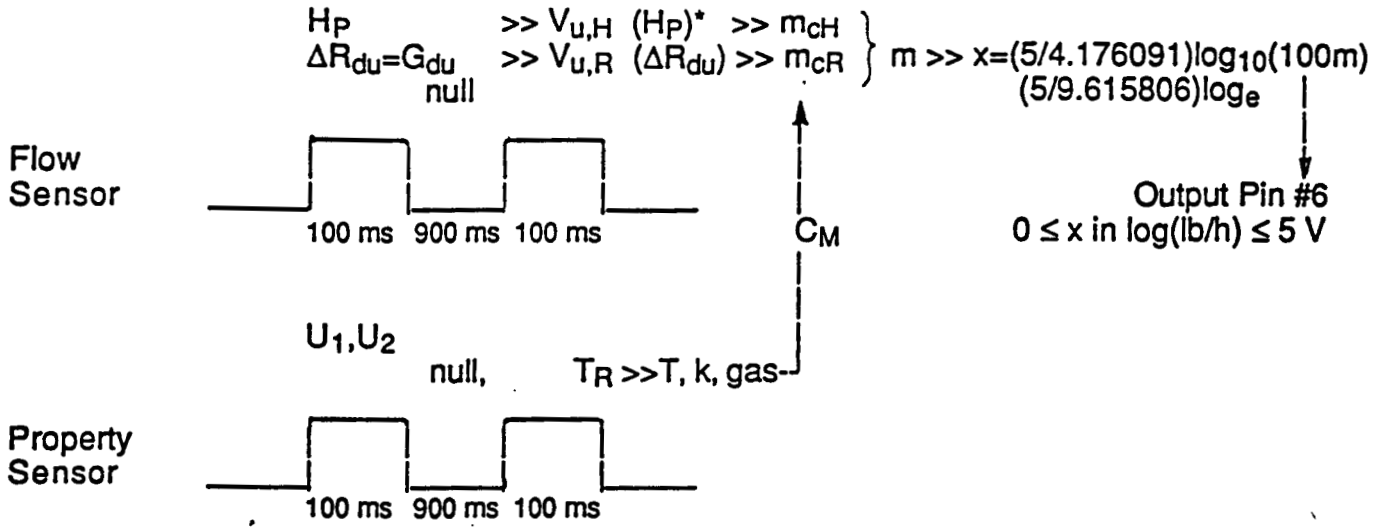

I/O is connected via the following pin numbers of the 13-pin connector:

#	INPUTS	OUTPUTS
1.	+5 V Digital	
2.	Digital Ground	
3.	+15 V Analog	
4.	Analog Ground	
5.	-15 Analog	O2, N2, H2, He, O3 or N3
6.		D/A Output - x
7.		D/A Return
8.		RS232 Transmit - U#,X,T,U_1,U_2, gas,G_{du},H_P,m CR LF **
9.		RS232 Receive - O2, ..., or N3
10.		RS323 Common
11.		Digital Ground
12.		Analog Ground
13.		Chassis Ground

Rev.: 21 Aug.'95

* The corresponding coefficients are upgradable on Serial EE PROM, 24C32

** Data string transmitted once/second; ASCII code: ±x.xxxxxxE±xx for each of the listed variables, which are comma-separated and of which each set is finished with a carriage return (CR) and a line feed (LF); received inputs: any of the first four X above for individual gases, but enter "N3" for N_2/He/H_2, or "O3" for O_2/He/H_2; the verification response is the same X as part of the transmitted string.

FIG. 15b. MASS FLOW SENSOR #2: SIMPLIFIED MEASUREMENT PROTOCOL AND INFORMATION FLOW CHART, LEADING TO ANALOG 0-5 VDC OUTPUT. Both sensors are pulsed at about 100 ms; the gas is reidentified during each cycle; the corresponding flow correction factor, C_M, is recomputed and reapplied to the flow sensor signal. The flow signal is downselected from two measurements as shown. The chosen mass flow, m, is then converted to its logarithm and converted to analog.

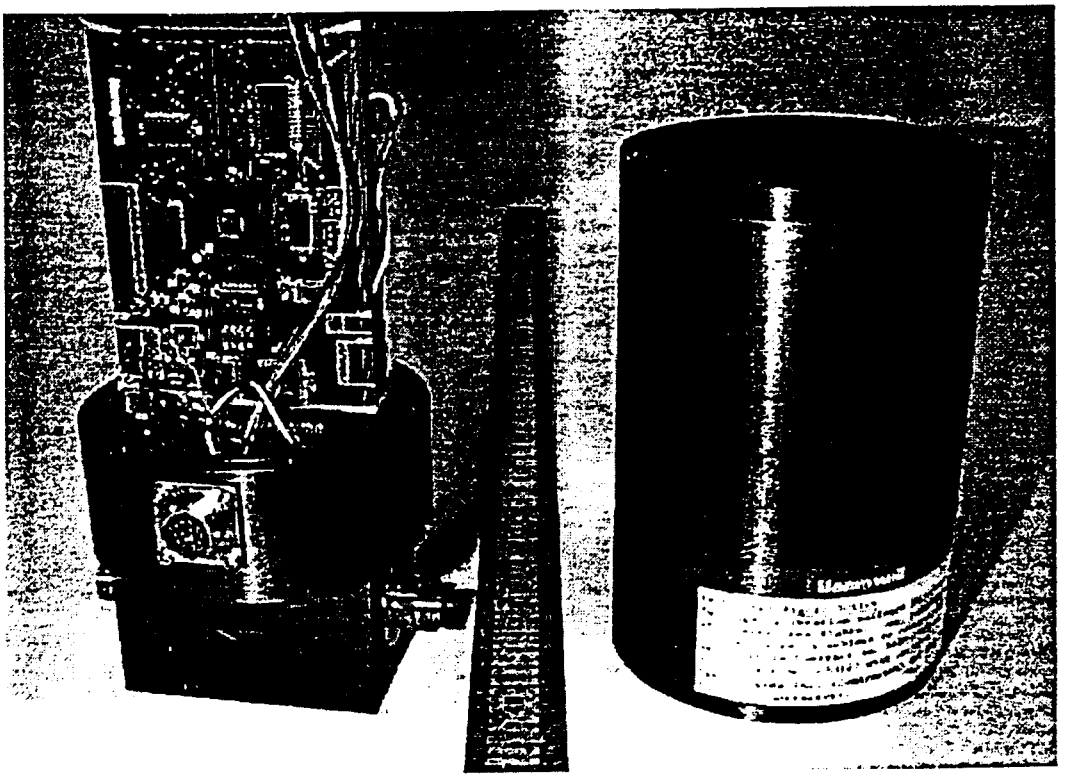

FIG. 16. PHOTOGRAPH OF SMART MASS FLOW SENSOR DEMONSTRATION UNIT, SHOWING THE IN- AND OUTLET FITTINGS IN THE LOWER LEFT BLOCK.

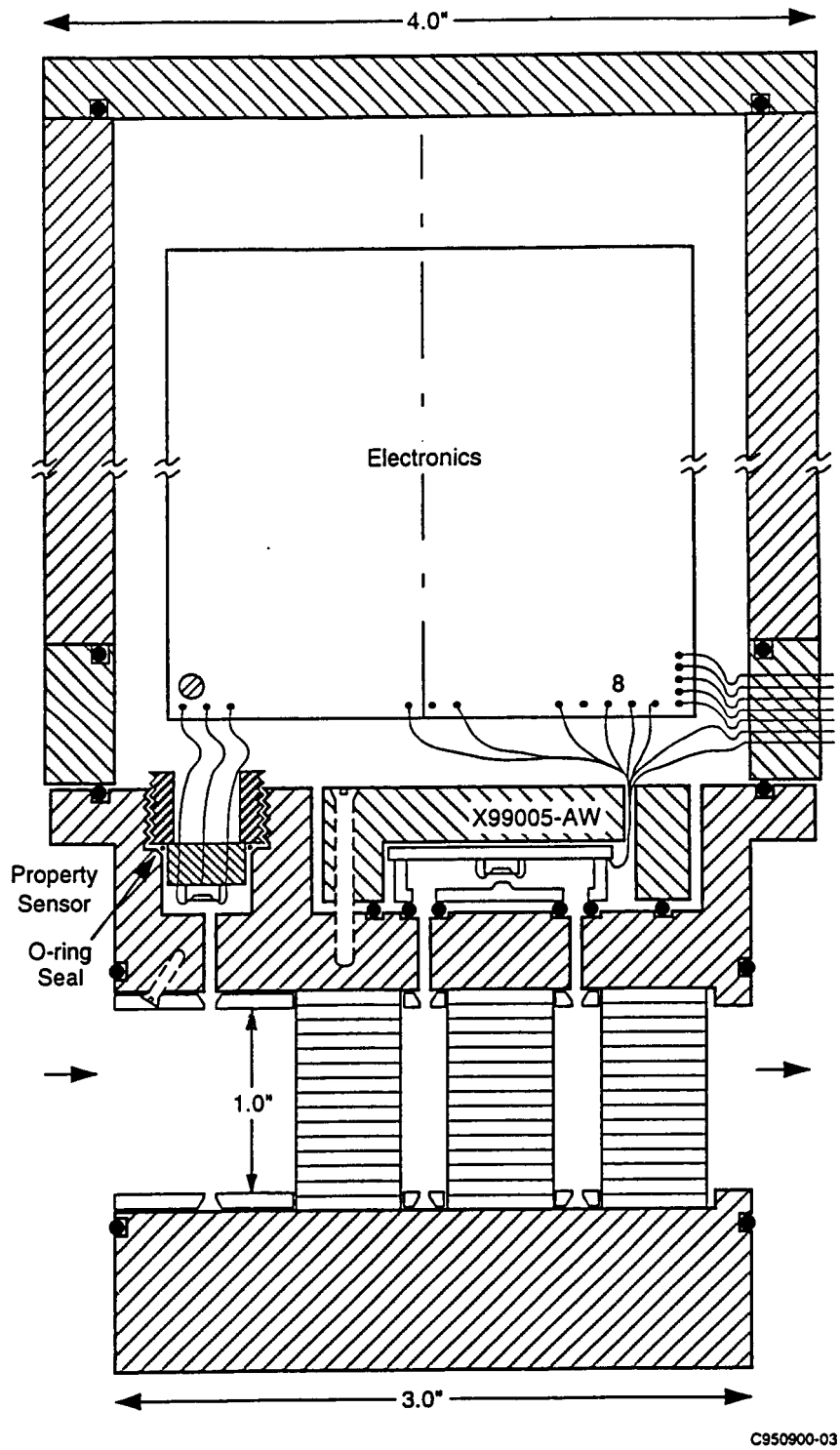

17

FIF. 4a. IMPROVED FLUID FLOW SENSING SYSTEM BASED ON A BYPASS ACROSS A LAMINAR FLOW RESTRICTION (CENTRAL HONEYCOMB). FLUID REACHES BOTH PROPERTY AND FLOW SENSORS DIRECTLY. A METAL BRACKET HOLDS THE FLOW SENSOR IN PLACE AGAINST FLUID PRESSURE, AND ITS LEADS ARE ACCESSIBLE W/O ADDITIONAL FEEDTHROUGHS.

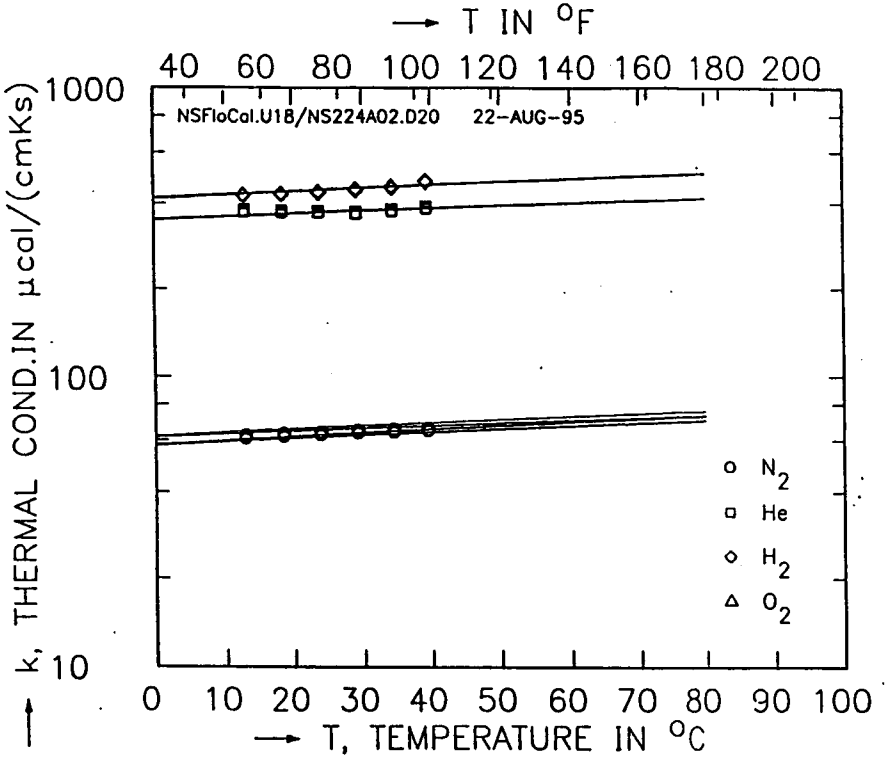

FIG. 18. THERMAL CONDUCTIVITY MEASUREMENT VIA CONST.ΔT_{htr}=30°C. LARGE SENSOR. DATA PRESSURE RANGE: 45–500 psia, CURVES FOR 45 AND 500 psia.

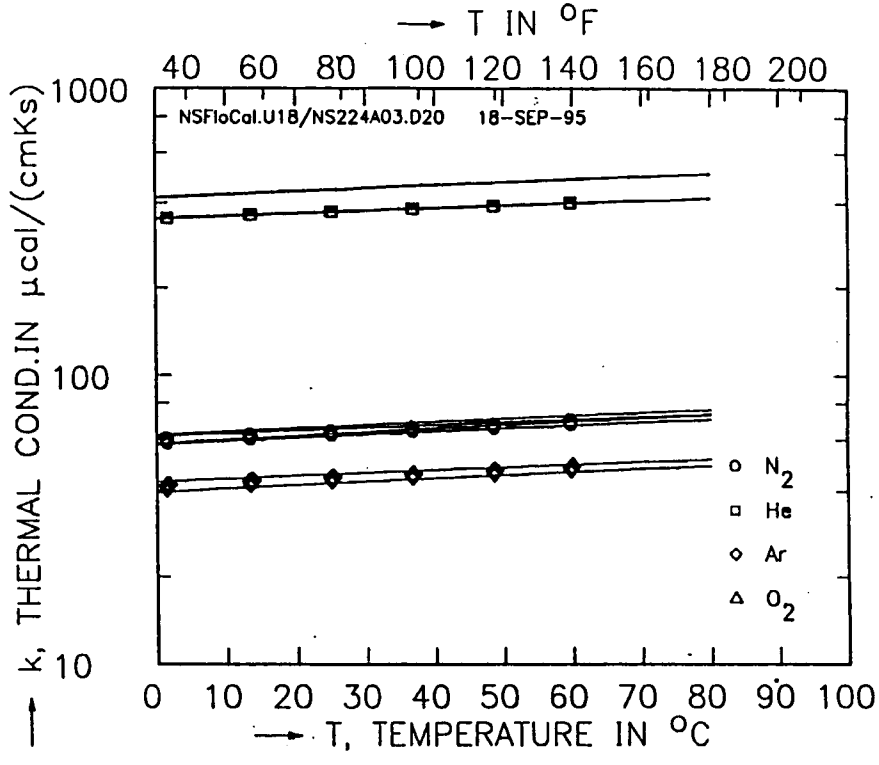

FIG. 18a. THERMAL CONDUCTIVITY MEASUREMENT VIA CONSTANT ΔT_{htr} DRIVE. LARGE SENSOR. PRESSURE RANGE: 45–500 psia FILE:C:NS224A03.D20

FNKx ± 0.2833% ± 1.973% TLS = 1.62

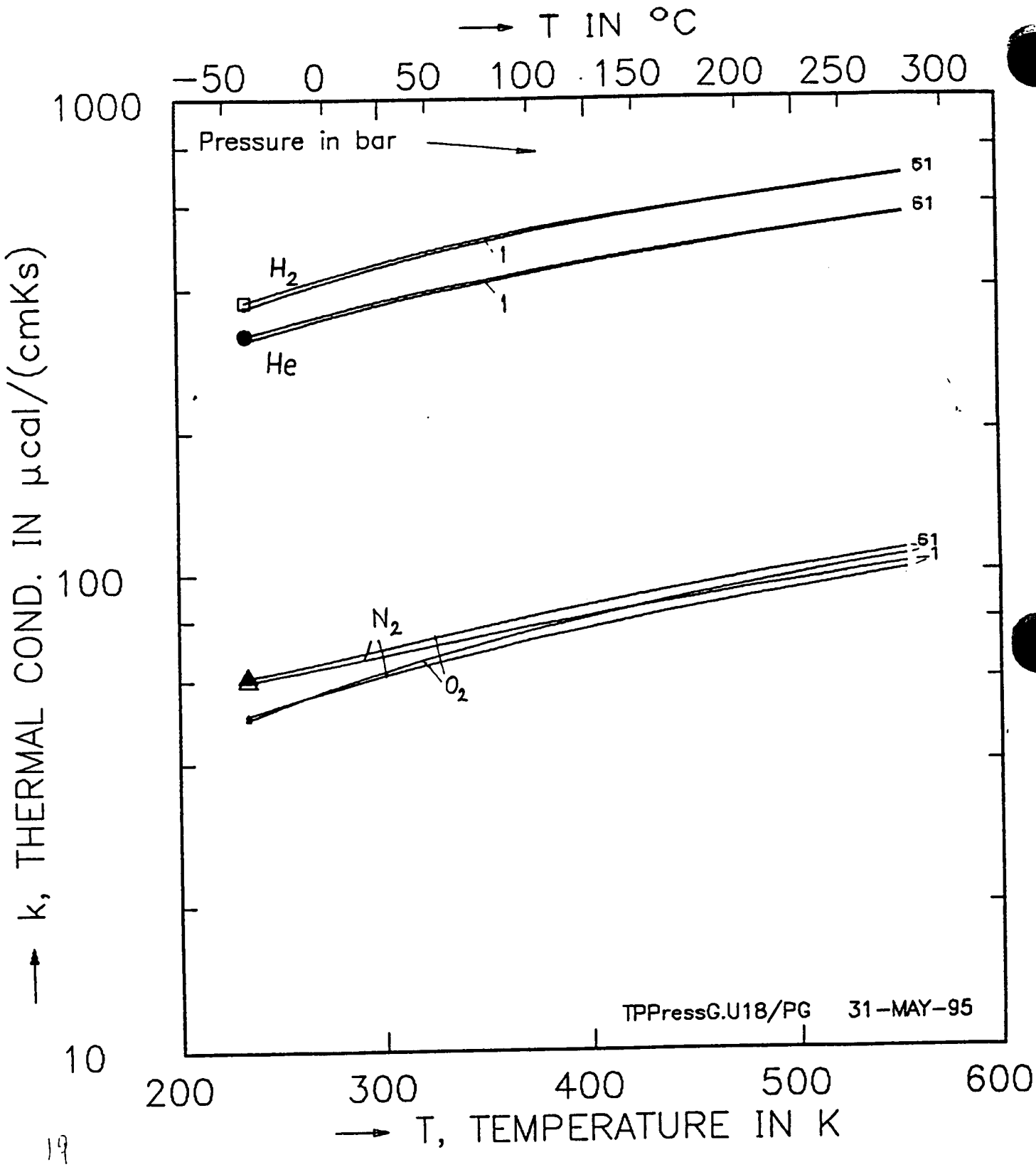

19

FIG. 1. THERMAL CONDUCTIVITY VS. TEMPERATURE OF H_2, He, N_2 AND O_2, AT 1 AND 61 bar OF PRESSURE.

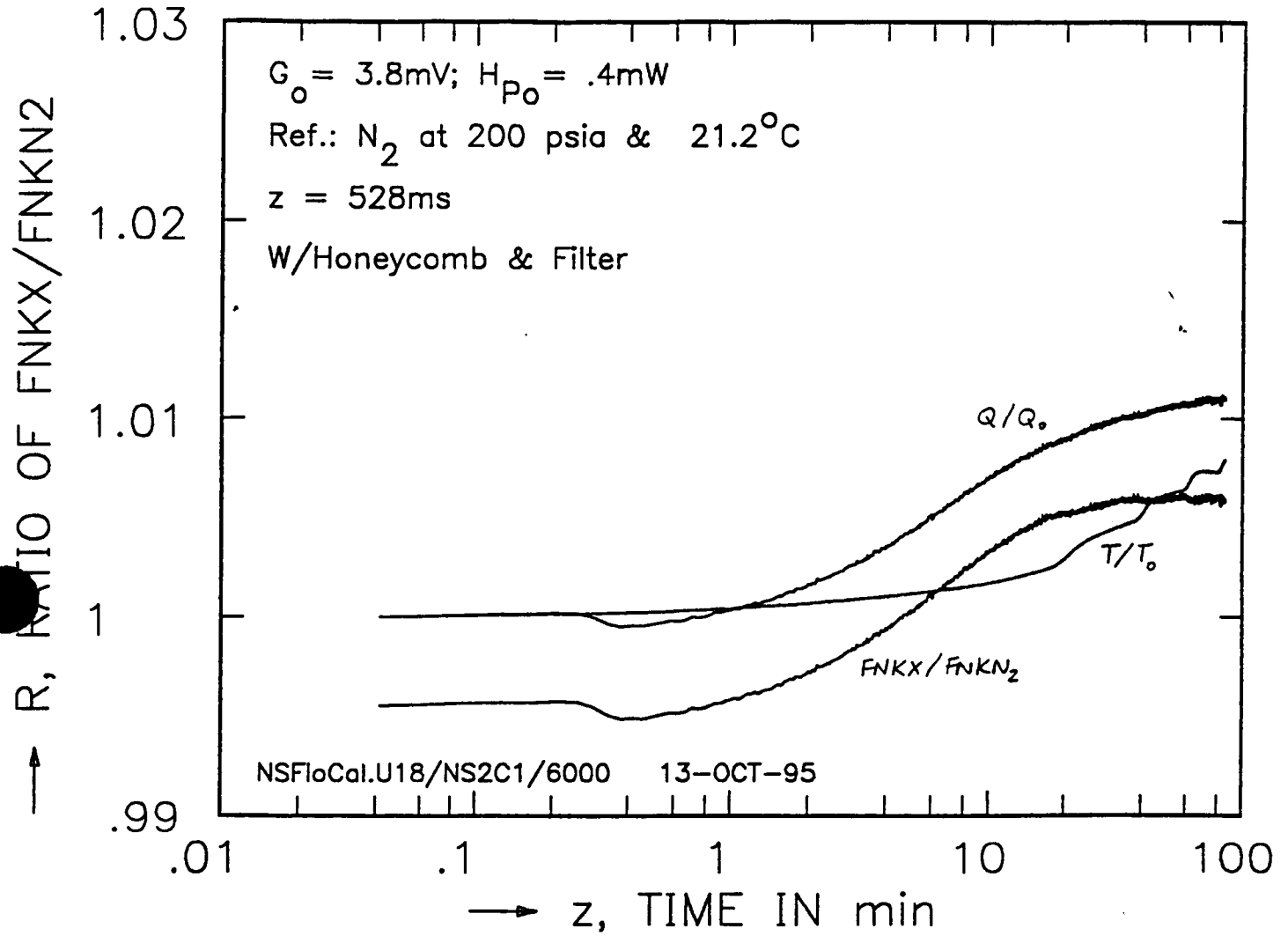

20a

FIG. 5. WARMUP TIME OF COMPENSATED FLOW SENSOR W/CONST.ΔT_{htr}=30°C DRIVE. START FROM COLD ELECTR. & SENSOR. #5 FILE: NS224N01.CSV, p = 1 bar, NO INSUL.

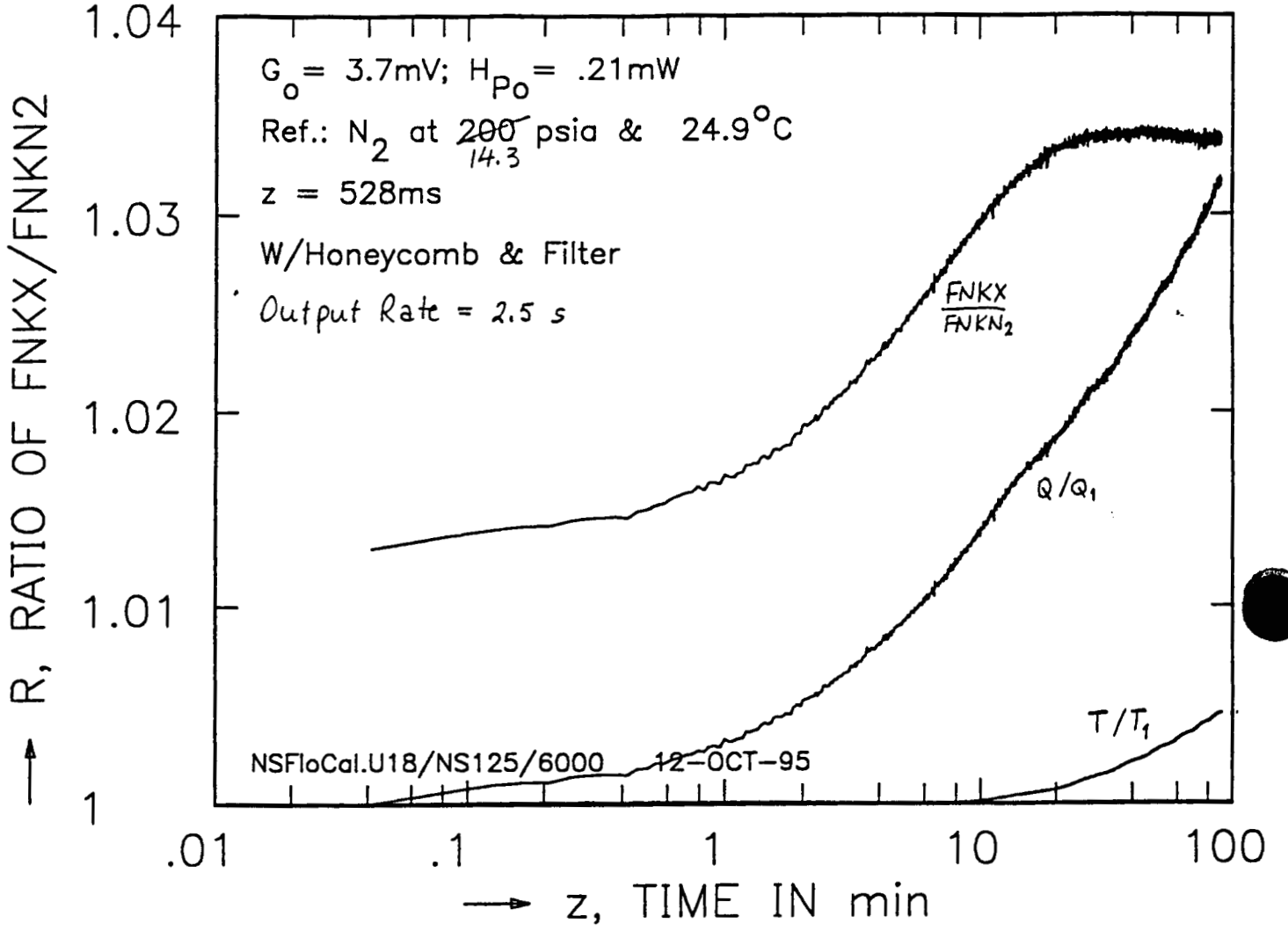

20

FIG. 5. WARMUP TIME OF COMPENSATED FLOW SENSOR W/CONST.ΔT_{htr}=30°C DRIVE. START FROM COLD ELECTR. AND SENSOR. #6 FILE: NS125N01.CSV, p = 1 bar

W/INSULATION. NO FLOW

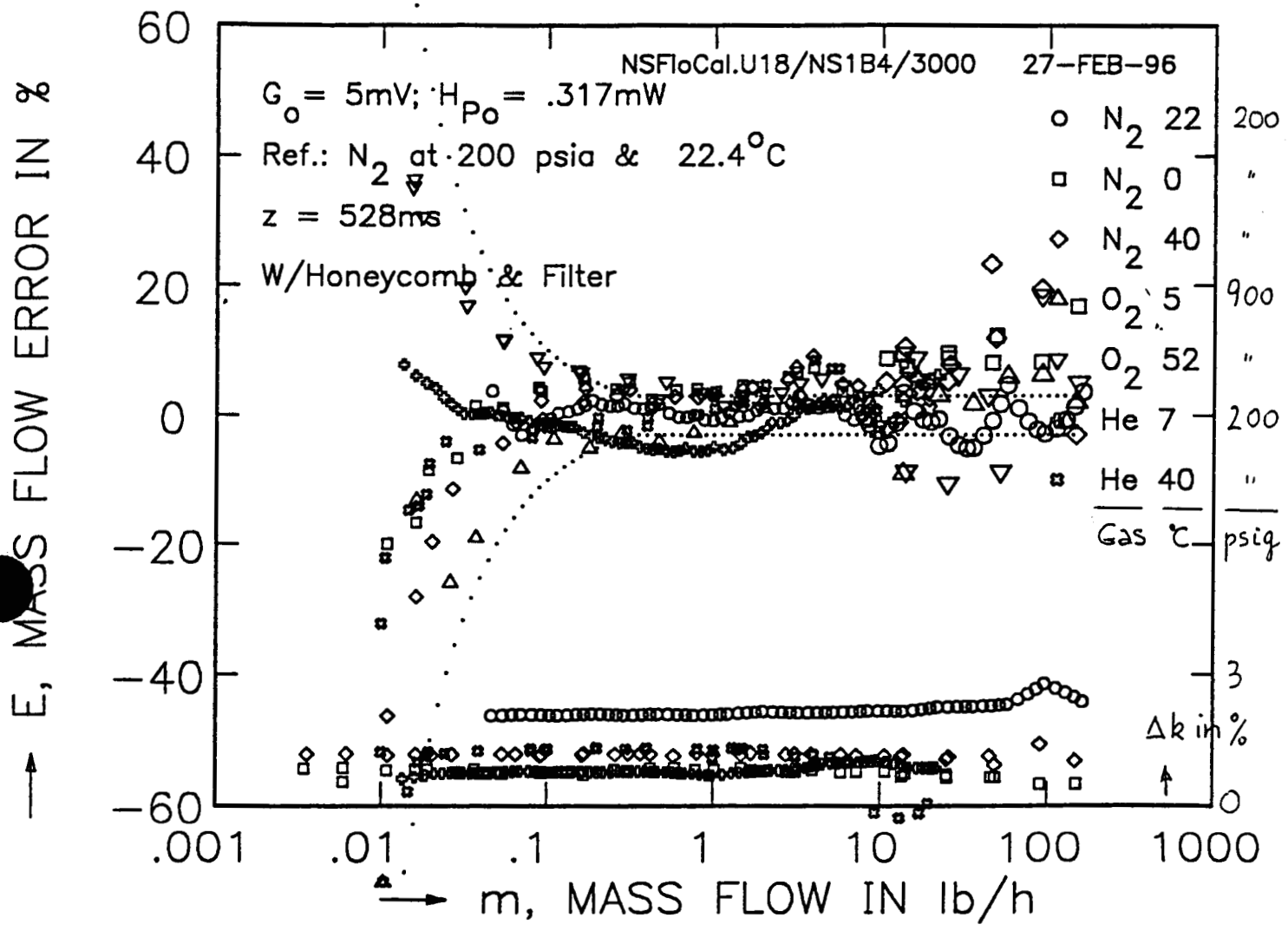

22

FIG. 4. MASS FLOW SENSOR MEASUREMENT ERROR, IMPR'TS: FILTER, AVERAGING, INDIV.G_o,T_6 1:.0055/−.8,2:.00500/−.6,4:.0056/−.6. NS1B4NT4/8/7.D20,0T3/2,HT3/4,ckt up lv C2=.94

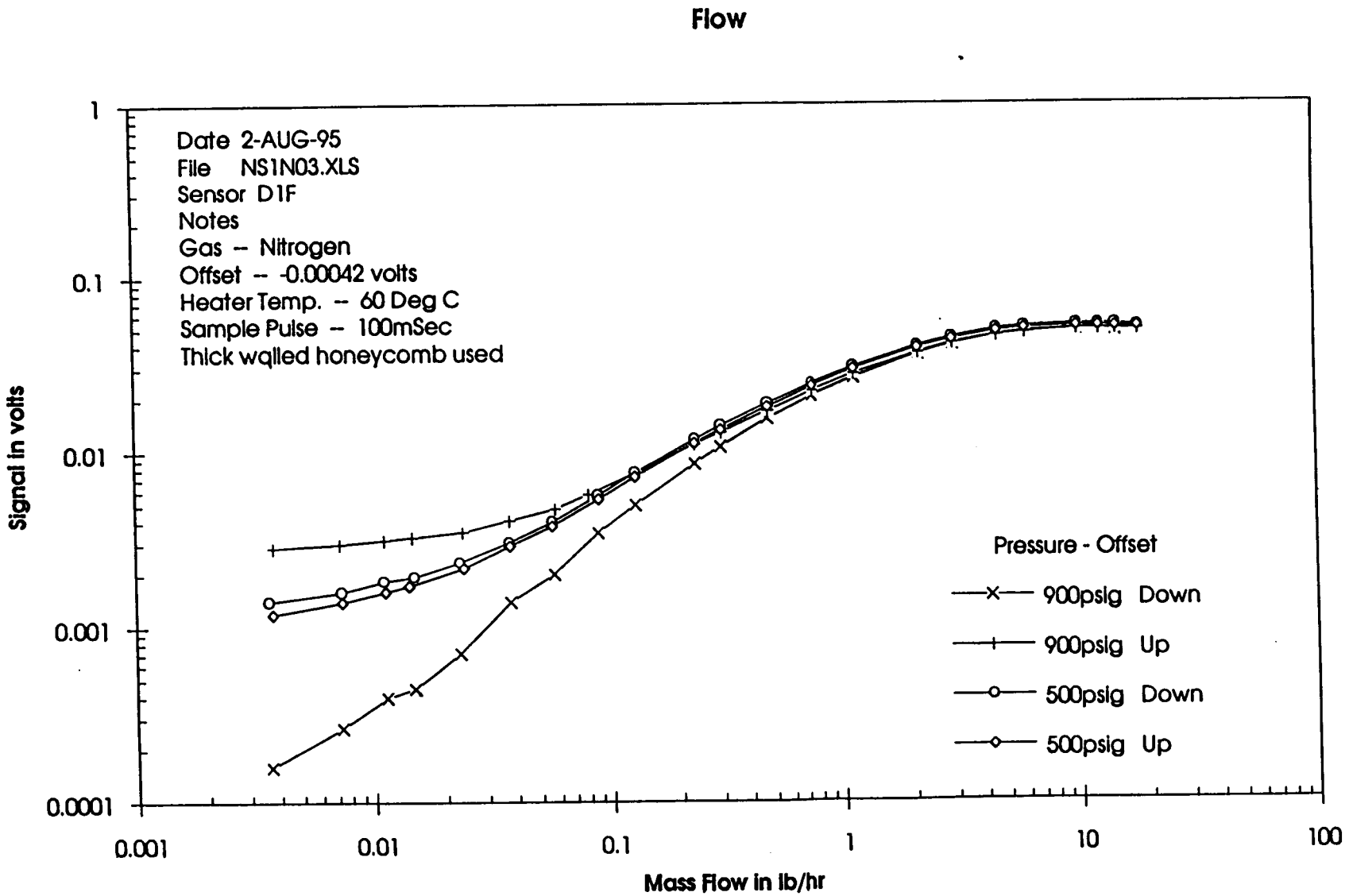

FIG. 21. PERFORMANCE OF FLOW MICROSENSOR UNIT#1 AFTER IMPLEMENTING DESIGN IMPROVEMENTS TO REDUCE THE INFLUENCE OF ORIENTATION.

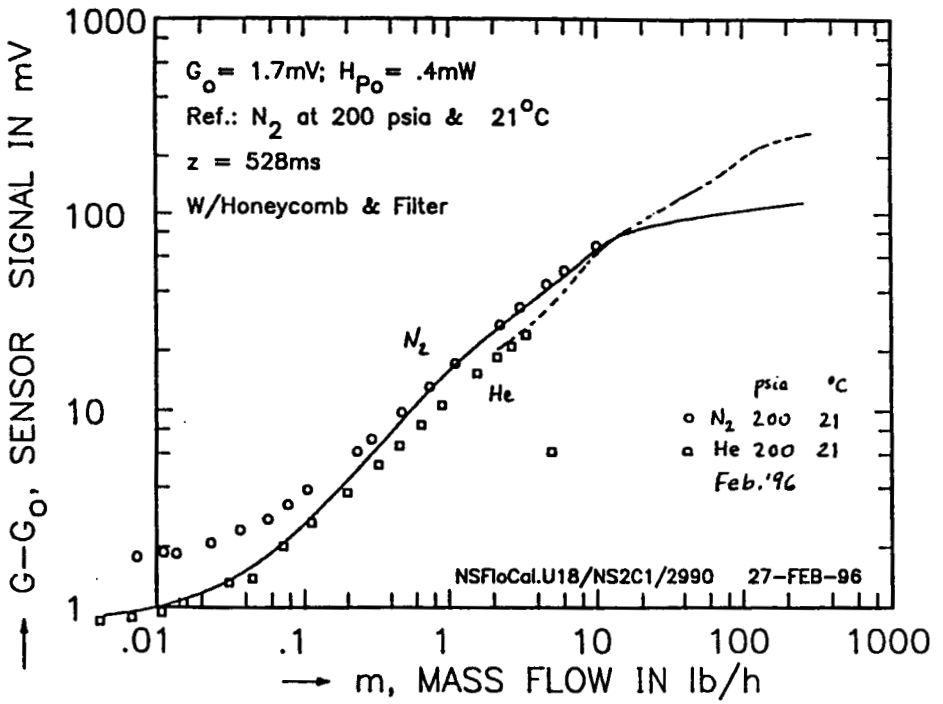

FIG. 23. MASS FLOW MEASUREMENT W/MICROSENSOR.
IMPR'TS: FILTER, AVERAGING, INDIV.G_o,T_6
1:.0037/−.1,2:.00170/1.8
#5 NS2C1N08.D20,H06,ckt up lv C2=.94

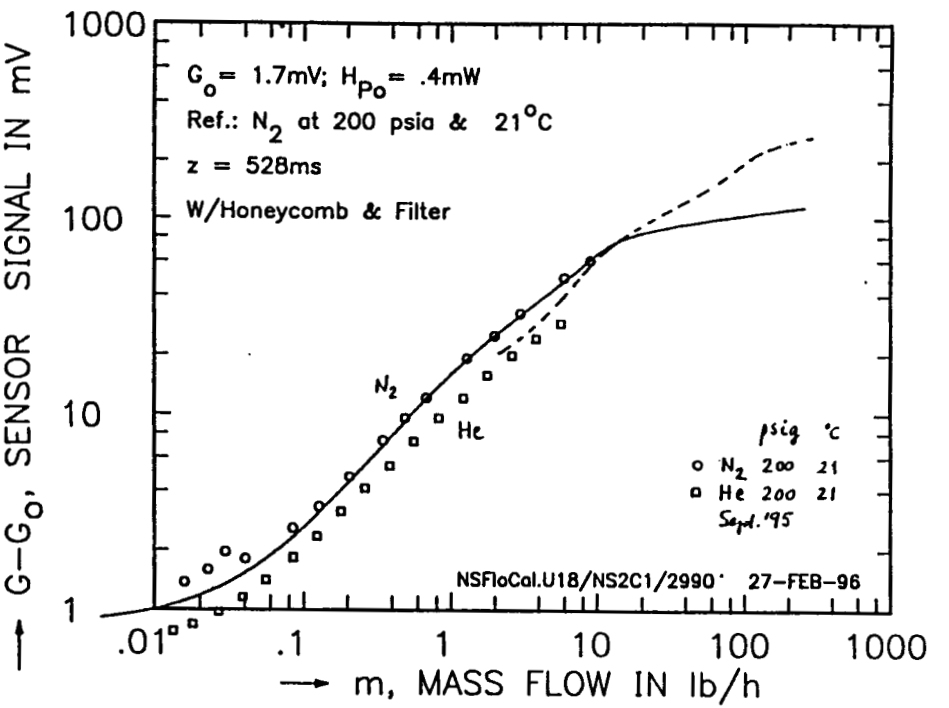

FIG. 24. MASS FLOW MEASUREMENT W/MICROSENSOR
IMPR'TS: FILTER, AVERAGING, INDIV.G_o,T_6
1:.0037/−.1,2:.00170/1.8
#5 NS1C1NT1.D20,HT1,ckt up lv C2=.94

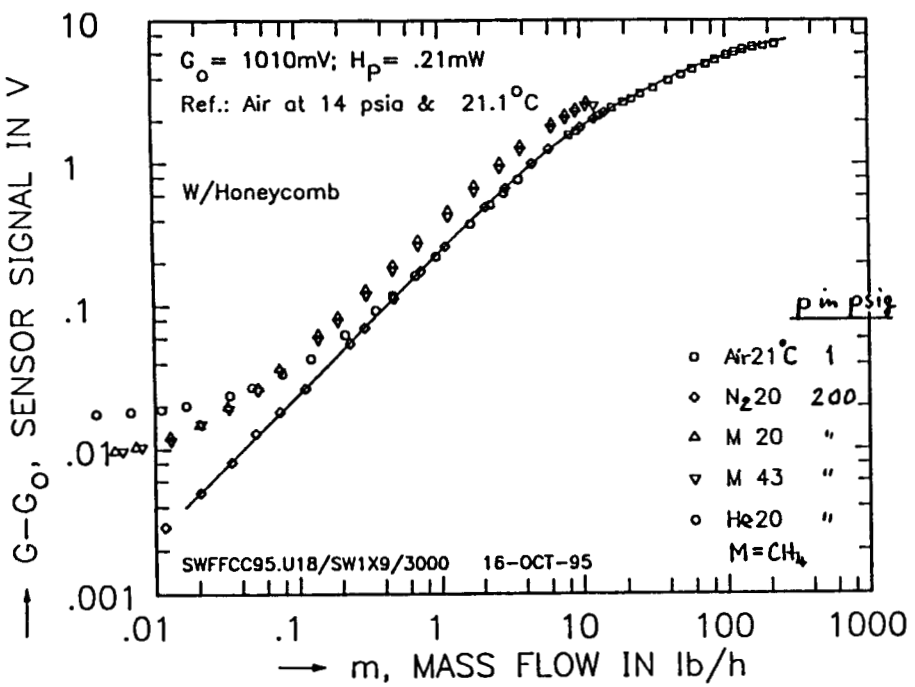

FIG. 25. MASS FLOW SENSOR X-99005 OUTPUT, WITHOUT COMPOSITION CORRECTION. BYPASS ACROSS 10 mm HCB.IN 25mmID PIPE. PROPERTY SENSOR SW129.

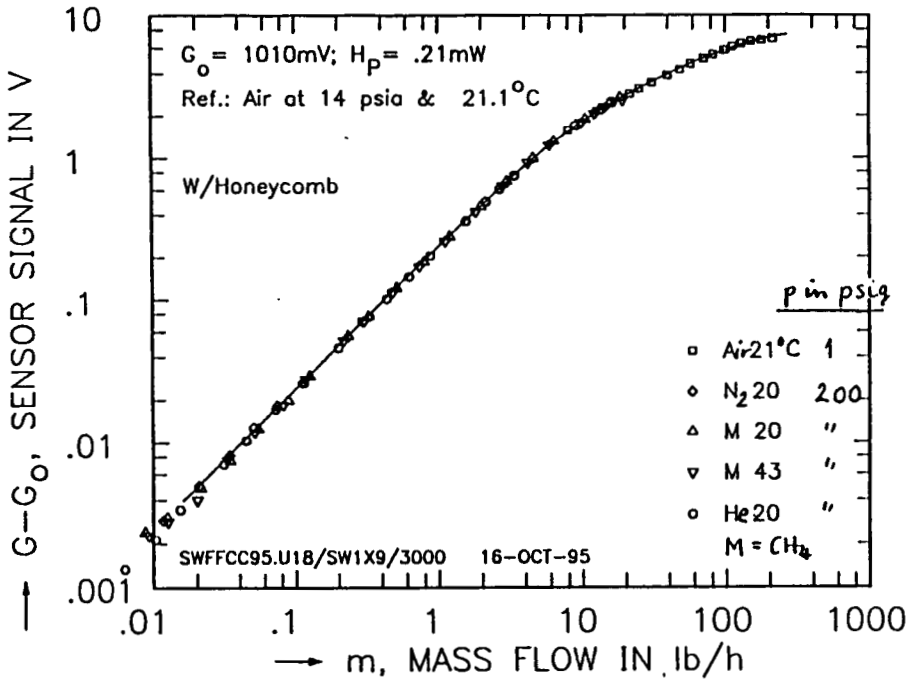

FIG.25a. MASS FLOW SENSOR X-99005 OUTPUT, WITH COMPOSITION CORRECTION (SW129). BYPASS ACROSS 10 mm HCB.IN 25mmID PIPE.

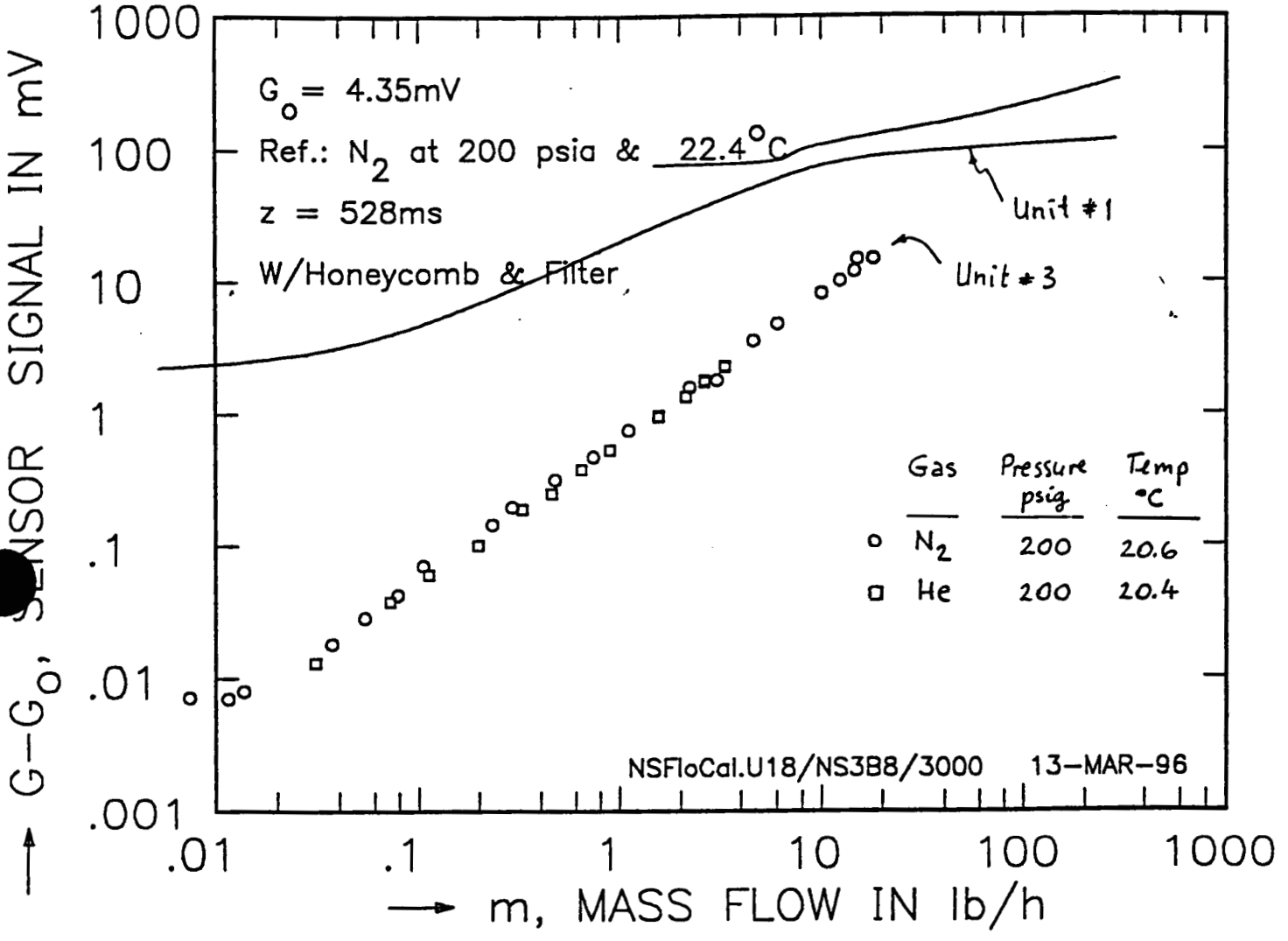

FIG. 26. MASS FLOW MEASUREMENT W/MICROSENSOR, IMPR'TS: BYPASS, AVERAGING, INDIV.G_o: 1:.00359, 2:.00435, 4:

#8 NS3B8N03.D20,H02; ckt up lv C2=.94

STRAIGHT FLOW CHANNEL OF 1" ID.

FIRE SAFETY ASPECTS OF Si_3N_4-Pt-BASED MICROBRIDGE FLOW SENSORS

by

U. Bonne, T. Stratton and R. Horning
Honeywell Sensor and System Development Center

May 20, 1992, rev. May 29, 1992

INTRODUCTION

The fire safety and flammability of Honeywell's flow micro-sensor[1,2,3] is described here from two points of view:

- The hazard resulting from operation in a flammable gas such as natural gas-air or hydrogen-air mixtures and

- The hazard resulting from operation in a pure, high pressure oxygen environment.

These hazards could be thought of, in the worst case, to lead to fires involving the sensor elements as ignitors of either the flammable mixture or of the sensor hardware itself.

To determine the severity of these hazards we checked whether:

1. The sensor heater, during normal operation, could ignite a surrounding gas mixture or

2. The sensor heater could ignite itself during normal operation, to burn in an oxygen atmosphere or

3. The sensor heater could ignite a gas mixture under abnormal operation or

4. The sensor heater could ignite itself during abnormal operation to burn in an oxygen atmosphere.

5. Any part of the sensor or its flow channel hardware could support combustion in air or in an oxygen atmosphere, if ignited by an external source.

The difference between normal and abnormal operation is defined, for the purposes of this review, by the difference in heater power: under normal conditions the approx. 50 x 100 µm sized heater is raised 60-160°C above ambient temperature, with about 2-6 mW of input power, and by applying less than 10V DC; under abnormal conditions, an over-voltage may first overheat and eventually vaporize the platinum thin film, and cause an electric spark and an open circuit.

DISCUSSION

In addressing the above five hazard modes, the physical evidence and experience which lead us to believe that this sensor is safe, is as follows:

1. Auto ignition temperatures of hydrocarbon-air mixtures range from 537°C for methane, 466°C for propane, to 206°C for n-nonane/n-hexadecane[4]. At these temperatures, large volumes of stoichiometric gas mixtures will eventually ignite. However, ignition by wires at these temperatures is much more difficult: a bare nickel or platinum wire needs to be heated to over 1000 and 1150°C, respectively[5] to achieve natural gas-air ignition under lean conditions, and still higher temperatures under stoichiometric or rich conditions. Given the smallness of the microbridge heater (i.e. well below even the quenching distance) and its normal operating temperature of less than 185 to 285°C, even under 125°C-under-hood-automotive ambient temperatures, ignition is extremely unlikely if the heater is operated at a peak absolute temperature of less than 200°C.

2. Reaction rates for Si_3N_4 to form SiO_2 and N_2 or NO_2 are so slow, even at 500°C, that combustion is not sustained. Evidence:
   a) The most energetic reaction, forming $3SiO_2 + 2N_2$, releases 473 kcal per mole of Si_3N_4[6] (465 kcal to form $3SiO_2 + 2NO_2$), or 158 kcal/mol of SiO_2 formed, which is less than released by the reaction: $Si + O_2 >> SiO_2 + 209$ kcal/mol.
   b) The Si-oxidation reaction can also not sustain itself, because its heat release rate is several orders of magnitude lower than the rate of heat dissipation by thermal conductivity into the surrounding oxygen atmosphere: The known "thin oxide layer" or reaction-limited oxidation rate of Si, at 500°C, through its adhering oxide, is $3.5 \cdot 10^{-7}$ µm/h, which is equivalent to $6 \cdot 10^{-7}$ cal/(h cm^2). The heat conduction rate, assuming only a 1000 °C/cm gradient, is over 8 orders of magnitude larger.
   c) The reaction-limited oxidation of Si_3N_4 at 1200 °C was computed to be 0.052µm/h[11], which still is equivalent to a factor of 1000x less than the heat dissipation rate.
   d) Even if oxidation occurs at high oxygen concentrations and temperatures, the forming oxide adheres to Si_3N_4 and SiO_2, as with the oxides of aluminum and stainless steel.

3. One abnormal condition of operation was tested. A microbridge flow sensor was introduced into a 0.8 stoichiometric natural gas-air mixture. An over-voltage applied to the heater, causing instant vaporization and a little spark; but no ignition of the combustible mixture resulted[7]. The applied heater voltage was 10x the normal level required for slow burnout, but was not sufficient to generate enough energy (10^{-5}J) to exceed the minimum ignition energy of $2 \cdot 10^{-4}$ J[6].

   The auto ignition temperatures of hydrocarbons with oxygen are only about 5°C lower than with air, except for butane (about

130°C lower)[4] and possibly propane (not listed in ref.4), but none is lower than 200°C.

4. The reasoning in above item 2 also holds here: while an over-voltage may disable the microbridge element (heater or sensor), the achieved local heating will not support a propagating combustion wave to reach the Si chip. Solid Si is not known to burn in an O_2 environment, unless ground and dispersed as a cloud of particles. Then its heat of combustion would be 209 kcal/mole[6].

5. The most vulnerable part of the exposed part of the sensor would be the honeycomb and screen(s) used to condition the flow. Therefore their composition was selected to not be flammable even in an oxygen atmosphere. Aluminum alloys 11XX-ANN (MIL-A-148) or 2024-T81 in foil[10] and 1100 or 2024-T4/T6 in wire form are rated for use in oxygen up to 1000psi in Rockwell's Materials Directory.[9] Other metals such as braze Cu and Ni, Ni-Cr-Fe wire, and Weld-wire Ni-based are also listed with ratings of up to 3000psi in oxygen and are candidate materials for screens.

The used 25 µm OD (0.001") gold wires to connect the sensor chip with the TO5 header are not viewed as a hazard in an oxygen or air environment.[9]

Fused zener diode barrier circuits can be added to the sensor input if a probability exists for the accidental application of voltages above those handled safely by the circuit (typically 30V), thus redering the circuit "intrinsically safe"[8]. The "internal" sensor and circuit are intrinsically safe since its maximum heater energy levels (<1mA x <15V), in case of malfunction, would be more than 1000x below the level needed to ignite combustible mixtures of hydrogen-air[8], in the presence of Al, Cd, Mg or Zn, or even of hydrogen-oxygen mixtures, with about 100x lower ignition energies, if the measurements with hydrocarbon-air and oxygen may be used as a guide.[5]

CONCLUSIONS

In conclusion, whether operating normally or under extreme (accidental) conditions, the hazard of having the Honeywell $Si_3N_4/Pt/Si$ flow sensor self-ignite or cause a combustible gas-air mixture to ignite is so small that it has not been measurable to date.

GAS FLOW SENSORS FOR SPACE APPLICATIONS
Phase I. Fabrication of Two Demonstration Units

1. EXECUTIVE SUMMARY

The purpose of this program was to demonstrate the performance of a thermal flow microsensor. It would be intended for the measurement of flows of helium, nitrogen, oxygen and hydrogen in both the ARPCS (Atmospheric Revitalization Pressure Control Subsystem) and in the FCS (Fuel Cell System), which have been using sensors that experienced high failure rates.

An existing sensor design was adapted for this project. Two sensors were built and tested, and delivered to Carleton for further tests, after improvements were made to overcome interferences by what was recognized as thermal microconvection.

In spite of the improvements, the test results indicate that not all performance attributes materialized, which had been predicted for operation at pressures up to 61 bar (900 psi), based on previous data of flow microsensor performance up to 4 bar (60 psia). The unforeseen factor that increasingly interfered as pressure was increased, was one caused by thermal microconvection currents generated by the sensor's microheaters. These caused both large, signal shifts as well as deterioration of the S/N ratio. Whereas the direct influence of these currents could be reduced significantly via implemented improvements[14], the ability of a single point flow sensor to meet the accuracy specifications over the large 15,000:1 dynamic flow range remained marginal.

Test results of these improved units, while meeting expectations in terms of the response time, power consumption, insensitivity to orientation up to 500 psi, and accuracy at flows below 5 lb/h, were disappointing as far as accuracies achieved with the high flow sensing approach (above 5 lb/h), labour-intensive adjustments of the matching of the high and low flow signals, flow signal errors resulting from the temperature difference between the flowing gas and the sensor block, in which the property and temperature sensors are mounted, the orientation sensitivity at 900 psig and signal noise, and the fact that the remaining orientation sensitivity also prevented us from differentiating between N_2 and O_2.

We therefore recommended that the direct, single-point flow measurement of Units#1 and 2 be replaced by a bypass, multiple-point flow sensing approach. Such recommendation was made on the basis of tests made with two such units, which not only showed predictable gas composition correction behaviour, a possibility to replace the heater power approach used at high flows by the more accurate differential approach over the the full flow range, but also a more linear and predictable output, enhanced S/N and the possibility of further reducing the effect of orientation-dependent, thermal microconvection, due to the beneficial influence of mounting the sensor chip in a well-defined, more constraining microchannel.

REFERENCES

1. D. Tessmann, Honeywell MICRO SWITCH, "Use of a Point Mass Flow Sensor to Measure Gas Flow Rates of up to 20L/min.," Sensors Expo-West, Anaheim, CA, 14-16 April 19924.

2. U. Bonne, "Fully Compensated Flow Microsensor for Electronic Gas Metering", Int'l Gas Res. Conf., Orlando, FL, 6-19 Nov. 92, accepted for publication.

3. U. Bonne and G. Havey, "Versatile Microbridge Flow Control Sensor Structure and Applications", 22nd Int'l Conf. Env. Syst., Seattle, WA, 13-16 July 92, accepted for presentation.

4. M.G. Zabetakis, "Flammability Characteristics of Combustible Gases and Vapors," Bulletin 627, USBM, US Gov't Printing Office, Washington, DC, 20402 (1965),Table 4, p.25.

5. B. Lewis and G. von Elbe, "Combustion Flames and Explosions of Gases," 1st Ed., Academic Press, NY, NY (1961) p. 365.

6. M.W. Chase et al, "JANAF Thermochemical Tables", 3rd Ed., (Dow Chemical Co.), ACS, AIP & NBS; J. Phys. Chem. Ref. Data 14 (1985) Suppl. 1.

7. U. Bonne et al, "Microstructure Sensors for Flow, Differential Pressure and Energy Measurement," IGT Symposium on "Natural Gas Energy Measurement," Chicago, IL, 30 April - 2 May, 1986, Proceedings.

8. P.J. Schram and M.W. Early, "Electrical Installations in Hazardous Locations," NFPA, Quincy, MA (1988), p.183ff and Fig. 4-31(attached).

9. G.A. Blackburn et al, "Materials Directory", Rockwell Int'l, Space Transportation Systems Div., IRD RA-366EA, Aug.1988.

10. Honeycomb structures of this material are available from Hexcel's Structural Products Division, phn.: (817) 274-2578.

11. SUPREM, Process Modeling Software Package, developed by Stanford University, licensed through Technology Modelling Associates Inc., Palo Alto, CA.

UB/jl
MBSafe92.W01 NASA Safety in O2/White Papers

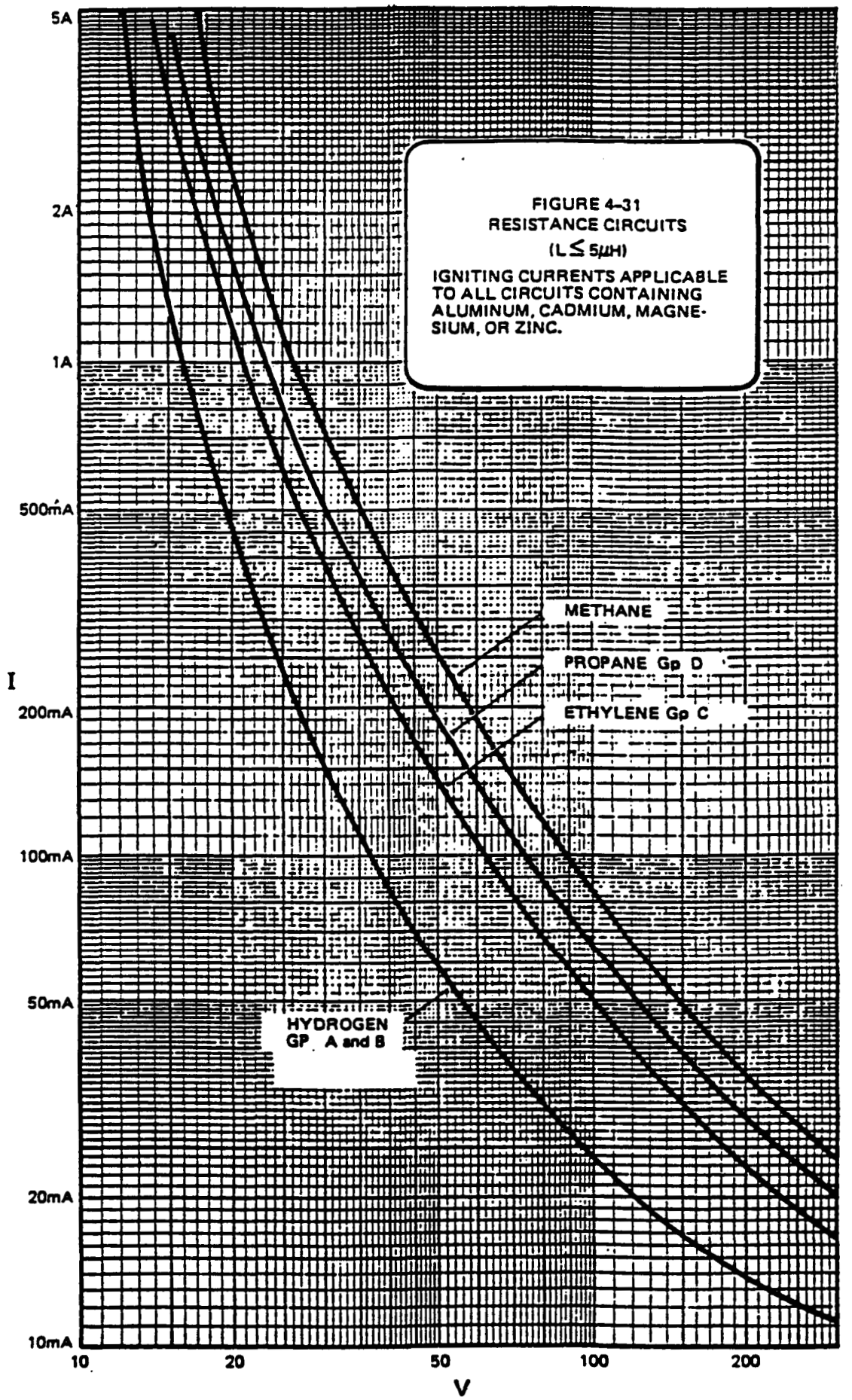

Figure 4–31. *Curve of resistance circuits, cadmium disc.*